



**This electronic thesis or dissertation has been  
downloaded from Explore Bristol Research,  
<http://research-information.bristol.ac.uk>**

*Author:*  
**Williams, Claire L**

*Title:*  
**The natural history of the autoimmune response to zinc transporter 8 (ZnT8) in type 1 diabetes**

**General rights**

Access to the thesis is subject to the Creative Commons Attribution - NonCommercial-No Derivatives 4.0 International Public License. A copy of this may be found at <https://creativecommons.org/licenses/by-nc-nd/4.0/legalcode> This license sets out your rights and the restrictions that apply to your access to the thesis so it is important you read this before proceeding.

**Take down policy**

Some pages of this thesis may have been removed for copyright restrictions prior to having it been deposited in Explore Bristol Research. However, if you have discovered material within the thesis that you consider to be unlawful e.g. breaches of copyright (either yours or that of a third party) or any other law, including but not limited to those relating to patent, trademark, confidentiality, data protection, obscenity, defamation, libel, then please contact [collections-metadata@bristol.ac.uk](mailto:collections-metadata@bristol.ac.uk) and include the following information in your message:

- Your contact details
- Bibliographic details for the item, including a URL
- An outline nature of the complaint

Your claim will be investigated and, where appropriate, the item in question will be removed from public view as soon as possible.



The natural history of the autoimmune  
response to zinc transporter 8 (ZnT8) in  
type 1 diabetes

Claire Louise Williams

A dissertation submitted to the University of Bristol in accordance with the requirements for award of the degree PhD in the Faculty of Health Sciences Bristol Medical School submitted October 2021.

Word Count: 63,223

## Abstract

---

Type 1 diabetes (T1D) results from progressive autoimmune-mediated destruction of insulin-producing beta ( $\beta$ )-cells in pancreatic islets. The most effective biomarkers used to predict the development of T1D are four islet autoantibodies that recognise  $\beta$ -cell antigens with high specificity. Islet autoantibodies can be detected years before diagnosis, but progression rate can vary from months to decades. Autoantibodies directed to zinc transporter 8 (ZnT8A) were discovered in 2007, are common in individuals that slowly and rapidly progress to T1D and are usually detected by radioimmunoassay, but characteristics of the response (affinity, IgG subclasses, epitope specificity) are under-investigated.

We hypothesised that (1) characterisation of ZnT8A responses prior and close to T1D onset utilising adapted radioimmunoassays will inform the pathogenesis of T1D (2) factors associated with loss of ZnT8A after T1D onset will be different to those at onset and may provide insights into ongoing  $\beta$ -cell destruction, and (3) a novel luciferase-based immunoprecipitation system (LIPS) assay could replace the radioimmunoassay for ZnT8A detection.

Prior to and close to T1D onset, ZnT8A responses are dynamic, showing loss or gain of autoantibody status and titre, and some alteration in affinity, epitope specificity, and IgG subclasses. There did not appear to be clear differences between individuals who slowly or rapidly progress to T1D. After T1D onset, ZnT8A were lost rapidly compared to other autoantibodies, but the non-genetic and genetic factors associated with ZnT8A at and after T1D onset were comparable. The LIPS assay offered improvement in sensitivity and specificity over the radioimmunoassay and identified a small additional subset of at-risk individuals with a 20-year T1D risk of 26%.

These studies provide the first in-depth analysis of ZnT8A throughout the autoimmune response in T1D, describe methods to examine ZnT8A characteristics, and detail the optimisation of an improved low blood volume test suitable for general population screening.

## Dedication & Acknowledgments

---

First and foremost, I would like to express my profound gratitude to all of my supervisors, Dr Anna E. Long, Dr Alistair J.K. Williams, and Professor Kathleen M. Gillespie, for their mentorship, invaluable advice, and encouragement throughout my PhD. All of whom believed in my ability to pursue an academic career from when I first joined the team as a Research Technician in 2014 and have since, invested in my development and have supported me all the way (even remotely)!

While I could not have asked for a better supervisory team, I would like to dedicate this thesis to my late supervisor, Dr Alistair J.K. Williams, in sincere appreciation of his life's work. I feel that no other thesis fully encapsulates all he developed and contributed to the T1D field over 30 years. I am extremely grateful for his mentorship, friendship, and time he dedicated to all early career researchers, including myself. Alistair is greatly missed, and it is with a heavy heart that I complete this PhD without his tremendous insight, experience, and high attention to detail.

I owe my deepest gratitude to Dr Anna E. Long. Not only have you been a superb primary supervisor, but you have also consistently been my guiding light and sounding board through a turbulent time in my life. You continually inspire me, boost my morale, and make me laugh! I am very proud to be your first PhD student, friend, and fellow Wagamama enthusiast! I also owe a great deal of gratitude to Professor Kathleen M. Gillespie, whose counsel, belief in me, and enthusiasm for my work have immeasurably prepared me for my future career and kept me going! Thank you also to Dr Becky Foster and Dr Ann Pullen for reviewing my work each year and for your collective counsel, insight, and advice.

Thank you to Diabetes UK for awarding me a PhD scholarship for this work, I have always been proud to represent this wonderful charity and have immensely enjoyed the yearly conferences and student networking days. I would also like to thank past and present faculty members of the Diabetes & Metabolism team (especially Georgina Mortimer and Olivia Ball) and the Learning & Research Building for their support, friendship, great sense of humour, lively laboratory environment, and affiliation for cake!

Last but not least, a massive thank-you goes to my partner of 12 years, Jake Murphy, and my parents, Karen and Stephen Williams. I could not have completed this PhD without your unconditional love, unwavering support, sacrifices for my education, and your steadfast belief I could do this (even when I did not!). A special thank-you to my two cat babies, Amber and Tootsie, for their company, affection, and distraction during my write-up.

## **Author's Declaration**

---

I declare that the work in this dissertation was carried out in accordance with the requirements of the University's Regulations and Code of Practice for Research Degree Programmes and that it has not been submitted for any other academic award. Except where indicated by specific reference in the text, the work is the candidate's own work. Work done in collaboration with, or with the assistance of, others, is indicated as such. Any views expressed in the dissertation are those of the author.

SIGNED: ..... DATE: .....October 2021.....

# Table of Contents

---

<b>Abstract.....</b>	<b>i</b>
<b>Dedication &amp; Acknowledgments .....</b>	<b>ii</b>
<b>Author’s Declaration .....</b>	<b>iii</b>
<b>Table of Contents .....</b>	<b>iv</b>
<b>List of Figures.....</b>	<b>xii</b>
<b>List of Tables .....</b>	<b>xix</b>
<b>Presentations &amp; publications that have arisen during the PhD Studentship to date ..</b>	<b>xxiii</b>
<b>Abbreviations .....</b>	<b>xxv</b>
<b>Chapter 1 - General introduction.....</b>	<b>1</b>
<b>1.1. Type 1 diabetes .....</b>	<b>2</b>
<b>1.2. Incidence .....</b>	<b>3</b>
<b>1.3. Clinical characteristics &amp; pathogenesis .....</b>	<b>4</b>
<b>1.4. Diabetes treatment &amp; management.....</b>	<b>6</b>
<b>1.5. Disease aetiology.....</b>	<b>8</b>
1.5.1. Genetics.....	8
1.5.1.1. HLA.....	9
1.5.1.2. Non-HLA.....	13
1.5.2. Environment.....	16
1.5.2.1. Viral infection.....	17
1.5.2.2. The hygiene hypothesis .....	17
1.5.2.3. The gut microbiome .....	18
1.5.2.4. Vitamin D.....	18
<b>1.6. Disease pathology .....</b>	<b>19</b>
1.6.1. Insulinitis.....	19
1.6.2. Tolerance, immune cells, autoimmunity, & T1D.....	21
1.6.2.1. Tolerance .....	22
1.6.2.2. T-cells & T1D .....	26
1.6.2.3. B-cells & T1D .....	32

1.6.3. Islet autoantibodies.....	43
1.6.3.1. Predicting T1D risk & progression using the presence of islet autoantibodies..	46
1.6.3.2. Characteristics of islet autoantibodies that further aids T1D risk prediction .....	51
1.6.3.3. Measuring islet autoantibodies .....	57
1.6.3.4. Islet autoantibody standardisation program (IASP) .....	62
<b>1.7. Zinc transporter 8 (ZnT8) &amp; T1D .....</b>	<b>63</b>
1.7.1. The function of ZnT8 .....	63
1.7.2. The <i>SLC30A8</i> gene.....	64
1.7.3. The structure of ZnT8 .....	66
1.7.4. Discovery & prevalence of autoantibodies to ZnT8 (ZnT8A) at T1D diagnosis.....	69
1.7.5. The initiation & development of the ZnT8A autoimmune response .....	71
1.7.5.1. Initiation of ZnT8 autoimmunity.....	71
1.7.5.2. ZnT8 as an autoantigen .....	72
1.7.6. Predicting diabetes using ZnT8A.....	74
1.7.7. ZnT8A as a biomarker of insulin secretory capacity after T1D onset .....	76
1.7.8. What benefits could new assays for ZnT8A detection offer for prediction? .....	77
<b>1.8. The Bart's-Oxford (BOX) family study .....</b>	<b>79</b>
<b>1.9. Project rationale .....</b>	<b>81</b>
1.9.1. Hypothesis.....	81
1.9.2. Aims .....	81
<b>Chapter 2 - Characterisation of the ZnT8 humoral response up to T1D onset .....</b>	<b>82</b>
<b>2.1. Introduction.....</b>	<b>83</b>
2.1.1. Hypothesis.....	84
2.1.2. Aims .....	84
<b>2.2. Characterisation of ZnT8A affinity.....</b>	<b>85</b>
2.2.1. Introduction of ZnT8A affinity for ZnT8.....	85
2.2.2. Materials & Methods.....	87
2.2.2.1. Populations for ZnT8A affinity studies.....	87
2.2.2.2. Recombinant ZnT8 protein for affinity studies .....	90

2.2.2.3. Radioimmunoassays (RIAs).....	91
2.2.2.4. RIA methodology for ZnT8A affinity studies.....	95
2.2.2.5. Statistical analysis .....	96
2.2.3. Results .....	97
2.2.3.1. Optimisation of the recombinant protein concentration curves .....	97
2.2.3.2. Defining ZnT8A affinity in new-onset T1D patients using the optimised protein concentration curve .....	100
2.2.4. Discussion .....	107
2.2.4.1. Main findings .....	107
2.2.4.2. Strengths, limitations, & future work.....	107
<b>2.3. Characterisation of ZnT8A IgG subclasses .....</b>	<b>111</b>
2.3.1. Introduction to islet autoantibody IgG subclasses .....	111
2.3.1.1. Hypothesis .....	117
2.3.1.2. Aims .....	117
2.3.2. Materials & Methods.....	118
2.3.2.1. Populations for autoantibody IgG subclass studies .....	118
2.3.2.2. Detection of ZnT8A, GADA, & IA-2A IgG subclasses by RIA .....	124
2.3.2.3. Statistical analysis .....	128
2.3.3. Results .....	129
2.3.3.1. Multiple autoantibody positive progressor sample set.....	129
2.3.3.2. New-onset T1D patient sample set.....	134
2.3.3.3. Screening T1D patients for quality control development sample sets .....	137
2.3.4. Discussion .....	142
2.3.4.1. Main findings .....	142
2.3.4.2. Strengths & limitations.....	143
2.3.4.3. Composition & characteristics of islet autoantibody IgG subclasses.....	146
<b>2.4. Characterisation of ZnT8A epitopes in C-terminal ZnT8 .....</b>	<b>149</b>
2.4.1. Introduction to B-cell epitopes of ZnT8.....	149
2.4.1.1. Hypothesis .....	152

2.4.1.2. Aims .....	152
2.4.2. Materials & Methods.....	153
2.4.2.1. Populations for ZnT8A epitope studies.....	153
2.4.2.2. Generation of mutant ZnT8 constructs for ZnT8A epitope studies .....	156
2.4.2.3. ZnT8A epitope studies by RIA .....	161
2.4.2.4. <i>SLC30A8</i> genotype determination.....	162
2.4.2.5. Statistical analysis .....	162
2.4.3. Results .....	163
2.4.3.1. Categorisation of ZnT8A reactivity to the major epitope (325) in slow & rapid progressors of T1D by <i>SLC30A8</i> genotype & age at onset.....	163
2.4.3.2. Categorisation of ZnT8A reactivity to the major epitope (325) in new-onset T1D patients by <i>SLC30A8</i> genotype & age at onset.....	166
2.4.3.3. Categorisation of ZnT8A reactivity to the major conformational epitope (REKK) according to ZnT8A specificity.....	172
2.4.3.4. Categorisation of ZnT8A reactivity to ZnT8's three C-terminal cysteines (C361, C364, & C368) according to ZnT8A specificity.....	181
2.4.4. Discussion .....	192
2.4.4.1. Main findings .....	192
2.4.4.2. Strengths & limitations.....	193
2.4.4.3. Epitopes of ZnT8 recognised by ZnT8A.....	196
<b>2.5. Characterisation of the ZnT8 humoral response from ZnT8A seroconversion...200</b>	
2.5.1. Materials & Methods.....	200
2.5.1.1. ZnT8A seroconversion population.....	200
2.5.2. Results .....	203
2.5.2.1. Determining ZnT8A specificity in the ZnT8A seroconversion population .....	203
2.5.2.2. Case study of the ZnT8A humoral response in two individuals that seroconverted under 10 years of age.....	204
2.5.2.3. Case study of the ZnT8A humoral response in four individuals that seroconverted between 10-15 years of age .....	207

2.5.2.4. Case study of the ZnT8A humoral response in four individuals that seroconverted with ZnT8A after 30 years of age .....	213
2.5.3. Discussion .....	218
2.5.3.1. Main findings .....	218
2.5.3.2. Strengths, limitations, & future work .....	219
<b>Chapter 3 - Characterisation of islet autoantibodies after T1D onset .....</b>	<b>222</b>
<b>3.1. Introduction .....</b>	<b>223</b>
3.1.1. Hypothesis .....	225
3.1.2. Aims .....	225
<b>3.2. Material &amp; Methods .....</b>	<b>225</b>
3.2.1. Population description .....	225
3.2.2. Genetic determination .....	229
3.2.3. Data transformation & statistical analysis .....	230
<b>3.3. Results .....</b>	<b>232</b>
3.3.1. Prevalence of autoantibodies at onset & longitudinal follow-up .....	232
3.3.2. Patterns of autoantibody titre over longitudinal follow-up .....	236
3.3.3. Non-genetic associations of autoantibody positivity at initial sampling & autoantibody loss at final sampling .....	239
3.3.3.1. Initial sampling .....	239
3.3.3.2. Final sampling .....	241
3.3.4. Genetic associations of autoantibody positivity at initial sampling & autoantibody loss at final sampling .....	248
3.3.4.1. GADA .....	250
3.3.4.2. IA-2A .....	250
3.3.4.3. ZnT8A .....	251
<b>3.4. Discussion .....</b>	<b>252</b>
3.4.1. Main findings .....	252
3.4.2. Islet autoantibody responses after T1D onset .....	253
<b>Chapter 4 - Development of Nluc-ZnT8 LIPS for ZnT8A detection .....</b>	<b>259</b>
<b>4.1. Introduction .....</b>	<b>260</b>

4.1.1. Bioluminescence & luciferase enzymes.....	261
4.1.2. Utilising luminescence for immunoassays.....	264
4.1.2.1. Luminescence immunoassays for islet autoantibody detection .....	264
4.1.3. Improving ZnT8A detection in plasma samples .....	267
4.1.4. Summary .....	268
4.1.5. Hypothesis.....	269
4.1.6. Aims .....	269
<b>4.2. Materials &amp; Methods .....</b>	<b>270</b>
4.2.1. Optimisation populations .....	270
4.2.1.1. Main optimisation sample set.....	270
4.2.1.2. IASP workshop optimisation sample sets .....	273
4.2.2. Matched serum & EDTA-preserved plasma population.....	274
4.2.3. Positivity threshold population .....	275
4.2.4. Validation populations .....	276
4.2.4.1. IASP2020 sample set.....	276
4.2.4.2. BOX.....	276
4.2.5. Optimised Nluc-GAD65 LIPS assay method .....	280
4.2.6. Nluc-tagged ZnT8 antigen constructs .....	281
4.2.7. Nluc-ZnT8 LIPS optimisation experiments for ZnT8A detection.....	282
4.2.8. Optimised Nluc-ZnT8 LIPS assay method .....	283
4.2.8.1. Assay buffers.....	283
4.2.8.2. Expression of Nluc-ZnT8 antigen .....	283
4.2.8.3. Preparation of Nluc-ZnT8 antigen .....	284
4.2.8.4. Optimised Nluc-ZnT8 LIPS assay methodology .....	285
4.2.9. Statistical analysis .....	287
4.2.9.1. Optimisation of the Nluc-ZnT8 LIPS assay .....	287
4.2.9.2. Establishing a positive threshold for the optimised Nluc-ZnT8 LIPS assay....	287
4.2.9.3. Sensitivity & specificity of the optimised Nluc-ZnT8 LIPS assay .....	288
4.2.9.4. Comparing the predictive utility of Nluc-ZnT8 LIPS & RIA .....	288

<b>4.3. Results .....</b>	<b>288</b>
4.3.1. Aim 1: Optimisation of a Nluc-ZnT8 LIPS assay for ZnT8A detection.....	288
4.3.1.1. Nluc-tagged ZnT8 antigen construct & antigen concentration .....	291
4.3.1.2. Concentration of Tween-20 in assay buffers.....	293
4.3.1.3. Nluc-tagged ZnT8 antigen construct & antigen incubation length .....	295
4.3.1.4. Nluc-ZnT8 LIPS assessment in the IASP2018 sample set.....	297
4.3.1.5. Expression & preparation of the Nluc-tagged ZnT8 antigen construct.....	304
4.3.1.6. Detection of luminescence .....	312
4.3.1.7. Summary of Nluc-ZnT8 LIPS assay optimisation .....	319
4.3.2. Aim 2: Investigate reagents to improve ZnT8A detection in EDTA-preserved plasma samples using the LIPS method. ....	320
4.3.2.1. Serum ZnT8A detection in the presence of EDTA with CaCl <sub>2</sub> or ZnCl <sub>2</sub> .....	320
4.3.2.2. Serum & plasma ZnT8A detection in the presence of 1mM ZnCl <sub>2</sub> .....	323
4.3.3. Aim 3: Establish a serum positivity threshold for the optimised Nluc-ZnT8 LIPS method.....	329
4.3.4. Aim 4: Evaluate the sensitivity and specificity of the optimised Nluc-ZnT8 LIPS method using new-onset T1D patients from BOX and blinded samples from the IASP2020 workshop .....	332
4.3.4.1. The sensitivity of Nluc-ZnT8 LIPS compared with RIA in new-onset T1D patients.....	332
4.3.4.2. The sensitivity and specificity of Nluc-ZnT8 LIPS in new-onset T1D patients & healthy schoolchildren.....	336
4.3.4.3. The sensitivity & specificity of Nluc-ZnT8 LIPS in the IASP2020 sample set .....	337
4.3.5. Aim 5: Evaluate the predictive utility of the optimised Nluc-ZnT8 LIPS assay compared with RIAs using serum samples from patients & first-degree relatives participating in the BOX study .....	339
<b>4.4. Discussion.....</b>	<b>341</b>
4.4.1.1. Main findings .....	341
4.4.1.2. Strengths & limitations.....	342
4.4.1.3. Optimisation of Nluc-ZnT8 LIPS.....	343

4.4.1.4. Validation of optimised Nluc-ZnT8 LIPS .....	344
4.4.1.5. Advantages of the LIPS assay & future applications .....	348
<b>Chapter 5 - General discussion .....</b>	<b>351</b>
<b>5.1. Prediction &amp; prevention of T1D .....</b>	<b>352</b>
<b>5.2. Islet autoimmunity &amp; residual <math>\beta</math>-cell function.....</b>	<b>362</b>
<b>5.3. Conclusion.....</b>	<b>366</b>
<b>Chapter 6 - References .....</b>	<b>369</b>
<b>Appendix A. ZnT8A affinity studies .....</b>	<b>401</b>
A.1. Generation of recombinant ZnT8 protein in-house .....	401
<b>Appendix B. ZnT8A IgG subclass studies .....</b>	<b>418</b>
B.1. Clones & source of monoclonal anti-human IgG subclass antibodies used in seminal T1D studies .....	418
B.2. GADA & IA-2A IgG subclass RIA standardisation .....	419
<b>Appendix C. ZnT8A epitope studies .....</b>	<b>426</b>
C.1. Cloning strategy to generate the ZnT8 construct encoding murine REKK (TGQ-) .....	426
C.2. Primer sequences of C-terminal ZnT8 mutations.....	430
<b>Appendix D. Characterisation of islet autoantibodies after T1D onset .....</b>	<b>432</b>
D.1. Seminal T1D studies reporting autoantibody prevalence.....	432
D.2. Prevalence of ZnT8RA & ZnT8WA at onset & longitudinal follow-up .....	436
D.3. Prevalence of autoantibodies at onset & longitudinal follow-up .....	437
D.4. Patterns of autoantibody titre over longitudinal follow-up .....	444
D.5. Non-genetic associations of longitudinal loss at final follow-up.....	455
<b>Appendix E. Development of Nluc-ZnT8 LIPS for ZnT8A detection.....</b>	<b>460</b>
E.1. Autoantibody detection in matched serum & EDTA-preserved plasma samples ....	460
E.2. Nluc-ZnT8 LIPS optimisation .....	461

## List of Figures

---

Figure 1:1 – Simplified schematic of Eisenbarth’s model of T1D pathogenesis (1986).....	5
Figure 1:2 – Schematic diagram of the MHC region on chromosome 6.....	9
Figure 1:3 – Simplified schematic of HLA class I & class II molecule structure .....	10
Figure 1:4 – HLA & Non-HLA genes that confer susceptibility to T1D identified from GWAS studies (2000-2009) .....	14
Figure 1:5 – Simplified diagram of the INS region on chromosome 11 .....	15
Figure 1:6 – Schematic of central tolerance .....	22
Figure 1:7 – Schematic of peripheral tolerance .....	23
Figure 1:8 – T-cell development & maturation .....	28
Figure 1:9 – B-cell development & maturation .....	34
Figure 1:10 – Schematic of a typical immunoglobulin molecule .....	36
Figure 1:11 – Human immunoglobulin isotypes .....	37
Figure 1:12 – Human IgG subclasses .....	38
Figure 1:13 – Schematic diagram of the pancreatic islet $\beta$ -cell illustrating the locations of the four major antigens that autoantibodies recognise: GAD65, IA-2, ZnT8, & insulin .....	44
Figure 1:14 – The predictive stages of T1D .....	47
Figure 1:15 – Summary of islet autoantibody characteristics that are associated with increased T1D risk .....	52
Figure 1:16 – Schematic diagram of the RIA .....	58
Figure 1:17 – Schematic diagram of the bridge-type ELISA .....	59
Figure 1:18 – Schematic diagram of the ECL assay .....	59
Figure 1:19 – Schematic diagram of the LIPS assay .....	61
Figure 1:20 – The structure of monomeric ZnT8 .....	67
Figure 2:1 – Basic methodology of the RIA for GADA, IA-2A, & ZnT8A detection.....	94
Figure 2:2 – ZnT8A affinity RIA plate set-up.....	95
Figure 2:3 – Optimisation of recombinant protein concentration curves for ZnT8A affinity studies (curve 1).....	97
Figure 2:4 – Optimisation of recombinant protein concentration curves for ZnT8A affinity studies (curve 2).....	98
Figure 2:5 – Optimisation of recombinant protein concentration curves for ZnT8A affinity studies (curve 3).....	99

Figure 2:6 – Categorisation of the major epitope (325) in new-onset T1D patients selected for affinity studies.....	100
Figure 2:7 – ZnT8A affinity competitive displacement curves in new-onset T1D patients according to radiolabelled ZnT8 antigen .....	102
Figure 2:8 – Proportion of high-moderate & low ZnT8A affinity responses for ZnT8RA, ZnT8WA, & ZnT8QA to corresponding ZnT8 antigen in new-onset T1D patients .....	103
Figure 2:9 – Proportion of high-moderate & low ZnT8A affinity responses to ZnT8 antigen across all ZnT8A responses according to ZnT8A titre (AU) in new-onset T1D patients .....	104
Figure 2:10 – ZnT8A affinity competitive displacement curves in new-onset T1D patients according to ZnT8A specificity & ZnT8 antigen .....	106
Figure 2:11 – Schematic diagram of the IgG subclass RIA.....	124
Figure 2:12 – GADA, IA-2A, & ZnT8A IgG subclass RIA plate set-up .....	125
Figure 2:13 – Basic RIA methodology for detection of GADA, IA-2A, & ZnT8A IgG subclasses.....	127
Figure 2:14 – GADA, IA-2A, ZnT8RA, & ZnT8WA IgG subclasses in the multiple autoantibody positive progressor sample set .....	131
Figure 2:15 – Overall frequency of GADA, IA-2A, ZnT8RA, & ZnT8WA IgG1-restricted & IgG-unrestricted responses in the multiple autoantibody positive progressor sample set.....	133
Figure 2:16 – IgG1 correlates with total IgG (PGS) & overall ZnT8A level (AU) in ZnT8R-reactive & ZnT8W-reactive new-onset T1D patients.....	134
Figure 2:17 – ZnT8A IgG subclasses in new-onset T1D patients.....	135
Figure 2:18 – The proportion of IgG1-restricted & IgG-unrestricted responses in ZnT8RA & ZnT8WA positive new-onset T1D patients .....	136
Figure 2:19 – Prevalence of GADA, IA-2A, ZnT8RA, & ZnT8WA IgG subclasses in the screening sample sets.....	138
Figure 2:20 – Correlation of IgG1 with total IgG (PGS) & overall autoantibody level (units) in GADA, IA-2A, ZnT8RA, & ZnT8WA screening sample sets.....	139
Figure 2:21 – Murine & human C-terminal ZnT8 residue alignment for conformational epitope mapping of ZnT8A .....	151
Figure 2:22 – Generation of ZnT8 mutant constructs by site-directed mutagenesis (SDM) & transformation into DH5 $\alpha$ E.Coli cells .....	156
Figure 2:23 – Cloning site, FASTA, & amino acid sequence of C-terminal ZnT8 (aa268-369) in the pCMVTnT vector.....	161
Figure 2:24 – Categorisation of the major epitope (325) in NPs, SPs, & RPs of T1D.....	163

Figure 2:25 – ZnT8A specificity profiles over longitudinal follow-up of NPs, SPs, & RPs.	165
Figure 2:26 – Categorisation of the major epitope (325) in new-onset T1D patients selected for epitope studies.....	166
Figure 2:27 – Correlation of R325-, W325-, & Q325-reactive ZnT8A in new-onset T1D patients .....	167
Figure 2:28 – SLC30A8 genotype & ZnT8A specificity to wild type ZnT8 variants by age at T1D onset.....	169
Figure 2:29 – The effect of the Q325 mutation on ZnT8RA & ZnT8WA binding according to overall ZnT8A specificity in new-onset T1D patients.....	171
Figure 2:30 – The effect of REKK-S, REKK-A, & murine-REKK mutations on ZnT8RA binding according to ZnT8A specificity in a subset of new-onset T1D patients.....	173
Figure 2:31 – The effect of the REKK-A mutation on ZnT8A binding according to ZnT8A specificity in new-onset T1D patients.....	175
Figure 2:32 – The effect of the REKK-A mutant on R325-reactive, W325-reactive, & Q325-reactive ZnT8A binding in new-onset T1D patients.....	176
Figure 2:33 – Categorisation of ZnT8A binding according to the median reduction in binding caused by REKK-A for the assessment of 349T .....	178
Figure 2:34 – The effect of the 349T mutation on ZnT8A binding according to the REKK-A binding & ZnT8A specificity in new-onset T1D patients .....	179
Figure 2:35 – The effect of the 349T mutant on R325-reactive & W325-reactive ZnT8A in new-onset T1D patients .....	180
Figure 2:36 – The effect of the C361S mutation on ZnT8A binding according to the ZnT8A specificity in new-onset T1D patients.....	182
Figure 2:37 – The effect of the C364S mutation on ZnT8A binding according to the ZnT8A specificity in new-onset T1D patients.....	183
Figure 2:38 – The effect of the C368S mutation on ZnT8A binding according to the ZnT8A specificity in new-onset T1D patients.....	184
Figure 2:39 – The effect of single cysteine-to-serine mutations on R325-reactive and W325-reactive ZnT8A binding in new-onset T1D patients.....	186
Figure 2:40 – The effect of the C361S/C364S & C361S/C368S double mutations on ZnT8RA binding according to ZnT8A specificity in a subset of new-onset T1D patients.....	187
Figure 2:41 – The effect of 360T on ZnT8A binding according to the ZnT8A specificity in new-onset T1D patients .....	189

Figure 2:42 – Dendrogram of ZnT8 mutational analysis by SLC30A8 genotype & binding to WT C-terminal ZnT8 .....	191
Figure 2:43 – Identifying ZnT8A seroconverters from FDRs in the BOX study .....	201
Figure 2:44 – Categorisation of the major epitope (325) in the ZnT8A seroconversion population .....	203
Figure 2:45 – Characterisation of the ZnT8A humoral response in Seroconverter 1 & 2.....	206
Figure 2:46 – Characterisation of the ZnT8A humoral response in Seroconverter 3 & 4.....	209
Figure 2:47 – Characterisation of the ZnT8A humoral response in Seroconverter 5 & 6.....	212
Figure 2:48 – Characterisation of the ZnT8A humoral response in Seroconverter 7 & 8.....	215
Figure 2:49 – Characterisation of the ZnT8A humoral response in Seroconverter 9 & 10...	217
Figure 3:1 – Distribution of longitudinal serum samples available from 577 individuals with T1D .....	227
Figure 3:2 – Autoantibody profiles at T1D onset .....	232
Figure 3:3 – Longitudinal autoantibody positivity over follow-up .....	233
Figure 3:4 – Prevalence of longitudinal autoantibody positivity characterised by autoantibody profiles at T1D onset.....	234
Figure 3:5 – The frequency of longitudinal autoantibody positivity .....	235
Figure 3:6 – Longitudinal GADA, IA-2A, & ZnT8A levels from T1D onset .....	237
Figure 3:7 – Non-genetic associations on autoantibody positivity at T1D onset .....	240
Figure 3:8 – Associations of co-existing autoantibodies on autoantibody positivity at T1D onset .....	241
Figure 3:9 – Non-genetic associations of autoantibody loss for GADA, IA-2A, & ZnT8A.	242
Figure 3:10 – Longitudinal GADA, IA-2A, & ZnT8A titres categorised into baseline quartiles at T1D onset.....	244
Figure 3:11 – Quartiles of autoantibody level at T1D onset over longitudinal follow-up for GADA, IA-2A, & ZnT8A (Violin plots).....	245
Figure 3:12 – Genetic associations of autoantibody positivity at initial sampling around T1D onset & autoantibody loss at final sampling after T1D onset.....	249
Figure 4:1 – Bioluminescent characteristics of Fluc, Rluc, Gluc, & Nluc luciferases .....	263
Figure 4:2 – Nluc-ZnT8 LIPS Validation: Positive threshold population.....	275
Figure 4:3 – Nluc-ZnT8 LIPS Validation: New-onset T1D patients.....	277
Figure 4:4 – Nluc-ZnT8 LIPS Validation: ZnT8A positive first-degree relatives .....	278
Figure 4:5 – Nluc-ZnT8 LIPS Validation: ZnT8A negative first-degree relatives .....	278
Figure 4:6 – sNluc- & Nluc-tagged ZnT8 antigen constructs.....	281

Figure 4:7 – Basic methodology of the optimised Nluc-ZnT8 LIPS assay .....	286
Figure 4:8 – Nluc-ZnT8 LIPS Optimisation: Nluc-R+W-ZnT8 antigen construct & concentration (SNR) .....	292
Figure 4:9 – Nluc-ZnT8 LIPS Optimisation: Concentration of Tween-20 in assay buffers (SNR) .....	294
Figure 4:10 – Nluc-ZnT8 LIPS Optimisation: Nluc-tagged ZnT8 antigen construct & antigen incubation length (SNR) .....	296
Figure 4:11 – Nluc-ZnT8 LIPS Optimisation: IASP2018 workshop ZnT8A specificity using monomeric ZnT8R/ZnT8W RIAs (AU) .....	299
Figure 4:12 – Nluc-ZnT8 LIPS Optimisation: IASP2018 workshop LIPS versus RIA using monomeric RIA AU or maximum RIA AU .....	300
Figure 4:13 – Nluc-ZnT8 LIPS Optimisation: LIPS & RIA AU in IASP2018 (AU) .....	301
Figure 4:14 – Nluc-ZnT8 LIPS Optimisation: Bland-Altman analysis comparing AU from LIPS & RIA (maximum) in the IASP2018 workshop .....	302
Figure 4:15 – Nluc-ZnT8 LIPS Optimisation: Preparation methods for the Nluc-R+W-ZnT8 dual heterodimer construct (SNR) .....	306
Figure 4:16 – Nluc-ZnT8 LIPS Optimisation: Preparation methods for the Nluc-R+W ZnT8 dual heterodimer construct (AU) .....	307
Figure 4:17 – Nluc-ZnT8 LIPS Optimisation: Preparation methods for the Nluc-R+W-ZnT8 dual heterodimer construct (AU correlation) .....	309
Figure 4:18 – Nluc-ZnT8 LIPS Optimisation: Freeze-thawing the Nluc-R+W-ZnT8 dual heterodimer construct (SNR) .....	311
Figure 4:19 – Nluc-ZnT8 LIPS Optimisation: Furimazine substrate concentration (LU/SNR) .....	313
Figure 4:20 – Nluc-ZnT8 LIPS Optimisation: Furimazine substrate incubation length with Nluc-R+W-ZnT8 dual heterodimer construct (SNR) .....	314
Figure 4:21 – Nluc-ZnT8 LIPS Optimisation: Furimazine substrate incubation length with Nluc-R+W-ZnT8 dual heterodimer construct (AU) .....	315
Figure 4:22 – Nluc-ZnT8 LIPS Optimisation: Logarithmic standard curve fit according to substrate incubation length (Log2 units) .....	317
Figure 4:23 – Nluc-ZnT8 LIPS: Serum ZnT8A detection in the presence of EDTA with & without CaCl <sub>2</sub> or ZnCl <sub>2</sub> (LU/SNR) .....	321
Figure 4:24 – Nluc-ZnT8 LIPS: Serum ZnT8A detection in the presence of 1mM ZnCl <sub>2</sub> (SNR) .....	324

Figure 4:25 – Nluc-ZnT8 LIPS: Serum ZnT8A detection in the presence of 1mM ZnCl <sub>2</sub> (AU)	325
Figure 4:26 – Nluc-ZnT8 LIPS: Matched serum & plasma ZnT8A detection in the presence of 1mM ZnCl <sub>2</sub> (LU/SNR)	327
Figure 4:27 – Nluc-ZnT8 LIPS: Matched serum & plasma ZnT8A detection in the presence of 1mM ZnCl <sub>2</sub> (AU)	328
Figure 4:28 – Nluc-ZnT8 LIPS Validation: Establishing a positive threshold in a cohort of healthy schoolchildren	331
Figure 4:29 – Nluc-ZnT8 LIPS Validation: ZnT8A level & positivity in new-onset T1D patients measured by LIPS & RIA by percentile positivity thresholds (97.5 <sup>th</sup> /99 <sup>th</sup> ) & Furimazine substrate incubation length in LIPS	334
Figure 4:30 – Nluc-ZnT8 LIPS Validation: ROC curve of ZnT8 LIPS and RIA in new-onset T1D patients & healthy schoolchildren	336
Figure 4:31 – Nluc-ZnT8 LIPS Validation: Kaplan-Meir survival analysis in FDRs	340
Figure A:1 – FASTA sequence of the cloning site of pET49b(+) vector with ZnT8 insert & flanking restriction enzyme recognition sites	402
Figure A:2 – Gel image of generating the ZnT8 insert for cloning into the pET49b(+) vector	403
Figure A:3 – Gel image of XmaI & XhoI double digest on the ZnT8 insert & pET49b(+) vector	404
Figure A:4 – Screening E. Coli colonies for ZnT8 insert on a 1% agarose gel	406
Figure A:5 – FASTA sequence of the cloning site of pET49b(+) vector with ZnT8 insert & sequencing primers	407
Figure A:6 – Gel image confirming the transformation of ZnT8/pET49b(+) into Rosetta <sup>TM</sup> (DE3)pLysS cells	408
Figure A:7 – SDS-PAGE gel showing the time course of expression of ZnT8 with GST tag in E.Coli Rosetta <sup>TM</sup> (DE3)pLysS cells	411
Figure A:8 – SDS-PAGE gel of FPLC eluted fractions	416
Figure B:1 – Prevalence of IgG subclasses in GADA & IA-2A T1D standardisation sample sets using the IgG detection thresholds	422
Figure B:2 – StDS between healthy schoolchildren & T1D patients in the GADA IgG subclass RIA	424
Figure B:3 – StDS between healthy schoolchildren & T1D patients in the IA-2A IgG subclass RIA	425

Figure C:1 – FASTA sequence of human C-terminal ZnT8 with the cloning strategy for generating the murine REKK (TGQ-) ZnT8 construct utilising flanking restriction enzyme recognition sites .....	426
Figure C:2 – Gel image of generating the ZnT8 murine REKK insert.....	427
Figure C:3 – Gel image of XhoI & HindIII double digest on the ZnT8 murine REKK insert & the ZnT8 pCMVTnT vector.....	428
Figure C:4 – FASTA sequence of human C-terminal ZnT8 with the successful cloning of ZnT8 murine REKK (TGQ-) into the pCMvTnT vector with the cloning and sequencing primers detailed.....	430
Figure D:1 – Longitudinal ZnT8RA & ZnT8WA levels from T1D onset .....	436
Figure D:2 – Longitudinal single GADA positive responses .....	439
Figure D:3 – Longitudinal single IA-2A positive responses .....	442
Figure D:4 – Longitudinal single ZnT8A positive responses.....	444
Figure D:5 – Increasing GADA titres after T1D onset.....	446
Figure D:6 – Increasing IA-2A titres after T1D onset.....	447
Figure D:7 – Increasing ZnT8A titres after T1D onset.....	448
Figure D:8 – Fold-change in GADA level corrected to the RIA positivity threshold over longitudinal follow-up (waxing-waning patterns) .....	450
Figure D:9 – Fold-change in IA-2A level corrected to the RIA positivity threshold over longitudinal follow-up (waxing-waning patterns) .....	451
Figure D:10 – QQ plots using raw autoantibody data to test for Gaussian distribution.....	452
Figure D:11 – Mean differences in GADA, IA-2A, & ZnT8A level between all combinations of longitudinal follow-up .....	454
Figure D:12 – Longitudinal autoantibody prevalence & titres according to T1DE categories of T1D age at onset .....	459
Figure E:1 – Nluc-ZnT8 LIPS Optimisation: Glycine-blocked PAS (GB-PGS) immunoprecipitate (SNR).....	462
Figure E:2 – Nluc-ZnT8 LIPS Optimisation: Purification of Nluc-R+W-ZnT8 dual heterodimer construct with ZnCl <sub>2</sub> (SNR).....	464
Figure E:3 – Nluc-ZnT8 LIPS Optimisation: Volume of 1mM methionine in Nluc-ZnT8 expression reaction mix (SNR/AU).....	467

## List of Tables

---

Table 1:1 – Central & peripheral tolerance mechanisms for developing T-cells & B-cells.....	25
Table 1:2 – Biochemical properties of human immunoglobulin isotypes .....	37
Table 1:3 – Biochemical properties of human IgG subclasses .....	39
Table 1:4 – Observations of human IgG subclasses .....	40
Table 1:5 – Prevalence of autoantibody frequency & combinations in 655 new-onset T1D cases & 761 healthy control subjects according to age .....	50
Table 1:6 – Summary of genetic associations with islet autoantibody positivity at different T1D stages.....	56
Table 1:7 – The codons for the major allele & SNPs in SLC30A8.....	66
Table 2:1 – ZnT8A affinity optimisation sample set .....	87
Table 2:2 – ZnT8A affinity new-onset T1D sample set .....	89
Table 2:3 – Optimisation of recombinant protein concentration curves for ZnT8A affinity studies. ....	91
Table 2:4 – Seminal T1D studies of IgG subclasses.....	113
Table 2:5 – Prevalence of GADA, IA-2A, & IAA IgG subclasses in autoantibody positive FDRs .....	114
Table 2:6 – Multiple autoantibody positive non-progressor sample set .....	120
Table 2:7 – Multiple autoantibody positive slow progressor sample set.....	120
Table 2:8 – Multiple autoantibody positive rapid progressor sample set .....	121
Table 2:9 – New-onset T1D patient ZnT8A sample set .....	121
Table 2:10 – Screening T1D patient sample set for GADA, IA-2A, ZnT8RA, & ZnT8WA IgG subclass RIAs.....	122
Table 2:11 – Quality control sample sets for GADA, IA-2A, ZnT8RA, & ZnT8WA IgG subclass RIAs.....	123
Table 2:12 – Summary of IgG subclass profiles in the multiple autoantibody positive progressor sample sets .....	133
Table 2:13 – The frequency of specific IgG subclasses in the T1D patient screening sample set .....	137
Table 2:14 – IgG subclass profiles between RPs & T1D patients (screening sample set) ....	139
Table 2:15 – Reproducibility of QC sample sets in GADA, IA-2A, & ZnT8RA/ZnT8WA IgG subclass assays during assay optimisation.....	141

Table 2:16 – Index sample or first ZnT8A positive sample & follow-up samples tested for ZnT8Q reactivity in NPs, SPs, & RPs .....	153
Table 2:17 – Cohort description of all T1D- & ZnT8A-associated variables in 71 new-onset T1D patients selected for ZnT8A epitope studies.....	155
Table 2:18 – PCR cycle for site-directed mutagenesis .....	157
Table 2:19 – Inventory of C-terminal ZnT8 mutant constructs.....	160
Table 2:20 – ZnT8A specificity to wild type ZnT8 according to SLC30A8 genotype .....	168
Table 2:21 – ZnT8A seroconversion case study population.....	202
Table 3:1 – Combinations of samples available that were tested for autoantibodies across all time categories .....	227
Table 3:2 – Cohort description & all variables investigated for association with autoantibody loss after onset of T1D.....	228
Table 3:3 – Minor allele frequencies of investigated SNPs in the T1D cohort .....	230
Table 3:4 – Linear trend & GLM assessment of variance over longitudinal follow-up for GADA, IA-2A, & ZnT8A responses .....	238
Table 3:5 –Autoantibody loss at final follow-up considering age at onset as quartiles versus T1DE categories.....	247
Table 4:1 – Main studies evaluating the performance of LIPS in detecting islet autoantibodies .....	265
Table 4:2 – Main optimisation sample set for Nluc-ZnT8 LIPS .....	271
Table 4:3 – IASP2016 optimisation sample set.....	273
Table 4:4 – Nluc-ZnT8 LIPS Validation: BOX evaluation population.....	279
Table 4:5 – Summary of the optimised Nluc-GAD65 LIPS assay for GADA detection .....	280
Table 4:6 – Summary of the Nluc-ZnT8 LIPS optimisation experiments.....	282
Table 4:7 – Nluc-ZnT8 LIPS optimisation experiments.....	290
Table 4:8 – Nluc-ZnT8 LIPS Optimisation: Summary of Nluc-ZnT8 LIPS & RIA IASP2018 results .....	303
Table 4:9 – Nluc-ZnT8 LIPS Optimisation: IASP2018 report.....	304
Table 4:10 – Summary of Nluc-ZnT8 LIPS assay optimisation.....	319
Table 4:11 – Positivity thresholds for monomeric ZnT8R/ZnT8W RIAs & Nluc-ZnT8 LIPS .....	329
Table 4:12 – Nluc-ZnT8 LIPS Validation: Summary of ZnT8A level & positivity in new-onset T1D patients & healthy schoolchildren using 97.5 <sup>th</sup> percentile thresholds in LIPS & RIA ..	337

Table 4:13 – Nluc-ZnT8 LIPS Validation: Initial IASP2020 report for in-house RIA & LIPS assays .....	338
Table 4:14 – Advantages of LIPS assays to conventional RIAs .....	348
Table A:1 – PCR recipe for ZnT8 cloning.....	402
Table A:2 – PCR recipe for screening E.Coli colonies for the ZnT8 insert .....	405
Table A:3 – Primers to confirm ZnT8 cloning into pET49b(+) vector .....	406
Table A:4 – SDS-PAGE methodology .....	412
Table A:5 – Methodology of purifying the ZnT8-GST fusion protein using a GSTrap™ column & FPLC (GE AKTA Prime System). .....	415
Table A:6 – Protein concentrations of eluted FPLC fractions quantified using the Qubit™ Protein Assay kit (Thermo).....	417
Table B:1 – Clones & source of monoclonal anti-human IgG-subclass antibodies used in seminal T1D studies.....	418
Table B:2 – T1D patient standardisation sample set .....	420
Table B:3 – IgG subclasses & total IgG in healthy schoolchildren for IgG detection thresholds .....	422
Table C:1 – PCR recipe & accompanying PCR cycle for generating ZnT8 murine REKK insert .....	427
Table C:2 – Primers used to confirm successful cloning of ZnT8 murine REKK into the ZnT8 pCMVTnT vector.....	429
Table C:3 – Primer sequences of C-terminal ZnT8 mutations .....	431
Table D:1 – Seminal T1D studies of islet autoantibody positivity after T1D diagnosis .....	435
Table D:2 – Cohort description of single GADA positives & all variables investigated for association with autoantibody loss after onset of T1D .....	437
Table D:3 – Descriptive statistics for levels of GADA over longitudinal follow-up in single GADA positives.....	438
Table D:4 – Linear trend and GLM assessment of variance over longitudinal follow-up in single GADA positives .....	439
Table D:5 – Cohort description of single IA-2A positives & all variables investigated for association with autoantibody loss after onset of T1D .....	440
Table D:6 – Descriptive statistics for levels of IA-2A over longitudinal follow-up in single IA-2A positives at T1D onset.....	441
Table D:7 – Cohort description of single ZnT8A positives & all variables investigated for association with autoantibody loss after T1D onset .....	443

Table D:8 – Descriptive statistics of GADA titres over longitudinal follow-up .....	453
Table D:9 – Descriptive statistics of IA-2A titres over longitudinal follow-up .....	453
Table D:10 – Descriptive statistics of ZnT8A titres over longitudinal follow-up.....	453
Table D:11 – Longitudinal GADA positivity & titre by autoantibody quartile at T1D onset .....	456
Table D:12 – Longitudinal IA-2A positivity & level by autoantibody quartile at T1D onset .....	457
Table D:13 – Longitudinal ZnT8A positivity & level by autoantibody quartile at T1D onset .....	458
Table E:1 – Autoantibody positivity in anonymised matched serum & plasma samples.....	460
Table E:2 – Nluc-ZnT8 LIPS Optimisation: Intra-assay & inter-assay variability of the logarithmic standard curve according to substrate incubation length.....	469

## Presentations & publications that have arisen during the PhD Studentship to date

---

### Published manuscripts unrelated to this PhD Studentship

Kozhakhmetova, A., Wyatt, R.C., Caygill, C.H., **Williams, C.L.**, Long, A.E., Chandler, K.A., Aikten, R.J., Wenzlau, J.M., Davidson, H.W., Gillespie, K.M., Williams, A.J.K. (2018) “A quarter of patients with type 1 diabetes have co-existing non-islet autoimmunity.” *Clinical & Experimental Immunology*. **192**(3): 251-258.

Church, D., Cardoso, L., Kay, R., **Williams, C.L.**, Freudenthal, B., Clarke, C., Harris, J., Moorthy, M., Karra, E., Gribble, F., Reimann, F., Burling, K., Williams, A.J.K., Munir, A., Jones, T.H., Fuhrer, D., Moeller, L.C., Cohen, M., Khoo, B., Halsall, D., Semple, R. (2018) “Assessment and Management of Anti-Insulin Autoantibodies in Varying Presentations of Insulin Autoimmune Syndrome.” *Journal of Clinical Endocrinology and Metabolism*. **103**(10): 3845-3855

### Published review articles related to this PhD Studentship

**Williams C.L.**, Long A.E., (2019) “What has zinc transporter 8 autoimmunity taught us about type 1 diabetes?” *Diabetologia*. **62**(11):1969-1976. [Review article selected as one of 5 “Up-front” articles in issue].

Long A.E., George, G., **Williams C.L.**, (2021) “Persistence of Islet Autoantibodies after diagnosis in Type 1 Diabetes.” *Diabetic Medicine*. [invited review accepted and awaiting publication].

### Planned manuscripts related to this PhD Studentship

**Williams, C.L.**, Mortimer, G.L.M., Fareed, R., Gillespie, K.M., Williams, A.J.K., Long, A.E. (2021) “The longitudinal loss of islet autoantibody responses after diagnosis of type 1 diabetes is determined by low autoantibody titres, early-onset, and genetic variants.” *Target journal: Clinical & Experimental Immunology* [submission planned early 2022].

**Williams, C.L.**, Lampasona, V., Gillespie, K.M., Williams, A.J.K., and Long, A.E. (2022) “A low-volume rapid Luciferase Immunoprecipitation System assay utilising a novel antigen to detect autoantibodies to zinc transporter 8 in type 1 diabetes provides an alternative to conventional radioimmunoassay.” *Target journal: To be decided* [submission planned early 2022].

## Abstracts related to this PhD Studentship

Gillespie, K.M., Long, A.E., **Williams, C.**, Becker, D.J., Libman, I.M., Wong, F.S., Casas, R., Steck, A.K., Rewers, M.J., Achenbach, P., Williams, A.J.K. (2016) “Is there regulation of the autoimmune response in slow progressors to type 1 diabetes?” (Poster Presentation). *The European Association for the Study of Diabetes (EASD)*, September 12-16, Munich, Germany [preliminary data and training period in Munich for Diabetes UK PhD Studentship 2017].

**Williams, C.L.**, Gillespie, K.M., Williams, A.J.K., Long, A.E. “What factors influence the persistence of autoantibodies to zinc transporter 8 (ZnT8A) in type 1 diabetes after diagnosis?” (Poster Presentation). *The 16<sup>th</sup> Immunology of Diabetes Society (IDS) Congress*, October 25-29, London, UK.

**Williams, C.L.**, Gillespie, K.M., Williams, A.J.K., Long, A.E. (2019) “Autoantibodies to zinc transporter 8 (ZnT8A) are more likely to persist after diagnosis in the presence of co-existing autoantibodies to glutamate decarboxylase (GADA) at type 1 diabetes onset.” (Poster Presentation). *Diabetes UK Professional Conference*, March 6-8, Liverpool, UK.

**Williams, C.L.**, Mortimer, G.L.M., Gillespie, K.M., Williams, A.J.K., Long, A.E. (2020) “High titre and older age-at-onset are predictors of persistent autoantibody responses to major autoantigens in type 1 diabetes modulated by HLA variants.” (Accepted for Poster Presentation). *Diabetes UK Professional Conference (cancelled)*, October 7, [published online in *Diabetic Medicine*].

**Williams, C.L.**, Roki, S., Lampasona, V., Gillespie, K.M., Williams, A.J.K., Long, A.E. (2020) “The last 9 amino acids of C-terminal ZnT8 forms a minor epitope for ZnT8 autoantibody responses in individuals with type 1 diabetes.” (Accepted for Poster Presentation). *Immunology of Diabetes Society (IDS) Congress (Virtual)*, October 15-18, Beijing, China, [abstracts were made available online].

Long, A.E., Grace, S.L., **Williams, C.L.**, Gillespie, K.M., Williams, A.J.K. (2020) “Assays that measure ZnT8A in EDTA plasma samples have low sensitivity.” (Accepted for Poster Presentation). *Immunology of Diabetes Society (IDS) Congress (Virtual)*, October 51-18, Beijing, China, [abstracts were made available online].

**Williams, C.L.**, Gillespie, K.M., Lampasona, V., Williams, A.J.K., Long, A.E. (2021) “A low-volume rapid luciferase immunoprecipitation system (LIPS) assay utilising a novel antigen to detect autoantibodies to zinc transporter 8 (ZnT8A) in type 1 diabetes provides an alternative to conventional radioimmunoassay.” (Poster Presentation with a 5-minute oral presentation) *Diabetes UK Professional Virtual Conference*, April 16-30, [awarded Basic Science Digital Poster Award].

**Williams, C.L.**, Roki, S., Lampasona, V., Gillespie, K.M., Williams, A.J.K., Long, A.E. (2021) “The last 9 amino acids of C-terminal ZnT8 forms a minor epitope for ZnT8 autoantibody responses in individuals with type 1 diabetes.” (Submitted September 20, awaiting outcome). *Immunology of Diabetes Society (IDS) Congress (Virtual)*, November 1-4, Nashville, USA, [abstract includes extra data than previous 2020 abstract].

## Abbreviations

---

- AA** – Amino acid
- ADAP** – Antibody detection by agglutination-PCR (polymerase chain reaction)
- ADCC** – Antibody-dependent cellular cytotoxicity
- AID** – Activation-induced deaminase
- AIRE** – Autoimmune regulator gene
- ANOVA** – Analysis of variance
- AR** – Assay reagent for Luminescence-based Immuno Precipitation System (LIPS) assays
- APC** – Antigen-presenting cell
- APS** – Ammonium persulfate
- ASK** – Autoimmune Screening for Kids
- AS95** – Assay sensitivity at 95% specificity
- ATP** – Adenosine triphosphate
- AU** – Arbitrary units
- AUC** – Area under the curve
- β-cell(s)** – Beta cell(s)
- B-cell(s)** – B cell(s) (lymphocytes)
- BCR** – B-cell receptor
- BDR** – Belgian Diabetes Registry
- BLAST** - Basic local alignment search tool
- BMI** – Body mass index
- BOX** – Bart’s-Oxford family study
- Bp** – Base pair
- Breg(s)** – B regulatory cell(s)
- CaCl<sub>2</sub>** – Calcium chloride
- CDC** – Centers for Disease Control and Prevention
- CDF** – Cation diffusion facilitator
- CPM** – Counts per minute
- ΔCPM** – Delta counts per minute
- CSR** – Class switch recombination
- CTD** – C-terminal domain

**CTLA-4** – Cytotoxic T lymphocyte antigen 4  
**CV** – Coefficient of variation  
**Cryo-EM** – Cryogenic electron microscopy  
**DAISY** – Diabetes Autoimmunity Study in the Young  
**DASP** – Diabetes Autoantibody Standardisation Program  
**DIPP** – Diabetes Prediction and Prevention  
**DKA** – Diabetic Ketoacidosis  
**DK** – Diabetic Kidney  
**DTT** – Dithiothreitol  
**EAE** – Experimental autoimmune encephalomyelitis  
**EB-PGS** – Ethanolamine-blocked Protein G Sepharose  
**EC** – Extracytoplasmic  
**ECL** – Electrochemiluminescence  
***E. Coli*** – Escherichia Coli  
**EDTA** – Ethylenediaminetetraacetic acid  
**ELISA** – Enzyme-linked immunosorbent assays  
**ENDIT** – European Nicotinamide Intervention Trial  
**FcR(s)** – Fc receptor(s)  
**Fc $\gamma$ R(s)** – Fc receptor(s) for IgG ( $\gamma$ ) antibodies  
**FDR(s)** – First degree relative(s)  
**Fluc** – *Firefly* luciferase  
**FOXP3** – Forkhead box P3  
**FPLC** – Fast protein liquid chromatography  
**GAD** – L-glutamic acid decarboxylase  
**GAD65** – Glutamic acid decarboxylase 65  
**GADA** – Glutamic acid decarboxylase autoantibodies  
**GB-PAS** – Glycine-blocked Protein A Sepharose  
**GLM** – Generalised linear model  
**Gluc** – *Gaussia* luciferase  
**GM-CSF** – Granulocyte-macrophage colony-stimulating factor  
**GRS** – Genetic risk score  
**GSIS** – Glucose-stimulated insulin secretion

**GWAS** – Genome-wide association study/studies

**HCl** – Hydrochloric acid

**HLA** – Human leukocyte antigen

**HR** – Hazard ratio

**HRV** – Human rhinovirus

**IAA** – Insulin autoantibodies

**IA-2** – Islet antigen 2

**IA-2A** – Islet antigen 2 autoantibodies

**IASP** – Islet Autoantibody Standardisation Programme

**IC** – Intracytoplasmic

**ICA** – Islet-cell autoantibodies

**ICI(s)** – Insulin-containing islet(s)

**IDS** – Immunology of Diabetes Society

**IFN $\gamma$**  – Interferon gamma

**Ig** – Immunoglobulin

**IgG-SSS** – IgG-Subclass Streptavidin Sepharose

**ISG(s)** – Insulin secretory granule(s)

**IL** – Interleukin

**IL2RA** – Interleukin 2 receptor alpha

**IPTG** – Isopropyl  $\beta$ -d-1-thiogalactopyranoside

**IQR(s)** – Interquartile range(s)

**JDF** – Juvenile Diabetes Foundation

**JM** – Juxtamembrane

**kDa** – Kilodalton

**LADA** – Latent Autoimmune Diabetes in Adults

**LB** – Luria-Bertanil

**LD** – Linkage disequilibrium

**LIPS** – Luminescence-based Immuno Precipitation System

**LLPC(s)** – Long-lived plasma cell(s)

**LU** – Light unit equivalents

**MAF** – Minor allele frequency

**mAutoab+ve** – Multiple autoantibody positive ( $\geq 2$  islet autoantibodies)

**MBP** – Maltose binding protein  
**MHC** – Major Histocompatibility Complex  
**MODY** – Maturity onset of the young  
**MS** – Multiple sclerosis  
**MTA** – Material Transfer Agreement  
**NCBI** – National Center for Biotechnology Information  
**NHS** – National Health Service (UK)  
**NHSt** – Natural History Study by TrialNet  
**NICE** – National Institute for Health and Care Excellence  
**NIH** – National Institute for Health  
**Nluc** – Nano Luciferase  
**Nluc-GAD65** – Nano Luciferase-tagged GAD65  
**Nluc-ZnT8** – Nano Luciferase-tagged ZnT8  
**NOD** – Non-obese diabetic (T1D mouse model)  
**NP(s)** – Non-progressor(s)  
**nPOD** – Network for Pancreatic Organ Donors with Diabetes  
**O/N** – Overnight  
**OR** – Odds ratio  
**PAS** – Protein A Sepharose  
**PCR** – Polymerase Chain Reaction  
**pGOLD™** – Plasmonic gold chip (Nirmidas Biotech, CA, USA)  
**PGS** – Protein G sepharose  
**PBS** – Phosphate buffered saline  
**PBST** – Phosphate buffered saline with 0.1% (v/v) Tween-20  
**PTP** – Protein tyrosine phosphatase  
**PTPN22** – Protein tyrosine phosphatase non-receptor 22  
**PTPS** – Pathway to Prevention Study (TrialNet)  
**Q325** – Glutamine (Q) encoded at aa325 of ZnT8  
**QC(s)** – Quality control(s)  
**R325** – Arginine (R) encoded at aa325 of ZnT8  
**RA** – Rheumatoid arthritis  
**REKK** – R<sub>332</sub>, E<sub>333</sub>, K<sub>336</sub>, and K<sub>340</sub> residues in ZnT8

**REML** – Restricted Maximum Likelihood

**RIA(s)** – Radioimmunoassay(s)

**RLD** – Reagent for luminescence detection

**RLU** – Relative light units

**Rluc** – *Renilla* luciferase

**ROC** – Receiver operator characteristic

**RP(s)** – Rapid progressor(s)

**RPM** – Rotations per minute

**RT** – Room temperature

**sAutoab+ve** – Single autoantibody positive ( $\geq 1$  islet autoantibody)

**SD** – Standard deviation

**SDM** – Site-directed mutagenesis

**SDS** – Sodium dodecyl sulfate

**SDS-PAGE** – Sodium dodecyl sulfate polyacrylamide gel electrophoresis

**SEM** – Standard error of the mean

**SLE** – Systemic lupus erythematosus

**SLMV** – Synaptic-like micro-vesicles

**SP(s)** – Slow progressor(s)

**sNluc** – Secretory Nano luciferase

**SNR** – Signal to noise ratio

**SLE** – Systemic lupus erythematosus

**SLMV** – Synaptic-like micro-vesicles

**SNP(s)** – Single nucleotide polymorphism(s)

**SOC** – Super optimal broth with catabolite repression

**S-S** – Streptavidin-Sepharose

**StDS** – Standard deviation score

**SWENDIC** – Southwest of England New-Diagnosed Collection

**T1D** – Type 1 diabetes

**T1DE** – Type 1 diabetes endotype

**T1DGC** – Type 1 diabetes genetic consortium

**T2D** – Type 2 diabetes

**TAE** – Tris base, acetic acid and Ethylenediaminetetraacetic acid (EDTA)

**TBST** – Tris buffered saline with 0.15% (v/v) Tween-20

**TBST-0.5%** – Tris buffered saline with 0.5% (v/v) Tween-20

**TBST-BSA** – Tris buffered saline (0.15% Tween-20) with 0.1% (w/v) bovine serum albumin

**T-cells(s)** – T cell(s) (lymphocytes)

**TCR(s)** – T-cell receptor(s)

**TEDDY** – The Environmental Determinants of Diabetes in the Young

**TEMED** – Tetramethylethylenediamine

**TGFβ** – Transforming growth factor beta

**Th(s)** – T helper cell(s)

**TMD** – Transmembrane domain

**TNFα** – Tumour necrosis factor alpha

**TNFβ** – Tumour necrosis factor beta

**Treg(s)** – T regulatory cell(s)

**TSPAN7** – Tetraspanin protein family member 7

**UCPCR** – Urinary C-peptide: creatinine ratio

**VDJ** – Variable, diversity, and joining

**VDR(s)** – Vitamin D receptor(s)

**VNTR** – Variable number tandem repeat

**VP1** – Enteroviral capsid protein 1

**W325** – Tryptophan (W) encoded at aa325 of ZnT8

**WHO** – World Health Organisation

**WT** – Wild-type

**ZnCl<sub>2</sub>** – Zinc chloride

**ZnT8** – Zinc transporter 8

**ZnT8A** – Zinc transporter autoantibodies

**ZnT8RA** – Zinc transporter 8 R (arginine)-specific autoantibodies

**ZnT8WA** – Zinc transporter 8 W (tryptophan)-specific autoantibodies

**ZnT8QA** – Zinc transporter 8 Q (glutamine) non-specific autoantibodies

# Chapter 1 - General introduction

---

---

## 1.1 Type 1 diabetes

---

Type 1 diabetes (T1D) results from the progressive autoimmune-mediated destruction of insulin-producing beta ( $\beta$ )-cells in the pancreatic Islets of Langerhans. After diagnosis, individuals must rely on a life-long supply of exogenous insulin to regulate glucose (1). The aetiology of T1D remains unknown. The complex interplay between genetic and environmental risk factors that influence autoimmunity creates phenotypic heterogeneity and a multifaceted disease (2). Ultimately T1D and other autoimmune conditions result from defects in the central and peripheral tolerance processes that prevent autoreactive (self-recognising) cells from entering circulation (3).

Currently, T1D accounts for ~10-15% of diabetes cases worldwide; incidence is increasing steadily at a rate of ~3-4% each year in the western world, with the highest increase observed in children aged <5 years (4-7). Although T1D remains the most common chronic disease of childhood-adolescence with two peaks of incidence around 5-7 years and pubescent age, T1D can occur at any age (4, 8, 9). At least 42% of genetically defined T1D cases are diagnosed in adulthood (>30 years; representing 4% of all diabetes cases after this age) which is clinically challenging to diagnose given the high prevalence of type 2 diabetes (T2D) in older adults (9-11). However, adult-onset T1D has not been as extensively studied and remains to be better characterised.

To assign disease risk, the detection of islet autoantibodies produced by self-reactive immune cells, directed to islet-specific proteins before the clinical manifestation of T1D, remain primary biomarkers of disease (12). These autoantibodies, detectable from months to decades prior to clinical onset of T1D, can aid (alone or in combination with genetic markers) identification of high-risk individuals for clinical trials and form a key clinical feature of

autoimmunity for T1D diagnosis. A combination of genetic predisposition and accelerated loss of immunological tolerance to  $\beta$ -cells in infants and children contributes to rapid disease progression within months to a few years, but islet autoimmunity in those with a slower progression to disease into adulthood are not fully understood (13-15).

---

## 1.2 Incidence

---

A meta-analysis of studies between 1990-2019 found that the worldwide incidence of T1D is 15 per 100,000 people (16). The highest incidence of T1D is mainly observed in westernised nations, including Finland, Sardinia, Sweden, and the United Kingdom (17, 18). Finnish, Sardinian, and Swedish children have the highest incidence of T1D (40-37 cases per 100,000 per year), compared with the United Kingdom (25 cases per 100,000 per year) (17-19). Overall, the prevalence of T1D in Europeans is 0.2-0.3% (20). China and India are among the countries with the lowest incidence rates of T1D (0.1 cases per 10,000 per year) (21). Within the United States of America, the incidence of T1D varies according to ethnicity; non-Hispanic whites had a higher incidence rate than Native Americans in individuals under 20 years (22, 23). However, advances in epidemiology surveillance have led to the identification of high T1D incidence in countries outside of the western world, such as Saudi Arabia (33.5 cases per 100,000 per year) (24, 25), with increasing incidences observed in China, India, and Egypt (18).

Epidemiological studies have reported evidence in support of environmental risk factors, including: 1) immigration causes shifts in T1D risk associated with the new country of residence instead of the native country (26-28), 2) a shift to earlier onset of disease (29), 3) increased incidence across all age groups (18), 4) greatest increments of incidence observed in previously low-income countries (30), and 5) increased incidence in countries with rapid economic growth (17, 31).

---

### 1.3 Clinical characteristics & pathogenesis

---

The clinical characteristics of T1D typically arise when  $\beta$ -cell mass becomes significantly reduced. The catabolic consequences of insulin deficiency and uninhibited fatty acid metabolism result in diabetic ketoacidosis (DKA), polyuria, weight loss, hyperglycaemia, and polydipsia (1, 4, 13). Approximately 15-67% of new-onset T1D presents with potentially life-threatening DKA, but this is more common in children (<4 years), individuals of lower socioeconomic status, and within developing countries (23, 32). Secondary complications include heart disease, kidney disease, peripheral artery disease (high amputation risk), and vascular retinopathy. More than 90% of T1D patients will be affected by significant vascular complications. Individuals with T1D have a 10-times higher risk for cardiovascular events than the general population and is the leading cause of morbidity and mortality in T1D (9, 33, 34).

Recent studies show that T1D individuals can preserve the ability to produce endogenous insulin, which even in small quantities, can significantly improve glycaemic control protecting from hypoglycaemia and microvascular complications (35, 36). At 5 years disease duration, 80% of T1D subjects had detectable endogenous C-peptide (a by-product of insulin synthesis) (37, 38), suggesting that most individuals retain some  $\beta$ -cell mass/function. Histological examination of T1D pancreases up to 50 years disease duration also supports this observation, but  $\beta$ -cell mass/function is highly variable (particularly <1-year disease duration) and appears related to age-at-onset (39-43). This evidence challenges Eisenbarth's original T1D pathogenesis model (1986), that proposed clinical onset of T1D manifests when  $\beta$ -cell mass/function is reduced by ~80-90% (26, 44) (**Figure 1:1**).

Three scenarios have since been hypothesised to occur in the preclinical phase that leads to the decline of  $\beta$ -cell mass/function and clinical T1D onset: (1) several relapsing-remitting phases of  $\beta$ -cell destruction but insulin secretion/C-peptide production remains stable, (2) a sudden decline in  $\beta$ -cell mass/function just prior or around clinical onset of T1D with low insulin secretion/C-peptide production, and (3) either regeneration of residual  $\beta$ -cells or formation/proliferation of new  $\beta$ -cells in the clinical diabetes phase enables microsecretion of insulin/C-peptide production (26).

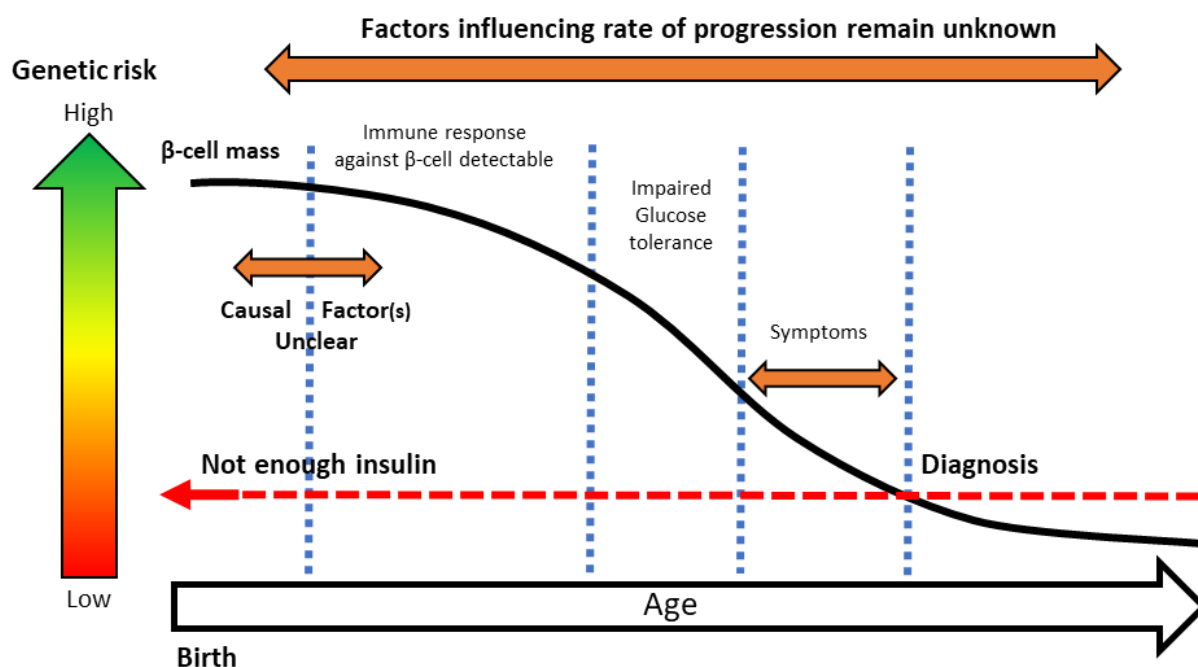


*Figure 1:1 – Simplified schematic of Eisenbarth's model of T1D pathogenesis (1986)*

Schematic adapted from Eisenbarth (1986) (44). The high-risk DR3/DR4 heterozygous genotype increases the risk of T1D. Faulty immune cell selection causes the release of self-reactive immune cells with resultant self-reactive autoantibodies directed to pancreatic  $\beta$ -cell specific proteins. These autoantibodies can be detected many years before T1D diagnosis. The factors that cause or influence the rate of progression from detectable autoantibodies to disease onset remain unknown.

---

## 1.4 Diabetes treatment & management

---

The discovery of insulin by Banting and Best a century ago remains the most significant therapeutic event for T1D. Whilst the delivery of exogenous insulin therapy, glycaemic control, and diabetes care has improved drastically, therapy often does not achieve desired glycaemic or metabolic targets. Additionally, the mortality rate, associated with a younger age-at-onset, remains 2-8 times higher in T1D compared to the general population (9, 45, 46). Additionally, limited access to insulin or healthcare across many parts of the world causes high T1D mortality (e.g., in Mozambique, the life expectancy of a T1D child is 7 months) (34).

In parts of the western world, advances in technology such as insulin pumps and continuous glucose monitors have further improved T1D management. Most recently, the automated closed-loop basal insulin delivery system (“the artificial pancreas”) is being trialed by the National Health Service (NHS) in 1000 UK patients (2021) (9, 47).

The misdiagnosis of diabetes can also heavily impact diabetes management (10-15% of young adults suffer from poor glycaemic control) if there is a significant delay to insulin treatment (10, 48). Clinical diabetes diagnosis is slow (due to the high prevalence and increasing incidence of T2D versus T1D in young adults), expensive, and is often based on time to absolute insulin deficiency and poor discriminatory clinical characteristics (10, 11, 19, 49). However, there are no predictive tests for insulin requirement. Islet autoantibodies may be informative and have been useful for discriminating other forms of diabetes (50-52) but can produce false-positive results (~half of autoantibody positives after age 30 will have T2D based on the 97.5<sup>th</sup> percentile of non-diabetic controls), cannot be conducted in clinical practice for rapid point-of-care testing, and are not available in less developed countries (10, 53).

## Chapter 1 - General introduction

The conversion of proinsulin to equimolar concentrations of insulin and cleaved C-peptide provides an avenue to determine endogenous insulin production accurately (13). The development of highly sensitive serum or urinary C-peptide assays (37, 39) enables clinicians to monitor residual  $\beta$ -cell function and endogenous insulin production in real-time. Post-meal urinary C-peptide: creatinine ratio (UCPCR) has surpassed the sensitivity of previous methods detecting C-peptide  $>0.002\text{nmol/mmol}$  in 80% of UK diagnosed T1D subjects ( $>5$  years diabetes duration). Additionally, most subjects that maintained clinically significant secretion of insulin (C-peptide of  $\sim 0.2\text{nmol/mmol}$ ) had better glycaemic control and a lower risk of complications and hypoglycaemia, but age and diabetes duration were independent predictors of C-peptide (38, 54). Children tend to lose C-peptide more rapidly after diagnosis than adults, particularly  $<1$ -year disease duration, suggesting that adults have greater residual  $\beta$ -cell function and may present with a less aggressive phenotype of autoimmunity (55-57). While these assays have greatly improved diabetes classification, diabetes management, and insulin therapy, a challenge of T1D research is an accurate, real-time, and non-invasive means of obtaining an accurate biomarker for  $\beta$ -cell destruction.

---

## 1.5 Disease aetiology

---

---

### 1.5.1 Genetics

---

Genome-wide association studies (GWAS) have identified >60 genetic loci that are associated with T1D risk in individuals of European ancestry (reviewed in (58)), and recently, 36 additional genes have been identified in a larger population inclusive of individuals with non-European ancestry (59). The overall genetic risk of T1D in the general population is around 0.4% (60, 61). Although autoimmunity is still a rare event, a combination of genetic susceptibility and environmental influence may impact the initiation of  $\beta$ -cell autoimmunity, particularly in early life (62, 63).

Unlike other autoimmune conditions, T1D lacks gender bias (64). As expected in a multifactorial condition, most T1D occurs in the general population, but there is some clustering within families, and lifetime T1D risk is dependent on familial relationship; ~3% mother, ~5% father, and 8% sibling (65). Monozygotic twins have >70% long-term genetic risk if one twin has T1D, with both twins having 30-40% risk of developing the disease (17, 66-68), whereas there is only a 6-10% long-term genetic risk in dizygotic twins which is comparable to non-twin siblings (6, 66). Collectively, this highlights the strong genetic predisposition for the disease, but genetics cannot be the primary cause of T1D. The familial heritability of genetic risk in T1D is ~50% associated with human leukocyte antigen (HLA) alleles and ~50% non-HLA gene loci (6, 63).

Distinct genetic factors may be important in different stages of disease progression, such as the initiation of  $\beta$ -cell autoimmunity, the production of the first islet autoantibody, or offering protection from disease progression (63).

### 1.5.1.1 HLA

In common with other autoimmune conditions, HLA genes in the human major histocompatibility complex (MHC), composed of *HLA Class I, II, and III* genes, remain the strongest genetic risk factors of T1D (23, 69) (**Figure 1:2**).

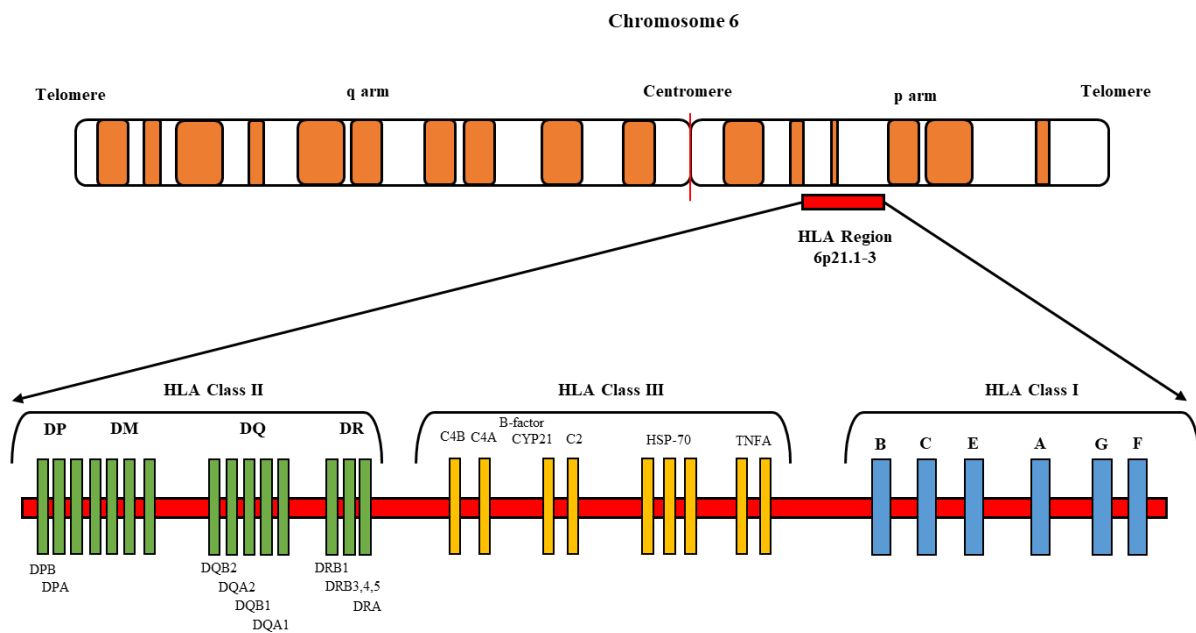


**Figure 1:2 – Schematic diagram of the MHC region on chromosome 6**

Schematic adapted from Lina Junior & Pratt-Riccio (70) but (6, 23) was used as additional sources of information. The MHC region is located on the short (p) arm of chromosome 6 (6p21.13) and can be divided into three subgroups: *HLA Class I, II, and III* genes. Genes in this region are involved in innate and adaptive immune responses through antigen presentation, the inflammatory process, and the complement cascade. The HLA region is composed of around 200 genes, but only half of which are thought to be expressed. The function of some *HLA* genes remains unknown.

The glycoproteins encoded by *HLA* genes are fundamental for binding and presenting peptides (antigen) on the cell surface to T-cell receptors (TCRs). This peptide presentation ultimately aids the body in differentiating between self and non-self (e.g., pathogen), which establishes self-tolerance, and initiates cellular (T-cells) and humoral (B-cells) immune responses. To carry out this function, *HLA* genes must be able to re-define their peptide-binding repertoire to accommodate biological diversity from both endogenous and exogenous sources (71, 72).

More than 15,000 genetic variants have been identified within the most polymorphic classical *HLA class I* and *II* genes (71, 72). Numerous variants of *HLA class I* and *II* genes are associated with T1D (20), but one study found that six single nucleotide polymorphisms (SNPs) in *HLA class III* genes were associated with T1D susceptibility adjusting for *HLA class II* (73).

Whilst the function and structure of HLA molecules are well established and highly homologous, the definitive role in the pathogenesis of T1D remains to be fully elucidated (74)

(Figure 1:3).

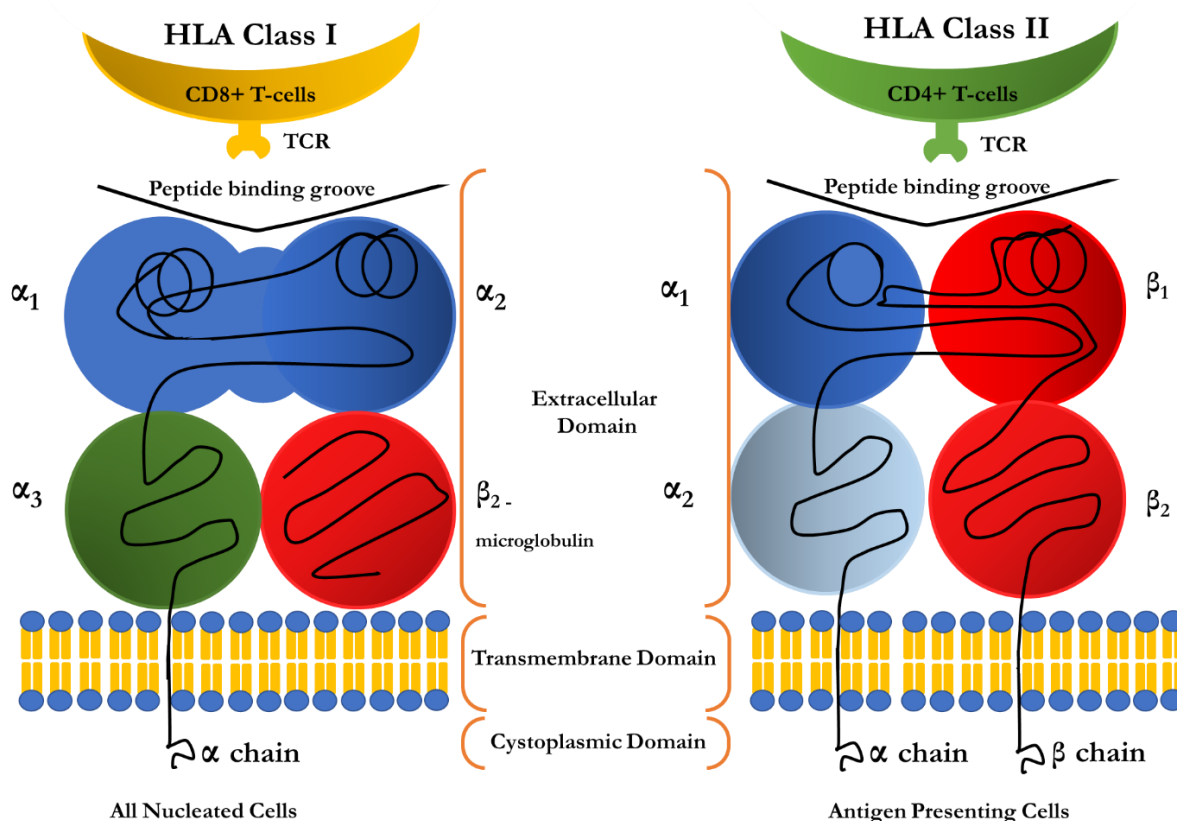


Figure 1:3 – Simplified schematic of HLA class I & class II molecule structure

Schematic was adapted from Schumacher *et al.* (2017) (75) and Wieczorek *et al.* (2017) (76). HLA Class I is a heterodimer consisting of a heavy polymorphic  $\alpha$  chain and a light monomorphic  $\beta_2$ -microglobulin chain (non-covalently linked) and presents endogenous antigen to CD8+ T-cells via the T-cell receptor (TCR) (77). Both classical (*DR*, *DP*, and *DQ*) and non-classical (*DO* and *DM*) *HLA class II* genes exist as dimeric transmembrane molecules that consist of alpha ( $\alpha$ ) and beta ( $\beta$ ) chains that differ primarily by variations in the N-linked glycosylations (77). Classical *HLA class II* genes exist as  $\alpha$ - $\beta$  heterodimers where the outer-membrane part of the molecule forms a groove for the antigenic peptide, which upon binding, transforms the molecule into its most stable form and presents exogenous antigen to CD4+ T-cells (77, 78).

### **1.5.1.1.1 HLA class I**

The 54 protein-coding *HLA class I* genes present endogenous antigen from the cytoplasm of cells, are ubiquitously expressed, and can be subdivided into classical (*A*, *B*, and *C*) and non-classical (*E*, *F*, and *G*) subtypes, but all HLA class I molecules play important roles in both innate and adaptive immune responses (79, 80).

Classical *HLA class I* genes are present on all nucleated cells in the body, shape the T-cell repertoire during T-cell maturation, present endogenous antigens to cytotoxic CD8<sup>+</sup> T-cells, and have limited polymorphic ability compared with class II genes. Therefore, they have pivotal roles in establishing self-tolerance and initiating antigen-specific T-cell mediated cytotoxicity (20, 23). Non-classical *HLA class I* genes are less polymorphic than their classical counterparts and largely function as immunoregulators (79, 81).

Despite strong linkage disequilibrium (LD) and the subsequent difficulty in investigating individual allele associations, all classical *HLA class I* genes have been linked to T1D in addition to, and independent of, the *HLA class II* genes. Adjusting for LD with *HLA class II*, the most highly T1D-associated classical *HLA class I* genes are *B\*39:06* (in LD with *C\*16:01*; predisposing odds ratio (OR): 10.3) and *B\*57:01* (protective OR: 0.2), but there are many others. Additional predisposing alleles include *A\*24:02*, *A\*02:01*, *B\*18:01*, and *C\*03:03* (OR range: 1.4-2.1). Additional protective alleles include *A\*11:01*, *A\*32:01*, *A\*66:01*, *B\*07:02*, *B\*44:03* (in LD with *C\*16:01*), and *B\*35:02* (OR range: 0.2-0.6) (23, 82-88). HLA class I molecules, given their role in target-cell recognition by CD4<sup>+</sup>/CD8<sup>+</sup> T-cells, are likely to influence the ongoing autoimmune response, which may modulate the rate of  $\beta$ -cell destruction. For example, *A\*24:02* is associated with rapid disease progression, specific islet autoantibody responses, early/complete  $\beta$ -cell destruction/function, and early T1D onset (87, 89-92).

### **1.5.1.1.2 HLA class II**

The 17 protein-coding *HLA class II* genes can be divided into classical (*HLA-DR*, *HLA-DQ*, and *HLA-DP*) and non-classical (*HLA-DM* and *HLA-DO*) subtypes within the D region (80). Classical *HLA class II* genes are expressed on professional antigen-presenting cells (APCs) of the innate (macrophages/dendritic cells) and adaptive (T-/B-cells) cells of the immune system and present exogenous antigen to CD4<sup>+</sup> T-cells (20, 77, 93). The interaction between antigen and CD4<sup>+</sup> T-cells via the TCR and co-receptor molecule CD4 activates CD4<sup>+</sup> T-cells which, subsequently leads to downstream activation or regulation of other immune cells through cell-to-cell interaction or release of soluble effectors (cytokines/chemokines) (20). Non-classical *HLA class II* genes are expressed intracellularly in lysosomal membranes and aid antigen peptide loading onto classical HLA Class II molecules for cell surface antigen presentation (20).

Classical *HLA-DR* and *HLA-DQ* genes are in strong LD, form haplotypes, and show the greatest association with T1D implicating the role of antigen presentation (self-antigen recognised as “foreign”) to CD4<sup>+</sup> T-cells in the disease (78, 94, 95). The genotype with the highest risk of T1D is heterozygous *HLA-DR3/DR4* or, more specifically, the haplotype inheritance of *HLA-DR3-DQ2* (*DRB1\*0301-DQB1\*0201*) on one chromosome and *HLA-DR4-DQ8* (*DRB1\*0401-DQB1\*0302*) on the other (69, 96, 97). Approximately 80-90% of T1D cases have at least one high-risk haplotype (*DR3/DR4/DQ2*) and between 30-50% have both, compared to ~2% in the general population (61, 95, 98). However, only 3-7% of children with these alleles develop diabetes (96, 99, 100).

The frequency of HLA class II risk genes varies widely between ethnic groups, with most multi-ethnic comparison studies reporting racial/ethnic differences, but to date, most studies have been conducted in Caucasian populations (23, 61). For example, whilst the *HLA-DR3* and

*DR4/DQ2* haplotypes are highly prevalent in Caucasian T1D cases, they are rare in Japanese T1D cases, and the *DRB1\*0405-DQB1\*0401* and *DRB1\*0901-DQB1\*0303* haplotypes are predominantly observed (101, 102). Additionally, evidence suggests that the rising incidence of T1D is accompanied by a decrease in the contribution of the *HLA-DR3-DQ2/DR4-DQ8* genotype to T1D risk (103), suggesting that variables independent of genetic susceptibility determine disease, which strengthens the argument for environmental influence.

It is also important to note that within the *DR/DQ* alleles are also haplotypes that are protective from disease. The most protective haplotypes are *DRB1\*1501-DQA1\*0102-DQB1\*0602*, *DRB1\*1401-DQA\*0101-DQB1\*0503*, and *DRB1\*0701-DQA1\*0201-DQB1\*0303* with *DQA1* and *DQB1* loci seemingly determining the degree of haplotypic risk (95, 96). To a lesser extent, *HLA-DP* molecules encoded by *DPA1* and *DPB1* genes have also been linked to T1D susceptibility in conjunction with, and additional to, *HLA-DR* and *HLA-DQ* (predisposing: *DPB1\*03:01* and *DPB1\*03:02*; protective: *DPB1\*04:02*) (104-108).

### **1.5.1.2 Non-HLA**

---

In GWAS, 57 *non-HLA* genes are associated with T1D risk (97), but many more have been identified (59) and are primarily implicated in immune cell function. The *non-HLA* genes that confer the highest T1D risk after *HLA* genes in order are *INS* (insulin), *PTPN22* (protein tyrosine phosphatase non-receptor 22), and *IL2RA* (interleukin 2 receptor alpha) (63, 109) (**Figure 1:4**): the *INS* gene is described further (**1.5.1.2.1**) as the gene also encodes a primary autoantigen in T1D. Since other *non-HLA* loci confer subtle effects on T1D disease susceptibility, increasingly combined genetic risk scores (GRS), in addition to islet autoantibody markers and clinical characteristics, are being applied to better discriminate T1D and T2D. Recently, this approach showed the highest diabetes discrimination using just 9 SNPs (7 *non-HLA* and 2 *HLA* SNPs that determine the high-risk *DR3/DR4* haplotypes) (110).

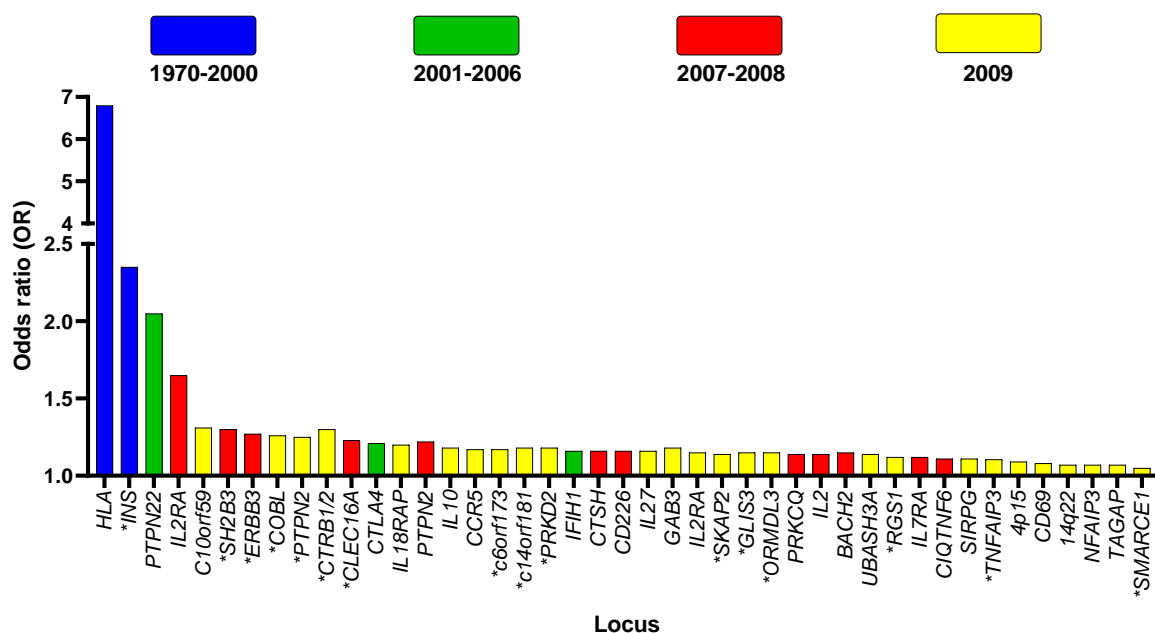


**Figure 1:4 – HLA & Non-HLA genes that confer susceptibility to T1D identified from GWAS studies (2000-2009)**

Figure adapted from Pociot *et al.* (2010) (111) and (112, 113) was used as additional sources of information. Colour denotes the time of discovery. Most significant HLA and non-HLA genetic loci are implicated in the immune system, with strong enrichment in lymphocyte and thymic enhancers. However, several non-HLA genes are expressed in pancreatic  $\beta$ -cells [denoted by an asterisk (\*)] and are likely related to  $\beta$ -cell function and/or preservation. For example, *TNFAIP3* protects from  $\beta$ -cell apoptosis, and *ERBB3* is involved in insulin production and metabolism.

### 1.5.1.2.1 INS

First described by Bell *et al.* (1984), the human insulin gene *INS* (IDDM2 locus located on chromosome 11p15) encodes pre-proinsulin, the predecessor of proinsulin/insulin, and confers 10% genetic susceptibility to T1D confirmed by GWAS (78, 114, 115). The genetic risk of the IDDM2 locus is due to a variable number tandem repeat (VNTR; 14-15bp G-rich unit ACAGGGGTGTGGGG) which is in absolute LD with a SNP (rs689) that influences transcription (116-118) (**Figure 1:5**).

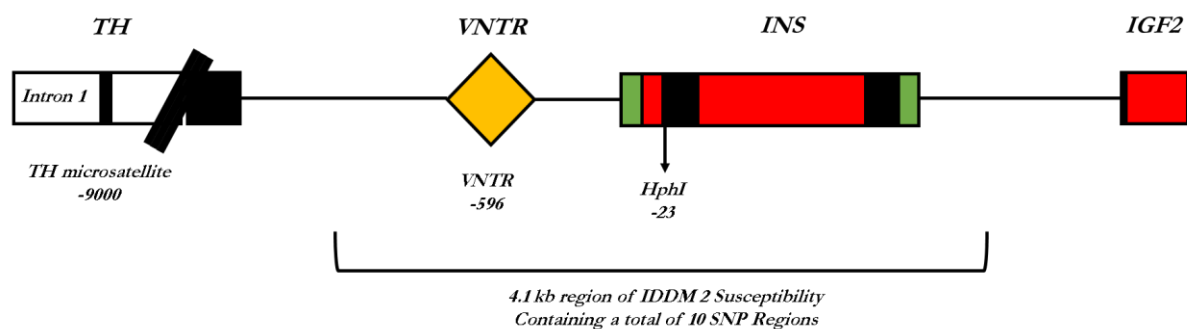


**Figure 1:5 – Simplified diagram of the *INS* region on chromosome 11**

Schematic adapted from Bennett *et al.* (1995) (119). The genes for tyrosine hydroxylase (*TH*)-insulin (*INS*)-insulin-like growth factor 2 (*IGF2*) region with the 4.1 kb of the IDDM2 susceptibility locus located on chromosome 11 (11p15). Red, black, and green indicate introns, exons, and untranslated regions, respectively. The two genetic variations that confer the greatest association for T1D (VNTR and linked rs689 SNP in *HphI*) are detailed using the 5' and 3' end boundaries for the VNTR first depicted by Bell *et al.* (1984) (114). There are 8 other SNPs within the IDDM locus that have more minor effects on T1D risk not detailed on this diagram.

The VNTR alleles can be divided into three classes according to the length of repeat units; short class I (26-63 repeats; average 570bps), intermediate class II (average 1320bps), and long class III (140-200 repeats; average 2470bps). Classes I and III are most common in Caucasian populations (114, 117). In Caucasians, homozygosity of short class I VNTR alleles confers ~2-5-fold increased risk for T1D (114, 120, 121). Conversely, the longer class III VNTR alleles are rare in Caucasian T1D cases and appear to be dominantly protective (120, 122). The protective T1D effect of long class III VNTR alleles may be explained by the 2-3-fold higher thymic expression of *INS* mRNA driven by *AIRE* (autoimmune regulatory gene) and lower pancreatic *INS* mRNA levels compared with class I VNTR alleles (119, 123). Thymic allelic variation of the VNTR locus has also been shown in foetal and childhood T1D cases, suggesting that disease modification through *INS* transcription can occur in early life (117). The transcription of *INS*, translation into pre-proinsulin protein (known T1D autoantigen and precursor of insulin), and immune tolerance of thymocytes (T-cell precursors) occurs in the thymus (120). Therefore, class III VNTR alleles likely protect against T1D through immune tolerance to pre-proinsulin (117, 123). However, it is important to appreciate the complex heterogeneity of this region, resulting in many combinations of VNTR alleles that can modulate disease susceptibility (120).

---

## 1.5.2 Environment

---

Environmental triggers could influence immune cell selection/tolerance,  $\beta$ -cell autoimmunity, autoantibody development, and/or modify genes that may ultimately influence T1D risk. It has long been evident that environmental factors must influence T1D risk from epidemiology studies (26, 63).

A plethora of environmental stimuli have been associated with the induction of T1D in early life (124). *In utero* development and childhood factors that have been linked to T1D risk are: commensal gut microbiota (125), birth weight (126), maternal immunity via placental transfer (127) or breast milk (128, 129), infections (e.g. enteroviruses)(130), dietary exposure to bovine milk insulin/proteins (infant feeding)(131-133), and Vitamin D deficiency (134). However, many studies have typically been small and included only high-risk (DR3/DR4) children with limited follow-up from birth (14). Consequently, the associations between environmental stimuli and T1D induction have often been modest, with contradictory findings between studies.

Presently, the ongoing TEDDY (The Environmental Determinants of Diabetes in the Young) study is best placed to fully evaluate the environmental influence on T1D development as high-risk (DR3/DR4) infants have been recruited since birth across six clinical centres in the USA and Europe and, are still prospectively followed up for the development of islet autoimmunity and/or T1D (135). Larger studies encompassing all ages and the genetically diverse with long-term follow-up are required to explain how environmental stimuli and genetic susceptibility continue to modulate disease risk throughout life. It is likely that some individuals are better able to regulate  $\beta$ -cell autoimmunity and/or have a greater capacity for  $\beta$ -cell regeneration/recovery (26, 124). Viral infection, hygiene hypothesis, gut microbiome, and Vitamin D are amongst the most heavily studied environmental factors in T1D research.

### **1.5.2.1 Viral infection**

---

The association between many viral infections and T1D induction have been studied at the serological and epidemiological level, but enteroviruses are the strongest and most clinically relevant (136, 137). A meta-analysis of 26 studies found evidence of enterovirus by molecular and/or immunological methods was >9 times higher in T1D cases, 3 times higher in children with islet autoimmunity, and was evident in longer-duration T1D cases. This suggests enteroviral infection could be involved in T1D induction and either persists in T1D or individuals with T1D are more susceptible to infection (130). Pancreas sections from living T1D donors (3-9 weeks duration) also showed evidence of enteroviral infection: the presence of enteroviral capsid protein 1 (VP1), hyperexpression of HLA class I in insulin-containing islets observed irrespective of VP1, and low-level enteroviral RNA (138). Nevertheless, the TEDDY study found no association between the first appearing islet autoantibody (seroconversion) or infection history in children who rapidly progressed to T1D (139).

### **1.5.2.2 The hygiene hypothesis**

---

The hygiene hypothesis was first proposed by Strachan (1989) (140), who observed an inverse relationship between hay fever transmission and household size, attributable to unhygienic contact between siblings and poor sanitation. The hygiene hypothesis proposes that lower infection rates in western countries (due to advances in healthcare/modern medicine, diet, sanitation, and living conditions) are causing the increasing incidences of allergy/autoimmune conditions (141). Greater exposure to infections/pathogens in early life has been shown to be protective of T1D (142), which has also been demonstrated through higher day-care attendance (143, 144) and later birth order (145). Additionally, population-based studies found that better sanitation, medium-to-high household crowding, and children sharing bedrooms or living with siblings appeared protective of T1D (146, 147).

### **1.5.2.3 The gut microbiome**

---

The gut microbiome, intrinsically linked to nutrition and immunity, encompasses the largest number of commensal microorganisms in humans. The gut microbiome is established in the neonatal period, develops over the course of 1-year, and stabilises in adulthood (148, 149). In infants, the gut microbiome is principally determined by the method of delivery which can have long-term effects (148, 150, 151), but intestinal biodiversity is highly diverse and dynamic throughout life as it is heavily influenced by diet (152). In large studies of T1D cases or at-risk children, reduced intestinal biodiversity was reported with evidence of intestinal dysbiosis (less favourable commensal organisms), increased intestinal permeability (increased exposure and transfer of dietary antigens), and differences in microbiome composition by age (highest <1 year of age) and geographical location (99, 125, 153, 154). Many of T1D's environmental influences could contribute to alterations to the gut microbiome leading to modifications in disease susceptibility such as immune system exposure to pathogens (immune tolerance/hygiene hypothesis) and diet/infant feeding (allergen exposure, immune tolerance, and/or maternal immunity) (148, 154).

### **1.5.2.4 Vitamin D**

---

In humans, vitamin D is predominantly synthesised endogenously in the dermal layer of the skin following ultraviolet B radiation. Calcidiol is the major form of circulating vitamin D and has the longest half-life (3-4 weeks). The enzyme 1-alpha-hydroxylase (CYB27B1) converts calcidiol into active vitamin D, which has a short half-life (2-5 hours) and exerts its function through the vitamin D receptor (VDR) expressed on all nucleated cells (155). Vitamin D has a pivotal role in skeletal health, but VDR and CYB27B1 are expressed on many cell types, including immune cells (e.g., activated B-/T-cells) and the pancreas. High calcidiol locally in the circulation is reportedly required for immunomodulation, enhanced immune cell function,

protection from infection, and has direct anti-proliferative, anti-activating, and apoptosis-inducing effects on activated B-/T-cells. Therefore, vitamin D deficiency may play a pivotal role in autoimmunity (156). In T1D, the EURODIAB substudy found that vitamin D supplementation in the first year of life decreased T1D risk by 33% across seven European countries (134). A meta-analysis of four large studies corroborated the protective effect of vitamin D supplementation in early childhood (157). However, two clinical trials found no association between vitamin D supplementation and  $\beta$ -cell function in new-onset T1D (158, 159).

---

## 1.6 Disease pathology

---

T1D is characterised by the presence of insulinitis, autoreactive immune cell infiltrate, and islet autoantibodies.

---

### 1.6.1 Insulinitis

---

Insulinitis is an inflammatory lesion of the islet of Langerhans and is considered a pathognomonic hallmark for T1D (160). Insulinitis is present in most children with recent T1D (<1 year) or individuals who progress rapidly to disease and is characterised by the presence of immune and inflammatory cells (161-163). Insulinitis was present in all T1D cases, and when studied, the islet immune cell infiltrate predominantly consisted of CD8+ T-cells followed by macrophages (CD68+), CD4+ T-cells, B-cells (CD20+), and plasma cells (CD138+) but FOXP3+ (Forkhead box P3) T regulatory cells (Tregs) were rare; findings from 279 islets from 28 subjects with recent-onset T1D post-mortem (<18 months; age range 1-23 years) and 1 recent-onset T1D subject acquired from surgical resection (18 months; age 42 years) compared to 16 controls (164). Cellular immunity is accompanied by islet antigen-specific autoantibodies (44) indicated by the presence of T-cells and B-cells in the immune cell infiltrate.

## Chapter 1 - General introduction

Insulinitis was first described by Schmidt (1902) (165) then later confirmed a hallmark of acute-onset T1D in children by Lecompte (1958) (166). The subsequent seminal study by Gepts (1965) (162) determined that insulinitis was present in 68% of acute T1D cases (15/22 aged 0.9-30 years with <1-year duration) which had sporadic peri- and intra-insular islet immune infiltrate. However, insulinitis was not present in chronic T1D cases (0/18 aged 13-47 years with 2-37 years duration), suggesting insulinitis was transient. Further pivotal studies by Gepts (1978) and Foulis *et al.* (1986) led to the identification that insulinitis (and immune cells) preferentially targets insulin-containing  $\beta$ -cells (163, 167).

Bottazzo *et al.* (1985) and Foulis *et al.* (1987) observed that hyperexpression of MHC class I was present in 92% of insulin-containing islets (but MHC class II expression was absent) in new-onset and longer duration T1D (up to 9 years) (168, 169). Later Foulis *et al.* (1991) showed that  $\beta$ -cell MHC class I hyperexpression was coupled with elevated interferon gamma (IFN $\gamma$ ) levels. The sequence of events hypothesised was: innate cells infiltrate>MHC class I hyperexpression>recruitment and activation of T-/B-cells>destruction of  $\beta$ -cells (170). Further studies have confirmed that insulinitis precedes T1D onset comparable to islet autoantibodies, as lesions were found in multiple autoantibody positive T1D-free individuals, but paucity of insulinitis was observed (171-173).

A meta-analysis (2014) of pancreatic histological studies showed that the prevalence of insulinitis was not as common as first thought (19% of 247 T1D cases and ~10% of derived islets) (174). Features of insulinitis (transient nature, heterogeneous distribution in islets, and parameters of limited patient populations) later prompted standardised diagnostic criteria: presence of  $\geq 15$  CD45+ cells immediately adjacent to or within  $\geq 3$  islets, predominant lymphocytic infiltration, and presence of insulin-negative  $\beta$ -cells (175).

Pancreata available for research remain rare due to improved disease management and declining autopsy rates (174). *In vivo/in vitro* study of human islets is also difficult due to their low abundance (1-2% of pancreatic volume), scattered presence throughout the tissue, and anatomical inaccessibility (173). Attempts to acquire pancreas biopsies from living donors (176-178) were initially considered safe but has been associated with inherent risks resulting in trial termination (174). Organised efforts by PannFinn and the Network for Pancreatic Organ Donors with Diabetes (nPOD) (179, 180) seek to provide large biobanks of high-quality tissue specimens from preclinical and clinical T1D to advance our understanding of disease pathology and technical prowess to study live islets (181).

It is important to acknowledge that the non-diabetic (NOD) T1D mouse model has been invaluable in elucidating molecular and cellular processes underpinning autoimmunity, but valid differences between human and mouse T1D etiopathologies have been raised as many promising mouse immunotherapies have failed to be translated in humans, reviewed in (182, 183).

---

### 1.6.2 Tolerance, immune cells, autoimmunity, & T1D

---

Several checkpoint processes termed “tolerance” exist in the development of immune cells that function to exclude cells recognising self or innocuous antigens from entering circulation and eliciting autoimmune-mediated destruction of healthy cells. The initiation and termination of immune responses are orchestrated by cell-signalling stimulatory/inhibitory molecules and specific T-/B-cells. Ultimately, autoimmunity results from the breakdown of tolerance and/or immune regulation mechanisms (184). Autoimmune-mediated destruction of pancreatic islets in T1D is predominantly driven by CD8<sup>+</sup> and CD4<sup>+</sup> T-cells. The role of innate immune cells and B-cells is less clear, but autoreactive T-cells and B-cells (accompanied by the presence of islet autoantibodies) have been identified before clinical onset (185, 186).

### 1.6.2.1 Tolerance

Tolerance of T-cells (cellular responses) and B-cells (humoral responses) is achieved by positive and negative selection of developing lymphocytes and can be broadly subdivided into central (**Figure 1:6**) and peripheral tolerance (**Figure 1:7**) (184).

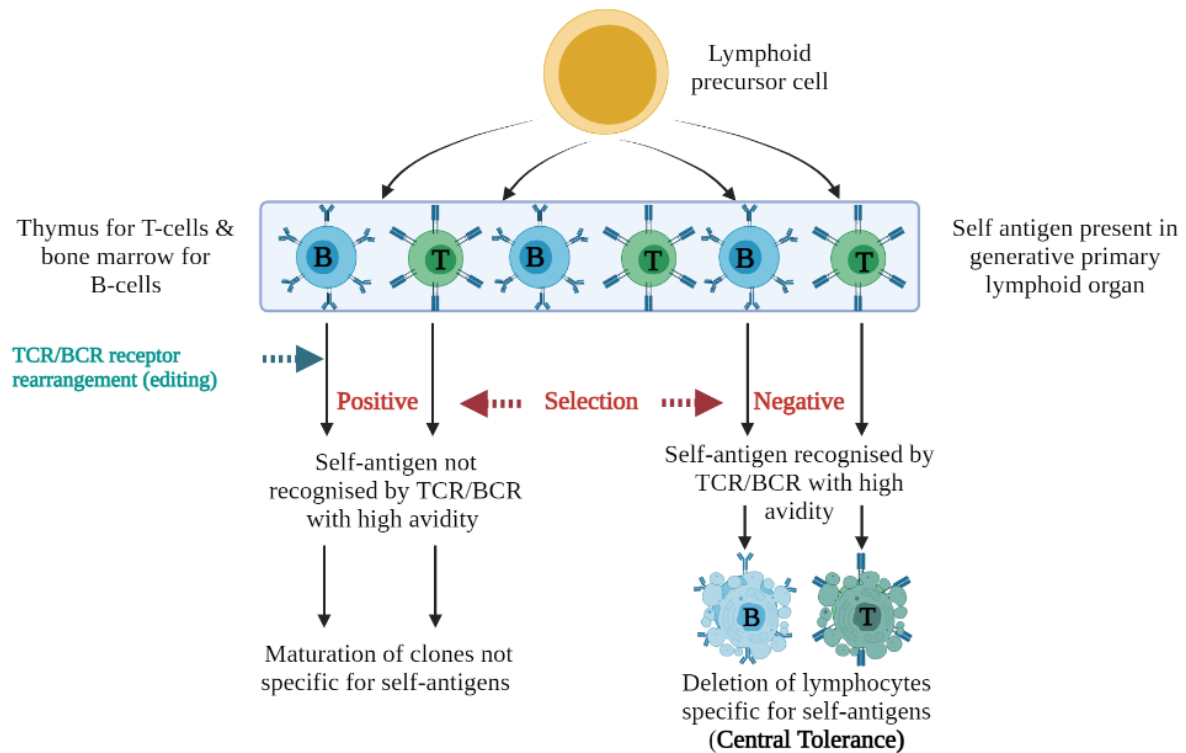


*Figure 1:6 – Schematic of central tolerance*

Simplified schematic adapted from Kindt, Goldsby, and Osborne (2006) (184) and created in BioRender.com. TCR: T-cell receptor; BCR: B-cell receptor. The random rearrangement of variable (V), diversity (D), and joining (J) gene segments that determine TCRs and BCRs can give rise to receptors that recognise self-antigen by chance in generative primary lymphoid organs (the thymus for T-cells and bone marrow for B-cells). Early immature T- and B-cells that do not recognise self-antigen with high avidity (strength of receptor-antigen binding) are positively selected for further maturation. In contrast, immature T- and B-cells that recognise self-antigen with high avidity are negatively selected (“deleted”) and undergo apoptosis to prevent the maturation of these auto-reactive cells. As central tolerance relies on the limited expression of self-antigens in the primary lymphoid organs, some self-recognising immature lymphocytes are released into the circulation. Therefore, efficient peripheral tolerance in secondary lymphoid tissues is paramount in the prevention of autoimmunity.

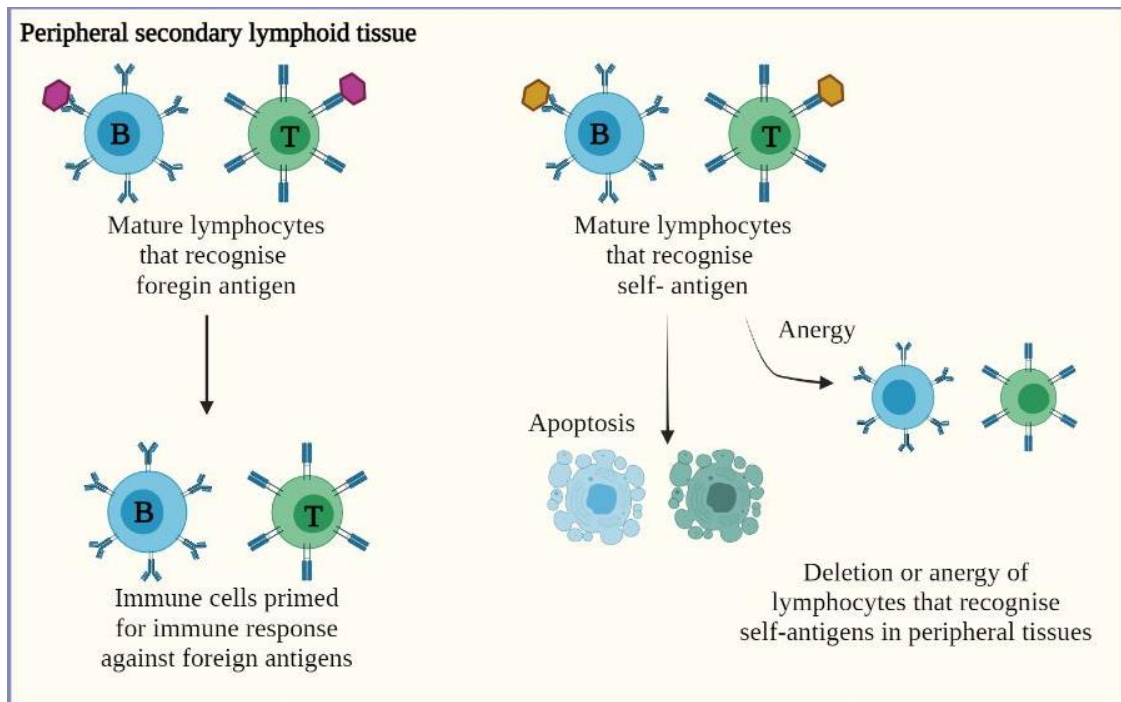


*Figure 1:7 – Schematic of peripheral tolerance*

Simplified schematic adapted from Kindt, Goldsby, and Osborne (2006) (184) and created in BioRender.com. Peripheral tolerance occurs in secondary lymphoid tissues (lymph gland, lymph node, or circulation) following the release of mature naïve lymphocytes from primary lymphoid organs (thymus for T-cells and bone marrow for B-cells). Peripheral tolerance in these tissues results if mature lymphocytes possess receptors (TCR/BCRs) that react with self-antigens. Self-recognising lymphocytes undergo anergy (inactive/unresponsive state) or apoptosis if self-antigen is recognised with high affinity/avidity.

The precise tolerance mechanisms in T-cell and B-cell development are slightly different (**Table 1:1**) and are not always successful. An estimated 95-98% of all immature T-cells (thymocytes) do not survive central tolerance (184). It is speculated that survival is proportional to the local expression of self-MHC ± self-antigen in the thymus and peripheral tissues (peripheral tolerance), which is tissue-specific (3). Despite the low success rate, there has been evidence of autoreactive T-cells in the periphery and re-activation of short-lived anergic T-cells under inflammatory conditions. Under “normal conditions,” these cells are controllable through inhibitory molecules. However, in autoimmunity, there could be a deficiency of these inhibitory molecules, developing T-cells could be less responsive to suppression, and/or autoreactive anergic T-cells are more likely to be re-activated, exacerbating autoimmune destruction (3, 187).

## Chapter 1 - General introduction

In contrast, around ~55-75% of early immature B-cells are autoreactive due to the arbitrary nature of B-cell receptor (BCR) gene recombination during central tolerance. This is reduced to ~20% in mature naïve B-cells following peripheral tolerance. However, as anergic B-cells comprise ~5-7% of peripheral B-cells and have a short half-life (~5 days), up to 50% of newly emerging B-cells are estimated to undergo anergy and are autoreactive (3, 188). Therefore, anergic B-cells could be a large source of autoreactive cells as they are not “deleted” after tolerance and, under inflammatory conditions, can be reactivated like anergic T-cells. Anergic B-cells have been shown to contribute to many autoimmune conditions such as T1D and systemic lupus erythematosus (SLE) (3). Additionally, transgenic mouse models have suggested CD4<sup>+</sup> T-cells play a pivotal role in eliminating peripheral autoreactive B-cells (189) but, genetics also appear to regulate B-cell tolerance, as single gene mutations and deficiencies of molecules involved in B-cell tolerance have been linked to autoimmunity and immunodeficiency (e.g. recombination-activating gene 1 and Bruton’s tyrosine kinase) (190).

No mechanistic consensus has been reached between tolerance and many autoimmune conditions (including T1D), but it is likely that multiple defects in the cellular and molecular processes lead to the breakdown of tolerance and, consequently, development of autoimmunity (187, 190).

T-cells	B-cells
<p><b>Central tolerance – Self-MHC</b></p> <p><u>Location:</u> thymus (outer cortex)  <u>Cells:</u> immature thymocytes (T-cell precursors)</p> <p><u>Positive selection:</u> following random TCR gene re-arrangement, thymocytes with expressed TCR (<math>\alpha\beta</math>) heterodimers that recognise/bind to self-MHC expressed on thymus epithelial cells are positively selected (MHC restriction). Failure of positive selection results in thymocyte apoptosis through cell signalling neglect.</p> <p><u>Negative selection:</u> remaining thymocytes will express TCRs (<math>\alpha\beta</math>) of different affinities for self-MHC. DCs &amp; M<math>\phi</math> bearing MHC I &amp; II interact with thymocyte clones bearing high-affinity TCRs for self-MHC <math>\pm</math> self-antigen expressed on thymic stromal cells. Under control of transcription regulators, there are three outcomes based on affinity for self-MHC <math>\pm</math> self-antigen*:</p> <ol style="list-style-type: none"> <li>1. thymocytes with high affinity are negatively selected &amp; undergo apoptosis.</li> <li>2. thymocytes with intermediate affinity later become Tregs.</li> <li>3. thymocytes with low affinity undergo further maturation (self-tolerance).</li> </ol>	<p><b>Central tolerance – Self-antigen</b></p> <p><u>Location:</u> bone marrow  <u>Cells:</u> immature B-cells</p> <p><u>Positive selection:</u> following random BCR gene re-arrangement, immature B-cells expressing a BCR (composed of IgM's heavy chain &amp; a surrogate light chain) with innocuous specificity for self-antigen further mature through BCR signalling &amp; once positively selected, cannot re-edit their BCR.</p> <p><u>Negative selection:</u> immature B-cells with BCRs that recognise self-Ag will high avidity undergo apoptosis or receptor re-editing to produce a non-self-reactive/innocuous BCR through a second attempt.</p>
<p><b>Peripheral tolerance – Self-antigen</b></p> <p><u>Location:</u> lymph node/lymph gland/periphery  <u>Cells:</u> naïve T-cells</p> <p><u>Negative selection:</u> anergy/apoptosis</p> <ul style="list-style-type: none"> <li>- Lymph node stromal cells expressing tissue-specific antigens mediate the deletion/apoptosis of naïve T-cells recognising self-antigen.</li> <li>- DC/M<math>\phi</math> or other APCs can induce anergy through inhibition of the mTOR pathway.</li> </ul>	<p><b>Peripheral tolerance – Self-antigen</b></p> <p><u>Location:</u> lymph gland/Lymph node  <u>Cells:</u> naïve B-cells</p> <p><u>Negative selection:</u> anergy/apoptosis/tolerance</p> <ul style="list-style-type: none"> <li>- Continued stimulation of self-antigen with the BCR inhibits proliferation/differentiation of naïve B-cells &amp; renders cells in an unresponsive/anergic state.</li> <li>- Somatic hypermutation of the BCR gene segments alters foreign-antigen specificity &amp; affinity. This process excludes clones with BCRs with low affinity for foreign antigen/binding to self-antigen resulting in apoptosis or anergy.</li> <li>- Soluble, low abundance, &amp;/or monomeric self-antigen can be tolerated/ignored.</li> </ul>

*Table 1:1 – Central & peripheral tolerance mechanisms for developing T-cells & B-cells*

MHC: Major histocompatibility complex; TCR: T-cell receptor; BCR: B-cell receptor; DC: dendritic cell(s) that function as antigen-presenting cells; M $\phi$ ; macrophage (innate immune cell) that function as antigen-presenting cells; mTOR: mammalian target of rapamycin; Treg: T regulatory cell. \* Negative selection efficiency seems to occur proportional to the antigen present in the thymus. Table composed of information from (3, 184, 187, 190).

## **1.6.2.2 T-cells & T1D**

---

### **1.6.2.2.1 T-cell maturation & development**

T-cells are derived from haematopoietic stem cells and mature in the thymus. Immature T-cell precursors (thymocytes) express a distinct TCR comprised of  $\gamma\delta$  or  $\alpha\beta$  chains. Thymocytes bearing  $\alpha\beta$ -TCRs have random specificity and become CD4<sup>+</sup>CD8<sup>+</sup>-double-positive. Thymocytes recognising self-MHC on thymic endothelial cells and have low-affinity for self-antigen are selected (central tolerance). Recognition of MHC Class II and Class I gives rise to single-positive CD4<sup>+</sup> and CD8<sup>+</sup> naïve thymocytes, respectively. Single-positive naïve thymocytes are released into the circulation to secondary lymphoid organs for the following events: peripheral tolerance > foreign-antigen exposure > activation/maturation > activated antigen-specific mature CD4<sup>+</sup> and CD8<sup>+</sup> T-cells (187, 191) (**Figure 1:8**).

In the blood and secondary lymphoid organs, ~30-40% are CD8<sup>+</sup>, which have a highly cytotoxic phenotype that mediates cell destruction/apoptosis, and ~60-70% are CD4<sup>+</sup>, designed “T helper (Th)-cells” that can activate and suppress cellular and humoral responses (187, 191). There are three functional subsets of Th-cells characterised by their secreted cytokines: Th1-cells [interleukin(IL)-2, tumour necrosis factor beta (TNF $\beta$ ), and IFN $\gamma$ ; pro-inflammatory phenotype], Th2-cells [granulocyte-macrophage colony-stimulating factor (GM-CSF), IL-4, IL-5, and IL-10; regulatory phenotype], and Th17-cells [IL-6, IL-17, and TNF alpha (TNF $\alpha$ ); pro-inflammatory phenotype particularly in tissues]. All Th-cells and the cytokines they release work antagonistically, and usually, one subset is dominant in responding to a particular antigen at any one time (191, 192). However, the immunological decision-making that governs a particular Th response is not clear.

## Chapter 1 - General introduction

During the development of T-cells, CD4<sup>+</sup>CD25<sup>+</sup> Tregs are also produced following upregulation and expression of FOXP3. Tregs are critical for immune regulation and can be divided into “natural” and “acquired” based on their origin. “Natural” Tregs arise from the thymus during central tolerance, have an intermediate affinity for self-MHC ± self-antigen when released into circulation, and exert immune suppression via cell-to-cell contact. “Acquired” Tregs arise in the periphery from naïve precursors during an immune response or following antigen-presentation from APCs (tolerogenic dendritic cells) and mediate immune suppression by releasing soluble factors such as IL-10 and transforming growth factor beta (TGFβ), which are potent independent mediators of immune suppression. Both types of Tregs become induced in an antigen-specific fashion against foreign-antigen and are pivotal in regulating immune responses (193-196).



### **1.6.2.2.2 T-cells in T1D**

It is widely accepted that the activation and expansion of autoreactive CD4<sup>+</sup> and CD8<sup>+</sup> T-cells play crucial roles in the orchestration, mediation, and final effector phase of  $\beta$ -cell destruction in T1D. This is unsurprising given the roles of both HLA and non-HLA alleles on immune system function and their association with T1D risk (185, 197).

Both HLA I and II molecules influence the specificity of the T-cell response in T1D (197). There has also been evidence that HLA-DQ molecules have differential (competitive) binding to  $\beta$ -cell antigenic epitopes thereby, having a direct mechanism for modulating the T-cell autoimmune response in T1D through regulatory or proinflammatory processes (94, 198). CD4<sup>+</sup> and CD8<sup>+</sup> T-cells were two of the three most prevalent cell types found in the insulitic lesion infiltrate in human islets (164). Additionally, hyperexpression of MHC class I in human donors suggests that  $\beta$ -cells may be directly capable of presenting self-antigen to autoreactive CD4<sup>+</sup>/CD8<sup>+</sup> T-cells, flagging them for autoimmune destruction, which may explain the predominance of CD8<sup>+</sup> T-cells in insulitis (185). Insulin and/or glutamic acid decarboxylase (GAD65)-reactive CD4<sup>+</sup> T-cells have also been expanded after isolation from pancreatic lymph nodes of deceased T1D subjects (199), but many varieties of islet autoantigen-reactive infiltrating T-cells have been identified in human T1D subjects (200).

Both CD4<sup>+</sup>/CD8<sup>+</sup> T-cells are also required for diabetes development in NOD mice (201). Analysis of the CD4<sup>+</sup> compartment showed that only Th1-cells express diabetogenic TCRs and dominate the response (202-204), but Th2-cells appear important for diabetes progression: IFN $\gamma$  deficiency did not prevent insulitis or diabetes (205), IL-10 production in islets accelerated diabetes progression (206), and Th2-induced autoimmunity to a single  $\beta$ -cell autoantigen led to antigen spreading (207). CD8<sup>+</sup> T-cells are the major effectors of  $\beta$ -cell destruction but are important later in the pathogenesis (208-210). Comparable to human

## Chapter 1 - General introduction

studies, CD8<sup>+</sup> T-cells isolated from NOD pancreatic lymph nodes identified insulin as the primary antigen targeted, and both CD8<sup>+</sup>/CD4<sup>+</sup> T-cells recognised an identical epitope on insulin's B-chain (211, 212).

Additionally, disturbed Treg function and/or lower frequency of Tregs may underline all autoimmune conditions as the absence of Tregs (mutations in FOXP3) in the congenital condition IPEX syndrome (immune dysregulation, polyendocrinopathy, enteropathy, X-linked) leads to aggressive autoimmunity (191, 193). However, it's unclear whether the number of Tregs is reduced in T1D due to contradictory findings, but studies have reported that FOXP3 expression, IL-2 responsiveness for activation/proliferation, and effector function is reduced or impaired in Tregs from T1D subjects (213-217). These findings, in conjunction with Treg-associated genetic susceptibility of T1D (e.g., non-HLA genes *cytotoxic T lymphocyte antigen (CTLA)-4* and *PTPN22*), implicates a failure of immune regulation in T1D. Similarly, NOD mice have low numbers of Tregs, and effector T-cells show resistance to Treg suppression over time. However, Treg transfer and IL-2 treatment attenuated diabetes (213, 218, 219).

Conclusive proof that T1D is a T-cell mediated autoimmune disease is evidenced by the recent success of a randomised control trial (RCT) that showed a single 14-day course of the T-cell-modulating anti-CD3 monoclonal antibody, Teplizumab, delayed T1D onset by ~2 years in first-degree relatives (FDRs) participating in TrialNet's Natural History study (NHSt) (220). After 6 years, Teplizumab continued to delay diabetes in these FDRs (50% remained diabetes-free) with improved  $\beta$ -cell function (C-peptide). The improvement in  $\beta$ -cell function was associated with an exhausted CD8<sup>+</sup> T-cell phenotype with weaker effector function (221). Teplizumab is the first non-antigen specific T-cell immunosuppressant therapy shown to be efficacious with a prolonged effect and limited side effects.

## Chapter 1 - General introduction

Recently, Telizumab has been the first secondary prevention immunotherapy proposed for FDA approval for T1D (2021), but as many previous T-cell immunotherapies have not shown lasting effects on  $\beta$ -cell function (222-225), T-cells are unlikely to be the sole driving force in T1D development. Mounting evidence suggests that  $\beta$ -cell dysfunction plays a pivotal role in the aetiology of both T1D and T2D (reviewed in (226)). Increasingly, combination immunotherapy regimens may enhance efficacy in T1D and several of these trials are ongoing with more anticipated in the future.

### **1.6.2.3 B-cells & T1D**

---

#### **1.6.2.3.1 B-cell maturation & development**

Derived from haematopoietic stem cells, B-cells mature in the bone marrow where after random rearrangement of variable, diversity, and joining (VDJ) gene segments (that later determine immunoglobulin (Ig) heavy and light chains), express a unique antigen-binding BCR, and are released into circulation as mature naïve B-cells to peripheral lymphoid tissues: spleen and lymph nodes. Within the marginal zones of these tissues, naïve B-cells encounter either soluble antigen (blood- or lymph-borne) or antigen presented on TCRs of activated Th-cells. Activated B-cells internalise and express antigen on MHC class I and II and then, with activated Th cells, migrate to the primary follicles to form germinal centres (184).

Within germinal centres, affinity maturation occurs to preferentially select mature B-cells expressing high-affinity BCRs for survival. Affinity maturation is determined through somatic hypermutation of V-domain genes that determine the antigen-binding site of secreted Ig. Somatic hypermutation is initiated by the B-cell specific activation-induced deaminase (AID) enzyme that induces point nucleotide substitutions by deamidating DNA cytosines. At the same time, AID also initiates class switch recombination (CSR), which in combination with cytokine signalling transmitted from Th-cells, determines secreted Ig isotype. In brief, AID generates double-strand DNA breaks in the switch (S) genes located downstream of the heavy chain constant (C) region ( $C\mu$  in naïve mature B-cells), resulting in intrachromosomal deletional recombination that changes the  $C\mu$  gene (encoding IgM) to either  $C\gamma$  (encoding IgG),  $C\alpha$  (encoding IgA), or  $C\epsilon$  (encoding IgE). The  $C\delta$  gene encoding membrane-bound IgD on naïve mature B-cells is excluded from CSR to maintain cell-surface IgD expression (227-229). Following affinity maturation and CSR, mature B-cells rapidly proliferate and differentiate into pre-determined Ig-secreting plasma cells and memory B cells (**Figure 1:9**).

## Chapter 1 - General introduction

Secreted Ig broadly has two purposes: to capture antigen for enhanced antigen presentation to other immune cells (amplifying antigen-specific immune responses) and to exist as soluble effectors that can individually bind and neutralise antigen (227). Memory B cells provide future Ig-mediated protection upon antigen-reencounter. Additionally, activated B-cells expressing antigen can act as an APC to further stimulate CD4<sup>+</sup>/CD8<sup>+</sup> T-cells via TCRs. The presence of antigen determines the lifespan of maturing B-cells; ~90% of naïve B-cells undergo apoptosis and only survive days to weeks (184).

There are also B-cells with a regulatory phenotype (Bregs) that play an important role in immune suppression, although the potential role of these cells in autoimmunity is not fully understood and are often overlooked (230). Bregs were first described in the B-cell deficient mouse model of experimental autoimmune encephalomyelitis (EAE) (231), where EAE exacerbation was attributed to the deficiency of IL-10 producing B-cells (232). Bregs primarily originate from naïve or memory B-cells, can control T-cell maturation, expand Tregs, and inhibit T-cell-mediated antibody secretion from germinal centres during B-cell development. Like Tregs, Bregs can exert immune regulation through TGF $\beta$  and IL-10. Therefore, deficiencies in Breg activity might lead to aberrant autoimmune responses especially considering the T-cell-dependent control of humoral immunity. The phenotype of Bregs appears to show plasticity, able to alter the expression of cell-surface molecules (233). Therefore, cell surface panels to identify these cells need to incorporate many Breg phenotypes but CD24<sup>high</sup>CD38<sup>high</sup>CD19<sup>+</sup> (immature cells) and CD27<sup>+</sup>CD24<sup>high</sup>CD148<sup>high</sup>CD48<sup>high</sup> (IL-10 producing Bregs), and CD27<sup>high</sup>CD38<sup>+</sup> (plasma cells) have been used in human subjects with autoimmunity such as SLE, and multiple sclerosis (MS) (234).

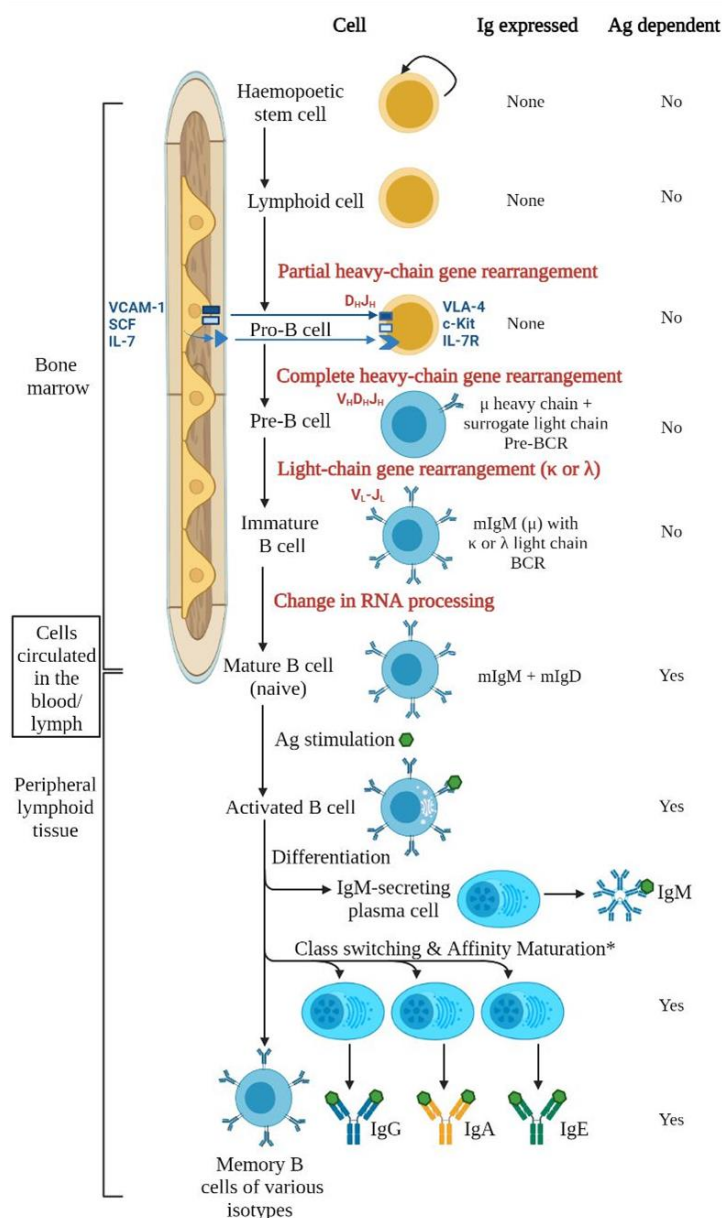


Figure 1:9 – B-cell development & maturation

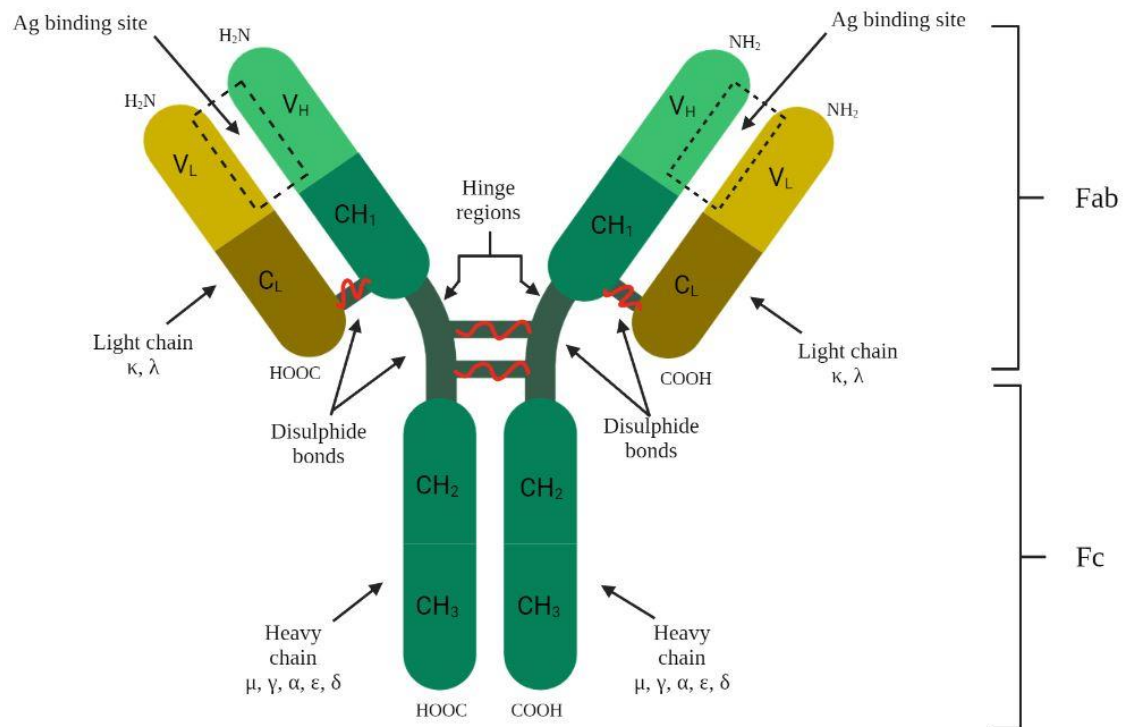
Image adapted & constructed using information from (184, 227, 235). Image created in BioRender.com. B-cell development begins in the bone marrow, where events occur independently of antigen. Proliferation and pro-B-cells into pre-B-cells require the microenvironment provided by bone marrow stromal cells. The interaction between vascular cell adhesion molecule 1 (VCAM-1) and integrin  $\alpha 4\beta 1$  (VLA-4) promotes the binding of c-kit to stem cell factor (SCF), which stimulates intracellular signaling in the pro-B-cell to express interleukin-7 receptor (IL-7R). IL-7R binds IL-7 released from stromal cells and induces the maturation of the pro-B-cell to pre-B-cells and are released from stromal cells. At the pre-B-cell stage, there has been VDJ gene segment rearrangement of the Ig DNA (RAG-1 & RAG-2) in the lymphoid cells, which forms the immature B-cell; first ( $D_H$ -to- $J_H$ ) and second ( $V_H$ -to- $D_H$ - $J_H$ ) rearrangement determines the heavy chain ( $\mu$  for IgM which forms pre-B-cell receptor, BCR) and light chain ( $\kappa$  or  $\lambda$ ), respectively which forms the BCR. A change in the RNA processing of the heavy chain primary transcript in the immature B-cell permits the production of two mRNAs, one encoding the membrane-form of IgM (mIgM) and one encoding membrane-bound IgD (mIgD). The co-expression of mIgM and mIgD signifies a mature B-cell that is released into circulation to peripheral lymphoid tissue (primarily the spleen or lymph nodes) where if the antigen is encountered and recognised by the BCR, mature B-cells undergo clonal expansion (secreting IgM) and differentiation into secreting plasma cells (which undergo further processes produce different Ig isotypes (IgG/IgA/IgE) specific for antigen with enhanced affinity\*) or memory B-cells (which mount rapid responses upon secondary encounter with antigen).

### **1.6.2.3.2 Antibody-secreting plasma cells**

Plasma cells can continuously and rapidly secrete Ig (commonly termed antibodies) but do not undergo further maturation/differentiation. Most plasma cells have a short half-life (3-4 days), but some can survive in the bone marrow for month-years and continue to secrete antibodies (236). Additionally, tissue-resident long-lived plasma cells (LLPCs) form an independent compartment of immunological memory which can persist for decades independent of B-cell precursors or residual antigen but are not intrinsically long-lived. Their survival is dependent on specialised niche microenvironments, but the cellular and molecular components that promote LLPC production or survival are not fully characterised in humans (237-239).

An antibody in its simplest form is a Y-shape glycoprotein that consists of 2 identical heavy (H;  $\mu$ ,  $\gamma$ ,  $\alpha$ ,  $\epsilon$ , or  $\delta$ ) and 2 identical light (L;  $\kappa$  or  $\lambda$ ) polypeptide chains that have NH<sub>2</sub>-terminal variable (V) and COOH-terminal constant (C) domains. The four chains are held together by covalent (disulphide) and noncovalent bonds, which form two identical halves of the molecule; H/L V domains form the Fab region with two identical antigen-binding sites, and the H/C domains form the Fc region, which determines the isotype, subclass, and function of the antibody (**Figure 1:10**) (227).

The Fc region binds to Fc receptors (FcR) expressed on effector or mediator cells, with most cells expressing several FcRs, which differ in their affinity for antibody-Fc. Antibodies cannot directly remove innocuous antigen, but the antibody-activation of different FcRs can activate multiple intracellular signalling pathways in a single cell, invoking many effector functions: antibody-dependent cellular cytotoxicity (ADCC: antigen-bound antibody binds to FcRs and mediates target destruction), antibody-dependent cellular phagocytosis (opsonisation of target for destruction), or complement-dependent cytotoxicity (activation of the complement cascade initiates target destruction and is the major effector of the humoral response) (184).



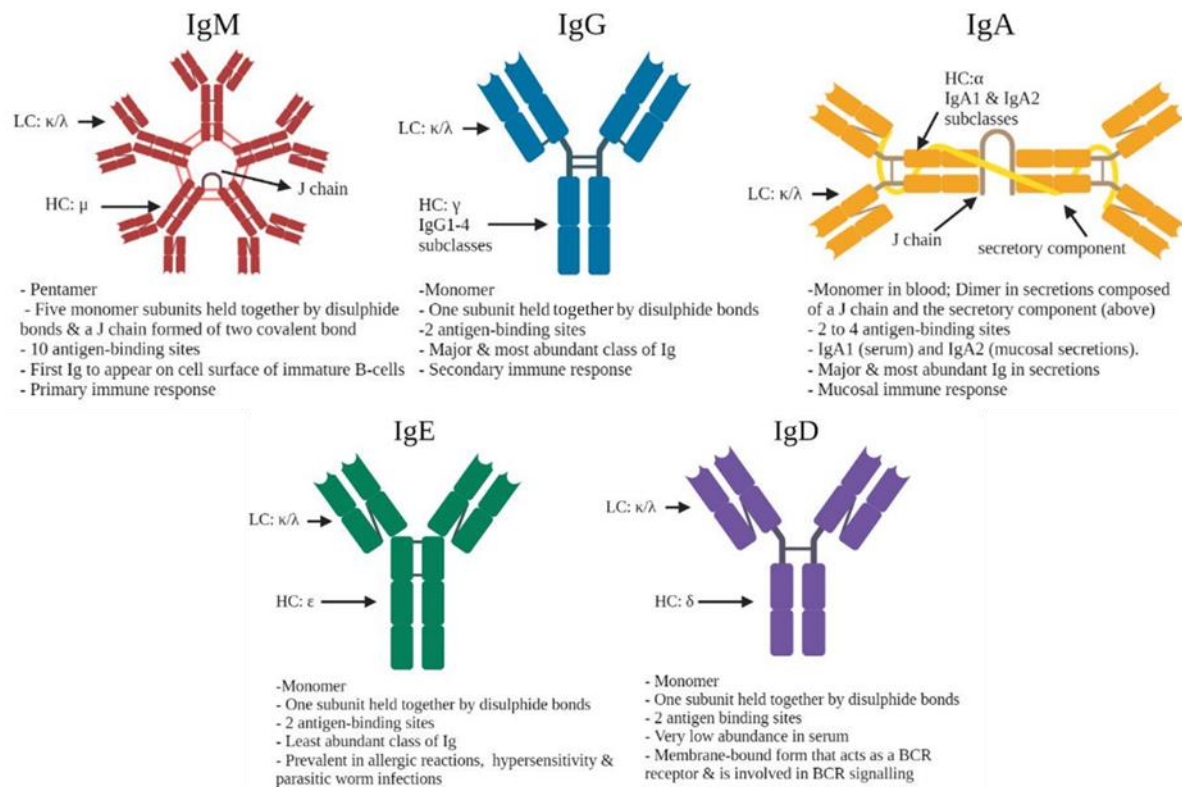
**Figure 1:10 – Schematic of a typical immunoglobulin molecule**

Image adapted from Alberts *et al* (2002) (236) and created in BioRender.com. A typical immunoglobulin (antibody) molecule is a Y-shape glycoprotein composed of 4 polypeptides (2 heavy and 2 light chains) held together by covalent (disulphide) and noncovalent bonds. One antibody molecule is bivalent with two identical antigen-binding sites formed by the N-terminus of both the light and heavy chains. An antibody can be divided into two; the variable (V) region composed of heavy (V<sub>H</sub>) and light (V<sub>L</sub>) chains with the antigen-binding site (Fab) and the constant (C) region composed onto of heavy chains (predominantly CH<sub>2</sub>/ CH<sub>3</sub>) that determine the antibody function and isotype (Fc). In humans, there are up to 5 heavy chains that determine the antibody isotype and function and 2 light chains.

### **1.6.2.3.3 Antibody isotypes & subclasses**

Humans have five antibody isotypes (IgM, IgD, IgG, IgA, and IgE) that have similar structures composed of Ig subunit(s) (**Figure 1:11**) but are highly specialised for their function (**Table 1:2**). IgM and IgD are expressed on mature naïve B-cells and function as BCRs, but only IgM is also secreted by plasma cells and is pivotal in primary responses. IgG is the most commonly produced antibody and is involved in secondary responses with a high capacity for neutralising antigen with four specialised subclasses. IgA is the most prevalent antibody in mucosal secretions and plays crucial roles in both primary and secondary responses in these regions with two specialised subclasses. IgE is primarily involved in allergic reactions, hypersensitivity, or parasitic worm infections (236).

## Chapter 1 - General introduction



**Figure 1:11 – Human immunoglobulin isotypes**

Image created in BioRender.com using material from (184, 227, 236).

	<b>IgM</b>	<b>IgG</b>	<b>IgA</b>	<b>IgE</b>	<b>IgD</b>
% in total blood	10	75	15	<1	<1
Normal serum level (mg/ml)	1.5	0.5-9*	0.5-3.0	0.0003	0.03
Molecular weight (kDa)	900	150	150-600*	190	150
Half-life (days)	5	8-23*	6	2.5	0.03
Present on cell membrane of mature B-cells	+	-	-	-	+
Activates complement	++	+	-	-	-
Crosses placenta	-	+	-	-	-
Binds to Fc receptors on phagocytes (macrophages & neutrophils)	-	+	-	-	-
Binds to mast cells & basophils	-	-	-	+	-
Mucosal transport	-	-	++	-	-

**Table 1:2 – Biochemical properties of human immunoglobulin isotypes**

Image created in BioRender.com using material from (184, 227, 236). \* Variation dependent on the specific subclass.

*IgG subclasses*

First described by Grey and Kunkel (1964), IgG can be further subdivided into four subclasses according to the prevalence observed in a healthy human western population: IgG1, IgG2, IgG3, and IgG4 (240, 241). Comparable to the generation of antibody isotypes, IgG subclasses are formed during CSR of mature B-cells where specific deletion recombination of switch (S) genes encode IgG subclass-specific heavy chain (C) regions; C $\gamma$ 1-4 encodes IgG1-IgG4. The IgG subclasses share >90% structural homology (**Figure 1:12**), and the ~10% difference in their Fc regions determines distinct effector functions, biochemical properties, and the type/affinity of FcR they recognise (Fc $\gamma$ R) (**Table 1:3**) (229, 240, 242).

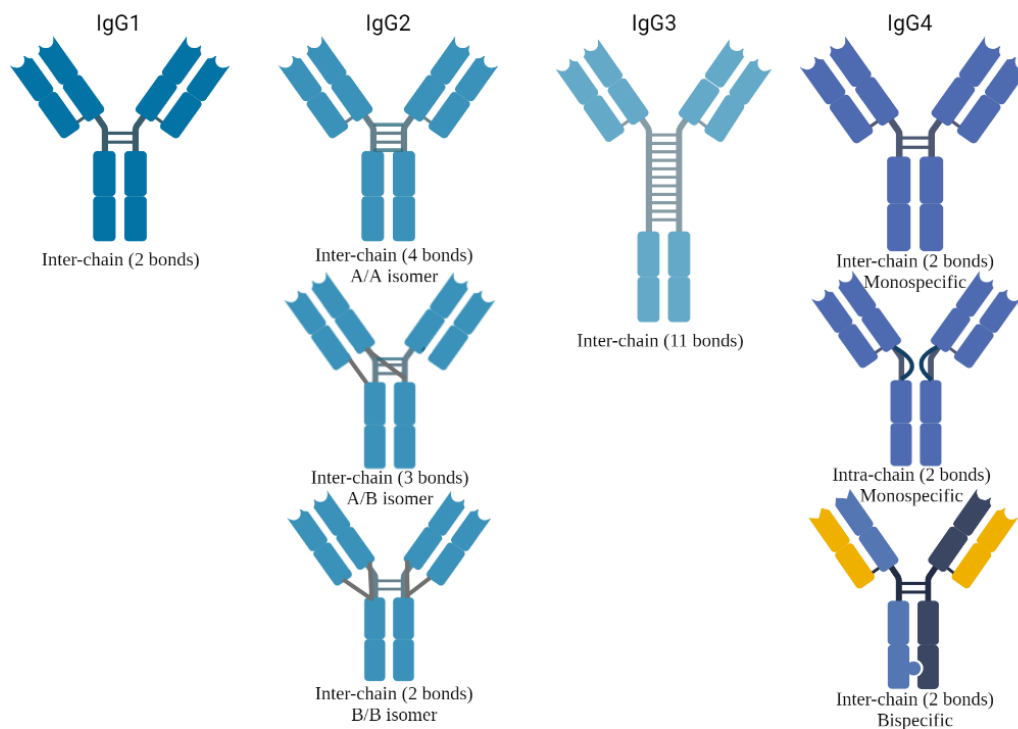


**Figure 1:12 – Human IgG subclasses**

Image was adapted from Vidarsson, Dekkers, and Rispens (2014) (243) and created in BioRender.com. There are four IgG subclasses, named in order of abundance found in a healthy western human population: IgG1-IgG4. These subclasses share >90% structural homology. They primarily differ by their hinge region and the N-terminus of the CH3 heavy chain. IgG1 has two inter-chain disulphide bonds in its hinge region. IgG2 can exist in three isomers (A/A, A/B/ & B/B) that vary according to the number and position of inter-chain disulphide bonds in the hinge region. IgG3 has 11 inter-chain disulphide bonds in its hinge region. IgG4 can exist in up to 3 different allotypes shown in this figure that can interchange randomly across 6 different variations with only 2 disulphide bonds in its hinge region. Most IgG4 in humans exist as inter-chain bispecific molecules (can bind two different antigens or two epitopes on the same antigen), which prevents IgG4 binding to multiple antigen regions and reduces antibody avidity. Therefore, IgG4 has been coined as a “blocking antibody,” which may be an evolutionary mechanism to modulate immune responses and a reason for the association between IgG4 & Bregs. The effector function and affinity for antigen of these IgG subclasses can vary significantly.

Biochemical Property	IgG1	IgG2	IgG3	IgG4
<b>General</b>				
Molecular mass (kDa)	146	146	170	146
Amino acids in the hinge region	15	12	62 <sup>a</sup>	12
Inter heavy chain disulphide bonds	2	4 <sup>b</sup>	11 <sup>a</sup>	2
Relative abundance (%)	60	32	4	4
Half-life (days)	21	21	~7/21 <sup>a</sup>	21
Placental transfer	++++	++	++/++++ <sup>a</sup>	+++
<b>Antibody response to</b>				
Proteins	++	+/-	++	++
Polysaccharides	+	+++	+/-	+/-
Allergens	+	(-)	(-)	++
<b>Function</b>				
Complement cascade activation	++	+	+++	-
Opsonisation	++++	++++	++++	-
<b>Fc receptors</b>				
FcγRI (high affinity)	+++	-	++++	++
FcγRII (low affinity)	+ / +++ <sup>c</sup>	+ / +++ / - <sup>c</sup>	++ / ++++ <sup>c</sup>	+ / +++ <sup>c</sup>
FcγRIII (low affinity)	++ / ++++ <sup>c</sup>	- / + <sup>c</sup>	++++	- / +++ <sup>c</sup>

*Table 1:3 – Biochemical properties of human IgG subclasses*

Adapted from Vidarsson, Dekkers, and Rispens (2014) (243) and Schroeder and Cavacini (2010) (227).  
<sup>a</sup> dependent on IgG3 allotype; <sup>b</sup> based on IgG2 A/A isomer. <sup>c</sup> differential binding to polymorphic variants of FcγR II and III, which are of lower affinity than FcγRI; IgG1 binds I/II/III; IgG2 preferentially binds II; IgG3 binds I/II/III; IgG4 binds I/II. +/+/+/+/+++ correlates to strength of subclass binding/reactivity. (-) absent. +/- refers to contradictory findings. Despite biochemical differences, all subclasses can neutralise antigen, can perform opsonisation (antibody-coating target cell for immune-mediated destruction and phagocytosis), and can activate the complement cascade (the major effector of the humoral response) (184).

Protein antigens usually trigger MHC Class II molecules on mature B-cells receiving Th-dependent antigen presentation via the TCR (T-cell dependent), which primarily elicit IgG1 and IgG3 responses but can also lead to IgG4 or IgE responses. T-cell-independent responses with polysaccharide/carbohydrate antigens predominantly elicit IgG2 responses. Chronic antigen stimulation, such as in allergic desensitisation (e.g., bee stings), elicits IgG4 responses. In mature B-cells, CSR can occur again, but the type of IgG produced is limited by the remaining heavy chain C<sub>γ</sub> genes from the previous CSR cycle, and therefore, chronic antigen exposure may continue to drive CSR cycles until only C<sub>γ</sub>4 genes remain and IgG4 are developed (242, 243).

The ability of IgG subclasses to potentially activate several FcγRs on effector or mediator cells could have therapeutic and/or pathogenic implications for disease (242). However, independent of considering FcγRs, many interesting IgG subclass-specific observations during an immune response, in autoimmune conditions, and deficiencies have been reported (**Table 1:4**).

<b>IgG</b>	<b>Observations</b>
<b>IgG1</b>	<ol style="list-style-type: none"> <li>1. Soluble &amp; membrane-bound Ag usually invoke IgG1 responses</li> <li>2. Most abundant &amp; commonly produced IgG</li> <li>3. IgG1 &amp; IgG4 pre-/post-transplant associated with allograft failure (kidney).</li> <li>4. IgG1-restricted responses observed in autoimmune diseases (T1D/SLE).</li> <li>5. Deficiency mirrors overall IgG deficiency, is associated with IgG3 deficiency, &amp; results in a shift to IgG3/IgG4 responses.</li> </ol>
<b>IgG2</b>	<ol style="list-style-type: none"> <li>1. Deficiency linked to increased susceptibility to bacterial infections</li> <li>2. Deficiency linked to other IgG subclass deficiencies (IgG4 &amp;/or IgA) &amp; usually results in a shift toward IgG1/IgG3 responses.</li> <li>3. IgG2 &amp; IgG4 deficiency common together</li> <li>4. Bacterial capsular polysaccharide Ag invokes IgG2-restricted responses.</li> </ol>
<b>IgG3</b>	<ol style="list-style-type: none"> <li>1. Potent pro-inflammatory antibody (explanation for shorter half-life) but an IgG3 allotype has a comparable half-life to IgG1 &amp; alters immunogenicity.</li> <li>2. More effective against HIV than IgG1.</li> <li>3. Highly present in bacterial/viral infections against protein Ag</li> <li>4. Most polymorphic IgG with 29 reported alleles</li> <li>5. With IgG1, IgG3 is primarily involved in viral infections &amp; is often the first appearing antibody.</li> <li>6. IgG3-dominant responses rare &amp; IgG3 deficiencies associated with other subclass deficiencies.</li> <li>7. IgG3-mediated immunotherapy may be advantageous in many diseases owing to its many unique properties.</li> </ol>
<b>IgG4</b>	<ol style="list-style-type: none"> <li>1. Usually present in chronic responses (continued Ag stimulation)</li> <li>2. Common in responses against allergens</li> <li>3. Production modulated by IL-10 &amp; restricted to Bregs, which directly implicates IgG4 in immune regulation.</li> <li>4. IgG4-dominated responses may occur towards therapeutic proteins &amp; IgG4 deficiencies are rare.</li> <li>5. Common in parasitic worm infections with high associated with asymptomatic infection.</li> <li>6. Elevated serum concentration &amp; tissue IgG4-positive plasma cells linked to a broad spectrum of diseases (IgG4-related disease) such as RA &amp; AP; 70-80% of AP &amp; 10% of pancreatic cancer cases had elevated IgG4.</li> <li>7. IgG4 is present in 5% of the general population; can be used as a diagnostic marker in combinations with other markers.</li> </ol>

*Table 1:4 – Observations of human IgG subclasses*

Information gleaned from (227, 234, 240, 243-253). SLE: systemic lupus erythematosus; HIV: human immunodeficiency virus; RA: rheumatoid arthritis; AP: acute pancreatitis.

#### **1.6.2.3.4 B-cells in T1D**

Unlike other autoimmune conditions such as rheumatoid arthritis (RA), evidence for the pathogenic role of B-cells, beyond generating islet autoantibodies, in human T1D is elusive. They could simply be markers of the loss of immune tolerance or, conversely, markers of immunomodulatory attempts. Both of these and the subsequent production of autoantibodies require activation from activated T-cells and, B-cells cannot activate naïve T-cells, which suggests B-cells cannot initiate autoimmunity but may contribute to the pathogenesis of T1D once initiated. Evidence for this has been found through the histological examination of T1D pancreases (254).

Analysis of the islet immune cell infiltrate ranked CD20+ B-cells as fourth overall but, they were predominantly found in the later stages of insulitis and were the most abundant cell type in inflamed islets, followed by CD8+ T-cells. This suggests that B-cells are recruited to the islets once  $\beta$ -cell destruction has begun, and B-cell numbers increase with the development of insulitis (164). However, in a follow-up study, individuals diagnosed <20years had CD20<sup>high</sup> and CD20<sup>low</sup> inflamed islets. Interestingly, CD20<sup>low</sup> islets were associated with a lower abundance of other infiltrating immune cells (255). In a larger cohort of pancreas donors, CD20<sup>high</sup> and CD20<sup>low</sup> profiles discriminated donors who were diagnosed <7years and >13years, respectively. Furthermore, the presence of insulin-containing islets (ICIs) was associated with an older age-at-onset suggesting that CD20<sup>low</sup>/older individuals have a less aggressive/rapid  $\beta$ -cell destruction as ~40% of adolescents had ICIs at diagnosis (42). Based on these profiles, two type 1 endotypes (T1DE) have been proposed with further evidence that CD20<sup>high</sup> islet profiles (<7years) had an aberrant expression of proinsulin which was cross-sectionally reflected through elevated serum proinsulin: C-peptide ratios in children <7years (43).

## Chapter 1 - General introduction

Despite mounting histological evidence, monoclonal anti-CD20 immunotherapy (Rituximab) that depletes most B-cells, only partially preserved  $\beta$ -cell function (serum C-peptide) and reduced insulin dose requirement over 1-year in a RCT of new-onset T1D by TrialNet (four infusions; <11 weeks T1D duration; aged 8-45 years) but these effects were not sustained at 2 years (256). This confirms that B-cells may play a role in human T1D but that T1D still occurs when B-cells are depleted and/or repeat dosing may be necessary for efficacy. Additionally, a B-/T-cell combination immunotherapy may enhance efficacy which has been successful in RA utilising Rituximab with T-cell suppressants, cyclosporin or methotrexate (257).

Despite a lack of consensus in the involvement of B-cells in human T1D, many findings have shown that B-cells are critical for the development of diabetes in NOD mice: B-cells act as APCs, initiate T-cells and insulinitis, and B-cell deficient mice were resistant to T1D, which was diminished when treated with NOD B-cells (258-260). Furthermore, anti-CD20, chronic anti-IgM antibody treatment, or anti-CD22 therapy were shown to either be protective or be effective at restoring normoglycaemia after onset (258, 261, 262). However, it was also shown that passive or maternal milk transfer of autoantibodies cannot cause disease and therefore, were shown not to be pathogenic (260, 263). Whereas, in humans, offspring of islet autoantibody positive T1D-affected mothers were protected from T1D (findings from BABYDIAB) (127). Many paradoxical findings between human and NOD T1D have been long debated, but overall, evidence points towards a role for B-cells in T1D, but further investigation is required (254, 264)

---

### 1.6.3 Islet autoantibodies

---

Initially, the identification of islet cell autoantibodies (ICA) by Bottazzo and Doniach (1974) was instrumental in characterising T1D as an autoimmune disease (265, 266). By the 1990s, autoantibodies directed against three major highly  $\beta$ -cell specific autoantigens, insulin (IAA) (267), glutamic acid decarboxylase 2 (GAD65A) (268), and islet antigen 2 (IA-2A) (269) had been identified. More recently, autoantibodies to zinc transporter 8 (ZnT8A) were discovered in 2007 and are now recognised as the fourth major autoantibody specificity (270). Research into additional autoantibody targets in  $\beta$ -cells is still ongoing. For example, in 2016, autoantibodies to the 36-kDa glycoprotein tetraspanin protein family member 7 (TSPAN7) was found in >30% of patients (266, 271).

One or more of the four major islet autoantibodies is present in at least 70% and up to >90% of new-onset T1D, but both frequency and combination of autoantibodies can vary by age (272-274). The prevalence of autoantibodies in descending order was GADA (75%), ZnT8A (58%), IA-2A (57%), and IAA (51%) in a large cohort of 655 new-onset T1D cases (<2 weeks duration) spanning a wide age range (0-39 years) using the 99<sup>th</sup> percentile of 761 healthy controls (275).

The autoimmune targeting of the proteins IA-2, ZnT8, and insulin are all directed at the insulin secretory granules (ISGs) within  $\beta$ -cells and their contents however, GAD65 is found in synaptic-like micro-vesicles (SLMC) within  $\beta$ -cells (**Figure 1:13**) (266). Although TSPAN7 is the most abundant TSPAN protein in islets and is found in the membrane of ISGs, TSPAN7 is ubiquitously expressed in islets, with expression in all islet cell types ( $\alpha$ ,  $\beta$ , and  $\delta$ ) (266, 276). The mechanism(s) by which these molecules become targets of islet autoimmunity is still not fully understood.

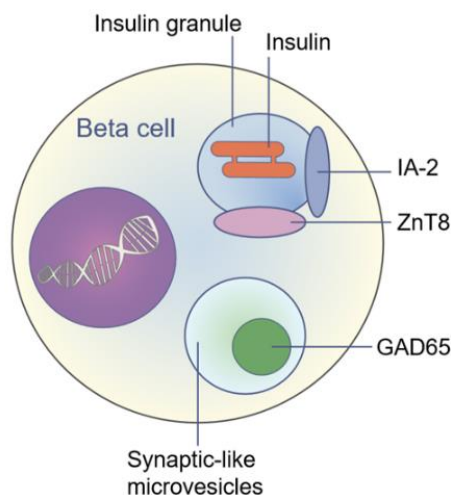


**Figure 1:13 – Schematic diagram of the pancreatic islet  $\beta$ -cell illustrating the locations of the four major antigens that autoantibodies recognise: GAD65, IA-2, ZnT8, & insulin**

Figure was taken from Williams and Long (2019) (277). Islet antigen 2 (IA-2), insulin, and zinc transporter 8 (ZnT8) are found within insulin secretory granules, but glutamic decarboxylase (GAD65) is found within synaptic-like micro-vesicles within the  $\beta$ -cell. The mechanism(s) by which these proteins become targets and are exposed to autoimmunity in T1D is not fully understood.

Much of what we understand about islet autoantibodies, the natural history of T1D, and T1D risk has been derived from prospective birth-cohorts of genetically at-risk children (defined by an FDR with T1D or HLA-genotype within the general population) that have primary aims in characterising the natural history of T1D, environmental determinants of T1D, and/or recruitment to clinical trials; DAISY (Diabetes Autoimmunity Study in the Young, USA)(278, 279), TEDDY (USA & Europe)(135), DIPP (Diabetes Prediction and Prevention; Finland)(280, 281), and BABYDIAB (Germany)(282).

Outside of birth-cohorts, other studies have longitudinally followed-up FDRs of subjects with T1D across a wide age range such as the Bart's-Oxford (BOX) family study (new-onset T1D <21 years and their FDRs, UK)(283), TrialNet (FDR aged 1-45 years or second-degree relative aged 1-20 years from 25 worldwide clinical centres across Europe, USA, Canada, Australia, and New Zealand)(284), and the Belgian Diabetes Registry (BDR)(new-onset T1D and their FDRs aged <40 years, Belgium)(285).

## Chapter 1 - General introduction

Collectively, these studies have contributed a plethora of information: patterns of autoantibodies (appearance, order, titre, combination, and number), age at autoantibody seroconversion, and genetic influence on autoantibody presence independent/in combination with T1D-susceptibility genes (286).

Humoral islet autoimmunity can develop in children as young as 6 months of age, with a peak incidence of seroconversion at 2-3 years and a probable second peak in puberty (287). The first autoantibodies at primary seroconversion in young children are typically IAA and/or GADA, and therefore, insulin and GAD65 are often regarded as primary targets of autoimmunity (288). In contrast, IA-2A and ZnT8A are rarely the only islet autoantibodies identified at primary seroconversion; data for ZnT8A are more limited (270, 289) but may develop in early life as ZnT8A have been found in children with either IAA or GADA by 3 years (287). IA-2A and ZnT8A often appear together in later childhood to adolescence in individuals positive for either GADA and/or IAA and are thought to be associated with a later stage in islet autoimmunity, appearing closer to T1D onset, and are regarded as secondary targets of autoimmunity. Therefore, IA-2A and ZnT8A can be used to identify individuals at the greatest risk of progressing to disease (275, 290-292).

Large prospective follow-up studies of high-risk FDRs from seroconversion to T1D onset encompassing young-onset and late-onset T1D found that age influences the autoantibody profile at onset (275, 287, 291). These studies also showed that the development of autoantibodies during the T1D prodrome occurs sequentially rather than simultaneously, indicative that the T1D humoral response spreads from one to multiple  $\beta$ -cell antigens but is heterogeneous (291, 293, 294). Nevertheless, the development of multiple autoantibody positivity ( $\geq 2$  autoantibodies; mAutoab+ve) confers the highest risk of T1D, up to 80% T1D risk within 10-15 years in childhood (287).

Further characterisation of prospective islet autoantibody responses has shown that the pattern of autoantibody appearances within those who develop multiple autoantibodies infers differential T1D risk (295). It is important to note that to date, most large prospective studies have followed high genetic risk infants from birth. Therefore, the T1D prodrome in adult-onset T1D and the general population (genetically diverse) is less defined but ongoing.

### **1.6.3.1 Predicting T1D risk & progression using the presence of islet autoantibodies**

---

Although islet autoantibodies are not considered pathogenic and are regarded as markers of islet autoimmunity, the predictive utility of islet autoantibodies for T1D has been known since ~1970s: in 15 ICA positive subjects, 2 developed diabetes per year over follow-up (265). Since the development of antigen-specific (biochemical) islet autoantibody tests (IAA, GADA, IA-2A, ZnT8A), the number of islet autoantibodies combined with clinical parameters of glucose tolerance has formed a suggested staging for presymptomatic T1D (96) (**Figure 1:14**). This staging system, based mainly on Eisenbarth's original T1D model, has aided the identification, monitoring, and recruitment of high-risk FDRs to clinical trials but has also greatly informed the natural history of T1D. Despite its robust value and defined stages, progression from stage 1 (mAutoab+ve with normal glucose tolerance) to 2 (mAutoab+ve with abnormal glucose tolerance) to 3 (clinical T1D diagnosis) remains highly heterogeneous (286, 296).

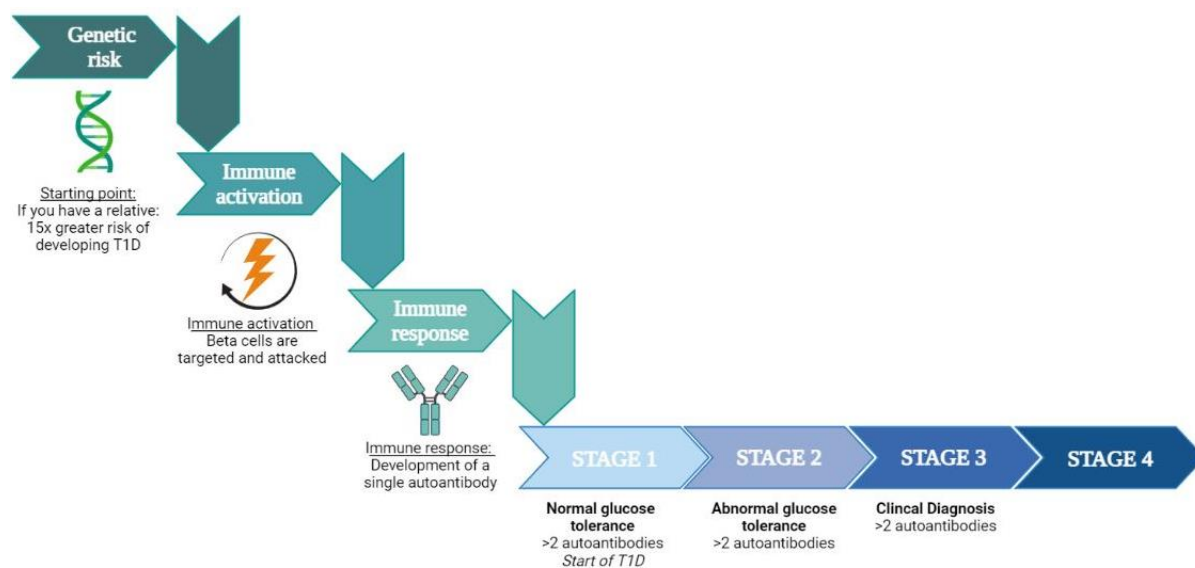


**Figure 1:14 – The predictive stages of T1D**

Image adapted from Bingley *et al.* (2018) (296) and created in BioRender.com. This staged system developed by TrialNet has been successfully employed to recruit individuals to clinical trials, with the most majority recruiting individuals at stage 3. Intervention and prevention clinical trials aim to identify and recruit individuals at stage 1 or stage 2 to induce immune tolerance, dampen the autoimmune response, and/or slow progression to clinical T1D.

In childhood, GADA and IAA are the most frequently detected islet autoantibody at seroconversion but are modified by age and genotype. IAA are associated with a younger age at seroconversion and the *HLA-DR4-DQ8* genotype. GADA are associated with an older age at seroconversion but are common over a wide age range, and the *HLA-DR3-DQ2* genotype (288, 297, 298). For example, in TEDDY children, IAA seroconversion appeared at a median age of 1.8 years versus 4.3 years for GADA. However, the first autoantibody (GADA or IAA) did not appear to be strongly associated with T1D risk or the risk of an additional autoantibody (mAutoab+ve) adjusting for age at seroconversion. Yet, IA-2A as the second autoantibody [hazards ratio (HR): 16.3 versus 5.4-6.4 for GADA/IAA/ZnT8A) and shorter time intervals between seroconversion and mAutoab+ve status, was associated with increased T1D risk (288).

Overall, T1D risk is highest in children that seroconvert aged <3 years (75% 10-year progression risk versus 61% >3years), with the high-risk genotype, *HLA-DR3/DR4-DQ8* (77%

versus 66% with other genotypes) and is correlated with increasing islet autoantibody number (287, 288, 297, 298). With each additional autoantibody, the risk of T1D increases six-fold (299) with the detection of mAutoab+ve in children implying 70-80% T1D risk within 10-15 years; symptomatic disease 15 years after seroconversion occurred in 13%, 62%, and 80% of children single, double, or triple autoantibody positive, respectively (287). Combining data from BABYDIAB, DAISY, and DIPP, comprising a total of 13,000 prospectively followed children, has shown that 80% of children who develop T1D aged <20 years, seroconverted before age 5 years (300). Whilst HLA genotypes influence T1D risk and autoantibody specificity at seroconversion, once mAutoab+ve, HLA-DR-DQ haplotypes do not appear to influence disease progression (301, 302). Despite this, utilisation of genetic tests has aided T1D risk stratification in prospective birth-cohorts and has identified relationships between T1D-associated genes with the initiation of islet autoantibody responses and tolerance mechanisms involved in T-/B-cell development (63, 303).

In prospective studies of FDRs encompassing a wide age range and follow-up period that largely preceded the birth-cohort studies, many findings have been consistent. For instance, BOX (12, 304), TrialNet (305, 306), and the BDR (307, 308) unanimously reported that T1D risk correlated with the number of islet autoantibodies and was highest in mAutoab+ve FDRs. For example, in the BDR, FDRs (aged <40 years), the 20-year T1D progression rate was 88% in mAutoab+ve FDRs compared with 54% in single autoantibody positive (sAutoab+ve) FDRs and was independent of age, total autoantibody number/specificities present, and HLA-DQ genotype. Additionally, this study corroborated an earlier report by BABYDIAB (287) by showing that the conversion from sAutoab+ve to mAutoab+ve was associated with a younger age at seroconversion, the presence of *HLA-DQ2/DQ8*, and persistent IAA positivity (291). Furthermore, independent of age (0-40 years), higher rates of progression in the presence of

## Chapter 1 - General introduction

IA-2A and/or ZnT8A were greater than in their absence, but GADA and IAA (with/without IA-2A) identifies early autoimmunity (309).

Collectively, the combined and present findings from prospective birth and FDR studies suggest that a similar autoimmune process occurs in the T1D prodrome in younger and older individuals (286). However, differences between islet autoantibody responses, age, and T1D risk have begun to emerge with greater follow-up and enhanced awareness of the prevalence of adult-onset T1D (at least 42% aged >30 years)(10, 11). For instance, TrialNet data indicates that the autoimmune response is more aggressive in children than adults. Compared to FDRs aged <20 years, FDRs >20 years had lower T1D risk once mAutoab+ve (stage 1/2) and at T1D onset (stage 3), had higher stimulated C-peptide, insulin resistance, and higher prevalence of sAutoab+ve responses (most commonly GADA) (305, 310, 311). This may be indicative of differential (but still heterogeneous) disease pathogenesis with slower progression and perhaps better clinical outcomes and/or diabetes management in adult-onset T1D.

Further evidence for slower T1D progression has come from the identification of “slow progressors” from numerous European and American studies. These individuals remain diabetes-free for at least 10 years following mAutoab+ve status and roughly comprise ~30% of autoantibody positive subjects in the studies. These individuals are typically diagnosed older (at least  $\geq 10$  years), but it is important to note that a fraction developed mAutoab+ve status in childhood, and therefore, slower progression may not be an exclusive characteristic of age at mAutoab+ve detection (312, 313).

The age group most often used for clinical trials is 10-39 years, although this may be changing as research and trials consider general population screening. However, the natural history of T1D remains best characterised in young children. Therefore, continued research is required to

understand risk in older ages. The BDR covers the age group mostly considered for clinical trials and has shown that testing for IA-2A  $\pm$  ZnT8A would still identify individuals at the greatest T1D risk independent of co-existing autoantibodies: IA-2A  $\pm$  ZnT8A identified 78% of rapid progressors (progressed to T1D <5 years) versus 62% without ZnT8A and 75% mAutoab+ve status considering IAA/GADA/IA-2A/ZnT8A (309). This suggests that screening for IA-2A and ZnT8A would be a cost-effective and sample saving strategy for identifying high-risk individuals for enrolment in clinical trials, but the sensitivity of this approach may be age-dependent as sensitivity was highest in older individuals (309). Despite this, the frequencies of all four main autoantibodies in the BDR new-onset T1D subjects aged 0-40 years shows that the frequency of GADA  $\pm$  IA-2A or IAA  $\pm$  ZnT8A is comparable, but interestingly, ZnT8A could replace IAA without loss of diagnostic sensitivity in individuals >10 years (275) (**Table 1:5**).

Antibody Status	Prevalence			
	New-onset cases			Controls
Age at onset (years)	0-9	10-19	20-39	0-39
	n=170 n (%)	n=223 n (%)	n=262 n (%)	n=761 n (%)
<b><math>\geq 1</math> autoantibody positive</b>				
<b>GADA, IA-2A, or IAA</b>	164 (96)*	207 (93)*	207 (79)*	24 (3)
<b>GADA, IA-2A, or ZnT8A</b>	162 (92) *	209 (94)*	206 (79)*	21 (3)
<b><math>\geq 2</math> autoantibodies positive</b>				
<b>GADA, IA-2A, and/or IAA</b>	138 (81)*¥	154 (69)*	129 (49)*	0 (0)
<b>GADA, IA-2A, and/or ZnT8A</b>	123 (72)*	162 (73)*	139 (53)	0 (0)

**Table 1:5 – Prevalence of autoantibody frequency & combinations in 655 new-onset T1D cases & 761 healthy control subjects according to age**

Table amended and data included from Vermeulen *et al.* (2011) (275). Data are expressed as n (%) unless otherwise depicted. \*  $p < 0.001$  versus control subjects. ¥  $p = 0.011$  versus combination with ZnT8A within the same age category. The data suggest that testing for ZnT8A could replace IAA without a loss of diagnostic sensitivity and that prevalence across age groups with these combinations are comparable.

### **1.6.3.2 Characteristics of islet autoantibodies that further aids T1D risk prediction**

---

Beyond detection of autoantibody positivity, many characteristics of islet autoantibody responses have increased and refined their predictive utility for T1D (**Figure 1:15**), which highlights the complexity of the antigen-specific humoral response. The humoral responses towards insulin, GAD65, and IA-2 have been better characterised than ZnT8 due to its more recent discovery (detailed later in **1.7**). Where ZnT8A has been reported, it has usually only been tested in samples with other autoantibodies prospectively collected from high-risk children. Therefore, the benefit of ZnT8A is inadequately defined (and a focus of this thesis) but is likely to be more informative in the future with studies expanding beyond childhood-onset T1D and into the general population (277).

	IAA	GADA	IA-2A	ZnT8A
Higher risk & rapid progression associated with autoantibody seroconversion <3yrs				
<b>Age &amp; order of appearance</b>	Commonly appears at seroconversion & is associated with higher risk in young children  No independent risk in mAutoab+ves	Commonly appears at seroconversion but is associated with risk in older individuals Seroconversion associated with slower progression to mAutoab+ve & T1D	Commonly appears closer to onset & is associated with higher risk across all ages & autoab profiles  Rare as the seroconversion ab	Commonly appears closer to onset & late childhood. Is associated with higher risk in sAutoab+ve but risk may be age-dependent.  Rare as the seroconversion ab
<b>Number</b>	Autoantibody persistence and increasing islet autoantibody number associated with risk regardless of antigen specificity, stage of disease, or high-risk genetic susceptibility.			
<b>Titre &amp; Persistent vs transient responses</b>	High titre associated with higher risk independent of age. Lower titres - higher risk of ab loss prior to onset  Persistent positivity associated with higher risk	High titre early after seroconversion (<1yr) associated with higher risk but titres may decrease up to onset.  Lower titres - higher risk of ab loss prior to onset	High titre - higher risk Loss of IA-2A prior to onset less common  Presence of IA-2A and/or ZnT8A +/- GADA or IAA is associated with higher risk independent of titre/age/genetics	No association found to date. Loss of ZnT8A prior to onset not known.
<b>Epitopes</b>	No high risk epitope identified	Middle and C-terminus of GAD65 -increased risk.  Removal of N-terminus improved assay specificity & sensitivity by 20%	IC domain of IA-2 & IA-2β	C-terminal ZnT8 domain  Major epitope determined by R325/W325 SNP stratifies risk
<b>Affinity</b>	High affinity associated with increased risk	High affinity associated with increased risk	No association found to date	High affinity associated with increased risk*
<b>IgG subclasses</b>	Presence of IgG2-IgG4 (unrestricted-IgG) responses -increased risk	IgG subclasses was not associated with risk	Presence of IgG2-IgG4 (unrestricted-IgG) responses - increased risk	Unknown

**Figure 1:15 – Summary of islet autoantibody characteristics that are associated with increased T1D risk**

Image adapted and expanded from So *et al.* (2021) (286) and created in BioRender.com. Islet autoantibody characteristics that have been associated with increased T1D risk and/or progression has predominantly been found in prospective studies of high-risk individuals (T1D-associated HLA Class II haplotypes in birth-childhood and/or FDRs). Findings depicted in the above figure has been derived from TEDDY (288, 295, 298, 301, 302, 314), BABYDIAB (282, 287, 289, 315-317), DAISY (318-320), TrialNet (284, 306, 318, 321-323), BOX (12, 90, 317, 324, 325), BDR (291, 292, 309), and the Barbara Davis Centre (BDC) and/or the Joslin Diabetes Centre (USA) (270, 292, 326-328), plus others (299, 329-332). \* Finding from a recent study by Jia *et al.* (2021) (333) using a ZnT8A ECL assay that has not been confirmed

### 1.6.3.2.1 Persistent versus transient autoantibody positivity

Further characterisation of autoantibody positivity profiles in genetically high-risk children has found that disease risk can be further stratified by different combinations of detectable autoantibodies, autoantibody titres, and patterns of autoantibody positivity profiles (persistent versus transient). For example, in mAutoab+ve children (high genetic risk) participating in

TEDDY, that seroconverted <2 years, had persistent positivity in at least one consecutive sample, and titres of IAA and IA-2A, but not GADA, had the highest T1D risk (295, 314). Conversely, in the BDR, the loss of IAA but not GADA, IA-2A, or ZnT8A in mAutoab+ve FDRs (aged 0-40 years) appeared to delay progression to disease (291).

#### **1.6.3.2.2 Antigenic epitopes recognised by islet autoantibodies**

Antibodies bind to 3D peptide domains of an antigen (“epitopes”). For GADA and IA-2A, specific epitopes of GAD65 and IA-2 have been shown to aid in predicting T1D risk (further detailed below) (286). However, a convincing high-risk epitope of insulin has not been found as IAA have been shown to recognise epitopes within insulin’s A- and B-chains and insulin’s precursor, proinsulin (316, 319, 334, 335). Epitopes of ZnT8 recognised by ZnT8A are predominantly located in the C-terminal domain and are further described in **2.4**.

#### **GADA/GAD**

L-glutamic acid decarboxylase (GAD) is the major enzyme involved in the biosynthesis of the critical inhibitory neurotransmitter, gamma-aminobutyric acid. GAD has two isoforms (GAD65/GAD67), but GAD65 is the major isoform and is comprised of NH<sub>2</sub>-terminal, middle, and COOH-catalytic domains (266). Full-length GAD65 [amino acid (aa)1-585] is generally used to detect GADA in T1D. However, epitope analysis showed that most of GADA recognise the middle- and COOH-catalytic domains and bind to the NH<sub>2</sub>-terminal poorly (286, 330, 336). Truncation of the NH<sub>2</sub>-terminal (aa1-96) in the conventional radioimmunoassay (RIA, described later **1.6.3.3**) led to improved assay specificity and discrimination of high-risk FDRs with a subsequent finding that GAD65(aa1-142) does not contribute to GADA recognition (324, 325). Intermolecular epitope spreading to the N-terminal closer to T1D may occur however after clinical onset, epitope specificity appears to stabilise up to 5 years (329, 330, 337).

IA-2A/IA-2

IA-2 is a member of the receptor-type protein tyrosine phosphatase (PTP) family, comprised of an extracytoplasmic (EC) domain, a transmembrane region, and an intracytoplasmic (IC) domain. The IC domain can be subdivided into juxtamembrane (JM) and PTP domains, but overall, the IC domain is the major region of IA-2 recognised by IA-2A in new-onset T1D however, IA-2A can also bind the PTP-region of the homologue IA-2 $\beta$  (266, 286, 326, 338). Reactivity to specific IA-2 epitopes have not been consistently associated with T1D risk, but the reactivity of IA-2A towards multiple IA-2 antigens aided the identification of high-risk individuals (286, 317, 339-341). Therefore, IA-2IC is primarily used to screen for IA-2A and IA- $\beta$ A is often only tested in IA-2A positive individuals to further stratify risk.

The function of IA-2 is only partially known; once  $\beta$ -cells are stimulated to secrete insulin, IA-2's EC domain is cleaved to promote mobilisation of ISGs to the plasma membrane and, in addition, translocates to the  $\beta$ -cell nucleus to regulate genes associated with ISG function and insulin secretion ( $\beta$ -cell function) (266, 342).

**1.6.3.2.3 Islet autoantibody affinity for antigen**

Antibody affinity refers to the strength of the antibody-antigen (epitope) interaction in the antigen-binding site. The mechanisms of affinity maturation were described previously (1.6.2.3.1) but to assess antibody affinity, competitive displacement immunoassays with structurally sound recombinant protein is the common method used (236, 286). High-affinity autoantibodies could reflect more advanced preclinical stages of autoimmunity.

High-affinity IAA has been consistently associated with multiple markers of high-risk such as progression to mAutoab+ve status, clinical T1D onset, the *HLA-DR4* haplotype, and a younger age at IAA seroconversion (316, 331, 343). Similarly, high-affinity GADA has also been

shown to be associated with mAutoab+ve progression, clinical T1D onset, the *HLA-DR3* haplotype, and was highest in the middle-/COOH-catalytic domains of GAD65 but was not associated with age at seroconversion in FDR and general population children (286, 344, 345). However, IA-2A affinity for IA-2/IA-2 $\beta$  has not been shown to be associated with progression or T1D risk in children prospectively followed since birth (346), but low-affinity IA-2A was rare. As previously outlined, ZnT8A affinity remains under-investigated and is further described in **2.2**.

#### **1.6.3.2.4 IgG subclasses of islet autoantibodies**

IgG subclasses in T1D are described in detail in **2.3**, but the seminal paper by Achenbach *et al.* (2004) found that the presence of IgG subclasses additional to IgG1 and autoantibody titre in IA-2A and IAA responses (but not GADA) was associated with increased disease risk (IA-2A HR: 3.3; IAA HR: 4.6) above just considering total IgG level. Additionally, there was a positive association of the number of IgG subclasses present and the level of IgG1 binding with autoantibody titres (determined by conventional PAS/PGS RIA), suggesting high titres aids in discriminating risk (317). To our knowledge, the ZnT8A IgG subclass response in T1D has not been reported and therefore, was a focus of this project.

### 1.6.3.2.5 Genetic associations of islet autoantibody positivity

Genetic associations of islet autoantibody responses at various stages of disease are summarised in **Table 1:6**.

Autoantibody	Preclinical association (seroconversion or progression)	T1D onset	After T1D onset*	Comments where applicable
<b>IAA</b>	- <i>HLA-DR4</i> (+) - <i>HLA-B*39</i> in <i>HLA-B*39</i> FDRs who developed GADA/IAA rapidly progressed	- <i>HLA-DR4</i> (+)	Cannot be investigated following exogenous insulin treatment.	- In BABYDIAB children aged >2years with the <i>HLA-DR4</i> genotype, GADA was more prevalent than IAA.
<b>GADA</b>	- <i>HLA-DR3</i> (+) - <i>HLA-B*39</i> in <i>HLA-B*39</i> FDRs who developed GADA and IAA rapidly progressed	- <i>HLA-DR3</i> (+)	- <i>HLA-DQA1</i> (-) - <i>HLA-DRB1</i> (+) - <i>HLA-DRA1</i> (+) - <i>DR3</i> (+) - <i>LPP/3q28</i> (+) - <i>IFIH1</i>	- ~30% of GADA+ve children in the TEDDY study did not have <i>HLA-DR3</i> genotype. - <i>LPP/3q28</i> was only associated with GADA positivity >3 years disease duration.
<b>IA-2A</b>	- <i>HLA-A*24</i> (-) - <i>HLA-A*24</i> in <i>HLA-DQ8</i> FDRs who developed IA-2A or ZnT8A rapidly progressed - <i>FCRL3</i> (-)	- <i>HLA-A*24</i> (-) - <i>HLA-DR4</i> (+)	- <i>HLA-DQA1</i> (+) - <i>HLA-A</i> (-) - <i>DR3</i> (-) - <i>DR4</i> (+) - <i>RELA/11q13</i> (+) - <i>FIBP</i> (+) - <i>FCRL3/1q23</i> (-) - <i>IL-27</i> - <i>PTPN22</i> (-)	- <i>HLA-DR4</i> only associated with IA-2A positivity at onset excluding IA-2A titre due to an interaction between <i>HLA-DR4</i> and IA-2A titre.
<b>ZnT8A (ZnT8R/ZnT8W)</b>	- <i>HLA-A*24</i> (-) - <i>HLA-A*24</i> in <i>HLA-DQ8</i> FDRs who developed IA-2A or ZnT8A rapidly progressed - <i>FCRL3</i> (-)	- <i>HLA-A*24</i> (-)	- <i>HLA-DQA1</i> (+) - <i>DR4</i> (+) - <i>FCRL3</i> (-) - <i>CTSH</i> (+)	- Genetic associations of ZnT8A may largely differ from GADA & IA-2A due to the more rapid loss of ZnT8A after T1D onset.

*Table 1:6 – Summary of genetic associations with islet autoantibody positivity at different T1D stages*

Sources include BOX, BABYDIAB, TEDDY, DIPP, and the BDR (90, 287-289, 291, 295, 297, 301, 347-350). Plus (+) and minus (-) denotes positive and negative associations with the allele associated with diabetes risk or major allele, respectively. \* Findings from 7,077 T1D cases from 4,135 families from the type 1 diabetes genetic consortium (T1DGC) with a median age at diagnosis of 9 years (range 0-52) and autoantibodies detected at a median of 7 years disease duration (range 0-63) but 25% was taken <3 years.

### **1.6.3.3 Measuring islet autoantibodies**

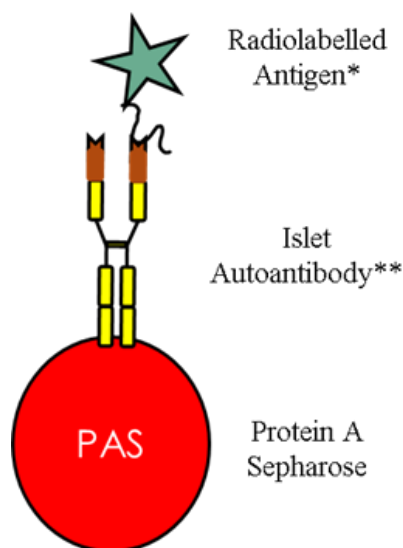
---

Before islet antigen-specific (biochemical) autoantibody assays in the 1990s, the gold-standard method for detecting islet autoimmunity and predicting disease risk were ICA assays. ICA staining can be observed in human pancreatic sections by indirect immunofluorescence (265, 351). Positivity is determined through sample titration and comparison to established Juvenile Diabetes Foundation (JDF) standards of known fluorescence intensity, expressed as JDF units. The international use of JDF standards improved ICA standardisation and protocol harmonisation between laboratories, but immunofluorescence assessment remains subjective (352-355).

The use of antigen-specific fluid-phase RIAs superseded ICA staining and remains the conventional method for measuring IAA, GADA, IA-2A, and ZnT8A (266, 356, 357). These assays involve incubation of serum with the appropriate radionuclide-labelled antigen fragments and subsequent immunoprecipitation of the radiolabelled-antibody complex by Protein G and/or Protein A Sepharose (PGS and/or PAS, respectively). Radiolabelled-antibody immunocomplexes are detected through scintillation detectors where residual radioactivity is expressed as counts per minute (CPM) and are proportional to autoantibody concentration (**Figure 1:16**).

Optimisation of RIAs has substantially improved the detection of islet autoantibodies in small quantities of serum. For example, IAA testing now only uses ~50µl per test (with confirmation of positive results) in comparison to 200-600µl before 1997 (356). Further characterisation of epitopes recognised by autoantibodies has increased RIA sensitivity and specificity with better disease prediction, particularly for IA-2A and GADA (266). The use of radioisotopes in autoantibody testing, however, has limited long-term sustainability. Radioisotopes are costly, have short shelf lives (radioactive decay), and are subject to tight regulations regarding storage

and disposal for safety and environmental reasons. Consequently, there is limited application of these assays in laboratory and clinical settings. To reach the goal of general population screening for at-risk individuals in the future, low-volume, rapid, and non-radioactive assays are required.



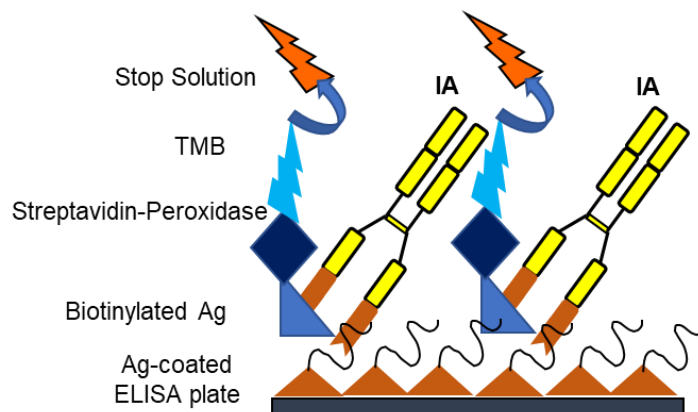
*Figure 1:16 – Schematic diagram of the RIA*

Image adapted from Williams and Long (2019) (277). \* GAD65 (aa1-585), IA-2IC (aa606-979), ZnT8 (aa268-369; monomeric peptides with either arginine (R) or tryptophan (W) encoded at the SNP site rs13266634) or Insulin. \*\* Islet autoantibodies specific to the recombinant antigen. Autoantibodies in serum specific to GAD65/IA-2/ZnT8 bind to [<sup>35</sup>S] or for insulin [<sup>125</sup>I] radiolabelled antigen. Immunocomplexes are then precipitated using Protein A Sepharose (PAS) to bind the Fc region of the autoantibody. The unbound excess radiolabelled antigen is excluded by serial wash and centrifugation steps. After the addition of MicroScint40 (PerkinElmer), residual radiation in counts per minute (CPM) is detected on a beta scintillation counter where CPM is proportional to the autoantibody level present in serum.

Other established methods for detecting antigen-specific autoantibodies that do not rely on radiolabelled-antigen tracers are solid-phase bridge enzyme-linked immunosorbent assays (ELISAs) (358, 359) and electrochemiluminescence (ECL) assays (266, 319, 360).

Routinely used and 1-day duration bridge-type ELISAs are commercially available through RSR Limited (Cardiff, UK; [www.rsrltd.com](http://www.rsrltd.com)) for GADA, IA-2A, and ZnT8A detection. In short, serum is incubated onto a microplate coated with recombinant antigen (solid-phase) and resultant immunocomplexes are detected through a biotin-streptavidin-peroxidase system which creates a colourogenic reaction that is detectable by an ELISA plate reader (358, 361,

362) (**Figure 1:17**). In contrast, the 2-day ECL assay utilises bivalent autoantibodies in serum to cross-link between an antigen with a Sulfo-TAG (Meso Scale Discovery [MSD], Rockville, MD, USA) and a biotinylated antigen to create immunocomplexes which are detected by an electrochemiluminescence signal on an MSD Sector Imager 2400 (363) (**Figure 1:18**). In both assays, the signal detected is proportional to autoantibody concentration.



**Figure 1:17 – Schematic diagram of the bridge-type ELISA**

Image adapted from Williams and Long (2019) (277). Ag: Antigen; ELISA: Enzyme-linked immunosorbent assay; IA: Islet autoantibody; TMB: 3,3', 5,5'-tetramethylbenzidine. Serum (25µl/well) is incubated onto a recombinant antigen-coated microplate. Anything unbound or in excess in serum is excluded through multiple washes and centrifugation steps. Next, the biotinylated antigen is incubated to allow streptavidin-peroxidase to bind. After multiple washes and centrifugation steps, TMB is added, which reacts with streptavidin-sepharose to create a colourimetric reaction that is terminated utilising the stop solution after 15 minutes. The residual signal can then be detected by an ELISA plate reader and is compared to a blank well containing TMB and stop solution only.

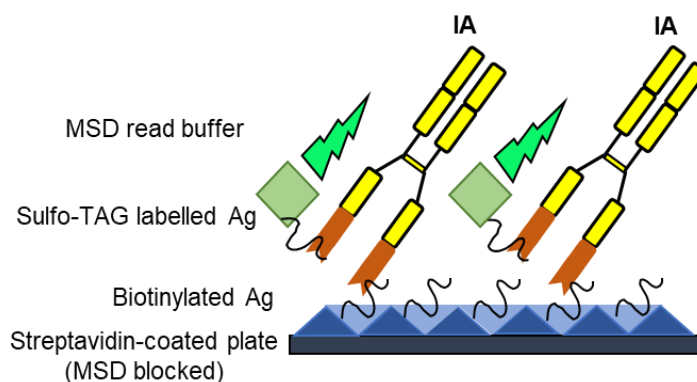


**Figure 1:18 – Schematic diagram of the ECL assay**

Image adapted from Williams and Long (2019) (277). Ag: Antigen; IA: Islet autoantibody; MSD: Meso Scale Discovery, Rockville, MD, USA. Bivalent IA in serum binds the Sulfo-Tag (MSD)-tagged antigen and the biotinylated antigen in solution (fluid-phase), which is mixed and incubated. Following incubation, the whole mixture is added to a blocked (with MSD blocker A buffer) streptavidin-coated plate. Following a series of wash and centrifugation steps to exclude unbound or excess antigen, MSD read buffer is added to give off an electrochemiluminescence signal detectable by an MSD Sector Imager 2400 where the signal is proportionate to IA in serum.

Although ELISAs and ECL assays are non-radioactive and have shown high performance (319, 358, 360-363), both have limitations that may hamper their use for general population screening. For example, ELISAs need a solid-phase that requires manufacturing recombinant protein, can obscure antigenic epitopes required for autoantibody binding, and uses up to ~50µl/per test. Low sample volume requirements are particularly important for testing capillary bleeds from young infants. Although ECL has more modest sample volume requirements (15µl/per test), serum requires acid treatment, streptavidin-coated plates must be prepared in advance, and per test, two separate antigens need preparation. However, recent protocol adaptations have resulted in multiplex-ELISA and -ECL assays to simultaneously detect 3-7 autoantibodies which show promising potential which may counteract their respective limitations (364, 365).

Collectively, there is a need for rapid, low-volume, non-radioactive, high performance, and simpler assay alternatives to replace RIAs and overcome the limitations of ELISA/ECL assays. The detection of multiple autoantibodies in a single test with the possibility of automation would be hugely advantageous for facilitating general population screening in the future.

#### **1.6.3.3.1 Methods in development for islet autoantibody detection**

More recently, luciferase immune precipitations system (LIPS) assays have sought to provide an inexpensive, low volume non-radioactive alternative to RIAs. The LIPS assay format is comprised of the same reagent constituents and steps as the fluid-phase RIAs but substitutes the antigen with a radioactive tracer for a NanoLuc<sup>TM</sup> luciferase reporter (Nluc) (**Figure 1:19**) (366).

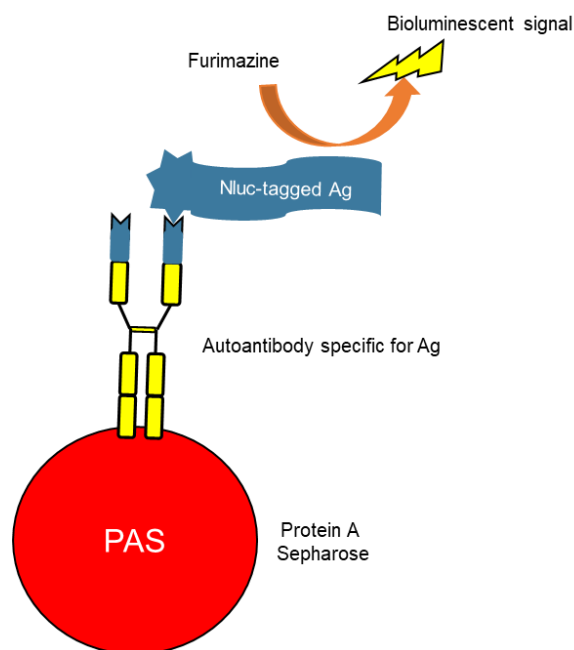


*Figure 1:19 – Schematic diagram of the LIPS assay*

Image adapted from Williams and Long (2019) (277). Autoantibodies in serum specific for islet antigen (Ag; GAD, IA-2, ZnT8R, ZnT8W, or insulin) bind to a Nanoluciferase-tagged (Nluc-) islet antigen. Immunocomplexes are then precipitated using Protein A Sepharose (PAS) to bind the Fc region of the autoantibody. Serial washes and centrifugation steps exclude unbound excess Nluc-tagged islet antigen. After adding the substrate Furimazine (Promega), a bioluminescent signal is produced and detected with a luminometer where the luminescence produced is proportional to the autoantibody level present in serum.

The major advantages of LIPS assays are the reduction in required serum volume (2 $\mu$ l versus 5-30 $\mu$ l by RIA), the long shelf-life of the Nluc-antigens (months versus weeks with radioisotopes), one-day duration (versus 2-3 days by RIA), and the use of widely available commercial reagents/equipment that many laboratories will have for conducting RIAs (366). One important consideration is that the placement of the Nluc- reporter in the antigen sequence may influence antigen conformation and subsequent autoantibody-antigen binding. A LIPS assay to detect IAA has been developed that correlated and matched the sensitivity and specificity of the IAA RIA in the Islet Autoantibody Standardisation Program (IASP) in 2015 and 2016 (described later **1.6.3.4**). However, large cohorts of at-risk individuals are required to fully elucidate the predictive utility of LIPS over RIA (366).

Another promising candidate for a low-volume non-radioactive immunoassay is antibody detection by agglutination-PCR (ADAP). In brief, antigen-specific antibodies in serum (2µl) are agglutinated by antigen-specific DNA conjugates, which enables DNA ligation and resultant quantification by qPCR. When compared to an FDA-approved RIA for detecting anti-thyroglobulin autoantibodies, ADAP offered a 1000-fold increased sensitivity. This assay offers several advantages over more conventional fluid-phase immunoassays: it's a simple method that only employs low volumes of standard PCR consumables, has enhanced sensitivity, and has a broad dynamic range (367). Over the last two IASP workshops, this ADAP method for GADA, IA-2A, IAA, and ZnT8A has been amongst the top-performing assays (data from IASP2018 (368); IASP2020 unpublished). However, the predictive utility is yet to be evaluated in at-risk populations, and few data have been published.

It is worth noting that both the LIPS and ADAP methodologies have scope to be multiplexed for the detection of multiple markers in a single test which alongside, multiplex-ECLs, make strong candidates for general population screening in T1D (368, 369).

### **1.6.3.4 Islet autoantibody standardisation program (IASP)**

---

International workshops to standardise autoantibody detection across laboratories began in 1985 with ICA assays that subsequently led to a standardised protocol with international standards that enhanced sensitivity (352, 370). Following the success of several workshops and the development of antigen-specific (biochemical) autoantibody RIAs in the 1990s, a collaboration between the Immunology of Diabetes (IDS) and the US Centers for Disease Control and Prevention (CDC) established the Diabetes Autoantibody Standardisation Program (DASP) in 2000 (351, 371, 372). The objective of DASP was to assess laboratory proficiency to harmonise assays worldwide and provide materials, technical support, and training for improving assay performance.

The first DASP proficiency programme was conducted in 2003 (372) with GADA, IA-2A, and IAA immunoassays, which has since improved laboratory concordance and protocol harmonisation (371-373). After the identification of ZnT8A in 2007, ZnT8A immunoassays were entered into DASP in 2011, but no formal assay harmonisation for ZnT8A to date has been conducted (374).

In 2013, DASP became the Islet Autoantibody Standardisation Programme (IASP) supported by the IDS and the National Institute for Health (NIH). IASP typically runs biennially and supplies uniquely coded samples from T1D cases and controls to participating laboratories for autoantibody detection. The results are centrally collected and analysed by the IASP committee to prevent bias prior to unblinding the data for researchers to conduct in-house analysis (375). These workshops also enable the performance of novel and new methodologies to be assessed.

---

## **1.7 Zinc transporter 8 (ZnT8) & T1D**

---

---

### **1.7.1 The function of ZnT8**

---

Zinc transporter 8 (ZnT8), part of the 10-member ZnT family, is encoded by the gene *SLC30A8*. ZnT8 is expressed moderately in kidney cells and pancreatic  $\alpha$ -cells, but unlike other ZnTs, ZnT8 is almost exclusively expressed in pancreatic  $\beta$ -cells, where zinc concentration is among the highest in the body; 70% of  $\beta$ -cell zinc content is contained in ISGs at ~10-20mM (376-380). It is not clear why ZnT8 is specifically expressed in pancreatic  $\beta$ -cells. However, it is thought that ZnT8 is highly specialised and is required to protect  $\beta$ -cells from oxidative stress, prevent zinc imbalance, and regulate insulin biosynthesis (381). Therefore, functional ZnT8 is essential for  $\beta$ -cell function and survival.

In  $\beta$ -cells, transport of  $Zn^{2+}$  ions from the  $\beta$ -cell cytoplasm into ISGs is crucial for the biosynthesis, storage, and secretion of insulin. In the endoplasmic reticulum and Golgi apparatus, two  $Zn^{2+}$  ions and one  $Ca^{2+}$  ion are complexed by histidine 30 in insulin's B-chain that ultimately ensures the hexameric structural stability of one proinsulin molecule. In ISGs, proinsulin is then converted to insulin facilitated by enzymes, and the insoluble hexameric crystallisation of insulin to form dense cores occurs, which requires up to 11  $Zn^{2+}$  ions supplied by ZnT8. Packaged within mature ISG vesicles, glucose-stimulated insulin secretion (GSIS) is required for the exocytosis of insulin from  $\beta$ -cells (376, 381-383). Unsurprisingly, ZnT8 and insulin are highly co-localised in  $\beta$ -cells (377, 378).

---

### 1.7.2 The *SLC30A8* gene

---

The *SLC30A8* gene located on chromosome 8 (8q24.11) contains 13 exons spanning ~226kb and encodes two ZnT8 protein isoforms (splice variants); full-length (aa1-369) and N-terminally truncated ZnT8 (aa50-369). Most studies focus on the full-length isoform, but direct evidence of differential function and cellular expression of these two isoforms has not been fully investigated (376, 379): one study showed no functional differences between the isoforms when expressed in *Pichia pastoris* yeast and incorporated into an *in vivo* transport assay (384).

A common SNP rs13266634 (C/T) in *SLC30A8*, causes a non-synonymous modification that changes the C-terminal amino acid 325 (aa325) to either arginine (R) or tryptophan (W) (385). This SNP is common in the general population with a minor allele (T encoding W) frequency of 0.31 in Europeans and has been linked to both main classifications of diabetes (386). The allele encoding R (homozygous CC genotype) at aa325 (R325) confers a minor risk of T2D (OR 1.07-1.18) linked to increased transporter activity with 12 loss-of-function mutations shown to offer a 65% reduction in T2D risk (387-393). However, in animal models, the

influence of ZnT8 on  $\beta$ -cell function and glucose homeostasis is less clear. Utilising the INS-1E rat cell line as a  $\beta$ -cell model, ZnT8 overexpression increased, but knock-down decreased,  $\beta$ -cell zinc accumulation, insulin content, and GSIS (378, 394). Whereas global ZnT8 knockout mice have shown inconsistent findings, but this could be due to differences in study parameters and/or the moderate ZnT8 expression in other tissues (395-397) as ZnT8  $\beta$ -cell specific knockout mice were glucose intolerant, had abnormal  $\beta$ -cell morphology with reduced zinc accumulation, and had both fewer and less dense ISGs from reduced insulin processing (398).

In T1D, the main effect of the rs1326634 SNP is on ZnT8A specificity (328). Individuals with the CC genotype (R325) rarely develop ZnT8 tryptophan-specific autoantibodies (ZnT8WA), and individuals with the TT genotype (W325) rarely develop ZnT8 arginine-specific autoantibodies (ZnT8RA) (328). Competitive displacement experiments with recombinant ZnT8 protein have shown that ZnT8A are truly specific for R325 or W325 (399).

Although *SLC30A8* does not influence T1D risk, the *SLC30A8* genotype or ZnT8A specificity may aid stratification of T1D risk in ZnT8A positive children (289, 328, 400); carriers of the CC genotype had an earlier age-at-onset (<5years) (401), but CC/TT had higher T1D risk than CT genotypes (289). Most of these studies have been conducted in Euro Caucasian populations, but the *SLC30A8* risk C allele is more common in African and Asian populations than Europeans (402), and therefore, risk stratification may be greater in these populations (94). Additionally, *SLC30A8* genotypes may also inform islet cell transplantation outcomes; the T allele (CT/TT genotypes) in combination with high body mass index (BMI) and *HLA-A\*24* positivity was associated with poor graft function but was independently associated with the failure to achieve insulin dependence and maintenance of C-peptide (403).

A second SNP in this region, rs16889462 (G/A), can encode glutamine (Q325) at this position but is only present in <1% of Europeans and while more common is still rare in other non-Caucasian ethnicities; up to 9% of African-Americans and 1-2% of Asian populations (385, 404). However, the reactivity of ZnT8A towards the naturally-occurring ZnT8-Q325 can be used to investigate ZnT8A responses not dependent on R325/W325 variants (non-specific) (405). All *SLC30A8* SNPs are summarised in **Table 1:7**.

	Major allele	Minor allele	Minor allele
Genomic codon	CGG	TGG	CAG
Relevant SNP	Common allele	rs13266634 MAF: 0.3	rs16889462 MAF <0.01 in Europeans
Encoded 325th amino acid	R Arginine	W Tryptophan	Q Glutamine

*Table 1:7 – The codons for the major allele & SNPs in SLC30A8*

Table taken from Williams and Long (2019) (277).MAF, minor allele frequency. These SNPs determine the protein sequence at amino acid 325 in the C-terminal of ZnT8. The major allele (encoding R325) is associated with increased risk of T2D; however, in T1D, this SNP influences autoantibody specificity to ZnT8 and can aid risk stratification of disease progression.

---

### 1.7.3 The structure of ZnT8

---

ZnT8 is a 369-aa (41-Dka) polytopic transmembrane protein with 6 transmembrane domains (TMD), a luminal facing histidine-rich loop, 8 exon regions, and cytoplasmic N-(NH<sub>2</sub>) and C-(COOH) terminal tails (**Figure 1:20**) (406, 407). *In vivo*, functional ZnT8 forms a dimeric structure from two 369aa monomers that facilitates Zn<sup>2+</sup> transport through proton [H<sup>+</sup>] antiport exchange and has signature Zn<sup>2+</sup> binding sites in the highly conserved TMD2/ 5; findings based on ZnT8 sequence alignment between mammalian and non-mammalian species (376, 408, 409).

The region determining R325/W325/Q325 through two SNPs is contained on a variable loop between two conserved secondary structures,  $\alpha$ -helix and  $\beta$ -sheet (410). Like other zinc transporters, the large C-terminal of ZnT8 is thought to be involved in the primary dimerization and stability of the transporter and therefore, is important for ZnT8's tertiary structure and cytosolic accessibility of ZnT8A (408).

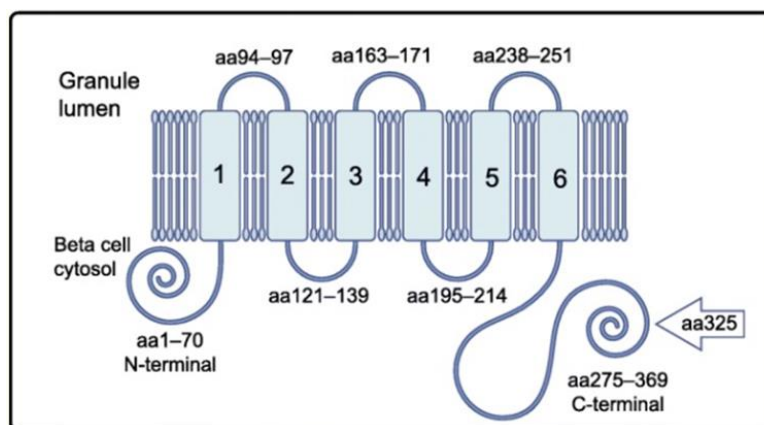


*Figure 1:20 – The structure of monomeric ZnT8*

This figure was taken from Williams and Long (2019) (277), which was adapted from Wenzlau *et al.* (2007) (270). ZnT8 is embedded within insulin secretory granule membranes and is a transmembrane protein. The C- and N-terminals are cytosolic, but the transmembrane domains (numbered 1–6) include three luminal regions, which are expressed extracellularly during insulin granule exocytosis. Functional ZnT8 is formed from two aa369 monomers where the C-terminal is thought to be essential for the primary dimerisation for ZnT8's tertiary structure.

The structure of ZnT8 can influence the epitopes of ZnT8A. Due to difficulties in purifying human ZnT8 protein, the structure of human ZnT8 has been primarily based on the 3D structure of the distantly related prokaryotic (*E. Coli*) cation diffusion facilitator (CDF) YiiP protein that shares only ~14-17% identical sequence homology with human ZnT8 with an overall homology of ~39.5% (411-414). Similar to human ZnT8, YiiP has 6 TMDs and C-terminal domains (CTD), but the mechanism of  $Zn^{2+}$  trafficking has been fully elucidated: binding of  $Zn^{2+}$  ions at the interface of the CTDs links the parallel-orientated monomers and induces an allosteric mechanism that causes two TMDs to swing out in a Y-shaped structure to trigger  $Zn^{2+}/H^{+}$  antiport. Given the several structural differences between human ZnT8 and YiiP, and the fact that bacterial CDF proteins only exports zinc when in excess whereas, eukaryotic ZnT8

## Chapter 1 - General introduction

appears to export zinc passively, it was not known if human ZnT8 utilises a similar allosteric mechanism to YiiP (410, 412-415).

Recently, the structure of human ZnT8 through cryogenic electron microscopy (cryo-EM) was evaluated (411). Researchers determined that each ZnT8 monomer housed four  $Zn^{2+}$  binding sites; the primary site in the highly conserved TMD2/5, the interfacial site between TMD2/3 (involving His-aa137) and the CTD (His-aa345) that modulates  $Zn^{2+}$  transport, and two “buried” sites in the cytosolic domain. Here,  $Zn^{2+}$  is chelated by conserved cysteine residues from the CTD [ $C_{361}XXC_{364}$  motif; specific for vesicular ZnTs (2/3/4/8) and highly conserved in mammals] and the His-Cys-His (aa52-54) motif of the N-terminal segment of the neighbouring monomer. The TMD of each monomer was also shown to have an allosteric mechanism undergoing large structural change to allow for alternating access to the primary  $Zn^{2+}$  site during the transport cycle that appears simply governed by the pH and  $Zn^{2+}$  concentrations on either side of the membrane (410, 411). The interchangeable availability and structural orientation of ZnT8 domains may be important for ZnT8A production and, the binding of ZnT8A to the CTD could have implications for ZnT8 function, insulin biosynthesis, and/or  $\beta$ -cell function.

As mentioned previously, R325W appears to influence the transport activity of ZnT8, and prior to cryo-EM of human ZnT8, a study that purified R325 and W325 variants also showed that the CTD  $C_{361}XXC_{364}$  motif had high affinity for  $Zn^{2+}$  but also found biophysical differences between variants. Compared with the heavily charged R325, W325 was less thermostable but had a higher dimerisation affinity (410). Presumably, the strength of ZnT8 dimerisation and the biophysical properties between the variants may influence the accessibility or downstream consequence of ZnT8A production and/or binding.

Collectively, there is evidence implicating the CTD in the structure and function of ZnT8 and that the two variants may have different biophysical properties that could influence ZnT8 function. However, there is currently no evidence to suggest ZnT8A directly impairs ZnT8 function or are pathogenic to  $\beta$ -cells.

---

#### 1.7.4 Discovery & prevalence of autoantibodies to ZnT8 (ZnT8A) at T1D diagnosis

---

Wenzlau *et al.* in 2007 identified ZnT8 and the *SLC30A8* gene using microarray mRNA expression profiling on human pancreas sections and islets for T1D autoantigen candidates. Of all candidate genes, ZnT8 (*SLC30A8*) ranked fourth for pancreatic and islet specificity. Subsequently, this research group developed an RIA to detect ZnT8A and found that ZnT8A were present in 60-80% of new-onset T1D patients dependent upon age-at-onset and <2% of healthy controls. Additionally, ZnT8A was found in up to 30% of individuals with other autoimmune disorders associated with T1D. The measurement of ZnT8A in new-onset T1D subjects increased sAutoab+ves by 26% (of those negative for GADA, IA-2A, and IAA) and mAutoab+ves by 10% (270). This led to the characterisation of ZnT8 as the fourth major autoantigen targeted in islet autoimmunity that is additive and independent of other islet autoantibodies.

Overall, several international studies have shown that around two-thirds of children are ZnT8A positive at diagnosis (274, 328); depending on the age group considered, the prevalence is comparable to IA-2A. The importance of ZnT8A as a biomarker in adult disease has not been fully assessed. A BDR study suggested that only half of those diagnosed >20 years are ZnT8A positive (275). This frequency is less than for GADA (65%) but comparable with IA-2A (45%) (416, 417). The contribution of ZnT8A in Latent Autoimmune Diabetes in Adults (LADA) is difficult to determine because the classification of LADA varies but typically are: insulin-

independent for at least 6 months after diagnosis, diagnosed aged >30 years, and have a T2D phenotype but are positive for at least one autoantibody, predominantly GADA (418, 419). Overall, ZnT8A prevalence in LADA subjects with confirmed GADA positivity ranged from 5-35%, comparable to IA-2A (327, 362, 420-423). However, ZnT8A and IA-2A are rarely found in adult diabetes with a T2D phenotype (1-2%) compared to GADA (5-10%), but the combined testing for all three autoantibodies is associated with clinical features (HbA1c/BMI), age-at-onset, and risk of multiple autoimmunity (292) which is useful, as ~25% of T1D subjects have co-existing non-islet autoimmunity (424). Additionally, there is evidence that ZnT8A screening reduces the cost of discriminating monogenic diabetes (51).

ZnT8A has also contributed to the observation that the natural history of humoral autoimmunity may be changing. In BOX (UK), between 1985 and 2002, the prevalence of IA-2A and ZnT8A at onset increased while GADA and IAA remained stable over time (274). This could indicate a shift towards a more aggressive form of disease, as IA-2A and ZnT8A tend to develop later in the pathogenesis. During the same period, the incidence of diabetes in young children has increased, and the proportion of probands with high genetic risk has reduced, suggesting an increase in environmental risk (7, 103). Lower genetic risk alleles, such as DQ6.4, may have become more common in people with T1D and contributed to increased ZnT8A. A Danish study covering a shorter time span (1997-2005) found no difference in IA-2A or GADA prevalence at diagnosis, but ZnT8A were not measured (425).

---

## 1.7.5 The initiation & development of the ZnT8A autoimmune response

---

Less than half of ZnT8 in functional/intact  $\beta$ -cells is accessible to immune surveillance. The whole protein or fragmented peptides are most likely to be accessible to the immune system upon  $\beta$ -cell death, although following granule exocytosis, during insulin secretion, the luminal transmembrane domains are exposed extracellularly (426).

### 1.7.5.1 Initiation of ZnT8 autoimmunity

---

At diagnosis, IAA, IA-2A, and GADA are associated with specific HLA Class II alleles contained within T1D risk genotypes (349, 427). In contrast, ZnT8A have not shown consistent HLA class II associations (347), except DQ6.4 in individuals with T1D (428). They are, however, associated with high diabetes risk (i.e., DR3/DR4) in FDRs. T-cell epitope scanning identified more putative ZnT8 epitopes for HLA-DQ2 than for -DQ8 or -DQ6.4 (94). An intermediate binding epitope for HLA-DQ2 was predicted to bind W325 but not R325, suggesting that this may contribute to differences in central tolerance for ZnT8. However, regardless of DQ type, people with diabetes had a higher frequency of proinflammatory ZnT8-specific CD4<sup>+</sup> T-cells than age- and HLA-matched non-diabetic individuals (186).

The predisposing *HLA-A\*24* allele was negatively associated with the presence of ZnT8A at and before diagnosis when age-at-onset was accounted for (90, 350). Studies of ZnT8 epitopes for CD8<sup>+</sup> T-cells have focused on the better characterised *HLA-A\*2*. There is some evidence that CD8<sup>+</sup> T-cells recognise a range of ZnT8 peptides across the transmembrane/loop and C-terminal regions in individuals with diabetes (429-431). This could suggest previous epitope spreading but may also reflect the technical challenge of detecting and characterising antigen-specific T-cell responses *ex vivo*. The number and phenotype of ZnT8-specific T-cells identified in people with and without diabetes appear to be similar, but functional differences

have been identified, such as greater ZnT8-stimulated IFN- $\gamma$  secretion by isolated CD8<sup>+</sup> T-cells from people with diabetes (432). Additionally, in T1D pancreases, compared with T2D or no diabetes pancreases, more ZnT8-specific (aa186-194) CD8<sup>+</sup> T-cells were present, suggesting that ZnT8-specific lymphocytes home to the pancreas preferentially. However, the ZnT8-specific CD8<sup>+</sup> T-cells had a more mature phenotype in children versus adults independent of disease status. As ZnT8 showed poor thymic expression, this study concluded that T-cell autoreactivity to ZnT8 was more likely to be caused by defective peripheral tolerance and/or a proinflammatory islet microenvironment (442).

### **1.7.5.2 ZnT8 as an autoantigen**

---

Although ZnT8A can be detected close to initiation of autoimmunity, alongside IA-2A, ZnT8A typically arise later in prediabetes and are more common in adolescents at diagnosis. Similarly, ZnT8 is also a target of autoreactive T-cells. In mice, transfer of ZnT8 C-terminal-specific CD4<sup>+</sup> T-cells only caused diabetes if insulinitis was present. Additionally, ZnT8-specific CD4<sup>+</sup> T-cells were only found in the pancreas, and lymph nodes of mice in advanced disease (433), supporting the observation that antigen spreading to ZnT8 is characteristic of the developing autoimmune response.

The limited accessibility of ZnT8 to immune surveillance in intact and/or functional  $\beta$ -cells suggests that the cytosolically accessible C-terminal plays a pivotal role in autoimmune responses to ZnT8. It has been shown that most mature ZnT8A responses recognise the C-terminal of ZnT8 with ~50% recognition in new-onset T1D cases studied in the original study versus only ~10% recognising the N-terminal (270). The rs13266634 SNP influencing ZnT8A specificity and subsequent competitive displacement experiments confirming R325/W325 ZnT8A specificity indicates that individuals respond to endogenous ZnT8 protein determined by their own genome. This has not been as easy to demonstrate for the other islet antigens

because they lack an amino acid polymorphism with such an obvious influence on the autoantibody response. In several populations, ZnT8A appear to cross-react with a viral protein from *Mycobacterium avium subsp. Paratuberculosis* (e.g. (434)) and ~50% of ZnT8A positive individuals have ZnT8A that recognise epitopes independent of aa325 (328). Therefore, molecular mimicry could contribute to the initial response to ZnT8, but more work is needed to evaluate this.

For other islet autoantibodies, epitope spreading has been demonstrated to occur during progression, and the identification of epitopes indicative of later stages of disease has improved the specificity of these markers and has informed autoantibody-antigen interactions (315, 324, 325, 341). However, ZnT8A responses prior to diagnosis are less well investigated, with reports primarily focused on new-onset T1D (270, 328, 404). In addition to the two SNPs located in C-terminal ZnT8 that form two critical epitopes (R325/W325) for ZnT8A recognition (328), a conformational ZnT8A epitope (dependent on residues R332, E333, K336, and K340 combined but independent of R325) (404) was characterised by comparison of human and mouse chimeric ZnT8 proteins. The importance of conformational epitopes to ZnT8A responses is also supported by the observation that linear 15aa ZnT8 peptides were insufficient to displace ZnT8A (400). The targeting of ZnT8 by autoreactive T-cells also appears to rely on conformational epitopes, with T-cells from carriers of *DR3-DQ2* and *DR4-DQ8* with T1D shown to target pools of overlapping 20-mer ZnT8 peptides spanning full-length ZnT8 (94, 186). If epitopes of ZnT8A associated with a higher risk of diabetes could be identified, these would aid prediction, but the pattern of epitope-specific responses before diagnosis in limited reports has not so far proved useful for risk stratification.

---

## 1.7.6 Predicting diabetes using ZnT8A

---

In Wenzlau's original 2007 report, the analysis of 43 individuals at high genetic risk followed prospectively showed that ZnT8A could stratify risk in those positive for IAA, GADA, or IA-2A alone (270). Subsequently, BABYDIAB (infants of T1D-affected parents) also showed that ZnT8A aids prediction of disease (found in 81% of children who progressed and was as frequent as IA-2A by the age of 3 at 4%) in the presence or absence of other islet autoantibodies but was more common in children with at least one other autoantibody (289). The much larger TrialNet dataset confirmed these findings in autoantibody positive FDRs and concluded that screening for ZnT8A should be included in prediction and prevention studies (318).

Several studies have shown that combined testing for IA-2A and ZnT8A identifies relatives who progress rapidly to disease and is a cost-effective screening strategy (275, 292, 309). For instance, in autoantibody positive (GADA, IA-2A, or IAA) FDRs from the BDR (aged <40 years), ZnT8A positivity +/- IA-2A had the highest 5-year progression rate at 45%, and ZnT8A/IA-2A were the strongest predictors of diabetes identifying 77% of rapid progressors (292). However, TEDDY reported that in sAutoab+ve high-HLA risk children (either GADA or IAA), the T1D risk was higher if IA-2A was the second appearing autoantibody (HR: 16.3) compared with ZnT8A (HR: 5.4), which was comparable with IAA or GADA (HR: 6.44) (288). However, the TEDDY study also reported that ZnT8A appeared at a median of 4-5 years which is later than BABYDIAB at 3-4 years (most likely due to the recruited of infants from the general population as opposed to FDRs) and conferred a five-fold increased risk of T1D progression compared to sAutoab+ves independent of specificity or genetics (288). Therefore, ZnT8A positivity could aid the enrolment of participants to secondary prevention trials in FDRs but is likely associated with age-at-onset and/or the genetic disposition of the population studied.

## Chapter 1 - General introduction

Further evidence for an age-dependent association for the predictive utility of ZnT8A in T1D includes a report from DAISY, which found that the benefit of considering ZnT8A in sAutoab+ves was only found when age-at-onset was >6 years (270). Additionally, in preselected FDRs participating in the European Nicotinamide Intervention Trial (ENDIT) who were positive for other islet autoantibodies, ZnT8A only added to risk prediction in relatives who were older or who were genetically lower risk (332). However, screening for ZnT8A is likely to benefit both young-onset and adult-onset T1D. For example, in 655 new-onset T1D spanning a wide age range (0-39 years), ZnT8A enabled 100% diagnostic specificity with 14% found single ZnT8A positive across childhood-onset and adult-onset (275).

Within identified mAutoab+ve “slow progressors” (progression >10 years), ZnT8A are frequently detected (312). This conflicts with studies that have shown ZnT8A develop late in preclinical diabetes (closer to onset) and are markers of high-risk. However, it should be noted that these “slow progressors” generally have a higher age-at-onset and have not been genetically preselected compared to the “rapid progressors” studied in predominantly genetically predisposed children. In fact, most studies of risk stratification for T1D have been conducted in relatives or individuals with high HLA class II risk (*DR3/DR4*; not associated with ZnT8A) with ZnT8A responses mostly characterised in children (274, 292, 328). The added predictive value of ZnT8A in the general population has not been fully assessed but is ongoing (e.g., in the German Fr1da study (435)). Despite contradictions, current evidence and recent reports suggest that screening for ZnT8A will provide additional information about risk, especially in adult-onset T1D or in older individuals in whom early autoimmune responses to insulin are waning.

Furthermore, many studies that have confirmed the predictive utility of ZnT8A have been conducted predominantly in Euro-Caucasian populations, but studies of non-Caucasian populations (new-onset and after onset T1D) also report a high prevalence of ZnT8A with the inclusion of ZnT8A benefitting the characterisation of islet autoimmunity (436-439) The measurement ZnT8A therefore, is merited in multiple populations to elucidate whether the predictive utility of ZnT8A differs across populations with different genetic pools and can aid the identification of T1D subpopulations (440).

---

### 1.7.7 ZnT8A as a biomarker of insulin secretory capacity after T1D onset

---

Another suggestion from the initial 2007 paper was that ZnT8A might be correlated with loss of insulin secretion because of ZnT8's high  $\beta$ -cell specificity and co-localisation with insulin (270). Following an initially successful pancreas transplant, ZnT8A have been associated with rapid onset of hyperglycaemia and eventual loss of graft function, making them a potentially important biomarker for predicting  $\beta$ -cell loss (441). Ongoing  $\beta$ -cell death is likely to drive levels of ZnT8A (270, 442), although low-level expression in non-functional  $\beta$ -cells or neighbouring alpha cells may also contribute.

After diagnosis, ZnT8A are lost more rapidly than GADA or IA-2A (443), while T-cell responses, particularly to the TMD, are lost within a few years post-diagnosis (430). This is important because if ZnT8A, which are easier to measure than T cells, reflect insulin secretory capacity and autoreactivity, they may be useful biomarkers for assessing/monitoring the efficacy of clinical trials.

A study showed that in a group of 15-34-year-olds with diabetes (71% type 1), high C-peptide at diagnosis correlated with prospective preservation of ZnT8A 5 years after diagnosis (444). Additionally, Nielsen *et al.* (2011) found that in children <16 years recruited from 15 centres across Europe and Japan, the *SLC30A8* genotypes CC and CT had higher stimulated C-peptide <1 year after diagnosis compared with TT, but this was primarily due to individuals with the TT genotype having lower stimulated C-peptide at the first visit (1-month) after diagnosis. Nielsen *et al.* also showed concordant loss of stimulated C-peptide and levels of ZnT8RA and ZnT8WA (445). However, another study in individuals with a younger age-at-onset showed that high positivity for ZnT8A at diagnosis was associated with lower C-peptide levels and increased insulin dose requirement 2 years after diagnosis, despite similar levels at disease onset (446). In a minority of individuals where ZnT8A persists for decades after diagnosis, cross-sectional studies have also failed to reach a consensus about the relationship between ZnT8A and C-peptide (447-449). The contrasting findings could be explained if age-at-onset influences this association. The hypothesis that ZnT8A could be used as a biomarker for therapeutic effect is attractive but is not strongly supported by current literature, but longitudinal analysis may be more conducive (36, 450).

---

### 1.7.8 What benefits could new assays for ZnT8A detection offer for prediction?

---

Internationally, RIAs for GADA and IA-2A have been harmonised but work to standardise the measurement of ZnT8A and IAA is ongoing (451). Most assays for ZnT8 investigate C-terminal epitopes recognised by ZnT8A (270, 328, 404). Since 2011, international ZnT8A RIA detection in IASP workshops have shown between ~50-70% sensitivity and  $\geq 98\%$  specificity dependent on the ZnT8 antigenic variant utilised (unpublished data). The main RIA development has been to create dimer ZnT8 antigen constructs of C-terminal ZnT8 (amino acid sequence 268-369) connected by a linking sequence to allow for the simultaneous measurement

of ZnT8A to the most common R325 and W325 ZnT8 variants in one test (438). In one Finnish study, the addition of a Q325 probe further increased RIA sensitivity (~2%) by reducing the number of antibody-negative children and adolescents (452). Alternative assays, such as the LIPS and ELISAs, have begun matching or even exceeding the specificity and sensitivity of RIAs for GADA, IA-2A, IAA, and ZnT8A, where reported and directly compared (362, 366, 373, 453).

The commercially available bridge-type ELISA from RSR Limited for ZnT8A(362), as well as GADA(358) and IA-2A detection (361), have shown comparable or enhanced sensitivity to RIAs. For ZnT8A, the ELISA utilises a C-terminal ZnT8 R325/W325 dimeric protein as the solid-phase, which is a well-validated recombinant protein that has consistently performed high in IASP workshops ( $\sim \geq 70\%$  sensitivity). Therefore, C-terminal epitopes are unlikely to preclude C-terminal reactive ZnT8A from binding. Although RSR's ELISAs can routinely be conducted in 1-day, recent adaptations to ZnT8A's protocol have reduced assay duration to ~4 hours without loss of sensitivity (362). Of note, however, is the reduced sensitivity observed in plasma versus serum samples stated on RSR's protocol (available via the website), but data was not available in the published report (362). In contrast, the detection of GADA and IA-2A in both calcium-treated plasma and serum by RSR ELISAs was comparable when studied (359) suggesting a ZnT8A-specific effect. RSR have also developed a GADA/IA-2A composite ELISA (361) and, more recently, a triple-plex (GADA/IA-2A/ZnT8A) ELISA that both show high sensitivity/specificity and highly correlate with RIA. The triple-plex ELISA is currently being utilised in the large-scale German Fr1da childhood screening study (364, 454).

Recently, a multiplex-ECL assay (incorporating GADA/IA-2A/ZnT8A and other non-islet autoantibodies) has been developed and have shown promising sensitivity and specificity with a high correlation with RIA. The single-ZnT8A ECL assay also shows that this method detects

high-affinity ZnT8A, which benefits the identification of high-risk individuals (333), and further adaptations the assay and antigen configuration has shown that ZnT8A directed to extracellular regions of ZnT8 (excZnT8) may precede IAA/GADA seroconversion, indicative of earlier ZnT8 humoral responses (455). Therefore, there is evidence that discrimination of ZnT8A and epitopes outside of the C-terminal may enhance assay performance and, importantly, aid in discriminating high-risk individuals.

There are, however, assays that have sought to establish the conformational structure of ZnT8 for non-linear ZnT8A epitopes. Wan *et al.* (2017) developed a novel assay using full-length ZnT8 (R325) in combination with proteoliposomes to detect ZnT8A on a plasmonic gold chip (pGOLD™; Nirmidas Biotech, CA, USA) (442). This assay has the potential to detect ZnT8A that recognise epitopes outside the C-terminal, but the need to use the pGOLD™ platform restricts the routine application of this assay due to costs. Future assay adaptations to investigate other epitopes, including post-translational protein modification, and that is validated on at-risk individuals, may improve disease prediction and should continue to be investigated.

---

## 1.8 The Bart's-Oxford (BOX) family study

---

The well-characterised population-based BOX family study, established in 1985, has recruited and prospectively followed individuals under 21 years with newly diagnosed T1D (probands; >95%) and their FDRs within the former Oxford Regional Health Authority in the UK (12, 424). Of those diagnosed with new-onset T1D, 86% provided serum samples close to diagnosis, and at present, around ~76% of the families are still in regular contact with the study (424). Currently, the study is comprised of ~3000 probands and ~6000 FDRs (6% sAutoab+ves and 2% mAutoab+ves) that were diabetes-free at study entry. The FDRs are annually followed

## Chapter 1 - General introduction

up for the development of diabetes by questionnaire. The BOX study is currently approved by the South Central – Oxford C. Research Ethics Committee. Participants provided informed, written consent and the study was performed according to the principles of the Declaration of Helsinki.

A total of 859 newly diagnosed (<3 months) probands were tested for all autoantibodies, but only 618 (71.9%) had genetic samples available because the collection of genetic samples started over a decade after samples for islet autoantibody testing (456). Of FDRs, the first available sample was tested for all autoantibodies (including ICA prior to 1996, GADA/IA-2A only after 1996 and after 2015, ZnT8A), and 5-year follow-up samples were screened for autoantibody positivity with ZnT8A tested in those positive for at least one other autoantibody; additional ZnT8A missing data were filled in as part of this PhD project (approximately 2500 results). Of 6000 FDRs, genetic samples were available from approximately 4000 (66.7%), and the HLA and non-HLA data were used where available.

The BOX study includes serum samples taken years before diagnosis, around the time of diagnosis, and many years after diagnosis. Therefore, these samples have been used to characterise ZnT8A responses which should yield information about disease progression/prediction, new-onset T1D, and the humoral response after T1D onset, respectively.

---

## 1.9 Project rationale

---

---

### 1.9.1 Hypothesis

---

Characterisation of the altered pattern of immune responses to ZnT8 and identification of antigen epitopes of ZnT8A during disease progression and after the clinical onset of type 1 diabetes will inform future therapies to delay disease.

---

### 1.9.2 Aims

---

1. To characterise the humoral autoimmune response to ZnT8 compared with GADA and IA-2A using samples taken before and close to diagnosis to better predict the risk of disease progression and understand longitudinal islet autoimmunity. Three characteristics of ZnT8A responses are established and explored in **Chapter 2** [affinity (**2.2**), IgG subclasses (**2.3**), and epitopes (**2.4**)] and are brought together to investigate responses in a subset of individuals (**2.5**).
2. To identify non-genetic and genetic factors associated with the loss of humoral autoantibody responses after the clinical onset of T1D (**Chapter 3**).
3. To optimise & validate a non-radioactive Luciferase Immunoprecipitation System (LIPS) method to detect ZnT8RA/ZnT8WA simultaneously (**Chapter 4**).

# **Chapter 2 - Characterisation of the ZnT8 humoral response up to T1D onset**

---

## **2.1 Introduction**

---

Detailed characteristics of islet autoantibody responses (affinity, IgG subclasses, and/or epitopes) have enhanced the predictive utility of other islet autoantibody responses (described previously **1.6.3.2**). It is clear that there are few studies on the characteristics of the ZnT8A humoral response outside of the three main epitope regions. It is hypothesised that characteristics of ZnT8A would be especially informative in at-risk individuals for T1D risk prediction. Therefore, this chapter of the project sought to optimise and/or further develop methods to investigate affinity, IgG subclasses, and epitopes of ZnT8A utilising RIA and begin to explore characteristics in subsets of at-risk relatives or new-onset T1D subjects. Finally, these characteristics were measured in a small number of ZnT8A positive individuals, repeatedly sampled before diagnosis.

### 2.1.1 Hypothesis

---

Characterisation of the humoral response to ZnT8 and identification of antigen epitopes of ZnT8A during disease progression and around the clinical onset of T1D will inform risk prediction and future therapies to delay disease.

---

### 2.1.2 Aims

---

1. To characterise the humoral autoimmune response to ZnT8 compared with GADA and IA-2A where possible using samples taken pre-, and around-diagnosis to better predict risk of disease progression.

- a. How strong is the antigen-antibody binding (affinity) and specificity of ZnT8A [ZnT8RA/ZnT8WA/ZnT8QA (non-specific)]?
  
- b. What type of IgG subclasses in ZnT8A responses compared with GADA and IA-2A are produced in progressors or new-onset T1D? Do the profiles discriminate slow from rapid progressors of disease?
  
- c. Which regions of C-terminal ZnT8 are important for ZnT8A binding in new-onset T1D?
  
- d. At ZnT8A seroconversion and follow-up, is there evidence of changes in specificity, titre, affinity, IgG subclasses, or epitopes recognised?

---

## 2.2 Characterisation of ZnT8A affinity

---

---

### 2.2.1 Introduction of ZnT8A affinity for ZnT8

---

Antibody affinity refers to the strength of the antibody-antigen (epitope) interaction. To assess the affinity of an antibody for its antigen, structurally sound recombinant protein reflective of *in vivo* conformation is crucial for maintaining epitope integrity. Studies of ZnT8A affinity for ZnT8 have been extremely limited, on small cohorts, have not encompassed all ZnT8A specificities, and are often precluded by the difficulty of producing soluble recombinant ZnT8 protein at high yields, which has led to many molecular expression/purification methods, with one requiring detergent solubilisation with strict drying/rehydration conditions (400, 442). Drawing robust conclusions and comparing between studies that have generated ZnT8 protein is difficult due to studies not investigating ZnT8A affinity, often do not report detailed structural protein analysis such as mass spectrometry, and up to very recently, modelling of human ZnT8 was based or predicted on the bacterial YiiP protein, and crucial differences have been highlighted (described previously **1.7.3**) (384, 410-415).

The seminal study by Skarstrand *et al.* (2015) expressed and purified a maltose-binding protein (MBP)-tagged ZnT8R and ZnT8W recombinant proteins (aa275-369; 0.001-100µg/ml), confirmed by mass spectrometry, and tested 12 ZnT8RA- and 12 ZnT8WA-specific new-onset T1D (diagnosed <15 years with high titre and reactivity to ZnT8Q excluded) by competitive displacement in monomeric ZnT8R/ZnT8W RIAs of [<sup>35</sup>S]-ZnT8 (aa268-369) antigen. Sera were diluted ~50% ZnT8A binding of the standard curve, equating to a median of ~500U/ml (range 360-653 U/ml). In ZnT8RA-specific and ZnT8WA-specific subjects, 10µg/ml protein was sufficient to displace radiolabelled ZnT8, but ZnT8WA affinity for ZnT8W appeared twice as high compared with ZnT8RA for ZnT8R. However, the maximum protein concentration (100µg/ml) caused almost complete inhibition of diluted ZnT8RA and ZnT8WA binding

## Chapter 2 - Characterisation of the ZnT8 humoral response up to T1D onset

(range 95-99%) independent of age-at-onset and HLA. Interestingly, ZnT8RA-specific subjects showed competitive displacement with ZnT8W recombinant protein [mean  $\pm$  standard error of the mean (SEM) (%):  $37 \pm 7$ ], but comparatively, ZnT8WA-specific subjects showed less binding inhibition with ZnT8R recombinant protein [mean  $\pm$  SEM (%):  $14 \pm 4$ ]. This suggests that ZnT8RA-specific responses may have less specificity due to a level of cross-reactivity that appeared absent for ZnT8WA-specific responses. Importantly, the possibility of autoantibodies cross-reacting to MBP in the sera was excluded (399).

In this PhD project, we first sought to optimise a ZnT8A affinity protein concentration curve by competitive displacement RIA, then utilising internal RIA quality controls (QCs) and anonymised new-onset T1D patient sera, we determined an arbitrary cut-off of high-moderate and low affinity determined by 50% ZnT8A reduced binding from radiolabelled ZnT8 antigen. We then used this method to evaluate the frequency of high-moderate and low affinity ZnT8A in new-onset T1D (n=27, sampled <3 months). Unlike other studies, we sought to investigate ZnT8A affinity by ZnT8A specificity (R325/W325/Q325), radiolabelled ZnT8 wild-type (WT) antigen used (ZnT8R/ZnT8W/ZnT8Q), and ZnT8A titre (from low to high), using a high-quality protein used in the well-performing commercial ELISA kit by RSR (362).

## 2.2.2 Materials & Methods

### 2.2.2.1 Populations for ZnT8A affinity studies

#### 2.2.2.1.1 ZnT8A affinity RIA optimisation sample set

The sample set utilised for the optimisation of the concentration curve for RIA affinity studies was tested using monomeric ZnT8RA RIA using 6 internal ZnT8 RIA QCs and/or 8 samples from fully anonymised T1D patients (**Table 2:1**). Age at sampling was available from 5 anonymised patients [median 26.1 years (range 21.0-28.3)]. No further information was available. Selected samples were of high volume and covered a range of ZnT8A specificity and titre.

Sample type (n)	ZnT8A categorisation of sample/s (n)	ZnT8RA Median AU (range)	ZnT8WA Median AU (range)	GADA Median DKunits/ml (range)	IA-2A Median DKunits/ml (range)
		n positive : 8	n positive : 5	n positive : 7	n positive : 6
<b>Anonymised T1D patients (8)</b>	ZnT8RA specific (3) ZnT8A non-specific (5)	56.3 (6.4-115.5)	21.2 (0.3-87.8)	275.1 (0.2-911.1)	223.4 (0.0-410.8)
<b>Internal RIA QCs (6)</b>	ZnT8RA/ZnT8WA- specific High (2)	130.0 (74.2-262.1)	90.8 (48.1-132.6)		
	ZnT8RA/ZnT8WA non-specific Medium (1)	33.9 (20.1-47.0)	23.2 (12.2-39.2)	-	-
	ZnT8RA/ZnT8WA- specific Low (2)	6.8 (3.5-10.6)	2.8 (1.9-4.6)		
	ZnT8RA/ZnT8WA Negative (1)	0.6 (0.3-1.6)	0.5 (0.2-1.6)		

*Table 2:1 – ZnT8A affinity optimisation sample set*

Optimisation of ZnT8A affinity curves was conducted on internal RIA QCs and/or ZnT8RA positive anonymised patients in the monomeric ZnT8RA RIA. High, moderate, and low refers to the ZnT8A titre of the internal QCs.

#### **2.2.2.1.2 New-onset T1D patient sample set**

High volume (>1ml) ZnT8RA/ZnT8WA positive new-onset (<3 months) T1D patients from BOX that encompassed different ZnT8A specificities and titres were selected for affinity studies [n=27; 15 males (55.6%); median age at diagnosis 8.8 years (range 3.0-17.8)] (**Table 2:2**). First, samples were tested and categorised according to ZnT8A specificity determined by the major epitope (aa325). Second, samples were tested for ZnT8A affinity towards radiolabelled WT ZnT8 antigens (R325/W325/Q325) where possible. Following affinity assessment, samples were categorised into high-moderate and low ZnT8A affinity based on the 50% competitive displacement of ZnT8A from radiolabelled ZnT8 antigen.

<b>Variable</b>	<b>Number (%)</b>
<b>Gender</b> (n=27)	
Male	15 (55.6)
Female	12 (44.4)
<b>Age at onset</b> (n=27)	
0-5 years	5 (18.5)
5-10 years	9 (33.3)
10-15 years	10 (37.0)
15-20 years	3 (11.1)
<b>Autoantibody</b> (n=27)	
IAA (n=23)	19 (82.6)
GADA (n=27)	23 (85.2)
IA-2A (n=27)	23 (85.2)
ZnT8A (n=27)	27 (100.0)
ZnT8RA	21 (77.8)*
ZnT8WA	20 (74.1)**
ZnT8QA	17 (63.0)***
<b>HLA Class II</b> (n=26)	
High (DR3-DQ2/DR4-DQ8)	11 (42.3)
Moderate (DQ2/DQ2, DQ8/DQ8, DQ2/X, DQ8/X)	11 (42.3)
Low (X/X, DQ6/X)	4 (15.4)
<b>HLA Class I</b>	
<i>HLA-A*24</i> Negative (n=24)	21 (87.5)
<i>HLA-B*18</i> Negative (n=24)	19 (79.2)
<i>HLA-B*39</i> Negative (n=24)	23 (95.8)
<b>Non-HLA SNPs</b>	
<i>SLC30A8</i> (n=25)	
CC	13 (52.0)
CT	7 (28.0)
<u>TT</u>	5 (20.0)

*Table 2:2 – ZnT8A affinity new-onset T1D sample set*

All data from genetic variables were available. Underlined genotype denotes the minor allele. ZnT8A affinity testing was prioritised for ZnT8RA and ZnT8WA over ZnT8QA. \*All ZnT8RA positive patients were tested for affinity to ZnT8R antigen. \*\* 19/20 (95.0%) ZnT8WA positive patients were tested for affinity to ZnT8W antigen. \*\*\* 14/17 (82.4%) ZnT8RA/ZnT8WA positive patients were tested for affinity to ZnT8Q antigen after the determination of reactivity towards ZnT8Q antigen.

### **2.2.2.2 Recombinant ZnT8 protein for affinity studies**

---

Experimental efforts to clone, express, and purify a ZnT8-GST fusion protein in-house for the purpose of ZnT8A affinity studies are presented in **Appendix A**. The strategy utilised was adapted for ZnT8 based on a previous body of work by Dr K. Elvers that successfully cloned IA-2 into a pET49b(+) vector then expressed and purified a IA-2-GST fusion protein in *E. Coli* Rosetta™(DE3)pLysS cells using a 5ml GSTrap™ FF column (Sigma) and fast protein liquid chromatography (FPLC); described in (457).

Cloning of ZnT8 into a pET49b(+) vector, transformation of ZnT8/pET49b(+) into *E. coli* Rosetta™(DE3)pLysS cells, and expression of ZnT8-GST fusion protein was successful using the developed IA-2 protocol. However, the preservation and purification of the expressed ZnT8-GST fusion protein required further optimisation. Due to time constraints, ZnT8R/ZnT8W dimeric protein® was acquired from RSR Limited (Cardiff, UK) for affinity studies. This is a high-quality protein used in their well-performing commercial ELISA kit (362). Stock aliquots of protein (0.652mg/ml) were further aliquoted to reduce freeze-thaw and kept at -80°C with a maximum of 2 freeze-thaw cycles before use. After thawing at RT, the protein was stored at 4°C and used within 24 hours.

#### **2.2.2.2.1 Optimisation of protein concentration curves for affinity studies**

Optimisation of recombinant protein concentration curves was tested on ZnT8RA positive samples from the affinity optimisation sample set using monomeric ZnT8R RIA and was later applied to ZnT8W/ZnT8Q RIAs. The first ZnT8 protein concentration curve was based on previous studies (399, 400), which reported that 100µg/ml was sufficient to displace all ZnT8A bound to radiolabelled ZnT8 antigen. From 100µg/ml, a 7-concentration curve was tested to fit easily on a 96-well plate. During optimisation, three 7-concentration curves were investigated (**Table 2:3**).

Description of protein concentration	Curve 1 ( $\mu\text{g/ml}$ )	Curve 2 ( $\mu\text{g/ml}$ )	Curve 3 ( $\mu\text{g/ml}$ )
<b>High</b>  <b>to</b>  <b>Low</b>	100	0.4	4.0
	25	0.1	0.5
	6.25	0.025	0.1
	1.56	0.0064	0.025
	0.39	0.0012	0.006
	0.097	0.0004	0.001
	0.0247	0.0001	0.0002
<b>No protein</b> <b>(Radiolabelled ZnT8 antigen only)</b>	0.0	0.0	0.0

Table 2:3 – Optimisation of recombinant protein concentration curves for ZnT8A affinity studies.

### 2.2.2.3 Radioimmunoassays (RIAs)

#### 2.2.2.3.1 Assay buffers

Tris buffered saline with Tween-20 (TBST) – 50mM Tris 150mmol/L NaCl, pH 7.3-7.4 with 0.15% v/v Tween-20.

TBST with 0.1% (w/v) bovine serum albumin (TBST-BSA).

#### 2.2.2.3.2 Generation of [35-S] radiolabelled antigens

Recombinant antigens of ZnT8 (aa268-369; monomeric peptides encoding either arginine (R) or tryptophan (W) at aa325 unless otherwise stated), GAD65 (aa1-585), and IA-2IC (aa606-979), encoded into pCMVTnT vectors (kindly supplied by Dr Vito Lampasona, San Raffaele Scientific Institute, Italy) were expressed and incorporated with L-[35-S]-methionine (1mCi; 37MBq; Perkin Elmer, Waltham, MA, USA) using an SP6 TnT *in vitro* transcription/translation kit (Promega, Madison WI, USA).

In detail, one microgram of recombinant antigen was incubated with 40 $\mu\text{l}$  of the SP6 master mix (containing amino acids excluding methionine, SP6 RNA polymerase and rabbit reticulocyte lysate) and 4 $\mu\text{l}$  L-[35-S]-methionine for 1.5 hours at 30°C. Unincorporated excess L-[35-S]-methionine was excluded using a 0.5ml NAP5<sup>TM</sup> desalting column (containing

Sephadex™G-25; GE Healthcare, Little Chalfont, UK). Column void volume and fractions were eluted and collected in TBST-BSA. To test for radioactivity, 2µl of all fractions with 200µl Microscint40 (Perkin Elmer) were prepared for detection on a TopCount plate scintillation counter (Perkin Elmer) following 2mins of optical shaking (set at 700 rotations per minute: rpm) at room temperature (RT). Incorporation of [35-S]-methionine with recombinant antigens was estimated based on the elution profile accounting for elution volumes and dilution factors. Accepted percentage incorporation for recombinant antigen is dependent on the number of methionines present in the peptide sequence and are typically  $\geq 30\%$  for GAD65 and  $\geq 10\%$  for IA-2 and ZnT8. Fractions containing purified incorporated recombinant antigen were pooled and stored at  $-70^{\circ}\text{C}$  for future use (458).

### **2.2.2.3.3 Basic RIA Method**

#### *Detection of GADA, IA-2A, and ZnT8A*

2µl of serum was plated in duplicate into a 96 deep-well plate (Sarstedt, Nümbrecht, Germany) and incubated with 20,000 ( $\pm 1,000$ ) counts per minute (CPM) of [35-S]-GAD65/IA-2IC/ZnT8R/ZnT8W antigen, diluted in TBST-BSA, overnight (19-21 hours) at  $4^{\circ}\text{C}$ . Immunocomplexes were precipitated using a 50% Protein A Sepharose (PAS; GE Healthcare) suspension in a 1-hour incubation on an orbital shaking platform (700rpm) at  $4^{\circ}\text{C}$ .

Excess unbound radiolabelled antigen was excluded by centrifugation (1500rpm at  $4^{\circ}\text{C}$  for 3 mins) and five serial washes in TBST. Samples were transferred from 96 deep-well plates to 96-well OptiPlates™ (Perkin Elmer) by multichannel pipetting, centrifuged, and aspirated for a 30µl end volume. Following the addition of 200µl Microscint 40 (Perkin Elmer) and orbital shaking for 15mins, remaining radiolabelled immunocomplexes were detected (5min/well time-lapse) using a TopCount plate scintillation counter (Perkin Elmer) expressed in CPM (**Figure 2:1**).

## Chapter 2 - Characterisation of the ZnT8 humoral response up to T1D onset

Logarithmic standard curves were used to determine units; GADA/IA-2A are expressed in Diabetic Kidney (DK) units/ml (451, 459), and ZnT8R/ZnT8WA are expressed as arbitrary units (AU). Internal QC samples of known autoantibody levels (1 negative and 3 positives of low, medium, and high titre) were also run in all assays on each deep-well plate to ensure assay reproducibility and performance were maintained.

Positivity thresholds were set at the percentiles of healthy controls for GADA (97th percentile of 1000 adults; 13.5 DK units/ml), IA-2A (98th of 500 schoolchildren; 1.4 DK units/ml) and ZnT8A (97.5th percentile of 523 schoolchildren; 1.8 AU) (274, 354). The sensitivity at 95% specificity (AS95) of these assays was assessed in the 2020 IASP workshop; 78% GADA, 74% IA-2A, 70% ZnT8RA, and 56% ZnT8WA (unpublished data).

Total Length of RIA: ~ 27 hours.

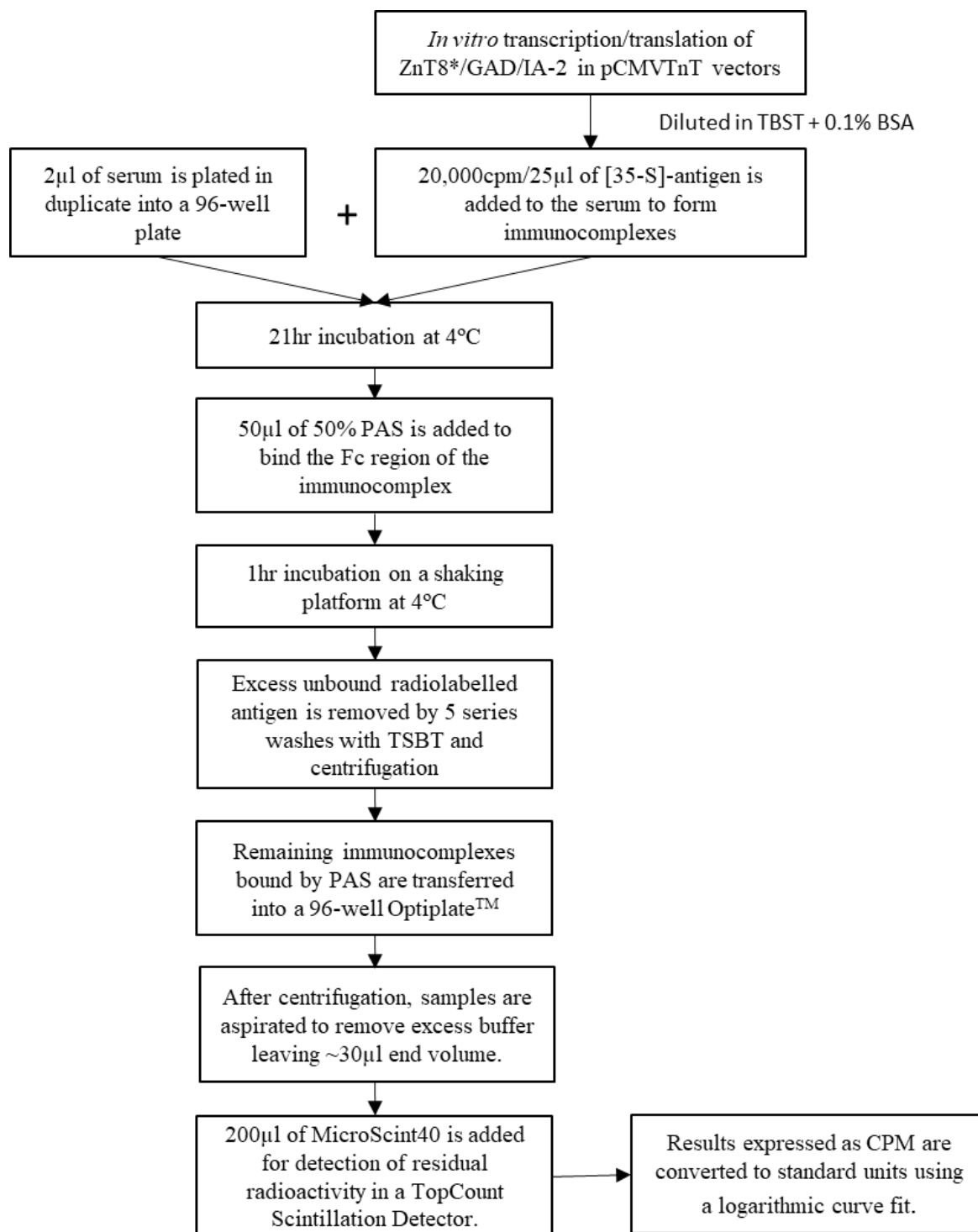


**Figure 2:1 – Basic methodology of the RIA for GADA, IA-2A, & ZnT8A detection**

\* Recombinant [35-S]-methionine radiolabelled ZnT8R/ZnT8W (aa368-369 encoding arginine (R) or tryptophan (W) at aa325). GAD65 (aa1-585) and IA-2 (aa606-979) antigens are synthesised in-house using a TnT SP6 Quick Coupled Transcription/Translation Reticulocyte System (Promega) with 30% and 10% incorporation deemed acceptable for GAD/ IA-2 and ZnT8A, respectively. CPM: counts per minute; PAS: Protein A Sepharose; TBST: Tris buffered saline with 0.15% Tween-20. Total assay length excludes *in vitro* transcription/translation preparation of antigen.

### 2.2.2.4 RIA methodology for ZnT8A affinity studies

The RIA method described previously (2.2.2.3) was adapted to include competition of radiolabelled ZnT8 antigen with 7 concentrations of RSR ZnT8R/ZnT8W dimeric protein® (Figure 2:2), and results were expressed in mean CPM. The mean CPM decreases as ZnT8A preferentially binds increasing concentrations of recombinant ZnT8 protein.

High-affinity antibodies require very little concentrations of protein to be displaced from the radiolabelled antigen (mean CPM reaches assay background at lower protein concentrations). Conversely, low-affinity antibodies require higher concentrations of protein to be displaced from the radiolabelled antigen (mean CPM remains high at higher protein concentrations).

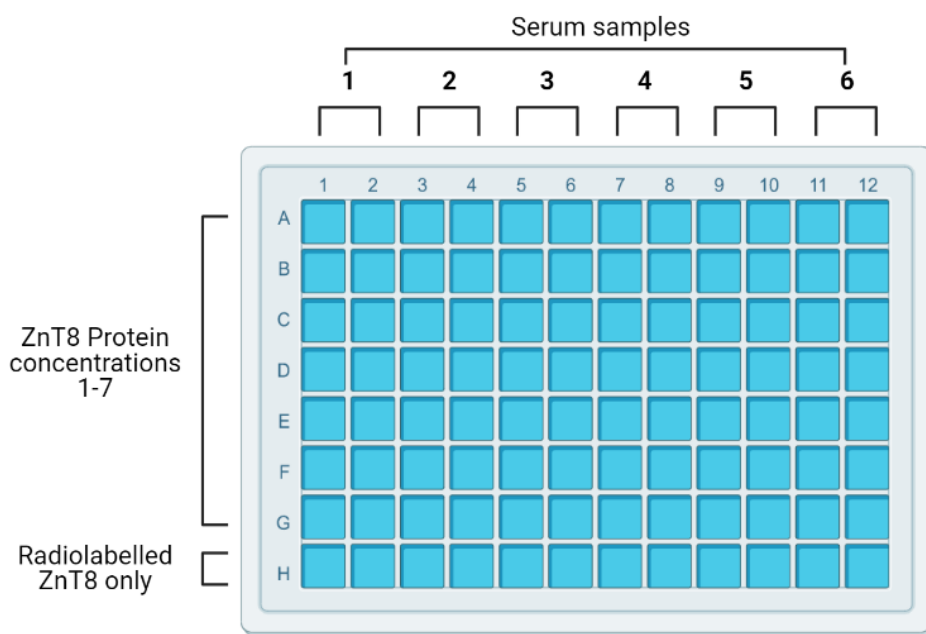


Figure 2:2 – ZnT8A affinity RIA plate set-up

Image created using BioRender.com. A total of 6 serum samples per 96 deep-well plate can be assayed. Rows A-G denotes wells of serum that are incubated with [<sup>35</sup>S]- ZnT8R/ZnT8W/ZnT8Q antigen and RSR recombinant ZnT8R/ZnT8W dimeric protein® in 7 concentrations. Row H denoted wells of serum that are only incubated with [<sup>35</sup>S]- ZnT8R/ZnT8W/ZnT8Q antigen. As ZnT8A preferentially binds the un-radiolabelled ZnT8 protein, competitive displacement curves can be generated using the mean CPM output of the RIA.

### **2.2.2.5 Statistical analysis**

---

The mean CPM was used to evaluate protein dissociation curves during optimisation of the protein concentrations. Following optimisation, to compare samples of varying ZnT8A titre, mean CPM was converted into percent binding, calculated by: mean CPM of wells containing recombinant protein  $\div$  mean CPM of wells without recombinant protein (radiolabelled ZnT8 antigen only)  $\times$  100.

Protein concentrations to displace ZnT8A binding from radiolabelled ZnT8 antigen by 50% was used to discriminate between high-moderate (0.006-0.025 $\mu$ g/ml) and low affinity ZnT8A (>0.025 $\mu$ g/ml). Proportions of high-moderate and low affinity were compared using Fisher's exact test. Protein concentrations were log transformed ( $\log_{10}$ ), and inhibition of radiolabelled ZnT8 antigen was assessed using nonlinear curve fit. Statistical analysis was performed in GraphPad PRISM (v. 9.2.0), and a  $p < 0.05$  was considered significant in all analyses.

## 2.2.3 Results

### 2.2.3.1 Optimisation of the recombinant protein concentration curves

During optimisation, ZnT8RA positive samples from the ZnT8A affinity optimisation sample set and the monomeric ZnT8RA RIA was used.

Curve 1 showed that in RIA QCs, a ZnT8 protein concentration of 0.4 $\mu$ g/ml was sufficient to fully displace ZnT8RA from radiolabelled ZnT8R antigen.

Independent of ZnT8RA titre in the QCs, a protein concentration of 0.4 $\mu$ g/ml was sufficient to displace ZnT8RA from radiolabelled ZnT8R antigen (**Figure 2:3**). In the low ZnT8RA-specific QC, the lowest concentration (0.0247 $\mu$ g/ml) reduced ZnT8A binding to assay background levels (~300-400CPM). Curve 2 used a maximum protein concentration of 0.4 $\mu$ g/ml, and ZnT8WA-specific QCs were excluded to preserve protein and sample, respectively.

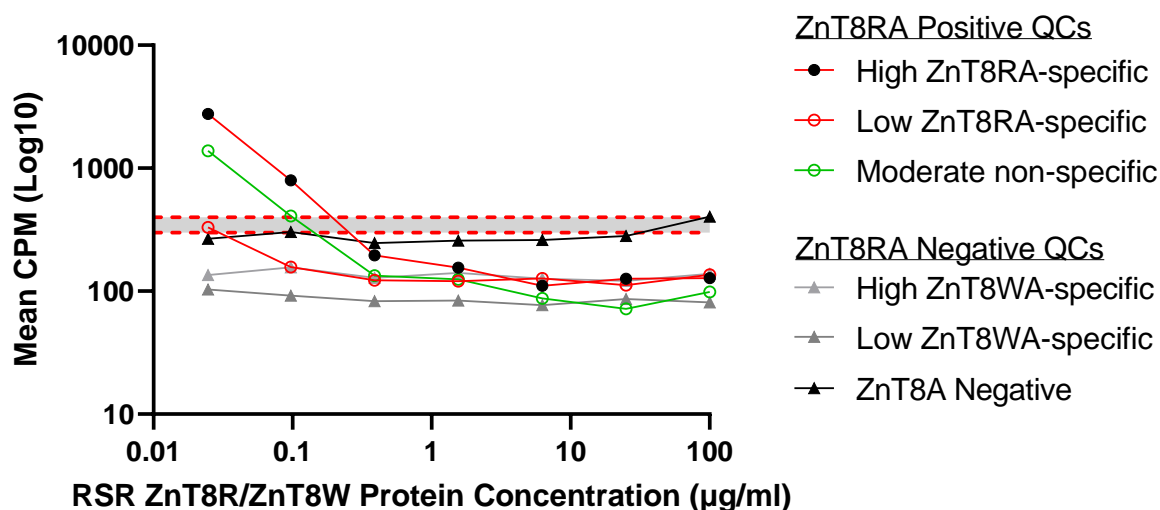


*Figure 2:3 – Optimisation of recombinant protein concentration curves for ZnT8A affinity studies (curve 1)*

Red dashed lines with grey fill denotes the assay background range (300-400CPM). In all ZnT8RA positive QCs, a maximum protein concentration of 0.4 $\mu$ g/ml was required to sufficiently displace ZnT8RA bound to radiolabelled ZnT8R antigen. Only 0.0247 $\mu$ g/ml (lowest concentration) was required to displace the binding of the low Zn8RA-specific QCs. All ZnT8WA-specific QCs and the ZnT8A negative QC remained within the assay background range.

Curve 2 showed that a ZnT8 protein concentration of  $\sim 0.4\mu\text{g/ml}$  was insufficient to fully displace ZnT8A from radiolabelled ZnT8R antigen in T1D patients with high ZnT8A titres.

Curve 2 appeared to increase affinity discrimination and included anonymised T1D patients. A maximum concentration of  $0.4\mu\text{g/ml}$  with approximately 4-fold protein concentration dilutions was sufficient to generate a curve and reduce ZnT8A binding in all QCs to background levels (**Figure 2:4A**). However, 2 high titre ZnT8A responses (1 ZnT8RA-specific and 1 non-specific) were not competitively displaced at  $0.4\mu\text{g/ml}$  (**Figure 2:4B**). Additionally, there was a plateau in most T1D patients at protein concentrations between  $0.0001$ - $0.0064\mu\text{g/ml}$ . Therefore, for curve 3, the concentration curve was slightly modified using a maximum concentration of  $4\mu\text{g/ml}$ .

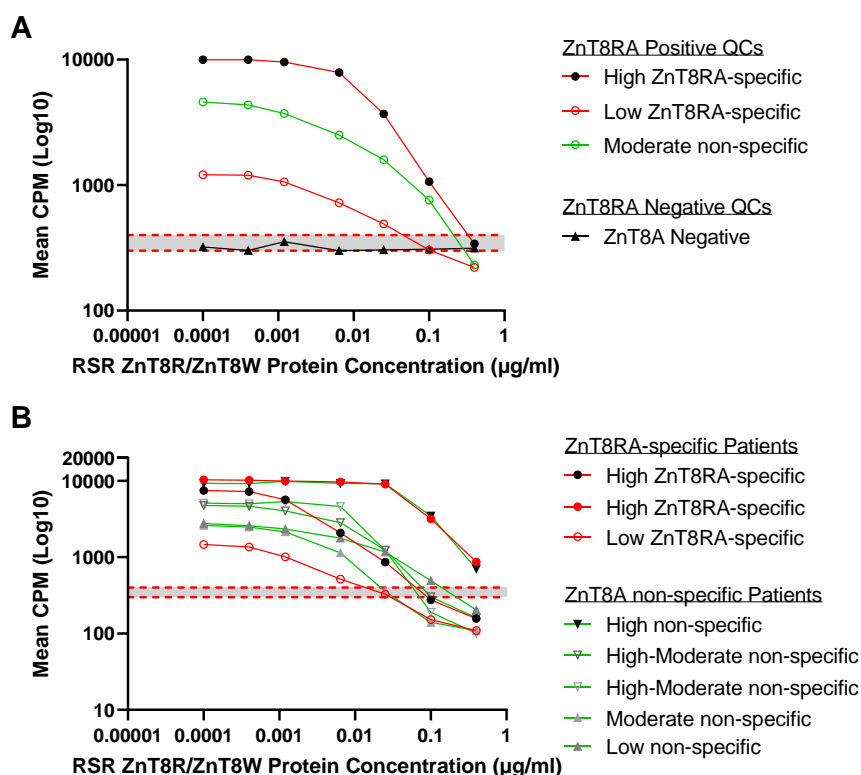


*Figure 2:4 – Optimisation of recombinant protein concentration curves for ZnT8A affinity studies (curve 2)*

Red dashed lines with grey fill denotes the assay background range (300-400CPM). In all ZnT8RA positive QCs, a maximum protein concentration of  $0.4\mu\text{g/ml}$  was sufficient to displace ZnT8RA bound to radiolabelled ZnT8R antigen (**A**). However, 2/8 T1D patients with high titre ZnT8RA responses were not fully competitively displaced at  $0.4\mu\text{g/ml}$  (**B**). Additionally, there was a plateau in most T1D patient ZnT8RA responses between  $0.0001$ - $0.0064\mu\text{g/ml}$  and therefore, the protein concentration curve required further modifications.

Curve 3 with a maximum protein concentration of 4µg/ml produced a desirable protein concentration curve.

Curve 3 was tested in a subset of the ZnT8A affinity optimisation sample set. Curve 3 competitively displaced all ZnT8RA positive QCs and 1 high titre T1D patient at the highest concentration (**Figure 2:5A**). The point at which low and high titre ZnT8RA positive samples were competitively displaced to assay background ranged between 0.1-4µg/ml. In this small sample set, the two high titre samples required higher concentrations of protein (0.5-4µg/ml) to be competitively displaced, which infers lower affinity. This preliminary data may suggest that titre and affinity may not be proportional. However, the logarithmic curve fit in all ZnT8A positive samples was high ( $R^2 > 0.97$ ; **Figure 2:5B**).

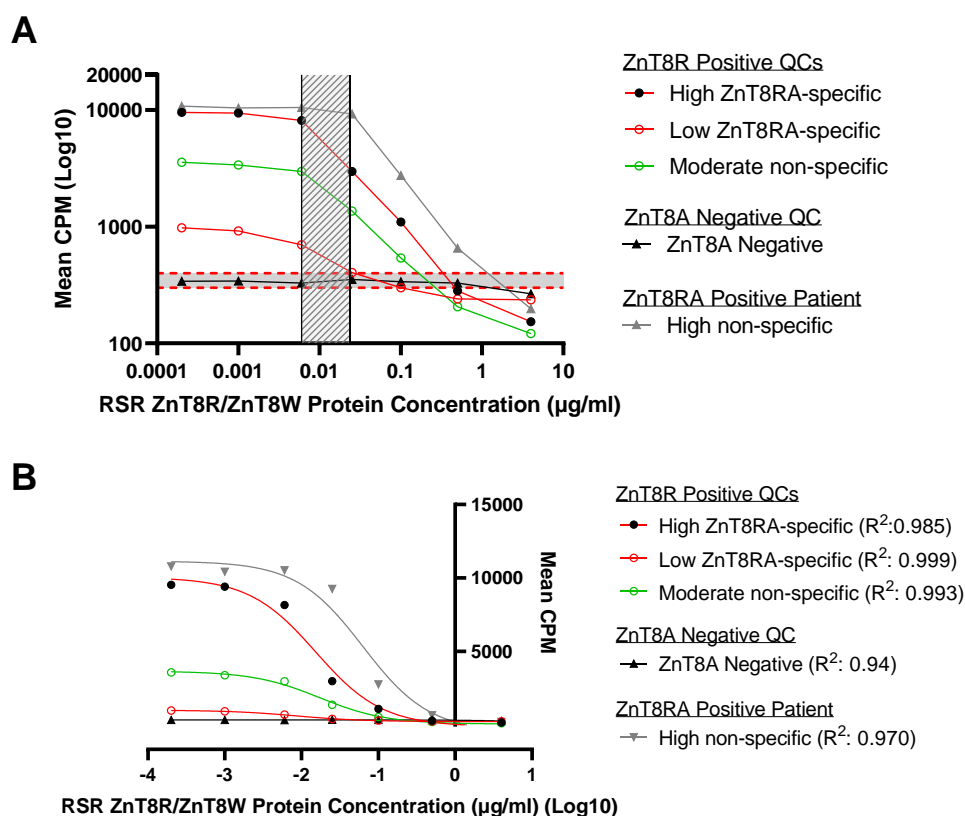


**Figure 2:5 – Optimisation of recombinant protein concentration curves for ZnT8A affinity studies (curve 3)**

(A): Red dashed lines with grey fill denotes the assay background range (300-400CPM). In all ZnT8RA positive samples, a maximum of 4µg/ml was sufficient to displace ZnT8RA bound to radiolabelled ZnT8R antigen. The protein concentration at the point where ZnT8A binding reached assay background range appeared to be within 0.006-0.025µg/ml, which may be associated with ZnT8A titre. High titre ZnT8A required a higher protein concentration to be competitively displaced. (B): The logarithmic curve fit of curve 3 was high ( $R^2 > 0.98$  in ZnT8A positive samples and 0.94 in the negative QC). This curve was used to further investigate ZnT8A affinity.

Curve 3 was further evaluated in the larger cohort of new-onset T1D patients with high-moderate and low ZnT8A affinity defined according to a 50% reduction in binding. In this optimisation experiment, 50% reduced binding was reached at protein concentrations 0.006-0.025µg/ml.

### 2.2.3.2 Defining ZnT8A affinity in new-onset T1D patients using the optimised protein concentration curve

The majority of new-onset T1D patients selected for ZnT8A affinity studies according to the major epitope (325) were non-specific.

Reactivity to the major epitope (aa325) of ZnT8A responses in 27 new-onset T1D patients was predominantly non-specific with 44.4% (n=12) reacting to all variants (R325/W325/Q325) and 25.9% (n=7) reacting to two variants. Overall, 77.8% (n=21), 74.1% (n=20), and 63.0% (n=17) reacted to R325, W325, and Q325 WT ZnT8, respectively (**Figure 2:6**).

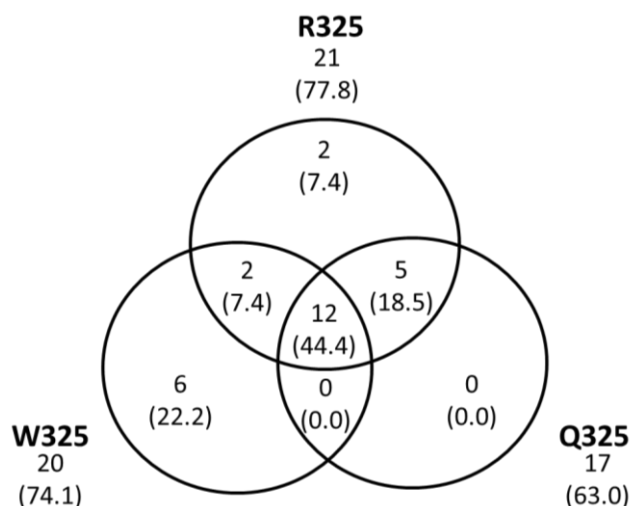


*Figure 2:6 – Categorisation of the major epitope (325) in new-onset T1D patients selected for affinity studies*

ZnT8A positivity profiles according to the major epitope region [R325 (77.8%), W325 (74.1%) and Q325 (63.0%)] WT ZnT8 antigen in 27 new-onset T1D patients sampled within 3 months of onset [15 male (55.6%); median age at diagnosis 8.8 years (range 3.0-17.8)]. Reactivity to all three 325 variants (R325/W325/Q325) comprised 44.4% (n=12) of the cohort and was categorised as ZnT8A non-specific responses. Due to the pre-selection of the cohort by monomeric ZnT8R/ZnT8W RIAs, as expected, there was no detection of Q325-specific responses.

Protein concentrations 0.006-0.025µg/ml displaced >50% of ZnT8A in the majority of new-onset T1D patients independent of ZnT8A specificity or ZnT8 antigen.

Of 21 ZnT8RA positive patients, competitive displacement of radiolabelled ZnT8R antigen by 50% was achieved by 0.006µg/ml in 1 patient (4.8%), by 0.025µg/ml in 16 patients (76.2%), and  $\geq 0.1\mu\text{g/ml}$  in 4 patients (19.1%) with 1 patient showing little to no competitive displacement (**Figure 2:7A**). Similarly, of 19 ZnT8WA positive patients, competitive displacement of radiolabelled ZnT8W antigen by 50% was achieved by 0.006µg/ml in 6 patients (31.6%), by 0.025µg/ml in 10 patients (52.6%), and  $\geq 0.1\mu\text{g/ml}$  in 3 patients (15.8%) (**Figure 2:7B**).

Whereas competitive displacement of radiolabelled ZnT8Q antigen in 14 ZnT8QA positive patients was more diverse: 50% displacement was achieved in 3 patients by 0.006µg/ml (21.4%), 6 patients by 0.025µg/ml (42.9%), and 5 patients  $\geq 0.1\mu\text{g/ml}$  (35.7%) with 1 patient showing little to no competitive displacement (**Figure 2:7C**). This could be due to using a ZnT8R/ZnT8W dimeric protein for competitive displacement but may suggest ZnT8A affinity differs according to the ZnT8 antigen and/or the specificity for the major 325 epitopes.

Nevertheless, independent of ZnT8A specificity, ZnT8A titre, and radiolabelled WT ZnT8 antigen used, the majority of ZnT8A was competitively displaced by 50% at protein concentrations 0.006-0.025µg/ml; 17/21 (81.0%) of ZnT8RA/ZnT8R, 16/19 (84.2%) ZnT8WA/ZnT8W, and 9/14 (64.3%) ZnT8QA/ZnT8Q. Based on the small sample size, ZnT8A affinity was categorised into two divisions, high-moderate (50% displacement by 0.006-0.025µg/ml) and low affinity ( $\geq 0.1\mu\text{g/ml}$ ) for further analysis.

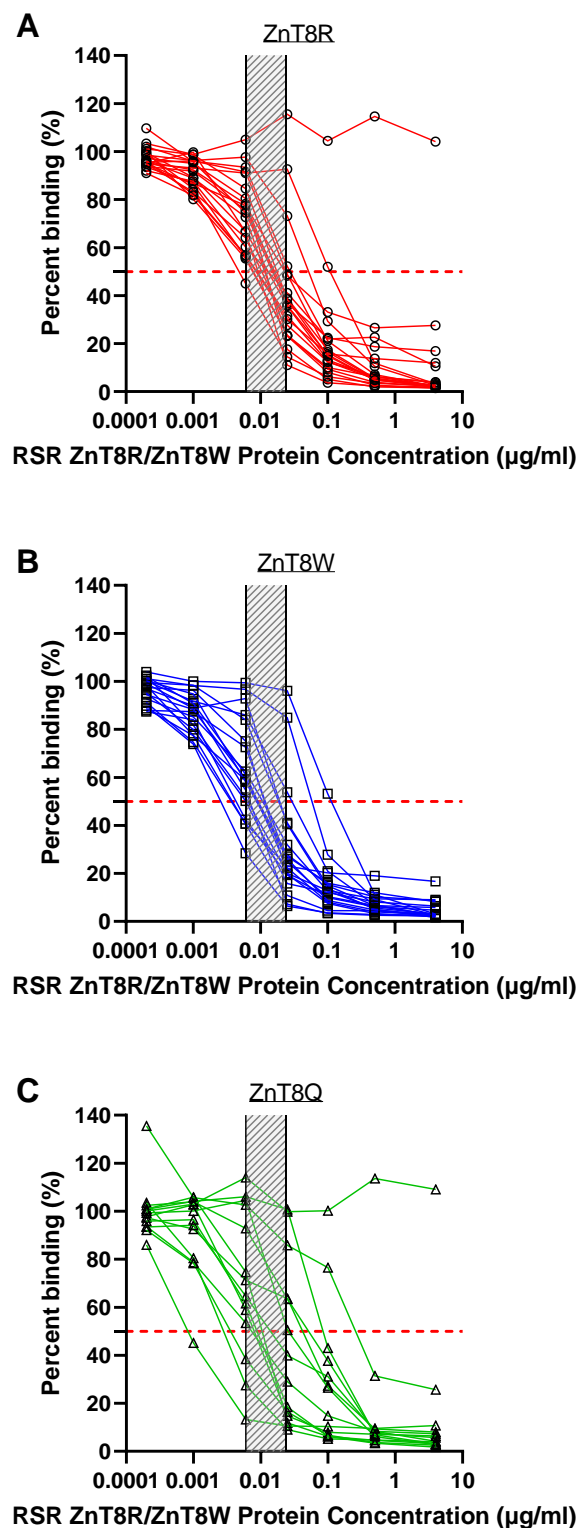


**Figure 2:7 – ZnT8A affinity competitive displacement curves in new-onset T1D patients according to radiolabelled ZnT8 antigen**

Red dashed line denotes 50% reduced ZnT8A binding. Hashed window denotes the protein concentration that discriminates high-moderate and low ZnT8 affinity for ZnT8 antigen [ZnT8R (R325), ZnT8W (W325), and ZnT8Q (Q325)]. From 27 T1D patients, 22/22 (100.0%) patients reactive to R325 was tested (A), 19/20 (95.0%) patients reactive to W325 was tested (B), and 14/17 (82.4%) patients reactive to Q325 was tested (C). The majority of all ZnT8A responses were competitively displaced from radiolabelled ZnT8 antigen at a protein concentration of 0.025µg/ml; 17/21 (81.0%) ZnT8RA/ZnT8R, 16/19 (84.2%) ZnT8WA/ZnT8W, and 9/14 (64.3%) ZnT8QA/ZnT8Q.

The majority of ZnT8A responses were of high-moderate affinity independent of ZnT8 antigen, but ZnT8A affinity was not associated with ZnT8A specificity or overall ZnT8A titre.

Overall, the majority of ZnT8A responses were of high-moderate affinity for ZnT8 antigen; 18/21 (85.7%) ZnT8RA/ZnT8R, 17/19 (89.5%) ZnT8WA/ZnT8W, and 9/14 (64.3%) ZnT8QA/ZnT8Q. There was no difference in the proportion of high-moderate and low affinity ZnT8A between ZnT8RA/ZnT8WA and ZnT8QA responses (p=0.104; **Figure 2:8**).

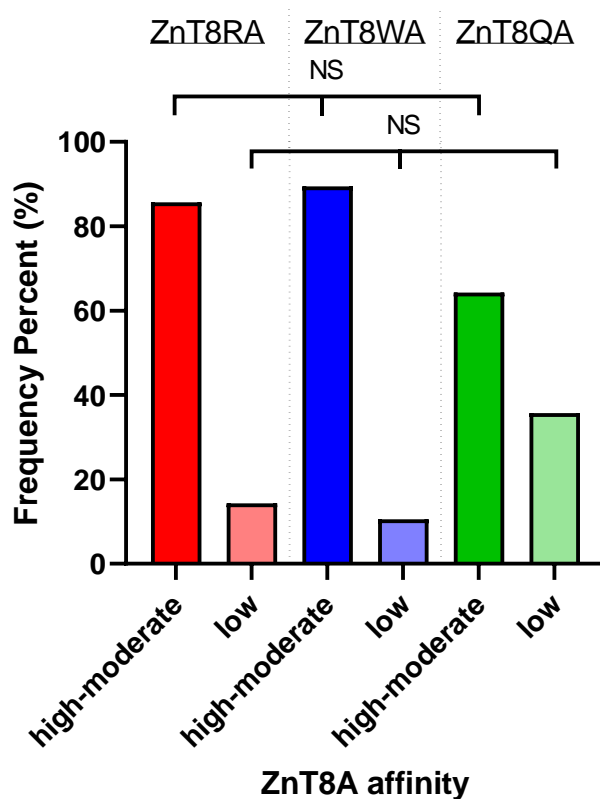


*Figure 2:8 – Proportion of high-moderate & low ZnT8A affinity responses for ZnT8RA, ZnT8WA, & ZnT8QA to corresponding ZnT8 antigen in new-onset T1D patients*

NS: Not significant. The majority of ZnT8A responses were of high-moderate affinity for ZnT8 antigen; 18/21 (85.7%) ZnT8RA/ZnT8R, 17/19 (89.5%) ZnT8WA/ZnT8W, and 9/14 (64.3%) ZnT8QA/ZnT8Q. There was no difference in the proportion of high-moderate versus low affinity ZnT8A responses between ZnT8RA/ZnT8WA and ZnT8QA responses (p=0.104).

Categorising ZnT8RA, ZnT8WA, and ZnT8QA responses together, the proportion of high-moderate and low affinity ZnT8A was also comparable in high-moderate and low titre ZnT8A defined as >20 and <20 AU by RIA based on medium-to-high and low RIA QCs (detailed in **Table 2:1** previously), respectively ( $p=0.675$ ; **Figure 2:9**). This suggests that high-moderate ZnT8A affinity may not always be associated with high titre ZnT8A and vice versa, low ZnT8A affinity with low titre ZnT8A, which would be expected.

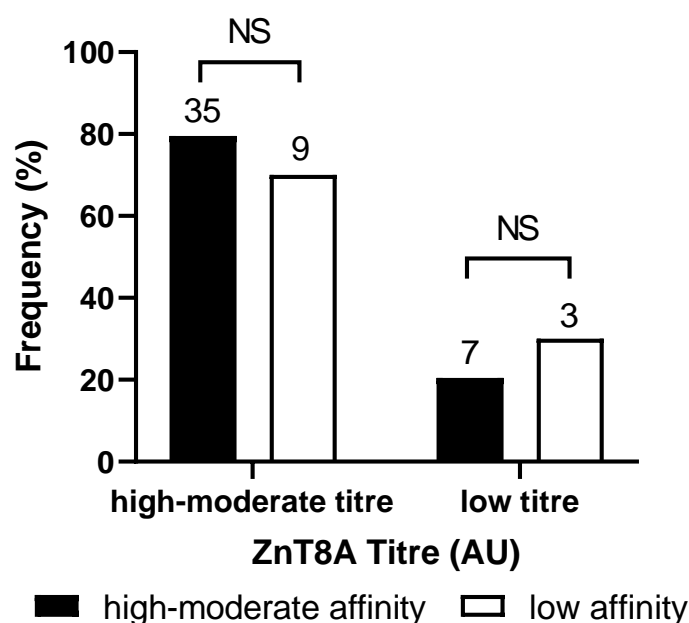


**Figure 2:9 – Proportion of high-moderate & low ZnT8A affinity responses to ZnT8 antigen across all ZnT8A responses according to ZnT8A titre (AU) in new-onset T1D patients**

NS: Not significant. The frequency (n above bars) as a percent of high-moderate and low ZnT8A affinity across ZnT8RA, ZnT8WA, and ZnT8QA responses according to ZnT8A titre. High-moderate ZnT8A titre is defined as >20 AU, and low ZnT8A titre is defined as <20AU based on the AU range of low, medium, and high internal RIA QCs. There was no difference in the proportion of high-moderate ZnT8A affinity according to ZnT8A titre ( $p=0.675$ ).

There was no difference in the proportion of high-moderate ZnT8A affinity according to ZnT8A specificity ( $p>0.05$ ) but there appeared to be a greater proportion of low affinity ZnT8QA/ZnT8Q in comparison to, ZnT8RA/ZnT8R and ZnT8WA/ZnT8W non-specific responses, but again, is possibly related to the ZnT8R/ZnT8W dimeric protein (data not shown). We decided to investigate ZnT8A affinity according to specificity and ZnT8 WT antigen utilised in more detail.

ZnT8A affinity according to ZnT8A specificity and radiolabelled ZnT8 antigen used suggests a range of affinity within new-onset T1D patients.

Grouping patients according to ZnT8A specificity shows some between-sample and between-patient heterogeneity in competitive displacement curves depending on the radiolabelled ZnT8 antigen. For instance, whilst only 8 patients, R325-specific (n=2; **Figure 2:10A**) and W325-specific (n=6; **Figure 2:10B**) responses have varying competitive displacement curves but the majority show 50% displacement at a protein concentration of 0.025µg/ml (87.5%; n=7) and 100% displacement at the maximal protein concentration of 4µg/ml.

In non-specific ZnT8A reactive to >1 variant [R325/Q325 (n=7) and R325/W325 (n=1)], the majority was displaced by 50% at 0.025µg/ml. However, in R325/Q325 patients, 1 showed little to no competitive displacement from either ZnT8R or ZnT8Q antigen (**Figure 2:10C/E**: open circles), 1 showed better competitive displacement of ZnT8R versus ZnT8Q antigen (**Figure 2:10 C/E**: grey triangles), and 1 showed better competitive displacement of ZnT8Q versus ZnT8R antigen (**Figure 2:10C/E**: red and green circles, respectively). This suggests that whilst ZnT8A may be non-specific and bind to >1 variant, ZnT8A may have different affinities dependent on the radiolabelled ZnT8 antigen.

Additionally, patients with non-specific ZnT8A reactive to all three variants (R25/W325/Q325) generally show competitive displacement at lower protein concentrations with either ZnT8R or ZnT8W (higher affinity) rather than ZnT8Q antigen (lower affinity) (**Figure 2:10F-H**). However, this could be due to utilising a ZnT8R/ZnT8W dimeric protein.

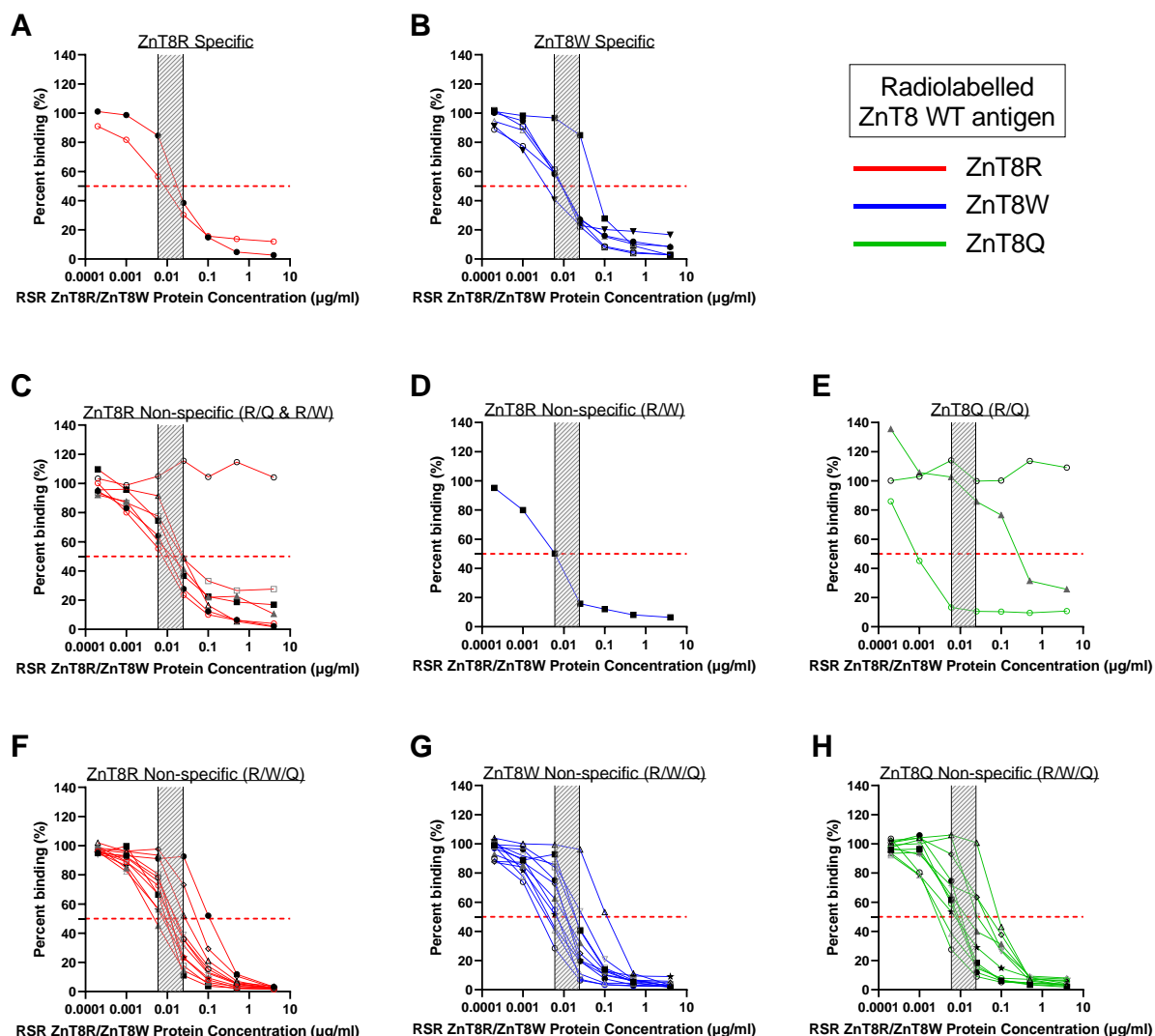


**Figure 2:10 – ZnT8A affinity competitive displacement curves in new-onset T1D patients according to ZnT8A specificity & ZnT8 antigen**

Red dashed line denotes 50% reduced ZnT8A binding. Hashed grey window denotes the protein concentration that has been used to discriminate high-moderate and low ZnT8 affinity for ZnT8 antigen. Corresponding symbols in graphs denote identical samples tested for ZnT8A affinity towards more than one radiolabelled WT ZnT8 antigen based on the specificity of the ZnT8A response. **A/C/F**: ZnT8RA versus ZnT8R antigen according to ZnT8A specificity; **B/D/G**: ZnT8WA versus ZnT8W antigen according to ZnT8A specificity; **E/H**: ZnT8QA versus ZnT8Q antigen according to ZnT8A specificity. Grouping of patients according to ZnT8A specificity shows heterogeneity in competitive displacement curves between patients and within patients depending on the ZnT8 antigen used; however, no strong conclusions can be drawn from this small cohort.

---

## 2.2.4 Discussion

---

### 2.2.4.1 Main findings

---

1. A maximum concentration of 4µg/ml RSR ZnT8R/ZnT8W dimeric protein® was sufficient to displace low and high titre ZnT8A binding to RIA assay background levels.
2. Protein concentrations 0.006-0.025µg/ml displaced >50% of ZnT8A in the majority of new-onset T1D independent of ZnT8A specificity or radiolabelled ZnT8 antigen. These two concentrations were used to discriminate high-moderate and low affinity ZnT8A.
3. The majority of ZnT8A responses were of high-moderate affinity independent of radiolabelled WT ZnT8 antigen, but ZnT8A affinity did not appear to be associated with ZnT8A specificity or overall titre.

### 2.2.4.2 Strengths, limitations, & future work

---

To our knowledge, this is the first investigation of ZnT8A affinity that has 1) utilised recombinant ZnT8 (ZnT8R/ZnT8W) protein that is well-validated and highly effective at binding ZnT8A with a consistently high sensitivity across many IASP workshops by ELISA (362), and 2) taken into account a range of ZnT8A titre and specificities by incorporating competitive displacement curves towards all three variants of ZnT8 antigen into the RIA.

The previous study to investigate ZnT8A affinity only investigated high titre R325- and W325-specific ZnT8A. The current study builds on this through the inclusion of non-specific ZnT8A, a range of ZnT8A titres, and the investigation of ZnT8A affinity towards all variants of radiolabelled ZnT8 antigen (R325/W325/Q325). However, the current study is limited by predominantly focusing on non-specific ZnT8A responses in 27 new-onset T1D patients, a future goal would be to investigate affinity in at-risk individuals and/or across all specificities

of ZnT8A in a larger cohort. However, data from the optimisation experiments demonstrated that affinity can be measured utilising a lower protein concentration of dimeric ZnT8R/ZnT8W protein than previously reported for monomeric MBP-ZnT8R and MBP-ZnT8W proteins: 4µg/ml versus 100µg/ml (399), showing that the dimeric protein was an efficient competitor for ZnT8A binding. Given the lower concentration required to displace ZnT8A and the observation that the majority of ZnT8A was displaced by 50% at 0.006-0.025µg/ml of dimeric ZnT8R/ZnT8W protein, it may be possible to categorise ZnT8A affinity utilising only 1-2 protein concentrations in future investigations. This would reduce serum volume requirements and cost by increasing the number of samples that can be assayed per 96-well plate.

Interestingly, there did not appear to be a relationship between ZnT8A titre and affinity, previously reported in other islet autoantibody responses (331, 345). In the TrialNet NHSt, Sosenko *et al.* (2013) reported that incorporating autoantibody titres into a risk score in mAutoab+ve FDRs considering IAA, GADA, IA-2A, ICA, and ZnT8A, enhanced T1D risk prediction (with/without adjustment for positivity status) above using the validated Diabetes Prevention Trial–Type 1 Risk Score (DPTRS) alone (460); DPTRS considers glucose tolerance, C-peptide, age, and BMI (299, 304). Overall, data from TrialNet highlights the importance of utilising autoantibody titre in assessing disease risk but that incorporating all these factors into a combined risk score should aid screening for high-risk individuals (460-462). Therefore, the consideration of all characteristics of ZnT8A responses in at-risk individuals is likely to be more informative than looking at each characteristic in isolation.

Another potential limitation of the current study is that all selected patients were mAutoab+ve, and therefore, affinity may differ between sAutoab+ve and mAutoab+ve ZnT8A responses. A very recent report by Jia *et al.* (2021) comparing ZnT8A detection by RIA and ECL in single ZnT8A positive children from the general population participating in ASK (Autoimmunity

Screening for Kids, BDC, USA) and DAISY, found that ECL positivity was associated with increased risk of progression compared to RIA (333). This was confirmed to be due to ECL's enhanced ability at detecting high-affinity ZnT8A over the RIA, comparable to previous findings for GADA and IAA (319, 360). Additionally, this study found that of 11 single ZnT8A RIA positives from 2547 DAISY children, only 3 were positive by ECL and later progressed to T1D. Therefore, single ZnT8A responses may be more likely to be of lower affinity and, by extension, lower risk, comparable with other sAutoab+ve responses (287, 323, 333, 463). In a TrialNet NHSt study, independent of all other islet autoantibodies, age (range 1-45 years), and HLA, FDRs with ZnT8A had a higher risk of T1D, but sAutoab+ve ZnT8A responses were found in 0.9% of relatives (318). While sAutoab+ve ZnT8A responses exist, they are rare, and individuals with this response are likely to be of lower T1D risk (based on many prospective studies). Therefore, to be of benefit, investigations of ZnT8A affinity are best applied in high-risk mAutoab+ves (287, 290).

Although we did not find an association between ZnT8A affinity and specificity, there was some evidence of differential displacement of radiolabelled antigen, particularly in non-specific ZnT8A responses. Differential displacement was also observed by Skarstrand *et al.* (2015) between R325- and W325-specific ZnT8A responses towards the corresponding monomeric MBP-tagged ZnT8 protein. This may be due to monoclonal and polyclonal B-cell responses and/or reactivity of ZnT8A to multiple C-terminal ZnT8 epitopes, but generally, ZnT8A affinity appears to vary even in very close proximity to T1D onset. For instance, specific epitopes of IAA and GADA were associated with high-affinity responses and T1D risk, but for IA-2A, low-affinity responses were rare prior to onset (316, 344-346). This could be due to IA-2A's association with rapid progression, appearing later in the preclinical stages, which may also be an anticipated outcome for ZnT8A, but a bigger sample set and further

intermolecular epitope mapping of ZnT8 in at-risk individuals over follow-up would be required to determine this.

The determination of IC<sub>50</sub> (half-maximal inhibitory concentration) and the reciprocal dissociation constant (K<sub>d</sub>; typically expressed in 1/mol) are conventionally used in affinity studies [e.g., (343, 344)]. Within the time constraints of the project, we were unable to ascertain the exact concentration of [35-S]-radiolabelled recombinant ZnT8 present in 2µl serum per well. Therefore, we used 50% inhibition of binding as a proxy for IC<sub>50</sub> in this thesis which was sufficient for optimising the protein concentration dissociation curves and discriminating low from high-moderate ZnT8A affinity in subsets of at-risk and new-onset T1D subjects.

Collectively, we can state that ZnT8A affinity varies at T1D onset but should be investigated before diagnosis, and in those analyses, ZnT8A specificity should be considered, but an association with titre and/or age cannot be excluded. Data on ZnT8A before T1D onset is limited, but preliminary data by Jia *et al.* (2021) suggests ZnT8A affinity aids T1D risk prediction in single ZnT8A responses, but these responses are rare in FDRs and are likely to be rarer in the general population, and comparison of ZnT8A affinity in mAutoab+ves is required to fully investigate whether ZnT8A affinity could inform or enhance the performance of ZnT8A detection methods in screening at-risk individuals. This type of study is feasible utilising the optimised protein concentration curve established in this project and samples from BOX.

---

## 2.3 Characterisation of ZnT8A IgG subclasses

---

---

### 2.3.1 Introduction to islet autoantibody IgG subclasses

---

The characterisation and the predictive utility of antigen-specific islet autoantibody IgG subclasses have been limited, conducted predominantly in European countries, and have largely comprised small cohorts of FDRs aged <20years. **Table 2:4** describes the largest IgG subclass investigations in T1D with the most comparable methodologies stemming from an initial report by Bonifacio *et al.* (1999), which has also been applied in this PhD project. These studies generally agree that GADA, IA-2A, and IAA responses are IgG1-dominant, IgG1 correlates with peak IgG responses (titre), IgG1 are the most stable IgG over follow-up, and the prevalence of IgG2-IgG4 was associated with the peak IgG response (titre) (244, 317, 464-467). However, even within these pre-selected studies, there are conflicting frequencies of IgG subclasses reported. These studies were predominantly conducted prior to the discovery of ZnT8A, and to our knowledge, there are no reports of ZnT8A IgG subclasses.

Chapter 2 - Characterisation of the ZnT8 humoral response up to T1D onset

Study (date) Autoab tested	Population & Subjects (n)	Method of IgG subclass detection	Prevalence of IgG subclasses (%)	Main Findings
<b>Bonifacio <i>et al.</i> (1999)§</b>  GADA IA-2A IAA	German BABYDIAB prospective birth cohort  26 autoab+ve children [median age at seroconversion 1.4yrs (range 0.5-5.4)]  44 controls utilised to generate StDS*	RIA & biotinylated murine monoclonal anti-human IgG subclass-specific secondary antibodies bound by Streptavidin Sepharose beads§	<u>GADA:</u> IgG1(65), IgG2(19), IgG3(12), IgG4(19).  <u>IA-2A:</u> IgG1(62), IgG2(19), IgG3(19), IgG4(0).  <u>IAA:</u> IgG1(96), IgG2(38), IgG3(38), IgG4(50).	1. Early IgG responses are IgG1-dominant. Peak IgG1 responses mirror and correlate with PAS/PGS in conventional RIA.  2. IgG2-IgG4 was more common at peak IgG. IgG2-IgG4 most abundant in IAA responses possibly related to insulin therapy with IgG4 dominating IgG1 in 4 children.
<b>Achenbach <i>et al.</i> (2004)§</b>  GADA IA-2A IAA	FDRs from Munich (Germany) & BOX (UK) family studies  180 non-diabetic FDRs autoab+ve (confirmed ≥2 f-up): [median age at 1 <sup>st</sup> sampling 14.5yrs (IQR 8.3-30.3); median f-up 5.9yrs (IQR 3.9-10.7)]  59/180 FDRs developed diabetes [median time to diabetes 3.6yrs (IQR 1.3-6.1)]	RIA & biotinylated murine monoclonal anti-human IgG subclass-specific secondary antibodies bound by Streptavidin Sepharose beads§ StDS used from Bonifacio <i>et al.</i> (1999)	<u>GADA:</u> IgG1(97), IgG2(24), IgG3(2), IgG4(34)  <u>IA-2A:</u> IgG1(94), IgG2(40), IgG3(5), IgG4(40)  <u>IAA:</u> IgG1(64), IgG2(24), IgG3(32), IgG4(26)	1. Spectrum of IgG2-IgG4 was related to titre & for GADA and IA-2A was related to reactivity to multiple epitopes.  2. Titre & the presence of IgG2-IgG4 in IA-2A (HR3.3) and IAA (HR4.6), was associated with increased diabetes risk.  3. Absence of considering IgG subclasses in hazard models significantly reduced model fit for predicting disease risk.
<b>Hoppu <i>et al.</i> (2004)<sup>a</sup></b>  GADA	FDRs (siblings) from the Childhood Diabetes in Finland (DiMe) Study  42 autoab+ve FDRs: [mean age at first sampling 9.5yrs (range 3.2–16.3)]  21/21 FDRs progressed/did not progress to diabetes over 12-year f-up  40 controls utilised to generate StDS*	RIA & monoclonal murine anti-human subclass-specific antibodies linked to streptavidin agarose	<u>(First sample – prog):</u> IgG1(100), IgG2(57), IgG3(14), IgG4(52)  <u>(First sample – non-prog):</u> IgG1(100), IgG2(81), IgG3(19), IgG4(76)	1. IgG1 (most dominant), IgG2/IgG4 more common than IgG3. IgG2/IgG4 more common in non-prog than prog but number of IgG subclasses was comparable between groups & correlated with titre. Number of IgG subclasses did not change over f-up.  2. Significant IgG spreading of IgG2 over f-up was observed in 7 prog, but this occurred in 3 non-prog.

Chapter 2 - Characterisation of the ZnT8 humoral response up to T1D onset

<p><b>Hoppu <i>et al</i> (2004)<sup>b</sup></b> IA-2A</p>	<p>FDRs (siblings) from the Childhood Diabetes In Finland (DiMe) Study</p> <p>34 autoab+ve FDRs: [mean age at first sampling 9.9yrs (range 4.2-17.3)].</p> <p>17/17 IA-2A+ve FDRs progressed/did not progress over 12-year f-up</p> <p>40 controls utilised to generate StDS*</p>	<p>RIA &amp; murine monoclonal anti-human subclass-specific antibodies linked to streptavidin agarose</p>	<p><u>(First sample – prog):</u> IgG1(82), IgG2(47), IgG3(6), IgG4(24)</p> <p><u>(First sample – non-prog):</u> IgG1(88), IgG2(18), IgG3(6), IgG4 (18).</p>	<p>1. IgG1 (most dominant), IgG2 more common in prog than non-prog but number of IgG subclasses was comparable between groups &amp; correlated with titre.</p> <p>2. Significant IgG spreading to IgG2-IgG4 in non-prog was observed over f-up.</p> <p>3. Half of FDRs had fluctuating positivity of IgG subclasses but IgG1 was constant.</p>
<p><b>Hoppu <i>et al.</i> (2004)<sup>c</sup></b> IAA</p>	<p>Type 1 Diabetes Prediction &amp; Prevention (DIPP) Study. High-HLA risk infants followed from birth.</p> <p>15 autoab+ve progressors [median age 1.0 (range 0.3-2.2)].</p> <p>30 autoab+ve non-progressors [median age 1.4 (range 0.6-3.6)].</p>	<p>RIA &amp; murine monoclonal anti-human subclass-specific antibodies linked to streptavidin agarose</p>	<p><u>All:</u> IgG1(96), IgG2 (56), IgG3(73), IgG4(33)</p>	<p>1. Positivity/titre remained stable in prog but decreased in non-prog.</p> <p>2. IgG1 most consistent over f-up &amp; IgG1/IgG2 appeared earlier than IgG4, but IgG3 &amp; higher IgG subclass number observed in prog. IgG1/IgG3 were frequently dominant in prog &amp; both correlated with titre.</p> <p>3. Absent IgG3 responses could be a marker of lower diabetes risk.</p>
<p><b>Seissler <i>et al.</i> (2002)</b> IA-2A</p>	<p>Recruited from the Deutsche Nicotinamide Intervention Study (DENIS)</p> <p>50 new-Dx T1D (&lt;7 days); [median age 9.4yrs (range 0.2-18.0)]</p> <p>32 autoab+ve FDRs (siblings) who were f-up a median of 68 months (range 24-92); 14 developed diabetes.</p>	<p>RIA &amp; monoclonal murine anti-human IgG-specific antibodies incubated with serum &amp; immunoprecipitated with NeutrAvidin agarose</p>	<p><u>New-Dx:</u> IgG1(98), IgG2(34), IgG3(26), IgG4(50)</p> <p><u>FDRs:</u> IgG1(59), IgG2(9), IgG3(16), IgG4(59)</p>	<p>1. In both groups, IgG1 only responses most common (42%/31%), followed by IgG1/IgG4 (22%/28%). Titre was comparable between groups, but only IgG1 was associated with higher titre.</p> <p>2. IgG4-only responses more common in non-prog than prog (50%/7%). Presence of IgG4 was associated with less disease risk versus IgG1; 6-year diabetes risk for IgG1 only (74%) vs IgG4 only (9%) responses.</p>

*Table 2:4 – Seminal T1D studies of IgG subclasses*

§ same methodology that was applied to this PhD project; <sup>abc</sup> same methodology; \* StDS; standard deviation score established IgG subclass-specific thresholds based on the SD of healthy controls; autoab+ve: autoantibody positive. Studies predominantly conducted in European-Caucasian populations & FDRs aged <20years who either progressed (prog) or did not progress (non-prog) to diabetes over follow-up (f-up). IgG subclasses are less defined in at-risk individuals >21 years & in new-onset T1D.

**Table 2:5** details the median prevalence (%) of IgG subclasses reported in FDRs of individuals with T1D or infants of parents with T1D in European populations. The prevalence of IgG subclasses in GADA and IA-2A responses appear comparable IgG1>IgG4>IgG2>IgG3. The detection of IgG2 and IgG4 are the most variable (range 19-57%), but the low frequency of IgG3 is generally consistent (range 2-4%). In contrast, IAA responses show a broad spectrum of IgG subclasses IgG1>IgG2≈IgG3≈IgG4, which was reported in most studies, but the prevalence varies between studies (range 24-73%).

Islet Autoab	IgG1 median % prevalence (range)	IgG2 median % prevalence (range)	IgG3 median % prevalence (range)	IgG4 median % prevalence (range)	Refs
GADA (Total n=217)	97 (65-100)	24 (19-57)	12 (2-14)	34 (19-52)	(244, 317, 464)
IA-2A (Total n=154)	82 (59-94)	19 (6-47)	6 (5-19)	24 (0-59)	(244, 317, 465, 467)
IAA (Total n=143)	96 (64-96)	38 (24-56)	38 (32-73)	33 (26-50)	(244, 317, 466)

*Table 2:5 – Prevalence of GADA, IA-2A, & IAA IgG subclasses in autoantibody positive FDRs*

The IgG subclass prevalence in autoantibody positive FDRs for GADA, IA-2A, and IAA previously reported (244, 317, 464-467). The prevalence (%) was calculated from reported data and used to demonstrate the median and range of prevalence reported.

The variability of reported IgG subclasses could be influenced by detection methods, clone or source of anti-human IgG subclass-specific antibodies, age at IgG subclass detection, or length of follow-up prior to T1D. There was a large international effort supported by the World Health Organisation (WHO) in 1986 to evaluate the specificity of commercially available anti-human monoclonal antibodies (468). Over time, commercially available clones of anti-human monoclonal antibodies have evolved and are now internally validated. Inevitably, different clones in the seminal T1D studies were utilised (notably anti-human IgG3; **Table B:1**; **Appendix B**). However, updated clones are likely to be more sensitive, and regardless of assay methodology, most studies in T1D report that the measurement of IgG subclasses has aided the discrimination of high-risk FDRs above total IgG detection (PAS/PGS) alone (317, 464-467)

but current data suggests IgG subclasses are more useful in IA-2A and IAA responses than GADA for predicting T1D risk.

GADA responses are largely comprised of IgG1, and the spectrum of IgG2-IgG4 subclasses was not found to be associated with increased T1D risk but was associated with multiple GAD epitope reactivity (N-, middle-, and C-terminus of GAD65 and GAD67) and higher GADA titres (317, 464). Titres of GADA were not independently associated with T1D risk (317). The prevalence of IgG2/IgG4 were more common than IgG3, and although not associated with T1D risk, some observations between FDRs who progressed to T1D compared to FDRs who did not progress over follow-up were reported: the seroconversion of IgG2 over follow-up was higher in progressors, but IgG2/IgG4 was more common in non-progressors (464).

IA-2A responses are also largely comprised of IgG1, but the spectrum of IgG2-IgG4 subclasses was associated with increased T1D risk (HR: 3.3; 100% of relatives with IgG2, IgG3, or IgG4 developed diabetes at 10 years follow-up versus 37% in IgG1-restricted responses), multiple IA-2 epitope reactivity (JM, PTP, and IA-2 $\beta$ ) (317), and higher IA-2A titres (317, 465). However, higher IA-2A titres and IA-2A reactive to IA-2 $\beta$  was also independently associated with T1D risk (317). It has also been observed that IA-2A reactive to JM, IgG1 prevalence, and IgG2-IgG4 spreading over follow-up was more common in progressors (465). There has also been an indication that IgG4-restricted IA-2A responses may be protective against T1D; the 6-year diabetes risk of IA-2A IgG4-restricted responses was 9% versus 74% in IgG1-restricted responses (467).

IAA responses are also largely comprised of IgG1, but the spectrum of IgG2-IgG4 subclasses was more prevalent than in GADA and IA-2A responses and was associated with increased T1D risk (HR: 4.6; 68% of relatives with IgG2, IgG3, or IgG4 developed diabetes at 10 years

follow-up versus 28% in IgG1-restricted responses) and higher IAA titres (317). However, higher IAA titres were also independently associated with T1D risk (317). It has also been observed that the prevalence of IgG3 in the first sample, IgG1- and IgG3-dominant responses, higher IgG1/IgG3 levels, and the number of subclasses (IgG2-IgG4) was higher in FDRs that progressed to T1D (466).

In the 1980-1990s, prior to characterising IgG subclasses in antigen-specific responses, ICA were characterised as polyclonal (kappa and lambda light chains), of IgG isotype, and were largely IgG1-restricted (>50-76%) with decreasing prevalence of IgG2>IgG3>IgG4 (24-50% combined) (246, 469-472). It was postulated that the IgG1-restriction, possibly reflective of monoclonal B-cell responses, may precede the clinical onset of T1D and could be a feature of autoimmunity as IgG1-restriction was also reported in other autoimmune conditions around this time such as autoimmune chronic active hepatitis and SLE (245, 246, 473). Therefore, the IgG1-dominance/restriction reported in T1D for GADA, IA-2A, and IAA responses may be a feature of autoimmunity. Thus, we can postulate that ZnT8A responses may be largely IgG1-dominant/restricted due to its later appearance in preclinical T1D, but the prevalence of IgG2-IgG4 is likely to be associated with high ZnT8A titres and T1D risk, comparable to IA-2A responses, as secondary targets of islet autoimmunity (290).

### **2.3.1.1 Hypothesis**

---

The ZnT8RA/ZnT8WA IgG subclass response will be IgG1 dominant like GADA and IA-2A responses, but specific IgG subclasses which will inform slow from rapid T1D progression.

### **2.3.1.2 Aims**

---

1. To evaluate ZnT8RA and ZnT8WA IgG subclass responses compared with GADA and IA-2A in slow and rapid progressors of T1D.
2. To evaluate ZnT8RA and ZnT8WA IgG subclass responses by ZnT8A specificity (aa325 reactivity) in a cohort of new-onset T1D (<3 months of diagnosis).
3. To explore assay standardisation and assess the reproducibility of IgG subclass assays through screening T1D patients <10 years disease duration for the development of quality control (QCs) samples and creating IgG subclass-specific positivity thresholds based on ~50 healthy schoolchildren.

---

## 2.3.2 Materials & Methods

---

### 2.3.2.1 Populations for autoantibody IgG subclass studies

---

To establish and evaluate the importance of ZnT8RA/ZnT8WA IgG subclasses in comparison to GADA and IA-2A, the following sample sets were used:

**1. Multiple autoantibody positive (mAutoab+ve) progressor:** The first mAutoab+ve sample available (index) and, where possible, a second follow-up sample from FDRs of the BOX study (previously described **1.8**) was tested for IgG subclasses based on autoantibody positivity (independent of titre). These samples were used to evaluate whether IgG subclass frequency was associated with progression to diabetes. Based on rate of progression from sample, these FDRs were categorised as non-progressors (NPs; diabetes-free by final follow-up; **Table 2:6**), slow-progressors (SPs; diabetes-free >10years; **Table 2:7**), and rapid-progressors (RPs; diabetes-free <5years; **Table 2:8**). Samples were primarily tested in Dr Peter Achenbach's laboratory in Munich (2-week training period) indicated in the tables. All data were expressed in mean  $\Delta$ CPM, but due to differences in assays between Munich/Bristol laboratories, there are differences in binding classified as positive [Munich: >32 (GADA), >16 (IA-2A), and >30 (ZnT8RA/ZnT8WA); Bristol: >100 for all].

**2. New-onset T1D patients:** To investigate whether the frequencies of ZnT8RA/ZnT8WA IgG subclasses are different at T1D onset, a subset of high volume (>1ml) ZnT8A positive new-onset T1D patients (n=18; <3 months of diagnosis) were tested. Samples were selected to encompass different ZnT8A titres and specificities and, where possible, matched for age-at-onset (**Table 2:9**).

**3. Screening T1D patients for IgG subclasses & quality control development:** After the initial testing of sample sets 1 and 2 (above), it became clear that for continued work, better assay controls were required. Therefore, to establish a sample set that could provide QC samples, a random selection of samples from T1D patients [ $<2$  years disease duration for ZnT8RA/ZnT8WA (encompassing all ZnT8A specificities) and  $<10$  years for GADA and IA-2A] and 1 NP (GADA only), with high serum volume ( $>1$ ml) and predominantly high autoantibody titres by RIA were screened for IgG subclasses (**Table 2:10**). Samples of high titre and short diabetes duration were selected to enhance the probability of detecting a spectrum of IgG subclasses, and for ZnT8A in particular, a shorter disease duration was preferable due to the rapid loss after onset previously reported (244, 443). Post-diagnosis IgG subclass responses have not been reported previously, and as these samples were predominantly high volume, these samples were selected for novelty and the likelihood of providing large pools of QCs for future use. Once established, samples subsequently used for QCs (**Table 2:11**) were run in all assays to evaluate assay reproducibility. An anonymised autoantibody negative control was used as a negative QC and was also run in all assays. No other information was available from this individual.

**4. Standardisation of IgG subclass RIAs:** Given the lower prevalence of IgG2-IgG4 in ZnT8RA/ZnT8WA responses, both the development of QCs and establishing IgG subclass-specific positivity thresholds was not possible. For GADA/IA-2A, however, ~50 high volume healthy schoolchildren were selected at random to develop IgG subclass-specific standard deviation score (StDS) thresholds. An StDS  $>3$  [previously described as positive (244)] detected 100% of IgG1 and total IgG (PGS) in GADA and IA-2A responses in T1D patients (**Appendix B.2**).

Chapter 2 - Characterisation of the ZnT8 humoral response up to T1D onset

Islet Autoab	n index sample	n f-up sample	Median (range) time between index and f-up sample (years)	Gender M/F	Median (range) age at sample (years)	Median (range) length of f-up (years)	Munich/Bristol testing
GADA	14	1	24.5*	6/8	17.1 (7.3-23.8)	18.7 (-0.8-54.7)↓	15/0
IA-2A	6	1	24.5*	1/5	15.9 (10.2-50.1)	23.1 (5.2-28.5)	7/0
ZnT8RA	9	1	24.5*	3/6	16.7 (5.7-65.9)	21.0 (3.5-31.0)↓	10/0
ZnT8WA	10	1	24.5*	4/6	16.4 (5.7-41.0)	14.1 (5.1-31.0)↓	11/0

*Table 2:6 – Multiple autoantibody positive non-progressor sample set*

\* Range not applicable; F-up: Follow-up; ↓ 3, 2, 1 without follow-up at last contact for GADA, ZnT8RA, and ZnT8WA, respectively. Slow progressors (SPs; total in BOX= 36) are defined as mAutoab+ve FDRs that remain diabetes-free for at least 10 years after mAutoab+ve was first detected (312). SPs that remain diabetes-free over follow-up have been classified into the non-progressors (NP) sample set.

Islet Autoab	n index sample	n f-up sample	Median (range) time between index and f-up sample (years)	Gender M/F	Median (range) sampling time before diagnosis (years)	Median (range) age at diagnosis (years)	Median (range) age at sample (years)	Munich/Bristol testing
GADA	9	1	27.4*	2/7	16.7 (10.4-27.8)	48.1 (22.9-68.0)	32.9 (6.21-40.2)	10/0
IA-2A	4	1	27.3*	2/2	14.5 (11.3-27.8)	41.3 (23.7-67.8)	26.8 (12.4-40.2)	4/0
ZnT8RA	5	1	4.0*	0/5	15.2 (10.4-27.8)	48.2 (30.6-68.0)	33.7 (20.0-40.2)	5/1
ZnT8WA	5	1	2.6*	2/3	13.4 (8.7-23.4)	28.1 (23.7-48.1)	15.6 (11.0-33.7)	5/1

*Table 2:7 – Multiple autoantibody positive slow progressor sample set*

\* Range not applicable; F-up: Follow-up. Slow progressors (SPs; total in BOX= 36) are defined as mAutoab+ve FDRs that remain diabetes-free for at least 10 years after mAutoab+ve was first detected (312). SPs that have progressed to diabetes over follow-up remain defined as a SP. Rough age-matching between GADA, IA-2A, and ZnT8RA/ZnT8WA IgG subclass testing was possible following seroconversion of ≥2 islet autoantibodies. BOX has the largest cohort of SPs identified to date.

Chapter 2 - Characterisation of the ZnT8 humoral response up to T1D onset

Islet Autoab	n index sample	n f-up sample	Median (range) time between index and f-up sample (years)	Gender M/F	Median (range) sampling time before diagnosis (years)	Median (range) age at diagnosis (years)	Median (range) age at sample (years)	Munich/Bristol testing
GADA	8	1	1.9*	4/4	1.3 (0.5-3.2)	24.4 (3.2-41.7)	22.37 (1.6-41.2)	9/0
IA-2A	5	1	1.9*	2/3	1.2 (0.5-1.6)	32.0 (13.5-41.7)	30.6 (12.0-41.2)	6/0
ZnT8RA	11	3	1.9 (0.8-2.4)	6/5	1.3 (0.5-4.3)	18.9 (3.2-41.7)	16.7 (1.6-41.2)	11/3
ZnT8WA	8	3	0.8 (0.5-2.4)	4/4	1.3 (0.5-4.3)	18.2 (11.7-41.7)	15.6 (10.6-41.2)	7/4

*Table 2:8 – Multiple autoantibody positive rapid progressor sample set*

\* Range not applicable; F-up: Follow-up. RPs (estimated total in BOX= ~25) are defined as mAutoab+ve FDRs that progress to disease within 5 years from when mAutoab+ve was first detected. Subsets of samples from RPs were selected based on serum volume availability. It was not possible to age match RPs between GADA, IA-2A, and ZnT8RA/ZnT8WA IgG subclass testing as RPs are generally of a younger age at sample and T1D onset suggestive of a more aggressive T1D phenotype compared to SPs and NPs.

ZnT8A specificity	n	Median (range) ZnT8A titre (AU)	Gender (M/F)	Median (range) age at diagnosis (years)
ZnT8RA-specific	3	7.8 (5.8-133.3)	1/2	8.2 (5.9-15.3)
ZnT8WA-specific	5	12.4 (3.1-207.6)	4/1	11.4 (3.3-12.7)
ZnT8RA/ZnT8WA non-specific	10	110.6 (4.9-260.0) *	8/2	10.41 (3.0-17.8)

*Table 2:9 – New-onset T1D patient ZnT8A sample set*

\* Median (range) across monomeric ZnT8RA and ZnT8WA RIAs. Samples were taken within 3 months of diagnosis and were selected to encompass different ZnT8A levels and specificities and where possible, matched for age at onset.

Chapter 2 - Characterisation of the ZnT8 humoral response up to T1D onset

<b>Islet Autoab</b>	<b>n individuals</b>	<b>n samples</b>	<b>Median (range) autoantibody titre*</b>	<b>Median (range) age at sample (years)</b>	<b>n diagnosed</b>	<b>Median (range) age at diagnosis (years)</b>	<b>Median (range) diabetes duration (years)</b>
<b>GADA</b>	10	12	190.8 (34.1-1159.4)	16.7 (10.2-39.7)	9	13.4 (4.7-29.4)	3.3 (1.3-10.3)
<b>IA-2A</b>	29	37	306.6 (79.0-504.2)	14.5 (6.9-44.7)	27	12.1 (5.9-39.0)	1.0 (0.4-6.4)
<b>ZnT8A</b>							
<i>ZnT8RA/ZnT8WA non-specific</i>	15	15	81.9 (13.0-137.6) **	12.2 (6.7-19.9)	15	11.6 (5.8-18.5)	0.8 (0.6-1.5)
<i>ZnT8RA-specific</i>	7	7	80.0 (20.7-122.8)	12.8 (10.7-15.6)	7	12.0 (10.1-15.0)	0.7 (0.6-1.5)
<i>ZnT8WA-specific</i>	3	4	63.5 (25.6-95.4)	12.4 (6.6-13.0)	3	11.5 (6.0-12.4)	0.7 (0.6-1.2)

*Table 2:10 – Screening T1D patient sample set for GADA, IA-2A, ZnT8RA, & ZnT8WA IgG subclass RIAs*

\* DK units/ml for GADA and IA-2A, and AU for ZnT8RA/ZnT8WA RIAs; \*\* Median (range) across monomeric ZnT8RA and ZnT8WA RIAs.

Chapter 2 - Characterisation of the ZnT8 humoral response up to T1D onset

Islet Autoab	Number of patients/samples	Gender (M/F)	Median age at diagnosis (yrs; range)	Median age at sample (yrs.; range)	IgG1 mean ΔCPM range	IgG2 mean ΔCPM range	IgG3 mean ΔCPM range	IgG4 mean ΔCPM range
GADA*	2/7	0/2	4.7 (4.7-14.9)	9.5 (8.4-16.6)	343-15749	2-485	32-1514	14-352
IA-2A*	4/5	2/2	10.9 (10.5-17.6)	11.4 (10.9-19.0)	10049-14961	35-5811	47-2570	0-470
ZnT8RA ZnT8WA	1	0/1	15.7	1.2	247.5-356 -18-31	5453-5740 2930-4734	48-70 3.5-58	293.5-297 114-190

*Table 2:11 – Quality control sample sets for GADA, IA-2A, ZnT8RA, & ZnT8WA IgG subclass RIAs*

From the GADA IgG subclass screening sample set (n=12), a total of 7 serum samples taken from two screened patients were pooled for two composite IgG subclass QCs\*: IgG1/IgG2 and IgG1/IgG3/IgG4 QCs. From the IA-2A IgG subclass screening sample set (n=60), a total of 5 serum samples (2 from one individual) from four screen patients were pooled for two composite IgG subclass QCs\*: IgG1/IgG2 and IgG1/IgG3/IgG4 QCs. From the ZnT8RA/ZnT8WA IgG subclass screening sample set (n=26), it was clear that detection of IgG subclasses (other than IgG1) for ZnT8A responses was rare even in ZnT8A responses of high titre (>100 AU) taken after T1D onset (<2 years). Due to assay costs and the high sample volume that the IgG subclass RIA requires, further screening of samples for QCs was deemed superfluous. However, one patient with a ZnT8A non-specific response had IgG2>IgG1 ≈ IgG4 response for the ZnT8R antigen but had IgG2>IgG4 response for the ZnT8W antigen. Therefore, this sample in all ZnT8RA/ZnT8WA IgG subclass assays as a positive QC. All samples selected for QCs were selected for high serum volume availability and a range of IgG subclass binding where possible. Once established, positive QCs were run in all assays and were used to evaluate assay reproducibility. An anonymised autoantibody negative control was used as a negative QC and was also run in all assays. No other information was available from this individual.

### 2.3.2.2 Detection of ZnT8A, GADA, & IA-2A IgG subclasses by RIA

The method for detecting GADA, IA-2A, and IAA IgG subclasses by RIA published previously (244, 317) was applied to ZnT8RA/ZnT8WA responses and was compared with GADA and IA-2A. The method replaces the PAS immunoprecipitate of the traditional RIA (**Figure 1:16**) with biotinylated IgG subclass-specific mouse anti-human monoclonal antibodies bound by Streptavidin Sepharose beads (Sigma Aldrich, Dorset, UK) (**Figure 2:11**). Commercially available mouse anti-human IgG subclass monoclonal antibodies used in this project for IgG1 (clone G17-1), IgG2 (clone G18-21), and IgG4 (clone FDC-14) were available from BD Biosciences, San Diego, USA, and were identical to the latest publication (317). However, for IgG3, a different clone (HP6047) from Invitrogen, Thermo Fisher, CA, USA, was employed. Non-specific binding was determined using a mouse anti-rat IgM monoclonal antibody (clone G53-238) from BD Biosciences.

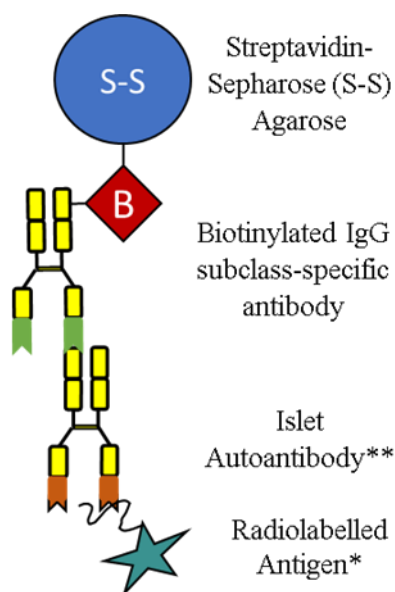


**Figure 2:11 – Schematic diagram of the IgG subclass RIA**

\* GAD65 (aa1-585), IA-2IC (aa606-979), ZnT8 (aa268-369; monomeric peptides with either arginine (R) or tryptophan (W)) or Insulin. \*\* Islet autoantibodies specific to recombinant antigen

Autoantibodies in serum specific to GAD65/IA-2/ZnT8 bind to radiolabelled antigen. Immunocomplexes are then precipitated using a biotinylated IgG subclass-specific secondary antibody and Streptavidin-Sepharose (S-S). Unbound excess radiolabelled antigen is excluded by serial wash and centrifugation steps. After the addition of MicroScint40 (PerkinElmer), residual radiation in counts per minute (CPM) is detected on a beta scintillation counter where CPM is proportional to the autoantibody level present in serum.

### 2.3.2.2.1 Assay buffers

Phosphate buffered saline (PBS) - 50 mM phosphate buffer and 150 mM NaCl, pH 7.4.

TBST

TBST-BSA

### 2.3.2.2.2 Generation of [35-S] radiolabelled antigens

The protocol detailed in 2.2.2.3.2 was followed to generate [35-S]-radiolabelled recombinant antigens (GAD65, IA-2, ZnT8R, and ZnT8W).

### 2.3.2.2.3 Preparation of serum samples

In a 96-deep well plate (Sarstedt), 2µl of serum sample was plated in duplicate per IgG subclass (IgG1, IgG2, IgG3, and IgG4), the anti-rat IgM negative control, and total IgG detection by ethanolamine-blocked Protein G Sepharose (EB-PGS) (**Figure 2:12**). Serum was incubated with 24,000 (± 1,000 CPM) of [35-S]-GAD65/IA-2/ZnT8 (encoding R325 or W325) antigen, diluted in TBST-BSA, overnight (19-21 hours) at 4°C. QCs for these assays were developed in 2.3.3.3.2.

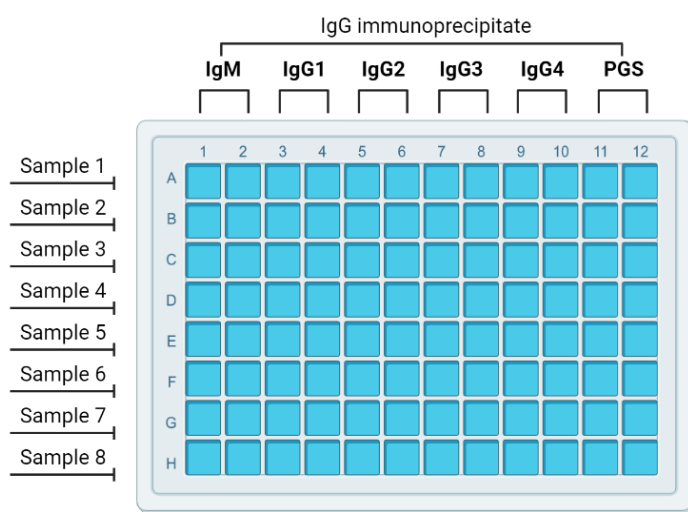


*Figure 2:12 – GADA, IA-2A, & ZnT8A IgG subclass RIA plate set-up*

Image created using BioRender.com. A total of 8 serum samples per 96 deep-well plate can be assayed. Columns 1-12 denote wells corresponding to the different IgG immunoprecipitates.

#### **2.3.2.2.4 Preparation of IgG subclass-specific immunoprecipitate**

Reported previously using the same method (244), the quantity of mouse anti-human monoclonal IgG subclass antibodies (5µg/well) and streptavidin beads (10µg/well) required to completely capture IgG in the reaction was determined by checkerboard titration for GADA and IA-2A. This was assumed sufficient for ZnT8A using the same volume of serum (2µl).

Biotinylated IgG subclass-specific mouse anti-human monoclonal antibodies (IgG1, IgG2, IgG3, and IgG4) and the mouse anti-rat monoclonal IgM at 5µl/well were incubated overnight (~18 hours) with 12.5µl/well of Streptavidin Sepharose (S-S; GE Healthcare) and 30µl/well PBS in 15ml Falcon tubes on an inverting rotatory wheel overnight at 4°C. After overnight incubation, each Falcon tube was washed once in PBS following centrifugation (1500rpm at 4°C for 3mins) and the supernatant was removed. This was repeated using TBST twice for a total of 3 washes. After the final wash, the supernatant was removed, and the bound IgG-Subclass-Streptavidin-Sepharose (IgG-SSS) pellet was resuspended in 53.75µl/well TBST.

#### **2.3.2.2.5 IgG subclass RIA methodology**

Prepared IgG-SSS at 50µl/well was added to wells corresponding to IgG1/IgG2/IgG3/IgG4 and anti-rat IgM. For detection of total IgG, 50µl/well of a 50% suspension of EB-PGS in TBST was added to the corresponding wells. After immunoprecipitates were added, the 96-well plate was centrifuged (1500rpm at 4°C for 3mins) and incubated at 4°C for 1hr on an orbital shaking platform (700rpm). Excess unbound radiolabelled antigen was excluded by centrifugation (1500rpm at 4°C for 3mins) and five serial washes in TBST. Samples were transferred from deep-well plates to 96-well OptiPlates™ (Perkin Elmer) by multichannel pipetting, centrifuged (1500rpm, at 4°C for 3mins), and aspirated for a 30µl end volume. Following the addition of 200µl Microscint40 (Perkin Elmer) and orbital shaking for 15mins, remaining radiolabelled immunocomplexes were detected (5min/well time-lapse) using a TopCount plate scintillation counter (Perkin Elmer) expressed in CPM (**Figure 2:13**).

Total Length of the IgG Subclass RIA: ~27 hours

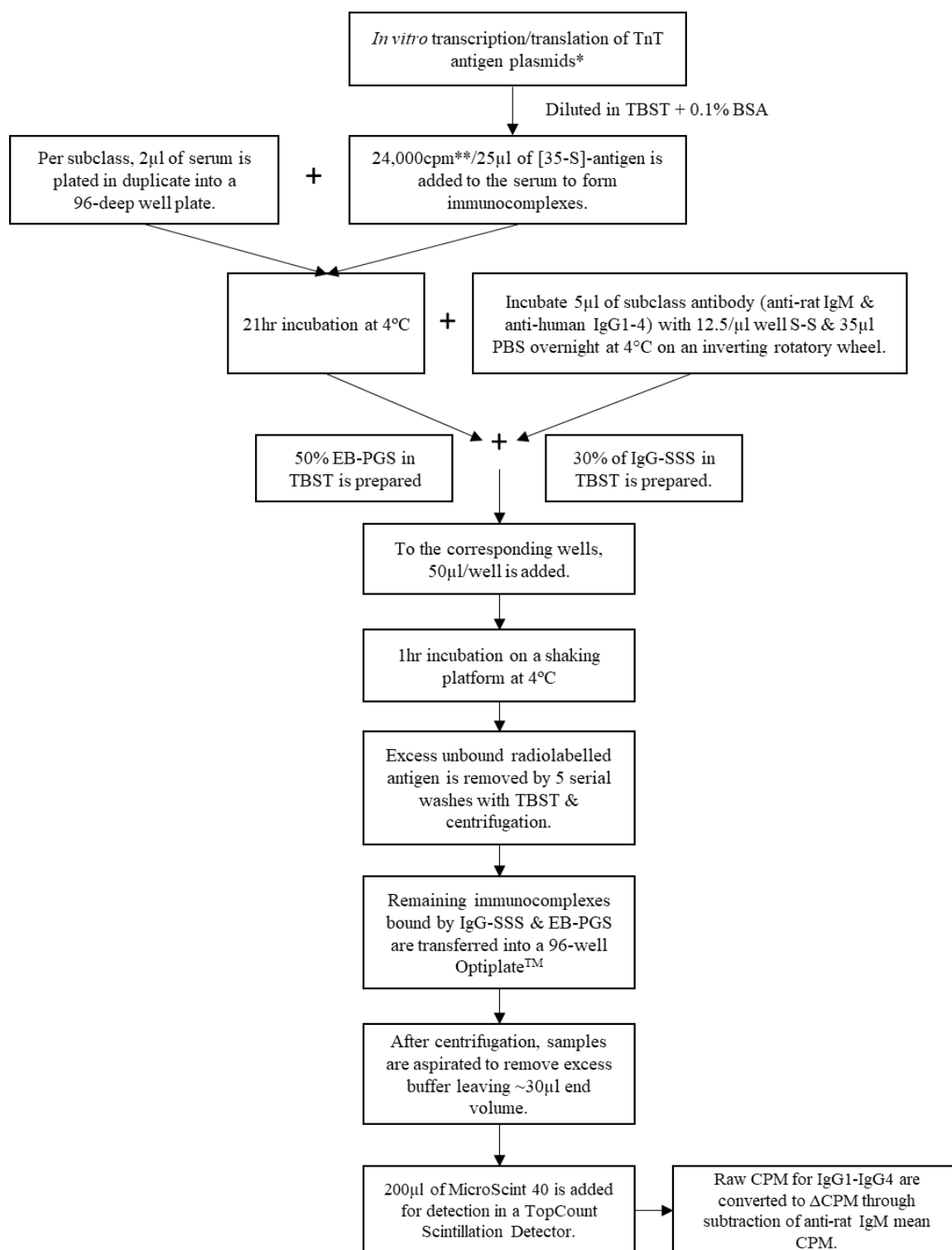


**Figure 2:13 – Basic RIA methodology for detection of GADA, IA-2A, & ZnT8A IgG subclasses**

\* Recombinant [35-S]-methionine radiolabelled GAD (aa1-585), IA-2IC (aa606-979) and ZnT8R/ZnT8W (aa368-369 encoding R or W at aa325) antigens are synthesised in-house using a TnT SP6 Quick Coupled Transcription/Translation Reticulocyte System (Promega) with 30% and 10% incorporation deemed acceptable for GAD/IA-2, and ZnT8A, respectively. CPM: counts per minute; EB-PGS: ethanolamine-blocked Protein G Sepharose; TBST: Tris buffered saline with 0.15% Tween-20; IgG-SSS: IgG-Subclass-Streptavidin-Sepharose. Total assay length excludes *in vitro* transcription/translation preparation of antigen.

### 2.3.2.3 Statistical analysis

---

To account for assay background, all data are expressed as mean delta CPM ( $\Delta$ CPM) for all IgG immunoprecipitates, calculated by: mean CPM of IgG subclass/PGS – anti-rat IgM mean CPM. Data collected in Munich (training period: predominantly applicable to the mAutoab+ve progressor sample set) and Bristol (during PhD project) were considered positive using different detection thresholds [Munich: >32 (GADA), >16 (IA-2A), and >30 (ZnT8RA and ZnT8WA); Bristol: >100 for all].

To compare between autoantibody responses in all progressor sample sets, responses were categorised into IgG1-restricted (IgG1 only) and IgG-unrestricted (IgG1 + any single or combination of IgG2-IgG4). Proportions of IgG subclass positivity with categorical variables were compared using the Chi-squared ( $\chi^2$ ) or Fisher's exact tests where appropriate. Assessing assay reproducibility through developed QCs, inter-assay variation of mean  $\Delta$ CPM was assessed using standard deviation (SD) and coefficient of variation [CV = (mean  $\Delta$ CPM  $\div$  SD)  $\times$  100 (%)]. Spearman's rank ( $r$ ) correlation test was used between IgG subclasses and total IgG determined either by PGS (mean  $\Delta$ CPM) in the IgG subclass RIA or units of autoantibody titre in the traditional RIA [for GADA and IA-2A (DK units/ml) and for ZnT8RA/ZnT8WA (AU)]. Statistical analysis was performed in GraphPad PRISM (v. 9.1.0) and an alpha value  $p < 0.05$  was considered significant.

---

## 2.3.3 Results

---

### 2.3.3.1 Multiple autoantibody positive progressor sample set

---

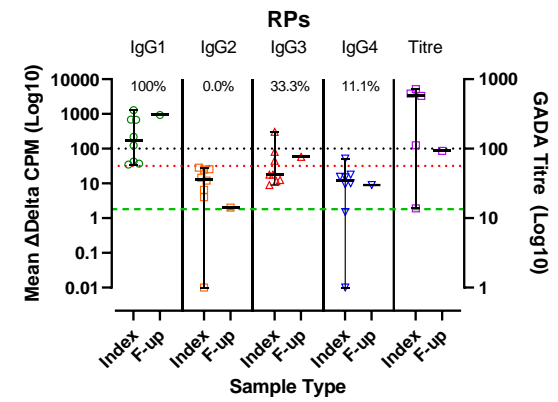
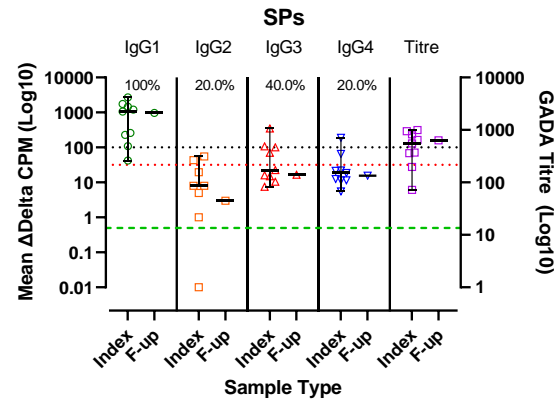
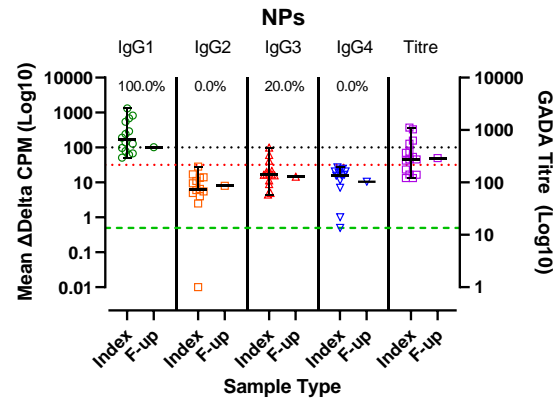
Using the mean  $\Delta$ CPM detection thresholds for data obtained in Munich or Bristol, the IgG subclass responses for GADA, IA-2A, ZnT8RA, and ZnT8WA in the mAutoab+ve progressor sample set is detailed in **Figure 2:14**. Small sample sizes did not allow for comparison, and therefore, results are purely descriptive.

In all sample sets, IgG1 was detected in all autoantibody positive samples for GADA, IA-2A, and ZnT8RA/ZnT8WA. In ZnT8RA responses, IgG3/IgG4 was detected in SPs (16.7%) and RPs (range 7.1-14.3%) but not NPs whereas, for ZnT8WA responses, IgG3/IgG4 was only present in RPs (18.2%). For both ZnT8RA and ZnT8WA, IgG2 was comparable across all progressors.

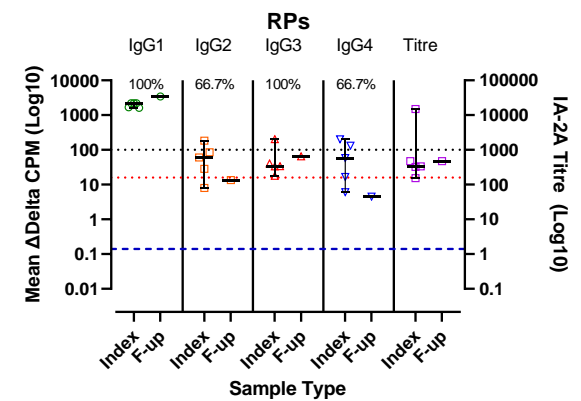
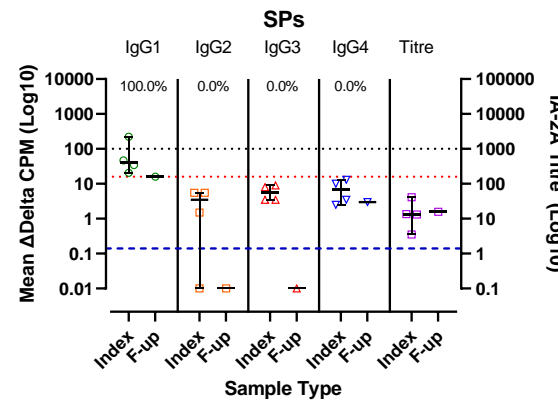
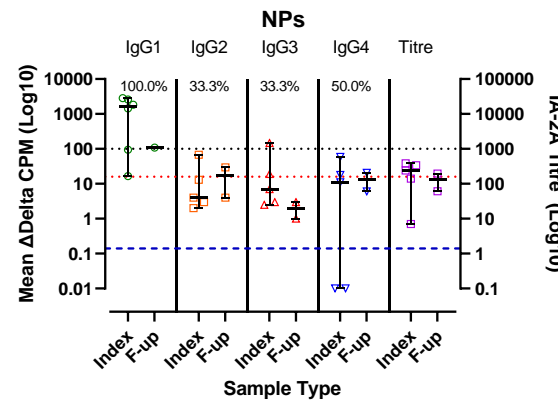
The prevalence of IgG2-IgG4 showed the greatest discrimination between SPs (0%) and RPs (range 66.7-100%) in IA-2A responses. Whereas IgG2-IgG4 prevalence in GADA responses was comparable between all progressors but IgG3 was more common than IgG2 or IgG4.

To compare between autoantibody responses in all progressor sample sets, responses were categorised into IgG1-restricted (IgG1 only) and IgG-unrestricted (IgG1 + any single or combination of IgG2-IgG4).

## GADA



## IA-2A



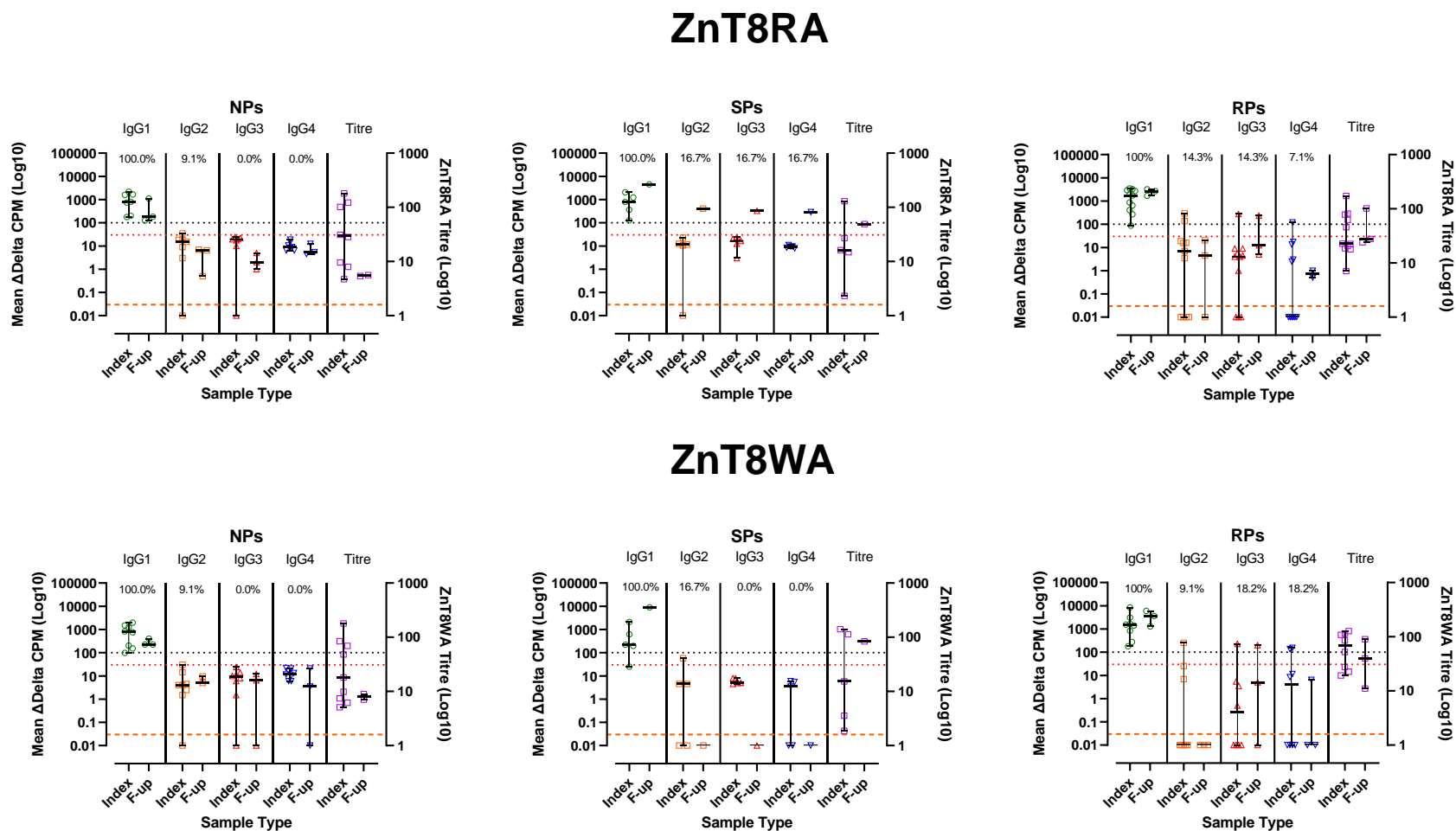


Figure 2:14 – GADA, IA-2A, ZnT8RA, & ZnT8WA IgG subclasses in the multiple autoantibody positive progressor sample set

NP: non-progressor; SP: slow progressor; RP: rapid progressor. Dotted lines: Munich (red) and Bristol (black) IgG subclass detection thresholds based on mean  $\Delta$ CPM. Dashed lines denote autoantibody titre positivity thresholds derived from conventional RIAs; GADA/IA-2A (DK units/ml) and ZnT8RA/ZnT8WA (AU). Despite the small sample sizes, GADA IgG subclasses showed some discrimination between progressor categories. IA-2A IgG subclasses offer the best discrimination between progressor categories. There may be subtle differences between ZnT8RA and ZnT8WA IgG subclass responses between categories of progressors with better discrimination observed for ZnT8WA IgG subclass responses. Small sample sizes violate  $\chi^2$  test assumptions.

The prevalence of IgG-unrestricted responses may discriminate slow and rapid progressors in IA-2A and ZnT8RA/ZnT8WA responses but not GADA responses.

The frequency (%) of IgG1-restricted versus IgG-unrestricted responses (positive by the respective mean  $\Delta$ CPM detection thresholds) are presented in **Figure 2:15**. The prevalence of GADA IgG-unrestricted responses showed some evidence of discriminating between categories of progressors: NPs 4/15 (26.7%); SPs 5/10 (50.0%); RPs 4/9 (44.4%). The prevalence of IA-2A IgG-unrestricted responses showed the most promising discrimination between SPs and RPs. Positive for any subclass (IgG2-IgG4): NPs 3/6 (50.0%); SPs 0/5 (0.0%); RPs 6/6 (100.0%). There was a much higher prevalence of IgG3 and a lower prevalence of IgG2 and IgG4 than anticipated (from previous studies **Table 2:5**) in GADA and IA-2A responses.

Whereas, ZnT8RA/ZnT8WA responses were largely IgG1-restricted with a comparable prevalence of IgG-unrestricted responses across all progressor categories but were highest in RPs. For ZnT8RA: NPs 1/10 (10.0%); SPs 1/6 (16.7%); RPs 3/14 (21.4%). For ZnT8WA: NPs 1/11 (9.1%); SPs 1/6 (16.7%); RPs 3/14 (21.4%). From this small data set, there could be a suggestion of ZnT8A IgG-unrestricted responses (spectrum of IgG2-IgG4) discriminating RPs from NPs/SPs.

All IgG subclasses were detected in selected mAutoab+ve FDRs, but differing frequencies were found according to the type of progressor and autoantibody response (**Table 2:12**). Based on the sample set size, it is unclear whether IgG subclass detection would be able to further discriminate SPs from RPs, but IA-2A followed by ZnT8RA/ZnT8WA appear the most promising whereas, IgG1-restricted GADA responses may be more common in NPs compared to SP or RPs.

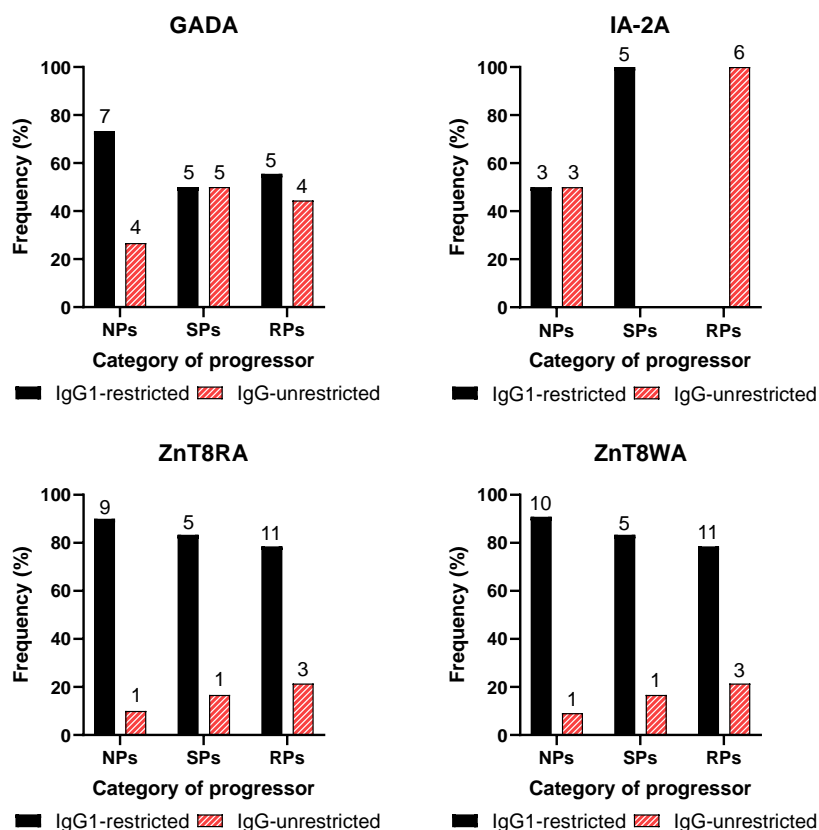


**Figure 2:15 – Overall frequency of GADA, IA-2A, ZnT8RA, & ZnT8WA IgG1-restricted & IgG-unrestricted responses in the multiple autoantibody positive progressor sample set**

Frequency percent (%) out of the total number of samples tested for IgG subclasses. The number of samples is denoted above bars. IgG1 only: IgG1-restricted responses; IgG1 + any single or combination of IgG2-IgG4: IgG-unrestricted response. GADA IgG subclasses are least likely to be informative in discriminating slow versus rapid progressors of disease. IA-2A IgG-unrestricted responses showed the most promising discrimination of rapid progressors. Similarly, there is a slight suggestion that ZnT8RA/ZnT8WA IgG-unrestricted responses may be higher in RPs versus SPs; however, a bigger sample set and/or additional longitudinal follow-up samples are needed.

Islet Autoab	Anticipated IgG response in FDRs	NPs	SPs	RP
<b>GADA</b>	IgG1>IgG4>IgG2>IgG3	IgG1>IgG3>IgG2>IgG4	IgG1>IgG3>IgG2~IgG4	IgG1>IgG3>IgG4
<b>IA-2A</b>	IgG1>IgG4>IgG2>IgG3	IgG1>IgG4>IgG2~IgG3	IgG1	IgG1>IgG3>IgG4>IgG2
<b>ZnT8RA</b>	Unknown (IgG1-dominant)	IgG1>IgG2	IgG1>IgG2~IgG3~IgG4	IgG1>IgG2~IgG3>IgG4
<b>ZnT8WA</b>	Unknown (IgG1-dominant)	IgG1>IgG2	IgG1>IgG2	IgG1>IgG3~IgG4>IgG2

**Table 2:12 – Summary of IgG subclass profiles in the multiple autoantibody positive progressor sample sets**

In GADA responses, IgG3 was the second most prevalent IgG subclass (as opposed to the last), and IgG4 was the least frequent IgG subclass (opposed to the second). In IA-2A responses, NPs had a similar IgG profile to what was anticipated, but SPs had IgG1-restricted responses, and IgG3 was the second most prevalent IgG subclass in RPs (as opposed to the last). IgG3 and IgG4 were higher in ZnT8RA responses from SPs and RPs, perhaps discriminating individuals with higher disease risk whereas, IgG3 and IgG4 in ZnT8WA were only present in RPs. Therefore, IgG subclasses in ZnT8A responses may aid the discrimination of high-risk individuals.

### 2.3.3.2 New-onset T1D patient sample set

A cohort of T1D patients was tested to investigate whether ZnT8A responses were less IgG1-restricted closer to T1D onset. This provided an opportunity to confirm previous findings regarding IgG1's relationship with different immunoprecipitates (PAS/PGS).

#### IgG1 in ZnT8RA and ZnT8WA responses correlates with total IgG & overall ZnT8A titre

The IgG1 mean  $\Delta$ CPM strongly correlated with the total IgG (PGS) mean  $\Delta$ CPM in all ZnT8RA-positive [n=13/28 (46.4%);  $r$  0.82 (95% CI: 0.49-0.95),  $p=0.0009$ ] and ZnT8WA-positive [n=15/28 (53.6%);  $r$  0.96 (95% CI: 0.87-0.99),  $p<0.0001$ ] patients (**Figure 2:16**).

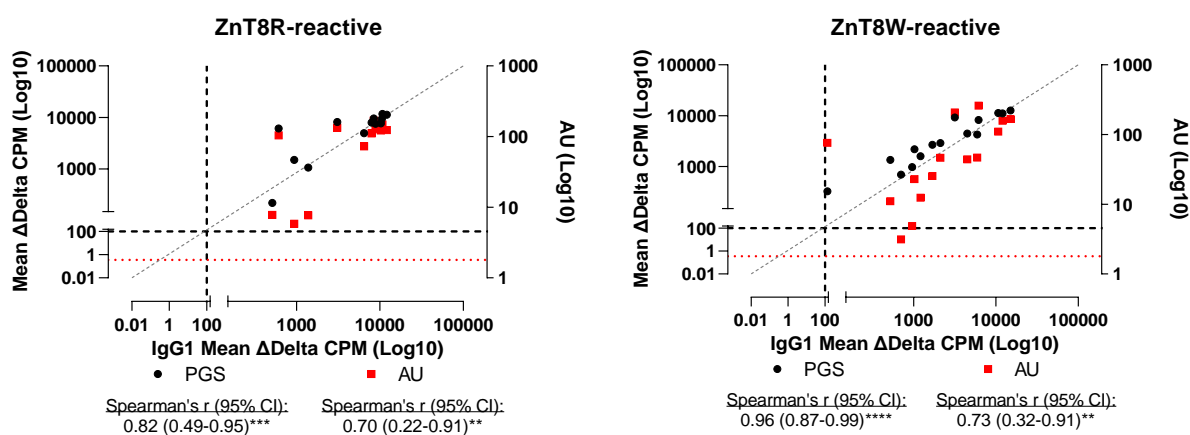
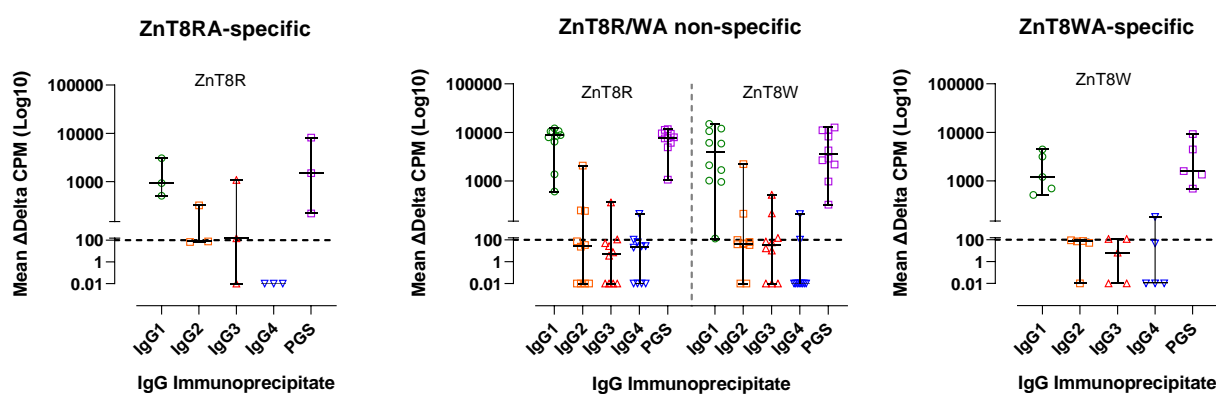


**Figure 2:16 – IgG1 correlates with total IgG (PGS) & overall ZnT8A level (AU) in ZnT8R-reactive & ZnT8W-reactive new-onset T1D patients**

From 28 new-onset T1D patients, 13 patients were ZnT8RA-reactive, and 15 were ZnT8WA-reactive. The patient categories were age-matched and encompassed a range of overall ZnT8A levels (AU by RIA) where possible. Binding of IgG1 (mean  $\Delta$ CPM) strongly correlated with total IgG (PGS) and overall ZnT8A level for ZnT8R-reactive ( $p=0.0009$  and  $p=0.01$ , respectively) and ZnT8WA-reactive ( $p<0.0001$  and  $p=0.003$ , respectively) responses.

New-onset T1D patients had comparable proportions of IgG1-restricted and IgG-unrestricted ZnT8RA and ZnT8WA responses regardless of overall ZnT8A specificity.

Independent of ZnT8A specificity, ZnT8RA/ZnT8WA responses were predominantly IgG1-restricted (n=16/28; 57.1%), but 12/28 (42.9%) new-onset T1D patients had IgG-unrestricted responses. In the 10 patients with ZnT8A non-specific responses, there was a similar prevalence of IgG-unrestricted responses towards ZnT8R and ZnT8W antigens (range 10-30%, n=1-3; **Figure 2:17**).



ZnT8A specificity	ZnT8 antigen	n	IgG1 (%)	IgG2 (%)	IgG3 (%)	IgG4 (%)	PGS (%)
ZnT8RA-specific	ZnT8R	3	100.0	33.3	66.6	0.0	100.0
ZnT8R/WA non-specific	ZnT8R	10	100.0	30.0	20.0	20.0	100.0
ZnT8R/WA non-specific	ZnT8W	10	100.0	20.0	30.0	10.0	100.0
ZnT8WA-specific	ZnT8W	5	100.0	0.0	20.0	20.0	100.0

*Figure 2:17 – ZnT8A IgG subclasses in new-onset T1D patients*

A subset of 28 ZnT8A positive new-onset T1D patients was tested for ZnT8RA and ZnT8WA IgG subclasses according to the ZnT8A specificity of the response; 3 ZnT8RA-specific, 10 ZnT8 non-specific, and 5 ZnT8WA-specific responses. A total of 13 patients were ZnT8RA-reactive, and 15 were ZnT8WA-reactive. The patient categories were age-matched and encompassed a range of ZnT8A titre (AU by RIA) where possible. A mean  $\Delta$ CPM >100 denoted by the black dashed line was used as the detection threshold of all IgG subclasses. A total of 12 patients (42.9%) had evidence of IgG-unrestricted responses, but 16 (57.1%) had IgG1-restricted responses independent of ZnT8A specificity.

There was no evidence of a difference between ZnT8RA and ZnT8WA positive patients and the type of IgG subclass response (IgG1-restricted versus IgG-unrestricted,  $p>0.999$ ; **Figure 2:18**). Similarly, IgG1 level was not associated with IgG1-restricted versus IgG-unrestricted responses in ZnT8RA or ZnT8WA responses ( $p>0.05$ ; data not shown). Therefore, the presence of other IgG subclasses may not always be related to IgG1 or overall ZnT8A titre.

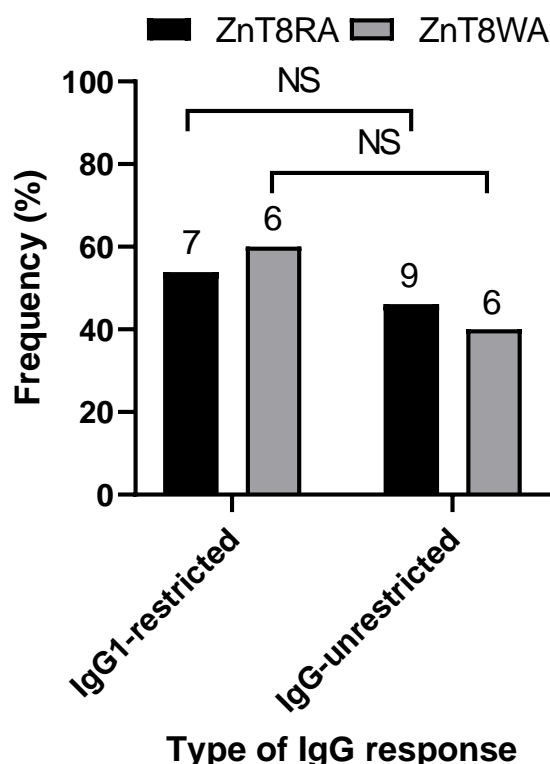


*Figure 2:18 – The proportion of IgG1-restricted & IgG-unrestricted responses in ZnT8RA & ZnT8WA positive new-onset T1D patients*

Frequency percent (%) out of the total number of samples tested for ZnT8RA/ZnT8WA IgG subclasses. The number of samples is denoted above bars. There was no difference in the type of IgG subclass response between ZnT8RA and ZnT8WA responses in new-onset T1D patients ( $p>0.999$ ), but there was almost an overall equal proportion of IgG1-restricted and IgG-unrestricted responses.

This subset of new-onset T1D patients indicates that there is a comparable proportion of IgG1-restricted and IgG-unrestricted responses in ZnT8RA and ZnT8WA positives. This was unexpected given the highly IgG1-restricted ZnT8RA/ZnT8WA responses obtained in the mAutoab+ve progressor sample set.

### 2.3.3.3 Screening T1D patients for quality control development sample sets

Sample sets from T1D patients were screened for IgG subclasses to develop QCs.

#### 2.3.3.3.1 Screening sample set

For GADA, IA-2A, and ZnT8RA/ZnT8WA IgG screening sample sets, a mean  $\Delta$ CPM >100 was considered positive to account for non-specific binding and assay background.

#### The prevalence of GADA and IA-2A IgG subclasses but not ZnT8RA/ZnT8WA allowed for the development of QCs.

The frequencies of specific IgG subclasses differed between autoantibody responses and did not appear related to age and/or range of titre (**Figure 2:19**). For all responses, IgG1 was the most dominant IgG and was detected in all samples. In order of prevalence: GADA: IgG1>IgG3>IgG4>IgG2; IA-2A: IgG1>IgG4>IgG3>IgG2; ZnT8RA: IgG1>IgG2>IgG3/IgG4; ZnT8WA: IgG1>IgG3>IgG2/IgG4 (**Table 2:13**). Confirming previous reports on GADA and IA-2A IgG subclass responses but with the addition of ZnT8RA/ZnT8WA responses, IgG1 correlated with PGS ( $p=0.012$ - $<0.0001$  for all responses) and overall autoantibody titre ( $p=0.0006$ - $<0.0001$  for all responses but ZnT8WA,  $p=0.06$ ) (**Figure 2:20**).

Islet Autoab	IgG1 (n; %)	IgG2 (n; %)	IgG3 (n; %)	IgG4 (n; %)
GADA (n=12)	12; 100.0	1; 8.3	7; 58.3	3; 25.0
IA-2A (n=37)	37; 100.0	12; 32.4	15; 40.5	19; 51.4
ZnT8RA (n=22)	22; 100.0	4; 18.2	1; 4.5	1; 4.5
ZnT8WA (n=19)	19; 100.0	1; 5.3	3; 15.8	1; 5.3

*Table 2:13 – The frequency of specific IgG subclasses in the T1D patient screening sample set*

The very low prevalence of IgG3 and IgG4 in individuals with <2 years disease duration prevented the development of ZnT8RA/ZnT8WA QCs to encompass all IgG subclasses. There was one individual with a ZnT8A non-specific response that had IgG2>IgG1 $\approx$  IgG4 response for ZnT8R but IgG2>IgG4 response for ZnT8W. This individual was used as a positive QC in further ZnT8RA/ZnT8WA IgG subclass assays.

## Chapter 2 - Characterisation of the ZnT8 humoral response up to T1D onset

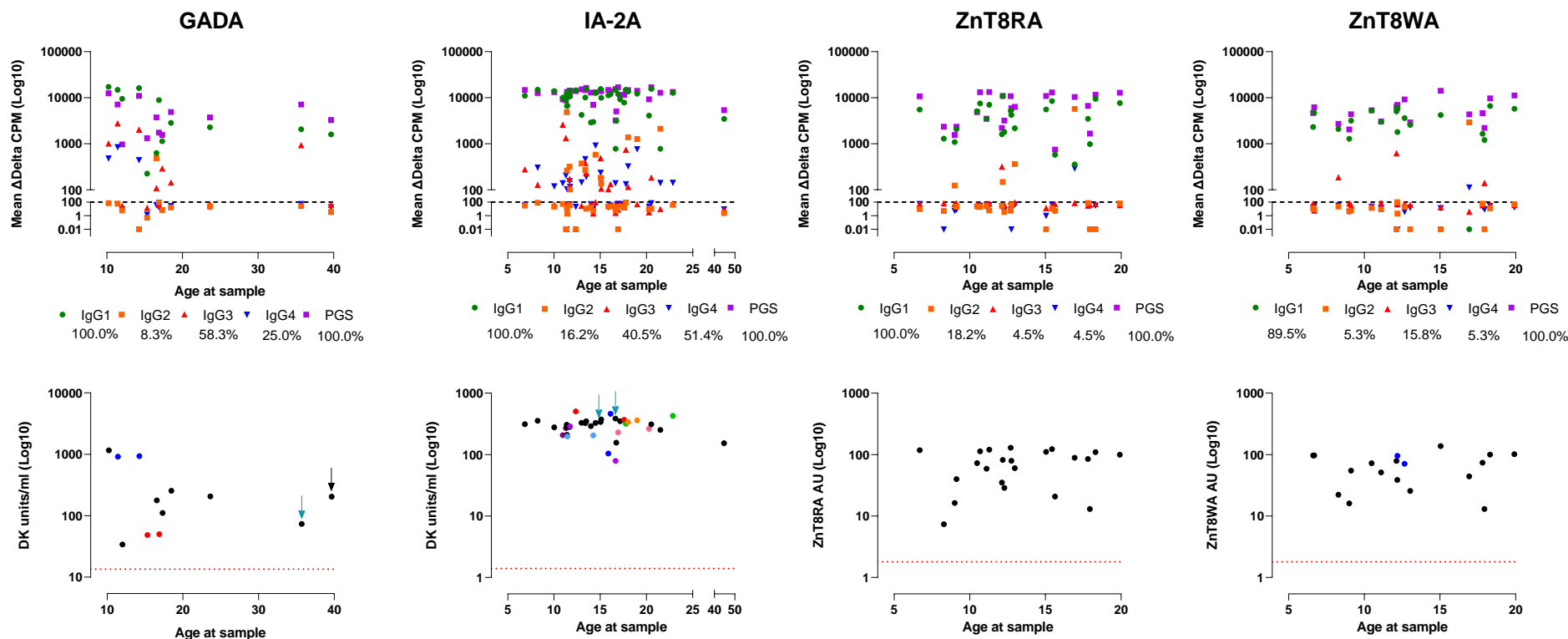


*Figure 2:19 – Prevalence of GADA, IA-2A, ZnT8RA, & ZnT8WA IgG subclasses in the screening sample sets*

GADA: pairs of coloured points denote samples from the same individual (<3 years apart); black arrows denote samples taken >10 years disease duration & remaining samples were taken 5-10 disease duration; teal arrows denote FDRs that have not progressed to disease at final follow-up. IA-2A: pairs of coloured points denote samples from the same individual (0.3-5.2 years apart); teal arrows denote FDRs that have not progressed to disease at final follow-up. ZnT8WA: pairs of coloured points denote samples from the same individual (<0.6 years apart). In order of prevalence: GADA: IgG1>IgG3>IgG4>IgG2; IA-2A: IgG1>IgG4>IgG3>IgG2; ZnT8RA: IgG1>IgG2>IgG3/IgG4; ZnT8WA: IgG1>IgG3>IgG2/IgG4. The IgG1 response for GADA, IA-2A and ZnT8RA/ZnT8WA appears to most closely resemble the overall autoantibody level obtained by conventional RIA.

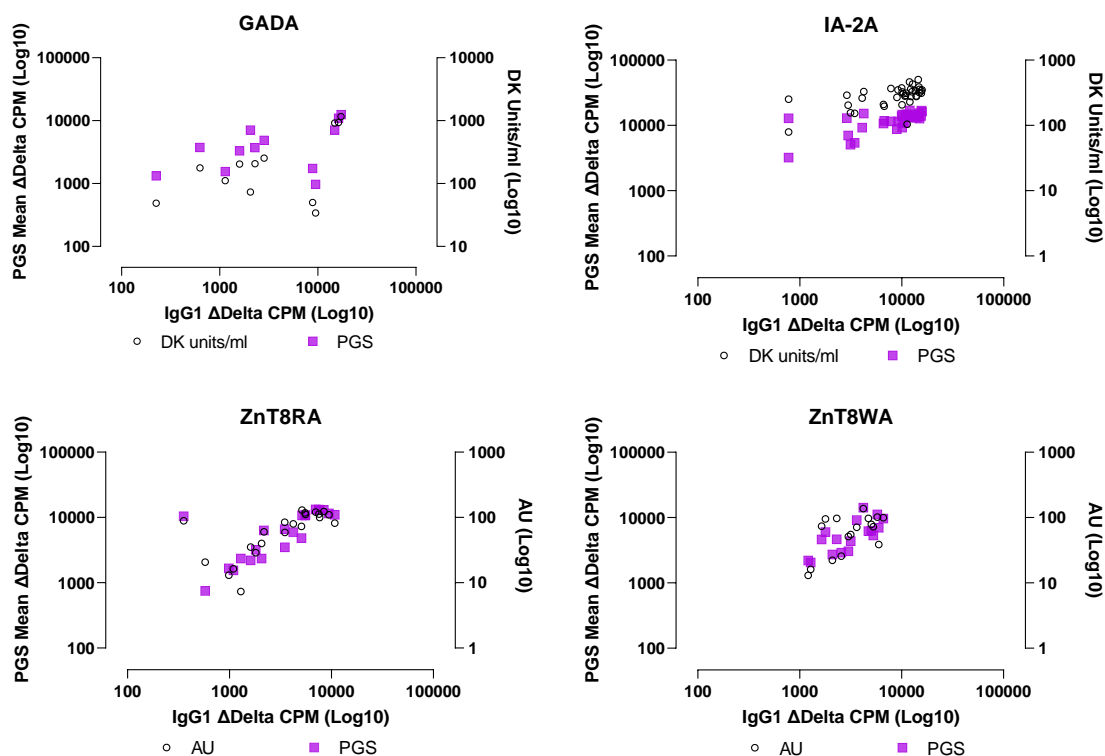


**Figure 2:20 – Correlation of IgG1 with total IgG (PGS) & overall autoantibody level (units) in GADA, IA-2A, ZnT8RA, & ZnT8WA screening sample sets**

Purple squares denote correlation between IgG1 and total IgG (PGS), and black open circles denote correlation between IgG1 and overall autoantibody level (DK units/ml for GADA and IA-2A; AU for ZnT8RA and ZnT8WA). The IgG1 response closely resembled total IgG and overall autoantibody level. For IA-2A and ZnT8RA/ZnT8WA but not GADA, the IgG1 response was correlated with PGS and overall autoantibody level [IA-2A:  $p < 0.0001$  and  $p = 0.0005$ , respectively; ZnT8RA: both  $p < 0.0001$ ; ZnT8WA:  $p = 0.0002$  and  $p = 0.02$ , respectively; GADA:  $p = 0.06$  and  $p = 0.07$ , respectively]. A correlation may be expected in a bigger sample set for GADA.

A summary comparing IgG subclass profiles between tested RPs (<5years before onset) and the T1D patient screening sample sets (range 0.4-10.3 years disease duration) showed similar profiles across all autoantibody responses (**Table 2:14**).

Islet Autoab	RPs	T1D Patients
<b>GADA</b>	IgG1>IgG3>IgG4 <5yrs from onset	IgG1>IgG3>IgG4>IgG2 <10.3yrs disease duration
<b>IA-2A</b>	IgG1>IgG3>IgG4>IgG2 <5yrs from onset	IgG1>IgG4>IgG3>IgG2 <6.4yrs disease duration
<b>ZnT8RA</b>	IgG1>IgG2≈IgG3>IgG4 <5yrs from onset	IgG1>IgG2>IgG3≈IgG4 <2yrs disease duration
<b>ZnT8WA</b>	IgG1>IgG3≈IgG4>IgG2 <5yrs from onset	IgG1>IgG3>IgG2≈IgG4 <2yrs disease duration

**Table 2:14 – IgG subclass profiles between RPs & T1D patients (screening sample set)**

The cross-sectional comparison between RPs and T1D patients have shown similar IgG subclass profiles for all autoantibody responses.

### **2.3.3.3.2 Quality control sample set**

The IgG subclass assays show good reproducibility using the mean  $\Delta$ CPM from quality control samples.

Screening T1D patients (<10 years disease duration) and the subsequent development of QCS, where possible, showed that mean  $\Delta$ CPM of positive QCs showed generally good reproducibility, typically regarded as <30% CV (**Table 2:15**). As expected, higher SD and CV was obtained in the negative QC, anti-rat IgM control, samples with low-level IgG subclass positivity, and samples negative for a particular IgG subclass.

Excluding the IgG subclasses that each QC is negative for, the two GADA positive QCs had CVs <30% (median CV of 12.9%). The two IA-2A positive QCs had CVs <30% (median CV of 6.4%), except for one IgG4 response, and the ZnT8RA/ZnT8WA positive QC had CVs <30% (median 3.4% and 33.4%, respectively), except for one very high IgG2 response.

In particular, the high variability in assay background observed justifies the inclusion of the anti-rat IgM and an autoantibody negative QC in the IgG subclass assays, as it adjusts for inter-assay variation, improves the reproducibility of the positive QCs, and by extension will benefit performing routine assays on other samples.

Chapter 2 - Characterisation of the ZnT8 humoral response up to T1D onset

Islet Autoab	QC sample	No. of tests	Anti-Rat IgM		IgG1		IgG2		IgG3		IgG4		PGS	
			Mean CPM	CV (%)	Mean Δ CPM	CV (%)	Mean Δ CPM	CV (%)	Mean Δ CPM	CV (%)	Mean Δ CPM	CV (%)	Mean Δ CPM	CV (%)
GADA	IgG1/IgG2	7	60.9	50.8	414.3	17.3	371.1	12.9	59.4	24.2	60.9	51.1	3560.9	10.4
	IgG1/IgG3/IgG4	7	378.6	129.1	16300.0	6.4	-272.8	-173.2	877.9	33.4	247.9	10.8	15150.8	8.5
	Negative§	6	58.2	30.9	43.6	39.8	0.5	119.7	160.4	156.8	2.6	346.3	310.9	83.8
IA-2A	IgG1/IgG2	8	505.8	49.1	14622.6	4.0	4649.7	22.2	193.0	240.4	-301.8	-90.9	13932.7	6.4
	IgG1/IgG2/IgG3/IgG4	8	246.1	34.5	15000.5	19.9	529.5	23.3	1789.4	25.5	759.2	49.8	15485.4	18.7
	Negative§	10	98.4	90.8	14.5	125.2	-16.2	-150.0	-17.4	-232.9	-20.6	-177.2	-6.9	-1174.2
ZnT8RA*	IgG1/IgG2/IgG4	2	54.5	44.1	301.5	25.3	5596.0	3.6	59.0	26.4	295.3	0.8	10164.5	3.2
	Negative§	1	75.5	-	17.5	-	11.0	-	31.5	-	14.0	-	50.5	-
ZnT8WA*	IgG2/IgG4	2	72.5	68.3	6.8	508.1	3836.8	33.4	30.8	125.3	151.8	35.6	5117.0	20.9
	Negative§	1	87.0	-	129.0	-	104.5	-	151.5	-	96.5	-	140.5	-

*Table 2:15 – Reproducibility of QC sample sets in GADA, IA-2A, & ZnT8RA/ZnT8WA IgG subclass assays during assay optimisation*

\* Sample was taken from the same individual with ZnT8A non-specific responses with a predominantly IgG2 response over other IgG subclasses. § Anonymised sample taken from the same individual. Dark grey: IgG subclass negative QCs; White: IgG subclass positive QCs. A higher standard deviation (SD) and coefficient of variation (CV, %) was obtained in the negative QC, anti-rat IgM control, samples with low-level IgG subclass positivity, and samples negative for a particular IgG subclass.

---

## 2.3.4 Discussion

---

This portion of work sought to evaluate the prevalence of ZnT8RA/ZnT8WA IgG subclasses in mAutoab+ve progressors and after T1D diagnosis (compared with GADA and IA-2A) but also new-onset T1D patients. To our knowledge, this is the first time that ZnT8A IgG subclasses have been investigated. IgG-unrestricted responses in ZnT8A responses were rare prior to onset but were more frequent close to onset.

### 2.3.4.1 Main findings

---

1. The prevalence of IgG subclasses in mAutoab+ve progressors of T1D indicated that ZnT8RA/ZnT8WA responses are largely IgG1-restricted but, the prevalence of IgG-unrestricted responses was highest in RPs. GADA responses had a more IgG1-restricted response in NPs, but IgG1-restricted/IgG-unrestricted responses were comparable between SPs and RPs. The prevalence of IA-2A IgG subclasses showed the greatest discrimination between T1D progressors, SPs IgG1-restricted responses versus RPs IgG-unrestricted responses.

2. In new-onset T1D, there was a comparable proportion of IgG1-restricted/IgG-unrestricted ZnT8RA/ZnT8WA responses regardless of ZnT8A specificity (aa325). The prevalence of IgG1-restricted/IgG-unrestricted responses did not appear related to the level of IgG1 binding. The presence of other subclasses additional to IgG1 may not always be associated with high ZnT8A titres.

3. All IgG subclasses were detected in GADA, IA-2A, and ZnT8RA/ZnT8WA positive T1D patients (sampled 1.5-10 years disease duration). The frequency of IgG subclasses enabled the development of two positive QCs for GADA and IA-2A RIA IgG subclass assays. The use of these QCs in a limited number of further assays generally showed good assay reproducibility (<30% CV) and can be used for future investigations.

4. In all autoantibody responses, IgG1 binding most closely resembled and correlated with total IgG (PGS) and overall autoantibody titre determined by conventional RIA.

### **2.3.4.2 Strengths & limitations**

---

This study benefits from the novel investigation of ZnT8RA/ZnT8WA IgG subclasses in mAutoab+ve T1D progressors compared to GADA and IA-2A) and included FDRs spanning a wide age range (3.2-66.0 years) with follow-up >30 years, and new-onset T1D patients (sampled <3 months of diagnosis with low risk of negative seroconversion). Previous studies of IgG subclasses in T1D were conducted prior to the discovery of ZnT8A (2007) and were either focused on mAutoab+ve children or FDRs with a shorter follow-up (median 5.9 years) and a younger age at IgG subclass detection (median 14.5 years). Therefore, the age range and long follow-up period is competitive and/or unique to the seminal IgG subclass studies in T1D (244, 317, 464-467).

Additionally, this study utilised clones of IgG subclass antibodies and an established IgG subclass RIA protocol published previously (244, 317) and replicated by other studies (464-466), participants from a well-characterised population-based family study, and a population of healthy schoolchildren (used to establish in-house conventional RIA positivity thresholds) to establish IgG subclass-specific positivity thresholds (where possible): 48-49 healthy schoolchildren for GADA and IA-2A IgG subclasses enabled the development of StDS thresholds.

Whilst other studies have developed StDS thresholds based on control subjects replicating the approach by Bonifacio *et al.* (1999) (244, 317, 464-466), this study uniquely includes efforts to further develop the method for routine screening of IgG subclasses by establishing QCs. Both GADA and IA-2A IgG subclass positivity thresholds and QC samples will benefit future

investigations. Further screening for ZnT8RA/ZnT8WA IgG subclasses will hopefully permit the development of pooled QCs and StDS thresholds.

The change in specific murine anti-human IgG subclass clones may be important in interpreting these results; clones of murine anti-rat IgM (G20-127) and anti-human monoclonal antibodies for IgG1 (G17-1), IgG2 (G18-21), and IgG4 (JDC-14) are identical and, from the same company (BD) between a seminal 2004 study and this present study (317). However, the 2004 IgG3 clone (G18-3), used in many studies between 1990-2000, was no longer available. Commercially available IgG3 such as HP6047 (Invitrogen/Sigma) used in the present study specifically binds the IgG3-specific hinge region. Whilst a comparison study may be lacking, one can assume that the increased frequency of IgG3 observed in this study could be related to improved specificity/sensitivity of the HP6047 clone. Therefore, previous diabetes risk prediction models may underestimate the value of IgG3. Owing to IgG3's unique characteristics compared with other IgG subclasses described previously (1.6.2.3.3), IgG3-mediated immunotherapeutics could be advantageous for many human diseases, including T1D and, warrants further mechanistic study (252). Therefore, accurate detection of IgG3 is important.

Furthermore, this study incorporated the immunoprecipitate PGS as a marker of total IgG in all assays as an additional approach to evaluate assay performance and developed a specific PGS-StDS threshold. This was not included in other published studies, but generally, the total IgG subclass binding roughly equated the total IgG (PGS) binding. This provided an important confirmation that sufficient IgG-SSS (5µg/well IgG Ab to 10µg/well streptavidin beads) was present between batches/assays to precipitate immunocomplexes; evident by 100% IgG1 detection by mean  $\Delta$ CPM or StDS thresholds (for GADA and IA-2A only).

It cannot be ruled out that different frequencies of IgG subclasses may be observed according to different antigenic epitopes previously found to be related to T1D risk (325, 339, 340). For instance, testing GADA IgG subclasses to N-terminally truncated GAD65 may improve non-specific binding in NPs/SPs, allowing for better discrimination of RPs (324, 325), but intermolecular epitope spreading to the N-terminus has been observed over follow-up (330, 337). However, reactivity to multiple GAD65 epitopes and the presence of IgG2-IgG4 was related to high GADA titres, but neither was related to T1D risk (317). Whereas in IA-2A responses, the presence of IgG2-IgG4 and reactivity to multiple IA-2-related epitopes was previously linked to high IA-2A titres and T1D risk (317). From our data, the ZnT8A IgG subclass response does not appear to be hugely promising for improving T1D risk, but ZnT8A specificity (325Q) may warrant further study.

Another limitation would be the small cohort size of mAutoab+ve FDRs. However, SPs are rare (312) and, the size of RPs/NPs is comparable to the other seminal studies (244, 317, 464-467). Other possible limitations are that the FDRs were not recruited and followed up from birth, not all FDR samples were tested for all positivity autoantibodies (precluded by serum volume availability), and the longitudinal IgG subclass responses couldn't be evaluated but maybe a future avenue of this work. Additionally, the at-risk FDRs investigated for ZnT8A were generally of older age compared with new-onset T1D patients, but there was not a strong indication that age may influence frequencies of specific IgG subclasses. Nonetheless, it cannot be ruled out that age at sampling could be an important confounder in ZnT8A IgG subclass responses, as production of IgG subclasses may be influenced by immune system maturation and ZnT8A are associated with older age (late childhood-adolescence but is also common in adults) (270, 275, 287, 289, 328). A large natural history study that longitudinally sampled individuals from ZnT8A seroconversion to T1D onset encompassing young- and adult-onset T1D would be required to fully evaluate this and its relation to T1D risk.

### **2.3.4.3 Composition & characteristics of islet autoantibody IgG subclasses**

It was confirmed that GADA, IA-2A, ZnT8RA/ZnT8WA IgG subclass responses are IgG1-dominant with all investigated FDRs and patients having detectable IgG1, independent of titre or other IgG. Additionally, we also showed that the IgG1 response mirrors and correlates with total IgG (PGS) and autoantibody titre (PAS) in all autoantibody responses (244, 317).

Prevalence of IgG2-IgG4 may indicate differences according to autoantibody specificity; IgG3 was more prevalent in GADA responses, IgG4 more prevalent in IA-2A responses, and IgG2 more prevalent in ZnT8RA/ZnT8WA responses. As anticipated, generally, a wider spectrum of IgG subclasses (unrestricted) was present closer to T1D onset in all autoantibody responses, particularly in ZnT8RA/ZnT8WA responses. This may suggest that prior to T1D onset, ZnT8RA/ZnT8WA IgG responses may be more likely to be IgG1-restricted but that close to T1D onset, become more IgG-unrestricted (IgG subclass spreading), possibly reflective of polyclonal B-cell responses, previously indicated in ICA/IA-2A/GADA responses (244, 246, 474) driven by chronic antigen stimulation.

Whilst predictive modelling was not applied, the ability of IA-2A IgG-unrestricted responses but not GADA to discriminate SPs/RPs was evident in our data (317). However, there was no evidence of the low-risk IgG4-restricted IA-2A response in NPs/SPs, previously reported as a protective response for T1D (467). It is possible that GADA IgG1-restricted responses may be more common in individuals less likely to progress to disease, which warrants a larger study, particularly encompassing single GADA responses which are associated with lower T1D risk (287, 288, 291).

The most striking difference in IgG subclass composition, compared with previous studies, was the higher IgG3 prevalence, often the second or third most prevalent IgG in all autoantibody responses. Whilst this is likely due to a more sensitive monoclonal antibody than previous studies (discussed earlier), there are also some alterations in the RIA IgG subclass method employed in this project compared to the original studies (244, 317) that may have influenced the frequency of IgG subclasses. For example, the use of modern plate washers in the present study allows an aqueous end volume of 30 $\mu$ l, which permits better scintillation of residual radioactivity. This is particularly important for low-level detection and likely contributed to the 100% IgG1 detection (independent of titre or response), not always previously reported (**Table 2:4** and **Table 2:5**) and therefore, higher end volumes may have compromised IgG subclass detection in previous studies.

Current conventional antigen-specific RIAs detect the majority of IgG subclasses through PAS and/or PGS immunoprecipitates: PAS preferentially binds the Fc region of human IgG1/IgG2/IgG4 (475, 476), and PGS binds the Fc region of all human IgG subclasses (IgG1/IgG2/IgG3/IgG4) (477). Therefore, the additive benefit of detecting individual IgG subclasses as a screening assay may be minimal in predicting disease risk but is clearly beneficial once identified as autoantibody positive by RIA. Removal of IgG subclass covariates from Cox proportional hazard models that accounted for conventional RIA detection significantly decreased the model fit in predicting disease risk (317). Therefore, the profiles of these subclasses may reflect mechanisms that underpin the pathogenesis or autoimmune prodrome of T1D that cannot be investigated by conventional RIA alone.

Despite this, RIA IgG subclasses are not widely conducted as they are costly in expense (5 times higher than conventional RIA per sample) and sample volume requirements (>25-50 $\mu$ l per islet autoantibody versus 5 $\mu$ l-20 $\mu$ l). Both can be particularly problematic in large-scale

screening trials and blood sample acquisition from infants/young children or by capillary blood sampling. However, in future investigations of ZnT8A IgG subclasses, an important next step would be screening large volume positive samples and samples from the general population to establish IgG subclass-specific positivity thresholds for ZnT8RA/ZnT8WA. The data gleaned from this for GADA and IA-2A shows that this would be worthwhile (**Appendix B.2**). Additionally, the detection of IgG subclasses after T1D onset was novel and although detection was performed for the purpose of establishing QCs here, the longitudinal follow-up of IgG subclasses after onset may also inform differing profiles of autoantibody loss which is particularly rapid in ZnT8RA/ZnT8WA responses (443) or indeed, provide insights into compartments of B-cells and/or residual  $\beta$ -cell function/mass (39, 237, 238, 449), and for GADA in particular, IgG subclasses may aid clinical diagnosis of diabetes in adults (478, 479).

---

## 2.4 Characterisation of ZnT8A epitopes in C-terminal ZnT8

---

---

### 2.4.1 Introduction to B-cell epitopes of ZnT8

---

In the original paper by Wenzlau *et al.* (2007) that identified ZnT8 as a major autoantigen in T1D, several ZnT8 antigen constructs were investigated by RIA in 277 new-onset T1D. Full-length ZnT8 (aa1-369) showed encouraging performance of ZnT8A binding (25% sensitivity, 98% specificity) but had >5% false-positive rate due to non-specific binding in a subset of 100 autoantibody negative non-diabetic controls. Due to the probability that ZnT8A cannot access the embedded transmembrane regions that make up half of ZnT8, monomeric or fusion ZnT8 antigen segments of the cytosolic and luminal regions were further investigated (270).

In T1D, the cytosolic N-terminal (aa1-74) had low sensitivity (8%), contributing to ~10% of ZnT8A reactivity. Whereas the cytosolic C-terminal (aa268-369) had the highest sensitivity (50%), contributing to ~80-90% of ZnT8A reactivity. Consequently, the C-terminal of ZnT8 was deemed the major region for ZnT8A reactivity in new-onset T1D (270, 480). The specificity of ZnT8A to the C-terminal was also confirmed; 9 high-level C-terminal-reactive ZnT8A were immunoprecipitated in the presence of 10 $\mu$ g His-tagged C-terminal ZnT8 protein which reduced serum ZnT8A binding by a mean  $\pm$  SEM of 93%  $\pm$  2.4%. Additionally, no reactivity was observed in these sera using the C-terminal of other zinc transporters expressed in islets that share substantial homology with ZnT8, ZnT3 (42%) and ZnT5 (22%) (270).

Reactivity of ZnT8A to variants of C-terminal ZnT8 was further investigated by RIA according to the SNP site (rs13266634/rs16889462) once implicated in T2D risk (328, 388-390). In 421 new-onset T1D, 61.5% were ZnT8A positive, and the prevalence was associated with age-at-onset: increased between 0.6-8 years, plateaued around 8-16 years, and decreased 16-50 years. In decreasing order, ZnT8A was reactive to C-terminal ZnT8 encoding R325 (53.2%), W325

(43.9%), and Q325 (33.7%). It was rare for subjects to be specific to just one C-terminal ZnT8 variant but was highly associated with the corresponding *SLC30A8* genotype: R325 (14.3%) with CC genotype, W325 (7.4%) with TT genotype, and Q325 (0.24%) with CT genotype. Subsequently, ZnT8A that recognised all C-terminal ZnT8 variants accounted for ~70% of ZnT8A were highly correlated and were associated with the *SLC30A8* heterozygous CT genotype. This suggested that the majority of ZnT8A responses are not dependent on the encoded aa325. Competitive displacement experiments with recombinant C-terminal ZnT8 (encoding R325/W325/Q325) confirmed that ZnT8A specificity was either dependent (specific) or independent on the encoded aa325 (non-specific) and could be categorised: R325-specific, W325-specific, and non-specific ZnT8A as Q325-specific responses were rare. Moreover, competitive displacement experiments with 20-mer C-terminal ZnT8 linear peptides were insufficient to displace ZnT8A suggesting that ZnT8A reactivity to C-terminal ZnT8 is reliant on conformational epitopes (328). This was also confirmed using short (aa318-331) and long (aa268-369) ZnT8 peptides to displace R325-specific and W325-specific ZnT8A from radiolabelled ZnT8 (aa268-369) (399).

To further elucidate conformational epitopes in C-terminal ZnT8, discrepant amino acids between murine (aa267-368) and human C-terminal ZnT8 (aa268-369) that share 78.4% homology (80/102 residues) were investigated since the conformation and functionality of ZnT8 *in vivo* should be conserved. The importance of the discrepant amino acids was shown as human ZnT8A from new-onset T1D did not recognise the murine ZnT8 C-terminal in >95% of subjects with <5% showing minimal ZnT8A binding. Humanising the 22 discrepant residues on murine C-terminal ZnT8 by site-directed mutagenesis (SDM) individually did not restore ZnT8A binding (480) (**Figure 2:21**). However, substituting segments of murine C-terminal ZnT8 to human C-terminal ZnT8 (404), the combined but not individual, humanisation of the murine C-terminal ZnT8 from residues T<sub>332</sub>/G<sub>333</sub>/Q<sub>336</sub>/- (340 absent) to residues R<sub>332</sub>, E<sub>333</sub>, K<sub>336</sub>,

## Chapter 2 - Characterisation of the ZnT8 humoral response up to T1D onset

and K<sub>340</sub> (REKK) restored ZnT8A binding independent of aa325 in T1D subjects. Therefore, these residues are thought to form a conformational epitope, but this was not observed for the related cluster V<sub>329</sub>, R<sub>332</sub>, E<sub>333</sub> and K<sub>336</sub>. It was concluded that there are likely other unrestricted epitopes (not dependent on aa325) that can be investigated using Q325 (404).

### Murine C-terminal ZnT8 (aa267-367)

KDFSILLMEGVPK**GLSYNSVKEI**ILAVDGV**ISVHS**LHIW**SLT**VNQVIL**SVHVATAAS****QDSQ****SVRTGIAQALS**  
**SFDLHSI**TIQ**IESAADQDP****SCLLCEDPQD**

### Human C-terminal ZnT8 (aa268-369)

KDFSILLMEGVPK**SLNYS**GVK**ELI**ILAVDGV**LSVHS**LHIW**SLT**MNQVIL**SAHVATAAS****RDSQ****VVREIAKALS**  
**SFTMHSI**TIQ**MES**PV**DQDPDCLFCEDP****CD**

*Figure 2:21 – Murine & human C-terminal ZnT8 residue alignment for conformational epitope mapping of ZnT8A*

Mouse and human ZnT8 alignment: Red/bold: discrepant amino acids; Pink: rs13266634/rs16889462 SNP site at aa325; Underlined: amino acids that contribute to major epitopes of ZnT8A; Black/bold: two serines that may be important for ZnT8A binding. Murine and human ZnT8 share 78.4% homology, but human ZnT8A does not bind mouse ZnT8, suggesting that the discrepant amino acids are important for ZnT8A in T1D. Humanising the individual 22 discrepant residues on murine C-terminal ZnT8 by site-directed mutagenesis (SDM) did not restore any ZnT8A binding in the T1D subjects. Substitution of the murine yellow segment in human ZnT8 containing 6 discrepant amino acids caused a minimal reduction in binding. Substitution of the blue and green murine segments in human ZnT8 containing 2 and 8 discrepant amino acids, respectively, abolished ZnT8A binding. Substitution of the murine grey segment in human ZnT8 containing 6 discrepant amino acids caused ~75% reduction in binding. Results and image adapted from Wenzlau *et al.* (2008 and 2011) (404, 480).

In this project, we investigated whether ZnT8A specificity (R325/W325/Q325) differed between FDRs that progressed slowly or rapidly to T1D. In new-onset T1D patients, we sought to confirm the major epitopes of ZnT8A (R325, W325, and REKK) through SDM of Q325 and REKK-to-alanine substitutions. This also involved confirming the effect of ZnT8A specificity, *SLC30A8* genotype, and age-at-onset, where appropriate. Additionally, considering the importance of core cysteines and the effect of Tween-20 on IA-2A/IA-2 $\beta$ A binding, we sought to investigate the three C-terminal cysteines specific to human ZnT8 on ZnT8A binding by SDM, as they may have important implications for assay performance and epitope recognition (341, 481). This has become increasingly intriguing as two of the three C-terminal cysteines (C<sub>361</sub> and C<sub>364</sub> in the highly conserved CXXC motif) have a high affinity for zinc and may aid in the allosteric mechanism of ZnT8 required for zinc trafficking (410, 411, 415). We also

investigated two novel truncations at aa360 and aa349 to investigate the removal of the three cysteines and ~20% of C-terminal ZnT8 on ZnT8A binding, respectively.

### **2.4.1.1 Hypothesis**

---

Confirmation of previously identified epitopes and characterisation of the unexplored cysteine-rich region of C-terminal ZnT8 will inform the ZnT8A humoral response and elucidate further conformational epitopes.

### **2.4.1.2 Aims**

---

1. To evaluate the major epitope (325) region and ZnT8A specificity in SPs and RPs.

In new-onset T1D patients (<3 months of diagnosis):

2. To evaluate the major epitope (325) region and the effect of Q325 on different ZnT8A specificities by *SLC30A8* genotype and age-at-onset.

3. For the assessment of the major conformational epitope REKK, investigate the structural integrity of mutating this region to serines or alanine compared with the murine equivalent (TGQ-).

4. To evaluate the major conformational epitope REKK (AAAA substitutions) and truncation of ZnT8 at aa349 by ZnT8A specificity.

5. To evaluate the cysteine-rich region of ZnT8 (C<sub>361</sub>, C<sub>364</sub>, C<sub>368</sub>, substituted for serine and truncation of ZnT8 at aa360) by ZnT8A specificity.

6. Perform heat map cluster analysis to identify clusters of patients with similar ZnT8A binding remaining after ZnT8 has been mutated or truncated.

## 2.4.2 Materials & Methods

### 2.4.2.1 Populations for ZnT8A epitope studies

#### 2.4.2.1.1 Multiple autoantibody positive progressor sample set

To investigate whether ZnT8A specificity differed between NPs, SPs, or RPs (previously described **2.3.3.1**) and changed over time, the major epitopes of ZnT8A (R325/W325/Q325) was investigated in a subset. The first mAutoab+ve sample (index sample) or first ZnT8RA/ZnT8WA positive sample and/or follow-up sample(s) was tested where possible.

A total of 16 (12 index and 4 first ZnT8A positive), 8 (4 index and 4 first ZnT8A positive), and 7 (all index) from NPs, SPs, and RPs were tested for Q325, respectively. From these subjects, a total of 7 NPs, 5 SPs, and 4 RPs had at least one follow-up sample available for Q325 testing and assessment of temporal changes in ZnT8A specificity (**Table 2:16**).

Progressor	n index/n first ZnT8A +ve sample	Gender M/F	Median (range) age at sample (yrs)	Median (range) of follow-up (yrs)	Median (range) time before diagnosis (yrs)	Median (range) age at diagnosis (yrs)	n with f-up samples/ n samples tested
<b>NPs (total=16)</b>	12/4	7/9	15.7 (2.6-50.1)	18.6 (3.2-29.1)	N/A	N/A	7/11
<b>SPs (total = 8)</b>	4/4	3/5	33.3 (7.3-42.0)	N/A	15.5 (11.3-27.8)	50.7 (18.9-68.0)	5/12
<b>RPs (total=7)</b>	7/0	2/5	30.4 (16.4-40.6)	N/A	3.7 (1.7-9.4)	32.9 (23.9-50.1)	4/7

*Table 2:16 – Index sample or first ZnT8A positive sample & follow-up samples tested for ZnT8Q reactivity in NPs, SPs, & RPs*

N/A: Not applicable; F-up: Follow-up. Either the mAutoab+ve sample (index) or first ZnT8A positive sample was tested from NPs, SPs, and RPs, and where possible, a subset of individuals with at least one follow-up sample was tested to access whether ZnT8A prevalence/specificity can change over time.

#### **2.4.2.1.2 New-onset T1D sample set**

Sera from 105 ZnT8A positive new-onset T1D patients [57 males (54.3%); median age at onset 10.5 years (range 1.9-19.3); sampled <3 months of diagnosis] were previously investigated for the effects of C-terminal single cysteine-to-serine mutations (C<sub>361</sub>S, C<sub>364</sub>S, and C<sub>368</sub>S) and two truncations (360T and 349T) on ZnT8RA/ZnT8WA binding by S. Rokni and Dr A.E. Long (2011-2013); 10 individuals had incomplete data across the 10 combined R325/W325 mutants and, 1 double cysteine-to-serine mutations were made (C<sub>361</sub>S/C<sub>368</sub>S with R325/W325 encoded) but not tested in the patient cohort.

Based on serum availability and the proportion of complete historical data, 71 new-onset T1D patients [43 males (60.6%); median age at onset 9.1 years (range 1.9-19.3)] (**Table 2:17** for complete cohort description) were selected for further ZnT8A epitope studies on 9 additional mutations made during this project and any missing data on the pre-existing 10 mutations were filled in. **Table 2:19** describes the total inventory of ZnT8 mutants and whether they were created/tested historically or during this project.

<b>Variable</b>	<b>Number (%)</b>
<b>Gender</b> (n=71)	
Male	43 (60.6)
Female	28 (39.4)
<b>Age at onset</b> (n=71)	
0-5 years	12 (16.9)
5-10 years	25 (35.2)
10-15 years	22 (31.0)
15-20 years	12 (16.9)
<b>Autoantibody</b> (n=71)	
IAA (n=61)	49 (80.3)
GADA (n=71)	57 (80.3)
IA-2A (n=71)	61 (85.9)
ZnT8A (n=71)	71 (100.0)
ZnT8RA	57 (80.3)
ZnT8WA	53 (74.6)
<b>HLA Class II</b> (n=70)	
High (DR3-DQ2/DR4-DQ8)	25 (35.7)
Moderate (DQ2/DQ2, DQ8/DQ8, DQ2/X, DQ8/X)	36 (51.4)
Low (X/X, DQ6/X)	9 (12.9)
<b>HLA Class I</b>	
<i>HLA-A*24</i> Negative (n=66)	54 (81.8)
<i>HLA-B*18</i> Negative (n=65)	55 (84.6)
<i>HLA-B*39</i> Negative (n=65)	59 (90.8)
<b>Non-HLA SNPs</b>	
<i>SLC30A8</i> (n=69) *	
CC	30 (43.5)
CT	27 (39.1)
TT	12 (17.4)

*Table 2:17 – Cohort description of all T1D- & ZnT8A-associated variables in 71 new-onset T1D patients selected for ZnT8A epitope studies*

All data from genetic variables were available. Underlined genotype denotes the minor allele.

### 2.4.2.2 Generation of mutant ZnT8 constructs for ZnT8A epitope studies

The generation of ZnT8 mutant constructs was conducted by SDM (Figure 2:22).

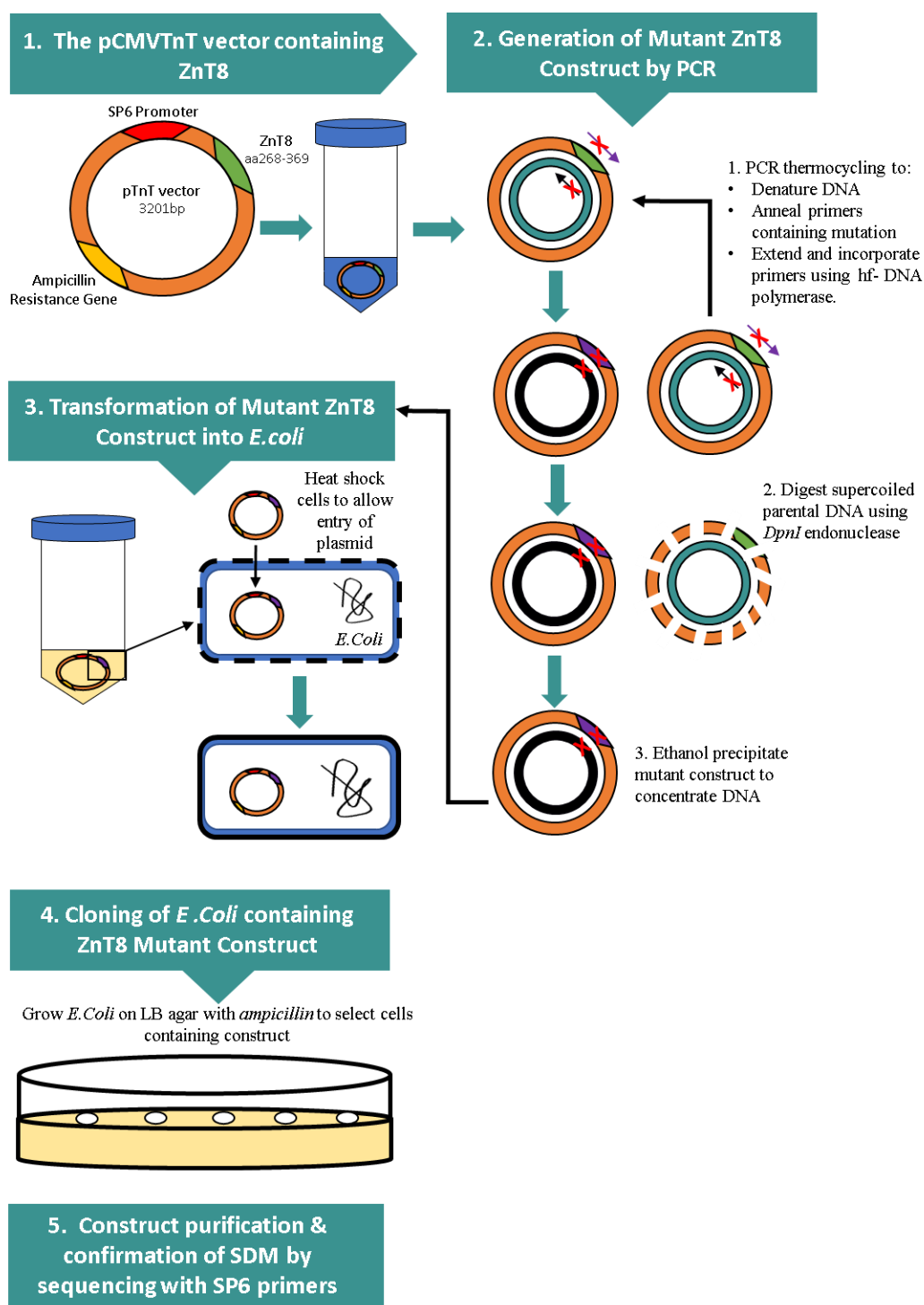


Figure 2:22 – Generation of ZnT8 mutant constructs by site-directed mutagenesis (SDM) & transformation into DH5a *E. coli* cells

The PCR thermocycling portion of this figure was adapted from the Agilent QuikChange II SDM Instruction Manual. Confirmation and sequencing of ZnT8 mutant constructs were conducted by Eurofins Genomics (Ebersberg, Germany) using 50-100ng/μl of the constructs.

**2.4.2.2.1 Site-directed mutagenesis (SDM)**

The pCMVTnT vectors containing WT C-terminal (aa268-369) monomeric ZnT8R or ZnT8W were kindly supplied by Dr V. Lampasona (Milan, Italy). SDM to replace selected amino acids with serine or alanine was performed according to the Agilent (Santa Clara, CA, USA) QuikChange II SDM Instruction Manual. Polyacrylamide gel electrophoresis (PAGE)-purified designed primers were resuspended in ddH<sub>2</sub>O for a working stock concentration of 100mM according to manufacturer instructions for all primers (Sigma Aldrich, Dorset, UK). An initial PCR reaction was conducted in a 50µl reaction volume containing 125ng of forward and reverse oligonucleotide primers (containing single mutations at desired sites) complementary to opposing strands of template DNA (WT ZnT8 R325/W325) and *PfuUltra* high-fidelity DNA polymerase (Agilent Technologies, Santa Clara, CA, USA) in a 35-temperature cycling program (**Table 2:18**).

PCR Step	Temperature (°C)	Length (seconds)	Cycles
Initial	95°C	30	
Denaturation	95°C	30	
Annealing	55°C	60	
Elongation	68°C	300	
DNA Preservation	5°C	∞	

*Table 2:18 – PCR cycle for site-directed mutagenesis*

Following PCR, non-mutated supercoiled template dsDNA was digested using 1µl of *DpnI* endonuclease (New England BioLabs) at 37°C for 2hrs. The remaining amplified DNA in a 51µl volume was precipitated with 100µl 100% Ethanol (Perkin Elmer) and 5µl 3M Potassium Acetate pH 3 (ThermoFisher), air dried, and then resuspended in 10µl sterile ddH<sub>2</sub>O.

#### **2.4.2.2.2 Transformation & purification of mutant ZnT8 constructs into *Escherichia Coli***

To 50µl of chemically competent DH5α *Escherichia Coli* (*E.Coli*) cells (Invitrogen, Waltham, MA, USA), 2µl of mutant ZnT8 plasmid (following SDM) was added and incubated on ice for 30mins. To allow entry of the mutant ZnT8 plasmid into *E.Coli* cells, the mixture was heat-shocked for 30secs at 42°C and placed back on ice for a further 2mins. 500µl sterile super optimal broth with catabolite repression (SOC) medium was added to the cells and incubated on a shaking platform at 225rpm for 1hr at 37°C.

To select cells containing the mutant ZnT8 plasmid, cells were spread onto Luria-Bertanil (LB) agar plates with 100µg/ml ampicillin (Sigma Aldrich, Dorset, UK) and incubated overnight at 37°C. To increase the yield of cells containing the mutant ZnT8 plasmid, resultant colonies were selected for further growth on fresh agar plates containing 100µg/ml ampicillin overnight (~16hrs) at 37°C. After incubation of select colonies with 5ml LB broth containing 5µl (100µg/ml) ampicillin overnight at 37°C on a shaking platform set at 225rpm, colonies containing the ZnT8 mutant plasmid were purified from *E.Coli* cells using a QIAprep Spin Miniprep Kit (Qiagen) according to manufacturer's instructions.

#### **2.4.2.2.3 Confirmation of ZnT8 mutations**

To confirm successful mutation(s), 50-100ng/µl of plasmid DNA was sequenced using a standard SP6 promoter primer (Eurofins Genomics, Ebersbery, Germany). Constructs containing a single mutation were confirmed using the basic local alignment search tool (BLAST) (482) available through the National Center for Biotechnology Information (NCBI). Plasmids containing single mutations were then used as template DNA for further SDM using primers designed to generate plasmids with multiple mutations and by repeating the process (2.4.2.2.1-2.4.2.2.3).

#### **2.4.2.2.4 Glycerol stocks for long-term storage of mutant ZnT8 constructs**

The addition of glycerol to bacterial plasmids maintains cell viability stably for many years when stored at -80°C (457). Single colonies of cells containing the mutant ZnT8 plasmid (confirmed by sequencing) were incubated in 5ml LB cultures containing 5µl ampicillin (100µg/ml) overnight at 37°C on a shaking platform (225rpm). Cells were then pelleted by centrifugation (3000xg for 10mins at RT) and resuspended in 1ml LB containing 15% glycerol. Glycerol stocks were then stored at -80°C to preserve plasmid DNA for future purification requirements.

### 2.4.2.2.5 Inventory of ZnT8 mutant constructs

**Table 2:19** details the total inventory of C-terminal ZnT8 mutations generated by SDM or cloning strategies (historically or during this project) in 71 new-onset T1D patients. This included the major epitopes at aa325 (R325/W325/Q325) and the major conformational epitope R<sub>332</sub>/E<sub>332</sub>/K<sub>336</sub>/K<sub>340</sub> (REKK). Double cysteine mutations, sequential REKK mutations, and human-to-murine REKK [TGQ-; threonine (T), glycine (G), glutamine (Q), deletion; made using a cloning strategy, detailed in **Appendix C.1**] were tested in a subset of the new-onset T1D cohort for the major ZnT8RA response to ascertain whether further testing was necessary. All primer sequences are detailed in (**Table C:3; Appendix C.2**).

Mutant(s)	Created by	Mutant available or generated	Historical data available			Data Generated			Total
			ZnT8R (n=57)	ZnT8W (n=52)	ZnT8R (n=57)	ZnT8W (n=52)	ZnT8Q (n=71)		
<b>C361S</b>	SDM	Available	57	52	-	-	-	71	
<b>C364S</b>	SDM	Available	57	52	-	-	-	71	
<b>C368S</b>	SDM	Available	19	52	38	-	-	71	
<b>C361S/C368S</b>	SDM	Available	0	0	31§	-	-	31	
<b>C361S/C364S</b>	SDM	Generated	-	-	31§	-	-	31	
<b>325Q</b>	SDM	Generated	-	-	-	-	71	71	
<b>R332S</b>	SDM	Generated	-	-	12**	-	-	12	
<b>RES</b>	SDM	Generated	-	-	12**	-	-	12	
<b>REKs</b>	SDM	Generated	-	-	12**	-	-	12	
<b>REKKS*</b>	SDM	Generated	-	-	12	-	-	12	
<b>R332A</b>	SDM	Generated	-	-	12**	-	-	12	
<b>REA</b>	SDM	Generated	-	-	12**	-	-	12	
<b>REKA</b>	SDM	Generated	-	-	12**	-	-	12	
<b>REKKA*</b>	SDM	Generated	-	-	57	52	71	71	
<b>Murine REKK §</b>	Cloning¥	Generated	-	-	12§	-	-	12	
<b>360-T</b>	Cloning↓	Available	56	51	1	1	-	71	
<b>349-T</b>	Cloning↓	Available	44	38	13	14	-	71	

*Table 2:19 – Inventory of C-terminal ZnT8 mutant constructs*

\* Constructs containing REKK mutations were created encoding R325, W325, and Q325; \*\* Sequential mutations for R332/E333/K336 were tested in a subset for ZnT8RA responses only (n=12) (data not shown) but REKK-S, REKK-A, and Murine REKK were first compared in the subset (n=12; results presented **Figure 2:30**) and REKK-A was chosen for further testing. § Human-to-murine REKK (TGQ-) was made by cloning (¥; detailed in **Appendix C.1**) and tested in a subset for ZnT8RA responses only (n=12). Four mutations and two truncations (↓) were available for ZnT8R and ZnT8W antigens encoded in the pCMVTnT vector (total mutant constructs=12). A further 13 mutations were created during this project to encompass all ZnT8A specificities to the polymorphic site (R325/W325/Q325). Some missing data of the historically made mutations were tested in this project to create a complete data set. Patients were selected for this project based on serum volume availability for further testing and the quantity of complete historical data.

The SP6 promoter, cloning site, and positions of all mutations (FASTA and amino acid sequence) of C-terminal ZnT8 in the pCMVTnT vector is detailed in **Figure 2:23**.

**FASTA:**

ATTAGGTGACACTATAGAATACAAGCTACTTGTCTTTTTGCACTCGAGAATTC  
GCCGCCACCATGGAGAAGGACTTCTCCATCTTACTCATGGAAGGTGTGCCAAAG  
AGCCTGAATTACAGTGGTGTGAAAGAGCTTATTTTAGCAGTCGACGGGGTGCTGT  
CTGTGCACAGCCTGCACATCTGGTCTCTAACAATGAATCAAGTAATTCTCTCAGC  
TCATGTTGCTACAGCAGCCAGCCGGGACAGCCAAGTGGTTCGGAGAGAAATTGC  
TAAAGCCCTTAGCAAAAGCTTTACGATGCACTCACTCACCATTGAGATGGAATCT  
CCAGTTGACCAGGACCCCGACTGCTTTTCTGTGAAGACCCCTGTGAC

**Amino acid sequence (aa268-369; 101aa):**

KDFSILLMEGVPKSLNSGVKELILAVDGVLSVHSLHIWLSLTMNQVILSAHVATAASR  
DSQVVRREIAKALSKSFTMHSLTIQMESPVDQDPDCLFCEDPCD

*Figure 2:23 – Cloning site, FASTA, & amino acid sequence of C-terminal ZnT8 (aa268-369) in the pCMVTnT vector*

Green highlight: SP6 promoter; Light blue highlight: beta globin leader sequence; grey highlight: cloning site; pink highlight: Kozak sequence; teal highlight: added start M (ATG) & E (GAG) codons. Dark blue highlight: the beginning of C-terminal ZnT8 (aa268) Red highlight: the end of C-terminal ZnT8 (aa369). Yellow highlight: rs13266634 SNP site encoding R325 (CCG), but codons for W325 and Q325 would be TGG and CAG, respectively. Orange, light blue, green, and purple indicates R332, E333, K336, and K340, respectively. Three black/underlined regions indicate the three C-terminal cysteines C361, C364, and C368.

### **2.4.2.3 ZnT8A epitope studies by RIA**

Once sequencing confirmed successful mutation(s), 1 microgram of ZnT8 mutant construct was used to generate [35-S]-radiolabelled ZnT8 mutant antigens and were tested by the standard RIA, detailed previously (2.2.2.3.2 and 2.2.2.3.3). All mutants were tested in parallel with WT ZnT8 antigen and are expressed as mean CPM.

Reactivity to Q325 was considered positive if greater than the 97.5<sup>th</sup> percentile of 523 healthy schoolchildren (>1.8AU) when applied to the same logarithmic standard curve as monomeric R325/W325 RIAs.

#### **2.4.2.4 *SLC30A8* genotype determination**

---

To investigate the influence of ZnT8A specificity towards WT and mutant ZnT8 antigen, the *SLC30A8* SNP (rs13266634) was considered. The *SLC30A8* genotype was not available for the mAutoab+ve progressor cohort but was available for 69/71 (97.2%) new-onset T1D patients. Genotype was determined by a Taqman™ SNP kit following the manufacturer's instructions (ThermoFisher).

#### **2.4.2.5 Statistical analysis**

---

Spearman's rank (r) correlation test was used to compare ZnT8A binding (AU) to WT ZnT8 antigens. Proportions of categorical variables were compared using the Chi-squared ( $\chi^2$ ) test or Fisher's exact test where appropriate. All ZnT8 mutants were tested in parallel RIAs with WT ZnT8 antigen with ZnT8A binding expressed in mean CPM to account for inter-assay variation. The median reduction in ZnT8A binding to mutant ZnT8 (**A**) as a percentage of ZnT8A to WT ZnT8 (**B**) was determined using the formula  $[(\mathbf{A} - \mathbf{B}) \div \mathbf{B} \times 100 (\%)]$ . Data were categorised by ZnT8A specificity to WT ZnT8 (R325-specific, W325-specific, and non-specific) once determined. One sample Wilcoxon tests were used to evaluate whether the median reduction in binding differed from WT (zero). One-way Kruskal-Wallis tests with a Dunn post-hoc test for multiple comparisons were used to evaluate differences in ZnT8A binding to mutant ZnT8 according to ZnT8A specificity. Statistical analysis was performed in GraphPad PRISM (v. 9.1.0), and  $p < 0.05$  was considered significant.

To evaluate all investigated ZnT8 mutants on ZnT8A binding in the total cohort, the R statistical program using the native heatmap() function allowing no additional scaling was used to generate a heat map to identify clusters of patients with comparable ZnT8A binding to mutant ZnT8 through hierarchical clustering to produce a dendrogram. For this analysis, the median reduction in binding to mutant ZnT8 was evaluated against the rank of ZnT8A binding

to WT ZnT8 antigen. The genotype of *SLC30A8* and ZnT8RA, ZnT8WA, ZnT8QA were scaled to values between -100 and +25 to match the range of median reduction for mutants. Dr A.E. Long conducted this analysis.

## 2.4.3 Results

### 2.4.3.1 Categorisation of ZnT8A reactivity to the major epitope (325) in slow & rapid progressors of T1D by *SLC30A8* genotype & age at onset

ZnT8A specificity was comparable between slow & rapid progressors, but ZnT8A titres & specificity may change over time in some individuals.

The proportions of ZnT8A reactive to WT ZnT8 antigen encoding R325, W325, or Q325 was comparable between NPs/SPs and RPs ( $p=0.676$ ; **Figure 2:24**).

Reactivity to all three 325 variants (R325/W325/Q325; non-specific ZnT8A) comprised the majority of ZnT8A responses in all progressors: 62.5% ( $n=10$ ) NPs, 50.0% ( $n=4$ ) SPs, and 57.1% ( $n=4$ ) RPs. None of the RPs had W325-specific responses but for SPs and NPs, the proportion of R325- and W325-specific responses was similar [18.8-28.6% ( $n=2-3$ )].

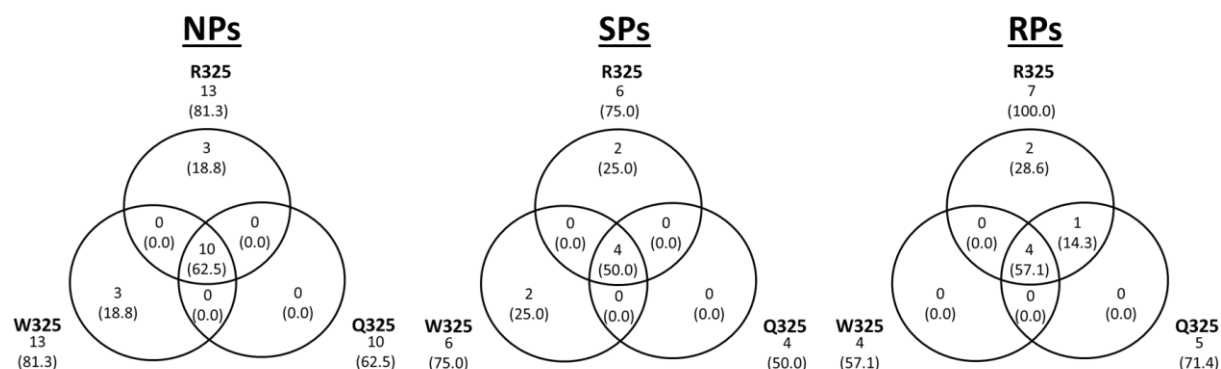


**Figure 2:24 – Categorisation of the major epitope (325) in NPs, SPs, & RPs of T1D**

The proportions of R325/W325-specific ZnT8A responses versus R325/W325/Q325 non-specific ZnT8As between NPs/SPs and RPs was comparable ( $p=0.676$ ).

## Chapter 2 - Characterisation of the ZnT8 humoral response up to T1D onset

Although ZnT8A specificity was comparable between all progressors, over longitudinal follow-up, there was evidence of interesting ZnT8A patterns according to the titre and reactivity towards WT ZnT8(325) antigen (**Figure 2:25**).

Of 7 NPs over a range of ages, 6 (85.7%) showed decreasing ZnT8A titre over follow-up and, of 5 individuals with non-specific ZnT8A in the first mAutoab+ve sample, 3 (60.0%) had differentially declining ZnT8A profiles according to the WT ZnT8(325) antigen (no. 3, 4, and 5).

In 5 SPs with longitudinal sampling, the ZnT8A patterns were less clear with heterogeneous changes in titre and reactivity to the WT ZnT8(325) antigen. Four of five (80.0%) showed some indication of modestly increasing ZnT8A titres to at least one 325 variant over follow-up. One individual (no.2) had an R325-specific ZnT8A response in the first mAutoab+ve sample (aged 15.3 years) but, over follow-up, developed non-specific ZnT8A (aged 16.3-20.8 years) and was later diagnosed (aged 30.6 years). This suggests that ZnT8A specificity to the 325 epitopes could change in some individuals during the disease course.

In 4 RPs with longitudinal sampling, 3 (75.0%) maintained the ZnT8A specificity of the first mAutoab+ve sample over time. In 3 (75.0%) individuals with non-specific ZnT8A in the first mAutoab+ve sample, 2 (50.0%; no.1/2) had high titre ZnT8A and were able to maintain this profile over time, but 1 (25.0%; no.3) individual with a moderate ZnT8A titre had fluctuating reactivity to the W325 ZnT8 antigen. This suggests that ZnT8A titres may influence the longevity of the ZnT8A response before T1D onset. However, the individual with a low-level R325-specific response in the mAutoab+ve sample could sustain the same ZnT8A level over follow-up (no.4).

The characteristics of ZnT8A (titre and specificity) appear to be heterogeneous, but data from this small cohort may suggest differences between progressors and warrants further investigation.

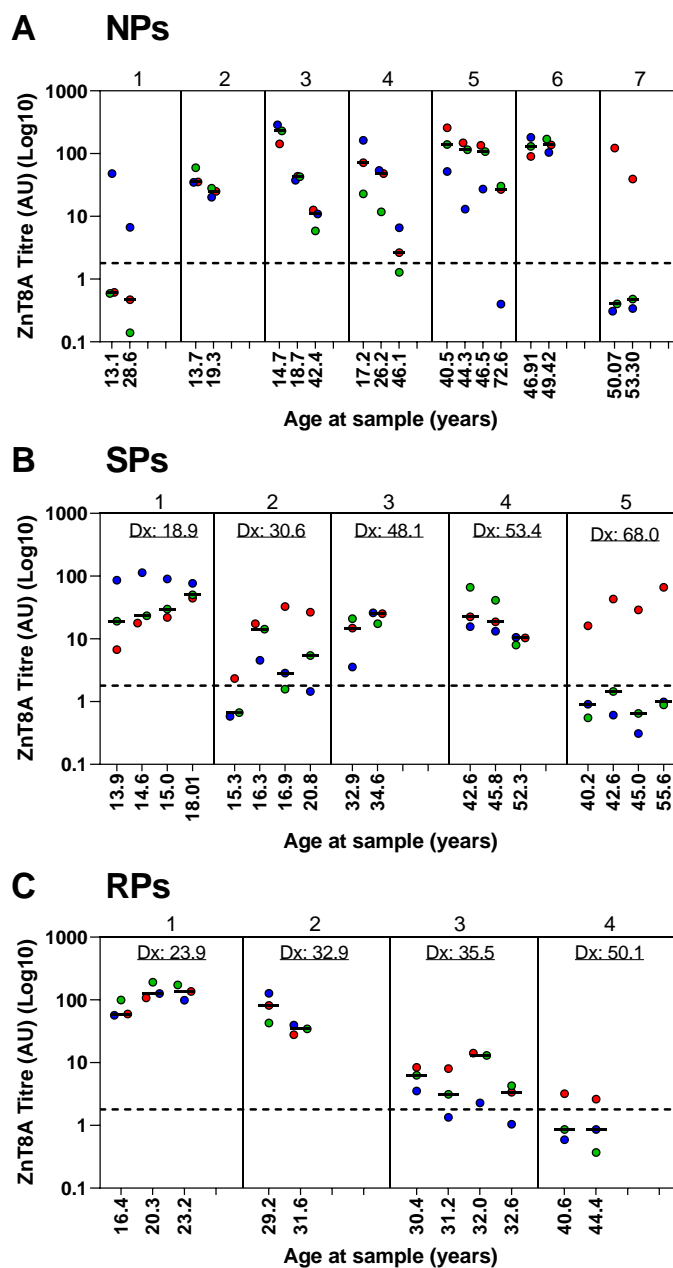


Figure 2:25 – ZnT8A specificity profiles over longitudinal follow-up of NPs, SPs, & RPs

Numbers 1-7 above the graphs denote individual progressors which are organised according to age at first sample (years). Red circles: reactivity to R325 ZnT8 WT antigen; Blue circles: reactivity to W325 ZnT8 WT antigen; Green circles: reactivity to Q325 ZnT8 WT antigen. Black horizontal bars denote median ZnT8A titre (AU) per sample. The black dashed line denotes the ZnT8A RIA positivity threshold at 1.8AU. ZnT8A specificity profiles in ZnT8A positive non-progressors (NPs; **A**), slow progressors (SPs; **B**), and rapid progressors (RPs; **C**) of T1D over longitudinal follow-up according to age at first sample with mAutoAb+ve status. For SPs and RPs, the age at diagnosis (DX) is detailed for context. Patterns between T1D progressors appears heterogeneous, but differences in ZnT8A titre and specificity over longitudinal follow-up may aid the discrimination of slow and rapid progressors of T1D.

### 2.4.3.2 Categorisation of ZnT8A reactivity to the major epitope (325) in new-onset T1D patients by *SLC30A8* genotype & age at onset

Confirmation that the majority of ZnT8A, according to the major epitope (325), are non-specific.

In 71 new-onset T1D patients, 80.3% (n=57), 73.2% (n=52), and 62.0% (n=44) had ZnT8A binding to WT ZnT8 antigen encoding R325, W325, and Q325, respectively, and 50.7% (n=36) reacted to all three variants. Reactivity to two 325 variants comprised 14.1% (n=10) of the cohort and 35.2% (n=25) produced specific ZnT8A responses: 16.9% (n=12) R325-specific and 18.3% (n=13) W325-specific. Due to the pre-selection of the cohort based on R325/W325 reactivity, there was no Q325-specific responses (**Figure 2:26**).

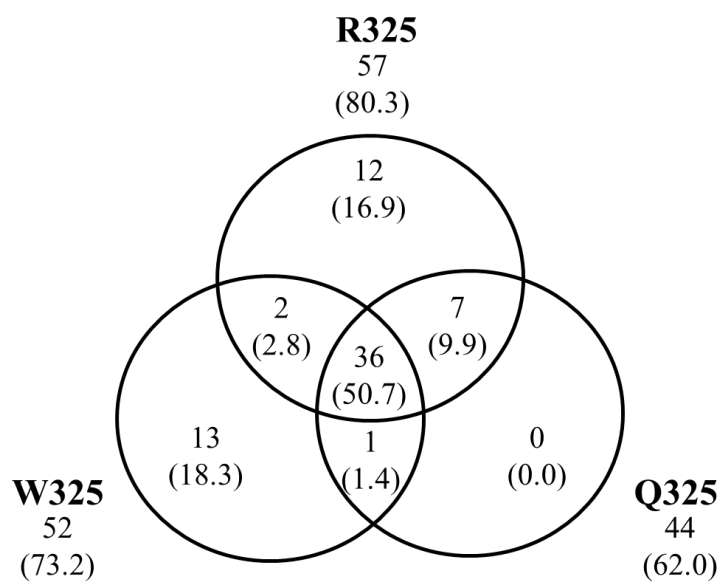


*Figure 2:26 – Categorisation of the major epitope (325) in new-onset T1D patients selected for epitope studies*

ZnT8A positivity profiles according to the major epitope region [R325 (80.3%), W325 (73.2%) and Q325 (62.0%) WT ZnT8 antigen] in 71 new-onset T1D patients sampled within 3 months of onset [43 males (60.6%); median age at onset 9.1 years (range 1.9-19.3)]. Due to the pre-selection of the cohort based on R325/W325 reactivity by respective monomeric RIAs, there was no detection of Q325-specific responses.

Confirmation that titres of R325-reactive & W325-reactive ZnT8A correlate with titres of Q325-reactive ZnT8A

Titres of R325-reactive (ZnT8RA) and W325-reactive (ZnT8WA) ZnT8A were highly correlated with levels of Q-reactive (ZnT8QA) ZnT8A [ $r$  (95% CI): ZnT8RA versus ZnT8QA 0.59 (0.40-0.72),  $p < 0.0001$ , **Figure 2:27A**; ZnT8WA versus ZnT8QA 0.62 (0.45-0.75),  $p < 0.0001$ , **Figure 2:27B**]. However, due to the presence of R325- and W325-specific ZnT8A, levels of ZnT8RA and ZnT8WA was not correlated [ $r$  (95% CI): 0.14 (-0.11-0.36),  $p > 0.05$ , **Figure 2:27C**].

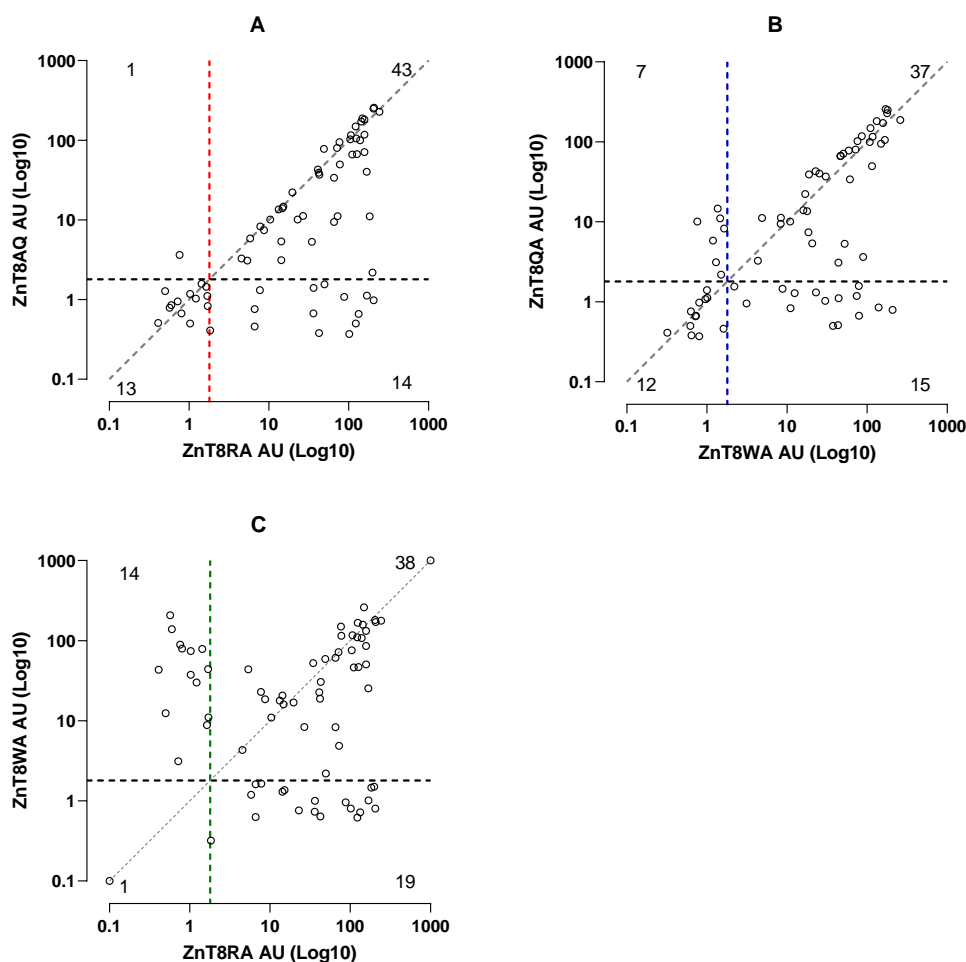


**Figure 2:27 – Correlation of R325-, W325-, & Q325-reactive ZnT8A in new-onset T1D patients**

Levels of ZnT8A (AU) in 71 new-onset T1D patients are plotted according to R325-, W325-, and Q325-reactivity. Levels of R325-reactive (ZnT8RA; **A**) and W325-reactive (ZnT8WA; **B**) ZnT8A were highly correlated with levels of Q-reactive (ZnT8QA) ZnT8A [ $r$  (95% CI): ZnT8RA versus ZnT8QA 0.59 (0.40-0.72),  $p < 0.0001$ ; ZnT8WA versus ZnT8QA 0.62 (0.45-0.75),  $p < 0.0001$ ]. Levels of ZnT8RA and ZnT8WA (**C**) was not correlated [ $r$  (95% CI): 0.14 (-0.11-0.36),  $p > 0.05$ ] due to R325- and W325-specific responses as well as, preferential binding to either antigen in some patients.

Confirmation that ZnT8A specificity to the major epitope (325) is associated with *SLC30A8* genotypes.

The relationship between ZnT8A reactivity to WT ZnT8 variants according to *SLC30A8* genotypes was investigated (**Table 2:20**). As expected, the specificity of ZnT8A was associated with *SLC30A8* genotypes. Non-specific ZnT8A that respond to all R325/W325/Q325 variants were most frequent in CT heterozygotes, lowest in TT homozygotes, and intermediate in CC homozygotes ( $p=0.0006$ ). Whereas R325- and W325-specific ZnT8A corresponded with genotypes containing the C allele ( $p=0.013$ ) and T allele ( $p=0.0002$ ), respectively.

The prevalence of R325-reactive ZnT8A was highest in the CC homozygotes and lowest in the TT homozygotes ( $p<0.0001$ ). However, the prevalence of W325-reactive ZnT8A was highest in the CT heterozygotes and was comparable between CC and TT homozygotes ( $p=0.0008$ ). As anticipated, the prevalence of Q325-reactive ZnT8A was highest in the CT heterozygotes and lowest in the TT homozygotes ( $p=0.0002$ ).

	n (69)	<i>SLC30A8</i> Genotype (rs13266634)			p value
		CC	CT	TT	
All variants	35 (50.7)*	30 (43.5)	27 (39.1)	12 (17.4)	0.0006
R325-reactive	55 (79.7)*	14 (40.0)	20 (57.1)	1 (2.9)	6.73x10 <sup>-11</sup>
W325-reactive	50 (72.5)*	30 (54.5)	24 (43.6)	1 (1.8)	0.0008
Q325-reactive	43 (62.3)*	15 (30.0)	23 (46.0)	12 (24.0)	0.0002
R325-reactive only	12 (17.4)	11 (91.7)	1 (8.3)	0 (0.0)	0.013§
W325-reactive only	13 (18.8)	0 (0.0)	3 (23.1)	10 (76.9)	0.0002§
R325/W325-reactive	1 (1.4)	1 (100.0)	0 (0.0)	0 (0.0)	¥
R325/Q325-reactive	7 (10.0)	4 (57.1)	3 (42.9)	0 (0.0)	¥
W325/Q325-reactive	1 (1.4)	0 (0.0)	0 (0.0)	1 (100.0)	¥

**Table 2:20 – ZnT8A specificity to wild type ZnT8 according to *SLC30A8* genotype**

Data are presented as n (%) unless otherwise stated. Of 71 new-onset T1D patients, 69 had *SLC30A8* genotype data. \* Categories with 1 missing data set. Data were analysed by  $\chi^2$  or Fisher's exact tests [§; comparing genotypes containing the C allele (CC/CT) and T allele (TT/CT)] where indicated]. ¥ Categories with frequencies less than 5 could not be compared.

Age at onset was not associated with *SLC30A8* genotype or ZnT8A specificity to the major epitope (325).

Age at onset (<10years versus >10years) was not associated with *SLC30A8* genotype (p=0.295; **Figure 2:28A**), ZnT8A reactive to any R325/W325/Q325 variant (p=0.509; **Figure 2:28B**), or the number of 325 variants recognised by ZnT8A (p=0.469; **Figure 2:28C**).

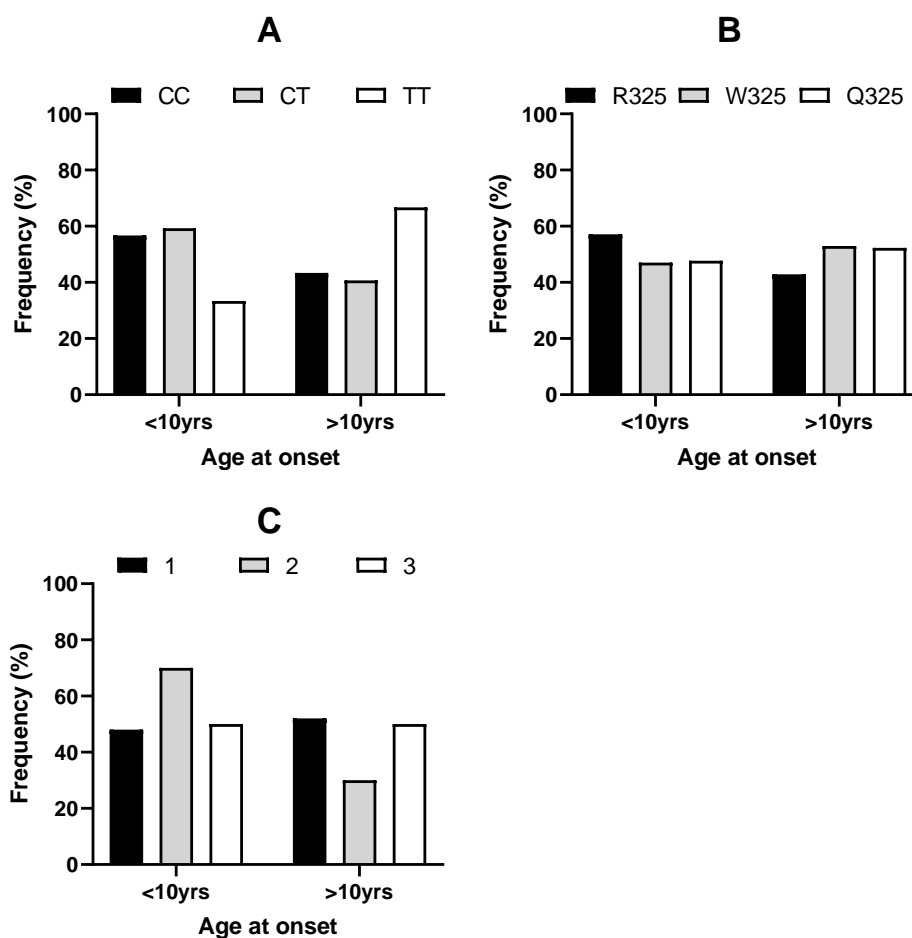


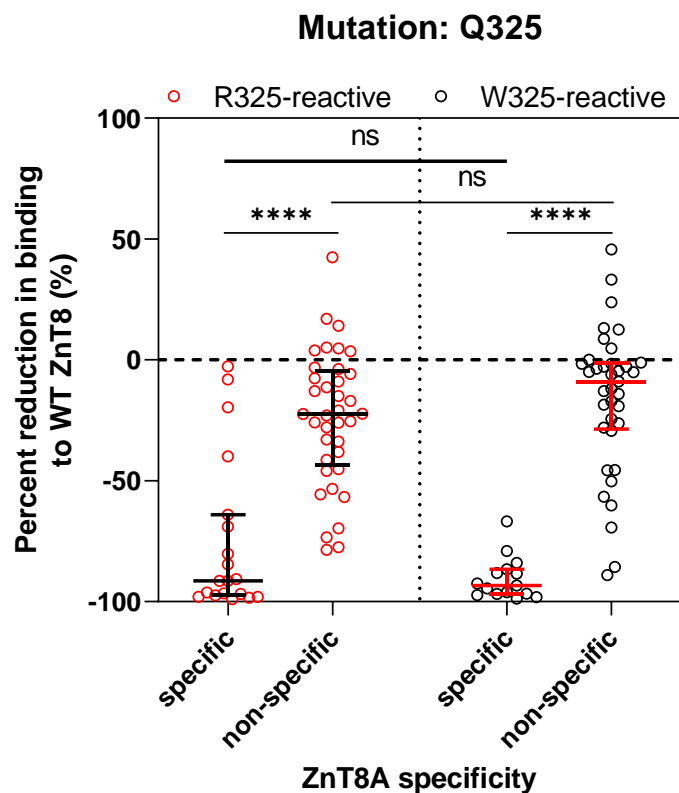
**Figure 2:28 – *SLC30A8* genotype & ZnT8A specificity to wild type ZnT8 variants by age at T1D onset**

Age at T1D onset [<10yrs (n=37) versus >10yrs (n=32)] by *SLC30A8* genotype (CC/CT/TT; n=69/71 with data available) was not associated with age at onset (**A**; p=0.295). Similarly, ZnT8A reactivity to R325/W325/Q325 variants (**B**; p=0.509) and the number of R325/W325/Q325 variants was not associated with age at onset (**C**; p=0.469). For resolution, bars denoting results from Chi-squared testing is not displayed on the graphs.

The 325Q mutation generally reduced ZnT8A binding in the majority of T1D patients but was most pronounced in R325- & W325-specific ZnT8A than non-specific ZnT8A.

The Q325 mutation caused a significant reduction in ZnT8RA and ZnT8WA binding ( $p=0.0009- <0.0001$ , **Figure 2:29**) but R325-specific and W325-specific ZnT8A had a higher median reduction in binding [median reduction 91.5-93.3% (range 2.7-98.9)] than non-specific ZnT8A [median reduction 9.0-22.4% (range +45.7-89.0)]. This indicates that these individuals are heavily reliant on encoded R325/W325 at the SNP site.

There was no evidence of differences between reduction in binding for R325-reactive versus W325-reactive ZnT8A categorised as specific or non-specific ZnT8A ( $p>0.05$ ). However, the effect of Q325 in all categories of ZnT8A specificity shows evidence of heterogeneity; 4 R325-specific ZnT8A maintained  $>50\%$  ZnT8A binding (not found in W325-specific ZnT8A), and in 7 non-specific ZnT8A, the Q325 mutation improved binding compared to WT ZnT8, which were discordant between ZnT8RA and ZnT8WA responses.



ZnT8A Specificity	ZnT8 WT antigen	n	Median reduction (%) in binding to WT ZnT8 (range)	P value*
R325-specific	ZnT8R	19	91.5 (2.7-98.9)	<0.0001
R325 non-specific	ZnT8R	38	22.4 (+42.4-78.5)	<0.0001
W325 non-specific	ZnT8W	38	9.0 (+45.7-89.0)	0.0009
W325 specific	ZnT8W	14	93.3 (66.8-98.7)	<0.0001

*Figure 2:29 – The effect of the Q325 mutation on ZnT8RA & ZnT8WA binding according to overall ZnT8A specificity in new-onset T1D patients*

NS: Not significant. Black dotted line: no change in ZnT8A compared with wild type (WT) ZnT8 antigen. Red/black bars denote median and interquartile ranges. \* Wilcoxon signed-rank test was used to evaluate change from zero in ZnT8A binding. One-way Kruskal-Wallis test with the Dunn post-hoc test was used to compare medians between categories. The Q325 mutation in all groups caused a significant reduction in ZnT8A binding ( $p < 0.0001$ - $0.0009$ ) but R325-specific and W325-specific ZnT8A had a higher median reduction in binding than non-specific ZnT8A ( $p < 0.0001$ ). This indicates that these individuals are heavily reliant on the encoded amino acid at the SNP site (aa325). There was no evidence of differences between R325/W325-specific and non-specific ZnT8A ( $p > 0.05$ ).

For further ZnT8A epitope investigation of other ZnT8 mutations, the T1D patients remained categorised by the specificity of their ZnT8A response and reactivity to R325/W325/Q325 WT ZnT8 antigens.

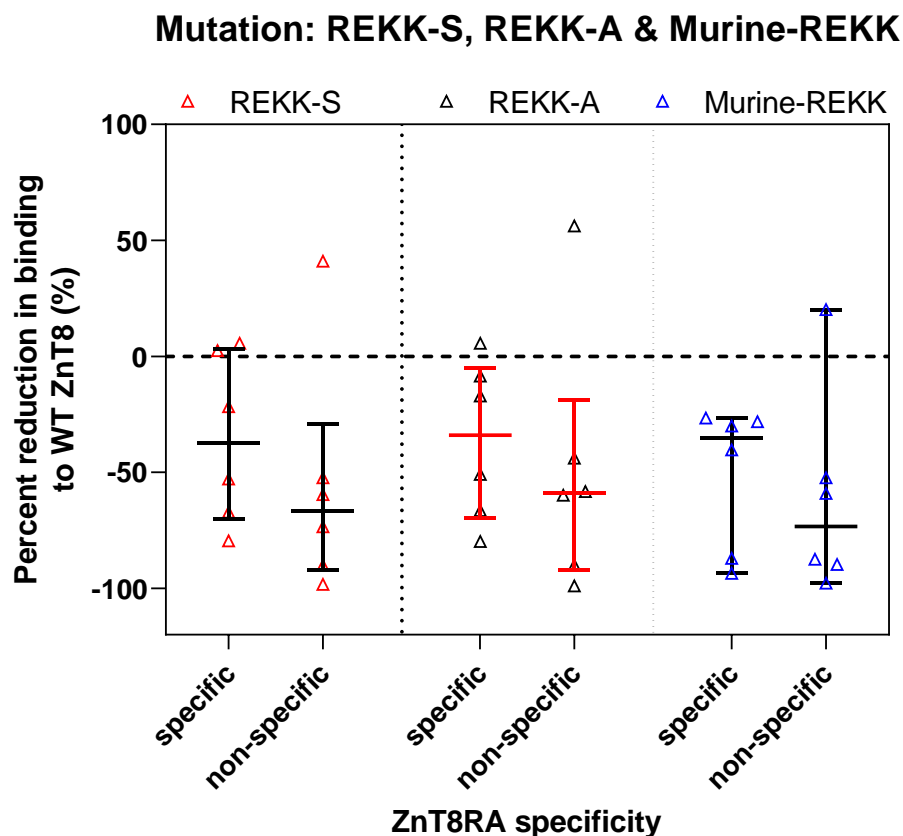
### **2.4.3.3 Categorisation of ZnT8A reactivity to the major conformational epitope (REKK) according to ZnT8A specificity**

---

The structural integrity of C-terminal ZnT8 was comparable between mutations REKK-S, REKK-A, and murine-REKK independent of ZnT8A specificity (325).

For the assessment of the REKK region (R<sub>332</sub>, E<sub>333</sub>, K<sub>336</sub>, and K<sub>340</sub>), first REKK-to-serine and REKK-to-alanine mutations were compared with murine-REKK (TGQ-) on ZnT8RA binding in a subset of T1D patients (n=12; 6 R325-specific and 6 non-specific ZnT8A).

The ability of ZnT8RA to bind REKK-serine, REKK-alanine, or murine-REKK ZnT8 constructs were comparable ( $p > 0.05$ ; **Figure 2:30**). Therefore, it was concluded that neither REKK-serine nor REKK-alanine ZnT8 mutants severely impacted the structural or epitope integrity for ZnT8RA binding greater than the naturally occurring murine-REKK sequence. Given that most studies use alanine for amino acid substitutions due to its neutrality, the mutant REKK-A was used for further investigation.



ZnT8A Specificity	ZnT8 WT antigen	ZnT8 mutant	n	Median reduction (%) in binding to WT ZnT8 (range)	P value*
R325-specific	ZnT8R	REKK-S	6	37.3 (+5.7-79.5)	0.0093
R325 non-specific	ZnT8R	REKK-S	6	66.5 (+41.0-98.2)	
R325-specific	ZnT8R	REKK-A	6	34.0 (+5.7-79.9)	0.0093
R325 non-specific	ZnT8R	REKK-A	6	59.1 (+56.3-99.0)	
R325-specific	ZnT8R	murine-REKK	6	35.2 (26.6-93.5)	0.0010
R325 non-specific	ZnT8R	murine-REKK	6	73.3 (20.1-97.7)	

**Figure 2:30 – The effect of REKK-S, REKK-A, & murine-REKK mutations on ZnT8RA binding according to ZnT8A specificity in a subset of new-onset T1D patients**

Black dotted line: no change in ZnT8A compared with wild type (WT) ZnT8 antigen. Red/black bars denote median and interquartile ranges. One-way Kruskal-Wallis test with the Dunn post-hoc test was used to compare medians between categories. There was no difference between the categories of ZnT8A specificity and ZnT8 mutant (REKK-S, REKK-A or murine-REKK) ( $p > 0.05$ ), but mutations did cause reductions ZnT8A binding greater than zero as expected (\* Wilcoxon signed-rank test). Therefore, it was concluded that neither REKK-serine nor REKK-alanine ZnT8 mutants severely impacted the structural or epitope integrity for ZnT8RA binding greater than the naturally occurring murine-REKK.

The REKK region is important for ZnT8A binding independent of ZnT8A specificity (325), but responses were heterogeneous.

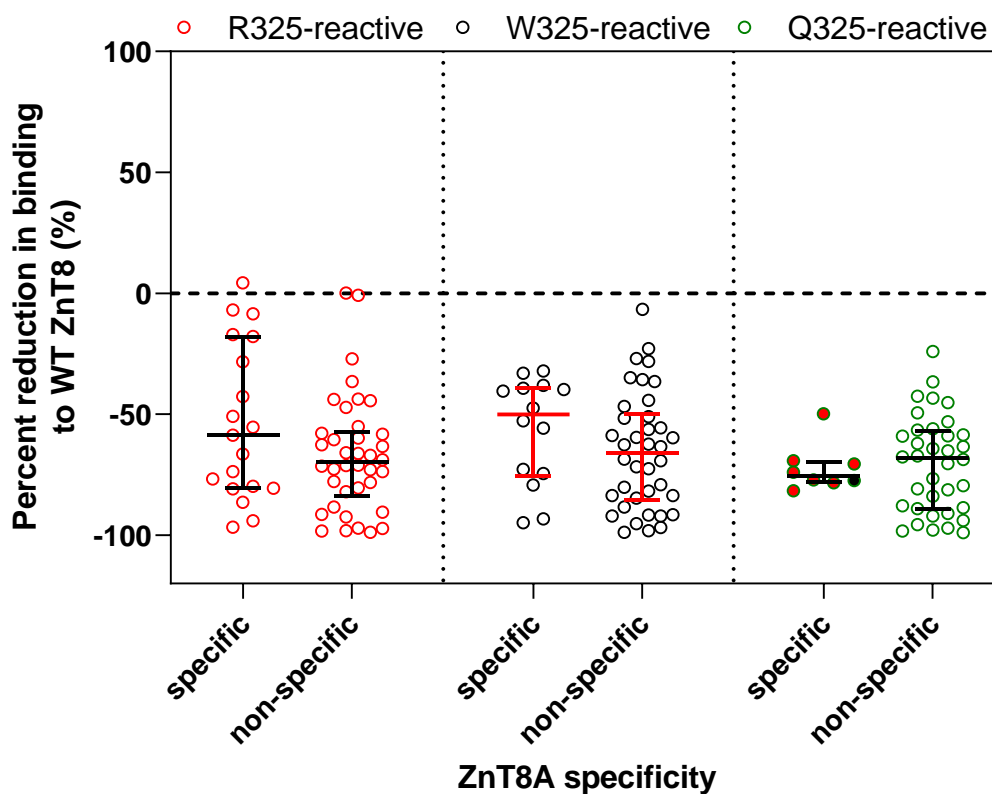
The REKK-A mutation caused a significant reduction in ZnT8RA, ZnT8WA, and ZnT8QA binding ( $p < 0.001$ ) independent of ZnT8A specificity ( $p > 0.05$  in all pairwise comparisons, **Figure 2:31**).

The median reduction in binding caused by the REKK-A mutation was comparable but there was evidence of heterogeneity between sera given the range of effect across ZnT8 WT antigen constructs ( $p < 0.0001$  for all) encoding R325 [56.8% (range 4.4-96.7)], W325 [66.0% (range 6.7-98.8)], or Q325 [68.2% (range 24.0-98.9)]. Similarly, the median reduction in binding caused by REKK-A was comparable in R325-specific [56.8% (range 4.4-96.7),  $p < 0.0001$ ] and W325-specific [50.1% (range 32.2-94.8),  $p < 0.0001$ ] responses.

Individuals R325/Q325-reactive and W325/Q325-reactive comprised a small portion of the cohort ( $n=8$ ; 11.3%), but a significant reduction was still observed [median reduction in binding 75.6% (range 49.9-81.6),  $p=0.0078$ ]. Binding to the REKK-A mutant when Q325 is present on all R325-reactive and W325-reactive ZnT8A was comparable regardless of specificity (data not shown). There were some R325/W325-specific ZnT8A responses with ZnT8A binding within 50% of WT: 7 R325-reactive, 7 W325-reactive, and 1 R325/Q325-reactive.

Although the REKK conformational epitope region is important for ZnT8A binding, mutating this region does not cause a unanimous effect for all patients as a total of 38 patients (53.5%) maintained  $>50\%$  ZnT8A binding towards REKK-A reactive towards R325 ( $n=15/57$ , 26.3%), W325 ( $n=16/52$ , 30.8%), and Q325 ( $n=7/44$ , 15.9%). Therefore, this region may not always be fully independent of the major 325 epitope region (**Figure 2:32**).

### Mutation: REKK-A



ZnT8A Specificity	ZnT8 WT antigen	n	Median reduction (%) in binding to WT ZnT8 (range)	P value*
R325-specific	ZnT8R	19	56.8 (4.4-96.7)	<0.0001
R325 non-specific	ZnT8R	38	69.9 (0.0-98.8)	<0.0001
W325-specific	ZnT8W	14	50.1 (32.2-94.8)	0.0001
W325 non-specific	ZnT8W	38	66.0 (6.7-98.8)	<0.0001
Q325-specific	ZnT8Q	8	75.6 (49.9-81.6)	0.0078
Q325 non-specific	ZnT8Q	36	68.2 (24.0-98.9)	<0.0001

*Figure 2:31 – The effect of the REKK-A mutation on ZnT8A binding according to ZnT8A specificity in new-onset T1D patients*

Black dotted line: no change in ZnT8A compared with wild type (WT) ZnT8 antigen. Red/black bars denote median and interquartile ranges. Filled red and black circles denote R325/Q325-reactive patients and W325/Q325-reactive patients, respectively. \* Wilcoxon signed-rank test was used to evaluate change from zero in ZnT8A binding. One-way Kruskal-Wallis test with the Dunn post-hoc test was used to compare medians between categories. The REKK-A mutation reduced ZnT8A binding ( $p < 0.0001$ - $0.0078$ ) independent of ZnT8A specificity ( $p > 0.05$ ).

## Mutation: REKK-A

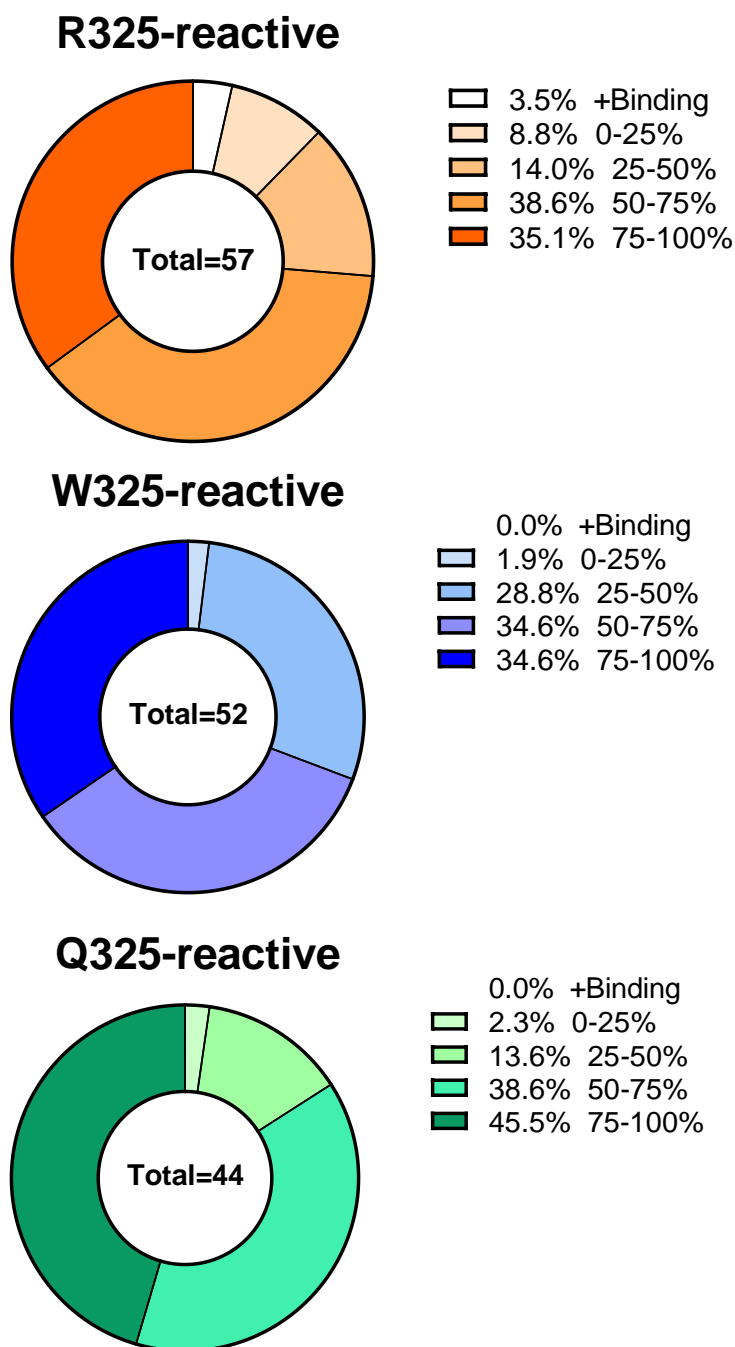


**Figure 2:32 – The effect of the REKK-A mutant on R325-reactive, W325-reactive, & Q325-reactive ZnT8A binding in new-onset T1D patients**

Proportions of the degree of decreased binding from wild-type (WT) ZnT8 antigen caused by REKK-A encoding R325, W325, or Q325 on R325-reactive, W325-reactive, and Q325-reactive ZnT8A, respectively is presented. Q328-reactive ZnT8A are all non-specific ZnT8A responses, whereas R325- and W325-reactive ZnT8A is a mixture of specific and non-specific ZnT8A responses. No difference was observed between R325-reactive, W325-reactive, or Q325-reactive ZnT8A ( $p > 0.05$ ) but 26.3% ( $n=15$ ), 30.8% ( $n=16$ ), and 15.9% ( $n=7$ ), respectively was able to maintain ZnT8A binding within 50% of binding to WT ZnT8 antigen.

Truncating C-terminal ZnT8 by 20% (349T) did not explain the heterogeneous ZnT8A binding observed in the REKK-A mutant

The 349T mutant resulted from a historic cloning error that removed the last 20 amino acids of C-terminal ZnT8, but the major epitopes (R325/W325/Q325 and REKK) remain present. To further investigate the heterogeneity of the ZnT8A binding caused by the REKK-A mutant, R325 and W325 categories of ZnT8A specificity were split according to the median reduction in binding with REKK-A (**Figure 2:33**) and compared with the median reduction in binding caused by the 349T mutant (**Figure 2:34**).

Truncating the last 20 amino acids caused a reduction in all categories of R325-reactive and W325-reactive ZnT8A ( $p=0.0156- < 0.0001$ ) independent of the effect of the REKK-A mutant. When adjusted for multiple comparisons, there was only a difference between R325-specific and non-specific ZnT8A that was most resistant to the REKK-A mutation when tested for the 349T mutation ( $p=0.0119$ ) (**Figure 2:34**; indicated by § symbols). However, generally non-specific ZnT8A appeared to have a higher median reduction in binding than R325- or W325-specific responses, possibly due to aa325 dependent epitope being unaffected by the truncation.

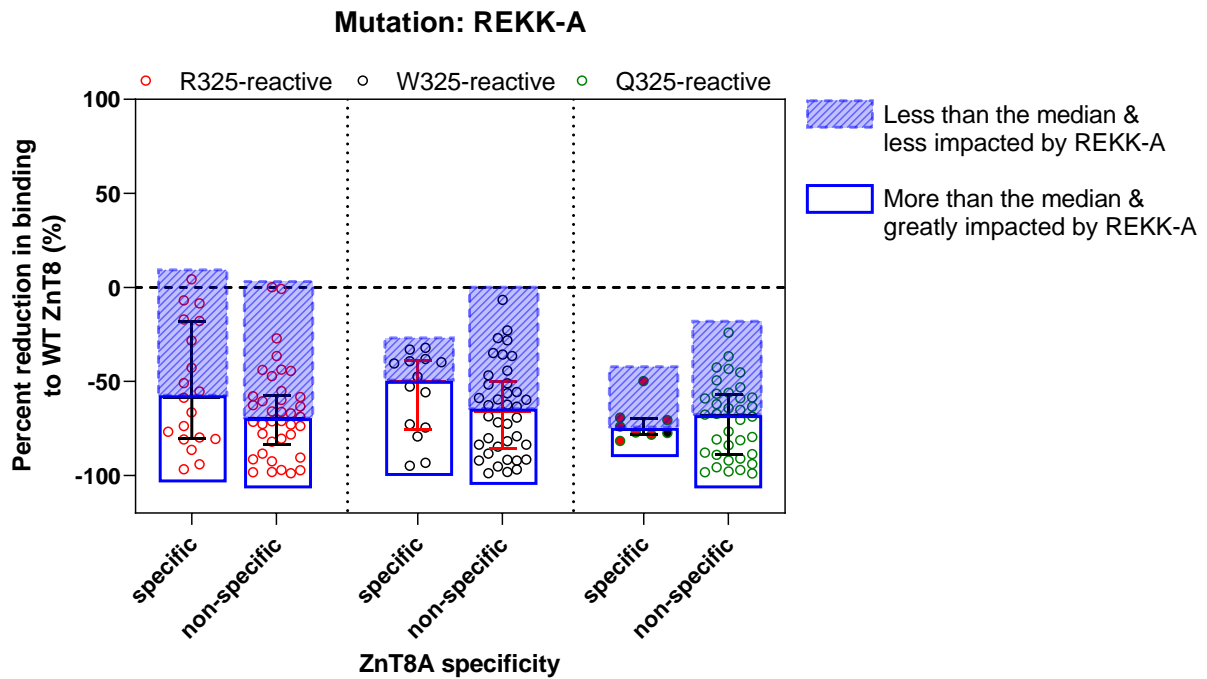
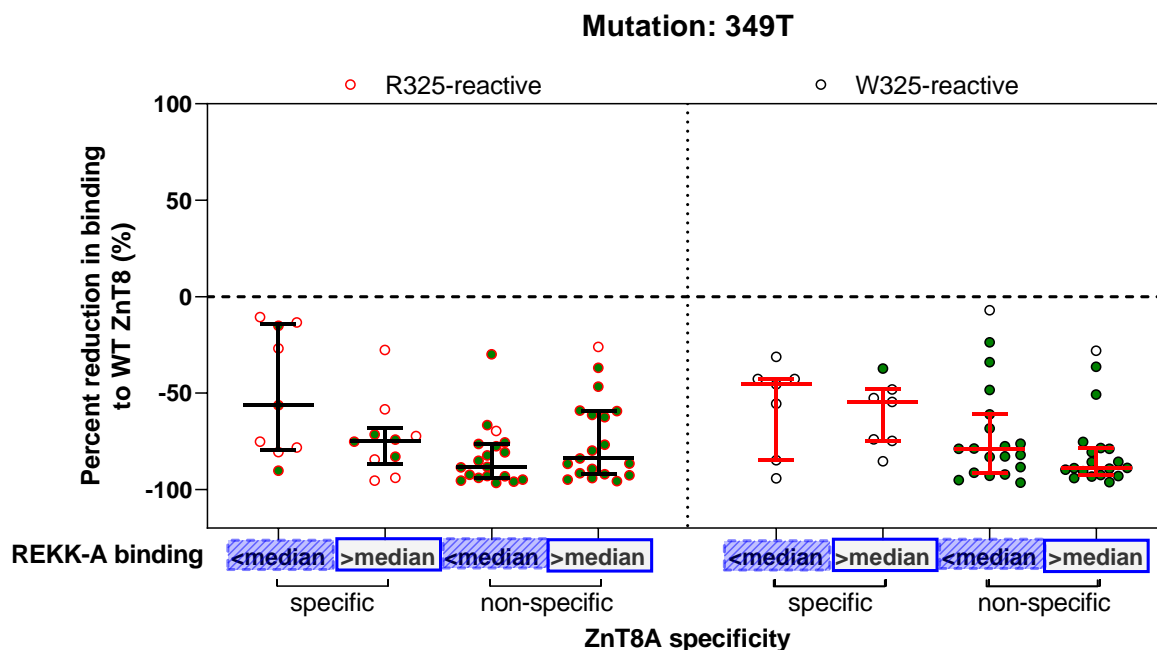


*Figure 2:33 – Categorisation of ZnT8A binding according to the median reduction in binding caused by REKK-A for the assessment of 349T*

Black dotted line: no change in ZnT8A compared with wild type (WT) ZnT8 antigen. Red/black bars denote median and interquartile ranges. Filled green circles denote all patients that also react to Q325 WT ZnT8 antigen. Patient ZnT8A responses were categorised according to the median reduction in binding across all ZnT8A specificities. Blue filled boxes denote ZnT8A responses less impacted by the REKK-A mutation (less than the median reduction in binding). Blue open boxes denote ZnT8A responses greatly impacted by the REKK-A mutation (greater than the median reduction in binding).



ZnT8A Specificity	ZnT8 WT antigen	Lower/higher than median reduction in binding to REKK-A	n	Median reduction (%) in binding to WT ZnT8 (range)	P value*
R325-specific	ZnT8R	< -56.8%	9	56.3 (10.6-90.2)	0.0039§
R325-specific	ZnT8R	> -56.8%	10	74.6 (27.6-95.5)	0.002
R325 non-specific	ZnT8R	< -69.9%	19	88.2 (29.9-96.6)	<0.0001§
R325 non-specific	ZnT8R	> -69.9%	19	83.9 (26.0-95.6)	<0.0001
W325-specific	ZnT8W	< -50.1%	7	45.4 (31.1-94.2)	0.0156
W325-specific	ZnT8W	> -50.1%	7	54.5 (37.3-85.3)	0.0156
W325 non-specific	ZnT8W	< -66.0%	19	78.8 (7.0-96.5)	<0.0001
W325 non-specific	ZnT8W	> -66.0%	19	88.2 (28.0-96.1)	<0.0001

**Figure 2:34 – The effect of the 349T mutation on ZnT8A binding according to the REKK-A binding & ZnT8A specificity in new-onset T1D patients**

Black dotted line: no change in ZnT8A compared with wild-type (WT) ZnT8 antigen. Red/black bars denote median and interquartile ranges. Filled green circles denote all patients that also react to Q325 WT ZnT8 antigen. \* Wilcoxon signed-rank test was used to evaluate change from zero in ZnT8A binding. One-way Kruskal-Wallis test with the Dunn post-hoc test was used to compare medians between categories. § only pairwise comparison that was significantly different when adjusted for multiple comparisons (p=0.0119).

Truncating C-terminal ZnT8 by 20% (349T) revealed that the majority of R325- & W325-reactive ZnT8A relied on the downstream 20 amino acids to bind (aa349-369) despite the presence of the major epitopes.

Interestingly, removing 20% of C-terminal ZnT8 (349T) still caused heterogeneous effects on ZnT8A binding but the majority of ZnT8A showed >50% reduced binding with comparable proportions between R325-reactive (n=48, 84.2%) and W325-reactive (n=40, 76.9%) ZnT8A (p=0.466; **Figure 2:35**).

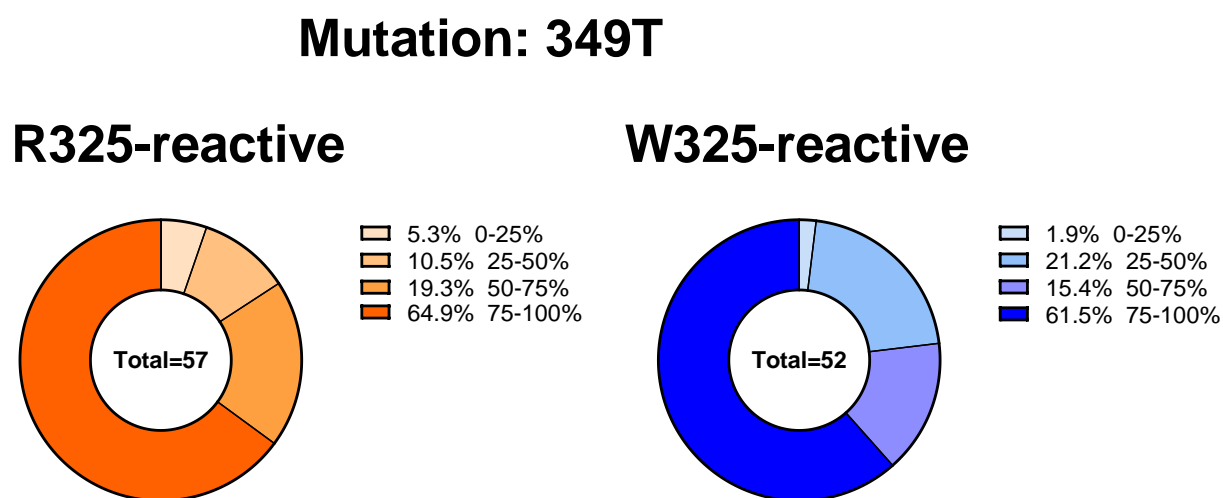


*Figure 2:35 – The effect of the 349T mutant on R325-reactive & W325-reactive ZnT8A in new-onset T1D patients*

Proportions of the degree of decreased binding from wild-type (WT) ZnT8 antigen caused by 349T encoding R325 or W325 R325-reactive and W325-reactive ZnT8A, respectively, are presented. In both categories, there is a mixture of specific and non-specific ZnT8A responses but, the majority of ZnT8A independent of specificity had a >50% reduced ZnT8A binding caused by the 349T truncation [R325-reactive n=48 (84.2%); W325-reactive n=40 (76.9%)]. However, a small proportion was able to maintain between 0-50% of the ZnT8A binding to WT ZnT8 antigen [R325-reactive n=9 (15.8%); W325-reactive n=12 (23.1%)]. No difference was observed in the proportions of patients who had less than or greater than 50% reduced binding between R325-reactive and W325-reactive ZnT8A (p=0.466).

This mutant has both the previously reported major epitopes present (the 325 and the REKK region), and therefore, the last 20 amino acids are clearly important for ZnT8A binding. However, 325 and REKK epitope regions may rely on the conformational structure provided by the last 20 amino acids. As cysteines provide support for protein structure through disulphide bonds, the 349T data supported the investigation into the effect of the three cysteines in C-terminal ZnT8 (C<sub>361</sub>, C<sub>364</sub>, and C<sub>368</sub>) on ZnT8A binding.

#### **2.4.3.4 Categorisation of ZnT8A reactivity to ZnT8's three C-terminal cysteines (C361, C364, & C368) according to ZnT8A specificity**

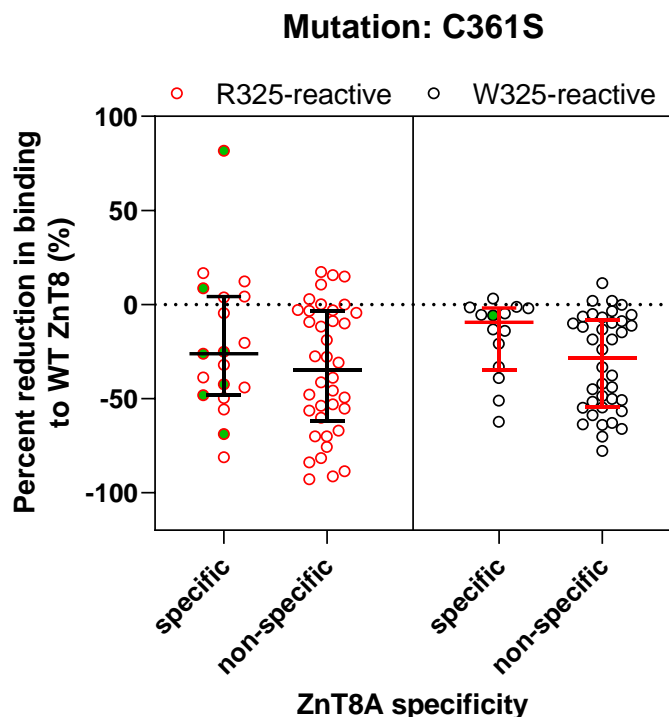
---

##### Single cysteine-to-serine mutations caused a reduction in ZnT8A binding independent of ZnT8A specificity.

The C361S mutation caused a significant reduction in R325-reactive and W325-reactive ZnT8A binding ( $p < 0.0001-0.018$ ) independent of ZnT8A specificity ( $p > 0.05$  in all pairwise comparisons), despite some evidence of heterogeneity in the degree of reduced binding (**Figure 2:36**).

The median reduction in binding caused by C361S was comparable for R325-specific and R325 non-specific ZnT8A responses [26.2% (range +81.6-81.2),  $p < 0.018$  and 34.9% (range +17.2-93.0),  $p < 0.0001$ , respectively]. Whilst the median reduction in binding in W325 non-specific ZnT8A responses was comparable with the R325-reactive responses [28.7% (range +11.3-77.8),  $p < 0.0001$ ], W325-specific ZnT8A was less effected by C361 [9.5 % (range +3.1-62.3),  $p = 0.0009$ ].

A total of 15/71 (21.1%) patients had improved ZnT8A binding above WT ZnT8 caused by the C361S mutation across all categories of ZnT8A specificity; R325-specific (n=4), R325/Q325 (n=2), W325-specific (n=1), R325/W325/Q325 non-specific (n=8).



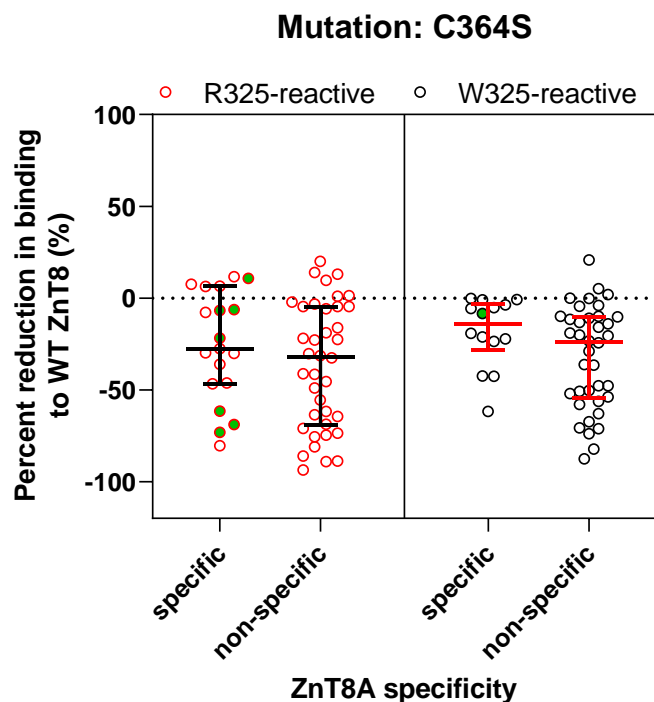
ZnT8A Specificity	ZnT8 WT antigen	n	Median reduction (%) in binding to WT ZnT8 (range)	P value*
R325-specific	ZnT8R	19	26.2 (+81.6-81.2)	0.018
R325 non-specific	ZnT8R	38§	34.9 (+17.2-93.0)	<0.0001
W325 non-specific	ZnT8W	38§	28.7 (+11.3-77.8)	<0.0001
W325-specific	ZnT8W	14	9.5 (+3.1-62.3)	0.0009

*Figure 2:36 – The effect of the C361S mutation on ZnT8A binding according to the ZnT8A specificity in new-onset T1D patients*

Black dotted line: no change in ZnT8A compared with wild type (WT) ZnT8 antigen. Red/black bars denote median and interquartile ranges. Filled green circles denote all patients with R325-specific and W325-specific responses that also react to Q325 WT ZnT8 antigen. § The vast majority (94.7%; n=36) of non-specific ZnT8A react to all three variants R325/W325/Q325 but includes 2 individuals (5.3%) with ZnT8A reactive to R325/W325. \* Wilcoxon signed-rank test was used to evaluate change from zero in ZnT8A binding. One-way Kruskal-Wallis test with the Dunn post-hoc test was used to compare medians between categories. No difference between pairwise comparisons was observed ( $p>0.05$ ).

Similar to C361S, comparable reductions in binding were observed for C364S (**Figure 2:37**) and C368S (**Figure 2:38**) in R325-reactive and W325-reactive ZnT8A ( $p<0.0001-0.0108$ ) independent of specificity ( $p>0.05$  for all pairwise comparisons); however, W325-specific ZnT8A was less effected by single C361S/C364S mutants [median reduction in binding 9.5-13.8% (range +3.1-62.3)] than other ZnT8A specificities but was comparable to all ZnT8A specificities for C368S [median reduction in binding 34.7% (+7.0-79.6)].

A total of 13/71 (18.3%) patients had improved ZnT8A binding above WT ZnT8 caused by the C364S mutation across all categories of ZnT8A specificity except W325-specific responses; R325-specific (n=4), R325/Q325 (n=1), and R325/W325/Q325 non-specific (n=8) (**Figure 2:37**).

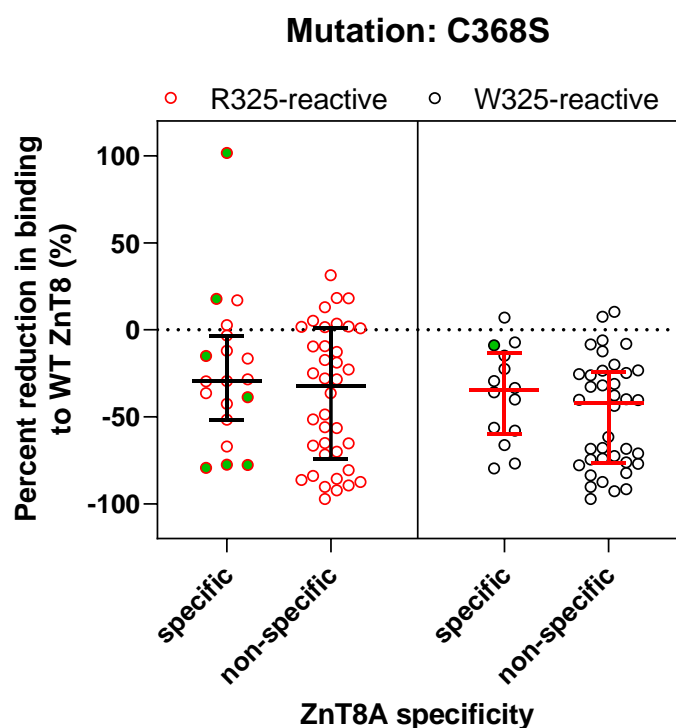


ZnT8A Specificity	ZnT8 WT antigen	n	Median reduction (%) in binding to WT ZnT8 (range)	P value*
R325-specific	ZnT8R	19	27.6 (+11.7-80.5)	0.0033
R325 non-specific	ZnT8R	38§	32.0 (+20.0-93.6)	<0.0001
W325 non-specific	ZnT8W	38§	23.9 (+20.7-87.5)	<0.0001
W325-specific	ZnT8W	14	13.8 (0.24-61.8)	0.0001

**Figure 2:37 – The effect of the C364S mutation on ZnT8A binding according to the ZnT8A specificity in new-onset T1D patients**

Black dotted line: no change in ZnT8A compared with wild type (WT) ZnT8 antigen. Red/black bars denote median and interquartile ranges. Filled green circles denote all patients with R325-specific and W325-specific responses that also react to Q325 WT ZnT8 antigen. § The vast majority (94.7%; n=36) of non-specific ZnT8A react to all three variants R325/W325/Q325 but includes 2 individuals (5.3%) with ZnT8A reactive to R325/W325. \* Wilcoxon signed-rank test was used to evaluate change from zero in ZnT8A binding. One-way Kruskal-Wallis test with the Dunn post-hoc test was used to compare medians between categories. No difference between pairwise comparisons was observed (p>0.05).

A total of 16/71 (22.5%) patients had improved ZnT8A binding above WT ZnT8 caused by the C368S mutation across all categories of ZnT8A specificity; R325-specific (n=2), R325/Q325 (n=2), W325-specific (n=1), and R325/W325/Q325 non-specific (n=11) (**Figure 2:38**).



ZnT8A Specificity	ZnT8 WT antigen	n	Median reduction (%) in binding to WT ZnT8 (range)	P value*
R325-specific	ZnT8R	19	29.3 (+101.7-79.3)	0.0108
R325 non-specific	ZnT8R	38§	32.4 (+31.3-97.2)	<0.0001
W325 non-specific	ZnT8W	38§	42.0 (+10.4-97.2)	<0.0001
W325-specific	ZnT8W	14	34.7 (+7.0-79.6)	0.0002

**Figure 2:38 – The effect of the C368S mutation on ZnT8A binding according to the ZnT8A specificity in new-onset T1D patients**

Black dotted line: no change in ZnT8A compared with wild type (WT) ZnT8 antigen. Red/black bars denote median and interquartile ranges. Filled green circles denote all patients with R325-specific and W325-specific responses that also react to Q325 WT ZnT8 antigen. § The vast majority (94.7%; n=36) of non-specific ZnT8A react to all three variants R325/W325/Q325 but includes 2 individuals (5.3%) with ZnT8A reactive to R325/W325. \* Wilcoxon signed-rank test was used to evaluate change from zero in ZnT8A binding. One-way Kruskal-Wallis test with the Dunn post-hoc test was used to compare medians between categories. No difference between pairwise comparisons was observed (p>0.05).

Overall, ~50-60% of R325-reactive and 40-71% of W325-reactive ZnT8A in new-onset T1D patients had greater than 25% reduced ZnT8A binding caused by single cysteine-to-serine mutations.

The proportion of new-onset T1D patients with R325-reactive and W325-reactive ZnT8A responses categorised by the percent reduction of ZnT8A binding between mutant (C361S, C364S, C368S) and WT ZnT8 is presented in **Figure 2:39**. In R325-reactive T1D patients (n=57 of 71), 33 (56.1%), 31 (54.4%), and 32 (56.1%) had a greater than 25% reduced ZnT8A binding caused by C361S, C364S, and C368S, respectively. In W325-reactive patients (n=53 of 71), 23 (43.4%), 21 (39.6%), and 37 (69.8%) had a greater than 25% reduced ZnT8A binding caused by C361S, C364S, and C368S, respectively. There was no difference in the proportion of patients who had less than or greater than 50% reduced binding between R325-reactive and W325-reactive ZnT8A for any of the single cysteine-to-serine mutations [C361S: >0.999; C364S: p=0.832; C368S: p=0.566].

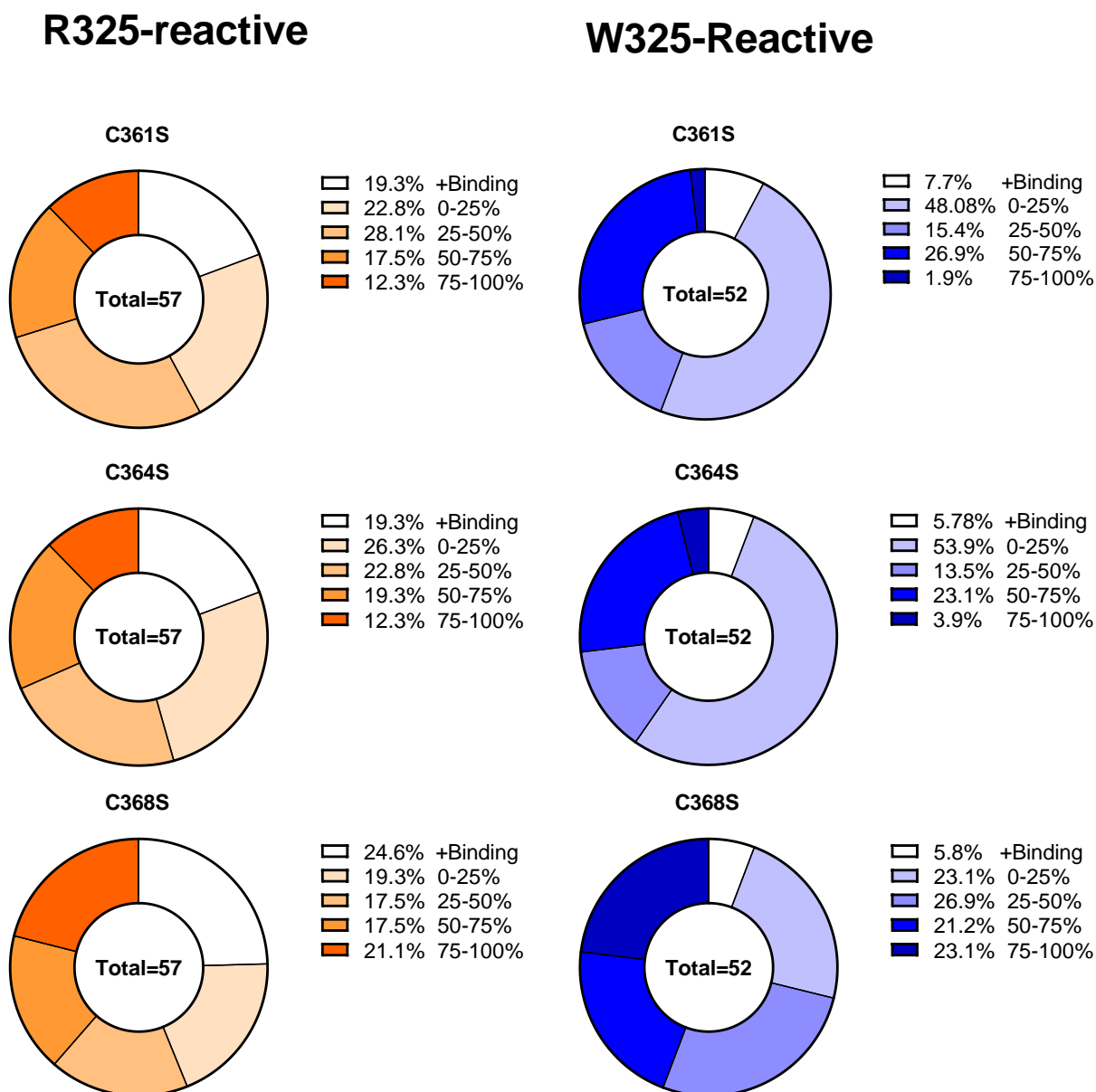
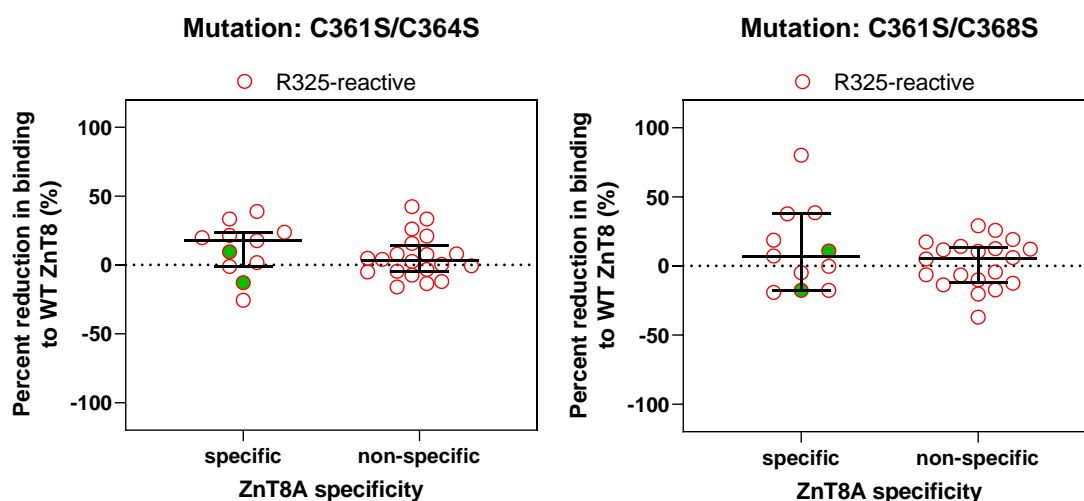


**Figure 2:39 – The effect of single cysteine-to-serine mutations on R325-reactive and W325-reactive ZnT8A binding in new-onset T1D patients**

No difference was observed in the proportions of patients who had less than or greater than 50% reduced binding between R325-reactive and W325-reactive ZnT8A for any of the single cysteine-to-serine mutations [C361S: >0.999; C364S: p=0.832; C368S: p=0.566].

Conflicting with the single cysteine-to-serine mutations, double cysteine-to-serine mutations had little impact on ZnT8RA binding in a subset of new-onset T1D patients.

Despite the effect of mutating individual cysteines, double cysteine-to-serine mutations (C361S/C364S and C361S/C368S) did not cause a significant reduction in ZnT8RA binding ( $p>0.05$ ) independent of ZnT8A specificity (**Figure 2:40**). Therefore, there does not appear to be a sequential effect of mutating more than one C-terminal cysteine, and it was not further investigated in ZnT8WA responses.



ZnT8A Specificity	ZnT8 WT antigen	ZnT8 Mutations	n	Median reduction (%) in binding to WT ZnT8 (range)	P value*
R325-specific	ZnT8R	C361S C364S	11	+17.6 (-25.5-+38.9)	NS
R325 non-specific	ZnT8R	C361S C364S	20	+3.3 (-15.6-+42.4)	NS
R325-specific	ZnT8R	C361S C368S	11	+7.2 (-19.1-+80.1)	NS
R325 non-specific	ZnT8R	C361S C368S	20	+5.6 (-37.0-+29.0)	NS

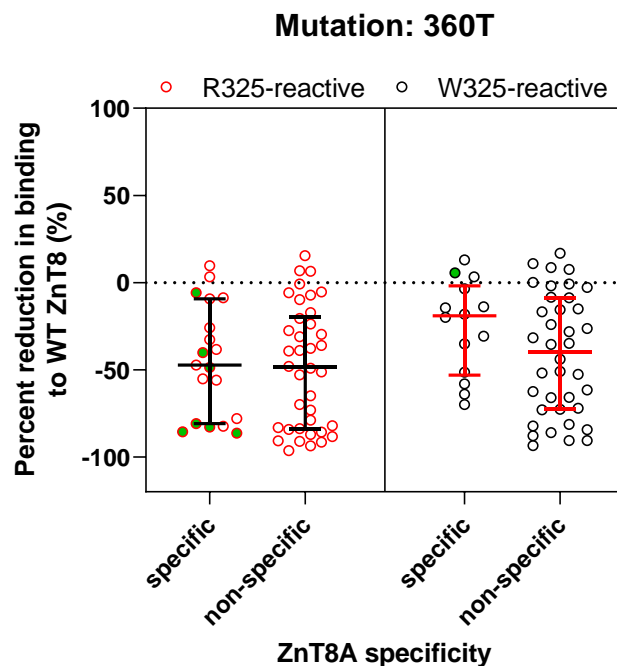
**Figure 2:40 – The effect of the C361S/C364S & C361S/C368S double mutations on ZnT8RA binding according to ZnT8A specificity in a subset of new-onset T1D patients**

NS: Not significant; Black dotted line: no change in ZnT8A compared with wild type (WT) ZnT8 antigen. Black bars denote median and interquartile ranges. Filled green circles denote all patients with R325-specific and W325-specific responses that also react to Q325 WT ZnT8 antigen. \* Wilcoxon signed-rank test was used to evaluate change from zero in ZnT8A binding. One-way Kruskal-Wallis test with the Dunn post-hoc test was used to compare medians between categories. No difference between pairwise comparisons was observed ( $p>0.05$ ).

Truncating C-terminal ZnT8 by 9 amino acids (360T) to remove all three cysteines had a comparable impact on ZnT8A binding as single cysteine-to-serine mutations.

The 360T truncation reduced R325-reactive and W325-reactive ZnT8A binding ( $p < 0.0001$ - $0.0031$ ) independent of specificity ( $p > 0.05$ ), despite some evidence of heterogeneity. The median reduction in binding was comparable for R325-specific [47.3% (range +9.7-86.4),  $p < 0.0001$ ] and R325 non-specific ZnT8A responses [48.6% (range +15.5-96.4),  $p < 0.0001$ ]. However, as observed for the single mutations, W325-specific ZnT8A was less effected [19.1% (range +13.0-69.4%),  $p = 0.0031$ ] but W325 non-specific ZnT8A responses was comparable to the R325 counterpart [39.6% (range +16.8-93.5),  $p < 0.0001$ ] (**Figure 2:41**).

Whilst it was speculated that the highly detrimental effect of 349T could have been due to the removal of cysteines (and resultant disulphide bonds) influencing the conformational structure of C-terminal ZnT8, the reduced effect of cysteine-specific removal (360T) suggests, the effect of 349T was not entirely related to the three C-terminal cysteines.



ZnT8A Specificity	ZnT8 WT antigen	n	Median reduction (%) in binding to WT ZnT8 (range)	P value*
R325-specific	ZnT8R	19	47.3 (+9.7-86.4)	<0.0001
R325 non-specific	ZnT8R	38§	48.6 (+15.5-96.4)	<0.0001
W325 non-specific	ZnT8W	38§	39.6 (+16.8-93.5)	<0.0001
W325-specific	ZnT8W	14	19.1 (+13.0-69.4)	0.0031

**Figure 2:41 – The effect of 360T on ZnT8A binding according to the ZnT8A specificity in new-onset T1D patients**

Black dotted line: no change in ZnT8A compared with WT ZnT8 antigen. Red/black bars denote median and interquartile ranges. Filled green circles denote all patients with R325-specific and W325-specific responses that also react to Q325 WT ZnT8 antigen. § The vast majority (94.7%; n=36) of non-specific ZnT8A react to all three variants R325/W325/Q325 but includes 2 individuals (5.3%) with ZnT8A reactive to R325/W325. \* Wilcoxon signed-rank test was used to evaluate change from zero in ZnT8A binding. One-way Kruskal-Wallis test with the Dunn post-hoc test was used to compare medians between categories. No difference between pairwise comparisons was observed (p>0.05).

Combining all C-terminal ZnT8 mutations on ZnT8A binding by heat map analysis elucidates the heterogeneous patterns that appear unrelated to ZnT8A specificity – evidence for subpopulations of co-existing ZnT8A?

Unbiased heat map analysis across all ZnT8 mutants by rank ZnT8A binding to radiolabelled WT ZnT8 antigen (R325/W325/Q325) and *SLC30A8* genotype was performed by Dr A.E. Long to identify clusters of new-onset T1D patients with similar ZnT8A binding profiles. Surprisingly, profiles clustered at the major SNP epitope region (325; according to the corresponding *SLC30A8* genotype(s)) first and was followed by the C-terminal cysteine and REKK regions (**Figure 2:42**). Aside from these 3 major clusters, a large degree of heterogeneity was still evident, inferring that in this new-onset T1D patient cohort, ZnT8A targeting of ZnT8 is highly variable. For instance, heterogeneity was observed for REKK, which was not previously reported. The clustering suggests the cysteine region could form a minor independent epitope for ZnT8A.

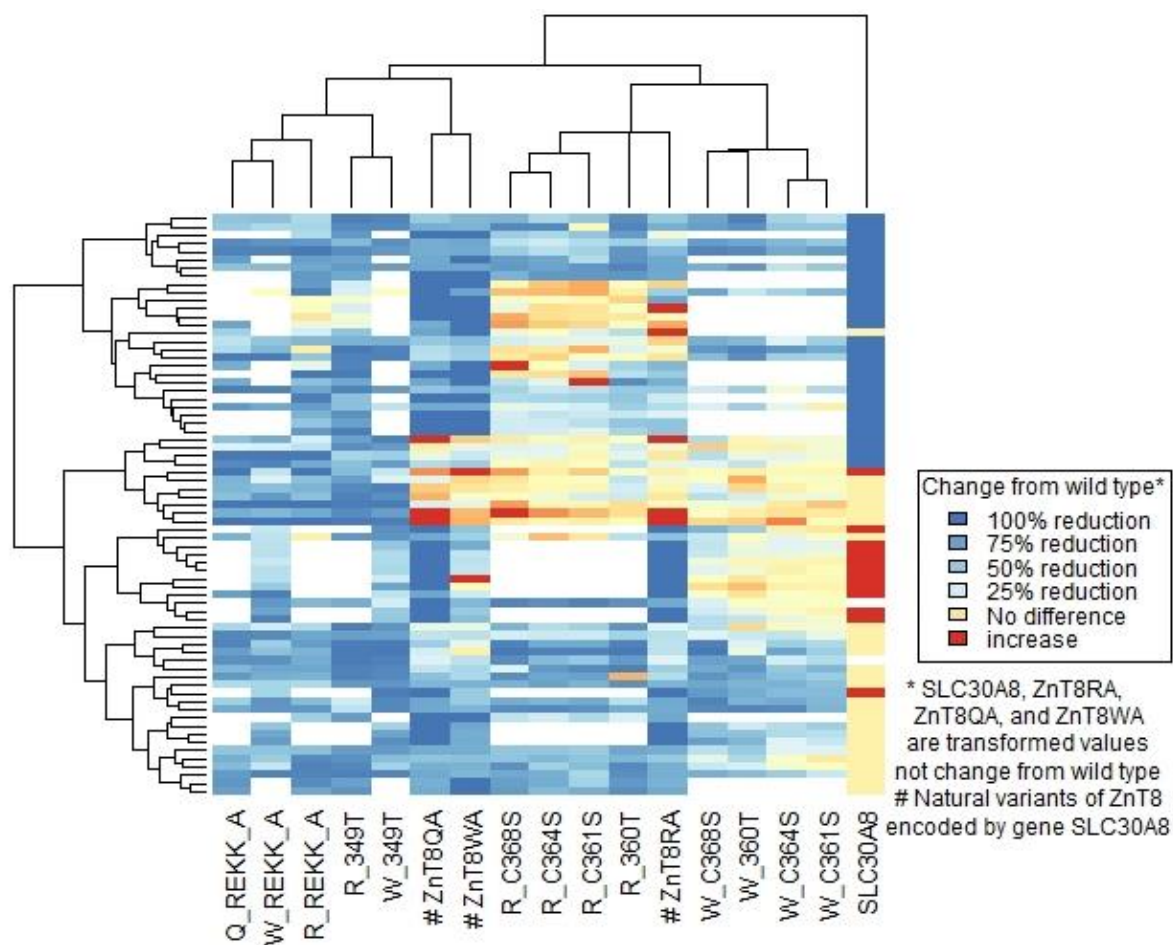


**Figure 2:42 – Dendrogram of ZnT8 mutational analysis by SLC30A8 genotype & binding to WT C-terminal ZnT8**

SLC30A8 genotype: blue (CC homozygous), yellow (CT heterozygous), and red (TT homozygous). Sera predominantly clustered by CC (R325) genotype or CT/TT (W325 ± R325) genotype, but this may have been driven by the testing strategy and preselection of ZnT8RA and ZnT8WA positives. Of the ZnT8A responses, two main clusters emerged. One contained 360T, C-terminal cysteine mutations, and ZnT8RA titre (rank), subdivided by R or W ZnT8A specificity. The main cluster contained REKK, 349T, ZnT8QA titre (rank), and ZnT8WA titre (rank). This suggests that the C-terminal cysteine and C360T have similar effects to each other but that the sera affected are different between ZnT8RA and ZnT8WA specificity. In contrast, REKK and 349T responses are distinct.

---

## 2.4.4 Discussion

---

### 2.4.4.1 Main findings

---

1. Many findings were confirmed in this study: the majority of ZnT8A according to the major epitope (325) are non-specific and bind more than one variant, titres of R325-reactive & W325-reactive ZnT8A do not correlate (due to R325- and W325-specific responses), and ZnT8A specificity (325) is associated with *SLC30A8* genotypes. Unlike other reports, both ZnT8A specificity and *SLC30A8* genotype was not related to age-at-onset when comparing under or over 10 years.

2. ZnT8A specificity (325) was comparable between SPs and RPs, but ZnT8A titres & specificity may change over time in some individuals. This suggests that 325 epitope spreading can occur prior to T1D onset or that ZnT8A can be polyclonal.

3. As expected, the 325Q mutation severely reduced ZnT8A binding in the T1D patients with R325- & W325-specific ZnT8A (median reduction in binding 92-93%). However, there were some reductions in non-specific ZnT8A (median reduction in binding 9-22%), suggesting that some of these individuals may have combined responses comprising a mix of R325- and W325-specific ZnT8A.

4. The REKK region is important for ZnT8A binding independent of ZnT8A specificity (325), but there was heterogeneous ZnT8A binding (range of reduced binding 0-99%).

5. The removal of 20% of C-terminal ZnT8 (downstream of aa349) revealed that 84.2% of R325-reactive ZnT8A and 76.9% of W325-reactive ZnT8A had <50% reduced binding compared to WT ZnT8 antigen. This suggests that the majority of ZnT8A either rely on

residues downstream of this to bind or that the residues downstream of aa349 are required for the structural integrity of ZnT8 for ZnT8A to bind.

6. Single cysteine-to-serine mutations generally caused ~30% reduced ZnT8A binding in R325-reactive ZnT8A and non-specific ZnT8A responses, but W325-specific ZnT8A was least affected by C361S and C364S (~9-13% reduced binding). In contrast, double cysteine-to-serine mutations did not impact ZnT8A binding in a subset of T1D patients.

7. Truncating C-terminal ZnT8 by 9 amino acids (360T) to remove all three C-terminal cysteines had a comparable impact on ZnT8A binding as single cysteine-to-serine mutations and was also independent of ZnT8A specificity.

8. Heat map clustering analysis indicated that epitope recognition of ZnT8A to previously identified epitopes and the C-terminal cysteine region investigated in this project are heavily heterogeneous with very few indications of specific clusters.

#### **2.4.4.2 Strengths & limitations**

---

To our knowledge, this is the first investigation of the major epitope (325) in FDRs that progress slowly or rapidly to diabetes. Whilst the overall ZnT8A specificity was comparable between progressors, longitudinal study of these individuals suggested titres of ZnT8A can be lost and that 325-epitope spreading and ZnT8A specificity may change. A large natural history study that longitudinally sampled individuals from ZnT8A seroconversion to T1D onset would be required to fully evaluate this and its potential for disease prediction.

Additionally, this is the only investigation of ZnT8A epitopes in new-onset T1D patients that includes consideration of the two major epitopes previously identified (R<sub>325</sub>/W<sub>325</sub>/Q<sub>325</sub> and

R<sub>332</sub>E<sub>333</sub>K<sub>336</sub>K<sub>340</sub>) but also considered the unexplored cysteine-rich region of C-terminal ZnT8 and the addition of two novel truncated ZnT8 constructs. From this, we were able to confirm many previous findings; the majority of ZnT8A are non-specific, titres of non-specific ZnT8A are correlated, the ZnT8A specificity is influenced by *SLC30A8* genotype (289, 328), and mutation of REKK decreased ZnT8A binding independent of ZnT8A specificity (404). Importantly though, we were able to capture the heterogeneity of ZnT8A binding towards these major epitopes in addition to, novel residues that has been lacking from previous reports and may suggest that ZnT8 antigen is presented to the immune system differentially.

Whilst this study cannot identify or conclude specific epitope recognition through non-biased clustering analysis, it does suggest that ZnT8A targeting of ZnT8 between new-onset T1D patients is truly heterogeneous and is not related to ZnT8A specificity (325). Of all studied ZnT8 mutants, the 325Q mutation was the only alteration influenced by ZnT8A specificity; 325Q abolished ZnT8A binding in R325-specific [median 91.5% (range 2.7-98.9)] and W325-specific [median 93.3% (range 66.8-98.7)] responses but was less pronounced in non-specific responses with stronger evidence of heterogeneity [R325-reactive median 22.4% (range +42.4 increase-70.5 decrease; W325-reactive median 9.0% (range +45.7 increase-89.0 decrease)]. To consider ZnT8A specificity across all mutational analyses is a novel approach. However, we were unable to replicate the association between older age-at-onset and reactivity to 325 ZnT8 variants, but this is unsurprising given the lack of T1D patients diagnosed >20 years and a smaller new-onset T1D sample set (328). Although the new-onset T1D patient cohort was of similar age-at-onset as reported studies (~9-14 years), the present study included FDRs that progressed to T1D aged >21-60 years (270, 328, 404). It cannot be ruled out that ZnT8A epitope recognition and maturation of ZnT8A responses prior to or around onset may differ by age; however, an age-at-onset association has only been reported for R325/W325 epitopes and was not investigated for the REKK epitope (328, 404).

A limitation of this present study and others is that primarily, ZnT8A epitope mapping has been conducted in Euro-Caucasian populations (>70%). It is likely that ZnT8A specificity/reactivity will differ in other populations that are currently under investigated. However, a high ZnT8A prevalence and an enhanced diagnostic sensitivity when ZnT8A is considered are increasingly reported in other populations, e.g., Argentinian, Chinese, and Japanese (436, 437, 483). The following may be expected in other populations: an increase in R325-reactive ZnT8A in populations with a higher prevalence of the risk C allele such as Africa and the Middle East (402), an increase in Q325-reactive ZnT8A in Africa given the higher frequency of rs16889462 (405) and by extension, different frequencies of R325-, W325-, and Q325- specific and non-specific ZnT8A. The minor allele frequency (MAF) of the TT allele in this patient cohort was 0.370, slightly higher than the global MAF of 0.2824 (currently based on 1094 worldwide individuals), which was anticipated in a cohort pre-selected for ZnT8WA positivity. The T1D-associated HLA genes may also influence ZnT8A specificity. For example, the preference of ZnT8RA rather than ZnT8WA at diagnosis in Swedes compared to non-Swedes was thought to be related to *HLA-DQ2* and *SLC30A8* CC genotypes (94). High and moderate risk HLA class II genotypes containing *HLA-DQ2* comprised 87.1% and therefore, we were unable to robustly investigate an association with HLA in our cohort.

Furthermore, a large limitation of this study is that we cannot elucidate the structural impacts of the ZnT8 mutants studied as we were unable to access molecular modelling expertise within the duration of this PhD project. However, this has not routinely been conducted in other epitope studies of islet autoantibodies, including ZnT8A (324, 325).

### **2.4.4.3 Epitopes of ZnT8 recognised by ZnT8A**

---

We have confirmed findings from the previously identified major epitopes [R325, W325, and REKK (conformational)] are important for ZnT8A binding; however, regarding the REKK region, we have utilised a different strategy. Wenzlau *et al.* (2011) exploited the discrepant residues between murine (aa267-368) and human C-terminal (aa268-369) ZnT8 by humanising the specific residues in murine C-terminal ZnT8 to restore ZnT8A binding. Here, we have used human C-terminal ZnT8 and investigated REKK through alanine substitution. The binding of ZnT8A towards mutated REKK (AAAA) was comparable to when the equivalent murine TGQ- was present. However, we can't rule out that TGQ-/AAAA may have entirely different structural consequences allowing/inhibiting ZnT8A accessibility. Nonetheless, alanine substitutions are widely used for SDM analysis as a small, neutral, and physiochemically innocuous amino acid (484). Therefore, alanine is unlikely to perturb the gross structure of C-terminal ZnT8 but will disrupt the  $\alpha$ -helix, which supports our decision to use this strategy.

Similarly, cysteines are usually substituted for serines due to their isosteric compatibility, and as the placement of the cysteines is within the cytosolic domain and not the hydrophobic core of ZnT8, this should be a well-tolerated substitution. This strategy was successfully applied to investigating the core/cytosolic cysteines in IA-2IC for IA-2A/IA-2 $\beta$ A binding in new-onset T1D from BOX by our research group previously (341). Whilst the cysteine-rich C-terminal region of ZnT8 now may have links to the function of ZnT8 with C<sub>361</sub>S/C<sub>364</sub>S exhibiting high affinity for zinc (410, 411, 415), it is not known whether bound ZnT8A-to-ZnT8 may have a pathogenic effect on  $\beta$ -cell function via inhibition of zinc trafficking into insulin secretory granules. Whilst islet autoantibodies are not thought to be pathogenic, for no other autoantibody has been shown to be directed towards an antigenic region that contains a SNP that influences autoantibody specificity (evidence of a true autoantigen) and a region that has now been linked

to the function of the protein (the allosteric mechanism of human ZnT8). To investigate the impact of the ZnT8A-ZnT8 interaction would require co-crystallisation for cryo-EM analysis and functional ZnT8 assays (480).

Whilst we were unable to include molecular modelling of the ZnT8 mutants explored in this project, now we have collected the data, a future avenue would be to confirm the structural impact of mutating/truncating ZnT8A around the REKK and cysteine-rich regions because the structural impact of the R325W has been investigated already. This naturally-occurring mutation/SNP site may influence the function of ZnT8 with different biophysical properties, and whilst there is no evidence for binding zinc directly, the site may be important for the allosteric mechanism of ZnT8 given the differences noted in transporter activity between the two variants (392, 410, 411, 415).

Although the intracellular cytosolic C-terminal of ZnT8A is responsible for the majority of ZnT8A reactivity, different epitopes within the cytosolic or extracellular regions of ZnT8 may be required for ZnT8A binding. In the original Wenzlau *et al.* (2007) study, the N-terminal accounted for 8-10% of ZnT8A reactivity. However, combining the N- and C-terminals into a single-chain construct (N/C) had comparable sensitivity to the C-terminal construct (43.3%) but did not capture all C-terminal reactive ZnT8A with a total of 70 (31.4%) discrepant samples. Despite this, the combination of N/C and C-terminal constructs identified 63% of T1D, a performance comparable to other islet autoantigens (GAD65/IA-2IC/insulin). The N/C construct, compared with full-length ZnT8, showed 77.1% agreement suggesting, that the transmembrane and short connecting luminal/cytosolic loop segments are not major regions for ZnT8A epitope recognition (270). However, a very recent report adapted the ECL assay to incorporate Fab-conjugated sulfo-tagged C-terminal ZnT8 to bind ZnT8A reactive to extracellular regions of ZnT8 (excZnT8), namely the cytosolic-accessible transmembrane/loop

segments. Utilising a positivity threshold set at the 99<sup>th</sup> percentile of 336 healthy controls (aged 0.7-51.0 years), ZnT8A directed to excZnT8 was present in 23.6% (74/313) in patients with T1D [median age 11.5 years (range 0.7-67.6); participants from the BDC and DAISY study] and recognised both R325/W325 polymorphic variants. In 30 children from DAISY that developed diabetes over longitudinal follow-up, 10 were positive by excZnT8 ECL, and interestingly, in all 10 children, this represented the seroconversion response and, therefore, appeared before IAA/GADA/IA-2A/ZnT8A (C-terminal). The *in vitro* binding of ZnT8A to excZnT8 in the membrane was also confirmed by immunofluorescence in the EndoC- $\beta$ H1 cell line (455). This study suggests that epitopes of ZnT8A outside of the C-terminal domain may represent the early phases of the ZnT8 humoral response in T1D which may identify at-risk individuals earlier than primary autoantigens GAD and insulin, but further studies are required to confirm this.

Moreover, ZnT8A epitopes buried within full-length ZnT8 may be important not just for IgG but for IgM and IgA binding. Shruthi *et al.* (2019) performed *in silico* B cell epitope prediction on full-length ZnT8 using four different modelling software followed by wet-lab validation of concordant cryptic epitopes (short peptides generally deeply buried and inaccessible for antibody binding) in T1D (n=109) and T2D (n=233) patients with/without complications utilising indirect ELISA to determine antibody isotypes (IgM, IgG, and IgA). Of the three concordant cryptic epitopes, one was in the N-terminus (aa33-46: NKDQCPRERPEELE), and two was in the C-terminus (the major polymorphic site aa321-327: TAAS[R/W]DS; aa352-360: ESPVDQDPD). A multi-epitope polypeptide of these three cryptic epitopes was synthesised and used in the indirect ELISA (NH<sub>2</sub>-NKDQCPRERPEELEGGGGTAAS[R]DSGGGGESPVDQDPD-COOH). Compared to normal glucose tolerant individuals (n=33), IgG and IgA reactivity to this polypeptide was decreased in T1D without complications, IgM was reduced in T1D subjects with retinopathy,

but in newly diagnosed T1D initiated on insulin therapy, IgA was increased, and IgM was decreased. Comparable to T1D subjects, T2D had decreased IgG, IgA, and IgM. Therefore, further investigation of ZnT8A epitopes would perhaps incorporate ZnT8A isotypes, at-risk FDRs, and/or longitudinal analysis of individuals 6-12 months after diagnosis. This design might further inform disease risk, and the latter might be informative regarding the rapid loss of ZnT8A after diagnosis (443).

---

## 2.5 Characterisation of the ZnT8 humoral response from ZnT8A seroconversion

---

This PhD project involved the development of methods to characterise the natural history of the ZnT8A humoral response utilising modified RIAs to investigate affinity, IgG subclasses, and epitopes. We sought to apply these methods to FDRs from BOX that, prior to T1D onset, seroconverted with ZnT8A over follow-up.

---

### 2.5.1 Materials & Methods

---

#### 2.5.1.1 ZnT8A seroconversion population

---

Of approximately 6000 FDRs that were diabetes-free at study entry in BOX, 70 FDRs provided at least two follow-up samples, and from which 13 seroconverted with ZnT8A over follow-up (**Figure 2:43**). Of these 13, 3 individuals were excluded from the study due to low sample volume or unconfirmed ZnT8A seroconversion. A total of 78/131 (55.7%) available samples from the remaining 10 individuals had ZnT8R/ZnT8W RIA data, of which 34 (43.6%) samples were selected for further characterisation based on maintained positivity and serum volume availability.

The cohort description of the ZnT8A seroconversion population is detailed in **Table 2:21**; [n=10; 3 males (30%); median age of ZnT8A seroconversion 14.6 years (range 2.7-40.6); median age at onset 27.1 years (range 8.7-68.0); median time from onset of ZnT8A seroconversion 10.4 years (range 3.2-27.8)]. This cohort is therefore, comprised of SPs (n=6; 60.0%) and RPs (n=4; 40.0%).

## Chapter 2 - Characterisation of the ZnT8 humoral response up to T1D onset

Genetic samples were available for 9/10 seroconverters and had HLA data. HLA Class II: 5 (55.6%) high risk (*DR3-DQ2/DR4-DQ8*) and 3 (44.4%) moderate risk (*DR3-DQ2/DR3-DQ2*, *DR4-DQ8/X*; X refers to any other haplotype). HLA Class I: 8 (88.9%) *HLA-A\*24* negative, 8 (88.9%) *HLA-B\*18* negative, and 8 (88.9%) *HLA-B\*39* negative. *SLC30A8* genotype data was unavailable.

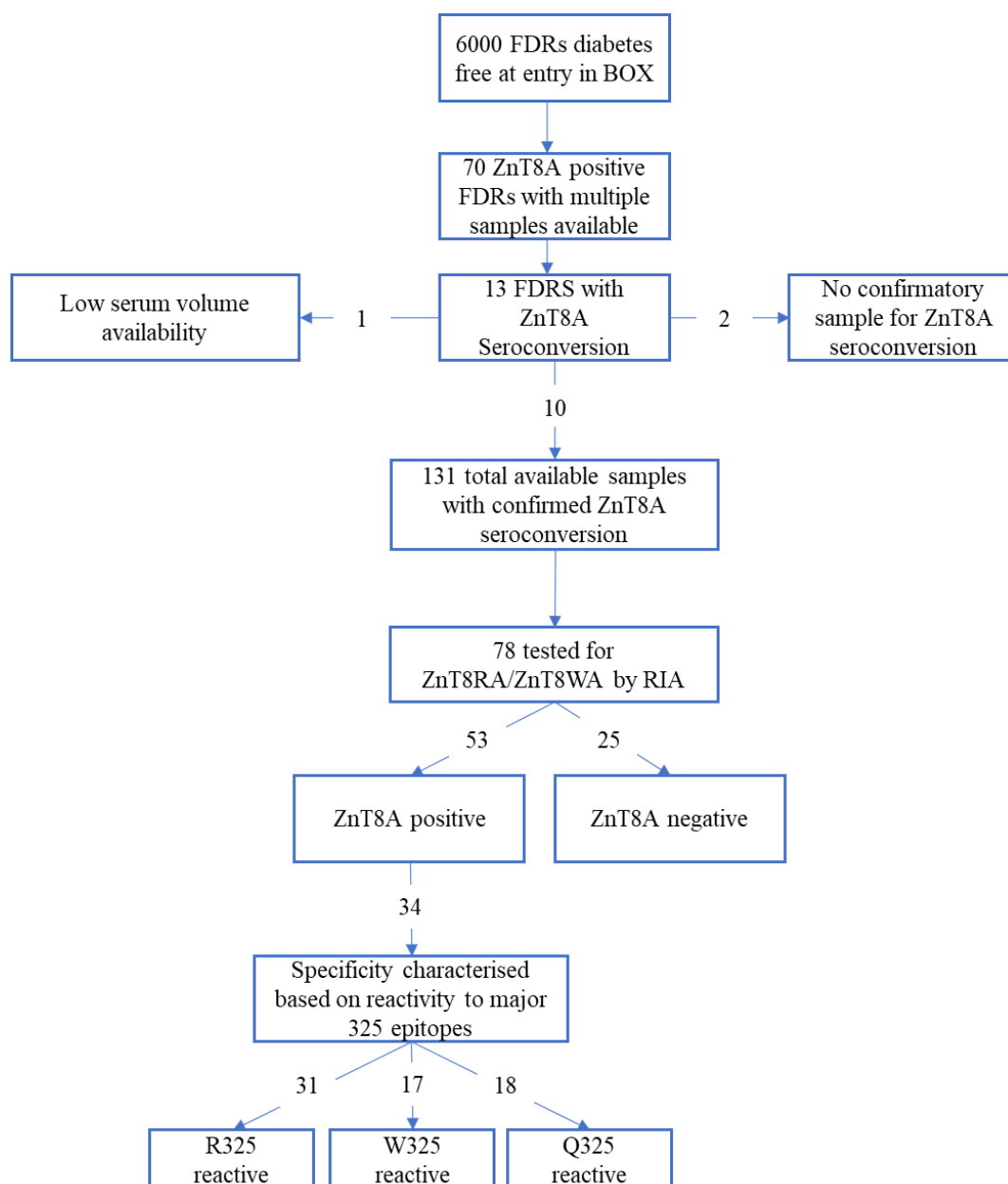


**Figure 2:43 – Identifying ZnT8A seroconverters from FDRs in the BOX study**

10 FDRs with confirmed ZnT8A seroconversion by ZnT8R/ZnT8W monomeric RIAs (in at least two sequential samples) were selected. A total of 78/131 (55.7%) available samples from the remaining 10 individuals had ZnT8R/ZnT8W RIA data, of which 34 samples were selected for further characterisation based on maintained positivity and serum volume availability.

Chapter 2 - Characterisation of the ZnT8 humoral response up to T1D onset

ID	Gender	Age at onset (yrs)	Number of available samples	Samples with RIA ZnT8A data	Number of samples ZnT8A positive	Age at ZnT8A Seroconversion	Time from onset of ZnT8A seroconversion (yrs)	Range of age at sampling (yrs)	Range of time before onset (yrs)
1*	F	8.7	17	6	2	2.7	6.0	(1.6-6.7)	(2.0-7.1)
2	M	12.8	16	9	7	9.6	3.2	(9.6-12.2)	(0.6-3.2)
3*	F	22.6	5	4	3	9.9	12.7	(9.9-35.4)	(1.3-12.7)
4*	M	23.7	3	3	2	12.4	11.3	(12.4-15.0)	(8.7-11.3)
5*	M	18.8	17	8	4	13.9	5.0	(7.3-18.0)	(1.0-11.6)
6*	F	30.6	10	7	6	15.3	15.3	(14.7-20.8)	(9.8-15.9)
7*	F	35.5	12	8	6	30.4	5.1	(30.4-35.5)	(0.0-5.1)
8	F	54.6	12	8	3	39.3	15.3	(39.3-50.6)	(4.0-15.3)
9	F	68.0	24	14	13	40.2	27.8	(40.2-55.6)	(12.4-27.8)
10*	F	50.11	15	11	7	40.6	9.5	(40.6-46.0)	(4.1-9.5)

*Table 2:21 – ZnT8A seroconversion case study population*

10 FDRs from the BOX study with high sample volume and confirmed ZnT8A seroconversion in at least two sequential serum samples were selected for ZnT8A characterisation (levels over time, major epitope specificity, affinity, and IgG subclasses). \* Denotes 7 individuals where the ZnT8A seroconversion sample was further characterised due to high sample volume. In the remaining 3 individuals, the closest sample to ZnT8A seroconversion (time between samples 0.6-1.91 years) was further characterised. This case study population comprises 6 SPs (60.0%) and 4 RPs (40.0%).

## 2.5.2 Results

### 2.5.2.1 Determining ZnT8A specificity in the ZnT8A seroconversion population

The majority of the ZnT8A seroconversion population produced non-specific ZnT8A in the first available sample & follow-up samples, but R325-reactive ZnT8A was the most prevalent.

Reactivity to the major epitope (encoded aa325) of ZnT8A responses in the first available sample (n=10) and all samples (n=34) from the ZnT8A seroconversion population is detailed in **Figure 2:44**. Non-specific ZnT8A that was reactive to all 3 variants (R325/W325/Q325) formed the majority of the ZnT8A response in both the first available sample (n=5; 50.0%) and all samples (n=15; 44.4%). There was also a similar proportion of R325-specific (n=4/14; 40.0/41.2%) and W325-specific (n=1/2; 10.0/5.9%) ZnT8A between the first available and all samples, respectively. There was no reactivity to two 325 variants in the first available sample but considering all available samples, 3 samples developed reactivity to two variants: R325/Q325 (n=2; 5.9%) and W325/Q325 (n=1; 2.9%).

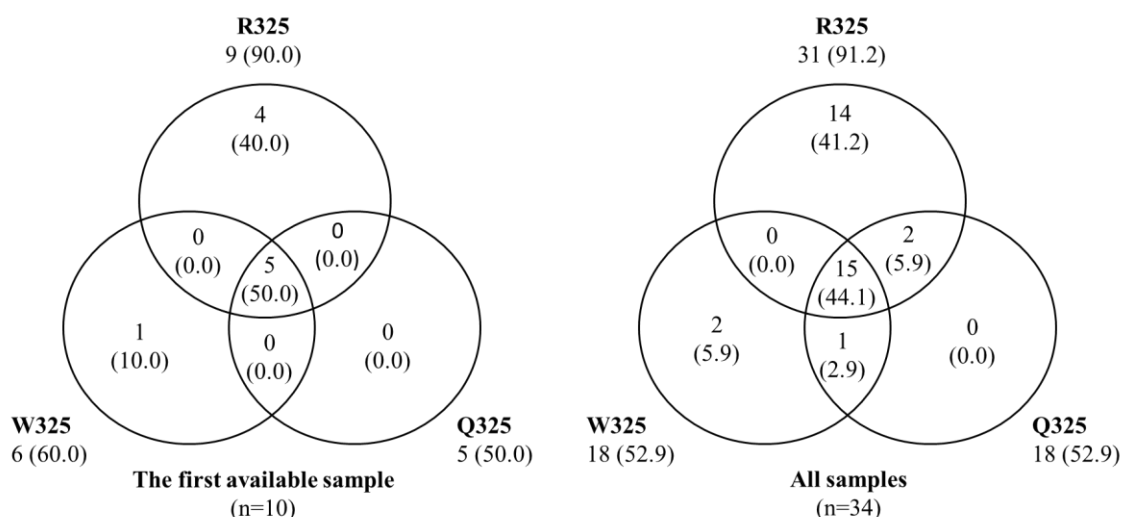


**Figure 2:44 – Categorisation of the major epitope (325) in the ZnT8A seroconversion population**

In the first available sample of the 10 individuals (7 of which was the ZnT8A seroconversion sample), 9 (90.0%) were R325-reactive, 6 (60.0%) were W325-reactive and 5 (50.0%) were Q325-reactive. Across all samples, 31 (91.2%) were R325-reactive, 18 (52.9%) were W325-reactive, and 18 (52.9%) were Q325-reactive. Non-specific ZnT8A that was reactive to all 3 variants (R325/W325/Q325) formed the majority of the ZnT8A response in both the first available sample (n=5; 50.0%) and all samples (n=15; 44.4%).

## **2.5.2.2 Case study of the ZnT8A humoral response in two individuals that seroconverted under 10 years of age**

---

### **2.5.2.2.1 ZnT8A Seroconverter 1**

ZnT8A Seroconverter 1 produced a ZnT8RA-specific response over two samples from the age of 2.7 years with a time interval of 0.4 years. However, within 1.4 years of the last ZnT8RA positive sample, the ZnT8RA response was lost and, the individual was subsequently diagnosed 4.8 years later at age 8.7 years (**Figure 2:45-1A**).

Further characterisation of the two ZnT8RA positive samples revealed that the ZnT8RA response was of high-moderate affinity (>50% competitive displacement by 0.025µg/ml protein concentration, **Figure 2:45-1B**), was IgG1-restricted (**Figure 2:45-1C**), and was more reliant on the R325 (60-70% reduced binding with Q325) and REKK (>90% reduced binding) major epitope regions to bind (**Figure 2:45-1D**). Interestingly, 360T impacted binding (30-70%) more than the drastic 349T (10-30%).

### **2.5.2.2.2 ZnT8A Seroconverter 2**

ZnT8A Seroconverter 2 produced a non-specific ZnT8A response over 6 samples from the age of 9.6 years with a time interval of 2.6 years. Within 0.6 years of the last ZnT8A positive sample, the ZnT8A response was lost and, the individual was diagnosed at age 12.8 years (**Figure 2:45-2A**). Two/three samples were further characterised.

The ZnT8A affinity was different according to the WT ZnT8 antigen. High-moderate affinity for W325 (>50% competitive displacement by 0.025µg/ml protein concentration, **Figure 2:45-2B**) but of low affinity for R325 and Q325 WT ZnT8 antigens (<50% competitive displacement by 0.025µg/ml). This may be related to higher titres of ZnT8WA compared with ZnT8RA, but ZnT8QA titre was comparable with ZnT8WA.

## Chapter 2 - Characterisation of the ZnT8 humoral response up to T1D onset

Testing of IgG subclasses in the two non-specific ZnT8A samples revealed differences between ZnT8RA and ZnT8WA IgG responses (**Figure 2:45-2C**). In the age 10 sample, ZnT8RA was IgG1-restricted, but the age 11 sample had IgG1 and IgG3. Conversely, for ZnT8WA, the age 10 sample had IgG1, IgG3, and IgG4, but the age 11 sample was IgG1-restricted. All non-IgG1 subclasses were of low level but were not unconvincing.

The ZnT8RA and ZnT8WA responses were heavily reliant on the REKK epitope to bind independent of whether R325 or W325 was present (>60-90% reduced binding), respectively. Interestingly, the two truncations at 360T (>70%) and 349T (>70%) produced a comparable effect on ZnT8RA and ZnT8WA binding as the REKK-A mutation. The mutation of Q325 had a greater effect on ZnT8WA binding (25-50% reduced binding) than ZnT8RA (+ positive binding) within the same sample (**Figure 2:45-2D**). This provides some evidence of non-specific ZnT8A responses targeting different regions of ZnT8 depending on encoded aa325.

Chapter 2 - Characterisation of the ZnT8 humoral response up to T1D onset

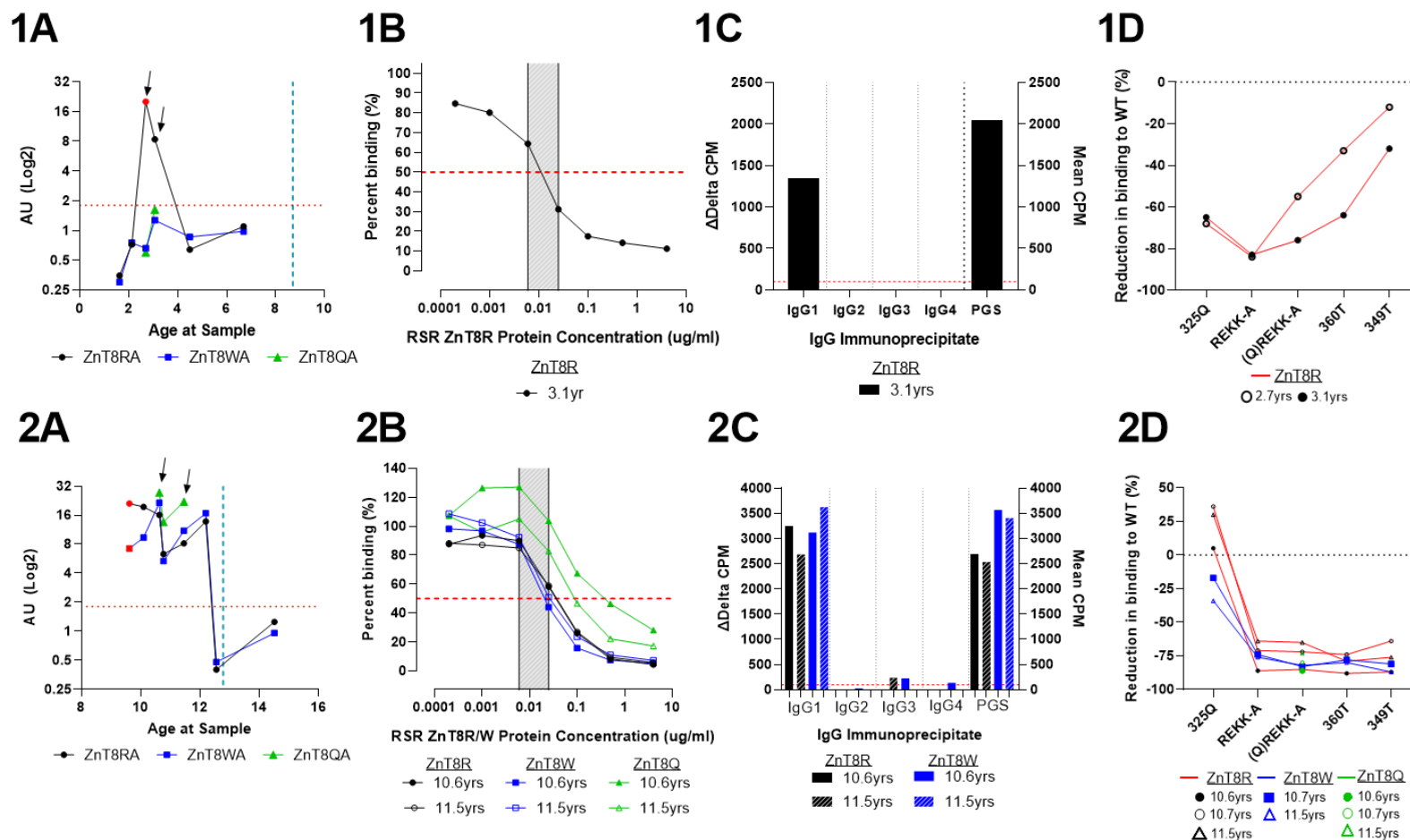


Figure 2:45 – Characterisation of the ZnT8A humoral response in Seroconverter 1 & 2

(A) Plots of ZnT8A titres over longitudinal follow-up for WT antigen encoding the major 325 epitopes; red symbols: first available ZnT8A positive sample and/or ZnT8A seroconversion sample; black arrows: samples selected for further characterisation (affinity, IgG subclasses and/or ZnT8A epitopes); blue dashed line: age at diagnosis; red dotted line: ZnT8A RIA positivity threshold (1.8 AU). (B) ZnT8A affinity plots for WT antigen encoding the major 325 epitopes: red dashed line: 50% reduced ZnT8A binding. (C) IgG subclass RIA for WT antigen encoding the major 325 epitopes; red dashed line denotes the detection threshold at 100 mean ΔCPM. (D) ZnT8A epitope plot of the major conformational epitope (REKK) encoding R325/W325 or Q325 and the two truncations (360T and 349T); black dashed line denotes zero change in ZnT8A binding compared to WT ZnT8.

### **2.5.2.3 Case study of the ZnT8A humoral response in four individuals that seroconverted between 10-15 years of age**

---

#### **2.5.2.3.1 ZnT8A Seroconverter 3**

ZnT8A Seroconverter 3 produced a non-specific ZnT8A response over 3 samples from the age of 9.9 years with a time interval of 11.4 years. Titres of ZnT8A reactive to all three 325 variants increased over the three samples, and within 1.3 years of the last ZnT8A positive sample, the individual was diagnosed at age 22.6 years (**Figure 2:46-3A**). Two/three samples were further characterised.

The ZnT8A affinity was comparable to variants of WT ZnT8 antigen (**Figure 2:46-3B**). Of the 3 samples tested for affinity towards R325/W325/Q325 (n=9 data points), 8 (88.9%) were of high-moderate affinity, but 1 (11.1%) was of low affinity towards R325 compared with W325/Q325, and this sample was the last ZnT8A positive sample prior to onset.

Similarly, of the three samples tested for IgG subclasses (R325/W325; n=6 data points), 5 were IgG1-restricted (83.3%), and 1 (17.7%) was IgG-unrestricted towards R325 with low-level binding of all IgG subclasses additional to IgG1 (mean  $\Delta$ CPM range 118.5-283.5). This IgG-unrestricted sample was the penultimate sample prior to onset (**Figure 2:46-3C**).

Epitope studies revealed some differences between ZnT8RA and ZnT8WA responses (**Figure 2:46-3D**). In the last two ZnT8A positive samples prior to onset, both ZnT8RA and ZnT8WA required the REKK major epitope for binding, which was comparable to the impact of 349T (>85%). However, ZnT8RA compared with ZnT8WA responses were less impacted by the 360T (60-70% versus >90%). In the first available sample, only the ZnT8RA response was investigated, which showed that both R325 (40-50%) and REKK (~30%) was important for binding, but the effect of 360T (60-70%) and 349T (>80%) was just as detrimental. Combined, this suggests that although an individual can have non-specific ZnT8A and can bind >1 325-variant, the epitopes recognised may be different depending on the 325-variant encoded.

Collectively for this individual, the ZnT8RA epitope specificity changed between age 9 and 20, and then between ages 20 and 21, just prior to diabetes onset, IgG-unrestricted responses emerged, with a further increase in titre, but a slight reduction in affinity, suggesting new B-cell clones were emerging.

#### **2.5.2.3.2 ZnT8A Seroconverter 4**

ZnT8A Seroconverter 4 produced a non-specific ZnT8A response over two samples from the age of 12.4 years with a time interval of 2.6 years. Titres of ZnT8A reactive to all three 325 variants increased over the two samples, and within 8.7 years of the last ZnT8A positive sample, the individual was diagnosed at age 23.7 years (**Figure 2:46-4A**). One/two samples were further characterised.

Based on positivity for R325/W325/Q325, samples reactive to R325 and Q325 were of low affinity, and samples reactive to W325 were of high-moderate affinity even though the last ZnT8A positive sample prior to onset had comparable titres between all three 325 variants (**Figure 2:46-4B**). The ZnT8A response towards R325/W325 was IgG1-restricted even in the high titre ZnT8WA positive sample (**Figure 2:46-4C**).

Different epitopes were important for ZnT8RA and ZnT8WA binding. The ZnT8RA response in the last available sample was reliant on the REKK epitope (>90% reduced binding), which was fairly independent of R325 (~40%); however, the ZnT8WA response was less reliant on the REKK epitope for binding (~30-40%). Encoding Q325 and mutating REKK caused a comparable effect on ZnT8RA and ZnT8WA (~50% reduced binding). Similarly, 360T and 349T caused ~20%-40%, and >90% reduced binding, respectively (**Figure 2:46-4D**). The REKK mutation and 349T are likely to impact ZnT8A binding differently because the reduction in binding with 349T was not related to reduction in binding with REKK (**Figure 2:34**), either could reveal or obscure linear or conformational epitopes upstream from aa349.

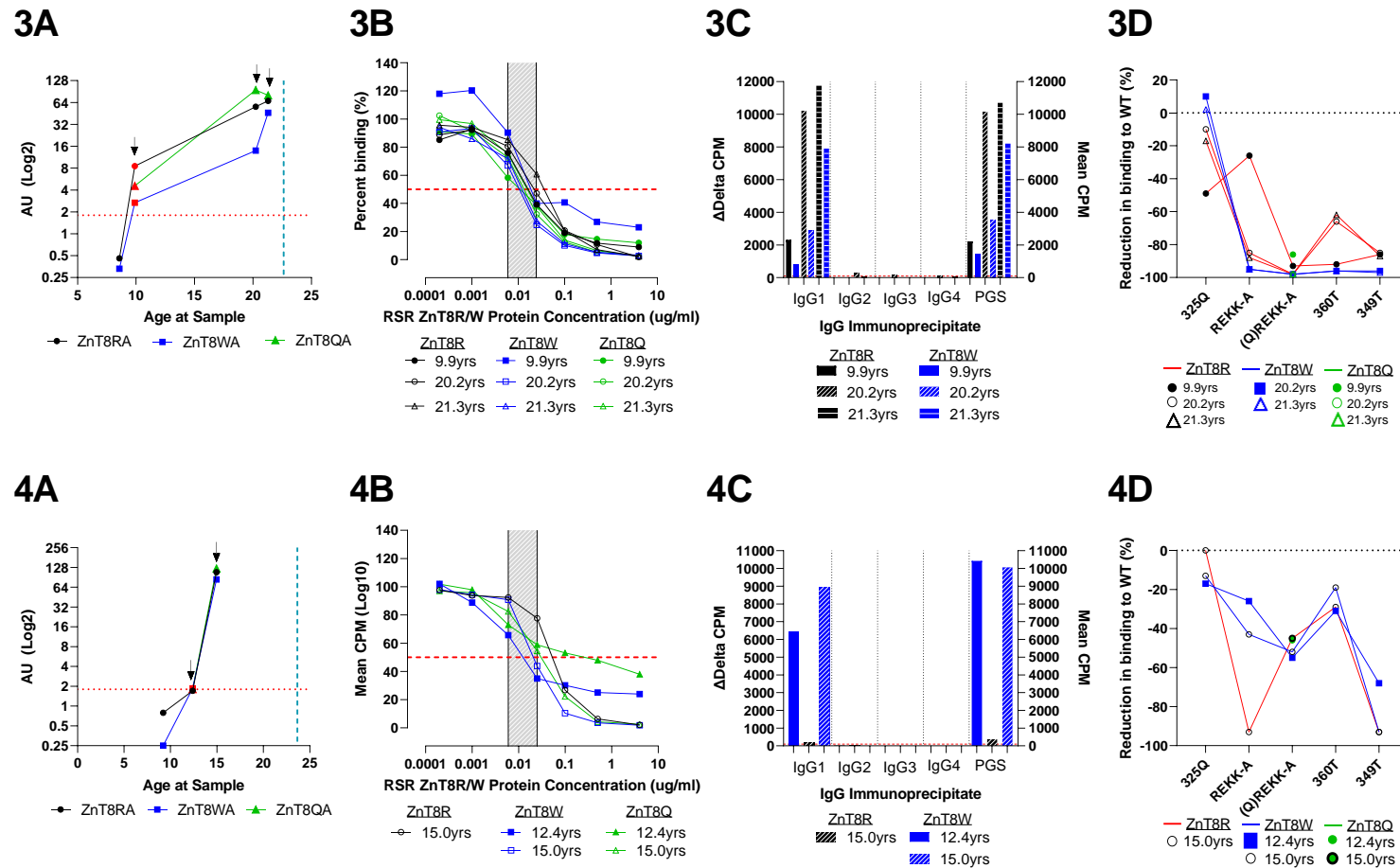


Figure 2:46 – Characterisation of the ZnT8A humoral response in Seroconverter 3 & 4

(A) Plots of ZnT8A titres over longitudinal follow-up for WT antigen encoding the major 325 epitopes; red symbols: first available ZnT8A positive sample and/or ZnT8A seroconversion sample; black arrows: samples selected for further characterisation (affinity, IgG subclasses and/or ZnT8A epitopes); blue dashed line: age at diagnosis; red dotted line: ZnT8A RIA positivity threshold (1.8 AU). (B) ZnT8A affinity plots for WT antigen encoding the major 325 epitopes: red dashed line: 50% reduced ZnT8A binding. (C) IgG subclass RIA for WT antigen encoding the major 325 epitopes; red dashed line denotes the detection threshold at 100 mean ΔCPM. (D) ZnT8A epitope plot of the major conformational epitope (REKK) encoding R325/W325 or Q325 and the two truncations (360T and 349T); black dashed line denotes zero change in ZnT8A binding compared to WT ZnT8.

### **2.5.2.3.3 ZnT8A Seroconverter 5**

ZnT8A Seroconverter 5 produced a non-specific ZnT8A response over four samples from the age of 13.9 years with a time interval of 4.1 years. Titres of ZnT8A reactive to all three 325 variants increased over the four samples with ZnT8WA>ZnT8RA>ZnT8QA, and within 0.9 years of the last ZnT8A positive sample, the individual was diagnosed at age 18.9 years (**Figure 2:47-5A**). Further characterisation in two/four samples revealed some interesting observations, particularly regarding ZnT8A epitopes.

The ZnT8A response in two/four samples was of high-moderate affinity for all 325 variants (**Figure 2:47-5B**). These two samples were also tested for ZnT8RA and ZnT8WA IgG subclasses which showed that the ZnT8RA was IgG-unrestricted (with low-level binding to at least one IgG2-IgG4) and ZnT8WA was IgG1-restricted despite being the dominant response (**Figure 2:47-5C**).

Testing of all four ZnT8A positive samples found that epitope recognition in the ZnT8RA and ZnT8WA response appeared distinct. The ZnT8RA response in the first three samples relied heavily on the REKK epitope (>90% reduced binding) independent of R325 (10-20%) and was similarly affected by 360T and 349T (both >90% reduced binding). However, the last sample prior to onset was less affected by the REKK mutant (60-70%), 360T (50-60%), and 349T (50-60%) but was more affected by R325 (~40%). Whereas the ZnT8WA response in the first three samples was more reliant on the W325 epitope (>80%) than the REKK epitope (20-30%) but combined removed all binding (>95%). ZnT8WA was less impacted by both truncations [360T (30-40%); 349T (30-60%)] than ZnT8RA. The ZnT8WA response in the last sample prior to onset showed similar profiles to the previous three samples but was less impacted by all mutants (40-70%) (**Figure 2:47-5D**). Combined, this suggests that whilst the ZnT8A response appears non-specific in this individual, the regions on ZnT8 that ZnT8RA and ZnT8WA targets seem to be distinct with some evidence of epitope spreading.

#### **2.5.2.3.4 ZnT8A Seroconverter 6**

ZnT8A Seroconverter 6 over 6 follow-up samples showed that the individual seroconverted with ZnT8RA at age 15.3 years then over 5.5 years, developed a non-specific ZnT8A response with increasing titres and ZnT8RA being the dominant response which attenuated by age 20.8 years. This individual was diagnosed ~10 years later at age 30.6 years (**Figure 2:47-6A**). Two-four samples that covered the peak and attenuating ZnT8A response were further characterised where possible.

Two samples were tested for ZnT8A affinity, 1 for R325/W325/Q325 and 1 for R325 only. The ZnT8RA and ZnT8WA responses were of high-moderate affinity, but the ZnT8QA response was of low affinity (**Figure 2:47-6B**). Both the ZnT8RA and ZnT8WA response was IgG1-restricted (**Figure 2:47-6C**).

The ZnT8RA and ZnT8WA samples after the ZnT8A seroconversion sample tested for epitope investigation was similarly impacted by the same mutations: Q325 (60-90%), REKK (>90%), Q-REKK (>90%), 360T (>70-80%), and 349T (>80%). This highlights the importance of the two major epitopes (325/REKK) and the presence of amino acids downstream of aa349 on ZnT8RA and ZnT8WA binding. However, the ZnT8RA-specific response in the seroconversion sample was less reliant on REKK (>40-50%) and 349T (~60%), more reliant on R325 (75-80%) and was comparably impacted by Q-REKK (>90%) and 360T (>70-80%) (**Figure 2:47-6D**). This may suggest epitope spreading in the ZnT8RA response over follow-up.

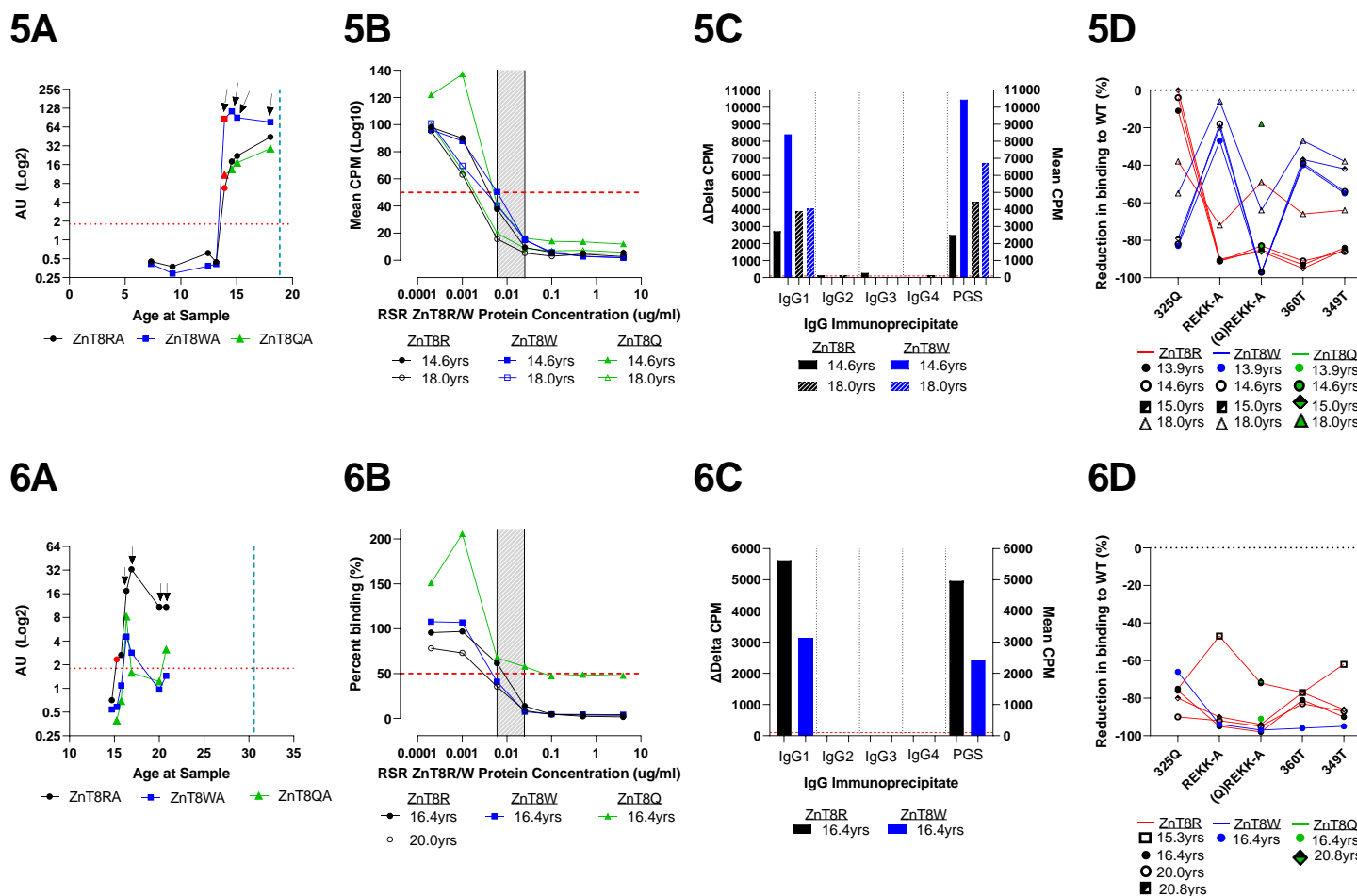


Figure 2:47 – Characterisation of the ZnT8A humoral response in Seroconverter 5 & 6

(A) Plots of ZnT8A titres over longitudinal follow-up for WT antigen encoding the major 325 epitopes; red symbols: first available ZnT8A positive sample and/or ZnT8A seroconversion sample; black arrows: samples selected for further characterisation (affinity, IgG subclasses and/or ZnT8A epitopes); blue dashed line: age at diagnosis; red dotted line: ZnT8A RIA positivity threshold (1.8 AU). (B) ZnT8A affinity plots for WT antigen encoding the major 325 epitopes: red dashed line: 50% reduced ZnT8A binding. (C) IgG subclass RIA for WT antigen encoding the major 325 epitopes; red dashed line denotes the detection threshold at 100 mean  $\Delta$ CPM. (D) ZnT8A epitope plot of the major conformational epitope (REKK) encoding R325/W325 or Q325 and the two truncations (360T and 349T); black dashed line denotes zero change in ZnT8A binding compared to WT ZnT8.

### **2.5.2.4 Case study of the ZnT8A humoral response in four individuals that seroconverted with ZnT8A after 30 years of age**

---

#### **2.5.2.4.1 ZnT8A Seroconverter 7**

ZnT8A Seroconverter 7 produced a non-specific ZnT8A response from the first available sample over seven samples from the age of 30.4 years with a time interval of 5.1 years. Titres of ZnT8A reactive to all three 325 variants fluctuated over follow-up, ZnT8RA increased and then was lost, ZnT8WA was only present in 3 samples and was lost twice over follow-up, ZnT8QA was present in five samples at lower titres but mirrored ZnT8RA/ZnT8WA responses. In the sample taken at onset at age 35.5 years, only ZnT8RA was present (**Figure 2:48-7A**). Further characterisation of up to five samples with fluctuating ZnT8A titres and responses revealed some interesting observations.

ZnT8RA (n=5), ZnT8WA (n=3), and ZnT8QA (n=4) positive samples were tested for ZnT8A affinity. Most ZnT8A responses were of low affinity across all specificities but were particularly marked in ZnT8QA responses. 1 sample in ZnT8RA and ZnT8WA responses was of borderline high-moderate affinity, but the sample was discordant between responses (**Figure 2:48-7B**).

All ZnT8RA responses tested were IgG1-restricted (n=5), and the majority of the ZnT8WA response were also IgG1-restricted (n=3) with 1 IgG-unrestricted sample with low-level IgG2 and IgG3 (**Figure 2:48-7C**).

All ZnT8RA responses tested for epitope investigation (n=5) were comparably reliant on select mutations but to varying degrees: Q325 (30-70%), REKK (>80%), Q-REKK (>80%), 360T (>80%), and 349T (>70%). Whereas, in the ZnT8WA responses tested for epitope investigation (n=3), 2 was not dependent on W325 (0% change) but over follow-up, in the peak ZnT8WA sample, became more reliant on W325 (~20-30%). The effect of the other mutations was comparable between ZnT8RA and ZnT8WA responses (**Figure 2:48-7D**).

#### **2.5.2.4.2 ZnT8A Seroconverter 8**

ZnT8A Seroconverter 8 firstly seroconverted with a very borderline positive non-specific ZnT8A response (R325/W325) at the age of 39.3 years, but over follow-up across 15.3 years, the ZnT8RA response was lost, and the ZnT8WA fluctuated up to onset at age 54.6 years (**Figure 2:48-8A**). The titres of ZnT8A remained low in all positive samples (<3 AU). The last ZnT8WA positive sample prior to onset was further characterised.

The ZnT8WA response was of low affinity, possibly related to the low titre (**Figure 2:48-8B**), IgG1-restricted (**Figure 2:48-8C**), and relied mainly on W325 being present (**Figure 2:48-8D**). The REKK mutant had a comparable effect in Q325 and Q-REKK mutations causing around 60-70% reduced binding, but the REKK epitope with W325 encoded caused ~20-30% reduced binding. The 360T and 349T had a comparable effect as Q325 and Q-REKK-A at around 60-70% reduced binding.

Chapter 2 - Characterisation of the ZnT8 humoral response up to T1D onset

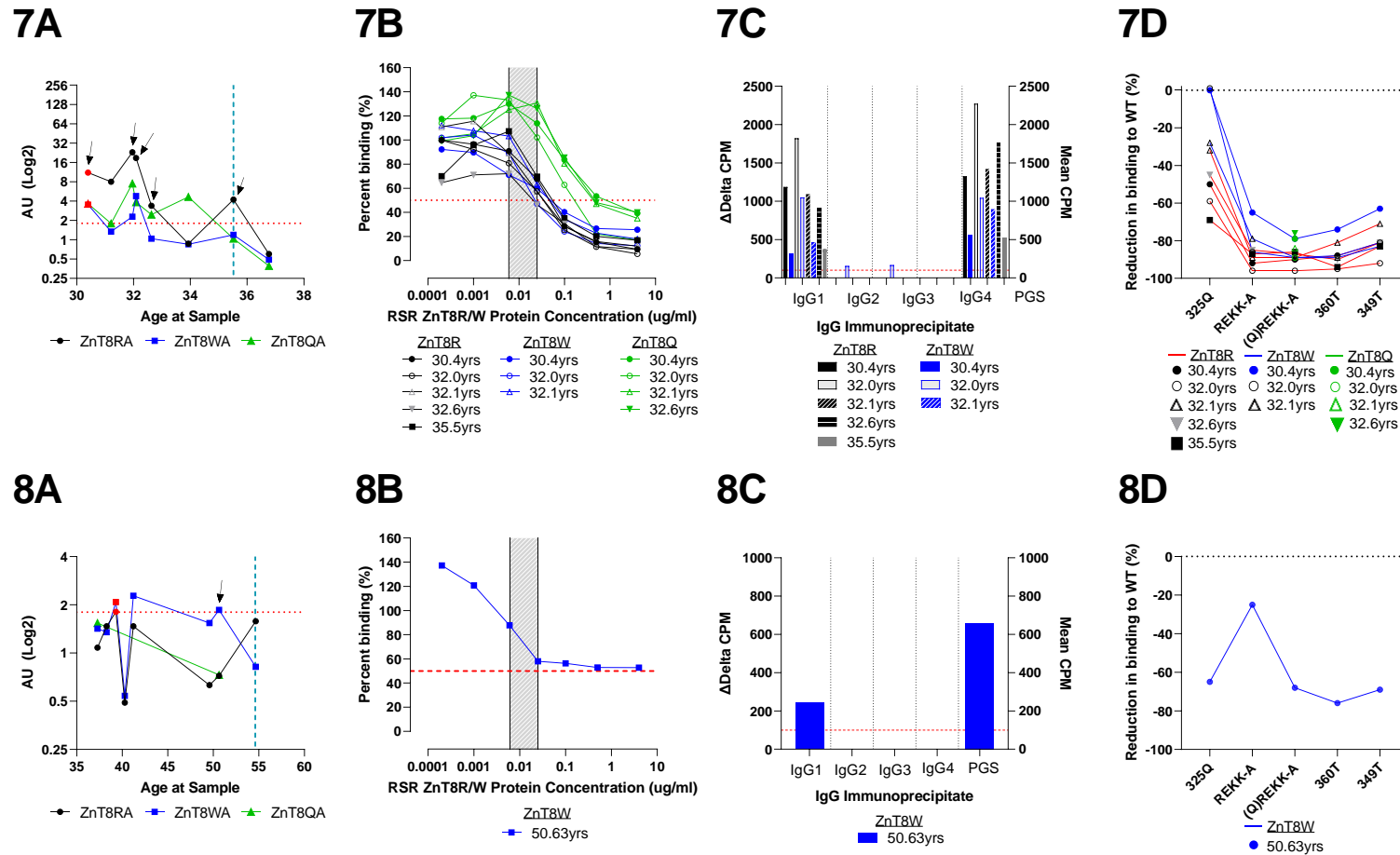


Figure 2:48 – Characterisation of the ZnT8A humoral response in Seroconverter 7 & 8

(A) Plots of ZnT8A titres over longitudinal follow-up for WT antigen encoding the major 325 epitopes; red symbols: first available ZnT8A positive sample and/or ZnT8A seroconversion sample; black arrows: samples selected for further characterisation (affinity, IgG subclasses and/or ZnT8A epitopes); blue dashed line: age at diagnosis; red dotted line: ZnT8A RIA positivity threshold (1.8 AU). (B) ZnT8A affinity plots for WT antigen encoding the major 325 epitopes: red dashed line: 50% reduced ZnT8A binding. (C) IgG subclass RIA for WT antigen encoding the major 325 epitopes; red dashed line denotes the detection threshold at 100 mean ΔCPM. (D) ZnT8A epitope plot of the major conformational epitope (REKK) encoding R325/W325 or Q325 and the two truncations (360T and 349T); black dashed line denotes zero change in ZnT8A binding compared to WT ZnT8.

#### **2.5.2.4.3 ZnT8A Seroconverter 9**

ZnT8A Seroconverter 9 produced a low-level ZnT8RA-specific response over seven samples from the age of 40.6 years with fluctuating patterns over follow-up with a time interval of 9.5 years. The ZnT8RA response was lost at age 48.8 years, and within 1.7 years, the individual was subsequently diagnosed at age 50.1 years (**Figure 2:49-9A**). The first available ZnT8A sample was further characterised.

The ZnT8RA response was of high-moderate affinity (**Figure 2:49-9B**), IgG1-restricted (**Figure 2:49-9C**), and was heavily reliant on R325 (~80%) and REKK (~80%) epitopes (**Figure 2:49-9D**). The effect of REKK was independent of whether R325 or Q325 was encoded (both ~80%). Both truncations 360T and 349 caused moderate reductions in ZnT8RA binding (~20-30%).

#### **2.5.2.4.4 ZnT8A Seroconverter 10**

ZnT8A Seroconverter 10 produced a high-moderate level ZnT8RA-specific response over 14 samples from the age of 40.7 years with fluctuating patterns over follow-up with a time interval of 27.4 years. The ZnT8RA response was lost at age 67.6 years, and within 0.4 years, the individual was subsequently diagnosed at age 68.0 years (**Figure 2:49-10A**). A selection of four samples at peak ZnT8RA responses, including the first available ZnT8RA positive sample, was further characterised where possible.

All four selected samples were of high-moderate affinity (**Figure 2:49-10B**), 3 of 4 were IgG1-restricted with one sample having low-level IgG2, IgG3, and IgG4 (**Figure 2:49-10C**), and were mainly reliant on R325 being encoded with >90% reduced binding caused by Q325 and Q-REKK mutations, compared to 50-65% reduced binding with REKK alone (**Figure 2:49-10D**). The 360T caused between 30-60% reduced binding across the four samples, and the 349T had a comparable effect as Q325 and Q-REKK mutants.

Chapter 2 - Characterisation of the ZnT8 humoral response up to T1D onset

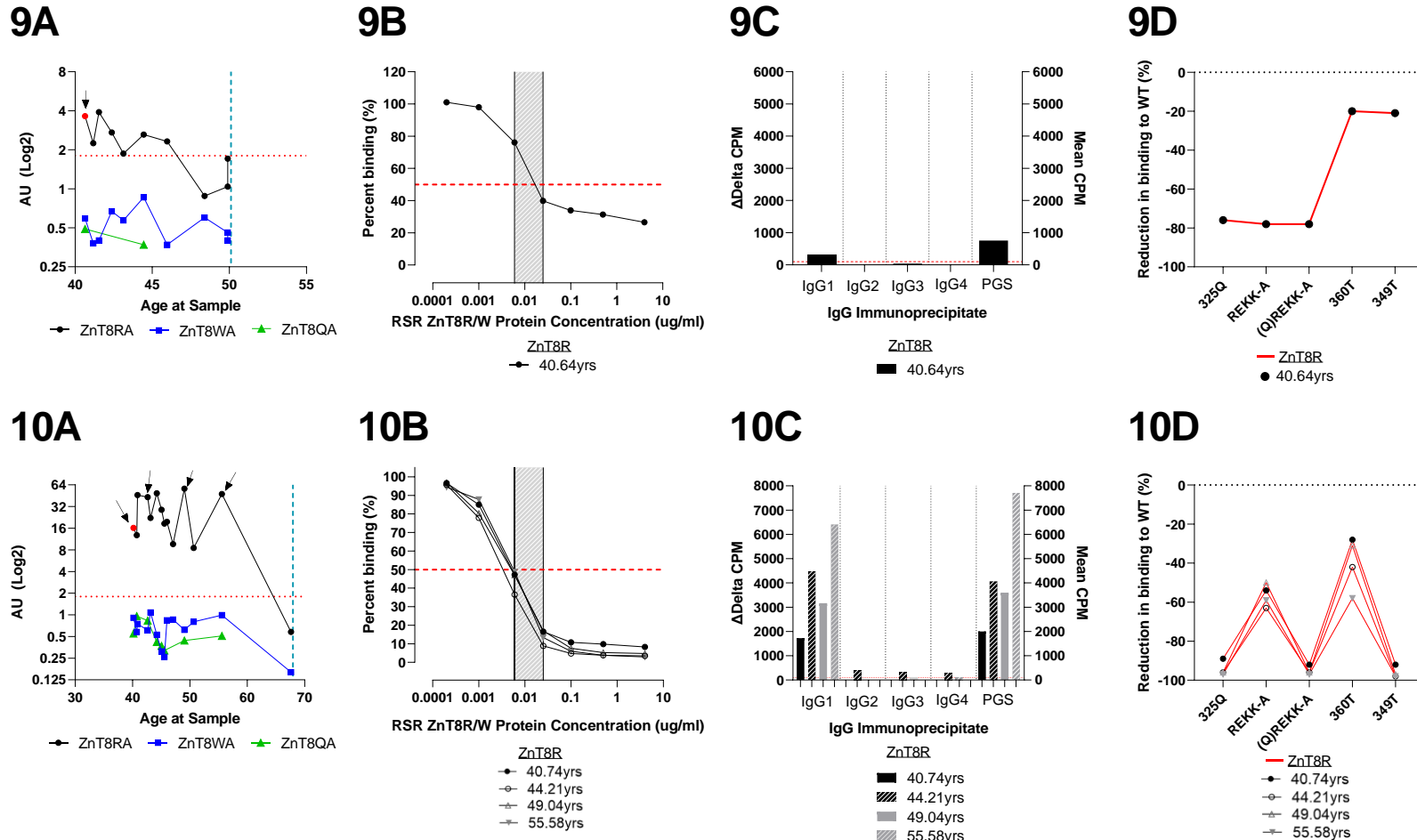


Figure 2:49 – Characterisation of the ZnT8A humoral response in Seroconverter 9 & 10

(A) Plots of ZnT8A titres over longitudinal follow-up for WT antigen encoding the major 325 epitopes; red symbols: first available ZnT8A positive sample and/or ZnT8A seroconversion sample; black arrows: samples selected for further characterisation (affinity, IgG subclasses and/or ZnT8A epitopes); blue dashed line: age at diagnosis; red dotted line: ZnT8A RIA positivity threshold (1.8 AU). (B) ZnT8A affinity plots for WT antigen encoding the major 325 epitopes: red dashed line: 50% reduced ZnT8A binding. (C) IgG subclass RIA for WT antigen encoding the major 325 epitopes; red dashed line denotes the detection threshold at 100 mean  $\Delta$ CPM. (D) ZnT8A epitope plot of the major conformational epitope (REKK) encoding R325/W325 or Q325 and the two truncations (360T and 349T); black dashed line denotes zero change in ZnT8A binding compared to WT ZnT8.

---

## 2.5.3 Discussion

---

### 2.5.3.1 Main findings

---

1. ZnT8A can be lost prior to T1D onset, occurring in at least two consecutive samples in 6/10 (60%) seroconverters which may be an age-independent response as this was observed over an age range of 2.7-40.7 years from either the seroconversion or first ZnT8A positive sample. In non-specific responses, the trend of decreasing/increasing ZnT8A level over longitudinal follow-up can differ according to R325/W325/Q325 WT reactivity.
2. Shifts in ZnT8A affinity were observed within individuals and prior to T1D onset (particularly evident in seroconverter 3, 5, and 6), can be different according to WT ZnT8 variant (R325/W325/Q325), and may be accompanied by changes in IgG subclasses and/or epitopes and therefore, may reflect the maturation of the ZnT8A response. However, in this small case study, dramatic shifts in ZnT8A affinity were not observed, but ZnT8A reactivity towards R325/W325 ZnT8 WT antigen was predominantly of high-moderate affinity.
3. In these individuals, the ZnT8A response was predominantly IgG1-restricted, but there was some indication in individuals with a non-specific ZnT8A response that different IgG subclasses may be directed to R325/W325 WT variants in the same sample.
4. In individuals with a non-specific ZnT8A response, ZnT8RA and ZnT8WA can rely on different ZnT8 epitopes to bind. This implies that these responses are polyclonal, i.e., ZnT8A derived from different B-cell clones rather than one monoclonal ZnT8A response that does not rely on the encoded residue at 325.

### **2.5.3.2 Strengths, limitations, & future work**

---

To our knowledge, this is the first case study series in at-risk individuals to incorporate many autoantibody characteristics for ZnT8A that has previously been associated with T1D risk in other islet autoantibody responses. Whilst we cannot draw robust conclusions from this small sample set, the novel approach applied does generate many questions and highlights many unknown aspects of the ZnT8 humoral response.

In regard to the loss of ZnT8A or decreasing ZnT8A titres prior to T1D onset observed in this case study, the prevalence of ZnT8A in new-onset T1D or after clinical T1D onset may be underestimated. An estimated ~70-80% of new-onset T1D (dependent on age) have ZnT8A, but this suggests that loss of ZnT8A prior to onset could occur in up to a third of individuals who progress, but not everyone who develops T1D may mount a ZnT8A response (270). Prospective birth-cohorts of genetically at-risk children to date have not reported observations of ZnT8A loss and only 15 mAutoab+ve relatives across a wide age range (0-40 years) lost ZnT8A, GADA, or IA-2A in the BDR, which was not associated with T1D risk, but this could be due to small sample size (291). Therefore, it is not clear whether loss of ZnT8A alters T1D risk. In TrialNet's Pathway to Prevention study (PTPS; mAutoab+ve relatives), of 1,522 ZnT8A positives at study enrolment, 15 (1%) lost ZnT8A over follow-up, which was associated with lower ZnT8A titres (485). This could provide some rationale as to why the predominantly low titre ZnT8A responses in the small ZnT8A seroconverter cohort were lost over follow-up prior to T1D onset. For individuals in BOX, we confirmed ZnT8A seroconversion through positivity in at least 2 follow-up samples, providing more evidence that these were true humoral responses towards ZnT8.

## Chapter 2 - Characterisation of the ZnT8 humoral response up to T1D onset

Presently, ZnT8A data is not consistently reported or tested in prospective studies of at-risk individuals prior to onset as it is only thought that ZnT8A stratifies T1D risk by identifying additional sAutoab+ve and mAutoab+ve individuals. However, TrialNet's PTPS indicates that loss of islet autoantibodies (considering all responses: GADA, IA-2A, IAA, ICA, and ZnT8A) can occur even in high-risk mAutoab+ve relatives at a prevalence around 1-5% (depending on specificity) (485). In this thesis, we only examined ZnT8A responses from seroconversion in individuals with multiple sampling, who developed T1D over follow-up, and was predominantly in individuals who developed ZnT8A <18 years (60%) but did encompass slow (60%) and rapid (40%) progressors with 2 (20%) individuals who convincingly regained ZnT8A, following a negative result, prior to onset. Collectively, loss of islet autoantibodies appears rare but increasing our understanding of "autoimmune remission" is critical for understanding the natural history of T1D and enrolment to prevention trials that target stage 1/2 (mAutoab+ve) at-risk individuals, but long duration follow-up encompassing all ages is required for future investigations.

The IgG response in ZnT8A seroconverters over follow-up prior to T1D onset continues to be largely IgG1-restricted; however, in select individuals with non-specific ZnT8A responses, there was evidence of low-level IgG-unrestricted responses towards R325/W325 WT ZnT8, but this did not appear to occur temporally in relation to T1D onset and was not observed in the peak ZnT8A titre sample. Whether the presence of IgG-unrestricted responses (independent of specific IgG subclasses) may infer greater T1D risk remains to be further elucidated, but it is unlikely that these responses are highly prevalent in at-risk individuals as evidenced from the SP/RPs also investigated in this project. However, the data from new-onset T1D patients suggests that IgG-unrestricted ZnT8A responses may be more common closer to onset.

## Chapter 2 - Characterisation of the ZnT8 humoral response up to T1D onset

Characterisation of the major epitope regions of ZnT8A in this case study provided some evidence to suggest that non-specific ZnT8A could be either monoclonal or polyclonal. In some cases, non-specific ZnT8A directed towards R325/W325 WT ZnT8 antigen were directed to the same (monoclonal) or different (polyclonal) epitopes inferring that they were produced from the same or different B-cell clones, respectively. The constitution of the non-specific ZnT8A response, therefore, may require further investigation, but the interaction between ZnT8A-ZnT8Q does help characterise non-specific ZnT8A. Additionally, this case study confirms the observations from new-onset T1D that ZnT8A responses between individuals appear very heterogeneous from seroconversion in SPs/RPs.

Could monoclonal/polyclonal non-specific responses and/or specific ZnT8A epitopes infer differential T1D risk and/or be informative for clinical trials? Larger studies that incorporate and are powered to examine characteristics of ZnT8A responses are required to understand whether individually or combined, they impact T1D risk prediction. The heterogeneity of the data collected from 10 individuals suggests that ZnT8 appears differentially presented to the immune system and that ZnT8-specific intervention strategies to delay progression may prove difficult.

Data presented in this study suggests that prior to T1D onset, ZnT8A responses are highly dynamic. Islet autoantibody responses also suggest ZnT8A is also dynamic after T1D onset. Compared to other autoantibody responses, ZnT8A is also lost more rapidly and can occur in as little as months from diagnosis (reported previously and shown later in this thesis **Chapter 3 -**) (443). But as many previous studies have been conducted cross-sectionally, they could not confirm whether those without ZnT8A after T1D onset ever had ZnT8A at or prior to T1D onset. This makes determining the degree of ZnT8A persistence after T1D onset difficult and was, therefore, an aim of this project.

# **Chapter 3 - Characterisation of islet autoantibodies after T1D onset**

---

### 3.1 Introduction

---

The four major T1D-associated autoantibodies (IAA, GADA, IA-2A, and ZnT8A) remain primary biomarkers for predicting future disease and are a distinctive clinical feature of islet autoimmunity. At the onset of clinically diagnosed T1D, >90% of people are positive for at least one of these autoantibodies (12, 270). The appearance of specific autoantibodies during the preclinical phase of disease and those present at onset are associated with particular HLA Class II genotypes, age-at-onset, gender (275, 287, 291, 486) and to a lesser degree, with HLA Class I and non-HLA genotypes (82, 487, 488).

Autoantibody prevalence after T1D diagnosis with a disease duration spanning 12 to 56 years (diagnosed between 0-56 years of age) generally report GADA as the most frequently detected autoantibody, followed by IA-2A and ZnT8A (where tested) (266, 489). The factors associated with autoantibody loss after diagnosis and what they tell us about ongoing autoimmunity are not clear: markers of continued autoimmune destruction on residual  $\beta$ -cells or the result of long-lived B cell immune compartments that may not rely on residual antigen for continued autoantibody production (237). Do the genetic drivers of autoantibody production change during disease from the known antigen-specific variants that influence disease progression/risk? Understanding why autoantibody positivity is lost or maintained post-diagnosis may help understand the ongoing loss of  $\beta$ -cells, and insulin production, after diagnosis.

Autoantibody positivity is inversely correlated with disease duration but was not found to strongly correlate with C-peptide (40, 443, 447-449, 490). However, there are conflicting findings in these studies, and therefore, the association between C-peptide/ $\beta$ -cell function and islet autoantibodies is not clear. Autoantibody prevalence after T1D onset has also shown

associations with a range of non-genetic (autoantibody specificity, number of autoantibodies, gender, age-at-onset, and disease duration at time of autoantibody detection) and genetic (HLA and non-HLA) factors (443, 491-493). Therefore, it is postulated that factors that influence the development of autoantibodies during the T1D prodrome may continue to drive humoral responses after T1D onset.

A literature review of the major studies that have contributed to the understanding of biochemical (GADA, IA-2A, and ZnT8A) autoantibody responses after T1D onset is summarised in **Table D:1; Appendix D**. These studies are often small, largely cross-sectional cohorts, and differ by many study design parameters (population, ethnicity, age-at-onset, duration of disease at the time of autoantibody detection, and autoantibody detection methods). Few studies have examined longitudinal autoantibody profiles in samples taken close at diagnosis with multiple sampling at longitudinal follow-up. A couple of longitudinal studies comprised only ~100 individuals diagnosed in childhood to adolescence with a follow-up of at least 10 years (443, 449, 493). We, therefore, sought to investigate autoantibody profiles and patterns in addition to non-genetic and genetic determinants of islet autoantibody loss in T1D subjects that provided both baseline (with confirmed autoantibody positivity status) and longitudinal follow-up samples in the BOX study.

---

### 3.1.1 Hypothesis

---

The factors that are associated with autoantibody responses at onset of T1D will be different from the factors associated with autoantibody loss or persistence after clinical onset of T1D.

---

### 3.1.2 Aims

---

1. To determine the longitudinal autoantibody profiles of ZnT8A, GADA, and IA-2A after onset of T1D.
2. To confirm the known non-genetic and genetic factors associated with autoantibody prevalence of ZnT8A, GADA, and IA-2A at onset of T1D.
3. To identify the non-genetic and genetic factors associated with the loss of autoantibody responses of ZnT8A, GADA, and IA-2A after onset of T1D.

---

## 3.2 Material & Methods

---

---

### 3.2.1 Population description

---

All participants of the BOX study (described previously **1.8**) that had a serum sample taken close to T1D onset [median 0.11 years (range-0.86-1.98)] and at least one longitudinal serum sample at follow-up [median 7.3 years (range 2-32)] were selected and tested for GADA, IA-2A and ZnT8A by in-house RIAs (previously described **1.6.3.3**) (12, 451); multiple longitudinal samples were tested until autoantibody negativity was determined using well-validated positivity thresholds (274, 356). Around ~3,000 data points were generated by in-house RIAs for GADA, IA-2A, ZnT8RA, and ZnT8WA longitudinal responses for this PhD project, the samples around T1D onset had available data. For the assessment of ZnT8A, the maximum ZnT8A result between ZnT8RA and ZnT8WA RIAs was used for analysis as responses over follow-up were comparable (**Figure D:1; Appendix D.2**).

### Chapter 3 - Characterisation of islet autoantibodies after T1D onset

A total of 577 [n males = 320 (55.5%); median age-at-onset 10.74 years (range 0.74-54.6)] autoantibody positive individuals at onset were identified. Data for IAA were available from 238 individuals [41.2% of cohort; n positive = 171/238 (71.8%)], where the onset sample was taken within 2 weeks of diagnosis prior to exogenous insulin treatment and was only included in the onset analysis. The detection of IAA is determined by RIA utilising A14-[125-I]-labelled human insulin  $\pm$  40 $\mu$ mol/L synthetic human insulin (ACTRAPID®, Novo Nordisk, Bagsværd, Denmark) and has been previously well described (343, 356, 494).

Overall, 290 (50.3%), 182 (31.5%), 88 (15.3%), and 17 (2.9%) individuals provided 1, 2, 3, and 4 follow-up samples, respectively; combinations of samples available for testing with the number tested for autoantibodies at all time points are detailed in **Table 3:1**. Data from 44/137 individuals that provided samples at onset and at 15-32 years disease duration have been previously published (449), but the remaining 93 individuals had additional samples that were not tested for autoantibodies in the previous publication. The incomplete autoantibody data was filled in and included in this project.

The total available serum samples for autoantibody detection at follow-up are detailed in **Figure 3:1**. Characteristics of the cohort with available data for variables investigated are detailed in **Table 3:2**.

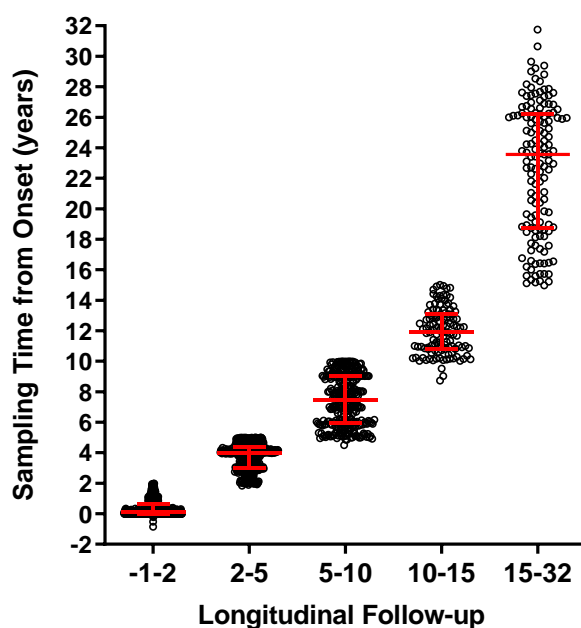
Number of Individuals from 577 cohort	Onset	2-5 years	5-10 years	10-15 years	15-32 years
17					
65					
20					
2					
1					
118					
5					
33					
14					
9					
3					
149					
66					
19					
56					*
<b>Total Samples</b>	<b>577</b>	<b>406</b>	<b>304</b>	<b>121</b>	<b>141</b>

Key:	
	4 follow-up samples
	3 follow-up samples
	2 follow-up samples
	1 follow-up samples

Table 3:1 – Combinations of samples available that were tested for autoantibodies across all time categories

\* Data from 44/137 individuals have been previously published by Williams *et al.* (2016) (449), but the remaining 93 individuals that provided a sample 15-32 years after onset had additional samples available which have not been previously published.



	Onset	Longitudinal Follow-up			
n samples	577	406	304	121	141
Median (IQR) sampling time from onset (years)	0.11 (0.00, 0.62)	3.96 (3.03, 4.37)	7.48 (5.94, 9.02)	12.00 (10.82, 13.08)	23.56 (18.76, 26.21)

Figure 3:1 – Distribution of longitudinal serum samples available from 577 individuals with T1D

The median and interquartile ranges (IQRs) for sampling time from onset (years) are detailed for each time category of longitudinal follow-up in the corresponding table.

<b>Variable</b>	<b>Number (%)</b>
<b>Gender</b> (n=577) Male Female	320 (55.5) 257 (44.5)
<b>Age at onset</b> (n=577) 0.74-7.52 years 7.52-10.73 years 10.73-13.76 years >13.76– 54.6 years	144 (25.0) 144 (25.0) 144 (25.0) 145 (25.0)
<b>Autoantibody</b> (n=577) IAA (n=238) GADA IA-2A ZnT8A ZnT8RA ZnT8WA	171 (71.8) 487 (84.4) 452 (78.3) 395 (68.5) 342 (59.3) 298 (51.6)
<b>HLA Class II</b> (n=501) High (DR3-DQ2/DR4-DQ8) Moderate (DQ2/DQ2, DQ8/DQ8, DQ2/X, DQ8/X) Low (X/X, DQ6/X)	159 (31.7) 269 (53.7) 73 (14.6)
<b>HLA Class I</b> <i>HLA-A*24</i> Negative (n=454) <i>HLA-B*18</i> Negative (n= 417) <i>HLA-B*39</i> Negative (n= 417)	376 (82.8) 364 (87.3) 385 (92.3)
<b>Non-HLA SNPs</b> <i>IFIH1</i> (n=469) <u>C</u> CT T <i>RELA</i> (FIBP) (n=432) C CT <u>T</u> <i>LPP</i> (n= 440) <u>A</u> AC C <i>FLCR3</i> (n=442) G AG <u>A</u> <i>SLC30A8</i> (n= 383) CC CT <u>TT</u>	59 (12.58) 215 (45.84) 195 (41.58) 280 (64.81) 133 (30.79) 19 (4.40) 99 (22.50) 213 (48.41) 128 (29.09) 159 (35.97) 199 (45.02) 84 (19.0) 179 (46.74) 168 (43.86) 36 (9.40)

**Table 3:2 – Cohort description & all variables investigated for association with autoantibody loss after onset of T1D**

All available results (n) for 577 individuals longitudinally followed-up from T1D onset to 32 years disease duration. For Non-HLA SNPs, underlined alleles identify the minor allele.

---

### 3.2.2 Genetic determination

---

All DNA samples with available data were extracted from whole blood or mouth swab samples and were whole genome amplified by a PCR-based protocol (Illustra GenomiPhi V2 DNA amplification kit; GE Healthcare). HLA Class II alleles were previously determined (n=501) by sequence-specific primers, described previously (495) and characterised into high [*DR3-DQ2:DR4-DQ8(DRBI\*03-DQAI\*0501-DQBI\*0201:DRBI\*04-DQAI\*0301-DQBI\*0302)*], moderate (*DQ8/DQ8*, *DQ8/X*, *DQ/X* and *DQ2/DQ2*), and low risk (*X/X* and *DQ6/X*), where *X* refers to any other haplotype. Individuals with the protective *DQ6/X* genotype were categorised into low risk and not excluded as the frequency was representative of the general population (n=4, 0.8% of 501). HLA Class I genotypes were previously determined for *HLA-A\*24* (n=454), *HLA-B\*18* (n=417), and *HLA-B\*39* (n=417) by sequence-specific primers previously described (496), were coded as binary variables (positive/negative).

Non-HLA SNPs for *IFIH1/2q24* (rs2111485 in LD with rs1990760, n=469), *RELA/11q13* (intron 4 of the *FIBP* gene; rs568617; n=432), *LPP/3q28* (rs1464510; n=440), and *FCRL3/1q23* (rs3761959; n=442) found to be associated with autoantibody positivity at follow-up (median 7 years) previously were also available (491, 497). For the assessment of ZnT8A loss, the *SLC30A8* SNP (rs13266634; n=383) that determines two major epitopes of ZnT8A was considered; n=67 (17.5%) out of a total of 383 was determined as part of this PhD project following manufacturer's instructions (ThermoFisher). The minor allele frequencies (MAF) of each SNP investigated for association with longitudinal autoantibody loss was of expected frequency within the general population (**Table 3:3**). All non-HLA SNPs were coded as binary variables (homozygous allele 1/homozygous allele 2) and the respective minor allele was compared to the major allele in multivariate analysis.

Non-HLA SNP	MAF-T1Dc (n)	GMAF or MAF-1000G*
IFIH1 C>T rs2111485	0.353 (469)	0.3632
RELA C>T rs568617	0.198 (432)	0.230*
LPP C>A rs1464510	0.467 (440)	0.4532
FCRL3 G>A rs3761959	0.415 (442)	0.4995
SLC30A8 C>T rs13266634	0.271 (383)	0.2824

*Table 3:3 – Minor allele frequencies of investigated SNPs in the T1D cohort*

The minor allele frequency (MAF) of non-HLA SNPs considered for association with longitudinal autoantibody loss in subjects with T1D (MAF-T1Dc; with available data) and the global MAF (GMAF) or MAF from the 1000 Genomes project (MAF-1000G\*) is detailed.

### 3.2.3 Data transformation & statistical analysis

Data were analysed using SPSS (v. 23) software and graphed using GraphPad PRISM (v.9.2.0). D'Agostino-Pearson normality omnibus K2 test was used to test for a Gaussian (normal) distribution. Proportions were compared using Chi-squared  $\chi^2$  tests or Fisher's exact tests where appropriate. Paired Wilcoxon tests were used to compare median autoantibody titres at onset and follow-up. Mixed-model effect generalised linear models (GLM) using a Restricted Maximum Likelihood (REML) fit and the Geisser-Greenhouse correction was applied to estimate a linear trend accounting for missing values and compare the mean variance of autoantibody titre over longitudinal follow-up, respectively. This modelling can be interpreted as a one-way Analysis of Variance (ANOVA) when missing values are random. Serum sampling from BOX is largely not predetermined.

Where indicated, descriptive statistics (mean, median, interquartile ranges (IQRs), standard deviation (SD), coefficient of variation (CV%) were used to investigate heterogeneity in autoantibody titres over longitudinal follow-up. Additionally, autoantibody titres were log transformed ( $\log_{10}$ ) to generate violin plots to identify subgroups.

### Chapter 3 - Characterisation of islet autoantibodies after T1D onset

Binary logistic regression was first used to confirm known associations (non-genetic and genetic) with autoantibody positivity at onset corrected for time of initial sampling (months; <2 years of onset) as a linear variable.

For analysis of autoantibodies after diagnosis, autoantibody loss was the metric used, i.e., the absence of an autoantibody that was present at diagnosis. Binary logistic regression was then used to determine the influence of non-genetic [gender, age-at-onset (as quartiles, compared to lowest quartile or as T1D endotype (T1DE) age: T1DE2 ( $\geq 13$  years) compared to T1DE1 (<7 years)), time of final sampling from onset (as quartiles, compared to the lowest quartile), autoantibody titre at onset (units as quartiles, compared to the highest quartile), number of- and combination of- autoantibodies at onset] and genetic covariates (binary and categorical) on autoantibody loss at final follow-up. All multivariate logistic regression models were applied adjusting for all covariates and confounders identified at the 10% significance level of univariate proportional testing. The Bonferroni correction was applied where applicable for multiple analyses. In all analyses, a two-tailed p-value <0.05 was considered significant.

### 3.3 Results

#### 3.3.1 Prevalence of autoantibodies at onset & longitudinal follow-up

Of 577 individuals prospectively followed, 84.4%, 78.3%, and 68.5% were positive at onset for GADA, IA-2A, and ZnT8A, respectively. Of the cohort, 16.3% had one, 36.2% had two, and 47.5% had three autoantibodies (**Figure 3:2**).

This study provided a novel opportunity to characterise longitudinal responses in single autoantibody positives (**Appendix D.3.1**), but given the small sample size, factors associated with responses could not be determined.

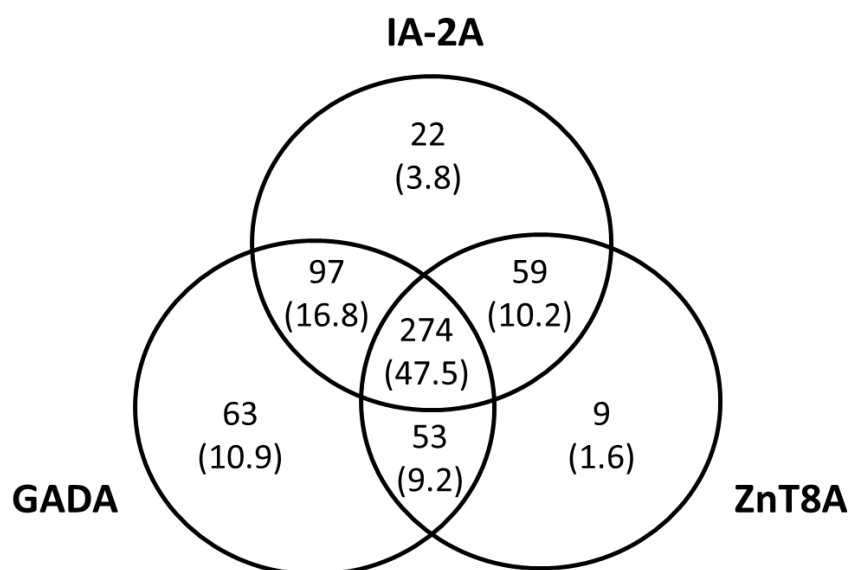


*Figure 3:2 – Autoantibody profiles at T1D onset*

Autoantibody positivity profiles for GADA, IA-2A, and ZnT8A (%) in 577 individuals sampled at the onset of T1D [median 0.11 years (range -0.86 to 1.98)] that also had at least one follow-up serum sample (2-32 years). In 238 individuals (41.2% of the total cohort), the onset sample was taken within 2 weeks of onset, enabling accurate detection of IAA in addition to GADA, IA-2A, and ZnT8A (n positive for IAA = 171/238; 71.8%). Positivity for GADA, IA-2A, and ZnT8A comprised 47.5% of the total cohort. GADA was the most prevalent in single autoantibody positives (67.0%), followed by IA-2A (23.4%) and ZnT8A (9.6%). The most frequent double autoantibody positive combination was GADA with IA-2A (n=97; 16.8%), followed by IA-2A with ZnT8A (n=59; 10.2%), and GADA with ZnT8A (n=53; 9.2%);, respectively.

Individuals positive for  $\geq$ two autoantibodies decreased over longitudinal follow-up, whereas single autoantibody positive and autoantibody negative subjects increased ( $p < 0.0001$ ; **Figure 3:3**). This corresponded with the loss of the T1D onset autoantibody profile over follow-up (45.6% 2-5 years, 61.5% 5-10 years, 74.4% 10-15 years, and 83.0% 15-32 years). Profiles containing GADA and/or IA-2A were more frequent over follow-up than those containing ZnT8A (**Figure 3:4**).

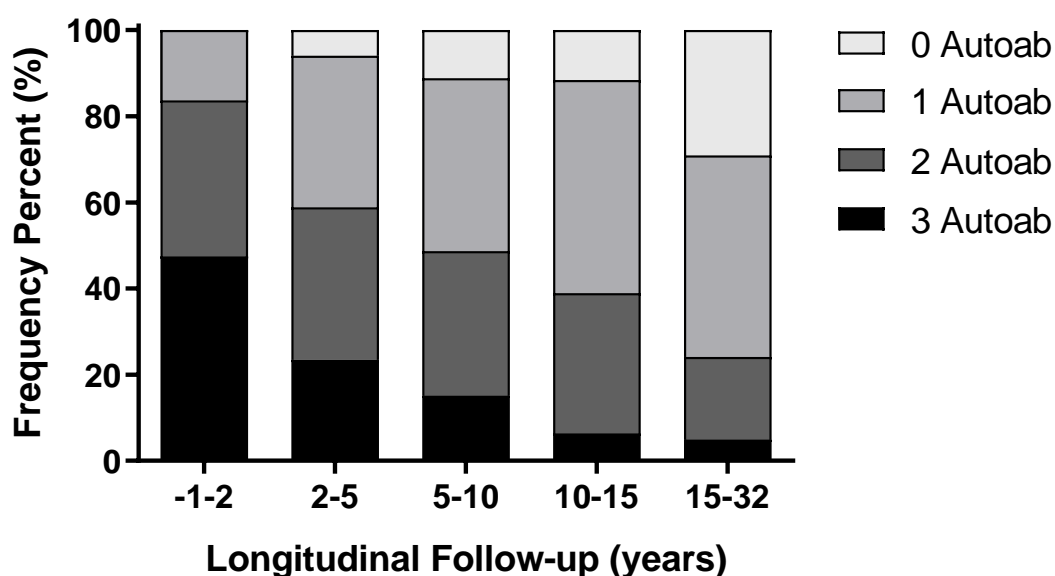


*Figure 3:3 – Longitudinal autoantibody positivity over follow-up*

Percentages derived from serum samples with complete autoantibody data for GADA, IA-2A, and ZnT8A at each time category. The proportion of subjects positive for three and two autoantibodies decreased from onset, and the proportion of subjects positive for 1 autoantibody or 0 autoantibodies increased from onset (both  $p < 0.0001$ ).

### Chapter 3 - Characterisation of islet autoantibodies after T1D onset

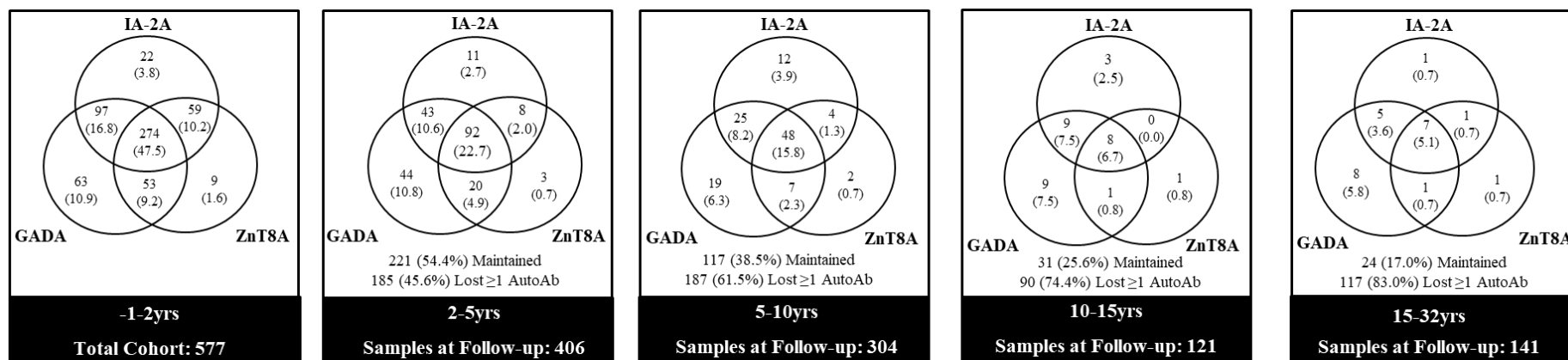


**Figure 3:4 – Prevalence of longitudinal autoantibody positivity characterised by autoantibody profiles at T1D onset**

Autoantibody positivity profiles for GADA, IA-2A, and ZnT8A in 577 individuals sampled at T1D onset [median 0.11 years (range -0.86 to 1.98)] that remained positive (%) by the onset autoantibody profile at longitudinal follow-up (range 2-32 years). The proportion of individuals losing  $\geq 1$  autoantibody at follow-up increased with increasing disease duration at follow-up ( $p < 0.0001$ ). Single GADA responses (5.8-10.8%) was more prevalent over longitudinal follow-up than single IA-2A (0.7-3.9%) and ZnT8A (0.7-0.8%) responses. Individuals positive for two autoantibodies, GADA/IA-2A positives (3.6-10.6%) was more prevalent over longitudinal follow-up than GADA/ZnT8A (0.7-4.9%) or IA-2A/ZnT8A (0.0-2.0%) responses. Individuals positive for all three major autoantibodies at onset, 5.1%-22.7% remained positive for all three autoantibodies over longitudinal follow-up. Autoantibody profiles containing ZnT8A were less frequent over longitudinal follow-up; therefore, testing for GADA and IA-2A after T1D onset will detect the majority of autoantibody positivity during disease.

Longitudinal autoantibody positivity showed distinct patterns according to antigen specificity. ZnT8A positivity was lost more rapidly than GADA and IA-2A whereas, GADA and IA-2A positivity was lost more gradually over follow-up (**Figure 3:5**).

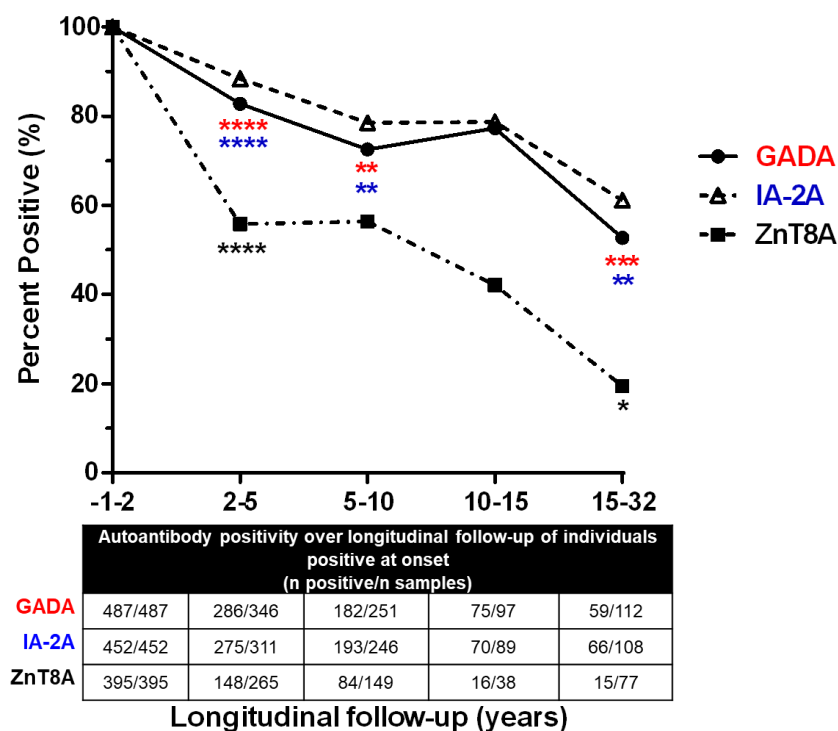


**Figure 3:5 – The frequency of longitudinal autoantibody positivity**

Percent positive (%) out of the number of serum samples available at longitudinal follow-up in individuals that were positive for GADA (n=487), IA-2A (n=452) and ZnT8A (n=395) around onset. Proportions of positivity for each autoantibody was compared to the previous longitudinal follow-up category. Red for GADA, Blue for IA-2A and Black for ZnT8A at significance; p values \* $<0.05$ , \*\* $<0.01$ , \*\*\* $<0.001$ , and \*\*\*\*  $<0.0001$ . The overall proportion of all autoantibody positives at each longitudinal follow-up category with complete data for GADA, IA-2A and ZnT8A compared to onset decreased ( $p_{corr} < 0.05-0.0001$ ).

In subjects positive for ZnT8A at onset (395/577; 68.5%), only 40.1% (150/374 with complete data) remained positive at final sampling [median 6.1 years (range 2-32)], with the greatest proportionate loss occurring within 5 years of onset (44.2%,  $p_{corr} < 0.0001$ ) and an overall loss of 80.5% at a disease duration  $\geq 15$  years ( $p_{corr} < 0.05$  compared with 10-15 years). In contrast, in subjects positive for GADA at onset (487/577; 84.4%), 70.8% (340/480 with complete data) remained positive at final sampling [median 7.9 years (range 2-32)], with only 17.3% loss

within 5 years of onset ( $p_{\text{corr}} < 0.0001$ ) and an overall loss of 47.3% at a disease duration  $\geq 15$  years ( $p_{\text{corr}} < 0.001$  compared with 10-15 years). Comparable to GADA, in subjects positive for IA-2A at onset (452/577; 78.3%), 76.8% (347/452) remained positive at final sampling [median 8.0 years (range 2-32)], with only 11.6% loss occurring within 5 years of onset ( $p_{\text{corr}} < 0.0001$ ) and an overall loss of 38.9% at a disease duration  $\geq 15$  years ( $p_{\text{corr}} < 0.01$  compared with 10-15 years).

---

#### 3.3.2 Patterns of autoantibody titre over longitudinal follow-up

---

In accordance with decreasing autoantibody prevalence, the median autoantibody titre for GADA, IA-2A, and ZnT8A also decreased as a function of increasing disease duration ( $p < 0.0001$ ) but high GADA and IA-2A titres were still observed at  $\geq 15$  years disease duration, which appeared rare for ZnT8A (**Figure 3:6**). Across a range of baseline titres, longitudinal autoantibody titres sequentially decreased over follow-up in most subjects [GADA: 365/487 (74.9%); IA-2A: 407/452 (90.0%); ZnT8A: 389/395 (98.5%)]. A minority of GADA and IA-2A positive subjects had higher autoantibody titres in at least one follow-up sample compared to onset (GADA:  $n=68$ , 14.0%; IA-2A:  $n=25$ , 5.5%) and/or had evidence of waxing-waning patterns of differing magnitudes from onset over at least two follow-up samples (GADA:  $n=69$ , 14.2%; IA-2A:  $n=26$ , 5.8%). However, only 6 (1.5%) ZnT8A positive subjects had a higher ZnT8A titre in at least 1 follow-up sample, and there was no evidence of waxing-waning patterns (**Appendix D.4**). Given the testing strategy, the re-emergence of autoantibodies after onset cannot be fully evaluated.

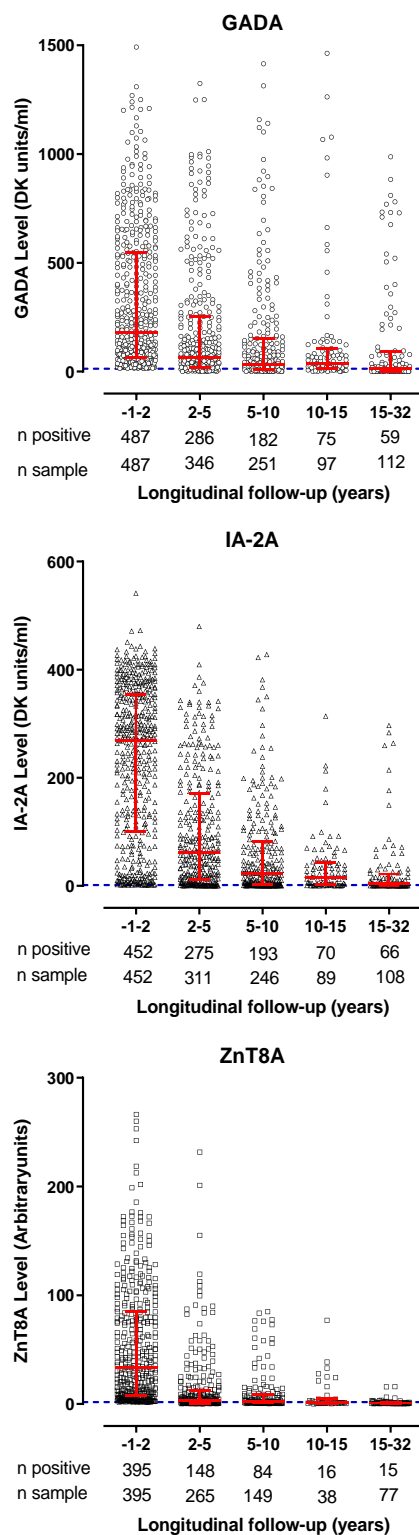


**Figure 3:6 – Longitudinal GADA, IA-2A, & ZnT8A levels from T1D onset**

Individuals positive for GADA, IA-2A, and ZnT8A by RIA out of a T1D cohort of 577 individuals that provided one sample at onset (-1-2 years) and at least one sample at longitudinal follow-up (2-32 years). Autoantibody levels are expressed as Diabetic Kidney (DK) units/ml for GADA and IA-2A and arbitrary units (AU) for ZnT8A. The number of samples positive for the respective autoantibody out of the samples with available data is detailed. Red error bars denote respective median units and interquartile ranges. Blue dashed line denotes positivity thresholds [GADA (13.5 DK units/ml), IA-2A (1.4 DK units/ml), and ZnT8A (1.8 AU)]. Autoantibody prevalence and median autoantibody titre at longitudinal follow-up compared to onset decreased as a function of increasing disease duration for all autoantibody responses corrected for multiple analysis ( $p_{\text{corr}} < 0.0001$ ).

As expected, there was strong evidence to suggest longitudinal autoantibody responses were not sampled from a Gaussian population ( $p < 0.0001$ ; **Figure D:10**; **Appendix D.4.3**). However, GLMs require normally distributed residuals, not normally distributed dependent variables; therefore, GLMs were explored to test other model assumptions. GLMs also suggested that there was evidence of a linear trend in decreasing autoantibody titres ( $p < 0.0001$ ), but the within-subject variance of mean autoantibody titres was highly unequal across categories of longitudinal follow-up (Geisser-Greenhouse  $\epsilon < 0.5$  in all responses; **Table 3:4**). Similarly, the between-subject variance of mean autoantibody titres was high in all autoantibody responses (GADA SD: 240.3; IA-2A SD: 83.0; ZnT8A SD: 27.1; **Appendix D.4.4** for full descriptive statistics). Unsurprisingly, the mean difference in autoantibody titre differed in most pairwise comparisons between time categories ( $p < 0.0001-0.05$ , **Figure D:11**; **Appendix D.4.4.1**). Autoantibody responses after onset are heterogeneous between individuals, and therefore, further predictive modelling using linear trend would be inappropriate.

<b>Linear trend &amp; mixed-model GLM assessment of variance over longitudinal follow-up</b>	<b>GADA</b>	<b>IA-2A</b>	<b>ZnT8A</b>
Linear trend across follow-up	$p < 0.0001$	$p < 0.0001$	$p < 0.0001$
Slope (95% CI)	-47.67 (-38.95, -56.40)	-47.36 (-43.23, -51.49)	-12.17 (-10.17, -14.18)
Means different across follow-up	$p < 0.0001$	$p < 0.0001$	$p < 0.0001$
Geisser-Greenhouse correction $\epsilon$	0.47	0.51	0.39
Total missing values (n)	1142	1054	1051

*Table 3:4 – Linear trend & GLM assessment of variance over longitudinal follow-up for GADA, IA-2A, & ZnT8A responses*

GLM: generalised linear model; CI: confidence interval.

---

### 3.3.3 Non-genetic associations of autoantibody positivity at initial sampling & autoantibody loss at final sampling

---

#### 3.3.3.1 Initial sampling

---

Non-genetic [gender, age-at-onset, and time of initial serum sampling (months); **Figure 3:7**] and the presence of co-existing autoantibodies (**Figure 3:8**) previously reported to be associated with GADA, IA-2A, and ZnT8A at onset were confirmed using adjusted multivariate logistic regression.

Positivity for GADA at onset was associated with female gender [OR 1.7,  $p=0.026$ ], an older age-at-onset  $\geq 11$  years [11-14 years OR 3.3,  $p=0.0004$ ;  $\geq 14$  years OR 6.1,  $p=1.3 \times 10^{-5}$ ], but not with the presence of co-existing autoantibodies ( $p>0.05$ ).

Positivity for IA-2A at onset was negatively associated with an older age-at-onset  $\geq 14$  years [OR 0.4,  $p=0.001$ ], but was positively associated with the presence of ZnT8A [OR 2.7,  $p=4.0 \times 10^{-6}$ ], and IAA [OR 2.8,  $p=0.003$  ( $n=283$ )].

Positivity for ZnT8A at onset was positively associated with age-at-onset between 8-11 years [OR 2.2,  $p=0.004$ ], IA-2A [OR 2.7,  $p=5.0 \times 10^{-6}$ ], and weakly with IAA [OR 1.9,  $p=0.045$  ( $n=282$ )] but, was negatively associated with initial sampling time [OR 0.6,  $p=0.009$ ]. This suggests that detection of ZnT8A decreases within 2 years of T1D onset.

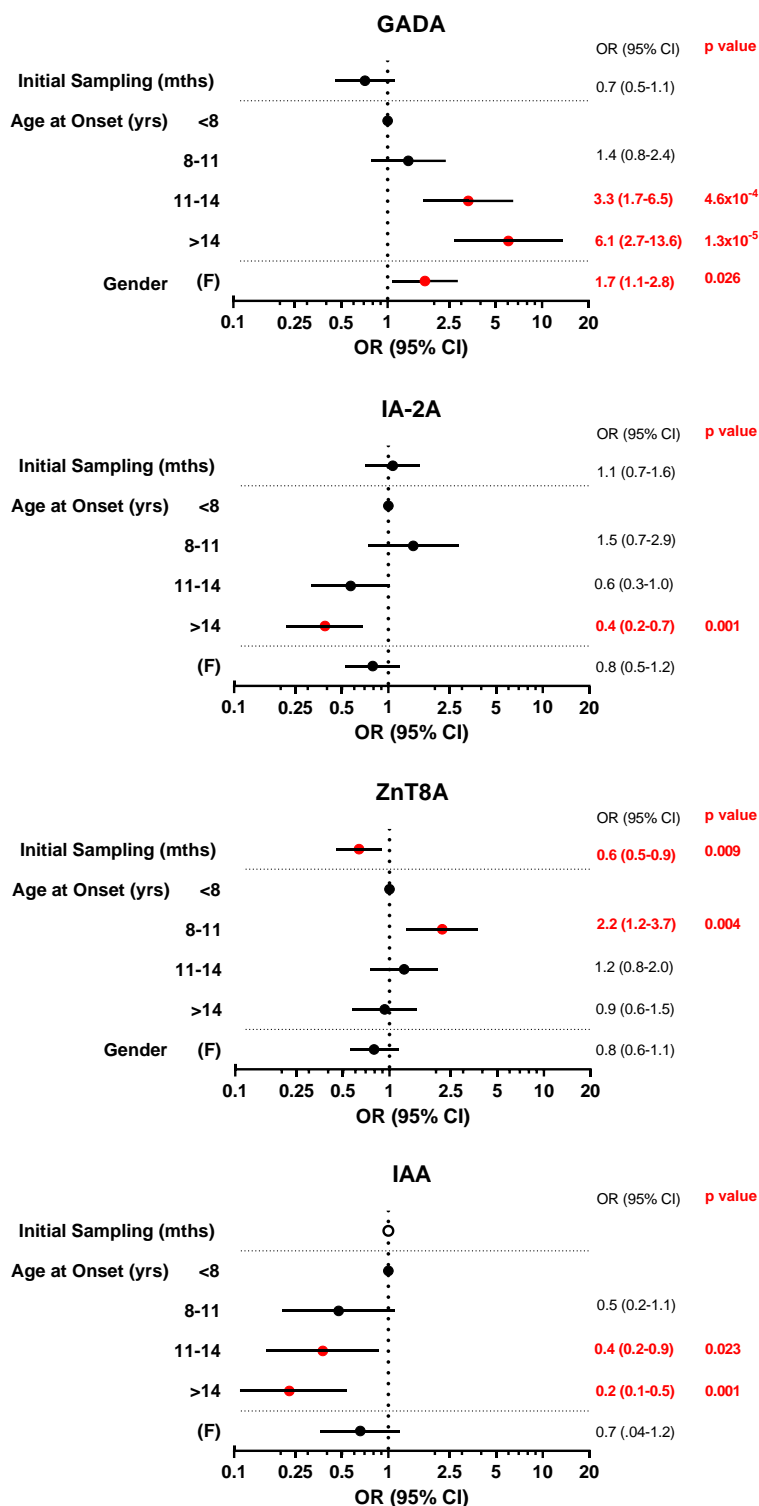
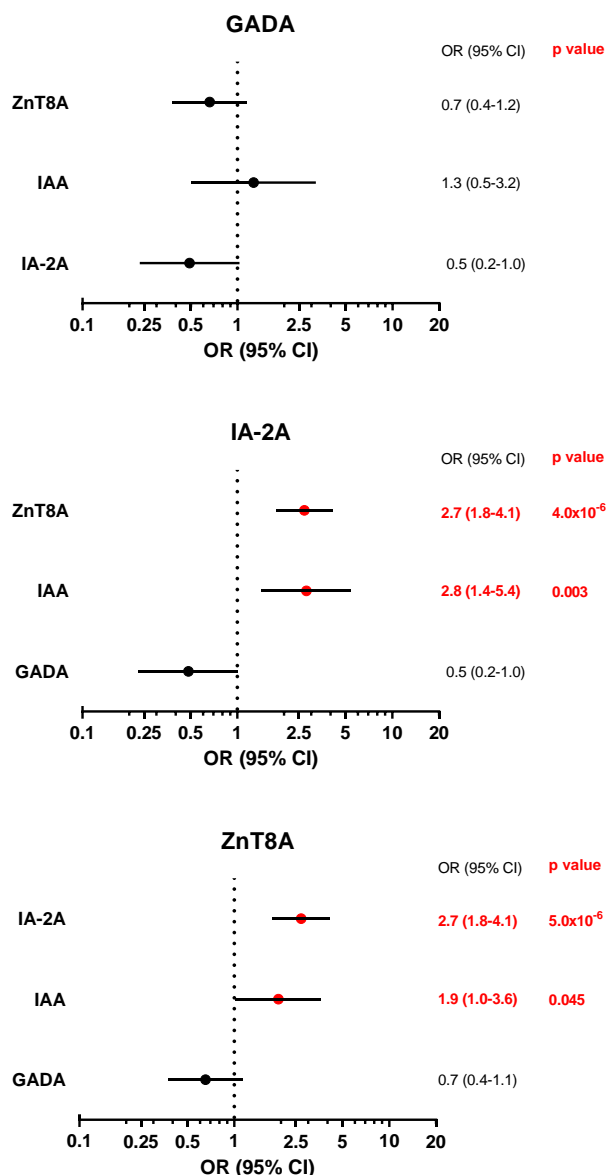


Figure 3:7 – Non-genetic associations on autoantibody positivity at T1D onset

OR: odds ratio; 95% CI: confidence interval; OR of 1 denotes the reference category of variable; ORs over 1 favour autoantibody positivity; red dots and text denote alpha significance (<0.05). ORs, CIs and p values were calculated from logistic regression models for autoantibody positivity at initial sampling time (months) adjusted for all non-genetic covariates (gender, age at onset, autoantibody level at onset, and initial sampling time (months) from onset. All subjects positive for these autoantibodies had complete non-genetic data at initial sampling (GADA n= 487; IA-2A n =452; ZnT8A n =395). The detection of IAA was only considered if sampling was taken within 2 weeks of diagnosis (n =238; 171; 71.8% positive), and therefore, models were unadjusted for initial sampling (open circle for non-applicable).



*Figure 3:8 – Associations of co-existing autoantibodies on autoantibody positivity at T1D onset*

OR: odds ratio; 95% CI: confidence interval; OR of 1 denotes the reference category of variable; ORs over 1 favour autoantibody positivity; red dots and text denote alpha significance (<0.05). ORs, CIs and p values were calculated from logistic regression models for autoantibody positivity at initial sampling time (months) adjusted for all non-genetic covariates (gender, age at onset, autoantibody level at onset, and initial sampling time (months) from onset). Autoantibody covariates were considered independently in all models; GADA, IA-2A and ZnT8A with IAA (n =283) and without IAA (n =577).

### 3.3.3.2 Final sampling

Multivariate analysis on the loss of GADA, IA-2A, and ZnT8A responses at final follow-up (range 2-32 years) adjusted for all non-genetic covariates are summarised in **Figure 3:9A/B**.

Gender was not associated with autoantibody responses at final follow-up independent of other covariates (p>0.05).

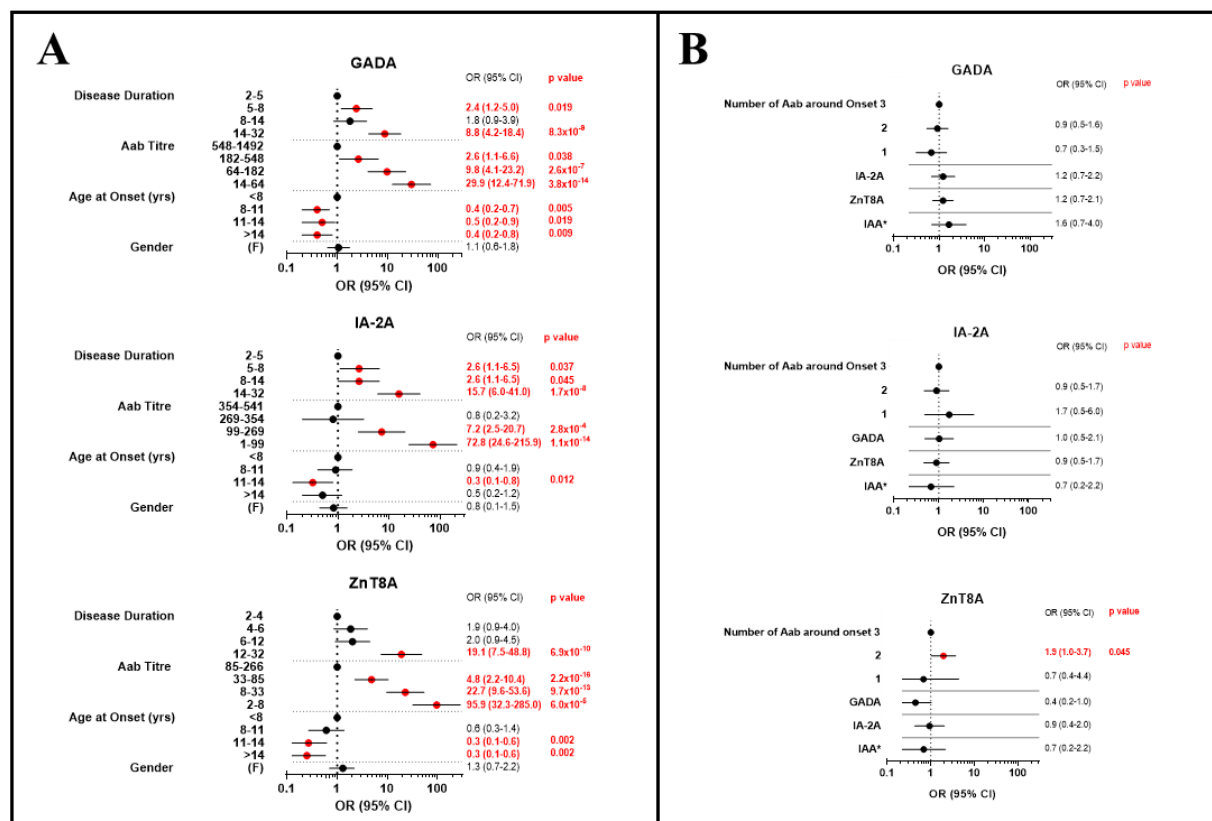


Figure 3-9 – Non-genetic associations of autoantibody loss for GADA, IA-2A, & ZnT8A

OR: odds ratio; 95% CI: confidence interval; OR of 1 denotes the reference category of variable; ORs over 1 favour autoantibody loss; red dots and text denote alpha significance (<0.05). ORs, CIs, and p values were calculated from multivariate logistic regression models for autoantibody loss at final sampling time (years) adjusted for all non-genetic covariates (gender, age at onset, quartile of baseline autoantibody titre at onset, and quartile of disease duration from onset (years) at final sampling. Complete non-genetic data was available for 481/487 GADA positive, 452/452 IA-2A, and 373/395 ZnT8A positive T1D subjects. (A) Multivariate non-genetic baseline model used for further analysis; lower autoantibody titres and higher disease duration at final sampling are positively associated with autoantibody loss for all responses. An older age-at-onset is negatively associated with autoantibody loss for GADA, IA-2A and ZnT8A above the age of 11 years. (B) Variables of co-existing autoantibodies were investigated independently (denoted by solid black lines), adjusting for variables detailed in the non-genetic baseline model. At onset, the presence or number of other islet autoantibodies did not strongly influence GADA, IA-2A or ZnT8A loss, but ZnT8A loss at final sampling was weakly associated with the presence of two autoantibodies compared to three autoantibodies.

### **3.3.3.2.1 Disease duration**

Quartiles of disease duration at final follow-up (years) were associated with GADA (OR range 1.8-8.8, p range=0.019- $8.3 \times 10^{-9}$ ), IA-2A (OR range 2.6-15.7, p range=0.037- $1.7 \times 10^{-8}$ ], and ZnT8A loss (only in >12-32 years OR 1.9-19.1, p= $6.9 \times 10^{-10}$ ) to differing degrees and was included in all multivariate analysis (**Figure 3:9A**). Whilst quartile of disease duration had differential effects on individual autoantibody responses when disease duration was considered in multivariate logistic regression as a linear variable (years), the risk of autoantibody loss per year was comparable across all autoantibody responses (GADA: OR 1.1; IA-2A: OR 1.2; ZnT8A: OR 1.2, p range= $6.98 \times 10^{-8}$ -  $4.78 \times 10^{-9}$ ]. This suggests that although ZnT8A is lost more rapidly than GADA and IA-2A, yearly disease duration had a similar effect on the risk of autoantibody loss at final follow-up.

### **3.3.3.2.2 Autoantibody titre at T1D onset**

Multivariate analysis confirmed that lower quartiles of autoantibody titres at onset were strongly associated with increased risk of autoantibody loss for GADA (OR 29.9, p= $3.8 \times 10^{-14}$ ), IA-2A (OR 72.8, p= $1.1 \times 10^{-14}$ ), and ZnT8A (OR 95.9, p= $2.2 \times 10^{-16}$ ) at final follow-up, independent of other covariates (**Figure 3:9A**). For GADA (p=0.038 to  $1.5 \times 10^{-16}$ ) and ZnT8A (p= $6.0 \times 10^{-5}$  to  $6.1 \times 10^{-18}$ ), quartiles of baseline autoantibody titre below the highest quartile were strongly associated with increased risk of autoantibody loss; however, for IA-2A, discrimination of risk was only observed between the upper two and lower two quartiles (p=0.00028 to  $1.1 \times 10^{-14}$ ). The influence of baseline autoantibody titre on autoantibody loss was also evident in all autoantibody responses when plotted by quartile despite the heterogeneity between individuals (**Figure 3:10**). However, no apparent groups of individuals who maintain their autoantibody response(s) were apparent, suggesting autoantibody loss occurs across all groups (**Figure 3:11**).

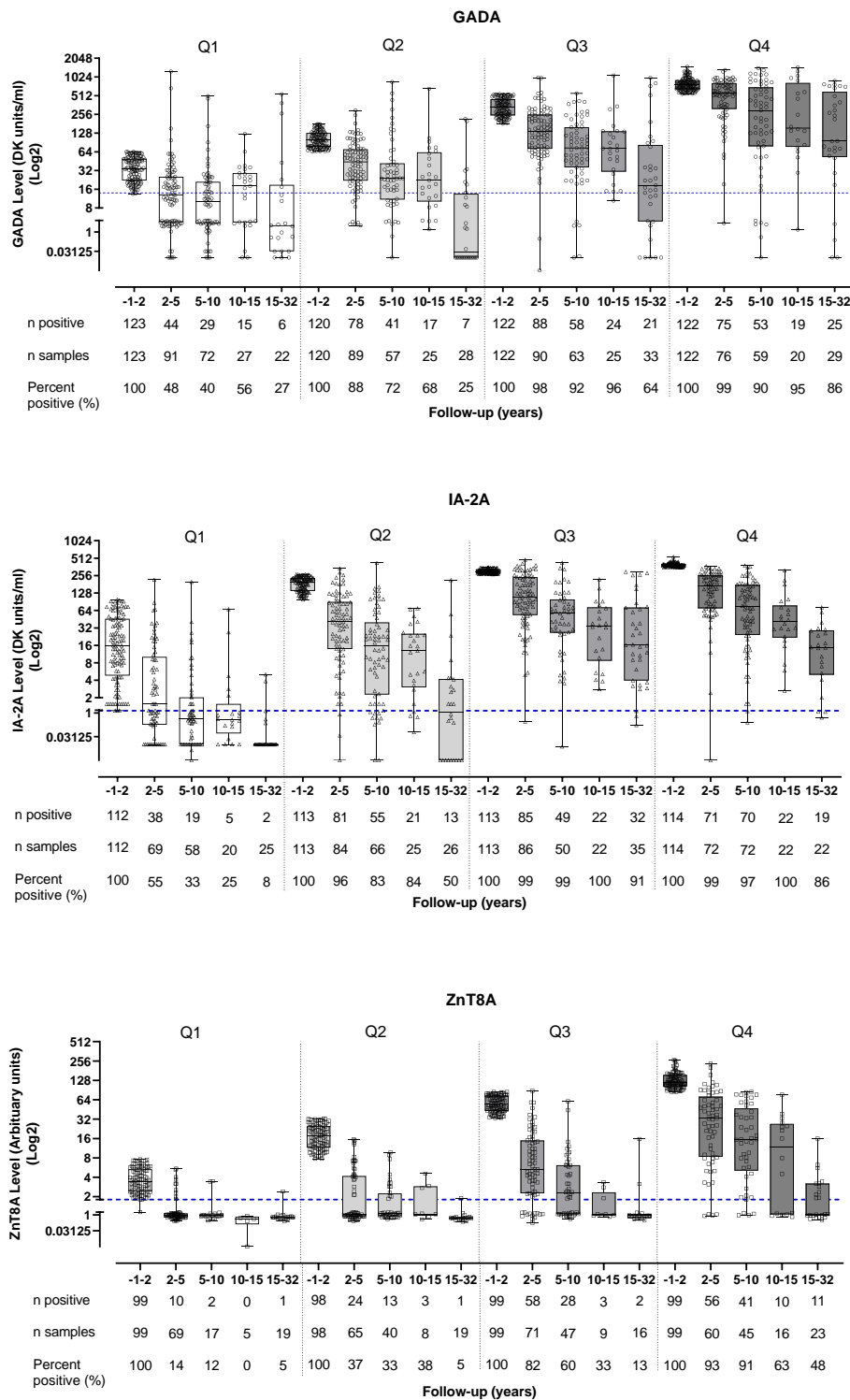


**Figure 3:10 – Longitudinal GADA, IA-2A, & ZnT8A titres categorised into baseline quartiles at T1D onset**

The prevalence of longitudinal autoantibody positivity in all autoantibody responses was higher in subjects with high quartiles of baseline autoantibody titre ( $p < 0.0001-0.05$ ). Independent of baseline titre, longitudinal autoantibody titres sequentially decreased over follow-up in most subjects [GADA: 365/487 (74.9%); IA-2A: 407/452 (90.0%); ZnT8A: 389/395 (98.5%)]. A minority of GADA and IA-2A responses had higher autoantibody titres in at least one follow-up and/or had evidence of wax-waning patterns of differing magnitudes in at least two follow-up samples. However, this was rare in ZnT8A responses. Given the testing strategy, the re-emergence of autoantibodies after onset cannot be fully evaluated.

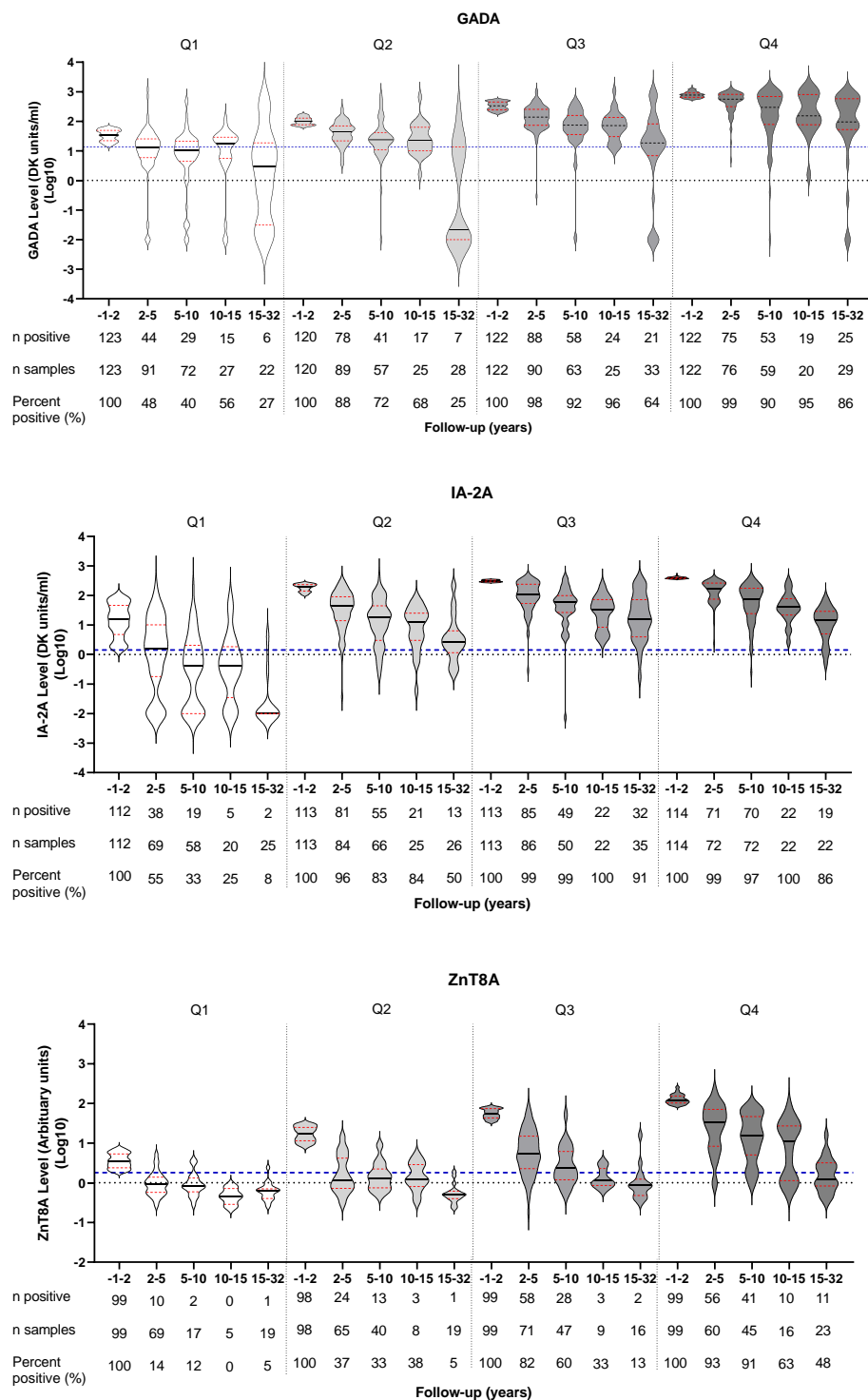


**Figure 3:11 – Quartiles of autoantibody level at T1D onset over longitudinal follow-up for GADA, IA-2A, & ZnT8A (Violin plots)**

Individuals positive for GADA (n=487), IA-2A (n=495) and ZnT8A (n=395) by RIA out of a T1D cohort of 577 individuals that provided one sample at onset (-1-2 years) and at least one sample at longitudinal follow-up (2-32 years), separated by quartiles of autoantibody level present at onset (Q1-Q4; lowest to highest). Violin plots denote the overall distribution of the data by smoothed kernel density (bar width) and show lines at the median and interquartile ranges at each time category. Blue dashed lines denote positivity thresholds for the respective autoantibody. The proportion of autoantibody positives decreased as a function of longitudinal follow-up for all quartiles of autoantibody level at onset (p<0.0001).

Importantly, the number of missing data points did not differ between the quartiles of titre at onset, suggesting that the influence of autoantibody titre on autoantibody loss at final follow-up was not due to skewed data (**Table D:11-Table D:13; Appendix D.5**).

### **3.3.3.2.3 Age at T1D onset**

An older age-at-onset considered as quartiles and compared to individuals diagnosed <8 years was associated with reduced autoantibody loss at final follow-up but, the pattern and strength of association were not uniform (**Figure 3:9A**). For GADA, an age-at-onset  $\geq 8$  years was associated with reduced GADA loss, with comparable odds across the upper age quartiles (OR range 0.4-0.5, p range=0.019-0.009). IA-2A loss was only less likely in individuals diagnosed between 11 and 14 years compared with individuals diagnosed <8 years (OR 0.3, p=0.012). In contrast, reduced ZnT8A loss was associated with an age-at-onset  $\geq 11$  years (OR 0.3, p=0.002).

When age-at-onset was considered as a binary variable according to T1DE age [T1DE2 ( $\geq 13$  years compared to T1DE1 (<7 years)], the overall log odds ratio associated with autoantibody loss at final sampling for all autoantibody responses was comparable to when age was considered as quartiles (OR range 0.3-0.4; p=0.004-0.011) (**Table 3:5**). Given the equal distribution of age at onset considered as quartiles, this was deemed more appropriate for multivariate analysis. However, the increased autoantibody loss in T1DE1 compared to T1DE2 subjects can be observed in **Figure D:12; Appendix D.5.2**, and there appeared to be no interaction between age and autoantibody titre at onset in relation to autoantibody loss at final follow-up (p>0.05).

Age at onset	GADA			IA-2A			ZnT8A		
	OR (95% CI)	p value	n	OR (95% CI)	p value	n	OR (95% CI)	p value	n
<b>Quartiles</b>									
≥8-11yrs vs <8yrs	0.4 (0.2-0.7)	5.0x10 <sup>-3</sup>	113 105	0.9 (0.4-1.9)	NS	127 120	0.6 (0.27-1.38)	NS	108 89
≥11-14yrs vs <8yrs	0.5 (0.2-0.9)	1.9x10 <sup>-2</sup>	126 105	0.3 (0.1-0.8)	1.2x10 <sup>-2</sup>	108 120	0.3 (0.1-0.6)	2.0x10 <sup>-3</sup>	91 89
≥14yrs vs <8yrs	0.4 (0.2-0.8)	9.0x10 <sup>-3</sup>	136 105	0.5 (0.2-1.2)	NS	97 120	0.3 (0.1-0.6)	2.0x10 <sup>-3</sup>	85 89
<b>T1DE</b>									
≥13yrs (2) vs ≤7yrs (1)	0.4 (0.2-0.7)	4.0x10 <sup>-3</sup>	138 82	0.32 (0.14-0.77)	1.1x10 <sup>-2</sup>	122 108	0.3 (0.1-0.7)	4.0x10 <sup>-3</sup>	103 78

*Table 3:5 –Autoantibody loss at final follow-up considering age at onset as quartiles versus T1DE categories*

NS: Not Significant; OR: odds ratio; 95% CI: confidence interval; OR of 1 denotes the reference category of variable; ORs over 1 favour autoantibody loss. ORs, CIs, and p values were calculated from logistic regression models for autoantibody loss at final sampling time (years) adjusted for all non-genetic covariates (gender, age at onset, autoantibody level at onset, and disease duration from onset (years) at final sampling. T1DE: type 1 diabetes endotype [<7yrs T1DE 1; >13yrs T1DE 2].

#### **3.3.3.2.4 Co-existing autoantibodies at T1D onset**

The presence of co-existing islet autoantibodies or number of islet autoantibodies at onset was not associated with the loss of GADA, IA-2A, or ZnT8A at final sampling adjusted for non-genetic covariates (**Figure 3:9B**). The presence of two autoantibodies, compared with three autoantibodies at onset, was only weakly associated with ZnT8A loss at final follow-up (OR 1.9;  $p=0.045$ ).

---

#### **3.3.4 Genetic associations of autoantibody positivity at initial sampling & autoantibody loss at final sampling**

---

Multivariate models with complete genetic data for autoantibody positivity at initial sampling (<2 years from onset) and autoantibody loss at final sampling adjusted for non-genetic covariates (gender, age-at-onset, baseline autoantibody titre, and disease duration), genetic variables were considered independently as categorical or binary variables as previously stated (**Figure 3:12**). This side-by-side comparison approach was used to investigate whether genetic drivers of autoantibody positivity at T1D onset are different and/or inversely associated with genetic drivers of autoantibody loss.

For interpretation of the figures, it is important to note that factors associated with autoantibody positivity at initial sampling appear on the right (OR>1), and factors negatively associated with autoantibody loss at final sampling appear on the left (OR<1).

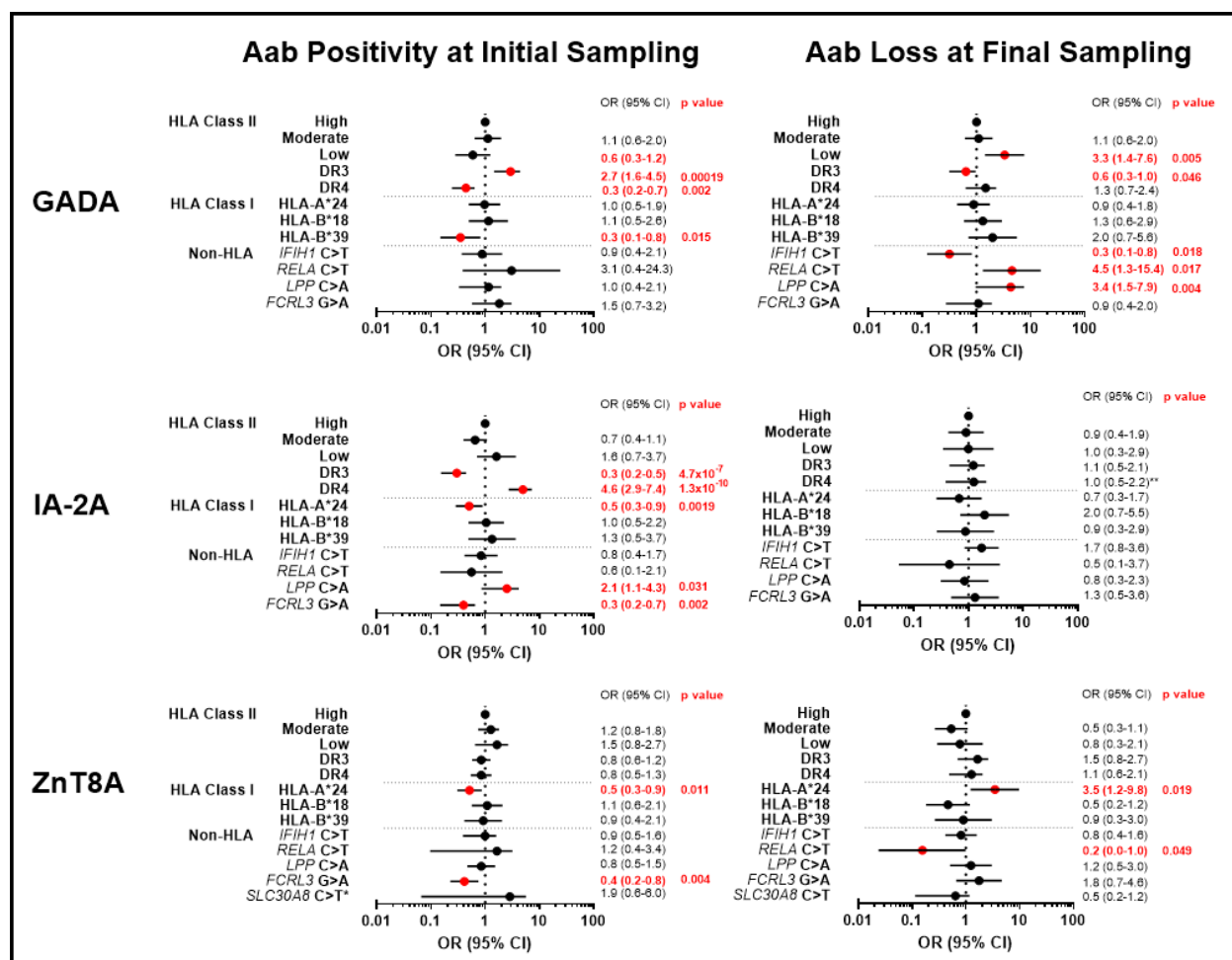


Figure 3:12 – Genetic associations of autoantibody positivity at initial sampling around T1D onset & autoantibody loss at final sampling after T1D onset

OR: odds ratio; 95% CI: confidence interval; OR of 1 denotes the reference category of variable; ORs over 1 favour autoantibody positivity at initial sampling or autoantibody loss at final sampling; red dots and text denote alpha significance (<0.05). ORs, CIs and p values were calculated from multivariate logistic regression models adjusted for all non-genetic covariates (Figure 3:9A) for initial and final sampling, including gender, age-at-onset, sampling time (months/years) and autoantibody titre at onset (final sampling only). All genetic covariates were considered independently in all models. The minor allele frequency (MAF) of non-HLA SNPs in this T1D cohort was comparable to the global MAF (GMAF) or MAF from the 1000 Genomes project (MAF-1000G\*) (Table 3:3) and minor alleles were compared to major alleles (major>minor).

### 3.3.4.1 GADA

---

At initial sampling, GADA positivity was not associated with HLA Class II risk genotypes but was strongly associated with the presence of DR3 [OR 2.7,  $p=0.00019$ ) and negatively with DR4 (OR 0.3,  $p=0.002$ ) when considered independently. The presence of HLA class I *HLA-B\*39* was negatively associated with GADA positivity (OR 0.3,  $p=0.015$ ). Investigated non-HLA SNPs were not associated with GADA positivity at initial sampling.

However, at final sampling, GADA loss was associated with low-risk HLA class II genotypes (OR 3.3,  $p=0.005$ ), possibly due to the reduced presence of at least one copy of DRB1\*03 that was weakly confirmed by the negative association with DR3 (OR 0.6,  $p=0.046$ ) when independently considered. Loss of GADA at final sampling was not associated with any HLA class I genotypes but was associated with 3 non-HLA SNPs; positively with the *RELA/11q13* T allele (OR 4.5,  $p=0.017$ ) and *LPP/3q28* A allele (OR 3.4,  $p=0.004$ ) but was negatively associated with the *IFIH1/2q24* T allele (OR 0.3,  $p=0.018$ ). Collectively, this suggests that individuals with DR3 and the diabetes risk allele of *IFIH1/2q24* were more likely to maintain GADA responses. In contrast, those with minor alleles of *RELA/11q13* and *LPP/3q28* linked to other autoimmune conditions were more likely to lose GADA.

### 3.3.4.2 IA-2A

---

At initial sampling, IA-2A positivity was not associated with HLA class II genotypes but was strongly associated with the presence of DR4 (OR 4.6,  $p=1.3 \times 10^{-10}$ ) and negatively with DR3 (OR 0.3,  $p=4.7 \times 10^{-7}$ ) when considered independently. The presence of HLA class I *HLA-A\*24* was negatively associated with IA-2A positivity (OR 0.5,  $p=0.0019$ ). IA-2A positivity at initial sampling was also associated with two non-HLA SNPs: positively with the *LPP/3q28* A allele (OR 2.1,  $p=0.031$ ) and negatively with the *FCRL3/1q23* A allele (OR 0.3,  $p=0.002$ ).

However, IA-2A loss at final sampling was not associated with any of the genotypes considered, independent of non-genetic covariates, but the presence of at least one copy of DR4 was negatively associated with IA-2A loss (OR 0.5,  $p=0.016$ ) when IA-2A titre at onset was excluded from the model. This was due to an interaction between DR4 and IA-2A titre (data not shown). Collectively, these results suggest that IA-2A positivity has distinct genetic associations at onset compared with after diagnosis, which differs from GADA responses. For example, compared with GADA, the minor allele of *LPP/3q28* was associated with the presence of IA-2A at diagnosis but was associated with GADA loss after diagnosis.

### 3.3.4.3 ZnT8A

---

At initial sampling, ZnT8A positivity was not associated with any HLA class II genotypes but was negatively associated with the presence of HLA class I *HLA-A\*24* (OR 0.5,  $p=0.011$ ) and the non-HLA *FCRL3/1q23* A allele (OR 0.4,  $p=0.004$ ). The *SLC30A8* genotype did not influence overall ZnT8A positivity but strongly influenced the specificity of the ZnT8A response. The T allele was strongly associated with the development of ZnT8WA (OR 7.7,  $p=5.8 \times 10^{-5}$ ) and strongly negatively associated with the development of ZnT8RA (OR 0.1,  $p=1.9 \times 10^{-7}$ ).

However, ZnT8A loss at final sampling was associated with the presence of *HLA-A\*24* (OR 3.5,  $p=0.019$ ). Only one non-HLA SNP showed a weak negative association with ZnT8A loss at final follow-up, the *RELA/11q13* T allele (OR 0.2,  $p=0.049$ ). This suggests that the negative association of *HLA-A\*24* and ZnT8A observed at diagnosis becomes stronger after diagnosis whereas, this was not observed in IA-2A responses. The minor allele of *RELA/11q13* may have opposite effects on ZnT8A and GADA responses.

---

## 3.4 Discussion

---

---

### 3.4.1 Main findings

---

1. Overall, autoantibody prevalence, number, and median autoantibody level decreased as a function of increasing disease duration in all autoantibody responses. In most subjects, autoantibody titres sequentially decreased over follow-up (range 74.9-98.5%) but the within-subject and between-subject variance were highly heterogenous. At  $\geq 15$  years disease duration, high GADA and IA-2A titres were still observed which was rare for ZnT8A responses.
2. ZnT8A responses were lost more rapidly over follow-up than GADA and IA-2A responses. At final follow-up across all autoantibody responses (median duration 7.3 years), only 40.1% remained positive for ZnT8A compared to 70.8% and 76.8% for GADA and IA-2A, respectively. The persistence of GADA and IA-2A positivity was comparable over follow-up.
3. The association of non-genetic [gender, age-at-onset, time of initial serum sampling (months), and the presence of co-existing autoantibodies] and genetic factors, previously reported to be associated with GADA, IA-2A, and ZnT8A positivity around T1D onset (<2 years duration), were confirmed using adjusted multivariate logistic regression models.
4. Logistic regression modelling identified that the principal non-genetic predictors of autoantibody loss at final sampling in order of increasing association were a younger age at onset <8 years, longer disease durations >5 years, and lower baseline autoantibody levels close to onset. The degree of autoantibody loss was not influenced by the number or combination of autoantibodies present around onset, but patterns were discriminated by antigen specificity.

5. Logistic regression modelling of genetic factors associated with autoantibody loss (independent of non-genetic covariates) revealed antigen-specific effects that differed from associations at the time of diagnosis. GADA loss was associated with low-risk HLA Class II genotypes and non-HLA loci for *RELA/11q13*, *LPP/3q28*, and negatively with *IFIH1/2q24*. IA-2A loss was not linked with any genetic factors considered. ZnT8A loss was associated with the presence of *HLA-A\*24* and weakly with *RELA/11q13*.

---

### 3.4.2 Islet autoantibody responses after T1D onset

---

Of those positive close to onset, 70.8%, 76.8%, and 40.1.% remained positive for GADA, IA-2A, and ZnT8A, respectively, at final follow-up (median duration 7.3 years). In individuals with  $\geq 15$  years duration, ZnT8A prevalence (14%) and level were low compared to GADA (43%) and IA-2A (48%), which were present at a range of levels. The rapid decline in ZnT8A, independent of R325W specificity during the first 10 years of disease, compared with GADA and IA-2A, has been reported previously (443, 492), but cross-sectional studies of long disease duration  $\geq 10$  years report contradictory frequencies of GADA, IA-2A, and ZnT8A (data limited) at follow-up.

Our data agree with the Barbara Davis Centre, showing that GADA and IA-2A are lost at a similar rate compared to ZnT8A with an overlapping follow-up period (12-57.1 years; n=282 autoantibody positivity was 21% GADA, 19.5% IA-2A, and 6.7% ZnT8A) (443). In the Golden Years survivor cohort (51-75 years disease duration; n=343), whilst GADA was the most prevalent autoantibody (48%), ZnT8A (24.6%) were more common compared with IA-2A (5.8%), which is in contrast to both the Barbara Davis Centre and our study (447). Additionally, the majority of remaining ZnT8A and IA-2A responses were only present at reduced levels (80-95% <50 units) compared with GADA (55.5% present >50 units) in the

Golden Years cohort, which may suggest at >50 years disease duration, a greater loss of IA-2A responses compared with GADA may be anticipated (447). It is important to consider that baseline autoantibody characteristics (positivity and level at onset) are unknown in those studies, and in other cross-sectional studies, which may account for some variability in autoantibody frequencies. The strength of our study was the ability to account for autoantibody positivity, and baseline autoantibody levels and these show a strong relationship with the longevity of humoral responses in a relatively large cohort.

Many studies agree that autoantibody prevalence decreases with disease duration. However, an older age-at-onset has only been confirmed for GADA positivity but not IA-2A (349, 491, 498) whereas, the one study investigating ZnT8A persistence found no association with age (491). The reason for the age-at-onset effect on longitudinal GADA, IA-2A, and ZnT8A found in this study is not clear but, may be due to a range of differences with our study such as the inclusion of individuals diagnosed older (>21 years), variations in disease duration at follow-up, longitudinal compared with cross-sectional sampling, or availability of baseline autoantibody level. Other factors could include differences in autoantibody detection protocols and additional cohort characteristics such as ethnicity and geographical location. Nonetheless, age-associated autoantibody positivity profiles during disease may in part be related to T1D endotypes (T1DE) recently described (43). Regardless of how age was considered in multivariate analysis (quartiles versus T1DE) in this study, a younger age at onset was associated with loss of autoantibody responses.

High-risk T1D-associated HLA Class II genotypes were not associated with autoantibody loss for GADA, IA-2A, and ZnT8A. However, low-risk HLA Class II genotypes were associated with GADA loss at final follow-up when compared with high-risk genotypes. This may be explained by the association between the *DRB1\*03* haplotype and GADA persistence,

consistent with other reports (349, 491, 498) because the low-risk category did not contain this haplotype. In contrast to other studies (499, 500), there was no association between DR4 and IA-2A persistence when adjusted for baseline level, probably due to the relationship of DR4 with IA-2A levels at onset (349). The ZnT8A response in our study was not associated with HLA Class II, but we were unable to study the protective allele DQ6.4 because of the low but expected frequency (0.4%) (94). Collectively, the highly predisposing HLA Class II genotypes for T1D risk that also strongly influence levels of specific autoantibodies at onset (especially IA-2A and IAA) do not have additional effects on humoral responses after clinical onset.

Type 1 diabetes-associated HLA Class I genotypes were not associated with loss of GADA or IA-2A, but the presence of *HLA-A\*24* was associated with loss of ZnT8A in adjusted models. This is in line with the negative association between *HLA-A\*24* and ZnT8A positivity we have previously observed at onset (90) and in first degree relatives (350), which may suggest that attenuation of humoral responses to ZnT8A in *HLA-A\*24* carriers continues after disease onset. The negative association of *HLA-A\*24* with IA-2A positivity at onset (90) was confirmed in the individuals analysed here but was not observed after clinical onset, inconsistent with a previous report (median 5 years disease duration; n=2,531 diagnosed  $\leq 17$  years) (498). Perhaps this was due to reduced statistical power, longer disease duration, an older range of age-at-onset, or the inability of the previous study to measure IA-2A positivity at diagnosis. The humoral phenotype of ZnT8A and IA-2A in carriers of *HLA-A\*24* after onset warrants further study.

A quarter of individuals with T1D have autoantibodies associated with non-islet autoimmunity, and therefore, SNPs associated with other autoimmune comorbidities are of interest (501). Genome-wide association studies reported links between *RELA/11q13* (rs568617 in high LD  $\geq 0.9 R^2$  with rs2231884) and Crohn's disease (502), *LPP/3q28* (rs1464510) and Coeliac

disease (503), *IFIH1/2q24* (rs2111485 in LD with rs1990760) with both T1D risk (504) and progression to T1D (505), and *FCRL3/1q23* (rs3761959) with autoimmune thyroid disease (506). These SNPs have also been linked with positivity for specific humoral responses 3 to 14 years after T1D onset in ~7,000 individuals from the type 1 diabetes genetic consortium (T1DGC; aged <17 years; median age at onset 8 years) (491). In age-at-onset and disease duration adjusted models, *RELA/11q13* and *FCRL3/1q23* SNPs was associated with IA-2A positivity, *LPP/3q28* SNPs was associated with GADA positivity, and *IFIH1/2q24* was associated with positivity for autoantibodies related to autoimmune gastritis and thyroid disease (491). However, *FCRL3/1q23* was strongly negatively associated with ZnT8A positivity when analysed in a subset of individuals sampled closer to onset (n=1,221; sampled <2 years disease duration with a median age of onset of 11 years) (491), which confirmed previous findings from a GWAS study also using T1DGC subjects (n=855; <2 years disease duration with a mean age at diagnosis 12 years) (347). Around onset (categorised as sampling within 2 years of diagnosis) in the present study, we were able to replicate the findings from both these studies. However, in contrast to Brorsson *et al.*, (2015)(491), we found that *RELA/11q13* and *LPP/3q28* were associated with GADA loss, but *IFIH1/2q24* was negatively associated with GADA loss and *RELA/11q13* was weakly negatively associated with ZnT8A loss. Despite the size difference in both cohorts (577 versus ~7000), the different effects of *RELA/11q13*, *LPP/3q28*, and *IFIH1/2q24* may be related to the present study having a longer follow-up period and correction for baseline autoantibody level rather than statistical power. The exclusive association of *IFIH1/2q24* with GADA responses in disease has not been previously reported.

Our study has certain limitations. We were unable to analyse the relationship between islet autoantibody data and C-peptide or clinical outcomes in this cohort. C-peptide data were available for only 100 individuals of whom, 44 had been published previously with no

association with autoantibodies at follow-up (449). Additionally, sequential samples after the loss of autoantibody responses were not tested, so we cannot comment on possible re-emergence or factors that may influence the waxing or waning of autoantibody positivity through more frequent sampling. Often only observed in small subsets of individuals, increasing or stable titres of GADA has also been reported in several studies, but usually, both IA-2A and ZnT8A titres decline with few reporting whether titres increase or stabilise (449, 493, 500).

Comprising only 1-2% of the pancreas, an estimated 10-20% of  $\beta$ -cell mass remains at T1D onset, but this is heterogeneous, related to age-at-onset, and may not reflect the clinical severity of disease (43, 173, 507). A growing body of evidence from histological examination of pancreatic tissue from individuals with long-standing (up to 50 years duration) T1D has demonstrated the presence of surviving insulin-containing  $\beta$ -cells (39, 42, 507). One study found evidence of ongoing  $\beta$ -cell destruction in the pancreases of long-duration T1D (range 4-67 years); however, the frequency of residual  $\beta$ -cells was higher in individuals with lower mean blood glucose independent of disease duration (508). However, pancreatic tissue sections from both healthy and T1D subjects suggests  $\beta$ -cell mass itself displays heterogeneity (26), and therefore, findings from T1D histological studies should be carefully considered. Nonetheless, residual  $\beta$ -cell presence and function have been further corroborated by the detection of serum or urinary C-peptide (a by-product of insulin synthesis) in individuals with long-standing T1D (>30 years duration) (37, 39, 40, 448, 449, 508). Collectively, it is plausible that the immunogenicity of residual  $\beta$ -cells may prolong autoantibody production to islet-specific antigens during disease.

Sustained islet autoantibody production by plasma cells in disease is unlikely to be due to constant replenishment of short-lived plasma cells through re-stimulation of memory B

lymphocytes. Tissue-resident LLPCs form an independent compartment of immunological memory which may be involved in long-duration T1D (237). LLPCs can persist for decades independent of B lymphocyte precursors or residual antigen but are not intrinsically long-lived. Their survival is dependent on specialised niche microenvironments, but the cellular and molecular components that promote LLPC production or survival are not fully characterised in humans; there is some evidence in other autoimmune diseases of LLPCs in inflamed target tissue (237-239).

Although islet autoantigens are highly expressed in pancreatic islets, ZnT8 expression is almost exclusive to islets in contrast to GAD and IA-2 that are found in specific cells of the nervous system (266). If residual antigen remains accessible to immune surveillance either by continued  $\beta$ -cell death or functional residual  $\beta$ -cells, the differential antigen expression may provide some rationale as to why ZnT8A are lost more rapidly than GADA or IA-2A. Exposure of ZnT8 may be possible during glucose-stimulated insulin secretion, but only one study has found an association between ZnT8A levels (but not GADA or IA-2A) and C-peptide in multivariate analysis in concurrent testing (448). Therefore, elucidating any relationship between islet autoantibodies and C-peptide/ $\beta$ -cell function requires simultaneous detection and prospective sampling in future studies. It is difficult to ascertain whether sustained islet autoantibody production occurs solely by LLPCs independent of stimulation by residual autoantigen or whether the level at diagnosis is related to  $\beta$ -cell mass. Understanding the role of islet autoantibodies and subsets of B lymphocytes before or after T1D onset may provide insights into autoimmune targeting of the  $\beta$ -cell that should benefit both prevention and intervention clinical trials and, therefore, merits further investigation.

# **Chapter 4 - Development of Nluc-ZnT8 LIPS for ZnT8A detection**

---

## 4.1 Introduction

---

Solid-phase immunoassays that use either immobilised antigen or antibody such as Western blotting and ELISAs have several limitations: reduced ability to detect conformational epitopes, high assay background that compromise specificity (often associated with antigen preparation techniques), higher sample volume requirements, and a limited dynamic range of detection. Whilst the fluid-phase RIA overcomes many hurdles of solid-phase immunoassays and has been the method of choice for (auto)antibody detection, the use of radioisotopes, among other required methodology steps such as multiple wash steps, prevent its widespread application (509).

Radioisotopes are expensive, highly regulated, and have limited shelf-life with both environmental and safety implications. Additionally, RIAs are labour-intensive, taking 1-3 days to complete, and to date, have not been developed to detect multiple antigen-specific (auto)antibodies simultaneously and, therefore, can still require substantial sample volumes. For example, detecting all major islet autoantibodies (IAA, GADA, IA-2A, and ZnT8A) can require up to ~70µl of sample for full confirmation of all results without a second sample. This limits the possibility for population-based screening and determination of islet autoimmunity in birth cohorts where blood volumes are often small. Since 2015, BOX has been conducting capillary sampling, and to date, 1380/2447 (56.4%) samples across all ages provided enough blood for >70µl serum for all islet autoantibody RIAs which is slightly reduced in samples from children aged under 5 years, 39/84 (46.4%). Therefore, fluid-phase immunoassays that replace the use of radionucleotides, reduce assay lengths, require less sample volume, and have the potential for multiple (auto)antibody detection are desirable. Luminescence-based assays that use luciferase reporters is a candidate format that may meet these desirable characteristics.

---

### 4.1.1 Bioluminescence & luciferase enzymes

---

Naturally occurring bioluminescence enzymes (luciferases) have been attractive candidates for reporters of cellular physiology due to their high sensitivity and lack of additional light amplification steps required (510-512). In the presence of adenosine triphosphate (ATP) and magnesium ions, luciferases oxidise the photo-emitting substrate luciferin into oxyluciferin in a broadly linear quantitative reaction (510, 511). The characteristics of all main luciferases are summarised in **Figure 4:1**. Firefly (Fluc) and Renilla (Rluc) luciferases have been most widely utilised as biosensors for a range of applications, including immunoanalysis, due to the high yields of engineered recombinant fusion proteins in bacterial and mammalian expression systems (510, 513).

The Fluc (61kDa), typically from *Photinus pyralis*, emits bioluminescence in the visible spectrum (peak at ~565nm) from a stable non-toxic and ATP-dependent reaction with D-luciferin. Although Fluc produces bioluminescence at high quantum yields (>88%) in a 1:1 ratio, it has a short half-life (~3hrs), can be inhibited by a range of compounds, and is often associated with high assay background, which compromises sensitivity and specificity (510, 511, 513, 514). The use of Rluc from the soft coral sea pansy *Renilla reniformis* has many advantages over Fluc. Rluc is a smaller (36kDa) ATP-independent enzyme with an enhanced thermostability, a longer half-life (4.5hrs), and a highly linear output spanning >7 orders of magnitude (509-511). Rluc catalyses the oxidative decarboxylation of the coelenterazine substrate with a peak emission at 480nm (510, 511). As Fluc and Rluc do not share homology, are active as monomers, and have distinct chemical reactions and peak emission spectra, they are often combined as co-reporters utilising a modified sequential detection protocol that reduces experimental and labour costs (512, 515).

Other luciferases from marine organisms of smaller size have exceeded the bioluminescent performance of Fluc and Rluc. *Gaussia* luciferase (Gluc; 20kDa; 460nm peak emission) from the copepod *Gaussia princeps* also acts on coelenterazine but is strongly resistant to heat and extreme pH and has a brighter bioluminescence (>1000-fold higher), offering enhanced sensitivity over Fluc/Rluc. However, Gluc requires natural secretion and decays rapidly. The half-life of Gluc *in vivo* is ~20-30mins, but the half-life can be extended to 6 days when secreted and stored in cell media at 4°C (511, 514, 516, 517). Despite an appreciatively good half-life, Gluc's light output decreases by 75% within 50 seconds compared with 50% within 90 seconds for Rluc and 50% after 10 minutes for Fluc (511, 514). A common limitation of utilising Gluc/Rluc is the coelenterazine substrate itself, which can be prone to chemical instability and autoluminescence (high backgrounds) (510, 517). Kinetically, the bioluminescence of Fluc is a glow-type, and Rluc/Gluc are flash-type luciferases that require luminometers equipped with injectors to detect the transient peak luminescence (510, 514).

Hall *et al.* (2012) sought to engineer and optimise a luciferase and substrate combination with superior biochemical and physical properties than Fluc/Rluc/Gluc and the coelenterazine substrate without compromising light emission efficiency. A small luciferase subunit (19kDa) known as NanoLuc (Nluc), from the deep-sea shrimp *Oplophorus gracilirostris* in combination with the furimazine substrate produces a brighter glow-type bioluminescent signal (460nm) with >2hr half-life, a specific activity 150-fold higher than Fluc/Rluc, and compared with Gluc, does not require natural secretion (510). With enhanced chemical and physical stability characteristics and improved expression in mammalian cells with little evidence of protein modifications, the NanoGlo® luciferase/substrate coupled system (Promega) kit utilising Nluc is a superior bioluminescence system (510, 518).

## Chapter 4 - Development of Nluc-ZnT8 LIPS for ZnT8A detection

Luciferase	Molecular Weight (kDa)	Organism	Chemical Reaction	Peak light emission ( $\lambda_{max}$ ; nm)	Luminescence Intensity	Half life (hrs)	Luciferase Stability <sup>a</sup>
<b>Fluc</b> <i>glow-type</i>	61	<i>Photinus pyralis</i>	D-luciferin $\xrightarrow{ATP + Mg^{2+}}$ oxyluciferin + AMP, PP <sub>i</sub> , CO <sub>2</sub>	565 	¥	3	7.3 ± 0.3
<b>Rluc</b> <i>flash-type</i>	36	<i>Renilla reniformis</i>	coelenterazine $\xrightarrow{O_2}$ coelenteramide +CO <sub>2</sub>	480 	0.51 ± 0.02¥ 2500§	4.5	99 ± 2
<b>Gluc</b> <i>flash-type &amp; naturally secreted</i>	20	<i>Gaussia princeps</i>	coelenterazine $\xrightarrow{O_2}$ coelenteramide +CO <sub>2</sub>	460 	6500§	0.33*	*
<b>Nluc</b> <i>glow-type</i>	19	<i>Oplophorus gracilirostris</i>	furimazine $\xrightarrow{O_2}$ furimamide +CO <sub>2</sub>	460 	75 ± 9¥	>2	11,000 ± 220

**Figure 4:1 – Bioluminescent characteristics of Fluc, Rluc, Gluc, & Nluc luciferases**

\* Gluc has a half-life of 0.33 hours in vivo and ~ 6 days in cell media once secreted and stored at 4°C; compared with Rluc with a 50% decay of luminescence at 90s, Gluc's decayed by 90% at 90s (514, 516); ¥ luminescence intensity from HEK293 cell lysates in reactions between luciferase enzymes and the compatible enzyme detailed normalised to the Fluc reaction (510); § luminescence emission expressed as counts per minute (CPS) for secreted flash-type luciferases (Gluc and Rluc), despite 2 orders of magnitude brighter bioluminescent signal from Gluc, Gluc decays rapidly (514). <sup>a</sup> Enzyme stability in HEK293 lysates (t<sub>1/2</sub>/min at 37°C) in luciferase reactions with compatible substrates (510); kDa: Kilodaltons; AMP: adenosine monophosphate; ATP: adenosine triphosphate; Mg<sup>2+</sup>; magnesium ions; PP<sub>i</sub>: pyrophosphate. Figure was adapted from (519) and (511) using (510), (514), and (516) as additional sources of information.

---

## 4.1.2 Utilising luminescence for immunoassays

---

Luciferase fusion proteins have been successfully engineered, produced at high yields, show high enzymatic activity, and have been utilised in studying protein-protein interactions (512) and metabolic processes such as gene expression (520). Luciferase-based Immuno-Precipitation System (LIPS) immunoassays have also been applied to detect and study antibodies in autoimmunity, infectious diseases, and cancers (509, 521, 522). Compared to conventional RIA, the LIPS immunoassay offers enhanced presentation of both linear and conformational antigenic epitopes and often have higher sensitivity, specificity, and dynamic range of detection with reduced diffusion times, enabling more rapid detection (522).

### 4.1.2.1 Luminescence immunoassays for islet autoantibody detection

---

To date, LIPS assays to detect GADA (453, 523), IA-2A (453, 521), ZnT8A (524), IAA (366, 525), and TSPAN7A (271) in T1D have been developed and reported (**Table 4:1**). The precise methodology varies between these studies (e.g., type of luciferase, vector, or expression system) and would benefit from protocol harmonisation and comparison in international workshops in the future, which have historically benefitted RIAs (371, 372, 374). However, generally, all studies report the promising potential of LIPS utilising Rluc, Gluc, or Nluc with good concordance with other conventional assays (RIA/ELISA) and either comparable or increased sensitivity to RIAs. This is especially promising when there is room for further improvement, with only one report (to date) utilising the superior bioluminescence system, Nluc/NanoGlo® luciferase/substrate coupled system (Promega). Liberati *et al.* (2018) not only found that performance between Nluc-LIPS and RIA was highly concordant in detecting IAA but also reported that LIPS identified additional FDRs that progressed to diabetes above RIA (366). This suggests that LIPS will be highly sensitive and will improve screening for high-risk individuals for intervention or clinical trials.

Study Autoantibody Methods	Luciferase & Antigen	Method details	Population studied	Performance
<b>Burbelo <i>et al.</i></b> (2008/10) - IA-2A - GADA & IA-2βA  LIPS vs RIA	Rluc  - IA-2 (601-979) - GAD65 (1-585) - IA-2β (662-1033)	Ag cloned into PREN2 vector & expressed in Cos1 cells. Serum (5μl) incubated with 1 x 10 <sup>7</sup> RLU of Rluc antigen. Positivity set at mean + SD of healthy controls.	- 150 T1D patients & controls (DASP2007) - 200-400 age- & gender-matched T1D patients & controls -Sweden	- IA-2A LIPS/RIA correlated by 80% - GADA LIPS/RIA was 100% concordant with 77.6% positivity. - IA-2β positivity in RIA was 51% and 62.5% in LIPS. - No difference in assay performance.
<b>Marcus <i>et al.</i></b> (2011) - GADA & IA-2A  LIPS vs RIA	Rluc  - GAD65 (1-585) - IA-2 (606-979)	Ag cloned into PREN2 vectors & expressed in Cos1 cells. Serum (2μl) incubated with 1.5x10 <sup>5</sup> RLU using local RIA methodology. Positivity based on pos/neg index.	- 150 T1D & controls - DASP2010	- LIPS/RIA SNR comparable. - LIPS/RIA highly correlate (R <sup>2</sup> 0.7-0.8) with high (95%) concordance. -Sensitivity and specificity of LIPS was identical or 1-2% higher than RIA.
<b>Ustinova <i>et al.</i></b> (2014) - ZnT8A  LIPS vs ELISA RSR™ Limited	Gluc  - ZnT8R-¥-ZnT8W dimer (aa268-369)	Secretion signal was added to the 5' end of the construct. Ag expressed in Tn5 cell line using the baculovirus expression system. Diluted serum (10μl at 1:10) incubated with 10-15x10 <sup>6</sup> RLU.	- 109 T1D patients - 123 age- & gender-matched controls - Estonia	Assay performance differed by age. - Adults AUC 0.79 in LIPS vs 0.78 in ELISA. - Children AUC 0.75 in LIPS vs 0.90 in ELISA.
<b>McLaughlin <i>et al.</i></b> (2016) - TSPAN7A  LIPS	Gluc  - Tspan7	Ag cloned into pCMVTnT vector & expressed in HEK293 cells. Serum (5μl) incubated with 10 <sup>6</sup> RLU. Positivity threshold based on mean + 3 SD of controls.	- 94 new-onset T1D - 52 controls - UK	40/94 positive (43%) and to date has not been compared to other detection methods.
<b>Liberati <i>et al.</i></b> (2018) - IAA  LIPS vs RIA	Nluc  - B chain-NLuc proinsulin - B chain-NLuc insulin	Ag subcloned in pCMVTNT vector and expressed in the Expi293™ expression system. Serum (2μl; ± synthetic ACTRAPID® insulin) was incubated with 10 <sup>7</sup> RLU. Positivity threshold set at 97.5th percentile of 186 schoolchildren.	- 80 T1D & 123 donors (Italy) - 186 healthy children (UK) - 53 FDRs (UK) - 136 FDRs (Belgium). - 150 T1D & controls (IASP2015-16)	- Both Nluc-Ags highly correlated with RIA ( $r = 0.87/0.83$ ). - High concordance (AUC: 0.89/0.91) - LIPS AS95 comparable to best performing assays (IASP) & identified more FDRs that developed diabetes than RIA.

Table 4:1 – Main studies evaluating the performance of LIPS in detecting islet autoantibodies

¥ linking sequence: GSGGSGSGGS; RLU: relative light units; FDR: First-degree relative.

## Chapter 4 - Development of Nluc-ZnT8 LIPS for ZnT8A detection

Previously, Dr R.C. Wyatt optimised a Nluc-GAD65 LIPS assay for GADA detection (PhD, University of Bristol, 2018; *manuscript in preparation*). The developed Nluc-GAD65 LIPS assay had several methodological advantages over its RIA counterpart: 1-day versus 2-day assay, 2µl versus 4µl sample volume, cheaper, and non-radioactive with comparable performance and methodology to RIA (unpublished data). This suggests that not only may LIPS have higher sensitivity than RIAs, but the advantages of LIPS would benefit general population screening and is a feasible RIA replacement.

In the case of a LIPS assay for ZnT8A detection, there has been one report using a Gluc-ZnT8R-ZnT8W heterodimer antigen which was evaluated in 232 T1D patients and 123 controls. The performance of this LIPS assay was comparable with, but not superior to, the ZnT8Ab commercial ELISA supplied by RSR™ Limited (ZnT8R/ZnT8W Dimeric Protein® as the solid-phase) (524). Several factors could have influenced this outcome, including the specific design of the antigenic fusion construct, the use of Gluc itself, or potential conformation/denaturation alterations to ZnT8 during cell secretion or purification, which may impact the ability of ZnT8A to bind. This assay also had poor specificity (68-78%) despite requiring a high Gluc-antigen concentration of 10-15 million relative light units (RLU) for clear discrimination of positive from negative sera (524).

Whilst the RSR™ Limited ELISA usually shows high sensitivity (~70%) and high specificity (>95%) in IASP programs and has been further optimised for rapid detection (~4hrs), the ELISA requires 50µl serum/test, which is 10 times greater than RIA and therefore, there is scope for a high-performance low-volume non-radioactive assay, that ideally would have enhanced scalability and potential for automation to facilitate large-scale population screening (362).

---

### 4.1.3 Improving ZnT8A detection in plasma samples

---

Aside from serum, the next commonly used sample type for islet autoantibody detection are plasma samples derived from whole blood treated with a preservative, primarily Ethylenediaminetetraacetic acid (EDTA). In whole blood, the presence of EDTA acts as an anti-coagulant by irreversibly binding (chelating) calcium through its two amine groups with two lone electrons (526). Owing to its chelating properties, EDTA also can bind metallic ions such as zinc and magnesium. A decrease in calcium or metallic ions can induce protein conformational changes, which are problematic for immunoassays reliant on antibody-antigen interaction. The importance of protein structure integrity and, by extension, conformational epitopes appear to be crucial for ZnT8A binding, which is evident from results presented in this PhD (2.4.3) and other reports (400, 404), and is further supported by the fact that detection of ZnT8A is particularly impeded in EDTA-preserved plasma compared with other islet autoantibodies. This is evident when autoantibody positive matched serum and EDTA-preserved plasma samples from BOX participants were tested by in-house RIAs (**Table E:1; Appendix E.1**) and has also been noted in the RSR™ Limited ELISA bridge-type ZnT8Ab ELISA protocol but was not presented in the report (362).

Improving ZnT8A detection in EDTA-preserved plasma samples utilising the Nuc LIPS assay methodology would therefore expand the application of the assay to multiple sample types. This is particularly important for the flexibility of utilising historical or available samples for studies in the future. For instance, some repositories may only have collected plasma, or in cases where serum/plasma was collected, and serum volume availability is low, plasma can be used as an alternative. In matched EDTA-preserved plasma and samples from BOX, we sought to investigate reagents to improve ZnT8A detection when developing the Nluc-ZnT8 LIPS assay.

---

#### 4.1.4 Summary

---

There is a need to develop and validate a Nluc LIPS assay for ZnT8A (Nluc-ZnT8) that meets or exceeds the performance of RIA and/or commercial ELISAs utilising a larger cohort of T1D patients (>109), controls (>123), and FDRs to evaluate disease risk. Dr Vito Lampasona (Milan, Italy) has developed and provided four novel Nluc-ZnT8 fusion constructs expressed from the mammalian embryonic kidney HEK293 cell line that provided the opportunity in this project to optimise and validate a Nluc-ZnT8 LIPS assay utilising the NanoGlo® (Promega) coupled kit. The optimised methodology for the Nluc-GAD65 LIPS assay was used as a template for the development of a Nluc-ZnT8 LIPS assay.

We, therefore, sought to develop a LIPS assay that would improve many aspects of the in-house monomeric ZnT8A RIAs; non-radioactive, cheaper, 2-day to 1-day duration, <10µl sample volume required, ZnT8RA/ZnT8WA simultaneous detection, increased sensitivity, and in the future, enhanced capacity for multiplexing and high-throughput screening with scalability for the potential for robotic automation with the ultimate goal of affordably screening large populations.

### 4.1.5 Hypothesis

---

The sensitivity and specificity of ZnT8A detection can be improved using novel Nluc-tagged ZnT8 antigen constructs in a LIPS assay format.

---

### 4.1.6 Aims

---

1. To investigate and compare novel Nluc-tagged ZnT8 antigen constructs, then utilising the best performing construct, optimise a Nluc LIPS assay for the measurement of ZnT8A (Nluc-ZnT8) using the NanoGlo® luciferase kit (Promega, Madison WI, USA).
2. Investigate reagents to improve ZnT8A detection in EDTA-preserved plasma samples using the Nluc-ZnT8 LIPS method.
3. Establish a serum positivity threshold for the optimised Nluc-ZnT8 LIPS method.
4. Evaluate the sensitivity and specificity of the optimised Nluc-ZnT8 LIPS assay using new-onset T1D patients from BOX, healthy schoolchildren, and blinded samples from the IASP2020 workshop.
5. Evaluate the predictive utility of the optimised Nluc-ZnT8 LIPS assay compared with RIAs using serum samples from patients and FDRs participating in the BOX study.

---

## 4.2 Materials & Methods

---

---

### 4.2.1 Optimisation populations

---

#### 4.2.1.1 Main optimisation sample set

---

For optimisation of Nluc-ZnT8 LIPS, known RIA ZnT8RA/ZnT8WA positive and negative samples from patients and controls, covering a range of ZnT8A titres, were required to assess assay background and ZnT8A binding across the dynamic range of the assay. The populations used for optimisation came from a range of studies: Southwest of England New-Diagnosed Collection (SWENDIC), BOX, and anonymised samples. Samples were predominantly selected for large sample volume availability (>1ml) and, where possible, encompassed all ZnT8A specificities. A mixture of these samples was run in all optimisation experiments alongside internal ZnT8RA/ZnT8WA RIA standards (at least 1 of 8 serial dilutions of a pool of high ZnT8RA/ZnT8WA positive T1D patient sera) and controls (n=6; 5 positive from T1D patients and 1 negative) (**Table 4:2**). The populations are described in detail in **4.2.1.1.1-4.2.1.1.4**.

Sample (n)	Study (n)	Gender n (%)	Median age at sample (range)	ZnT8RA median AU (range)	ZnT8WA median AU (range)	GADA median units/ml (range)	IA-2A median units/ml (range)
<b>Patients</b>	SWENDIC (7) Δ	M: 4 (57.1) F: 3 (42.9)	24.0 (17.0-33.0)	57.2 (4.4-80.2)	50.2 (4.5-84.3)	163.9 (4.6-607.3) ¥	1200.8 (2.3-2758.1) ¥
	Anonymised (5)	-	-	3.2 (0.3-50.7)	0.3 (0.2-61.5)	496.8 (268.5-1133.1) §	229.6 (0.0-406.5)
<b>Healthy Controls</b>	BOX (4)	M: 2 (50.0) F: 2 (50.0)	43.8 (20.0-60.6)	0.6 (0.4-1.3)	0.6 (0.3-1.5)	0.2 (0.0-3.4) §	1.3 (0.0-2.8) §
	Blood donors (13)	M: 2 (15.4) F: 11 (84.6)	42.1 (28.4-61.1)	0.26 (0.13-0.8)	0.4 (0.2-0.7)	0.0 (0.0-88.0) ***§	0.0 (0.0-3.6) ***§
	Anonymised (4)	Not known	Not known	0.3 (0.2-0.3)	0.5 (0.4-0.5)	0.0 (0.0-0.0) §	0.0 (0.0-0.0) §
<b>Internal Controls</b>	High (2)*			130.0 (74.2-262.1)	90.8 (48.1-132.6)		
	Medium (1)			33.9 (20.1-47.0)	23.2 (12.2-39.2)		
	Low (2)*			6.8 (3.5-10.6)	2.8 (1.9-4.6)		
	Negative			0.6 (0.3-1.6)	0.5 (0.2-1.6)		

**Table 4:2 – Main optimisation sample set for Nluc-ZnT8 LIPS**

Serum from patients with T1D was selected from SWENDIC and fully anonymised cohorts based on high sample volume and positivity for ZnT8RA and/or ZnT8WA by monomeric RIAs. Healthy controls who had not developed diabetes at the time of sampling were selected based on high sample volume from BOX (n=4; 2 of these individuals showed some low-level IA-2A positivity) and healthy blood donors (n=13). Δ Samples taken a median of 31 days from diagnosis (range 14-89). Internal controls used for ZnT8R and ZnT8W RIAs comprise pooled patient sera diluted in autoantibody negative human serum; \*High and low internal controls are ZnT8RA- or ZnT8WA- specific, whereas the medium is positive for both ZnT8RA and ZnT8WA and is non-specific. \*\* 1 positive for GADA only. \*\*\* 1 positive for IA-2A only. ¥ indicates WHO units/ml from historical GADA/IA-2A RIAs. § indicates DK units/ml from current GADA/IA-2A RIAs.

#### **4.2.1.1.1 The SWENDIC study**

The SWENDIC study is comprised of newly diagnosed T1D patients that were recruited from 14 centres in South-West England. Serum samples were taken <1 year from diagnosis [median duration 26 days (range 5-322)] from 106 patients [median age 15 years (range 17-41)] and were previously tested for ZnT8RA and ZnT8WA to help develop the monomeric RIAs in 2011. These sera were already found to be positive for GADA and IA-2A by well-validated local RIAs at this time. Seven high-volume (>1ml) ZnT8RA/ZnT8WA positive patients were selected for the main optimisation sample set encompassing different ZnT8A specificities and levels.

#### **4.2.1.1.2 The Bart's-Oxford (BOX) study**

The BOX study is described in 1.8. Four ZnT8A negative FDRs that had not progressed to diabetes within 10 years of follow-up with large serum bleeds (>10ml) available were randomly selected as healthy controls.

#### **4.2.1.1.3 Healthy control blood donors**

Serum from a cohort of 526 anonymised healthy blood donors [277 (52.7%) male; median age at sample 42.9 years (range 17.2-69.2)] collected in 1998 from the UK Blood Donor Service (Bristol/Avonmouth, UK) with data for all major islet autoantibodies was available (**Table 4:2**). These individuals were anonymised, and therefore, it is not known whether individuals later progressed to diabetes. A random selection of 13 healthy blood donors was selected based on higher serum volume availability (>1ml) for select optimisation experiments.

#### **4.2.1.1.4 Anonymised samples**

A selection of RIA ZnT8RA and/or ZnT8WA positive T1D patients (n=5; 3 were diagnosed between 18.0-40.0 years) were available and were likely taken close to diagnosis. A random selection of 4 healthy controls (autoantibody negative) was also available.

### 4.2.1.2 IASP workshop optimisation sample sets

#### 4.2.1.2.1 A subset of samples from IASP2016

To investigate the incubation lengths [2.5 hours versus overnight (O/N; 20-21 hours) of Nluc-R+W-ZnT8 heterodimer and dual heterodimer constructs, a subset of 19 ZnT8A positive samples from IASP2016 were selected to increase sample size; 16 new-onset T1D patients, 1 healthy control (found incorrectly positive by RIA previously), and 2 dilutions from a positive pool of T1D patient serum. As this experiment could potentially take the LIPS assay from a one-day to a two-day assay like the RIAs, a bigger sample set would give greater confidence in the experimental outcome.

The 19 ZnT8A positive samples were selected based on serum availability and, where possible, a range of different ZnT8A specificities and levels determined by the monomeric ZnT8RA/ZnT8WA RIAs (**Table 4:3**).

IASP2016 Specimen Type	ZnT8A Specificity					
	ZnT8RA-specific		ZnT8WA-specific		ZnT8RA-ZnT8WA non-specific	
	ZnT8RA median AU (range)	ZnT8WA median AU (range)	ZnT8RA median AU (range)	ZnT8WA median AU (range)	ZnT8RA median AU (range)	ZnT8WA median AU (range)
<b>New-Onset T1D (n=16)</b>	4.2 (2.8-9.3) n=5	0.5 (0.2-1.5) n=5	0.4 (0.3-0.6) n=2	9.2 (9.1-9.3) n=2	13.7 (3.8-149.4) n=9	5.6 (2.7-14.1) n=9
<b>Negative Controls (n=1)</b>	-	-	-	-	4.94 - n=1	4.41 - n=1
<b>Dilutions from a positive pool of patient serum (n=2)</b>	3.1 - n=1	1.5 - n=1	-	-	10.6 - n=1	4.8 - n=1

*Table 4:3 – IASP2016 optimisation sample set*

These IASP2016 workshop samples were selected based on serum volume availability and, where possible, a range of different ZnT8A levels and specificities determined by the monomeric ZnT8RA and ZnT8WA RIAs. This sample set was used to increase the sample size when optimising the length of Nluc-R+W-ZnT8 (heterodimer and dual heterodimer) incubation length [2.5 hours or overnight (O/N; 20-21 hours)] (**4.3.1.3**).

#### **4.2.1.2.2 All samples from IASP2018**

The Nluc-ZnT8 LIPS assay, prior to full optimisation, was entered into the IASP2018 workshop to assess assay performance (sensitivity and specificity) and laboratory concordance with other ZnT8A detecting methods. The 2018 workshop comprised 150 serum samples: 43 new-onset T1D patients, 7 mAutoab+ve, and 90 negative controls. The samples were blinded at the time of testing and independently analysed by the IASP committee.

---

#### **4.2.2 Matched serum & EDTA-preserved plasma population**

---

A cohort of fully anonymised matched serum and EDTA-preserved plasma samples (n=27) was available from a historical collection and were selected for investigating reagents to improve ZnT8A detection in the presence of EDTA. Only the autoantibody status of these samples was known.

To investigate reagents to improve ZnT8A binding in the presence of EDTA in the LIPS assay, 19/27 anonymised matched serum, and EDTA-preserved plasma samples were used. Of the 19 selected, 7 (36.8%) were mAutoab+ve, 4 (21.1%) were sAutoab+ve, and 8 (41.5%) were autoantibody negative considering GADA, IA-2A, IAA, and ZnT8RA/ZnT8WA by RIA. Serum samples from the main optimisation sample set were also treated with EDTA and included in these experiments for additional assessment.

### 4.2.3 Positivity threshold population

Autoantibody positivity thresholds in a population of 523 anonymised healthy schoolchildren [279 (53.4%) male; median age 11.3 years (range 9.0-13.8); 464 (88.7%) of Caucasian ethnicity] recruited from schools in Oxford and Windsor (1989-1991) were set at the 97.5<sup>th</sup> percentile for ZnT8RA and ZnT8WA monomeric RIAs at 1.8AU (354, 527). Samples with sufficient volume were used to establish the Nluc-ZnT8 LIPS positivity threshold once optimised (n=521/523 (99.6%), which included all 17 ZnT8A positive schoolchildren; 6 ZnT8RA-specific, 3 ZnT8WA-specific, and 8 ZnT8A non-specific responses) (**Figure 4:2**).

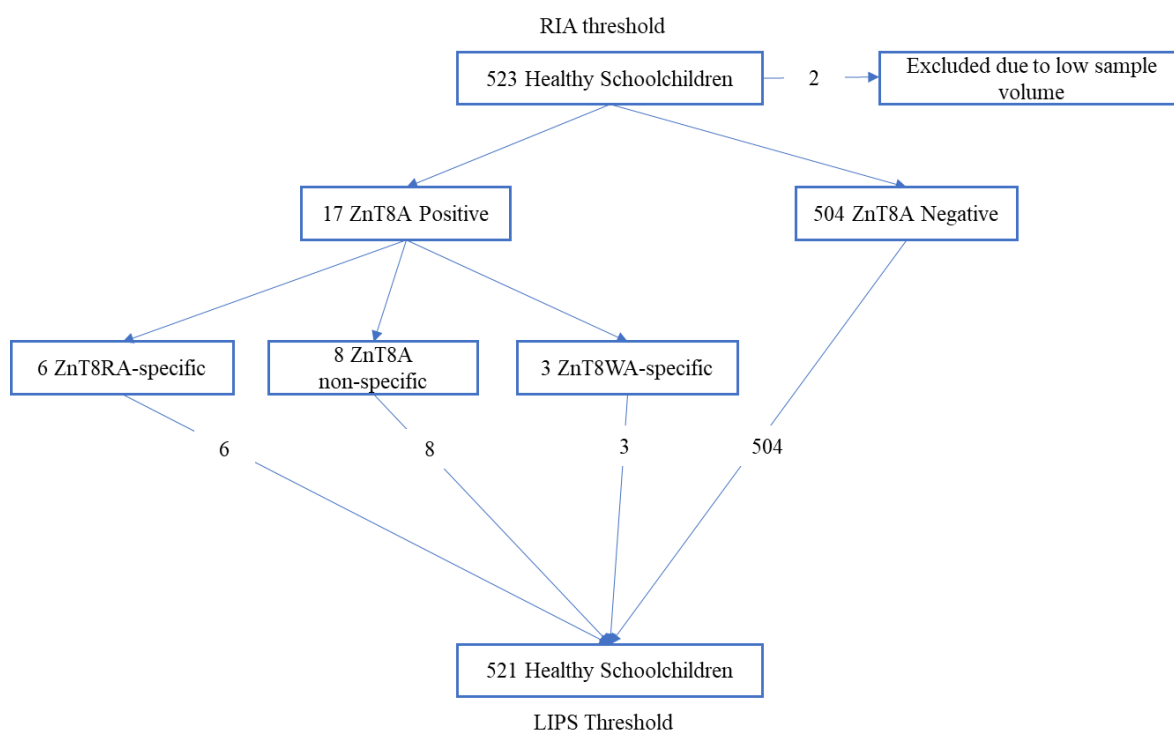


**Figure 4:2 – Nluc-ZnT8 LIPS Validation: Positive threshold population**

Positivity thresholds at the 97.5<sup>th</sup> and 99<sup>th</sup> percentiles were compared with RIA for Nluc: Furimazine incubation lengths of 5 seconds and 15 minutes (summarised in **Table 4:11; 4.3.4**). Following analysis, the 97.5<sup>th</sup> percentile (0.22AU) was used as a threshold to assess the performance (sensitivity and specificity) and validate the optimised Nluc-ZnT8 LIPS assay using samples from BOX.

---

## 4.2.4 Validation populations

---

### 4.2.4.1 IASP2020 sample set

---

The optimised Nluc-ZnT8 LIPS assay was entered into IASP2020 to evaluate the sensitivity and specificity of the method. The IASP2020 workshop comprised 150 serum samples: 38 new-onset T1D patients, 12 mAutoab+ve, and 90 negative controls. The samples were blinded at the time of testing.

For comparison of assays in-house, a ZnT8-R+W heterodimer RIA was entered into this workshop to compare the RIA method using a ZnT8 heterodimeric antigen with the Nluc-R+W-ZnT8 dual heterodimer LIPS (all constructs supplied by V. Lampasona, Milan, Italy). At the time of the workshop (January 2020), both the ZnT8-R+W heterodimer RIA and Nluc-R+W-ZnT8 dual heterodimer LIPS assays had preliminary thresholds set at the 97.5<sup>th</sup> percentile (n=150/521 healthy schoolchildren) of 0.5AU and 0.4AU, respectively.

### 4.2.4.2 BOX

---

To further investigate the sensitivity and specificity and the predictive value of the optimised Nluc-ZnT8 LIPS assay, serum samples from participants of the BOX study were selected. Samples were selected based on available RIA ZnT8RA and ZnT8WA data to compare between assays directly. Samples from new-onset T1D patients in BOX were tested for ZnT8RA/ZnT8WA by RIA 2011-2012 after the monomeric RIAs had been optimised in Bristol. However, ZnT8RA/ZnT8WA data in FDRs have predominantly been tested in individuals already positive for at least one autoantibody (GADA, IA-2A, IAA, and/or ICA). The cohort description of selected new-onset T1D and FDRs used for Nluc-ZnT8 LIPS validation is summarised in **Table 4:4**.

#### 4.2.4.2.1 New-onset T1D patients

Sera with sufficient sample volume from 573 new-onset T1D patients sampled within 3 months of diagnosis [318 male (55.5%); median age at onset 11.3 years (range 1.0-54.9)] were randomly selected from 741 new-onset T1D patients with available ZnT8RA/ZnT8WA RIA data. The 573 patients were largely comprised of ZnT8RA/ZnT8WA positives, but a selection of ZnT8RA/ZnT8WA negatives was included to evaluate whether the Nluc-ZnT8 LIPS assay would have a higher sensitivity than the monomeric ZnT8R/ZnT8W RIAs [n positive=388 (67.7%); n negative=185 (32.3%)] (**Figure 4:3**).

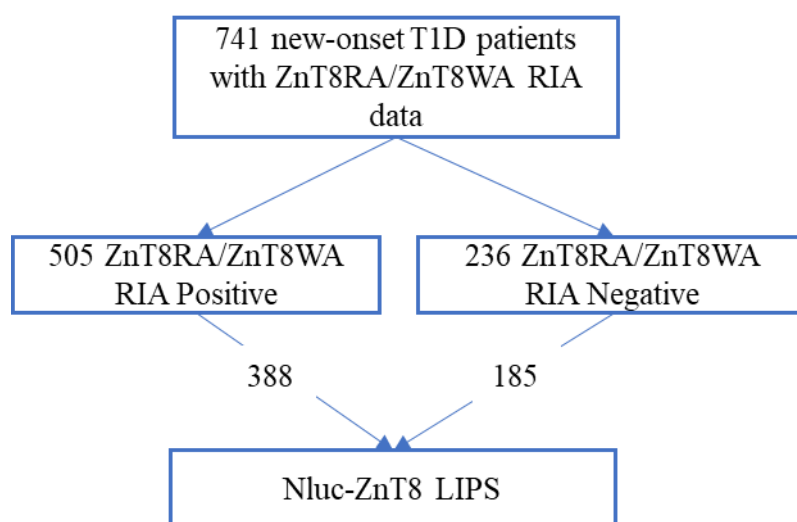


*Figure 4:3 – Nluc-ZnT8 LIPS Validation: New-onset T1D patients*

#### 4.2.4.2.2 ZnT8A positive first-degree relatives

Sera with sufficient sample volume from 48 [25 male (52.1%); median age at sample 13.6 years (range 1.3-65.9); median follow-up 20.0 years (range -0.1-33.7)] ZnT8A positive FDRs were randomly selected from 93 ZnT8A positive FDRs with available ZnT8RA/ZnT8WA RIA data. Of the 49 FDRs, 35 developed diabetes over follow-up [18 male (51.2%); median age at onset 16.5 years (range 3.2-59.9)] (**Figure 4:4**). A higher proportion of ZnT8A positive FDRs that developed diabetes over follow-up was selected to assess disease risk prediction of Nluc-ZnT8 LIPS above ZnT8RA/ZnT8WA RIAs combined.

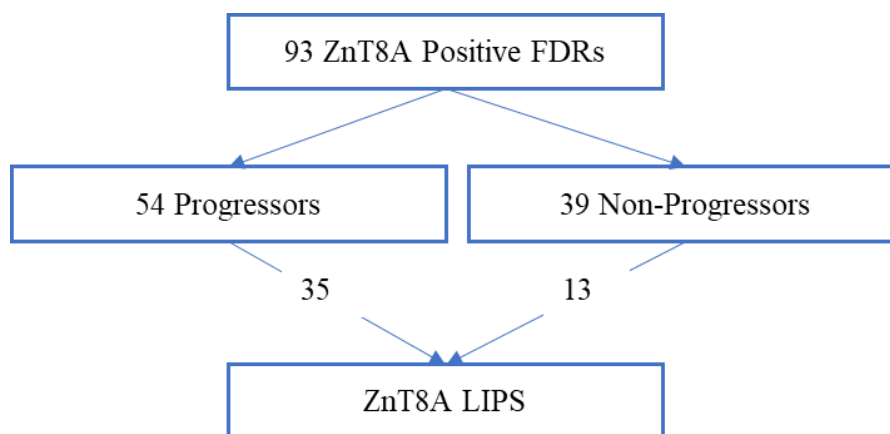


*Figure 4:4 – Nluc-ZnT8 LIPS Validation: ZnT8A positive first-degree relatives*

#### 4.2.4.2.3 ZnT8A negative relatives

Sera with sufficient sample volume from 684 [361 male (52.8%); median age at sample 15.5 years (range 0.0-66.0); median follow-up 19.6 years (range -0.7-33.9)] ZnT8A negative FDRs were randomly selected from 2,222 ZnT8A negative FDRs with available ZnT8RA/ZnT8WA RIA data. Of the 684 FDRs, 165 developed diabetes over follow-up [103 male (62.4%); median age at onset 12.7 years (range 1.0-75.2); median follow-up 21.1 years (0.3-33.2)] (**Figure 4:5**). A higher proportion of ZnT8A negative FDRs that developed diabetes over follow-up was selected to assess disease risk prediction of Nluc-ZnT8 LIPS above the monomeric ZnT8R/ZnT8W RIAs.

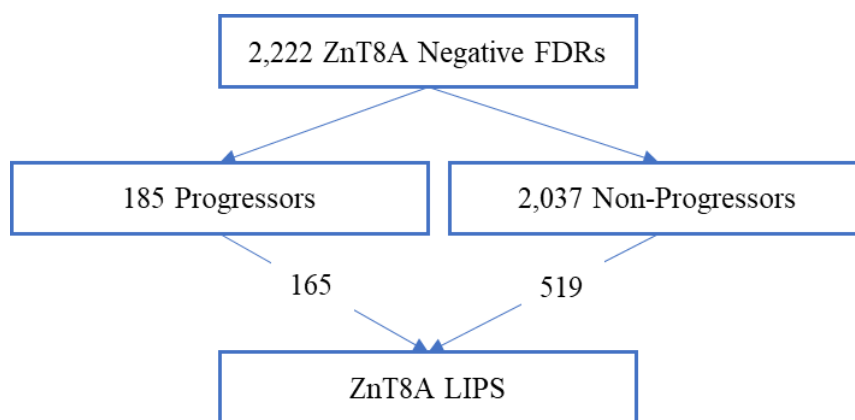


*Figure 4:5 – Nluc-ZnT8 LIPS Validation: ZnT8A negative first-degree relatives*

Chapter 4 - Development of Nluc-ZnT8 LIPS for ZnT8A detection

	New-onset T1D patients n=573		ZnT8A positive FDRs n=49		ZnT8A negative FDRs n=684	
	ZnT8A positive n=388	ZnT8A negative n=185	Progressors n=35	Non-progressors n=13	Progressors n=165	Non-progressors n=519
Male/female (% male)	222/166 (57.2)	98/87 (53.0)	18/17 (51.4)	7/6 (53.9)	103/62 (62.4)	258/261 (49.7)
Median age at onset (years; range)	11.2 (1.3-20.8)	11.7 (1.0-54.9)	16.5 (3.2-59.9)	-	12.7 (1.0-75.2)	-
Median age at sample (years; range)	11.2 (1.3-20.8)	11.7 (1.1-54.7)	14.4 (1.6-44.4)	11.4 (1.3-60.0)	14.1 (1.1-64.1)	15.0 (0.0-66.0)
Median diabetes duration or follow-up (years; range)	0.0 (-0.2-0.1)	0.0 (-0.2-0.2)	19.7 (0.4-32.3)	21.1 (-0.1-32.3)	21.1 (0.3-33.2)	19.4 (-0.7-33.9)
ZnT8RA (%)	347 (89.4)	-	31 (88.6)	12 (92.3)	-	-
ZnT8WA (%)	291 (75.0)	-	28 (80.0)	10 (76.9)	-	-
ZnT8RA/ZnT8WA (%)	388 (100.0)	-	35 (100.0)	13 (100.0)	-	-
ZnT8RA-specific (%)	97 (25.0)	-	7 (20.0)	3 (23.1)	-	-
ZnT8WA-specific (%)	41 (10.6)	-	4 (11.4)	1 (7.7)	-	-
ZnT8A non-specific (%)	250 (64.4)	-	24 (68.6)	9 (69.2)	-	-
Single autoantibody positive ± ICA* (%)	8 (2.1)	53 (28.6)	3 (8.6)	1 (7.7)	36 (21.8)	192 (37.0)
Positive for multiple (≥2) autoantibodies	380 (97.9)	114 (61.6)	32 (91.4)	12 (92.3)	17 (10.3)	13 (2.5)
GADA (%)	325 (83.8)	144 (77.8)	31 (88.6)	12 (92.3)	40 (24.2)	130 (25.0)
IA-2A (%)	324 (83.5)	106 (57.3)	23 (65.7)	9 (69.2)	9 (5.5)	20 (3.9)
IAA/n* (%)	176/234 (75.2)	71/121 (58.7)	22/35 (62.9)	6/9 (66.7)	26/117 (22.2)	69/447 (15.4)
ICA**/n with data (%)	156/215 (72.6)	51/123 (41.5)	18/25 (72.0)	4/9 (44.4)	6/123 (4.9)	57/472 (12.1)
Biochemical autoantibody negative ± ICA* (%)	-	18 (9.7)	-	-	112 (67.9)	314 (60.5)

**Table 4:4 – Nluc-ZnT8 LIPS Validation: BOX evaluation population**

\* IAA data only considered if the sample was taken before onset or within 2 weeks of diagnosis before exogenous insulin treatment. \*\* Islet Cell antibody (ICA) considered positive >20 juvenile diabetes foundation (JDF) used as positivity threshold in the European Nicotinamide Intervention Trial (ENDIT) (299); ICA positivity with 1 other biochemical autoantibody (GADA, IA-2A, IAA, or ZnT8A) has a comparable risk of T1D to single biochemical autoantibody positives.

### 4.2.5 Optimised Nluc-GAD65 LIPS assay method

The methodology of the Nluc-GAD65 LIPS assay (developed by Dr R.C. Wyatt) was used as a template for developing the Nluc-ZnT8 LIPS assay (**Table 4:5**).

Step of Assay	Nluc-GAD65 LIPS Method
<b>Assay Buffers</b>	<ul style="list-style-type: none"> <li>• Tris buffered saline with 0.5% (v/v) Tween-20 (TBST-0.5%).</li> <li>• Reagent for Luminescence Detection (RLD) - Furimazine substrate diluted 1:50 in NanoGlo® LIPS Assay Buffer supplied in the NanoGlo® coupled kit (Promega).</li> </ul>
<b>Expression of Nluc-tagged GAD65 Antigen</b>	<ul style="list-style-type: none"> <li>• 1 microgram of Nluc-GAD65 antigen in a pCMVTNT vector was incubated for 1.5 hours at 30°C with reagents from the SP6 <i>in vitro</i> transcription/translation coupled kit (Promega); 40µl reticulocyte master mix &amp; 2µl 1mM methionine.</li> <li>• After incubation, the Nluc-GAD65 antigen is purified using a NAP5™ desalting column (GE Healthcare) &amp; TBST-0.5% containing 0.1% BSA (v/v).</li> <li>• Luminescence activity (light units, LU) was detected by a LB 960 microplate luminometer Centro XS3 (Berthold Technologies, GmbH &amp; Co. KG, Bad Wildbad, Germany) using 2µl of the reaction mix &amp; 40 µl of RLD. 10µl aliquots are stored at -70°C &amp; freeze-thaw cycles are limited.</li> </ul>
<b>Serum sample</b>	<ul style="list-style-type: none"> <li>• 1µl of serum plated in duplicate into a 96-deep well plate.</li> </ul>
<b>Nuc-tagged GAD65 antigen preparation for LIPS</b>	<ul style="list-style-type: none"> <li>• Nluc-GAD65 antigen is diluted in TBST-0.5% to achieve <math>3.8-4.2 \times 10^6</math> LU in a 25µl volume.</li> <li>• Serum samples are incubated with diluted Nluc-GAD65 antigen for 2.5 hours at RT.</li> </ul>
<b>Precipitating immunocomplexes</b>	<ul style="list-style-type: none"> <li>• 6.25µl/well of PAS (25% suspension washed &amp; resuspended with TBST-0.5% in a 50µl volume) is added &amp; incubated with serum samples for 1 hour at 4°C on a shaking platform (~700rpm).</li> <li>• After incubation, excess antigen is excluded by 5 washes with TBST-0.5%, then transferred into a 96-well OptiPlate™ (Perkin Elmer) &amp; aspirated to remove excess buffer.</li> </ul>
<b>Detecting luminescence</b>	<ul style="list-style-type: none"> <li>• 40µl of RLD was injected, mixed for 5 seconds/well &amp; read for relative LU at 2 seconds/well using the LB 960 microplate luminometer Centro XS3 (Berthold Technologies).</li> <li>• Arbitrary units (AU) were calculated using a logarithmic standard curve.</li> </ul>

Table 4:5 – Summary of the optimised Nluc-GAD65 LIPS assay for GADA detection

## 4.2.6 Nluc-tagged ZnT8 antigen constructs

There were two Nluc-tagged ZnT8 antigen constructs kindly supplied by Dr Vito Lampasona (Milan, Italy) that differed by the position of Nluc, the number of monomeric C-terminal (aa268-369) ZnT8 sequences, and type of Nluc in the pCMVTnT vector: non-secretory Nluc or secretory Nluc (sNluc) produced by the kidney HEK293 cell line (**Figure 4:6**).

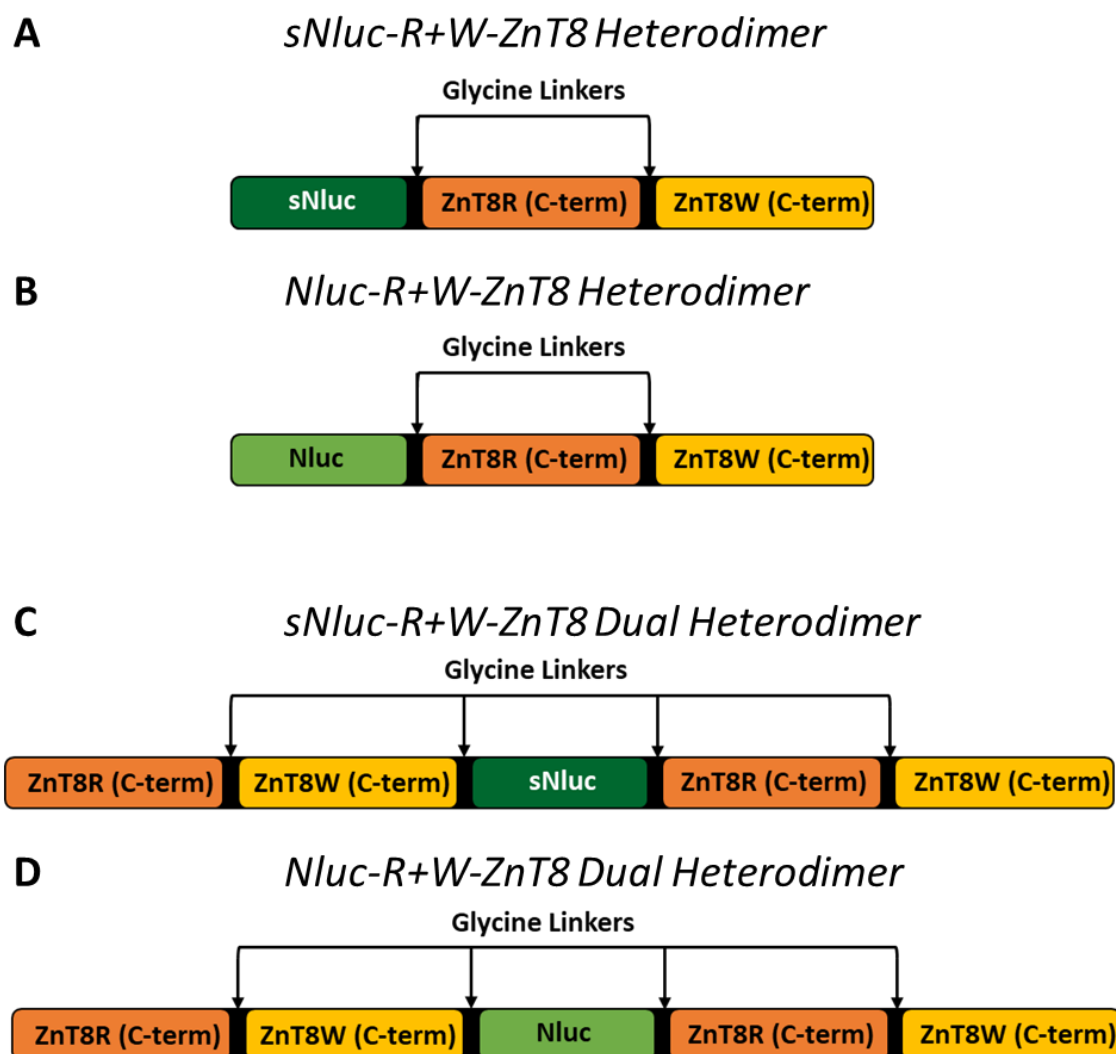


*Figure 4:6 – sNluc- & Nluc-tagged ZnT8 antigen constructs*

The first luciferase-tagged antigen construct was a single *Nano* luciferase (Nluc)- or secretory Nluc (sNluc)-tagged R+W-ZnT8 heterodimer comprised of two single C-terminal (aa268-369) ZnT8 monomers encoding 325R (ZnT8R) and 325W (ZnT8W) sequences with the luciferase reporter placed at the N-terminus (A/B, respectively). The second was a Nluc- or sNluc- tagged R+W-ZnT8 Dual heterodimer comprised of four C-terminal (aa268-369) ZnT8 monomers encoding two ZnT8R and two ZnT8W sequences with the Nluc placed in the middle of the construct (C/D, respectively). All constructs are encoded into a pCMVTnT vector. This construct schematic was adapted from materials supplied by Dr Vito Lampasona (Milan, Italy).

### 4.2.7 Nluc-ZnT8 LIPS optimisation experiments for ZnT8A detection

To develop a Nluc-ZnT8 LIPS method with high sensitivity and specificity, several assay conditions were investigated using samples from the optimisation populations (**Table 4:6**).

<b>Portion of Assay</b>	<b>Condition Assessed</b>
<b>Expression of Nluc-tagged ZnT8 antigen</b>	<ul style="list-style-type: none"> <li>• Nluc-or sNluc-tagged ZnT8 antigen.</li> <li>• Nluc-R+W-ZnT8 heterodimer or Nluc-R+W-ZnT8 heterodimer antigen.</li> <li>• Buffer &amp; method used to purify Nluc-ZnT8 antigen.</li> <li>• Freeze-thawing Nluc-ZnT8 antigen</li> </ul>
<b>Nluc-tagged ZnT8 antigen preparation for LIPS</b>	<ul style="list-style-type: none"> <li>• Concentration of dilute Nluc-ZnT8 antigen.</li> <li>• Concentration of Tween-20 in TBST during incubation of Nluc-ZnT8 antigen with sample.</li> <li>• Antigen incubation length of Nluc-ZnT8 antigen with sample.</li> </ul>
<b>Precipitating immunocomplexes</b>	<ul style="list-style-type: none"> <li>• Unblocked Protein A Sepharose (PAS) or glycine-blocked PAS (GB-PGS).</li> <li>• Concentration of Tween-20 in TBST during removal of excess Nluc-ZnT8 antigen.</li> </ul>
<b>Detecting luminescence</b>	<ul style="list-style-type: none"> <li>• The concentration of the substrate in RLD (Promega)</li> <li>• Length of substrate incubation prior to LU detection.</li> </ul>

*Table 4:6 – Summary of the Nluc-ZnT8 LIPS optimisation experiments*

---

## 4.2.8 Optimised Nluc-ZnT8 LIPS assay method

---

After optimisation (presented in **4.3.1.1-4.3.1.7**), the finalised assay methodology is detailed (below) with a summary of the adaptations made for Nluc-ZnT8 LIPS compared to the optimised Nluc-GAD65 LIPS method (presented in **Table 4:10**).

### 4.2.8.1 Assay buffers

---

Phosphate buffered saline with Tween-20 (PBST) – One 5g tablet of GIBCO™ PBS dissolved in 500ml ddH<sub>2</sub>O (10mmol/l Phosphate, 2.68mmol/l Potassium Phosphate, and 150mmol/l NaCl), pH 7.45 with 0.1% v/v Tween-20.

Tris buffered saline with Tween-20 (TBST-0.15%) – 50mM Tris, 150mmol/L NaCl, pH 7.3-7.4 with 0.15% v/v Tween-20.

Tris buffered saline with Tween-20 (TBST-0.5%) – 50mM Tris, 150mmol/L NaCl, pH 7.3-7.4 with 0.5% v/v Tween-20.

TBST-0.15% with 0.1% (w/v) bovine serum albumin (TBST-BSA).

Reagent for Luminescence Detection (RLD) – Furimazine substrate diluted 1:50 in NanoGlo® LIPS Assay Buffer (NanoGlo® Luciferase Assay System, Promega).

Assay Reagent (AR) – RLD diluted to 1:150 with TBST-0.15%.

### 4.2.8.2 Expression of Nluc-ZnT8 antigen

---

One microgram of recombinant Nluc-R+W-ZnT8 dual heterodimer antigen encoded into a pCMVTnT vector (kindly supplied by Dr Vito Lampasona, Milan, Italy; the construct with the most promising ZnT8A binding) was incubated with 40µl of the SP6 master mix (Promega) and 1-4µl of 1mM methionine (dependent on plasmid concentration; nuclease free water (Promega) was used to make up a final 50µl reaction mixture) for 2 hours at 30°C.

## Chapter 4 - Development of Nluc-ZnT8 LIPS for ZnT8A detection

At RT, the 50µl volume of neat reaction mix is diluted with 250µl PBST (dilution factor 0.16), gently mixed by inverting, and a 25µl aliquot is added to a well of a 96-well OptiPlate™ (Perkin Elmer). The diluted reaction mix is then serially diluted; 1:250 (2µl + 498µl PBST), 1:2,500 (10µl of 1:250 + 90µl PBST), and 1:25,000 (10µl 2,500 + 90µl PBST). All serial dilutions were mixed by gentle inverting and 25µl in duplicate was taken and added to 6 additional wells of a 96-well OptiPlate™ (Promega).

To detect luminescence activity, 40µl of RLD (Furimazine diluted 1:50 with NanoGlo® LIPS Assay buffer, Promega) is added to each well and the 96-well plate is loaded into a Bertold Centro XS3 luminometer (Bertold Technologies GmbH and Co. KG, Bad Wildbad, Germany). The luminescence activity by the Bertold is expressed as light unit equivalents (LU) in a program set to read each well for 2 seconds. After the multiplication of the LU by the dilution factor of the serial dilutions between  $3 \times 10^8$  and  $7 \times 10^8$  LU is typically obtained whilst the 2µl of neat reaction mix reaches the maximum detection limit at  $2 \times 10^9$ . The initial dilution of the neat reaction mix is then aliquoted into 10µl aliquots and stored at  $-70^\circ\text{C}$ . Whilst the luciferase-tagged ZnT8 construct remains stable for more than 6 months at  $-70^\circ\text{C}$ , each 10µl aliquot is thawed once prior to use in an assay as freeze-thawing the antigen reduced ZnT8A detection (see results presented in **4.3.1.5.2**).

### **4.2.8.3 Preparation of Nluc-ZnT8 antigen**

---

A 10µl aliquot of diluted reaction mix of Nluc-R+W-ZnT8 dual heterodimer antigen is thawed at RT, diluted 1:100 in TBST-0.5% buffer, and slowly filtered through a 0.45µM filter unit (Sigma) using a 1ml syringe (ThermoFisher). The filtered Nluc-R+W-ZnT8 dual heterodimer antigen is diluted to 4M ( $\pm 0.2 \times 10^6$ ) in TBST-0.15% in a 25µl volume with the addition of 40µl of RLD.

#### **4.2.8.4 Optimised Nluc-ZnT8 LIPS assay methodology**

---

1µl of serum was plated in duplicate into a 96-deep well plate (Sarstedt) and incubated with 4M ( $\pm 0.2 \times 10^6$ ) LU of filtered and diluted Nluc-R+W-ZnT8 dual heterodimer antigen in TBST-0.15%, for 2.5 hours at RT. Immunocomplexes were precipitated using a 25% PAS suspension (GE Healthcare; 6.25µl/well) in a 1-hour incubation on an orbital shaking platform (700rpm) at 4°C. Excess unbound Nluc-R+W-ZnT8 dual heterodimer antigen was excluded by centrifugation (1500rpm at 4°C for 3mins) and five serial washes in TBST-0.5%. Samples were transferred from 96-deep well plates to 96-well OptiPlates™ (Perkin Elmer) by multichannel pipetting. Plates were then centrifuged (1500 at 4°C for 3mins) and aspirated for a total end volume of 30µl. Fresh AR is made (1:50 Furimazine substrate diluted in NanoGlo® LIPS Assay Buffer further diluted 1:3 with TBST-0.15%) and injected into each well in a 40µl volume immediately prior to LU determination using the Bertold Centro XS3 luminometer and a standardised detection protocol; inject 40µl AR, shake 5 secs/well, detect LU 2 secs/well (**Figure 4:7**).

A local logarithmic standard curve developed for the monomeric ZnT8R/ZnT8W RIAs was used to determine and express ZnT8A binding (proportional to LU output) as arbitrary units (AU). Internal RIA QC serum samples of known ZnT8A levels and specificity including autoantibody negatives were run on all plates to ensure assay reproducibility and performance are maintained. The positivity threshold was set at the 97.5th percentile of 521 healthy schoolchildren [median age 11.3 years (range 9-13.8)] (354); 0.22AU. The AS95 was 78% assessed by the IASP2020 workshop using the 97.5<sup>th</sup> percentile of 92 schoolchildren tested at the time of the workshop (0.4AU).

Total Assay Length ~8 hours.

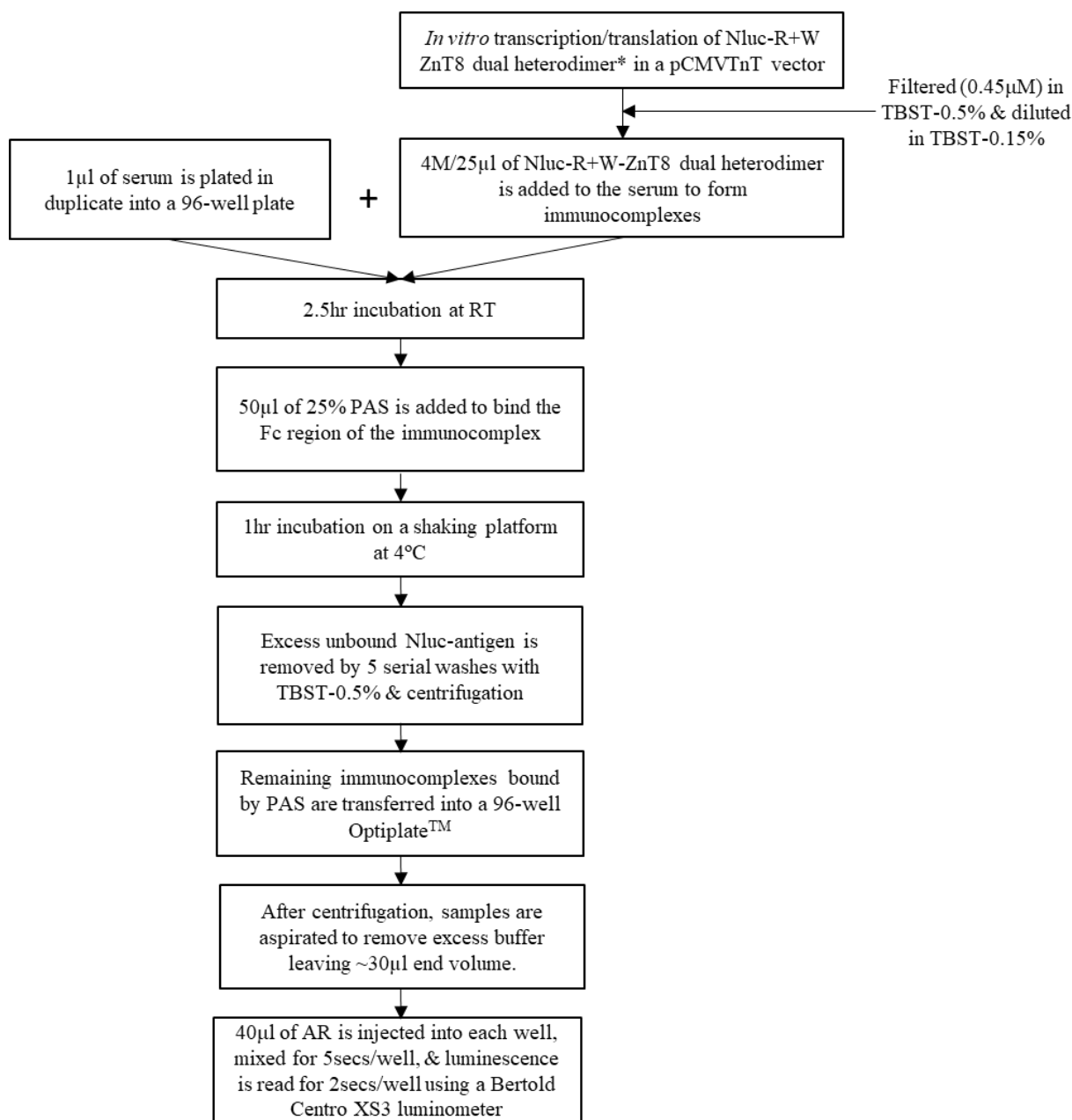


**Figure 4:7 – Basic methodology of the optimised Nluc-ZnT8 LIPS assay**

\* Recombinant NanoLuc(Nluc)-R+W-ZnT8 dual heterodimer is synthesised in-house using a TnT SP6 Quick Coupled Transcription/Translation Reticulocyte System (Promega) with a  $3.0-7.0 \times 10^8$  relative light units (RLU) expected range; RT: room temperature; PAS: Protein A Sepharose; TBST-0.15%: Tris buffered saline with 0.15% Tween-20. TBST-0.5%: Tris buffered saline with 0.5% Tween-20. Total assay length excludes *in vitro* transcription/translation preparation of antigen.

---

## 4.2.9 Statistical analysis

---

All statistical analysis was conducted using GraphPad PRISM (v. 9.1.0), and an alpha value  $p < 0.05$  was considered significant.

### 4.2.9.1 Optimisation of the Nluc-ZnT8 LIPS assay

---

Results from the optimisation experiments were analysed using mean LU/median LU (interquartile ranges; IQRs) or signal to noise ratios (SNR; mean LU of sample  $\div$  mean LU of negative controls) and/or AU where a full logarithmic standard curve was included. For each experiment, either LU or SNR was chosen to be presented based on the most accurate representation of the data and what led to decision making. Median LU (ZnT8A binding level) or SNR between categories was compared using paired Wilcoxon signed-rank and Spearman's rank correlation tests using the Bonferroni correction for multiple analyses where appropriate. Intra- and inter-assay variation between replicates was assessed using the coefficient of variation (CV) calculation [ $100 \times (\text{standard deviation (SD)} \div \text{mean LU})$ ] in select experiments when two or more independent assays were conducted.

### 4.2.9.2 Establishing a positive threshold for the optimised Nluc-ZnT8 LIPS assay

---

Spearman's rank ( $r$ ) correlation was used to compare AUs obtained in the optimised Nluc-ZnT8 LIPS assay with ZnT8RA/ZnT8WA RIAs (using the maximum AU between RIAs). Bland-Altman analysis was used to identify outliers outside of the 95% CI of agreement between assays.

### **4.2.9.3 Sensitivity & specificity of the optimised Nluc-ZnT8 LIPS assay**

---

Spearman's rank ( $r$ ) correlation was used to compare AUs obtained in the different substrate incubation lengths (5-seconds versus 15-minutes) in the optimised Nluc-ZnT8 LIPS assay with ZnT8RA/ZnT8WA RIAs (using the maximum AU between RIAs) using positivity thresholds set at the 97.5<sup>th</sup> and 99<sup>th</sup> percentiles of 521 healthy schoolchildren in 573 new-onset T1D patients. The sensitivity and specificity of the optimised Nluc-ZnT8 LIPS assay (using the 5-second incubation 97.5<sup>th</sup> percentile of 521 healthy schoolchildren) were assessed by receiver operator curve (ROC) analysis in 573 new-onset T1D patients and the IASP2020 sample set.

### **4.2.9.4 Comparing the predictive utility of Nluc-ZnT8 LIPS & RIA**

---

Kaplan-Meir survival curve analysis was used to predict disease risk, and the Mantel-Cox log-rank test was used to compare survival curves between categories.

---

## **4.3 Results**

---

### **4.3.1 Aim 1: Optimisation of a Nluc-ZnT8 LIPS assay for ZnT8A detection**

---

Optimisation experiments were conducted in a stepwise fashion of altering one condition (unless otherwise stated) from the optimised Nluc-GAD65 LIPS template protocol (**Table 4:7**).

Chapter 4 - Development of Nluc-ZnT8 LIPS for ZnT8A detection

Results	Condition Assessed	Expression & Purification of Ag	Ag	Ag concentration (LU/25µl) & incubation	Immuno-precipitate	Removal of excess Nluc-Ag Buffer	Substrate concentration & incubation	Conclusion
4.3.1.1	Nluc- or sNluc-tagged Ag & Ag Concentration	Nluc-Ag prepared according to Nluc-GAD65 LIPS protocol. Neat sNluc-Ag (HEK293 cell supernatant).	<b>Nluc- and sNluc- R+W ZnT8 heterodimer &amp; dual heterodimer</b>	<b>6M, 4M &amp; 2M</b> in TBST-0.5%  Incubated for 2.5hrs (RT)	6.25µl/well PAS. Washed with TBST-0.15%-BSA & incubated for 1hr (4°C)	TBST-0.5%	1:50 (Promega) & incubated 5s/well	Nluc-tagged Ag constructs at a concentration of 4M LU.
4.3.1.2	Concentration of Tween-20 in assay buffers	Nluc-Ag prepared according to Nluc-GAD65 LIPS protocol.	Nluc-R+W-ZnT8 heterodimer	4M in <b>TBST-0.15% or TBST-0.5%</b>  As above	As above. <b>Washed with TBST (0.15%)-BSA or TBST (0.5%)-BSA</b>	<b>TBST-0.15% or TBST-0.5%</b>	As above	TBST-0.15% for Nluc-Ag incubation & immunoprecipitation. TBST-0.5% for removal of excess Nluc-Ag.
4.3.1.3	Nluc-Ag Construct & Incubation Length	As above	<b>Nluc-R+W-ZnT8 heterodimer &amp; dual heterodimer</b>	4M in TBST-0.15%  <b>Incubated for 2.5hrs or 20-21hrs (RT)</b>	As above. Washed with TBST-0.15%-BSA & incubated for 1hr (4°C)	TBST-0.5%	As above	Nluc-R+W-ZnT8 dual heterodimer incubated for 2.5hrs at RT.
Appendix E.2.1	Glycine-blocked PAS (GB-PAS) immuno-precipitate	As above.	Nluc-R+W-ZnT8 dual heterodimer	4M in TBST-0.15%  Incubated for 2.5hrs (RT)	6.25µl/well <b>PAS or GB-PAS.</b> As above.	As above	As above	PAS.
4.3.1.4	<b>IASP2018 assessment</b>	As above.	As above	As above	6.25µl/well PAS. As above.	As above	As above	LIPS showed higher sensitivity than RIAs, but assay background may compromise specificity.

Chapter 4 - Development of Nluc-ZnT8 LIPS for ZnT8A detection

<b>Appendix E.2.2.1</b>	Purification of Nluc-Ag with ZnCl <sub>2</sub>	<b>Buffer with 0mM, 0.1mM, or 1mM ZnCl<sub>2</sub> (v/v)</b>	As above	As above	As above	As above	As above	Purification buffer without ZnCl <sub>2</sub> .
<b>4.3.1.5.1</b>	Preparation of Nluc-Ag by 0.45µM filtration (Milan protocol)	<b>Nluc-Ag prepared with or without column purification.</b>	As above	<b>4M neat in TBST-0.15% or 4M diluted 1:100 in TBST-0.5% &amp; filtered (0.45µM) into TBST-0.15%</b>  As above.	As above	As above	As above	No column purification with 4M diluted 1:100 in TBST-0.5% & filtered (0.45µM) into TBST-0.15%; Milan protocol
<b>Appendix E.2.2.2</b>	Quantity of 1mM methionine in Nluc-Ag expression mix	<b>Expression reaction with 2µl or 5µl 1mM methionine.</b> Nluc-Ag prepared without column purification	As above	4M of dilute (1:100 in TBST-0.5%) & 0.45µM filtered Nluc-Ag in TBST-0.15%  As above	As above	As above	As above	2-5µl can be used dependent on Nluc-Ag plasmid concentration. The quantity of methionine had very little effect.
<b>4.3.1.5.2</b>	Freeze-thawing of Nluc-Ag	Nluc-Ag expressed without column purification	As above	As above <b>Dilute Nluc-Ag freeze-thawed 1, 2, or 3 times</b>	As above	As above	As above	1 freeze-thaw.
<b>4.3.1.6.1</b>	Concentration of Substrate	As above	As above	As above with 1 freeze-thaw	As above	As above	<b>1:50 (Promega) to 1:100 or 1:150 with TBST-0.15%</b>	Substrate concentration reduced from 1:50 to 1:150 with TBST-0.15%.
<b>4.3.1.6.2</b>	Substrate Incubation Length	As above	As above	As above	As above	As above	1:150 with TBST-0.15% & incubated <b>5s/well vs 15mins/well</b>	5-second substrate incubation length.

*Table 4:7 – Nluc-ZnT8 LIPS optimisation experiments*

### 4.3.1.1 Nluc-tagged ZnT8 antigen construct & antigen concentration

---

To identify the optimal Nluc-tagged construct and concentration, the Nluc- and sNluc- ZnT8 heterodimer (Nluc-R-W-ZnT8) and dual heterodimer (R-W-Nluc-R-W-ZnT8) antigen constructs were tested at concentrations of 2M, 4M, and 6M LU using the optimised Nluc-GAD65 LIPS protocol. Samples included from the main optimisation sample set:

- 5 Internal ZnT8 RIA standards
- 6 Internal ZnT8 RIA controls (5 positive and 1 negative)
- 3 Anonymised healthy negative controls

The sNluc-R+W-ZnT8 heterodimer construct was on average  $1.7 \times 10^5$ ,  $1.9 \times 10^5$ , and  $4.8 \times 10^4$  LU higher than the Nluc-R+W-ZnT8 heterodimer across all samples at antigen concentrations of 6M, 4M, and 2M, respectively. Similarly, the sNluc-R+W-ZnT8 dual heterodimer construct was on average  $3.3 \times 10^5$ ,  $1.7 \times 10^5$ , and  $1.2 \times 10^5$  LU higher than the Nluc-R+W-ZnT8 dual heterodimer at an antigen concentration of 6M, 4M, and 2M, respectively. The median LU of internal controls was only weakly different between Nluc- and sNluc- constructs for both heterodimer and dual heterodimer configurations across all antigen concentrations ( $p < 0.05$ ).

The advantage of increased overall ZnT8A binding in the sNluc-R+W-ZnT8 constructs was counteracted by a higher assay background and lower median SNRs across all antigen concentrations; median SNR range 7.4-9.4 in sNluc-R+W-ZnT8 constructs compared with 9.1-18.2 in the Nluc-R+W-ZnT8 constructs (**Figure 4:8**). This reduced the dynamic range within the assay and, by extension, the discrimination between ZnT8A negative and positive samples. In addition to poorer assay performance, the expression yield (confirmed by Dr Lampasona) of the sNluc-R+W-ZnT8 constructs was also lower than the corresponding Nluc-R+W-ZnT8 constructs. The superior assay performance of Nluc- constructs with greater discrimination between positive and negative samples) could be related to better antigen expression *in vitro*.

Within Nluc-R+W-ZnT8 heterodimer and dual heterodimer constructs, an antigen concentration of 4M offered the greatest median SNR. The median SNR at 4M LU for Nluc-R+W-ZnT8 heterodimer was 19.3 (range 0.6-236.3) compared with 18.7 (range 0.7-232.7) and 16.41 (range 0.6-202.8) for 2M and 6M, respectively. Similarly, the median SNR at 4M for Nluc-R+W-ZnT8 dual heterodimer was 10.9 (range 0.6-120.7) compared with 7.3 (range 0.67-99.6) and 9.0 (range 0.6-102.7) for 2M and 6M, respectively.

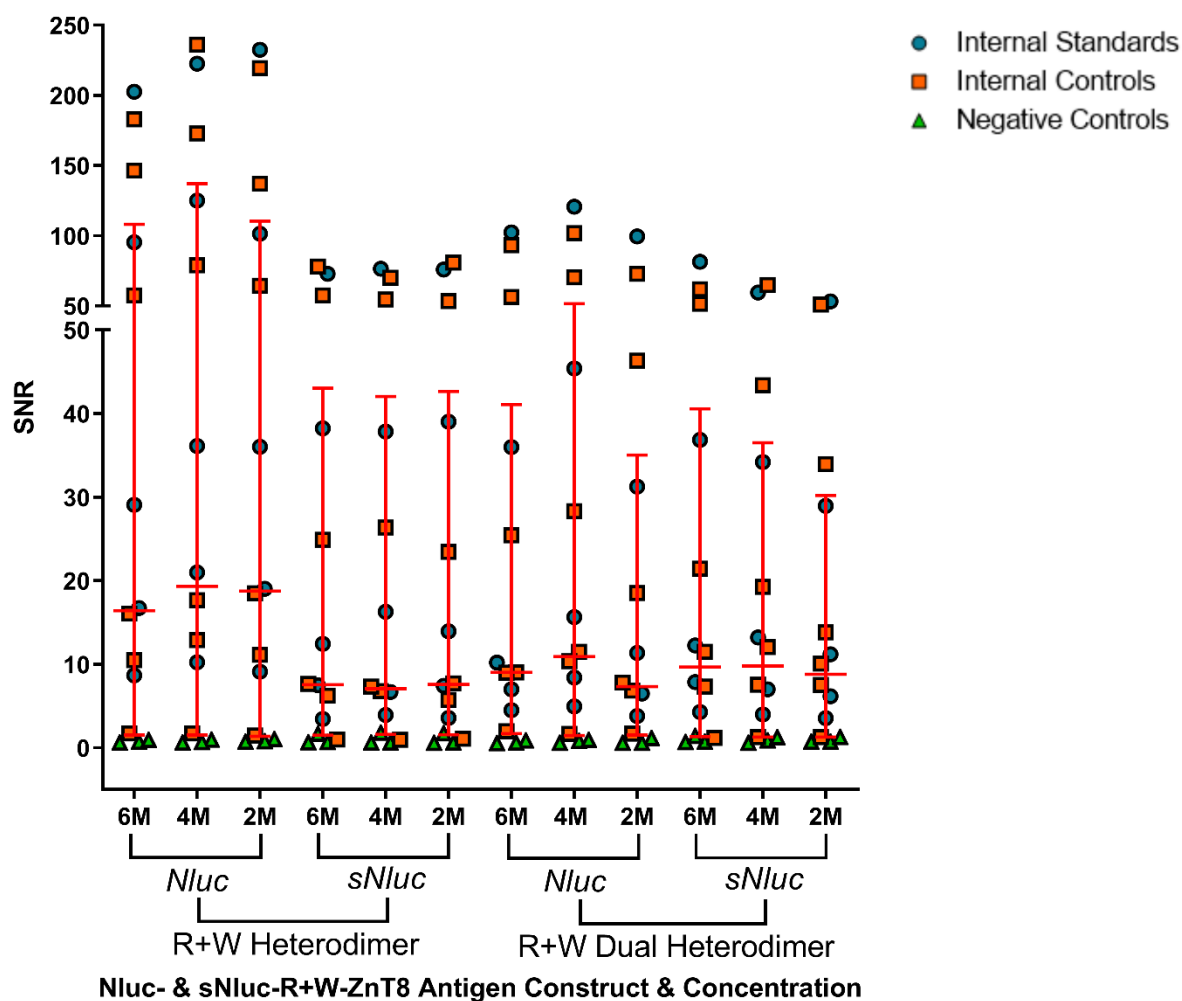


**Figure 4:8 – Nluc-ZnT8 LIPS Optimisation: Nluc-R+W-ZnT8 antigen construct & concentration (SNR)**

A plot of signal to noise ratio (SNR) obtained from testing Nluc- and secretory (s)Nluc- tagged-R+W-ZnT8 heterodimer and dual heterodimer constructs at concentrations of 2M, 4M, and 6M LU/25µl TBST-0.5%. Nluc-tagged ZnT8 constructs were tested according to the optimised Nluc-GAD65 LIPS protocol, and sNluc-tagged ZnT8 constructs were tested neat from the supernatant of HEK293 cells with the remainder of the optimised Nluc-GAD65 LIPS protocol followed. Red bars denote median and interquartile ranges.

**Experimental conclusion:** The Nluc-R+W-ZnT8 heterodimer and dual heterodimer constructs at a concentration of 4M offered the maximum ZnT8A binding accounting for assay background (SNR) in the optimisation population. Despite a higher SNR for the Nluc-R+W-ZnT8 heterodimer versus dual heterodimer in this assay, the performance of the Nluc-R+W-ZnT8 heterodimer and dual heterodimer constructs was further investigated later (**4.3.1.3**) to select the superior antigen construct after the concentration of Tween-20 in assay buffers was tested to lower assay background (**4.3.1.2**); LU in the negative controls ranged from  $2.4 \times 10^3$ - $1.6 \times 10^4$  LU at a concentration of 4M for both Nluc-R+W-ZnT8 heterodimer and dual heterodimer constructs.

#### **4.3.1.2 Concentration of Tween-20 in assay buffers**

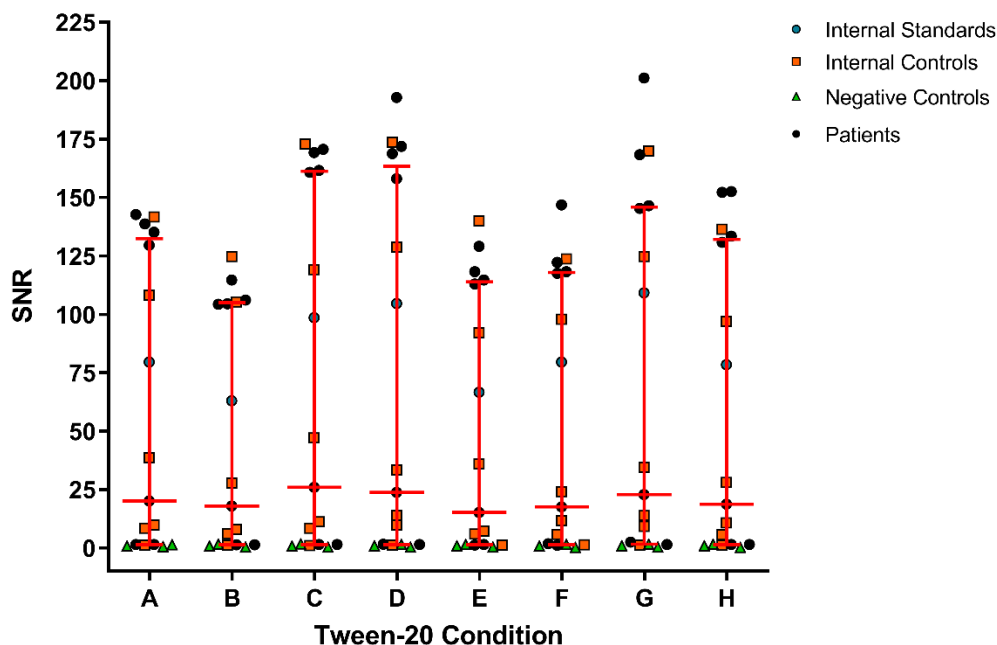
---

At a concentration of 4M LU, the Nluc-R+W-ZnT8 heterodimer construct was incubated and assayed in TBST buffer containing 0.15% or 0.5% Tween-20 (v/v) in six different combinations to reduce assay background. The remainder of the optimised Nluc-GAD65 LIPS protocol was followed. To investigate this, two independent experiments were conducted and included samples from the main optimisation sample set:

- 1 Internal ZnT8 RIA standard
- 6 Internal ZnT8 RIA controls (5 positive and 1 negative)
- 3 Anonymised healthy controls
- 6 T1D patients

Overall, the median LU binding across the six combinations of TBST assay buffer containing 0.15% or 0.5% Tween-20 (v/v) at different stages of the Nluc-ZnT8 LIPS assay was comparable. Conditions that offered the highest SNR were C [median SNR 25.9 (range 0.46-172.9)], D [median SNR 23.8 (range 0.3-192.8)], and G [median SNR 22.89 (range 0.3-201.1)] compared with A at standard conditions [median SNR 20.2 (range 0.5-142.7)] (**Figure 4:9**).

Although no significant difference between C, D, and G in pairwise Wilcoxon signed-rank tests was found ( $p>0.05$ ), condition D was selected for the practical advantage of using 0.15% Tween-20 TBST for the preparation of antigen and PAS immunoprecipitate and 0.5% Tween-20 TBST for the removal of excess unbound antigen.



Stage of Assay	A	B	C	D	E	F	G	H
Ag	0.15	0.50	0.15	0.15	0.50	0.50	0.15	0.50
PAS	0.15	0.15	0.50	0.15	0.50	0.15	0.50	0.50
Wash	0.15	0.15	0.15	0.50	0.15	0.50	0.50	0.50

**Figure 4:9 – Nluc-ZnT8 LIPS Optimisation: Concentration of Tween-20 in assay buffers (SNR)**

A plot of signal to noise ratio (SNR) obtained from testing the concentration of Tween-20 in TBST buffer at either 0.15% or 0.5% (v/v) in different combinations within the stages of the LIPS assay (A-H; A refers to the ZnT8A RIA protocol and H refers to the optimised Nluc-GAD65 LIPS assay protocol) in two independent experiments using the Nluc-R+W-ZnT8 heterodimer construct. Stages of assay; Ag (antigen incubation buffer), PAS (PAS washing buffer), and wash (removal of excess antigen buffer). Red bars denote median and interquartile ranges.

**Experimental conclusion:** TBST with a lower Tween-20 concentration (0.15% v/v) benefitted ZnT8A binding during Nluc- antigen incubation and a higher Tween-20 concentration (0.5% v/v) benefitted removal of excess unbound Nluc- antigen and reduced assay background. The concentration of Tween-20 in the TBST buffer used for washing the PAS immunoprecipitate had little effect on ZnT8A binding or assay background. Condition D offered the greatest compromise between ZnT8A binding and assay background and was also more practically straightforward to implement.

### **4.3.1.3 Nluc-tagged ZnT8 antigen construct & antigen incubation length**

To investigate whether a longer Nluc-R+W-ZnT8 antigen incubation would improve assay sensitivity and specificity, the Nluc-R+W-ZnT8 heterodimer and dual heterodimer constructs at a concentration of 4M LU, was incubated in TBST-0.15% for 2.5 hours or 20-21 hours (overnight; O/N) at RT in two independent experiments. The remainder of the optimised Nluc-GAD65 LIPS protocol was followed. To increase the sample size of ZnT8A positives and negatives, this assay included both samples from the main optimisation sample set, ZnT8A positive samples from the IASP2016 workshop, and ZnT8A negative healthy schoolchildren:

- 4 Internal ZnT8 RIA standards
- 6 Internal ZnT8 RIA controls (5 positive and 1 negative)
- 6 Anonymised healthy negative controls
- 4 Healthy schoolchildren
- 8 T1D patients
- 16 ZnT8A positive IASP2016 samples
  - 16 New-onset T1D patients
  - 1 Negative control
  - 2 Dilutions from a positive pool of T1D patient serum

Regardless of incubation length, the median LU of the Nluc-R+W-ZnT8 dual heterodimer construct was superior to the Nluc-R+W-ZnT8 heterodimer construct ( $p < 0.0001$ ), but SNR was comparable between constructs at each incubation length ( $p > 0.05$ ). However, O/N incubation, compared with 2.5hr incubation, had reduced SNR for both Nluc-R+W-ZnT8 constructs due to increased assay background (non-specific binding) in the negative controls ( $p < 0.0001$ ; **Figure 4:10A**).

Despite the comparable SNRs between constructs, the Nluc-R+W-ZnT8 dual heterodimer identified two additional low-moderate level ZnT8A positives in new-onset T1D patients with better discrimination of low-level ZnT8A from negative controls (**Figure 4:10B** presents SNR <10); median SNR 2.3 (range 0.3-49.2) Nluc-R+W-ZnT8 dual heterodimer versus median SNR 1.5 (range 0.2-51.4) in the Nluc-R+W-ZnT8 heterodimer.

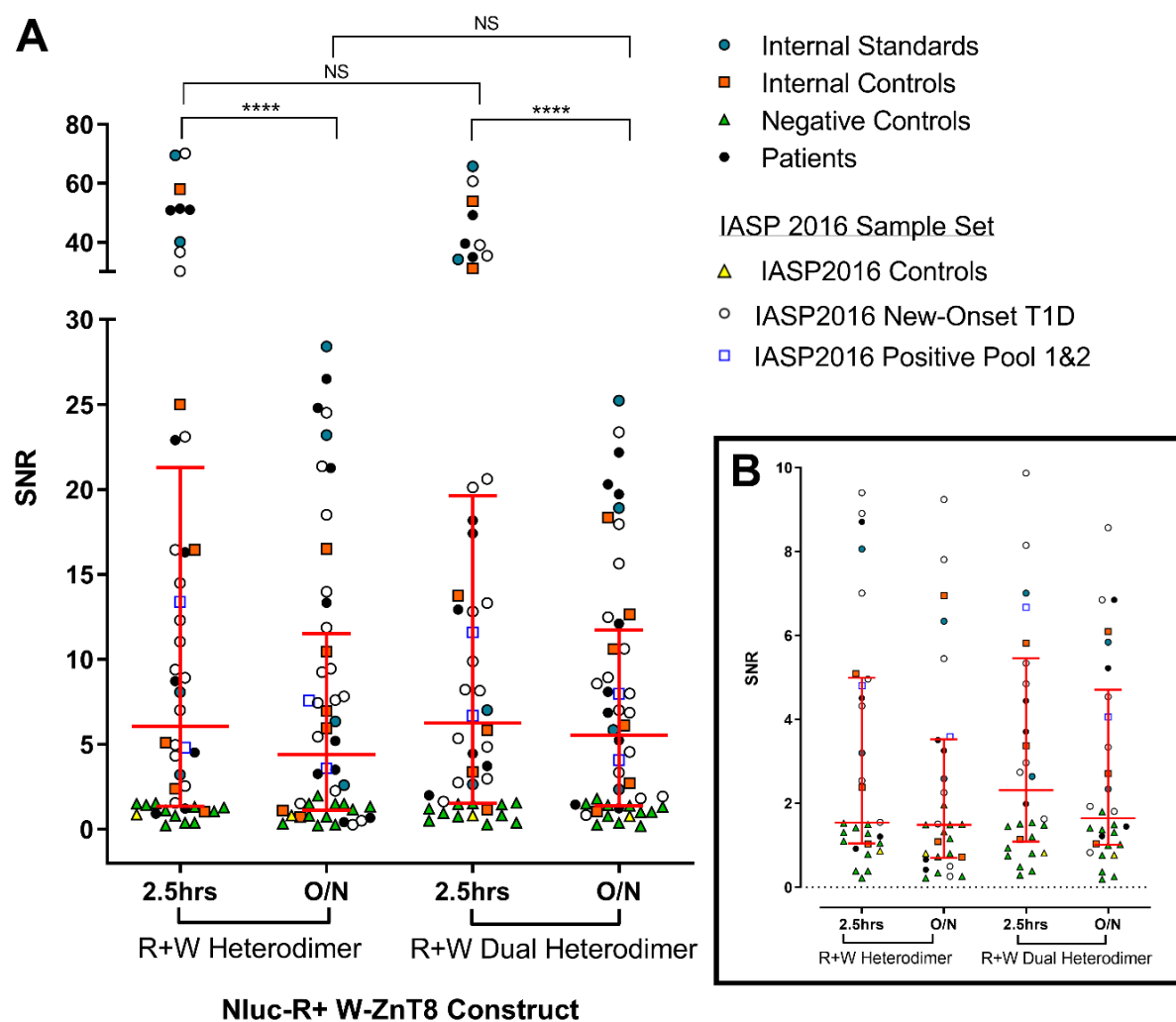


**Figure 4:10 – Nluc-ZnT8 LIPS Optimisation: Nluc-tagged ZnT8 antigen construct & antigen incubation length (SNR)**

Plots of overall (**A**) and low level (**B**; <10) signal to noise ratio (SNR) were obtained from testing Nluc-R+W-ZnT8 heterodimer and dual heterodimer constructs at a concentration of 4M LU/25µl TBST-0.15% and incubating with 1µl of serum for 2.5hrs or 20-21 (O/N; Overnight) at RT. Immunoprecipitate was washed with TBST-0.15%, and excess Nluc-tagged ZnT8 antigen was excluded using TBST-0.5% buffer (condition D from previous optimisation experiment). \*\*\*\*p<0.0001 by pairwise Wilcoxon signed ranked tests. Red bars denote median and interquartile ranges. NS: Not Significant less than alpha value 0.05; \*p<0.05; \*\*\*\*p<0.0001 by pairwise Wilcoxon signed-rank tests.

**Experimental conclusion:** An Nluc-R+W-ZnT8 antigen incubation length of 2.5hrs at RT offered greater ZnT8A binding and lower assay background compared with an O/N incubation at RT. The Nluc-R+W-ZnT8 dual heterodimer construct had improved SNR compared to the Nluc-R+W-ZnT8 heterodimer construct, which was particularly evident in low-moderate level ZnT8A positive new-onset T1D patients. The Nluc-R+W-ZnT8 dual heterodimer construct incubation at 2.5hrs at RT was selected for further optimisation experiments.

#### **4.3.1.4 Nluc-ZnT8 LIPS assessment in the IASP2018 sample set**

---

To assess the performance of the Nluc-ZnT8 LIPS assay during optimisation, the assay protocol (as of 13/08/2018) was entered into the IASP2018 workshop. The Nluc-R+W-ZnT8 dual heterodimer at a concentration of 4M LU was incubated for 2.5hrs at RT in TBST-0.15%. Following PAS immunoprecipitation, excess unbound Nluc-ZnT8 antigen was removed using TBST-0.5%. The remainder of the optimised Nluc-GAD65 LIPS protocol was followed. The full internal logarithmic RIA ZnT8A standard curve (n=8) was used in all assays to determine AU. The IASP2018 samples were blinded at the time of testing but was comprised of a total of 140 serum samples: 43 new-onset T1D patients, 7 mAutoab+ves, and 90 negative controls.

##### **4.3.1.4.1 Preliminary positivity threshold for IASP2018**

For the IASP2018 workshop, 92/523 healthy schoolchildren used to establish the monomeric ZnT8R/ZnT8W RIA thresholds was used to develop a preliminary positivity threshold for Nluc-ZnT8 LIPS (1.1AU at the 97.5<sup>th</sup> percentile). The 97.5 percentile of these 92 schoolchildren by RIA was 1.7AU and 2.1AU in ZnT8RA and ZnT8WA RIAs, respectively. This was comparable to the established 1.8AU threshold obtained in the total 523 schoolchildren population.

#### **4.3.1.4.2 IASP2018 sample set**

Raw data from either monomeric ZnT8R/ZnT8W RIA (CPM) and LIPS (LU) could not be directly compared, but when independently ranked and compared, there was a significant difference between the methods ( $p < 0.05$ - $0.0001$ ). This could be due to differences in the ability of the methods in detecting all ZnT8A specificities; however, when the maximum CPM from both monomeric ZnT8R/ZnT8W RIAs as a composite measure of all ZnT8A was compared to LU in LIPS, the difference in the methods was still apparent ( $p < 0.0001$ ).

The AUs derived from the same logarithmic standard curve in both monomeric ZnT8R/ZnT8W RIAs confirmed that the IASP2018 workshop included a range of ZnT8A specificities [ZnT8RA-specific (n=7); ZnT8WA-specific (n=4); ZnT8A non-specific (n=20)] with significant differences in AU ( $p < 0.05$ ) and an overall correlation of 0.6 (95% CI: 0.4-0.67;  $p < 0.0001$ ) between the two RIA assays (**Figure 4:11**).

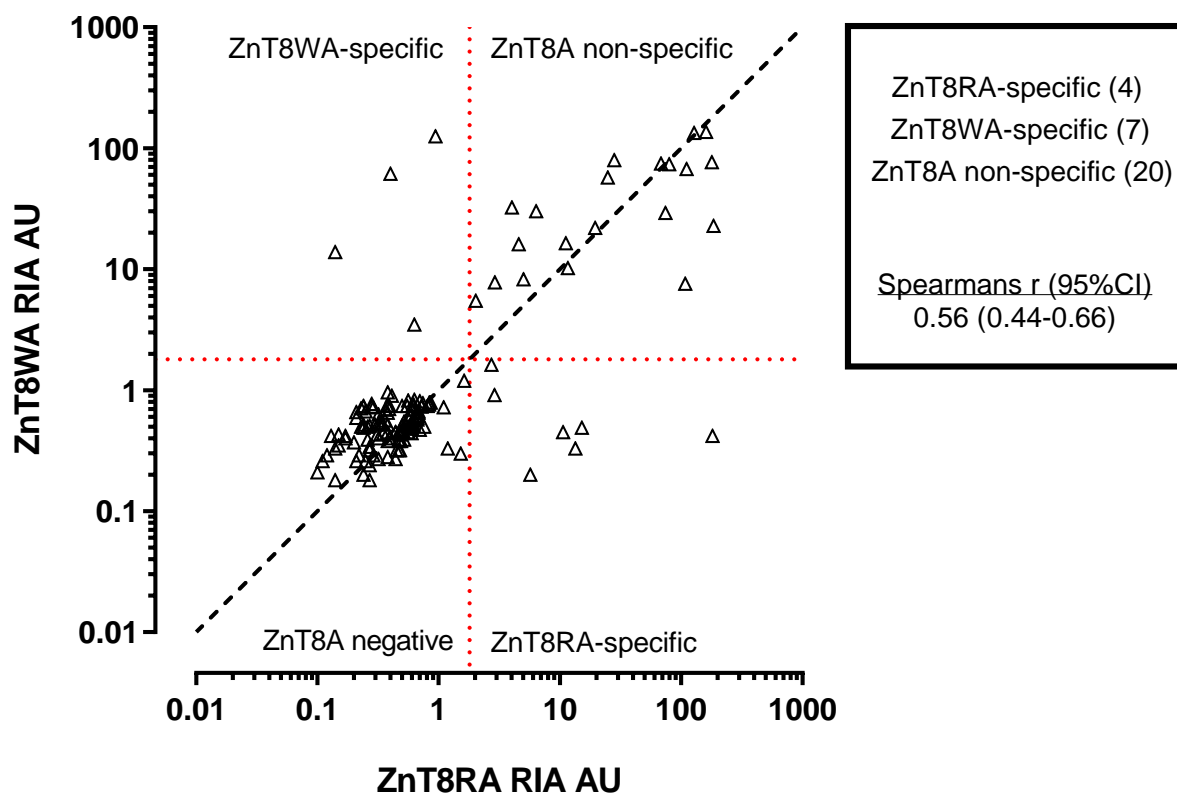


*Figure 4:11 – Nluc-ZnT8 LIPS Optimisation: IASP2018 workshop ZnT8A specificity using monomeric ZnT8R/ZnT8W RIAs (AU)*

A scatter plot of arbitrary units (AU) derived from the same logarithmic standard curve (8 serial dilutions from a pool of ZnT8A positive serum) in the IASP2018 workshop sample set of 140 blinded samples (43 new-onset T1D, 7 mAutoab+ves, and 90 negative controls). The scatterplot highlights the presence of ZnT8A positive samples with different ZnT8A specificities [ZnT8RA-specific (n=7); ZnT8WA-specific (n=4); ZnT8A non-specific (n=20)]. Whilst there is a significant correlation ( $p < 0.0001$ ), the different specificities of ZnT8A reinforce the AU differences between the monomeric RIAs ( $p < 0.05$ ). Red dotted lines denote positivity thresholds at the 97.5<sup>th</sup> percentile of 523 healthy schoolchildren (1.8AU). Black dashed line denotes linearity where  $X=Y$ .

Due to the presence of all ZnT8A specificities in the workshop, the maximum ZnT8A RIA AU was a better comparator to the Nluc-ZnT8 LIPS assay with improved correlation [0.8 (95% CI 0.7-0.9);  $p < 0.001$ ; **Figure 4:12A**] compared to the monomeric RIA AU [ZnT8RA RIA 0.7 (95% CI 0.6-0.7); ZnT8WA RIA 0.7 (95% CI 0.5-0.7); **Figure 4:12B**] as the Nluc-R+W-ZnT8 dual heterodimer construct should bind all ZnT8A specificities. However, the AUs between RIA (monomeric ZnT8R/ZnT8W or maximum ZnT8R/ZnT8W AU) and LIPS show that the AUs cannot be directly compared due to the dynamic range of the assays being different. Confirmed when independently ranked and compared ( $p < 0.0001$ ) (**Figure 4:13**).

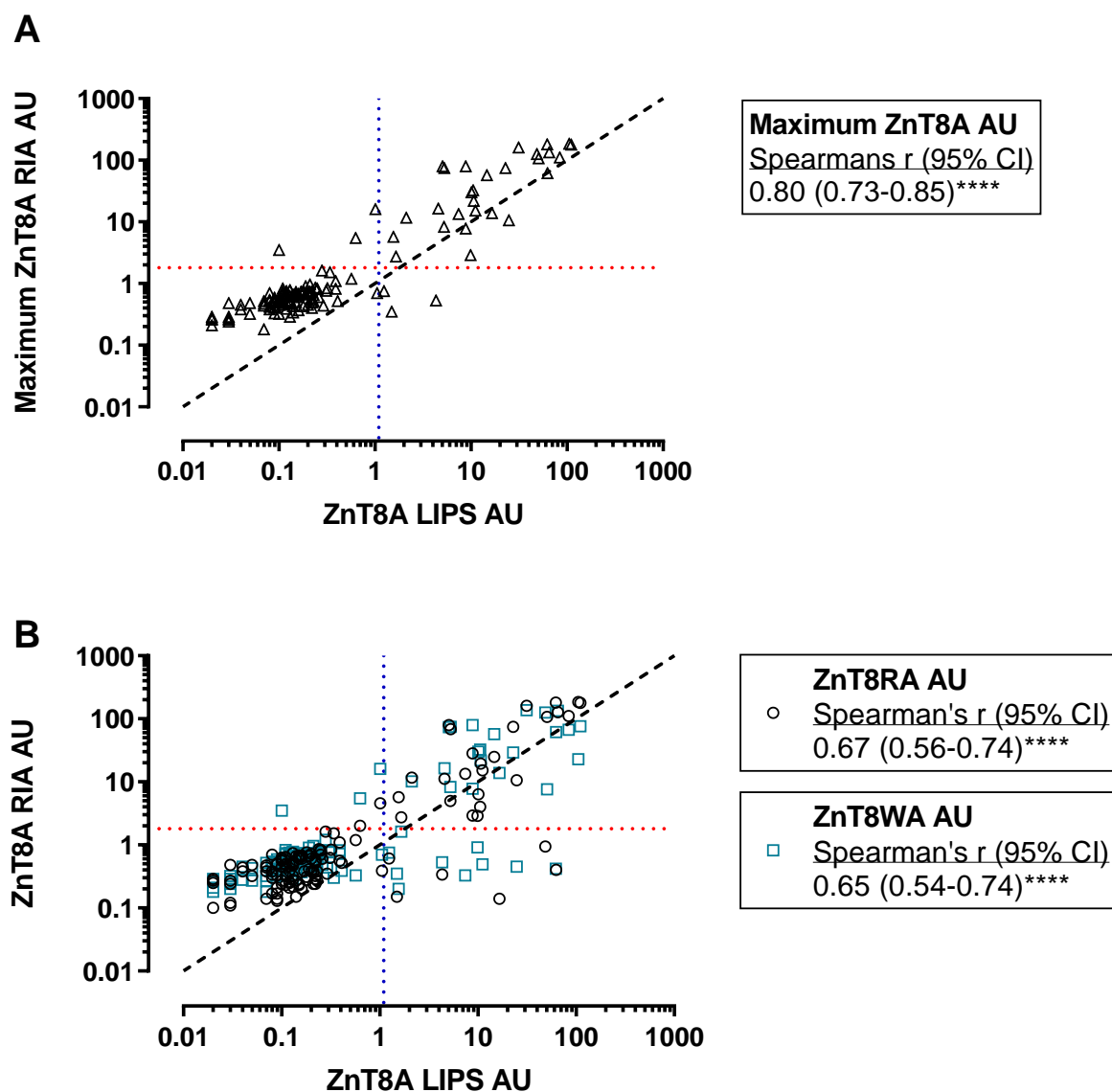


*Figure 4:12 – Nluc-ZnT8 LIPS Optimisation: IASP2018 workshop LIPS versus RIA using monomeric RIA AU or maximum RIA AU*

Scatter plots comparing arbitrary units (AU) obtained in Nluc-ZnT8 LIPS and RIA by either monomeric ZnT8RA and ZnT8WA RIA (A), or maximum AU obtained in either monomeric (ZnT8RA/ZnT8WA) RIA (B) in the IASP2018 sample set of 140 blinded samples (43 new-onset T1D, 7 mAutoab+ves, and 90 negative controls). Due to a mixture of ZnT8A specificities (ZnT8RA-specific; ZnT8WA-specific; ZnT8A non-specific) in the IASP2018 workshop, the maximum ZnT8A AU obtained by RIA better correlates with Nluc-ZnT8 LIPS than AU from monomeric RIAs, as the Nluc-R+W-ZnT8 antigen construct should bind all ZnT8A specificities. Red dotted lines denote positivity thresholds at the 97.5<sup>th</sup> percentile of 523 healthy schoolchildren (1.8AU) for RIAs. The blue dotted line denotes the preliminary positivity threshold for Nluc-ZnT8 LIPs at 1.1AU. \*\*\*p<0.001; \*\*\*\*p<0.0001.

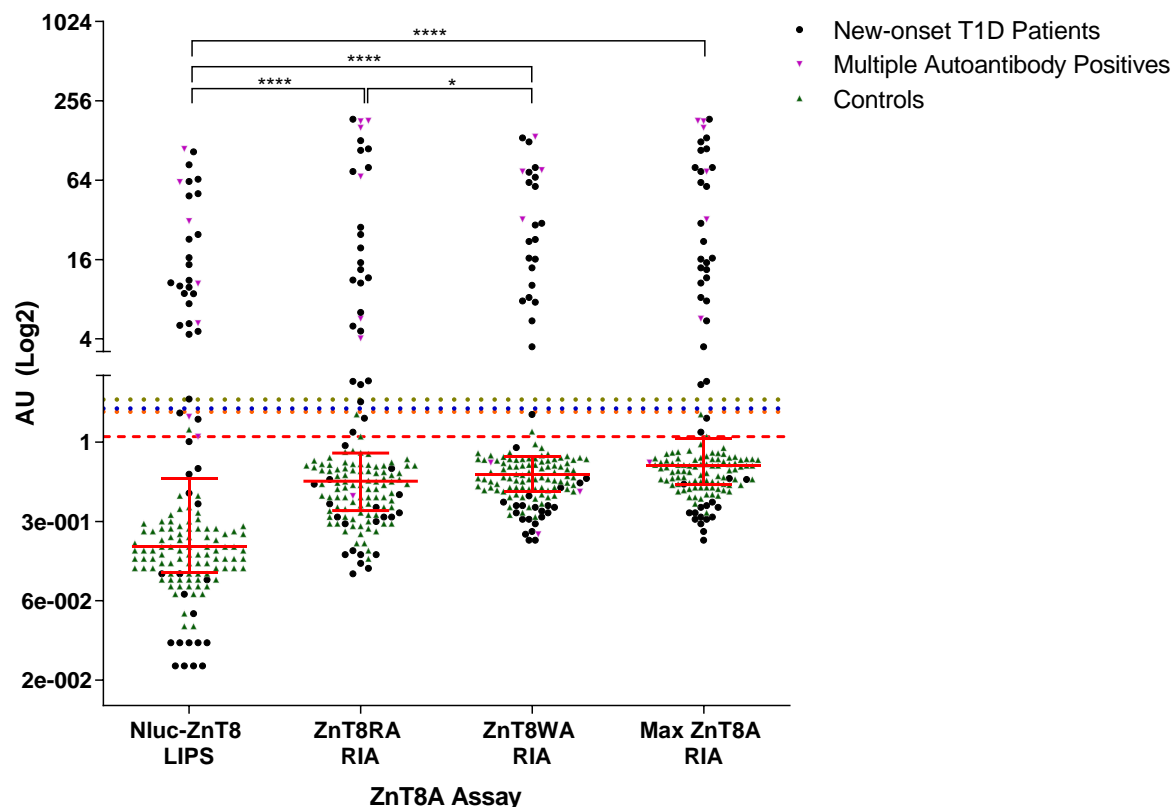


**Figure 4:13 – Nluc-ZnT8 LIPS Optimisation: LIPS & RIA AU in IASP2018 (AU)**

A plot of arbitrary units (AU; Log<sub>2</sub> scale) was obtained from testing 140 blinded serum samples from the IASP2018 workshop in the Nluc-ZnT8 LIPS assay and the monomeric ZnT8RA and ZnT8WA RIAs. To account for all ZnT8A specificities, the maximum ZnT8 RIA AU is used as a composite measure of ZnT8A compared to the Nluc-ZnT8 LIPS assay. The IASP2018 workshop was comprised of 43 new-onset T1D patients (black circles), 7 mAutoab+ves (purple triangles), and 90 negative controls (green triangles). Red dashed line: preliminary Nluc-ZnT8 LIPS positivity threshold (1.1AU; n=92 schoolchildren); Orange dotted line: ZnT8RA RIA preliminary threshold (1.7AU; n=92 schoolchildren); Yellow dotted line: ZnT8WA RIA preliminary threshold (2.7AU; n=92 schoolchildren); Blue dotted line: 97.5<sup>th</sup> percentile of the validated ZnT8RA and ZnT8WA RIA (1.8AU; n=523 schoolchildren). Red bars denote median and interquartile ranges. \*p<0.05 and \*\*\*\*p<0.0001 by pairwise Wilcoxon signed-rank tests

Bland-Altman analysis of the AU differences by IASP specimen type (new-onset T1D, mAutoab+ves, and negative controls) between Nluc-ZnT8 LIPS and the maximum AU from ZnT8R/ZnT8W RIAs identified discrepancies in negative controls (n=2; **Figure 4:14A**) and new-onset T1D (n=5; **Figure 4:14E**) but not mAutoab+ves (**Figure 4:14C**). The Nluc-ZnT8 LIPS method obtained lower AU than RIA overall, but this was expected given that the median AU, preliminary threshold, and assay detection limit was lower (**Figure 4:14B/D/F**).

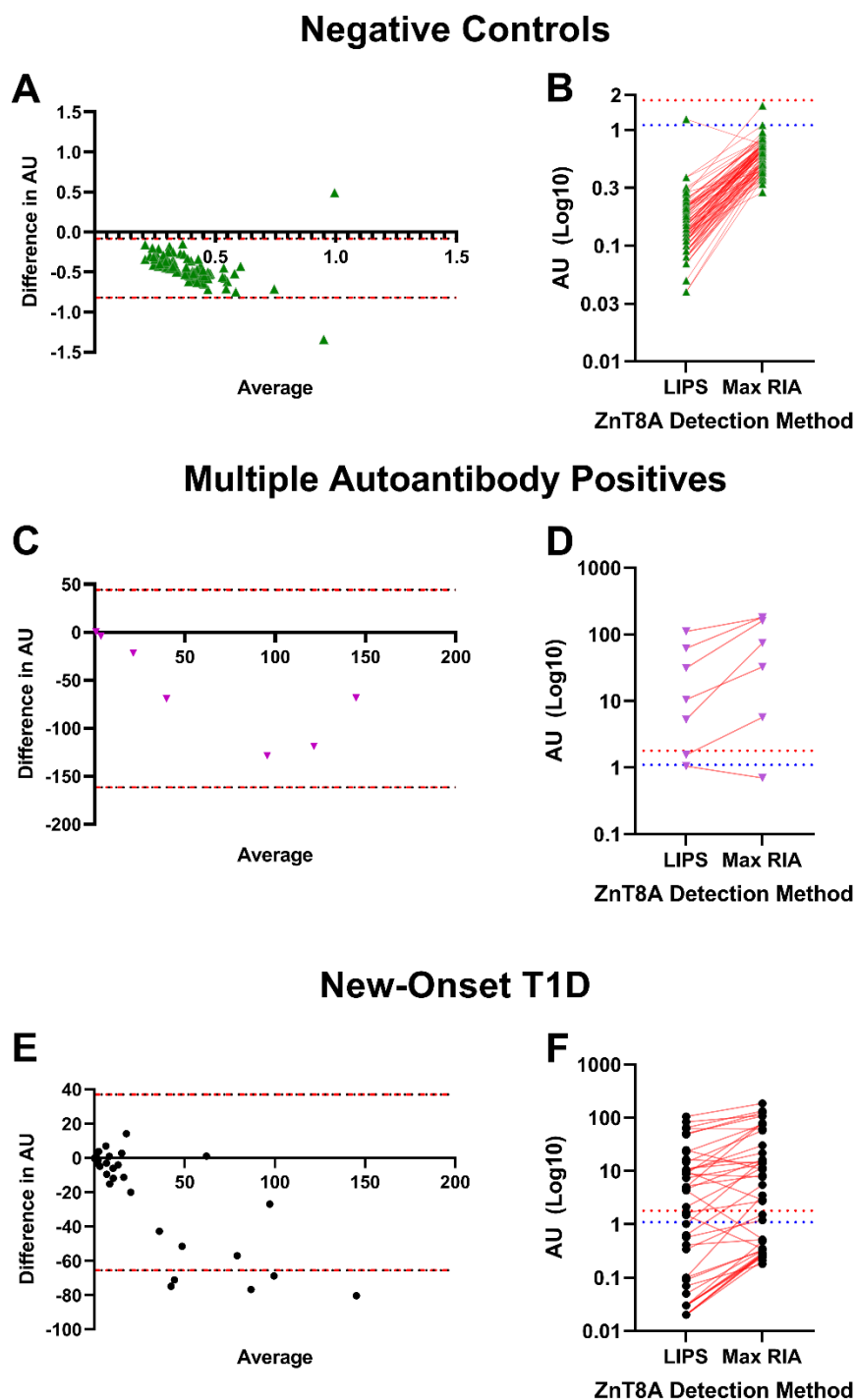


**Figure 4:14 – Nluc-ZnT8 LIPS Optimisation: Bland-Altman analysis comparing AU from LIPS & RIA (maximum) in the IASP2018 workshop**

Bland-Altman and paired aligned plots comparing the difference in Nluc-ZnT8 LIPS AU with the maximum ZnT8A AU obtained in either ZnT8R or ZnT8W monomeric RIAs [difference in AU calculated (LIPS AU-RIA Maximum AU) compared with average AU between both methods] in the IASP2018 sample set [negative controls (n=90; **A/B**); multiple autoantibody positives (n=7; **C/D**); new-onset T1D (n=43; **E/F**)]. A negative difference in AU indicates AU is greater in LIPS versus RIA. Overall, LIPS had lower AU than RIA for negative controls, multiple autoantibody positives and new-onset T1D. Incorrect categorisation of positive versus negative AU occurred in 1 negative control (RIA correctly identified all 90 negative controls), 0 mAutoab+ves (LIPS correctly identified all 7 mAutoab+ves versus 6 in RIA) and 19 new-onset T1D (24 identified correctly by LIPS versus 25 in RIA but 5 samples were discrepant between the methods).

## Chapter 4 - Development of Nluc-ZnT8 LIPS for ZnT8A detection

The performance of Nluc-ZnT8 LIPS and ZnT8R/ZnT8W RIAs are summarised in **Table 4:8**.

Overall, the Nluc-ZnT8 LIPS assay had higher sensitivity than the monomeric ZnT8R/ZnT8W RIAs, identifying 24 new-onset T1D patients compared with 21 and 20 in the ZnT8R and ZnT8W RIAs, respectively. However, using the maximum AU obtained between ZnT8R/ZnT8W RIAs showed that the RIAs identified a total of 25 new-onset T1D with 5 discrepant new-onset T1D samples between the methods: LIPS identified 2 additional new-onset T1D (4.7% of 43) that neither RIA identified, and the RIAs identified 3 new-onset T1D (0% of 43) that the LIPS assay did not identify.

Additionally, Nluc-ZnT8 LIPS identified all 7 mAutoab+ves compared with 6, 4, and 6 in the ZnT8R RIA, ZnT8W RIA, and ZnT8R/ZnT8W RIAs (maximum AU), respectively. However, 1 negative control was incorrectly identified positive by the Nluc-ZnT8 LIPS assay compared with the RIAs, which compromised assay specificity (98.9%). Both monomeric ZnT8R/ZnT8W RIAs correctly identified all negative controls and achieved 100% specificity.

IASP Specimen Type	n	n positive by Nluc-ZnT8 LIPS (%)	n positive by ZnT8R RIA (%)	n positive by ZnT8W RIA (%)	n positive by ZnT8R/ZnT8W RIA (max) (%)
New-onset T1D patients	43	24 (55.8)	21 (48.8)	20 (46.5)	25 (58.1)
Multiple autoantibody positives	7	7 (100.0)	6 (85.7)	4 (57.1)	6 (85.7)
Negative controls	90	1 (1.1)	0 (0.0)	0 (0.0)	0 (0.0)

*Table 4:8 – Nluc-ZnT8 LIPS Optimisation: Summary of Nluc-ZnT8 LIPS & RIA IASP2018 results*

Combining the new-onset T1D patients and mAutoab+ves to assess sensitivity encompassing at-risk samples, Nluc-ZnT8 LIPS was shown to have a higher area under the curve (AUC), AS95, and accuracy when analysed by the IASP committee, despite the one incorrectly identified negative control (**Table 4:9**).

Assay	Sensitivity (%)	Specificity (%)	AUC <sup>1</sup>	AS95 <sup>2</sup>	Accuracy <sup>3</sup>
<b>Nluc-ZnT8 LIPS</b>	62	98.9	0.733	72	85.7
<b>ZnT8R RIA</b>	54	100	0.688	60	83.57
<b>ZnT8W RIA</b>	48	100	0.571	52	81.43

*Table 4:9 – Nluc-ZnT8 LIPS Optimisation: IASP2018 report*

<sup>1</sup> Total Area Under the Curve (AUC) derived from Receiver Operating Characteristics (ROC) analysis; <sup>2</sup> Percent Sensitivity at 95% specificity (AS95) derived from ROC analysis; <sup>3</sup> Percent Accuracy: Number of T1D samples (new-onset and multiple autoantibody positives; n=50) identified as positive + Number of controls identified as negative ÷ number of T1D samples reported (n=50) + number of controls reported (n=90). The samples were all blinded at the time of testing and were independently analysed by the IASP committee.

**Experimental conclusion:** Results from IASP2018 showed that the Nluc-ZnT8 LIPS assay prior to full optimisation had superior sensitivity and accuracy than both monomeric ZnT8R/ZnT8W RIAs but showed discrepancies when results from both assays were combined and considered as the maximum RIA ZnT8RA/ZnT8WA level. Further optimisation of reducing assay background should alleviate the potential for false positives, but overall, the Nluc-ZnT8 LIPS assay (still undergoing optimisation) showed promising potential for detecting ZnT8A using a novel Nluc-R+W-ZnT8 dual heterodimer antigen without the requirement for radionuclides.

### **4.3.1.5 Expression & preparation of the Nluc-tagged ZnT8 antigen construct**

#### **4.3.1.5.1 Purification & preparation of the Nluc-tagged ZnT8 construct**

L

In the IASP2018 workshop, the Nluc-ZnT8 LIPS assay conducted by international collaborator Dr Lampasona's laboratory (Milan, Italy) using the same Nluc-R+W-ZnT8 dual heterodimer construct showed higher sensitivity and specificity; correctly identifying an additional 5 new-onset T1D patients [Milan n=29 (67.4%); Bristol n=24 (55.8%)] and all negative controls [Milan n=90 (100%); Bristol n=89 (98.9%)].

## Chapter 4 - Development of Nluc-ZnT8 LIPS for ZnT8A detection

When the protocols were reviewed, a key difference was the removal of the NAP5<sup>TM</sup> antigen purification step. Instead, after expression of the Nluc-R+W-ZnT8 dual heterodimer construct (identical to the Nluc-GAD65 LIPS protocol), the reaction mix is serially diluted in PBS (GIBCO® ThermoFisher)-0.1% Tween-20 (v/v) (PBST) to 1:250, 1:2,500, and 1:25,000 for LU detection (RLD; 1:50, Promega). Following LU detection, the remaining reaction mix is diluted 1:250 in PBST and stored at -70°C in 10µl aliquots. For use in an assay, 1x10µl aliquot is thawed, diluted 1:100 in TBST-0.5%, filtered through a 0.45µM filter unit (Sigma), and diluted to 4M LU/25µl with RLD (1:50; Promega). Therefore, the preparation of the Nluc-R+W-ZnT8 dual heterodimer construct according to the optimised Nluc-GAD65 LIPS protocol (NAP5<sup>TM</sup> column antigen preparation) was compared to Milan's protocol (0.45µM filter unit antigen preparation) in two independent assays following the remainder of the optimised Nluc-ZnT8 LIPS protocol entered originally in IASP2018.

These assays included the full internal ZnT8 RIA standard curve (n=8) for AU determination where the 1.1AU preliminary positivity threshold was re-applied, samples from the main optimisation sample set, and samples from the IASP2018 workshop with the most discrepant ZnT8A binding between Bristol and Milan protocols:

- 8 Internal ZnT8 RIA standards (AU determination)
- 6 Internal ZnT8 RIA controls (5 positive and 1 negative)
- 9 New-onset T1D patients
- 3 Anonymised healthy controls
- 22 Samples from the IASP2018 workshop
  - 15 New-onset T1D patients
  - 5 Multiple autoantibody positives
  - 2 Negative controls

The median LU was higher using Milan's 0.45 $\mu$ M filter unit protocol [ $3.0 \times 10^5$  (range  $1.1 \times 10^4$ - $2.2 \times 10^6$ )] than Bristol's NAP5<sup>TM</sup> purification protocol [ $2.0 \times 10^5$  (range  $1.5 \times 10^4$ - $2.2 \times 10^6$ )] for preparing the Nluc-R+W-ZnT8 dual heterodimer construct ( $p < 0.0001$ ). Consequently, there was improved discrimination between T1D patients and negative controls, reflected in improved median SNRs irrespective of the level of ZnT8A binding with little to no compromise in assay background, indicative of enhanced sensitivity and specificity (**Figure 4:15A/B**;  $p < 0.0001$ ).

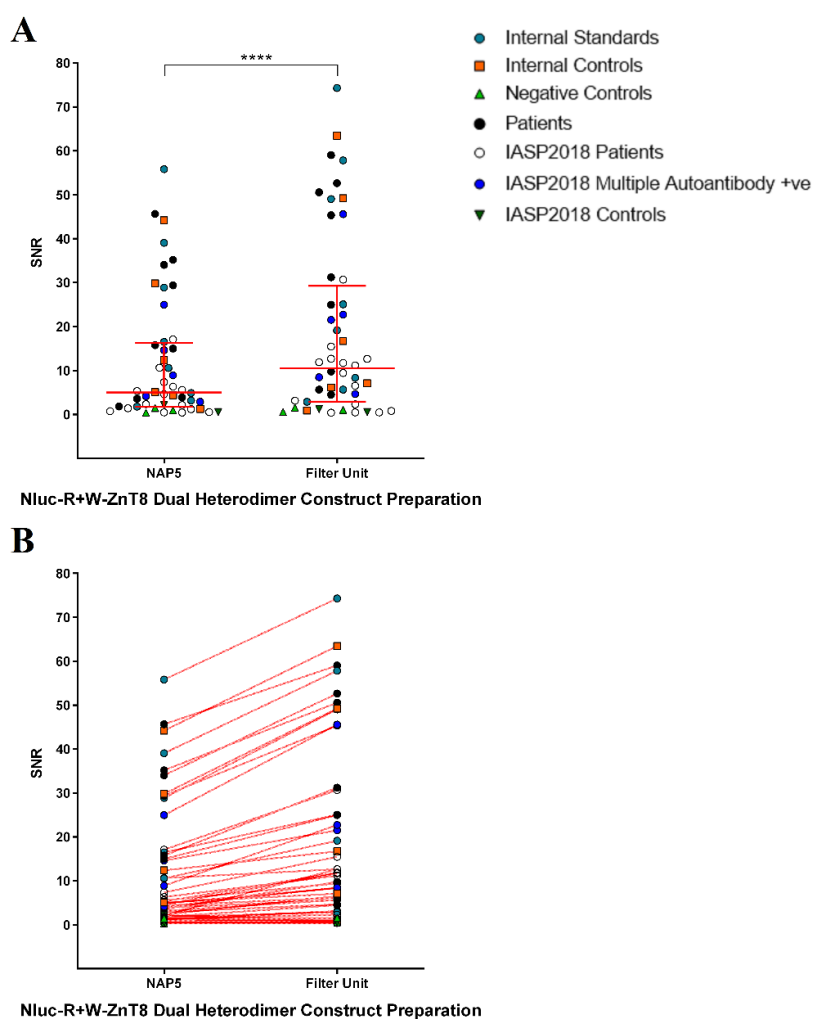


**Figure 4:15 – Nluc-ZnT8 LIPS Optimisation: Preparation methods for the Nluc-R+W-ZnT8 dual heterodimer construct (SNR)**

Plots of overall (A) and paired (B) signal to noise ratios (SNR) from comparing the preparation of the Nluc-R+W-ZnT8 dual heterodimer construct using NAP5<sup>TM</sup> column purification (optimised Nluc-GAD65 LIPS protocol in Bristol) with using a 0.45 $\mu$ M filter unit to dilute the construct to 4M LU/25 $\mu$ l excluding the requirement for purification (Milan's Nluc-ZnT8 LIPS protocol developed by Dr Vito Lampasona's laboratory). Each data point represents four replicates from two independent experiments. Red bars denote the median and interquartile ranges. \*\*\*\* $p < 0.0001$  by pairwise Wilcoxon signed-rank test.

Despite increased binding (LU) relative to the background (SNR), the ordinal ranking of AUs obtained from the logarithmic standard curve was not substantially different between Nluc-R+W-ZnT8 dual heterodimer construct preparation methods ( $p > 0.05$ ; **Figure 4:16**).

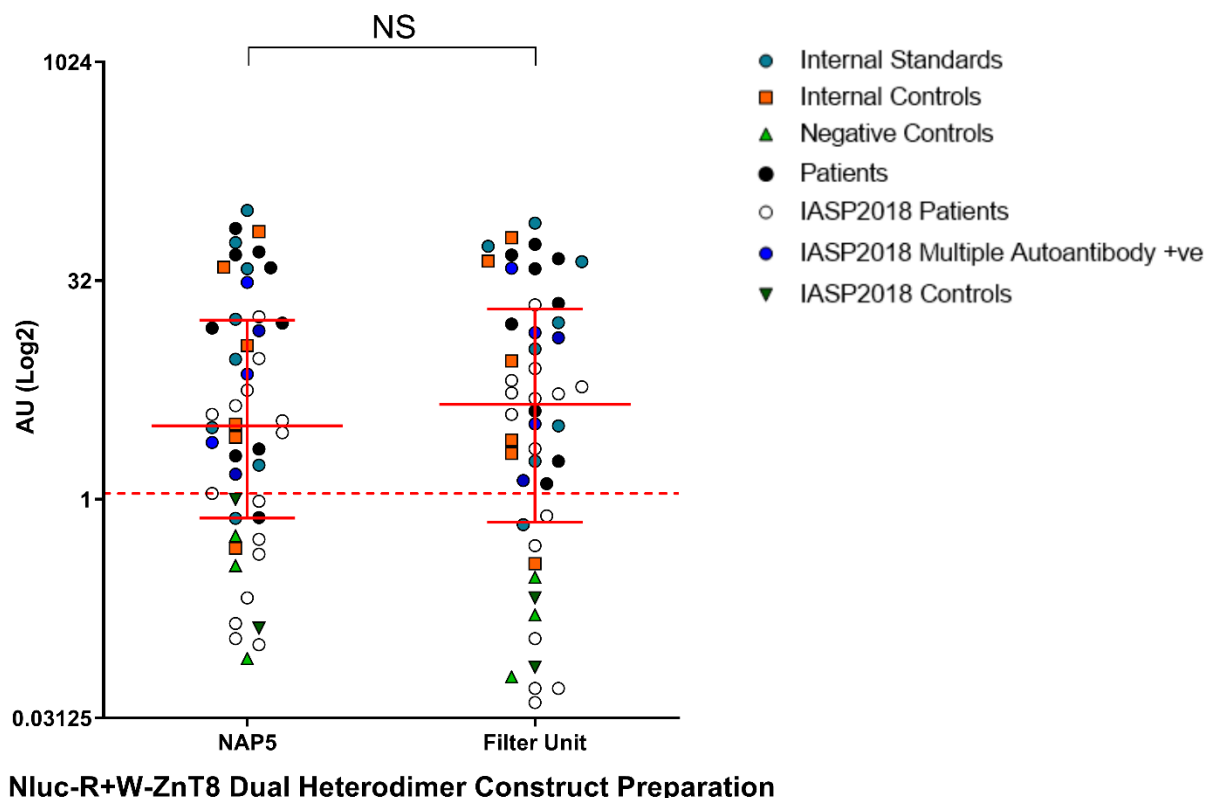


*Figure 4:16 – Nluc-ZnT8 LIPS Optimisation: Preparation methods for the Nluc-R+W ZnT8 dual heterodimer construct (AU)*

A plot of arbitrary units (AU) on a Log<sub>2</sub> scale obtained from the validated ZnT8 RIA logarithmic standard curve ( $n=8$  serial dilutions of a ZnT8A positive pool using negative human serum) comparing the preparation of the Nluc R+W ZnT8 Dual Dimer construct using NAP5™ column purification (optimised Nluc-GAD65 LIPS protocol in Bristol) with using a 0.45µM filter unit to dilute the construct to 4M LU/25µl excluding the requirement for purification (Milan’s Nluc-ZnT8 LIPS protocol developed by Dr Vito Lampasona’s laboratory). Each data point represents four replicates from two independent experiments. Red bars denote the median and interquartile ranges. The red dashed line denotes the preliminary positivity threshold of 92 healthy schoolchildren set at the 97.5<sup>th</sup> percentile of 1.1AU entered for IASP2018. NS: Not significant less than alpha value 0.05 by pairwise Wilcoxon signed-rank test.

## Chapter 4 - Development of Nluc-ZnT8 LIPS for ZnT8A detection

In the main optimisation sample set, Bristol's NAP5™ purification method identified 8/9 (88.9%) new-onset T1D and Milan's 0.45µM filter unit purification method identified all 9 (100%). Both methods had concurrent findings for the internal standards (7/8 positive; 87.5%), internal controls (5/6 positive; 83.3%), and anonymised healthy controls (0/3 positive, 0.0%). In the IASP2018 workshop sample set, both Nluc-R+W-ZnT8 dual heterodimer antigen preparation methods correctly identified all mAutoab+ves (n=5, 100%) and negative controls (n=2, 100%) but showed discrepancies in the new-onset T1D samples. Out of 15 new-onset T1D samples, 7 were identified positive by both methods (46.7%), 6 were identified as negative by both methods (40.0%), and 2 (13.3%) were discrepant by both methods; 1 borderline positive (1.1 AU) and 1 negative (1.0 AU) by Bristol's NAP5™ purification method but both were positive by Milan's 0.45µM filter unit purification method (2.2AU and 6.6AU, respectively). Therefore, Milan's 0.45µM filter unit antigen preparation method identified two additional new-onset T1D cases in the IASP2018 sample set [Milan n=9 (60.0%) versus Bristol n=7 (46.7%)].

Whilst there are two discrepant samples across the whole sample set analysed (main optimisation and select IASP2018 workshop sample sets), the two antigen preparation method protocols were highly correlated ( $p < 0.0001$ , **Figure 4:17**). This suggests that whilst there may be an advantage to Milan's antigen preparation protocol in select samples, the majority have comparable results between methods.

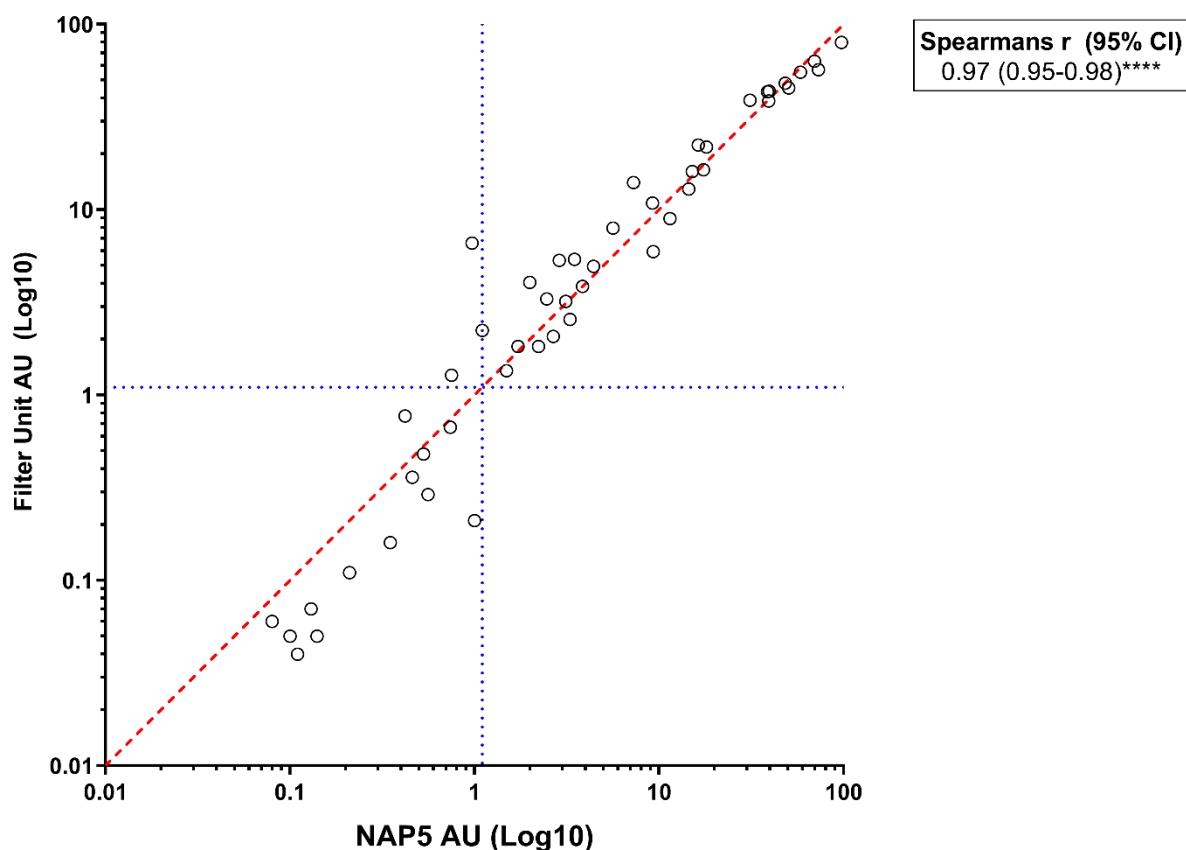


*Figure 4:17 – Nluc-ZnT8 LIPS Optimisation: Preparation methods for the Nluc-R+W-ZnT8 dual heterodimer construct (AU correlation)*

Scatter plot of arbitrary units (AU) on a Log<sub>10</sub> scale obtained from the validated ZnT8 RIA logarithmic standard curve (n=8 serial dilutions of a ZnT8A positive pool using negative human serum) comparing the preparation of the Nluc-R+W-ZnT8 dual heterodimer construct using NAP5<sup>TM</sup> column purification (optimised Nluc-GAD65 LIPS protocol in Bristol) with using a 0.45 $\mu$ M filter unit to dilute the construct to 4M LU/25 $\mu$ l excluding the requirement for purification (Milan's Nluc-ZnT8 LIPS protocol developed by Dr Vito Lampasona's laboratory). Each data point represents four replicates from two independent experiments. The blue dotted line denotes the preliminary positivity threshold of 92 healthy schoolchildren set at the 97.5<sup>th</sup> percentile of 1.1AU entered for IASP2018. The red dashed line denotes linearity where X=Y. Both methods were highly correlated regardless of sample type (identity removed to display overall correlation for the full sample set tested) despite two discrepant samples from the new-onset T1D IASP2018 sample set: \*\*\*\*p<0.0001.

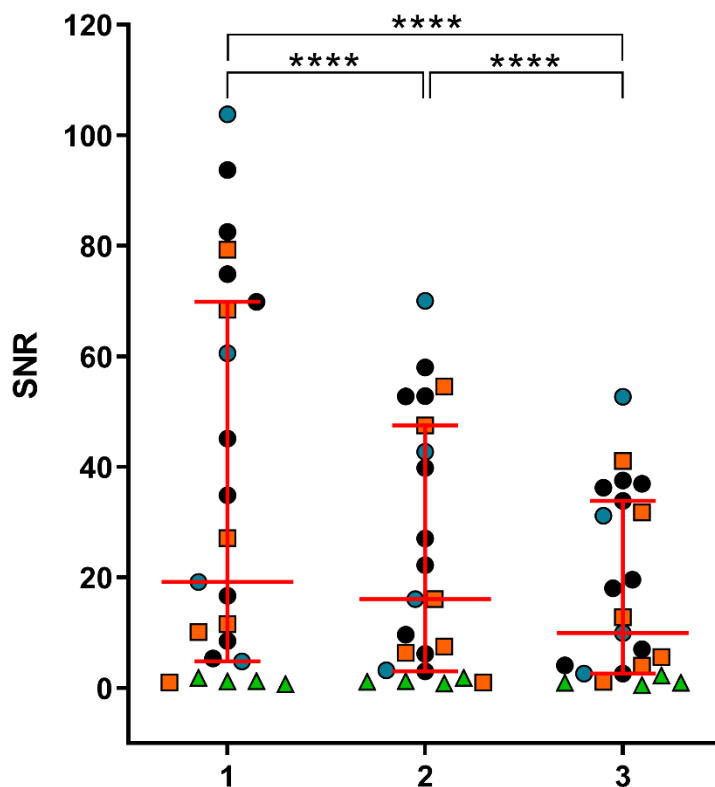
**Experimental conclusion:** The 0.45 $\mu$ M filtration protocol for preparing the Nluc-R+W-ZnT8 dual heterodimer construct used for the Nluc-ZnT8 LIPS assay in Milan increased ZnT8A binding (LU), assay performance (SNR; higher ZnT8A binding and lower assay background), and AU positivity determination in select samples. In addition to being a less time-consuming method with increased performance, adopting the Milan protocol favoured assay harmonisation and concordance between two international laboratories for ZnT8A detection.

#### **4.3.1.5.2 Freeze-thawing the prepared Nluc-tagged ZnT8 construct**

To investigate whether the Nluc-R+W-ZnT8 dual heterodimer construct could be used beyond 1 freeze-thaw cycle following expression, dilution, and filtration, 2 and 3 freeze-thaw cycles were tested using the Nluc-ZnT8 LIPS method currently optimised. This assay included samples from the main optimisation sample set:

- 4 Internal ZnT8 RIA standards
- 6 Internal ZnT8 RIA controls (5 positive and 1 negative)
- 9 T1D patients
- 4 Anonymised healthy negative controls

The median LU of freeze-thawing the Nluc-R+W-ZnT8 dual heterodimer construct indicated a biphasic pattern, increasing from 1 [ $4.5 \times 10^5$  (range  $1.7 \times 10^4$  -  $2.5 \times 10^6$ )] to 2 [ $5.6 \times 10^5$  (range  $2.9 \times 10^4$  -  $2.5 \times 10^6$ );  $p > 0.05$ ] freeze-thaw cycles and decreasing from 2 to 3 [ $4.1 \times 10^6$  (range  $2.2 \times 10^4$  -  $2.2 \times 10^6$ );  $p < 0.0001$ ] freeze-thaw cycles. The discrimination between new-onset T1D patients and healthy negative controls appeared visually to decrease with increasing freeze-thaw cycles. The reduced sensitivity and specificity were corroborated by SNR but the decrease in median SNR was linear with increasing freeze-thaw cycles; 1 [19.2 (range 0.7-103.8)]; 2 [16.1 (range 0.8-70.1)]; 3 [10.0 (range 0.5-52.7)];  $p < 0.0001$  for all pairwise Wilcoxon signed-rank tests (**Figure 4:18**).



**Number of Nluc-R+W-ZnT8 Dual Heterodimer Construct Freeze-thaw Cycles**

*Figure 4:18 – Nluc-ZnT8 LIPS Optimisation: Freeze-thawing the Nluc-R+W-ZnT8 dual heterodimer construct (SNR)*

A plot of signal to noise ratio (SNR) comparing one freeze-thaw cycle (standard) to two and three freeze-thaw cycles once the Nluc-R+W-ZnT8 dual heterodimer construct has been expressed, diluted and filtered (0.45µM filter unit) at a concentration of 4M LU/25µl. Red bars denote the median and interquartile ranges. NS: Not Significant less than alpha value 0.05; \*\*\*p<0.001; \*\*\*\*p<0.0001 by pairwise Wilcoxon signed-rank test.

**Experimental conclusion:** Increasing the number of freeze-thaw cycles above 1 (standard protocol) reduced ZnT8A binding and increased assay background. Therefore, to ensure optimal performance, each aliquot of frozen Nluc-R+W-ZnT8 dual heterodimer must only be thawed once before use in a LIPS assay.

### **4.3.1.6 Detection of luminescence**

---

#### **4.3.1.6.1 Substrate concentration**

The Furimazine substrate is routinely prepared in a 1:50 dilution with NanoGlo® LIPS Assay Buffer (supplied by Promega in the NanoGlo® Luciferase coupled assay kit). To reduce experimental costs, dilutions in TBST-0.15% (1:100; 1:150) was evaluated against loss of assay performance.

To confirm results, two independent experiments were conducted according to the optimised Nluc-ZnT8 LIPS protocol and included samples from the main optimisation sample set:

- 4 Internal ZnT8 RIA standards
- 6 Internal ZnT8 RIA controls (5 positive and 1 negative)
- 9 T1D patients
- 5 Healthy negative controls

The median LU gradually increased from 1:50 (Promega) to 1:100 and 1:150 substrate concentrations [1:50 median LU  $2.6 \times 10^5$  (range  $2.1 \times 10^4$ -  $2.0 \times 10^6$ ); 1:100 median LU  $2.9 \times 10^5$  (range  $2.4 \times 10^4$ - $2.5 \times 10^6$ ); 1:150 median LU  $3.1 \times 10^5$  (range  $2.6 \times 10^4$ - $2.1 \times 10^6$ )]. When independently ranked and compared, rank order of mean LU was substantially different (**Figure 4:19A**;  $p < 0.0001$ - $0.01$ ). However, there was no evidence of a difference in SNR when diluting the standard 1:50 [median SNR 6.9 (range 0.6-54.2)] further with TBST-0.15% at 1:100 [median SNR 6.6 (range 0.6-56.5)] or 1:150 [median SNR 6.6 (range 0.5-44.3)] (**Figure 4:19B**).

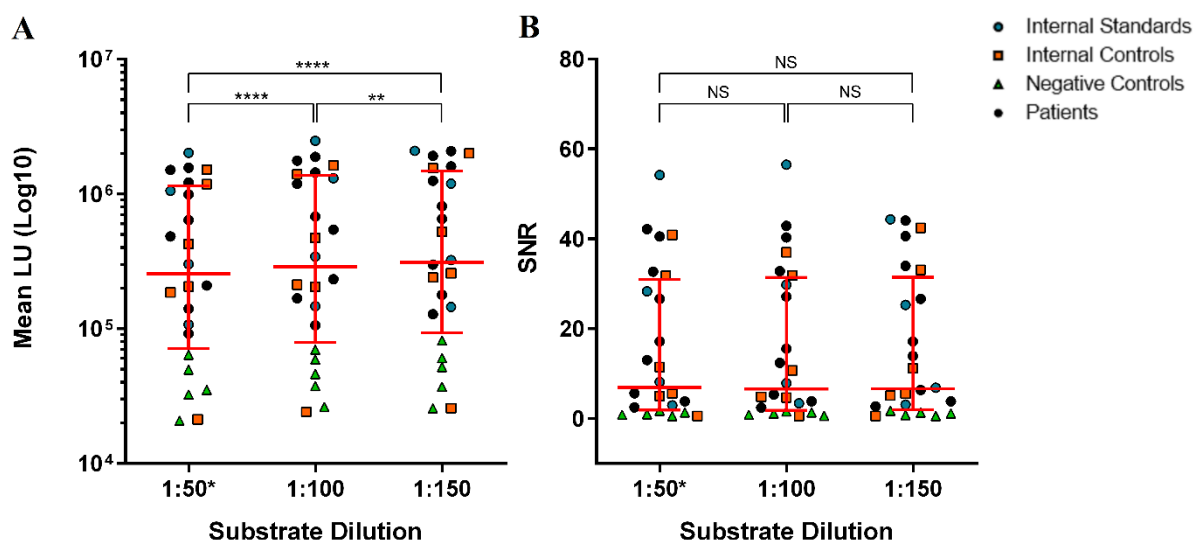


**Figure 4:19 – Nluc-ZnT8 LIPS Optimisation: Furimazine substrate concentration (LU/SNR)**

Plots of light units (LU; **A**) and signal to noise ratio (SNR; **B**) from investigating the Furimazine substrate concentration at the standard 1:50 (\* with NanoGlo® LIPS Assay Buffer supplied in the NanoGlo® Luciferase Assay System (Promega), 1:100 with TBST-0.15% and 1:150 with TBST-0.15%. The remainder of the optimised Nluc-ZnT8 LIPS protocol was followed. Each data point represents four replicates from two independent experiments. Red bars denote median and interquartile ranges. NS: Not Significant less than alpha value 0.05; \*\* $p < 0.01$ ; \*\*\*\* $p < 0.0001$  by pairwise Wilcoxon signed-rank tests.

**Experimental conclusion:** The standard Furimazine substrate concentration of 1:50 (Promega) can be diluted to 1:150 with TBST-0.15% without loss of ZnT8A binding or higher assay background.

#### 4.3.1.6.2 Substrate incubation length

To investigate the optimal Furimazine substrate incubation length with Nluc-R+W-ZnT8 dual heterodimer construct, the standard incubation length of 5-seconds was compared with 15-minutes and 60-minutes over two independent experiments. Wells were shaken for 5-seconds before LU detection (2secs/well). These assays included the full internal ZnT8 RIA standard curve (n=8) for AU determination and samples from the main optimisation sample set:

- 8 Internal ZnT8 RIA standards (AU determination)
- 6 Internal ZnT8 RIA controls (5 positive and 1 negative)
- 12 T1D patients
- 4 Anonymised healthy negative controls
- 13 Healthy blood donors

The median LU across substrate incubation lengths with the Nluc-R+W-ZnT8 dual heterodimer indicated a slightly biphasic pattern, increasing from 5-seconds [ $1.8 \times 10^5$  (range  $1.5 \times 10^4$ - $1.8 \times 10^6$ )] to 15-minutes [ $2.3 \times 10^5$  (range  $2.2 \times 10^4$ - $2.3 \times 10^6$ )] and marginally decreasing from 15-minutes to 60-minutes [ $2.3 \times 10^5$  (range  $2.1 \times 10^4$ - $2.3 \times 10^6$ )]. When independently ranked and compared, the rank order of mean LU was substantially different ( $p < 0.0001$ ) between all combinations (data not shown). The difference in rank may be explained by a small decrease in median SNR over greater incubation lengths; 5-seconds, 6.5 (range 0.5-63.3), 15-minutes, 5.7 (range 0.5-55.2), and 60-minutes 5.9 (range 0.5-58.2). When ranked, the SNR of samples between 5-seconds and 15/60-minutes was distinct ( $p < 0.0001$ ); however, the rank SNR between 15-minutes and 60-minutes was comparable ( $p > 0.05$ ) (**Figure 4:20**).

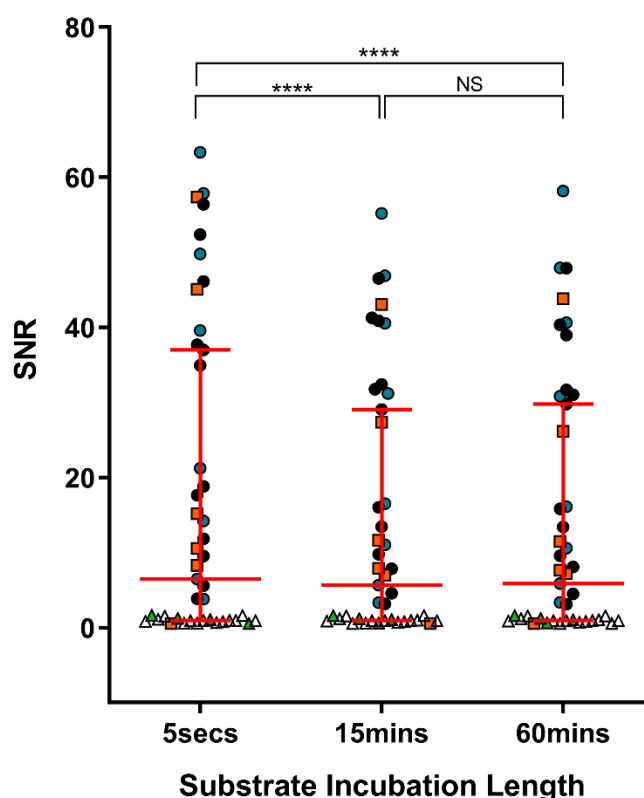


**Figure 4:20 – Nluc-ZnT8 LIPS Optimisation: Furimazine substrate incubation length with Nluc-R+W-ZnT8 dual heterodimer construct (SNR)**

A plot of signal to noise ratio (SNR) from investigating the Furimazine substrate incubation length at the standard 5 seconds with orbital shaking per well, 15 minutes with 5 seconds orbital shaking per well and 60 minutes with 5 seconds orbital shaking per well. The remainder of the optimised Nluc-ZnT8 LIPS protocol was followed. Each data point represents four replicates from two independent assays. Red bars denote median and interquartile ranges. NS: Not Significant less than alpha value 0.05; \*\*\*\* $p < 0.0001$  by pairwise Wilcoxon signed-rank tests.

There was some evidence of improved median CV between replicates between 5-seconds and a longer incubation duration on average; 5-seconds median CV 6.1% (range 0.5-44.3), 15-minutes median CV 5.4% (range 0.1-34.2) and 60-minutes median CV 5.4% (range 0.1-34.2) (**Table E:2; Appendix E**). This may suggest a longer incubation length improves replicate data for each sample (tested in duplicate) and thereby may reduce the repeat of samples due to poor replicates.

When calculated from a logarithmic standard curve, the rank AUs across all incubation lengths were comparable ( $p > 0.05$ ; **Figure 4:21**), which suggests that the differences in raw data observed (LU/SNR) do not substantially alter the standardised AU derived for each sample. Nevertheless, the minor differences in SNR and no difference in AU across incubation lengths reinforces that the Nluc:Furimazine bioluminescent reaction at 1:150 dilution remains chemically stable for at least 1 hour under the optimised Nuc-ZnT8 LIPS protocol.

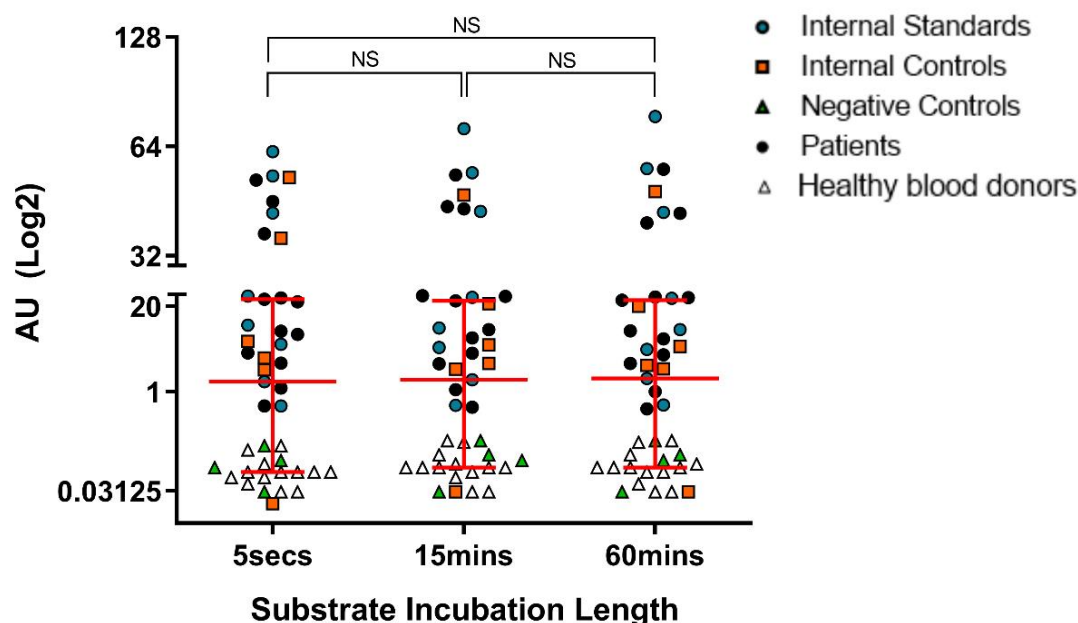


**Figure 4:21 – Nluc-ZnT8 LIPS Optimisation: Furimazine substrate incubation length with Nluc-R+W-ZnT8 dual heterodimer construct (AU)**

Plots of arbitrary units (AU) from investigating the Furimazine substrate incubation length at the standard 5 seconds with orbital shaking per well, 15 minutes with 5 seconds orbital shaking per well and 60 minutes with 5 seconds orbital shaking per well. The remainder of the optimised Nluc-ZnT8 LIPS protocol was followed. Each data point represents four replicates from two independent assays. Red bars denote median and interquartile ranges. NS: Not Significant less than alpha value 0.05 by pairwise Wilcoxon signed-rank tests.

When analysing the logarithmic curve fit from the standard curves obtained in the two experiments, there was evidence of a greater curve fit ( $>95\% R^2$ ; **Figure 4:22**) and, in most cases, improved intra- and inter-assay variability (lower CV%) obtained in longer incubation lengths, suggesting that a longer substrate incubation length may reduce the assay variability between sample duplicates and over multiple experiments. This is particularly important in obtaining an accurate and reproducible standard curve to generate AUs for positivity determination.

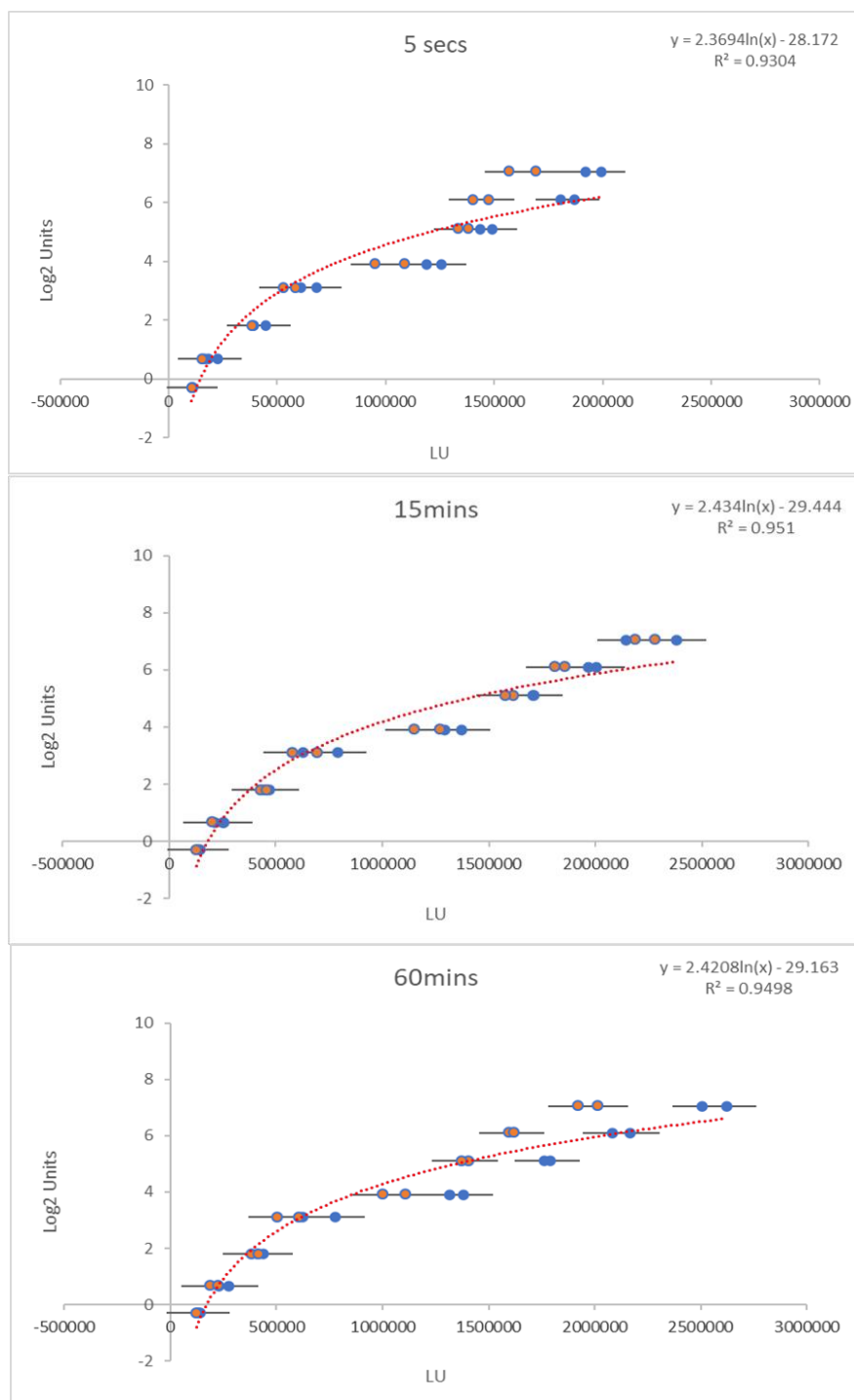


**Figure 4:22 – Nluc-ZnT8 LIPS Optimisation: Logarithmic standard curve fit according to substrate incubation length (Log2 units)**

Plots of internal ZnT8 standards (n=8) set against its Log2 units by Furimazine substrate incubation length. Red dotted line: logarithmic curve fit for four replicates obtained in two independent experiments; Orange dots: experiment 1 duplicates; Blue dots: experiment 2 duplicates; horizontal error bars denote standard error of the mean. The standard error of the mean within each experiment was reduced between duplicates (intra-assay) and inter-assay variation was improved ( $R^2 > 95\%$ ) in both experiments in substrate incubations lengths greater than 5 seconds. The 15-minute incubation length shows the lowest variation with overlapping points across both experiments. Incubations of 5 seconds and 15 minutes were further investigated during assay validation in a large cohort as 60-minute incubations would reduce the ability to conduct this assay in 1-day and in a high-throughput capacity.

**Experimental conclusion:** The bioluminescent signal of Nluc and Furimazine diluted at 1:150 remains chemically stable up to 1hr under the optimised conditions of the Nluc-ZnT8 LIPS assay. The AUs derived from the full logarithmic standard curve indicated no differences between substrate incubations lengths when independently ranked. Nonetheless, a substrate incubation length greater than the standard 5 seconds produced better replicate data, a greater logarithmic curve fit, and improved AU discrimination of the top 3 standards with very little difference in AU of the negative population. As a 60-minute substrate incubation length would drastically reduce the ability to conduct the Nluc-ZnT8 LIPS assay in 1-day and in a high-throughput capacity, the 5-second- and 15-minute incubations were assessed in a bigger sample cohort during assay validation to fully assess the potential benefit of a longer substrate incubation length.

### 4.3.1.7 Summary of Nluc-ZnT8 LIPS assay optimisation

Portion of Assay	Nluc-GAD65 LIPS Protocol	Optimised Nluc-ZnT8 LIPS Protocol
<b>Expression of Nluc-antigen</b>	<ul style="list-style-type: none"> <li>Reaction mix incubated for 1.5 hours at 30°C.</li> <li>Nluc-Ag was purified using NAP5™ desalting columns &amp; TBST-0.5% buffer.</li> </ul>	<ul style="list-style-type: none"> <li>Reaction mix incubated for 2 hours at 30°C.</li> <li>Nluc-Ag is serially diluted in PBST with 0.1% Tween without need for column purification.</li> </ul>
<b>Preparation of Nluc-antigen</b>	<ul style="list-style-type: none"> <li>10µl Nluc-Ag aliquots are thawed &amp; diluted in TBST-0.5% at RT to <math>3.8 \times 10^6</math> – <math>4.2 \times 10^6</math>.</li> </ul>	<ul style="list-style-type: none"> <li>10µl Nluc-Ag aliquots are thawed, diluted 1:100 with TBST-0.5% &amp; filtered through a 0.45µM filter unit.</li> <li>Filtered Nluc-Ag is diluted in TBST-0.15% at RT to <math>3.8 \times 10^6</math> – <math>4.2 \times 10^6</math>.</li> </ul>
<b>Precipitating immunocomplexes</b>	<ul style="list-style-type: none"> <li>6.25µl/well PAS; 25% suspension washed 4 times in TBST-0.5%.</li> </ul>	<ul style="list-style-type: none"> <li>6.25µl/well PAS; 25% suspension washed 4 times in TBST-BSA.</li> </ul>
<b>Detecting luminescence</b>	<ul style="list-style-type: none"> <li>Substrate: 40µl/well; 1:50 Furimazine substrate diluted in NanoGlo® LIPS Assay Buffer (Promega).</li> <li>Detection: Read 5-seconds after substrate injection at 2s/well.</li> </ul>	<ul style="list-style-type: none"> <li>Substrate: 40µl/well; 1:50 furimazine substrate in NanoGlo® LIPS Assay Buffer (Promega) further diluted 1:3 with TBST-0.15% for an end concentration of 1:150.</li> <li>Assay sensitivity &amp; specificity was further evaluated at substrate incubations lengths of 5-seconds (standard) &amp; 15-minutes using new-onset T1D &amp; healthy schoolchildren during assay validation.</li> </ul>

Table 4:10 – Summary of Nluc-ZnT8 LIPS assay optimisation

---

### 4.3.2 Aim 2: Investigate reagents to improve ZnT8A detection in EDTA-preserved plasma samples using the LIPS method.

---

#### 4.3.2.1 Serum ZnT8A detection in the presence of EDTA with CaCl<sub>2</sub> or ZnCl<sub>2</sub>

---

The treatment of EDTA-plasma samples with calcium chloride (CaCl<sub>2</sub>) have previously been investigated for GADA and IA-2A detection in RSR<sup>TM</sup> Limited ELISA bridge-type ELISAs. Treated CaCl<sub>2</sub>-plasma had high and comparable sensitivity to detection in serum, and detection was higher by ELISA than RIA (359). To investigate whether some ZnT8A binding can be restored in the presence of EDTA as a proof of principle for EDTA-preserved plasma, serum was incubated with Nluc-R+W-ZnT8 dual heterodimer antigen in TBST-0.15% buffer containing 1mM EDTA in the absence or presence of 1mM, 5mM, or 10mM CaCl<sub>2</sub> or zinc chloride (ZnCl<sub>2</sub>, considering ZnT8's function) in two independent experiments. A 1mM EDTA concentration was selected to mimic the estimated concentration of EDTA present in 1µl of sample as 1-2mg/ml EDTA is typically added to 3-5ml of whole blood at sample collection. The two independent experiments included samples from the main optimisation sample set (below) and were conducted before substrate dilution and incubation length optimisation experiments.

- 4 Internal ZnT8 RIA standards
- 6 Internal ZnT8 RIA controls
- 9 T1D patients
- 4 Anonymised healthy negative controls

Overall, the median LU binding and SNR was substantially decreased in the presence of 1mM EDTA in the Nluc-R+W-ZnT8 dual heterodimer antigen incubation TBST-0.15% ( $p < 0.0001$ ), irrespective of the presence of CaCl<sub>2</sub> or ZnCl<sub>2</sub> at concentrations of 1mM, 5mM, or 10mM ( $p < 0.0001$ ) (**Figure 4:23A/B**).

Both LU and SNR was utilised to interrogate the data as LU gives a better impression of the overall effects across all levels of ZnT8A binding and SNR considers the ratio between ZnT8A binding and assay background.

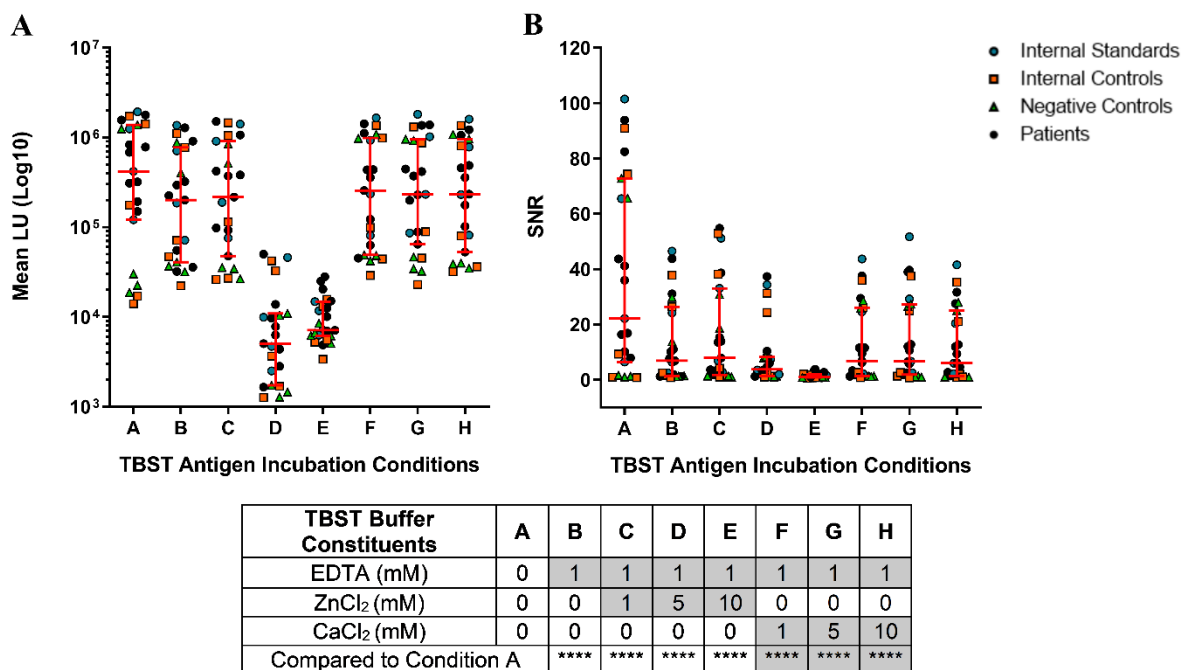


**Figure 4:23 – Nluc-ZnT8 LIPS: Serum ZnT8A detection in the presence of EDTA with & without CaCl<sub>2</sub> or ZnCl<sub>2</sub> (LU/SNR)**

Plots of light units on a Log<sub>10</sub> scale (LU; **A**) and signal to noise ratio (SNR; **B**) from investigating the presence of 1mM EDTA in the absence or presence of 1mM, 5mM or 10mM CaCl<sub>2</sub> or ZnCl<sub>2</sub> during sample incubation with Nluc-R+W-ZnT8 dual heterodimer antigen in TBST-0.15%. Each data point represents four replicates from two independent assays. These assays were conducted before optimising the Furimazine substrate dilution and incubation length (bioluminescence detection). The remainder of the optimised Nluc-ZnT8 LIPS protocol was followed. Red bars denote median and interquartile ranges. \*\*\*\*p<0.0001 by pairwise Wilcoxon signed-rank tests.

The presence of 1mM EDTA alone reduced the median LU by 47.8% from 4.2x10<sup>5</sup> (range 1.4x10<sup>4</sup>-1.9x10<sup>6</sup>) to 2.0x10<sup>5</sup> (range 2.2x10<sup>4</sup>-1.4x10<sup>6</sup>) and median SNR by 31.0% from 22.1 (range 0.7-101.5) to 6.8 (range 0.8-46.5). The presence of EDTA not only decreased the ability of ZnT8A to bind ZnT8 in T1D patients but also increased assay background in the negative controls. Due to this, the discrimination between T1D patients with low-level ZnT8A and negative controls was particularly diminished, explaining the SNR reduction.

## Chapter 4 - Development of Nluc-ZnT8 LIPS for ZnT8A detection

In the presence of 1mM EDTA, the addition of 1mM, 5mM, or 10mM CaCl<sub>2</sub> did little to recover any ZnT8A binding [1mM median LU  $2.6 \times 10^5$  (range  $2.9 \times 10^4$ -  $1.7 \times 10^6$ ); 5mM median LU  $2.3 \times 10^5$  (range  $2.3 \times 10^4$ -  $1.8 \times 10^6$ ); 10mM median LU  $2.3 \times 10^5$  (range  $3.2 \times 10^4$ -  $1.6 \times 10^6$ )] relative to the assay background [1mM median SNR 6.8 (range 0.8-43.6); 5mM median SNR 6.6 (range 0.7-51.7); 10mM median SNR 6.1 (range 0.8-41.5)].

In the presence of 1mM EDTA, the addition of 1mM ZnCl<sub>2</sub> but not, 5mM, or 10mM appeared to recover some ZnT8A binding [1mM median LU  $2.2 \times 10^5$  (range  $2.6 \times 10^4$ - $1.5 \times 10^6$ ); 5mM median LU  $5.0 \times 10^3$  (range  $1.3 \times 10^3$ - $5.0 \times 10^4$ ); 10mM median LU  $7.1 \times 10^3$  (range  $3.4 \times 10^3$ - $2.8 \times 10^4$ )] relative to the assay background [1mM median SNR 7.9 (range 1.0-54.7); 5mM median SNR 3.7 (range 0.9-37.3); 10mM median SNR 0.9 (range 0.4-3.7)].

**Experimental conclusion:** The presence of 1mM EDTA reduced the binding of ZnT8A in all ZnT8A positive serum samples and increased the assay background in negative controls. Despite the reduction in ZnT8A binding, patients with high levels of ZnT8A can still be identified in the presence of EDTA, but the ability to discriminate low-level ZnT8A positive patients from negative controls is diminished. The presence of 1mM ZnCl<sub>2</sub> offered the best improvement against the effects of EDTA out of all the tested conditions. Therefore, 1mM ZnCl<sub>2</sub> was selected to investigate ZnT8A binding in the anonymised matched serum and EDTA-preserved plasma samples.

### **4.3.2.2 Serum & plasma ZnT8A detection in the presence of 1mM ZnCl<sub>2</sub>**

To investigate whether the addition of 1mM ZnCl<sub>2</sub> in the Nluc-R+W-ZnT8 dual heterodimer antigen incubation TBST-0.15% buffer can improve ZnT8A detection in either serum or EDTA-preserved plasma samples, samples from the optimisation population and a subset (n=19 of 27) of the BOX participants with matched serum and EDTA-preserved samples were selected and tested in two independent experiments.

#### **4.3.2.2.1 1mM ZnCl<sub>2</sub> in serum (main optimisation sample set)**

The two independent experiments included the full internal logarithmic RIA ZnT8A standard curve (n=8) for AU determination and samples from the main optimisation sample set (below). These experiments were conducted before substrate dilution and incubation length optimisation experiments.

- 8 Internal ZnT8 RIA standards (AU determination)
- 6 Internal ZnT8 RIA controls (5 positive and 1 negative)
- 9 T1D patients
- 5 Anonymised healthy negative controls

Overall, the median LU binding and SNR was substantially decreased in the presence of 1mM ZnCl<sub>2</sub> in the Nluc-R+W-ZnT8 dual heterodimer antigen incubation TBST-0.15% buffer (both  $p < 0.0001$ ). The presence of 1mM ZnCl<sub>2</sub> reduced the median SNR from 12.5 (range 0.6-62.4) to 4.43 (range 0.8-47.2) (**Figure 4:24**). The presence of 1mM ZnCl<sub>2</sub> in serum not only decreased the ability of ZnT8A to bind ZnT8 in T1D patients but also increased assay background in the negative controls. Due to this, there was a decreased ability to identify between T1D patients (particularly those with low-level ZnT8A) and healthy controls.

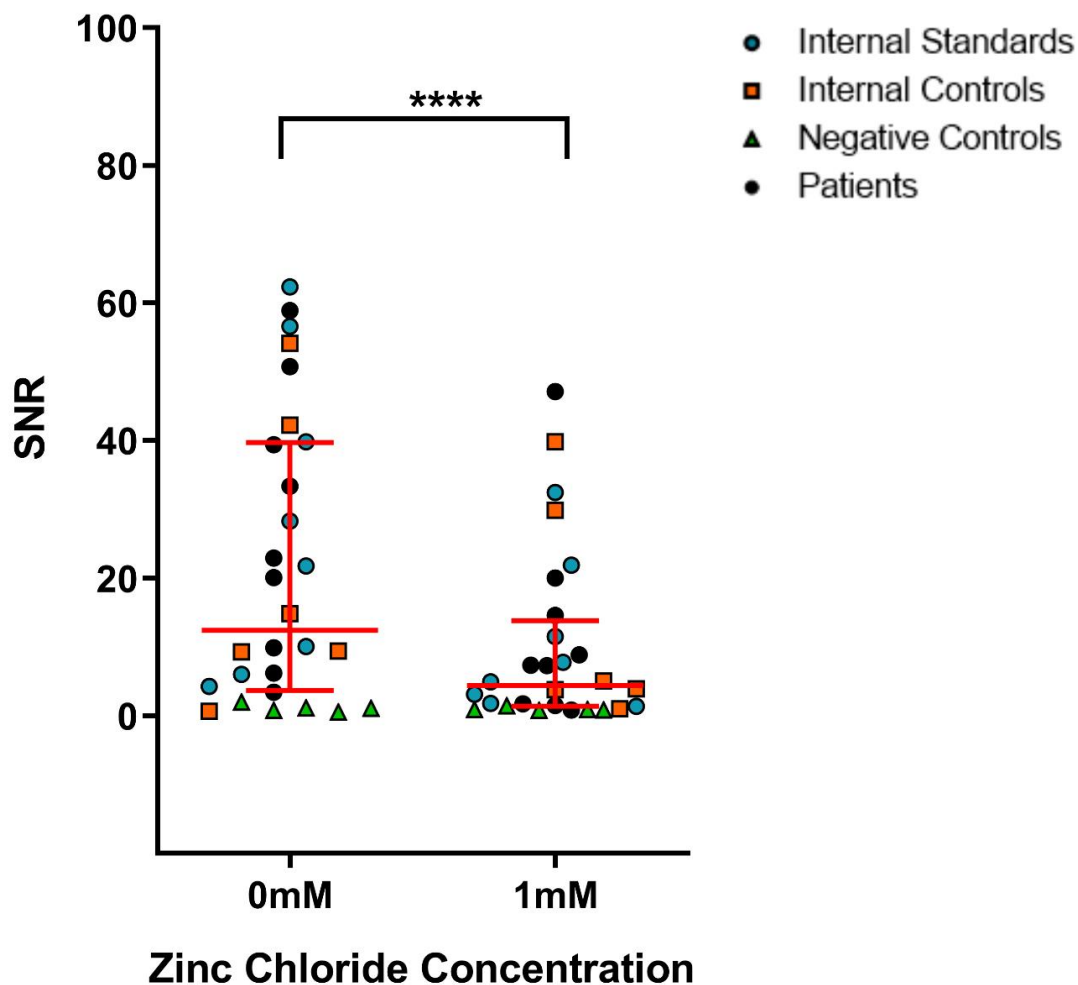


*Figure 4:24 – Nluc-ZnT8 LIPS: Serum ZnT8A detection in the presence of 1mM ZnCl<sub>2</sub> (SNR)*

A plot of signal to noise ratio (SNR) from investigating the presence of 1mM ZnCl<sub>2</sub> during sample incubation with Nluc-R+W-ZnT8 dual heterodimer antigen in TBST-0.15% buffer. Each data point represents four replicates from two independent assays. These assays were conducted before optimising the Furimazine substrate dilution and incubation length (bioluminescence detection). The remainder of the optimised Nluc-ZnT8 LIPS protocol was followed. Red bars denote median and interquartile ranges. \*\*\*\*p<0.0001 by pairwise Wilcoxon signed-rank tests.

Despite the reduction in median LU and SNR, there was some evidence to suggest that the presence of 1mM ZnCl<sub>2</sub> may better separate the logarithmic standard curve with slightly improved the curve fit and median AU determination overall (p=0.028, **Figure 4:25**). However, there may be the potential for false positives and false negatives within the healthy negative and T1D patient populations, respectively.

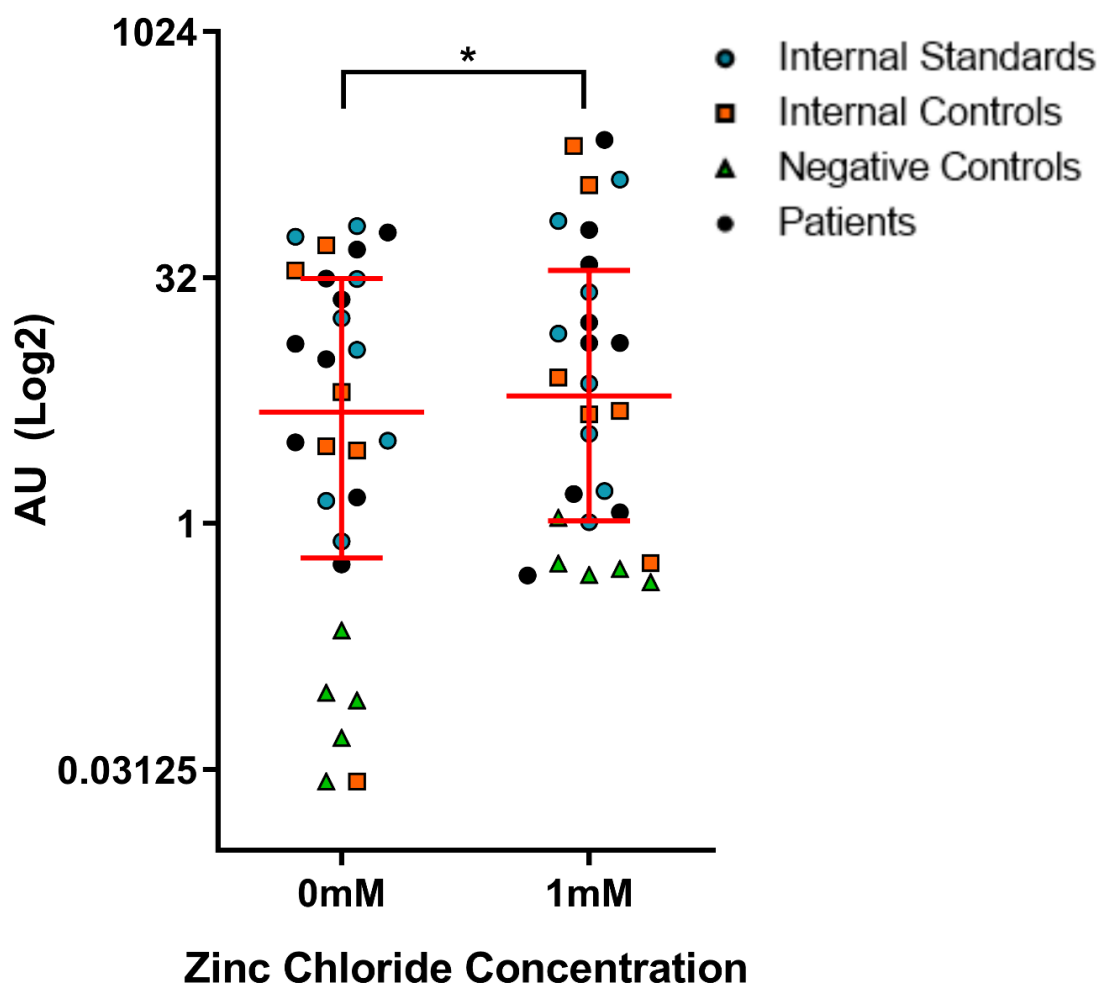


*Figure 4:25 – Nluc-ZnT8 LIPS: Serum ZnT8A detection in the presence of 1mM ZnCl<sub>2</sub> (AU)*

A plot of arbitrary units (AU) on a Log<sub>2</sub> scale investigating the presence of 1mM ZnCl<sub>2</sub> during sample incubation with Nluc-R+W-ZnT8 dual heterodimer antigen in TBST-0.15% buffer. Each data point represents four replicates from two independent assays. These assays were conducted before optimising the Furimazine substrate dilution and incubation length (bioluminescence detection). The remainder of the optimised Nluc-ZnT8 LIPS protocol was followed. Red bars denote median and interquartile ranges. \*p=0.028 by pairwise Wilcoxon signed-rank tests.

**Experimental conclusion:** The presence of 1mM does not appear to improve the discrimination between T1D patients and healthy negative controls or overall assay performance. There was some suggestion that the ZnT8A binding in select samples and curve fit to the internal ZnT8 RIA logarithmic standard curve may generally improve with 1mM ZnCl<sub>2</sub>, but as the assay background was higher, this may compromise the false positive/negative determination in T1D patient and healthy populations.

#### **4.3.2.2.2 1mM ZnCl<sub>2</sub> in matched serum & EDTA-preserved plasma samples**

To investigate whether the addition of 1mM ZnCl<sub>2</sub> in the Nluc-R+W-ZnT8 dual heterodimer antigen incubation TBST-0.15% buffer can improve ZnT8A detection in plasma compared with serum, a subset of the BOX matched serum, and EDTA-preserved samples were selected (n=19 out of 27; 11 positive for  $\geq 1$  autoantibody; 3 ZnT8A positive) and tested in two independent experiments. These experiments were conducted before substrate dilution and incubation length optimisation experiments. Both LU and SNR was utilised to interrogate the data as LU gives a better impression of the overall effects across all levels of ZnT8A binding, and SNR considers the ratio between ZnT8A binding and assay background.

Replicating the findings from investigating 1mM ZnCl<sub>2</sub> in serum samples from the main optimisation sample set, the presence of 1mM ZnCl<sub>2</sub> decreased the median LU from  $2.5 \times 10^4$  (range  $1.1 \times 10^4$ - $1.4 \times 10^6$ ) to  $1.3 \times 10^4$  (range  $7.3 \times 10^3$ - $2.1 \times 10^5$ ) ( $p < 0.0001$ , **Figure 4:26A**). When ranked and compared, the median SNR was not different ( $p > 0.05$ ) between the absence [median 0.9 (range 0.4-49.0)] or presence [median 1.5 (range 0.8-23.8)] of 1mM ZnCl<sub>2</sub> which indicates a parallel decrease in binding across all samples (**Figure 4:26B**).

In the matched EDTA-preserved plasma samples, the presence of 1mM ZnCl<sub>2</sub> increased both the median LU from  $3.6 \times 10^4$  (range  $1.4 \times 10^4$ - $1.1 \times 10^6$ ) to  $1.1 \times 10^5$  ( $2.4 \times 10^4$ - $7.5 \times 10^5$ ) and the median SNR from 1.3 (range 0.5-37.6) to 12.7 (2.8-85.6) ( $p < 0.0001$ , **Figure 4:26A/B**).

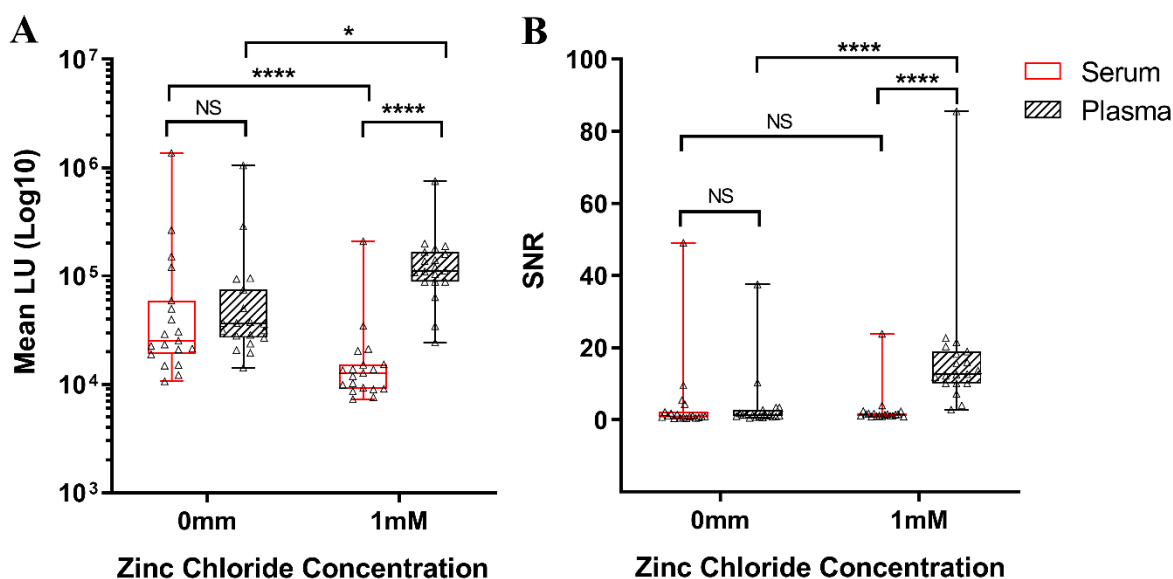
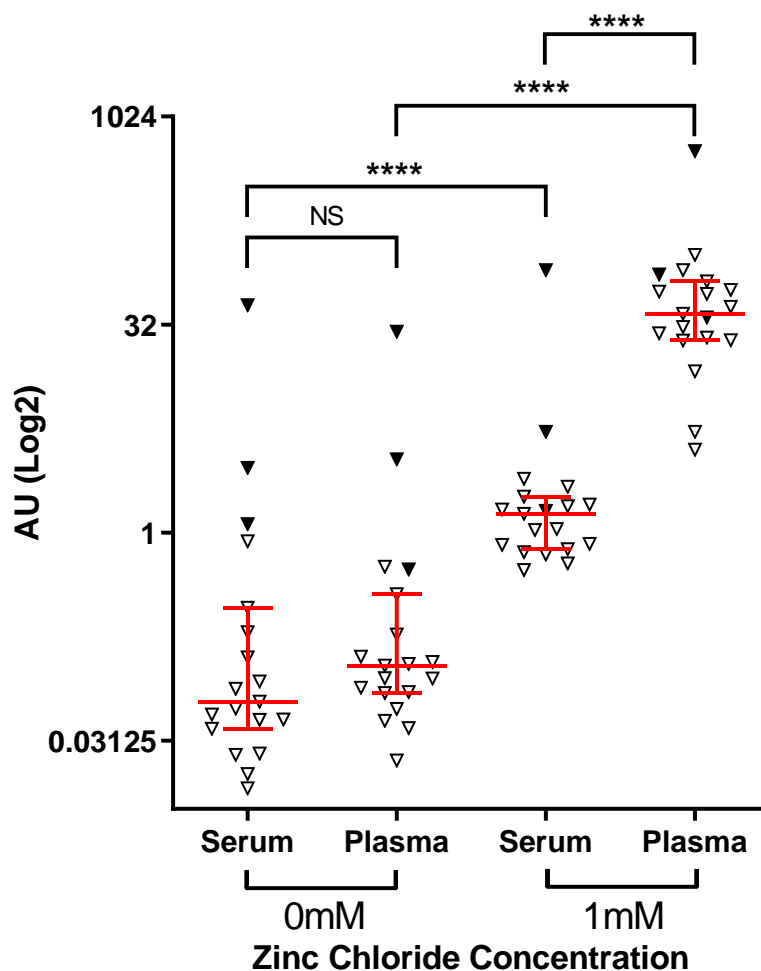


Figure 4:26 – Nluc-ZnT8 LIPS: Matched serum & plasma ZnT8A detection in the presence of 1mM ZnCl<sub>2</sub> (LU/SNR)

Plots of light units on a Log<sub>10</sub> scale (LU; **A**) and signal to noise ratio (SNR; **B**) from investigating the presence of 1mM ZnCl<sub>2</sub> during sample incubation with Nluc-R+W-ZnT8 dual heterodimer antigen in TBST-0.15% buffer. Each data point represents four replicates from two independent assays. These assays were conducted before optimising the Furimazine substrate dilution and incubation length (bioluminescence detection). The remainder of the optimised Nluc-ZnT8 LIPS protocol was followed. Red and black bars denote median and interquartile ranges. NS; Not significant; \* $p < 0.05$  ( $p = 0.018$ ); \*\*\*\* $p < 0.0001$  by pairwise Wilcoxon signed-rank tests.

When applied to a logarithmic standard curve, the increased LU binding and SNR gained from the presence of 1mM ZnCl<sub>2</sub> did not produce superior AU determination compared to standard conditions but compromised the ability to detect ZnT8A positives from ZnT8A negatives with a reduced range of detection. The AUs between matched serum and plasma under standard assay conditions was comparable overall, but in one individual with lower-level ZnT8A by RIA, positivity in plasma would likely be lost by Nluc-ZnT8 LIPS ( $p > 0.05$ ; **Figure 4:27**).



*Figure 4:27 – Nluc-ZnT8 LIPS: Matched serum & plasma ZnT8A detection in the presence of 1mM ZnCl<sub>2</sub> (AU)*

A plot of arbitrary units (AU) from investigating the presence of 1mM ZnCl<sub>2</sub> during sample incubation with Nluc-R+W-ZnT8 dual heterodimer antigen in TBST-0.15% buffer. Each data point represents four replicates from two independent assays. These assays were conducted before optimising the Furimazine substrate dilution and incubation length (bioluminescence detection). The remainder of the optimised Nluc-ZnT8 LIPS protocol was followed. Black filled triangles denote ZnT8A positive samples by RIA; Clear triangles denote ZnT8A negative samples by RIA; Red and black bars denote median and interquartile ranges. NS; Not significant; \*\*\*\*p<0.0001 by pairwise Wilcoxon signed-rank tests.

**Experimental conclusion:** The presence of 1mM ZnCl<sub>2</sub> did not increase the ability to detect ZnT8A positivity in EDTA-preserved plasma samples. Despite the improved median LU binding and SNR in EDTA-preserved plasma samples compared with serum samples, the AU determined by a full logarithmic standard curve showed that 1mM ZnCl<sub>2</sub> did not result in improved ZnT8A detection between positive and negative samples. For both EDTA-treated serum and EDTA-preserved plasma samples, the standard protocol (without ZnCl<sub>2</sub>) offers the most optimal conditions for ZnT8A detection.

### 4.3.3 Aim 3: Establish a serum positivity threshold for the optimised Nluc-ZnT8 LIPS method

Samples (n=521) with sufficient sample volume from 523 healthy schoolchildren that were used to establish the in-house ZnT8R/ZnT8W RIA thresholds were used to establish the Nluc-ZnT8 LIPS positivity threshold. Of 523, 504/506 (99.6%) RIA ZnT8A negatives and 17/17 (100.0%) RIA ZnT8A positives were tested in Nluc-ZnT8 LIPS. Samples were tested concurrently at substrate incubation lengths of 5-seconds and 15-minutes to evaluate the differences in AU derived at the 97.5<sup>th</sup> and 99 percentiles (**Table 4:11**).

Assay	n	AU at the 97.5 <sup>th</sup> percentile (n positive)	AU at the 99 <sup>th</sup> percentile (n positive)
ZnT8R RIA	523	1.8 (14)	2.2 (6)
ZnT8W RIA	523	1.8 (11)	2.1 (5)
ZnT8R/ZnT8W RIA	523	1.8 (17)	2.2 (8)
Nluc-ZnT8 LIPS 5-second substrate incubation length	521	0.22 (14)	0.28 (6)
Nluc-ZnT8 LIPS 15-minute substrate incubation length	521	0.30 (15)	0.54 (6)

*Table 4:11 – Positivity thresholds for monomeric ZnT8R/ZnT8W RIAs & Nluc-ZnT8 LIPS*

Comparing the AUs derived from the same logarithmic standard curve between monomeric ZnT8R/ZnT8W RIAs (maximum AU) and Nluc-ZnT8 LIPS suggested that there was slightly better correlation with a substrate incubation length of 15-minutes [ $r$  (95% CI) = 0.55 (0.48-0.61),  $p < 0.0001$ ], than 5-seconds [ $r$  (95% CI) = 0.46 (0.39-0.53),  $p < 0.0001$ ] (**Figure 4:28A/C**). However, Bland-Altman analysis revealed that only 2/521 healthy schoolchildren (0.4%) were outside the 95% CI of agreement which was concurrent between substrate incubation lengths (**Figure 4:28B/D**). This suggests that whilst the 15-minute incubation length may improve the correlation with RIA, the differences in AU between substrate incubation lengths are marginal (n=519; 99.6% concordance).

Despite only two discrepant samples by Bland-Altman analysis, there are discrepancies in sample positivity between Nluc-ZnT8 LIPS and the monomeric RIAs (table in **Figure 4:28**). At the 97.5<sup>th</sup> percentile, of 17 RIA ZnT8A positives, only 5 (29.4%) and 6 (35.3%) were identified as positive in LIPS in substrate incubation lengths of 5 seconds and 15-minutes, respectively. At the 99<sup>th</sup> percentile, of 8 RIA ZnT8A positives, 4 (50.0%) were identified as positive in LIPS at either substrate incubation length. In the 504 ZnT8A RIA negatives defined by the 97.5<sup>th</sup> percentile, 495 (98.2%) were confirmed negative, but 9 (1.8%) were positive in LIPS (concurrent between substrate incubation lengths). Similarly, of the 513 RIA ZnT8A negatives defined by the 99<sup>th</sup> percentile, 511 (99.6%) were confirmed negative, but 2 (0.4%) were positive in LIPS, which was also concurrent between substrate incubation lengths.

Overall, a total of 20-21 (3.8-4.0% of 521) samples at the 97.5<sup>th</sup> percentile and 6 (1.2% of 521) at the 99<sup>th</sup> percentile was discrepant between RIA and LIPS over both substrate incubation lengths. This suggests that most of the discrepant samples at the 97.5<sup>th</sup> percentile are of low-level AU. The substrate incubation length did not heavily influence the outcome of the positivity threshold. Only 1 additional ZnT8A RIA positive sample was identified positive in LIPS which was found in the incubation length of 15-minutes but not 5-seconds at the 97.5<sup>th</sup> percentile but otherwise were identical.

**Experimental conclusion:** Positivity percentiles are heavily influenced by the level gained in the positive population and the discrepant samples prevent the direct comparison between assays. While there was no substantial evidence suggesting that the substrate incubation length influenced the positivity threshold, due to better intra- and inter-assay variation, both substrate incubations lengths were evaluated for the condition that offered the maximum sensitivity and specificity.

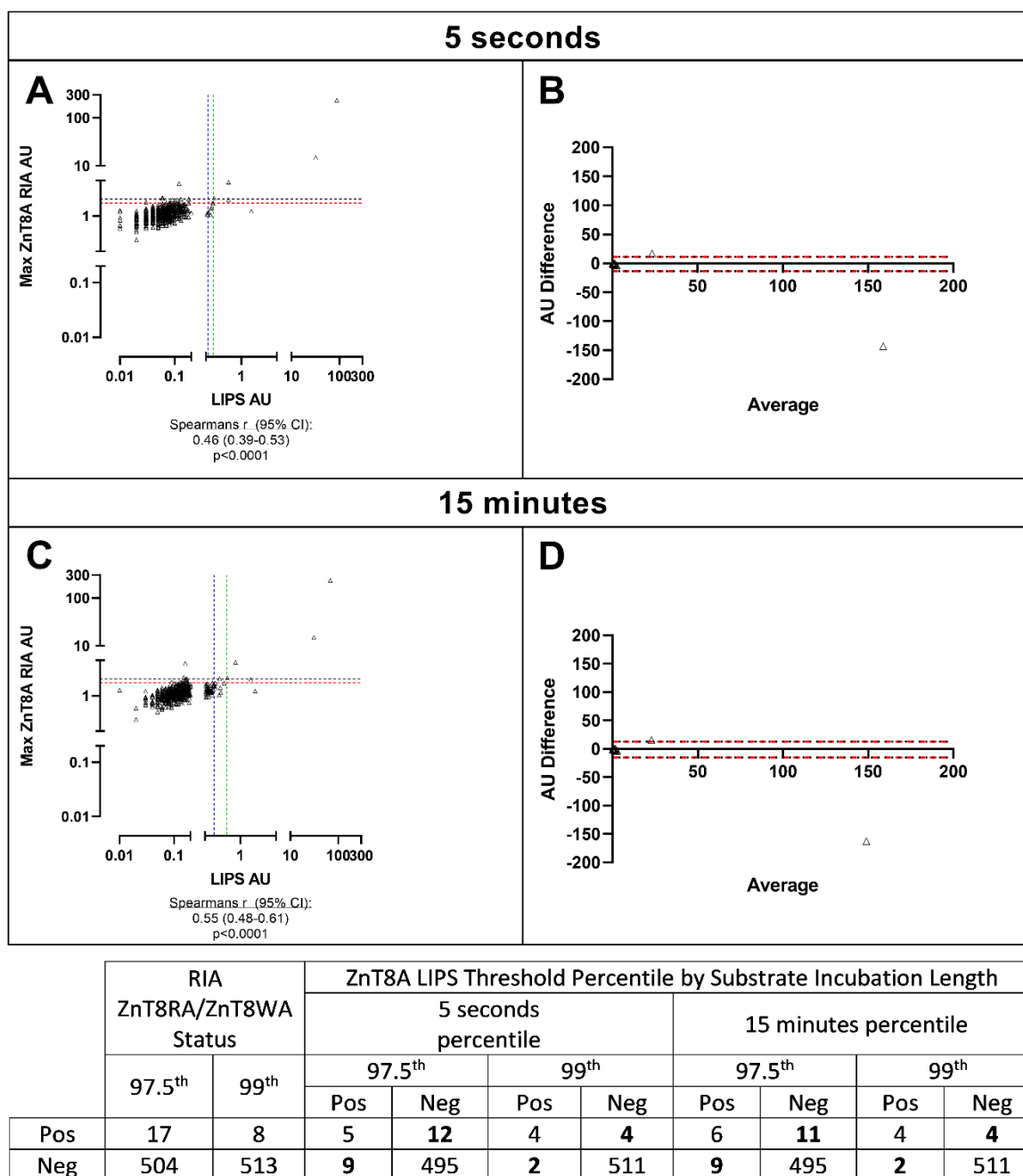


**Figure 4:28 – Nluc-ZnT8 LIPS Validation: Establishing a positive threshold in a cohort of healthy schoolchildren**

Scatter plots and Bland-Altman plots for Furimazine substrate incubation lengths of 5 seconds (A/B, respectively) and 15 minutes (C/D, respectively) in 521 healthy schoolchildren. Red and black dashed lines on A/C denote the ZnT8RA/ZnT8WA RIA 97.5<sup>th</sup> and 99<sup>th</sup> percentiles, respectively. Blue and green dashed lines on A/C denote the Nluc-ZnT8 LIPS 97.5<sup>th</sup> and 99<sup>th</sup> percentiles, respectively. Red dashed lines on B/D denote the 95% confidence intervals of agreement by Bland-Altman analysis. A substrate incubation length of 15 minutes showed a slightly higher correlation with RIA (55%) than 5 seconds (46%), both  $p < 0.0001$ . Bland-Altman analysis identified 2 samples outside the 95% confidence intervals of agreement in both substrate incubation lengths. At the 97.5<sup>th</sup> percentile in RIA and LIPS, 20 and 21 discrepant samples were identified at 5 seconds and 15-minute substrate incubation lengths, respectively (highlighted in bold). At the 99<sup>th</sup> percentile in RIA and LIPS, 6 discrepant samples were identified in both substrate incubation lengths suggesting, the discrepant samples at the 97.5<sup>th</sup> percentile are of low-level AU.

---

#### 4.3.4 Aim 4: Evaluate the sensitivity and specificity of the optimised Nluc-ZnT8 LIPS method using new-onset T1D patients from BOX and blinded samples from the IASP2020 workshop

---

##### 4.3.4.1 The sensitivity of Nluc-ZnT8 LIPS compared with RIA in new-onset T1D patients

---

To further evaluate the potential benefit of longer Furimazine substrate lengths (5-seconds versus 15-minutes) and a higher positivity threshold (97.5<sup>th</sup> versus 99<sup>th</sup> percentile) in the Nluc-ZnT8 LIPS assay, assay sensitivity was assessed between RIA and LIPS in 573 new-onset T1D patients from the BOX study.

At both a 5-second and 15-minute substrate incubation length, derived AUs showed high and near identical, correlation with the maximum RIA AUs [5-seconds  $r$ : 0.89 (0.87-0.90); 15-minutes  $r$ : 0.90 (0.89-0.91); both  $p < 0.0001$ ]. This suggests very little difference in AUs derived between the substrate incubations lengths (**Figure 4:29A/C**).

The sensitivity of positivity thresholds between RIA and LIPS assays by substrate incubation length were compared at the 97.5<sup>th</sup> [1.8AU RIA versus 0.22AU (5-seconds)/0.30AU (15-minutes) LIPS] and 99<sup>th</sup> [2.15AU RIA versus 0.28AU (5-seconds)/0.54AU (15-minutes) LIPS] percentiles. At the 97.5<sup>th</sup> percentile, both substrate incubation lengths in LIPS had equal sensitivity, identifying 365/387 new-onset T1D patients (94.3%) found positive by RIA (**Figure 4:29A/C**). At the 99<sup>th</sup> percentile, the sensitivity of LIPS was reduced through the loss of 7 [358/387 (92.5%)] and 11 [354/387 (91.5%)] RIA positive new-onset T1D patients for the 5-second and 15-minute substrate incubation lengths, respectively (**Figure 4:29B/D**). Therefore, to capture most of the new-onset T1D patients found positive by RIA, the 97.5<sup>th</sup> percentile was preferable to the 99<sup>th</sup> percentile.

#### Chapter 4 - Development of Nluc-ZnT8 LIPS for ZnT8A detection

Of 387 new-onset T1D patients found positive by RIA at the 97.5<sup>th</sup> percentile, 22 (5.7%) and 23 (5.9%) were not identified by LIPS in the 5-second and 15-minute substrate incubation lengths, respectively. However, in the 186 new-onset T1D patients found negative by RIA, the LIPS assay identified an additional 32 (17.2%) and 30 (16.1%) patients in the 5-second and 15-minute substrate incubation lengths, respectively. Combined, the proportion of new-onset T1D patients found negative by RIA and LIPS was comparable for both substrate incubation lengths [5-seconds (154/186, 82.8%); 15-minutes (155/186, 83.3%)]. Collectively, there was very little difference in overall assay sensitivity between substrate incubation lengths; a total of 397/395 was identified as positive, and 176/178 was identified as negative in substrate incubation lengths of 5-seconds and 15-minutes, respectively.

Additionally, levels of ZnT8A (AU) captured by RIA or LIPS were not correlated with age-at-onset (RIA  $r$  0.01 (95% CI: -0.07-0.1); LIPS  $r$  0.02 (95% CI: -0.06-0.1); both  $p > 0.05$ , data not shown).

**Conclusion:** To capture the majority of new-onset T1D patients found positive by RIA, favour assay harmonisation with other Nluc- LIPS assays, and omit a time-consuming step in the assay that does not greatly benefit assay sensitivity, the 97.5<sup>th</sup> percentile at a substrate incubation length of 5-seconds (0.22AU) was selected for full assay validation assessment in IASP2020 and FDRs from the BOX study.

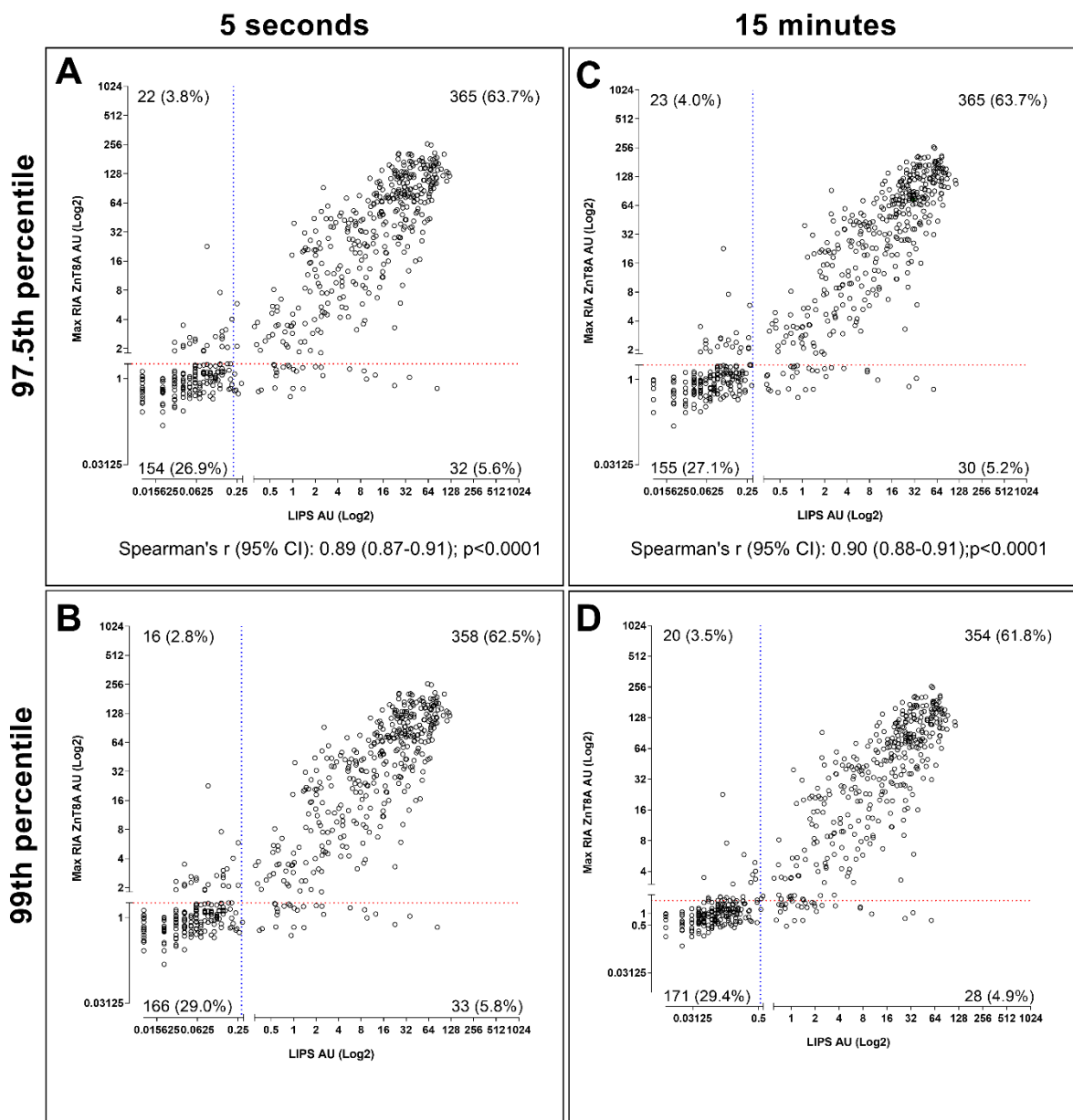


**Figure 4:29 – Nluc-ZnT8 LIPS Validation: ZnT8A level & positivity in new-onset T1D patients measured by LIPS & RIA by percentile positivity thresholds (97.5<sup>th</sup>/99<sup>th</sup>) & Furimazine substrate incubation length in LIPS**

Scatter plots of ZnT8A AU levels on a Log2 scale and positivity thresholds at 97.5<sup>th</sup> and 99<sup>th</sup> between RIA (maximum ZnT8RA/ZnT8WA AU) and Nluc-ZnT8 LIPS at Furimazine substrate incubation lengths of 5 seconds (A/B, respectively) and 15 minutes (C/D, respectively). Red dashed line denotes RIA thresholds (1.8 AU 97.5<sup>th</sup> and 2.15 AU 99<sup>th</sup>) and blue dashed lines denotes Nluc-ZnT8 LIPS thresholds [0.22 AU (97.5<sup>th</sup>) and 0.28 AU (99<sup>th</sup>) for 5-second substrate incubation length; 0.30 AU (97.5<sup>th</sup>) and 0.54 AU (99<sup>th</sup>) for 15-minute substrate incubation length]. The number (%) of 573 new-onset T1D patients are also detailed in each quadrant.

#### Chapter 4 - Development of Nluc-ZnT8 LIPS for ZnT8A detection

The LIPS derived AUs in both substrate incubation lengths highly correlated with the maximum RIA AU ( $r = 0.89-0.90$ ,  $p < 0.0001$ ). There was very little difference in overall assay sensitivity between substrate incubation lengths (395-397 new-onset T1D patients found positive and 176-178 found negative). The LIPS assay identified 94.3% new-onset T1D patients found positive by RIA and 82.8-83.3% new-onset T1D found negative by RIA. The LIPS assay identified an additional 5.7-5.9% of patients found negative by RIA. The highest sensitivity in LIPS was observed in the 5-second Furimazine substrate incubation length at the 97.5<sup>th</sup> percentile (0.22AU).

#### 4.3.4.2 The sensitivity and specificity of Nluc-ZnT8 LIPS in new-onset T1D patients & healthy schoolchildren

##### The Nluc-ZnT8 LIPS assay offers some improvement in assay sensitivity and specificity over monomeric ZnT8R/ZnT8W RIAs

The ROC curve analysis was used to evaluate the ability of the Nluc-ZnT8 LIPS assay to detect new-onset T1D patients (n=573) from healthy schoolchildren (n=521) compared with ZnT8R/ZnT8W RIAs. The AUC for LIPS was 0.82 (95% CI: 0.80-0.85, p<0.0001) and for ZnT8R/ZnT8W RIAs combined was 0.79 (95% CI: 0.76-0.82, p<0.0001). This suggests the Nluc-ZnT8 LIPS assay offers some improvement in assay sensitivity and specificity over the monomeric RIAs (**Figure 4:30**).

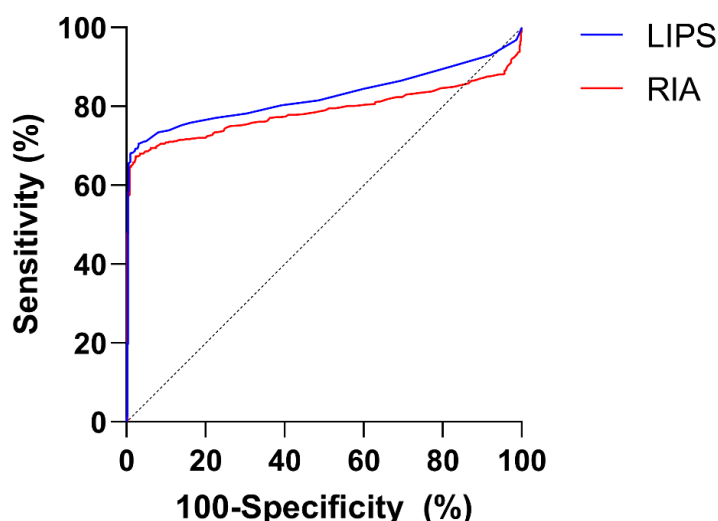


**Figure 4:30 – Nluc-ZnT8 LIPS Validation: ROC curve of ZnT8 LIPS and RIA in new-onset T1D patients & healthy schoolchildren**

ROC curve analysis on 573 new-onset T1D patients and 521 healthy schoolchildren. ROC-AUCs for LIPS was slightly improved at 0.82 (95% CI 0.80-0.85, p<0.0001) compared with RIA (ZnT8RA/ZnT8WA) at 0.79 (95% CI: 0.76-0.82, p<0.0001). At 95% specificity, LIPS had a sensitivity of 71.2%, and RIA had a sensitivity of 68.6%.

The sensitivity and specificity of LIPS at the 97.5<sup>th</sup> percentile threshold (0.22AU) was 69.3% (95% CI: 65.4-72.9) and 97.3% (95% CI: 95.5-98.4), respectively. The sensitivity and specificity of RIA at the 97.5<sup>th</sup> percentile threshold (1.8AU) was 67.9% (95% CI: 64.0-71.6) and 96.6% (95% CI: 94.6-97.8), respectively. At 95% specificity, the LIPS assay had a sensitivity of 71.2%, and the RIAs had a sensitivity of 68.6%.

**Table 4:12** summarises ZnT8A positivity and level in the cohorts of new-onset T1D patients and healthy schoolchildren between the assays. Despite differences in assay dynamic detection range, the data reinforces that LIPS offers slightly improved sensitivity and specificity over the monomeric RIAs.

ZnT8A Assay	Patients n=573		Healthy schoolchildren n=521	
	n positive (%)	Median AU (range)	n positive (%)	Median AU (range)
<b>Nuc-ZnT8 LIPS</b>	397 (69.3)	15.3 (0.2-123.0)	14 (2.7)	0.3 (0.2-87.2)
<b>ZnT8R/ZnT8W RIAs</b>	387 (67.5)	42.8 (1.8-260.0)	18 (3.5)	2.3 (1.8-230.4)

*Table 4:12 – Nluc-ZnT8 LIPS Validation: Summary of ZnT8A level & positivity in new-onset T1D patients & healthy schoolchildren using 97.5<sup>th</sup> percentile thresholds in LIPS & RIA*

#### **4.3.4.3 The sensitivity & specificity of Nluc-ZnT8 LIPS in the IASP2020 sample set**

A higher sensitivity was obtained by Nluc-ZnT8 LIPS compared with monomeric or dimeric ZnT8R/ZnT8W RIAs.

At the time of testing the IASP2020 sample set (January 2020), a preliminary threshold of 0.4AU based on the 97.5<sup>th</sup> percentile of 150/521 healthy schoolchildren was established using the optimised Nluc-ZnT8 LIPS method. Additionally, the R+W-ZnT8 dimer RIA was entered by the department into IASP2020 to compare the assay performance to Nluc-ZnT8 LIPS based on more compatible antigen configurations than the monomeric RIAs (all constructs supplied by V. Lampasona); a preliminary threshold set at 0.5AU was based on the same 150/521 healthy schoolchildren used to evaluate the Nluc-ZnT8 LIPS method.

Analysis by the IASP committee of in-house assays found all assays (LIPS, dimeric RIA, and monomeric RIAs) had 100% specificity, correctly identifying 90 negative controls. Additionally, R+W-ZnT8 dimeric LIPS and RIA had comparable sensitivity, but both were more sensitive than the monomeric RIAs. This is most likely due to the composite binding of all ZnT8A specificities in one test. However, the Nluc-ZnT8 LIPS assay correctly identified all 12 mAutoab+ves which was 2 additional to the R+W-ZnT8 RIA, increasing sensitivity by 4% overall and 2% at 95% specificity (**Table 4:13**).

Assay	New-onset T1D (n=43)	Multiple autoantibody positives (n=12)	Negative controls (n=90)	AS95 <sup>1</sup>
	n positive (%)	n positive (%)	n positive (%)	
<b>ZnT8R RIA</b>	20 (46.5)	10 (83.3)	0 (0.0)	70.0
<b>ZnT8W RIA</b>	22 (51.2)	6 (50.0)	0 (0.0)	56.0
<b>ZnT8R+W RIA</b> <sup>§</sup>	26 (60.5)	10 (83.3)	0 (0.0)	76.0
<b>Nluc-ZnT8 LIPS</b>	26 (60.5)	12 (100.0)	0 (0.0)	78.0

**Table 4:13 – Nluc-ZnT8 LIPS Validation: Initial IASP2020 report for in-house RIA & LIPS assays**

<sup>1</sup> Percent Sensitivity at 95% specificity (AS95) derived from ROC analysis. <sup>§</sup> ZnT8R+W dimer construct was kindly supplied by Dr V. Lampasona (Milan, Italy). At the time of testing (January 2020), both the ZnT8R+W dimer RIA and Nluc-R+W-ZnT8 dual heterodimer LIPS had preliminary positivity thresholds set (based on 92 healthy schoolchildren) at 0.5 AU and 0.4 AU, respectively. Overall, assays using dimeric ZnT8 constructs had a slightly higher positivity. This is most likely due to the composite binding of R- and W-specific ZnT8A in one test.

---

#### 4.3.5 Aim 5: Evaluate the predictive utility of the optimised Nluc-ZnT8 LIPS assay compared with RIAs using serum samples from patients & first-degree relatives participating in the BOX study

---

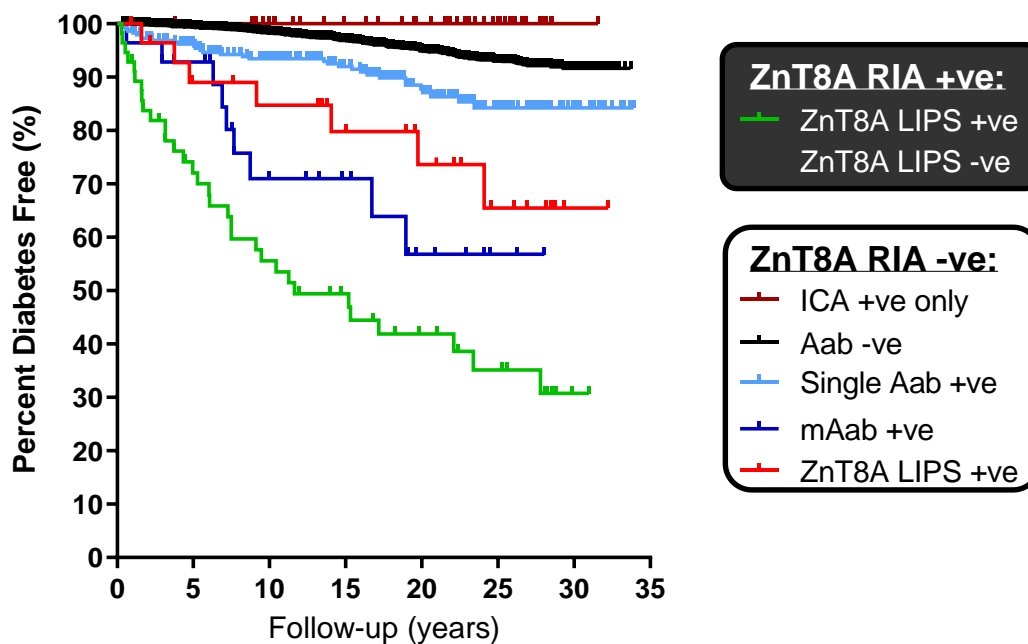
The Nluc-ZnT8 LIPS assay discriminates diabetes risk greater than monomeric ZnT8R/ZnT8W RIAs and identifies individuals with a similar diabetes risk to multiple autoantibody positives.

In 56 relatives that tested positive by both Nluc-ZnT8 LIPS and monomeric RIAs (max AU), the 20-year diabetes risk was 58.1% (95% CI: 45.0-69.2) (**Figure 4:31**). There were only four relatives that the monomeric RIAs found positive that the Nluc-ZnT8 LIPS assay did not identify, and, of these, 2 relatives slowly progressed to diabetes over a 20-year follow-up (data excluded from **Figure 4:31**). In relatives that tested negative by both monomeric RIAs, Nluc-ZnT8 LIPS identified a subset of 30 relatives with a 20-year diabetes risk of 26.3% (95% CI: 4.7-56.1).

Considering the detection of GADA, IA-2A, IAA, and/or ICA, relatives found ZnT8A positive by both monomeric RIAs and Nluc-ZnT8 LIPS had a comparable diabetes risk to mAutoab+ve relatives excluding ZnT8A: 20-year diabetes risk of 43.2% (95% CI: 18.0-66.3),  $p > 0.05$ . However, relatives found ZnT8A positive by both assays or by Nluc-ZnT8 LIPS alone, had a higher diabetes risk than sAutoab+ve [GADA/IA-2A/IAA: 20-year diabetes risk 12.9% (95% CI: 4.1-23.1),  $p < 0.0001$ ], single ICA positive [20-year diabetes risk 0.0% (95% CI: N/A),  $p < 0.0001$ ], and autoantibody negative [20-year diabetes risk 5.1% (95% CI: 3.0-7.9),  $p < 0.0001$ ] relatives.

The 5.1% 20-year diabetes risk observed in autoantibody negative relatives (193 progressed to diabetes over follow-up) can be largely explained by the prevalence of T2D [n=97; 67 males (69.1%); median age at diagnosis 52.7 years (range 29.8-75.2); 48 (49.5%) progressed <10 years of follow-up and 49 (50.5%) progressed >10 years of follow-up] but a subset of

autoantibody negative T1D subjects [n=10; 7 males (70.0%); median age at onset 20.4 years (range 5.1-63.4); 6 (60%) progressed <10 years of follow-up, and 4 (40%) progressed >20 years of follow-up], and 1 individual with maturity onset of the young (MODY) (female; age at diagnosis 29.7 years; 14.5 years of follow-up) also contributed to diabetes risk observed in the analysis.



	0	5	10	15	20	25	30	P value	20-yr diabetes risk (%)	Category
n	56	35	27	19	15	10	2	§	58.1	ZnT8A LIPS +ve
n	4	4	4	4	2	1	1	*	*	ZnT8A LIPS -ve
n	46	45	39	35	30	15	2	<0.0001	0.0	ICA +ve only
n	4287	3822	3379	2704	1679	877	167	<0.0001	5.1	Aab -ve
n	296	247	220	178	118	54	13	<0.0001	12.9	Single Aab +ve
n	28	25	15	11	7	3	1	NS	43.2	MAab +ve
n	30	24	21	16	13	8	2	0.0044	26.3	ZnT8A LIPS +ve

**Figure 4:31 – Nluc-ZnT8 LIPS Validation: Kaplan-Meier survival analysis in FDRs**

\* Only 2/4 positive by RIA but negative by Nluc-ZnT8 LIPS later progressed to disease & is not plotted for resolution § Reference category for Mantel-Cox test. NS: Not significant. Relatives positive by both Nluc-ZnT8 LIPS and monomeric ZnT8R/ZnT8W RIAs had a 20-year diabetes risk of 58.1%, comparable to diabetes risk in multiple autoantibody positives (mAutoab+ve) determined by GADA/IA-2A/IAA RIAs with/without ICA at 43.2%. The Nluc-ZnT8 LIPS assay identified a subset of relatives with a 20-year diabetes risk of 26.3% compared with ZnT8R/ZnT8W RIAs, which carried a higher diabetes risk than single autoantibody positive relatives determined by GADA/IA-2A/IAA RIAs with/without ICA at 12.9%. Single ICA positive relatives (biochemical autoantibody negative) carried the lowest 20-year diabetes risk at 0% compared with a 5% 20-year diabetes risk if negative for all autoantibody tests. However, this can be largely explained by 97 relatives that developed T2D but also includes 10 autoantibody negative T1D relatives and 1 maturity onset of the young (MODY) relative.

---

## 4.4 Discussion

---

Experiments described in this chapter investigated whether a low-volume, rapid and optimised Nluc-ZnT8 LIPS assay utilising a novel Nluc-R+W-ZnT8 dual heterodimer antigen to detect ZnT8A in T1D provides a non-radioactive alternative to conventional RIA(s). The performance of the optimised Nluc-ZnT8 LIPS assay against in-house monomeric ZnT8R/ZnT8W RIAs was evaluated using a population of healthy schoolchildren to set a common positivity threshold, new-onset T1D patients, and FDRs from the well-characterised BOX study, and two international IASP workshops (2018/2020) that comprised T1D patients, mAutoab+ves, and negative controls.

### 4.4.1.1 Main findings

---

1. The low-volume, rapid, and optimised Nluc-ZnT8 LIPS assay offered higher sensitivity than either ZnT8R/ZnT8W monomeric RIAs, and ZnT8A levels were highly correlated utilising the maximum ZnT8A level (AU) between monomeric RIAs.
2. Addition of CaCl<sub>2</sub> or ZnCl<sub>2</sub> to EDTA-treated serum or EDTA-preserved plasma in the Nuc-ZnT8 LIPS assay did not improve ZnT8A binding or detection of positivity.
3. A positivity threshold from a population of healthy schoolchildren showed that the greatest sensitivity of the Nluc-ZnT8 LIPS assay was achieved using a Furimazine substrate incubation length of 5-seconds at the 97.5<sup>th</sup> percentile with derived AUs correlating up to 90% with monomeric RIAs (maximum AU).
4. The sensitivity and specificity of Nluc-ZnT8 (R+W-R+W) LIPS was greater than monomeric (ZnT8R/ZnT8W) or dimeric (ZnT8R+ZnT8W) RIAs evaluated in blinded samples from IASP2020.

5. Relatives found positive by Nluc-ZnT8 LIPS and/or monomeric ZnT8R/ZnT8W RIAs combined had the highest 20-year diabetes risk which was comparable to mAutoab+ve relatives determined by other biochemical autoantibody RIAs. However, Nluc-ZnT8 LIPS identified additional relatives not identified by either monomeric RIA that had a higher 20-year diabetes risk than sAutoab+ves, thereby increasing mAutoab+ve detection.

#### **4.4.1.2 Strengths & limitations**

---

This study benefits from several novel aspects: Nluc-R+W ZnT8 dual heterodimer construct, the inclusion of a large number of both new-onset T1D and FDRs from the well-characterised population-based BOX study that encompassed all ZnT8A specificities, the direct comparison between LIPS and RIAs using common positivity thresholds based on a cohort of healthy schoolchildren recruited from a localised geographical area (Oxford/Winsor), and the blinded/unbiased evaluation of LIPS and RIA performance in two international IASP workshops (2018/2020). Although T1D subjects sampled <3 months of diagnosis can inform assay sensitivity with minimised false positivity, the inclusion of FDRs also permitted the assessment of the predictive utility of the assays in relatives with a long-term follow-up spanning 30 years which is rare in T1D cohorts. Whilst these FDRs have not been prospectively followed up since birth (opposed to BABYDIAB and TEDDY studies (135, 528)) and may not reflect disease risk in the general population, the FDRs encompassed a wide age range which may inform progression in both childhood-onset and adult-onset T1D.

Limitations of this study include the pre-selection of samples based on available monomeric ZnT8R/ZnT8W RIA data, differences in sample selection between assays, and the limited number of assays conducted to assess experimental conditions. However, experimental replication was not always feasible due to sample volume availability, cost of resources, and time efficiency. Nonetheless, two experiments were conducted when a large adaptation was

being assessed or was deviating from other optimised protocols (e.g., Nluc-tagged antigen construct selection, incubation length, and preparation) and included a larger sample set where possible.

#### **4.4.1.3 Optimisation of Nluc-ZnT8 LIPS**

---

A range of experimental conditions was assessed during Nluc-ZnT8 LIPS optimisation to increase ZnT8A detection and reduce assay background for clear discrimination between positive and negative populations.

Firstly, it was elucidated that sNluc-R+W-ZnT8 antigen constructs had a higher background (non-specific binding) than Nluc-R+W-ZnT8 antigen constructs, which may be related to the purification process of the HEK293 cell supernatant or level of antigen secretion/expression. However, ZnT8A binding in the positive RIA internal standards and QCs was comparable between sNluc- and Nluc-R+W-ZnT8 constructs, indicating that the structural integrity of sNluc-R+W-ZnT8 constructs was of compatible configuration for ZnT8A to bind. Nluc-R+W-ZnT8 constructs offered greater antigen expression with a more straightforward method of preparation. There was a slight indication that the Nuc-R+W-ZnT8 dual heterodimer may detect ZnT8A greater than the Nluc-R+W-ZnT8 heterodimer, particularly at the low-level range (<10 AU), but overall, the difference between the Nluc-R+W-ZnT8 heterodimer constructs was marginal. Nevertheless, the utilisation of R+W heterodimeric fusion antigen constructs not only reduced labour cost/time and sample volume requirements through simultaneous ZnT8RA/ZnT8WA detection but presumably contributed to the increased sensitivity of Nluc-ZnT8 LIPS above monomeric ZnT8R/ZnT8W RIAs, which is in line with other reports (436, 443); DASP2013 unpublished data.

Secondly, the purification and preparation of the Nluc-R+W-ZnT8 dual heterodimer antigen through a 0.45 $\mu$ M filtration, compared to the NAP5<sup>TM</sup> column purification, not only improved assay performance (SNR; higher ZnT8A binding and lower assay background) and AU positivity determination in select samples but also reduced labour time (saving ~1.5hrs) and cost (~£0.5/filter unit versus ~£4.7/column at current costs).

Other beneficial assay amendments included altering the Tween-20 concentration in TBST at different assay stages (0.15% during antigen incubation and 0.5% during removal of excess unbound antigen) and reducing the substrate concentration from 1:50 to 1:150, reducing assay costs without loss of assay performance.

Conversely, there were also many investigated conditions that did not severely improve assay performance, such as the presence of ZnCl<sub>2</sub> or CaCl<sub>2</sub> in EDTA-treated serum or EDTA-preserved plasma, presence of ZnCl<sub>2</sub> during Nluc-R+W-ZnT8 antigen purification, the quantity of methionine during *in vitro* transcription/translation of Nluc-R+W-ZnT8 antigen, or glycine-blocking PAS. Only the freeze-thawing of the Nluc-R+W-ZnT8 antigen once filtered and diluted was detrimental to assay performance and, therefore, should only be thawed once before use. There was an indication that longer substrate incubation (15mins/well versus 5sec/well) may benefit intra- and inter-assay variation and was assessed in new-onset T1D & healthy schoolchildren during assay validation.

#### **4.4.1.4 Validation of optimised Nluc-ZnT8 LIPS**

---

The LIPS method was first described by Burbelo *et al.* (2008) for detection of IA-2A utilising Rluc, which was extended to IA-2 $\beta$ A and GADA by the same research group in 2010 (521, 523). Subsequent studies by Marcus *et al.* (2011; Gluc), Ustinova *et al.* (2014; Gluc), McLaughlin *et al.* (2016; Gluc), and Liberati *et al.* (2018; Nluc) have since reported LIPS

methodology for the detection of GADA/IA-2A, ZnT8A (R+W), TSPAN7A, and IAA, respectively (271, 366, 453, 524). Principally, these assays were evaluated in new-onset T1D patients and controls (age/gender-matched where possible) and generally, these studies either report good concordance or increased sensitivity to conventional methods, predominantly RIA. Only Liberati *et al.* (2018) has evaluated the performance of Nluc-LIPS in the context of disease prediction through IAA detection in FDRs from BOX and Belgium cohorts; more FDRs that progressed to T1D were identified with Nluc-LIPS compared with RIA.

Regarding LIPS ZnT8A detection, this is the first time Nluc-ZnT8 antigens have been used, with only one previous study using a Gluc strategy. Utilising an R+W-Gluc heterodimer antigen secreted from the insect Tn5 cell line, Ustinova *et al.* (2014) compared the LIPS method to the commercially available RSR<sup>TM</sup> Limited ELISA. The assay concordance was age-dependent and was lower in children: adults AUC 0.79 in LIPS versus 0.78 in ELISA; children AUC 0.75 in LIPS versus 0.90 in ELISA. Whilst the report does not detail the age cut-offs defining these populations, it could be possible that opposed to PAS/PGS immunoprecipitation that detects IgG only in RIA/LIPS, the RSR<sup>TM</sup> Limited ELISA detects IgG as well as IgM and IgA isotypes which may play a bigger role in the ZnT8A response in younger individuals. Despite these age-related variations, the assay showed high sensitivity (78.6-87.3%) but poor specificity (68.7-78.0%) between patients and controls. This study highlights the potential of LIPS, but the high assay background, most likely due to the Gluc/coelenterazine chemical reaction itself, is problematic and high even when a concentration of 10-15M LU of Gluc-antigen was required to achieve clear discrimination between the populations.

The major advantage of this current study was utilising the superior bioluminescence system (Nuc/Furimazine, Promega) and a different strategy opposed to Gluc/cell line secretion, which offered many advantages; expression of Nluc-ZnT8 antigen through *in vitro*

## Chapter 4 - Development of Nluc-ZnT8 LIPS for ZnT8A detection

transcription/translation, enhanced expression requiring only ~2hrs and 4M RLU of antigen, greater chemical stability of Nluc/Furimazine, reduced autoluminescence/background, reduced risk of protein modifications, and brighter and longer-duration bioluminescence. Therefore, the Nluc-ZnT8 LIPS method developed in this PhD project did not suffer from poor specificity but offered a high sensitivity ranking in the top 3 of ZnT8A assays in IASP2020, alongside collaborator Dr V. Lampasona's laboratory (Milan) utilising the Nluc-ZnT8 LIPS harmonised protocol that resulted in 100% concordance (unpublished data).

The only modification to the Nluc-R+W-ZnT8 heterodimer antigen that may be worth investigating is a Nluc-N-terminal/C-terminal-R+W-ZnT8 heterodimeric construct. However, it is unlikely to greatly improve the assay as the N-terminal is thought to only contribute to ~10% of ZnT8A reactivity (270), may only contribute an additional 2% not identified by a ZnT8R/ZnT8W heterodimer (443), and the configuration may obscure antigenic recognition of ZnT8A and lower sensitivity. Additionally, the Nluc-ZnT8 LIPS assay developed in this project identified a greater proportion of FDRs that progressed to T1D over follow-up than the monomeric RIAs which, may be reduced if the N-terminal reactivity is associated with early ZnT8A humoral responses and/or lower T1D risk. The characterisation of ZnT8A epitope spreading prior to T1D outside of ZnT8's C-terminus is unknown.

Regarding the major ZnT8A epitope region, most assays choose not to incorporate the Q325 variant/ZnT8QA reactivity due to its relatively low prevalence (~30-40% sensitivity in IASP2016/2018 workshops by RIA). Andersson *et al.* (2013) tested for R325/W325/Q325-reactive ZnT8A in 3165 new-onset T1D (<18 years) utilising separate RIAs, but sensitivity was comparable when only R325/W325-reactive ZnT8A was considered (~50-60%) as ZnT8Q-specific ZnT8A was not detected and R325/W325 captured ZnT8R-/ZnT8W-specific and non-specific ZnT8A (428). Collectively, it is unlikely that the performance of the Nluc-

## Chapter 4 - Development of Nluc-ZnT8 LIPS for ZnT8A detection

ZnT8 LIPS assay could be enhanced through ZnT8 antigen alteration based on current knowledge.

Further assay adaptations that may improve Nluc-ZnT8 LIPS performance is modifying the format to a bridge-type LIPS assay for simultaneous measurement of IgM, IgA, and IgG isotypes, comparable to the RSR<sup>TM</sup> Limited bridge-type ELISA. A bridge-type LIPS would require in-house production of well-validated and conformationally sound ZnT8 protein for the solid-phase. The strategy employed to generate recombinant ZnT8 protein in this thesis appears promising but requires further optimisation but generating large quantities of stable ZnT8 with high ZnT8A bioactivity has been problematic and requires detergent solubilisation with strict drying/rehydration conditions (442). However, such stringent protocols may not be feasible in a high-throughput or, automated setting and will increase experimental expense over the fluid-phase LIPS.

This PhD project sought to provide a non-radioactive replacement to conventional RIAs and the data gleaned provides strong evidence that the LIPS assay is a viable option with scope for further adaption for general population screening.

#### 4.4.1.5 Advantages of the LIPS assay & future applications

The LIPS assay has several advantages over RIA (Table 4:14).

RIA	LIPS
2-day duration	1-day duration
3-week shelf life of L-[35-S]-methionine tagged ZnT8 antigen	At least 6-month shelf life of Nluc-tagged ZnT8 antigen (data not shown)
5µl sample (dimeric) or 10µl sample (monomeric) required	2µl sample required
Radioactive – cost, safety, & environmental impact with regulatory legislation	Non-radioactive – cheaper, safer, & less environmentally harmful without regulations
50-70% sensitivity & 98-100% specificity*	67-76% sensitivity & 99-100% specificity**
Automation conducted in some laboratories but costly	Automation is not currently conducted but is likely to be more cost-effective
Lower adaptability & scalability for large-scale population screening.	Enhanced adaptability/scalability for large-scale population screening
Comparable consumables & methodology; laboratories set up for RIA can easily adapt to LIPS.	

*Table 4:14 – Advantages of LIPS assays to conventional RIAs*

\* DASP 2013/2014 & IASP 2015-2020; \*\* IASP2018/2020. DASP/IASP performance taken from committee laboratory performance reports. Biennial DASP/IASP workshops cannot be directly compared due to differences in sample sets. A review of ZnT8A detection across multiple methods has not been conducted to date.

Whilst long-term follow-up of FDRs has invaluable added to predicting future disease risk and our understanding of the natural history of T1D, the mortality rate (2-8 times higher than the general population) and high presentation of DKA around diagnosis (15-67%, highest in children <4 years), demand earlier detection of islet autoimmunity in the general population (9, 32, 34). This would ideally only require small volume fingerprick capillary sampling that can be facilitated through postal collection. Therefore, rapid small-volume non-radioactive assays that meet the demand of large-scale population screening are required. Not only does the LIPS assay generally perform better than in-house RIAs, but the LIPS assay meets these requirements and overcomes some obstacles that have prohibited screening for islet autoimmunity in the general population.

For instance, the utilisation of different luciferase enzymes with different emission spectra can permit the simultaneous measurement of >1 autoantibody (GADA/IA-2A/ZnT8A/IAA) which

is not possible with RIA (beta radiation: GADA/IA-2A/ZnT8A; gamma radiation: IAA). Alternatively, incubation of samples with Nluc-tagged GAD/IA-2/ZnT8 and/or insulin LIPS (multiplex) with one emission spectra can be used as a primary screening strategy and, if positive, can be confirmed by individual tests (singleplex) for a more accurate determination of risk. For instance, a ZnT8A/IA-2A composite LIPS assay may be a cost-effective screening strategy as, when reviewed in an RIA, did not reduce sensitivity below singleplex RIAs (529).

A screening strategy that has proven beneficial for the large-scale Fr1da childhood-screening study utilises a GADA/IA-2A/ZnT8A 1-day triple-screen ELISA before performing singleplex RIAs to confirm all positive autoantibody results (364, 454). Whilst this ELISA is a rapid test that can be performed by automation and has shown good sensitivity/specificity, the assay cannot determine antigen-specificity until confirmed by RIA, and IAA detection cannot be integrated, relying solely on RIA (364, 454). Therefore, radioisotope use remains a necessity, and the sample volume required ranges from ~50µl but could require up to ~100-200µl following confirmation. This limits the determination of islet autoimmunity in small volume capillary samples, which are more frequent in infants/children. In the Fr1da study, 94.6% of children provided a sample with sufficient volume for screening and confirmatory islet autoantibody testing using a multiplex RSR ELISA and an individual IAA test, but samples were taken by primary care teams and not the most cost-effective strategy of self-collection by post (454).

The 4- or 7-plex ECL assay has modest sample volume requirements (~6-15µl), high correlation with single ECL/RIAs with high sensitivity/specificity and included markers of other autoimmune conditions, that are present in ~25% of T1D cases (365, 424). However, the assay did not include ZnT8A, has a 2-day assay duration, and requires expensive specialised equipment. Additionally, the method requires serum acid treatment and several preparation

steps (per autoantibody detection involves two antigen preparations and streptavidin-coated plates to be made in advance). These methodology steps may hamper large-scale high-throughput screening and/or the possibility for automation. Whilst the ECL assay does efficiently detect high-affinity autoantibodies and, by extension, identifies high-risk individuals most likely to progress to T1D, which is an advantage over RIAs and ELISAs that detect both low- and high-affinity autoantibodies, the method has not shown it can be conducted well in other laboratories (360, 363, 530).

More recently, LIPSTICKS technology coupled with luciferase-fused proteins has shown promise in rapid detection of immunocomplexes within minutes using magnetic neodymium sticks to detect luciferase-labelled antibodies bound to protein A/G-coated paramagnetic beads (369, 522). This has been used in a range of autoimmune, infectious, and other diseases such as head and neck squamous carcinoma with relatively accurate discrimination and potential for detecting multiple antigens (369, 522, 531). However, further assay improvements are necessary to improve sensitivity and specificity for use in large cohorts. This less labour-intensive, time-consuming luminescence assay with potential applications for diagnostic and research testing would be extremely advantageous for the development of rapid point-of-care testing that meets the required criteria, has potential for assay harmonisation between clinical and research laboratories, and accelerated testing using a hand-held luminometer for large-scale screening (369, 522, 532).

To date, the optimised and validated Nluc-ZnT8 LIPS assay, developed in this PhD, is being incorporated into a triple-screen Nluc-GAD/IA-2/ZnT8 LIPS assay (with singleplex assays for confirmation of positivity) to investigate the prevalence of islet autoantibodies in the general population and is being integrated into new prospective study contracts to ultimately replace the RIAs and perform high throughput general population screening in the future.

# Chapter 5 - General discussion

---

In this study, a Nluc-ZnT8 LIPS method to detect ZnT8A was optimised and validated, and assays based on conventional RIAs were developed and used to investigate characteristics of ZnT8A throughout the pathogenesis of T1D. Longitudinal follow-up of individuals revealed that ZnT8A responses are dynamic, showing loss or gain of autoantibody status and titre, some alteration in affinity, epitope specificity, and IgG subclasses, particularly in those with non-specific ZnT8A. In the small number of individuals analysed, no clear differences were observed between slow and rapid FDRs regarding ZnT8A specificity and IgG subclasses. Before diagnosis, compared with RIA, the Nluc-ZnT8 LIPS assay identified a small additional subset of FDRs who had a 20-year T1D risk of 26%. At diagnosis, there was a large degree of ZnT8A epitope specificity directed to C-terminal ZnT8, the breadth of IgG subclasses was more common, and ZnT8A positivity was negatively associated with *FCRL3/1q23* (<2 years disease duration). The Nluc-ZnT8 LIPS assay offers some improvement in assay sensitivity and specificity over RIA at diagnosis. After onset, ZnT8A was lost more rapidly, and this was associated with lower baseline titres, younger age-at-onset, disease duration at sampling, and the presence of *HLA-A\*24* and weakly negatively with *RELA/11q13*

---

## 5.1 Prediction & prevention of T1D

---

Despite the advances in insulin pharmacokinetics, insulin delivery technology, and improved diabetes management over the last 20 years, the majority of childhood-onset and adult-onset T1D are unable to achieve long-term glycaemic control (45, 533-535). To date, there is no conclusive proof that residual  $\beta$ -cells can regenerate or recover from autoimmune destruction in humans after T1D onset (507, 508). Therefore, alternative immunotherapeutic strategies are aimed at T1D prevention in the asymptomatic preclinical stages of the disease: initiation of  $\beta$ -cell autoimmunity (primary) or prevent/delay progression to T1D after detection of  $\beta$ -cell autoimmunity (secondary) (533). To date, only one secondary immunotherapeutic agent,

Telizumab (a T-cell modulating anti-CD3 monoclonal antibody), in a single 14-day course, has been shown to be efficacious in delaying progression to T1D with a prolonged effect on  $\beta$ -cell function in high-risk FDRs (220, 221). Previous and current intervention therapies rely on the ability to detect islet autoimmunity early in the disease pathogenesis.

The measurement of four major islet autoantibodies (IAA, GADA, IA-2A, and ZnT8A) remain the most reliable biomarkers of islet autoimmunity for the identification of at-risk individuals. The presence of multiple (>2) islet autoantibodies has been pivotal in identifying high-risk individuals (T1D risk after 15 years for a single autoantibody 13% versus 80% with triple autoantibodies) (287) and has informed the predictive preclinical stages of T1D (96). This staging system has facilitated the recruitment of at-risk individuals to clinical trials and, the monitoring of these individuals has greatly informed the natural history of T1D (296). Additionally, awareness of diabetes risk by participating in these trials has beneficially reduced DKA around T1D onset, particularly in young-onset T1D (536). Predominantly, these studies have been conducted in prospective birth cohorts of genetically at-risk children (FDR with T1D or HLA-genotype) or cross-sectional cohorts of high-risk FDRs of T1D subjects. However, the cross-sectional observation of FDRs only captures 10-15% of all T1D cases as most subjects do not have a T1D-affected FDR (533, 537). Therefore, efforts to screen for at-risk individuals in the general population without genetic preselection is a growing area of interest.

To date, general population studies show multiple islet autoantibodies are present in ~0.3% of subjects (536) versus ~3% in FDRs (data from >180,000 FDRs aged 2.5-45 years participating in TrialNet) (538). Although sporadic and familial T1D cases have shown comparable clinical characteristics and autoantibody profiles at onset (539, 540), suggestive of analogous pathogenesis, the difference in autoantibody prevalence has a tremendous cost, feasibility, and labour implications for whole population screening of islet autoimmunity (533). Additionally,

the remaining heterogeneity in disease progression rates to T1D onset (months to decades), even once multiple autoantibody positivity has been determined, also makes identifying high-risk individuals on a mass scale more difficult as some will require long-term follow-up if slowly progressive. However, advances in islet autoantibody detection methods have enhanced the probability of conducting general population screening in the future (286, 533).

In the short term, the developed Nluc-ZnT8 LIPS assay presented in this thesis allows for the direct replacement of the fluid-phase conventional ZnT8R/ZnT8W RIAs. This was demonstrated through the improvement in assay performance (sensitivity/specificity) and high correlation between LIPS and RIA in new-onset T1D patients but, there was evidence to suggest that the Nluc-ZnT8 assay will identify additional at-risk individuals. Whilst the Nluc-ZnT8 LIPS assay offers many methodological advantages to RIAs and increases the feasibility of general population screening (described previously **4.4.1.5**), the assay does not have a greater capacity for automation than RIAs in its current format. A future avenue of this work would be to adapt the Nluc-ZnT8 LIPS assay into a bridge-type plate format. This could be achieved by incorporating a ZnT8R/ZnT8W protein solid-phase to exclude the need for immunoprecipitation and multiple wash/centrifugation steps. Adopting this assay format would capture IgG, IgA, and IgM isotypes, reduce labour time even further, and could be robotically operated. The strategy to produce ZnT8 protein in this PhD project requires further optimisation, but this avenue may warrant further investigation in a larger cohort of at-risk and/or new-onset T1D subjects as preliminary results from bridge-type Nluc-coronavirus (COVID-19) and Nluc-IA-2 LIPS assays by the Diabetes & Metabolism team and other collaborators at the University of Bristol (UK) and Dr V. Lampasona's laboratory (Milan, Italy), for the detection of humoral responses to the SARS-CoV-2 virus and IA-2, are promising (unpublished data).

Currently, the LIPS (366, 518, 523-525), ECL (333, 360, 363, 530), and ADAP (367, 368) methods show the most promise for general population screening as all have shown high performance in single-plex and multi-plex configurations. There is unlikely to be a single assay utilised for general population screening in the future, and the method of choice will likely depend on sample volume and/or cost requirements. However, the determination of islet autoantibodies by different methods has historically benefitted further assay optimisation, understanding of antibody-antigen interactions, and/or inter-laboratory concordance, mainly attributable to the valiant efforts of the DASP/IASP committee and the participating laboratories over many years (371-375, 453). Therefore, the availability of various immunoassays should not be detrimental to the international and collective goal of population screening. Nonetheless, groups with comparable methods, where possible, should collaborate to harmonise protocols to benefit comparisons between studies and maintain high intra- and inter-laboratory concordance (451, 459).

Undoubtedly, detection of islet autoantibodies in at-risk or general populations will always be important for T1D risk assessment, but the further characterisation of islet autoantibody responses beyond a simple binary presence/absence metric (transient positivity, sAutoab+ves versus mAutoab+ves, titre, affinity, epitope specificity, and IgG subclasses) enhances T1D risk prediction and therefore, should also be integrated in autoantibody positives to further stratify risk (287, 316, 317, 320, 331, 344, 345). These characteristics pertaining to ZnT8A humoral responses are comparatively under-investigated and were a large focus of this project.

We would anticipate that the predictive utility of ZnT8A is likely age-dependent, with a higher risk associated with a younger age at ZnT8A seroconversion, based on current knowledge (294, 320). However, the development of islet autoimmunity remains to be fully characterised in older individuals, although late-onset T1D appears to have similar islet autoantibody profiles

at diagnosis but a later age at seroconversion and possibly a less aggressive autoimmune response (42, 43, 275, 294). Based on current data at diagnosis, ZnT8A is common in both childhood- and adult-onset T1D with an estimated 14-26% positive for ZnT8A only (270, 275). Systematic longitudinal ZnT8A detection from seroconversion without pre-selection for mAutoab+ve, age, or genetics (DR3/DR4) is required to fully elucidate many facets of the ZnT8A response during T1D pathogenesis and its implications for T1D prediction/progression.

Reports from TEDDY showed that loss of islet autoantibodies in children was associated with lower T1D risk in mAutoab+ve children, but ZnT8A were not measured in all longitudinal samples (295, 314). Therefore, it is unclear how often ZnT8A are lost in individuals who slowly or rapidly progress to T1D. The data presented in this thesis has shown ZnT8A can be lost in both SPs and RPs across a wide age range, suggesting that further clarification is needed for effective T1D prediction models that incorporate ZnT8A.

Previously, the BDR study reported that the presence of, but not titres of ZnT8A (determined by RIA using a ZnT8R/ZnT8W heterodimer) and/or IA-2A were independent predictors of T1D progression in mAutoab+ve relatives (aged <40 years) (291). Relatives persistently autoantibody positive and/or mAutoab+ve progressed more rapidly to T1D more often than those transiently autoantibody positive and/or who remained sAutoab+ve over follow-up. However, the study reported that only loss of IAA was associated with a delayed T1D progression rate, but ZnT8A was only tested in 8.7% of relatives negative for GADA, IA-2A, and IAA (291), due to the reportedly low prevalence of single ZnT8A responses from previous studies of relatives (292, 294). As a result, this study only captured 4 relatives with either single IA-2A or ZnT8A responses and was unable to investigate the loss of ZnT8A relative to T1D progression. We know that single autoantibody responses appear to reflect an earlier stage of islet autoimmunity, and individuals with any single islet autoantibody are at lower T1D risk

overall (314). As ZnT8A commonly appears in individuals with at least one other autoantibody, many studies opt for this testing strategy, it is not clear how prevalent single ZnT8A responses are prior to T1D onset. Additionally, the complete picture of all ZnT8A humoral responses from seroconversion up to T1D onset for T1D prediction is not fully understood. Data emerging from the general population ASK study of >20,000 children has shown that single ZnT8A responses may be present in ~0.6% (333), but the frequency in high-risk children and/or relatives is infrequently reported.

In addition to ascertaining the true prevalence of single ZnT8A responses prior to onset, elucidating the affinity of ZnT8A may be important for T1D risk as a recent report showed that the discrimination of high-affinity single ZnT8A responses by ECL identified children with higher T1D risk (a subset from the ASK/DAISY studies (333)). This study showed that single ZnT8A responses were more likely to be of lower titre compared to titres in mAutoab+ve responses, but an interaction between affinity and titre was not observed. Affinity and titre are often regarded as markers of increasing humoral autoimmunity, but in T1D, only titres of IAA and IA-2A are associated with T1D risk independent of other factors (317), but ZnT8A titres in relation to T1D risk has not been reported. Based on the data presented in this thesis, a convincing relationship between ZnT8A affinity and titre was not evident, which is comparable to other islet autoantibody responses, but should be further elucidated (316, 331, 343-346).

High-affinity autoantibodies appear to be associated with mAutoab+ve status and/or a younger age at seroconversion (316, 317, 331, 343-345). This may explain why we found that ZnT8A were predominantly of high-moderate affinity as affinity was investigated in small subsets of mAutoab+ve at-risk and new-onset T1D subjects, predominantly aged <21 years. Principally IA-2A responses have also been shown to be of high affinity (346), and therefore, secondary humoral responses may be more likely to undergo complete affinity maturation, perhaps

supporting the independent association of ZnT8A and IA-2A with rapid progression to T1D. In contrast, a mixture of low/high affinity has been reported in GADA/IAA responses (343, 344). In the mAutoab+ve ZnT8A seroconversion case study population (n=10), there was little difference of large changes in affinity and where detected, lower affinity appeared related to the radiolabelled WT ZnT8 antigen used and/or ZnT8A specificity, but affinity maturation (low>high) in GADA, IAA, and IA-2A responses over follow-up in relatives has been observed, predominantly in at-risk children (316, 344, 346). However, like other islet autoantibody responses (316, 344), we would expect single ZnT8A responses to be of lower affinity and, by extension, be more likely to be lost and of lower T1D risk. Both high- and low-affinity ZnT8A in single ZnT8A responses were reported (333), and therefore, assessment of ZnT8A affinity in single ZnT8A responses may be more beneficial for identifying high-risk individuals. However, there is not currently enough evidence to ascertain whether T1D prediction studies are likely to benefit from ZnT8A affinity assessment but as older onset and/or sporadic T1D in the general population are being investigated, ZnT8A affinity may be important for both disease sensitivity and specificity in future investigations, where single false positives may be problematic. For this, the development of methods to detect high-affinity ZnT8A without large sample volume requirements is essential. Bridge-type assay formats that incorporate solid-phase and fluid-phase antigens are best placed to discriminate high-affinity autoantibodies as shown by the ECL method for GADA, IAA, and ZnT8A detection (319, 333, 360, 530). However, liquid-phase assays that can use only two different competitive protein concentrations to discriminate high- and low-affinity ZnT8A, as suggested in this thesis, may be suitable tests. This assay format has successfully been developed for IAA affinity to reduce cost and serum volume requirements previously (343).

It is important to consider that determination of high-affinity ZnT8A and/or advances in ZnT8A detection methods may also require identifying specific epitope(s) of ZnT8 as found for IAA

and GADA (316, 344). Within the C-terminal, three major epitopes have been identified, two associated with the rs13266634 SNP and one conformational that appears to be independent of each other: R325, W325, REKK (findings from new-onset T1D patients) (328, 404, 480). However, considering all epitopes in 72 new-onset T1D patients in this thesis showed that some patients were affected by both mutations in the major epitope sites. Characterisation of these major epitope sites in FDRs prior to diagnosis revealed that a subset of individuals with non-specific ZnT8A responses had differential epitope specificity to R325 or W325 WT ZnT8 antigen. This suggests a proportion of non-specific ZnT8A may result from polyclonal B-cell clones directed to many ZnT8 epitopes. Expanding upon this, the effects of C-terminal mutations on ZnT8A binding in all patients was heterogeneous. Therefore, it is highly unlikely that a single high-risk epitope specificity can be identified in C-terminal ZnT8 for T1D risk prediction.

The proposal from predictive modelling of ZnT8 has suggested 3 short cryptic (buried) B-cell epitopes, and recent data supporting that ZnT8A recognise extracellular regions of ZnT8 suggests that other areas of ZnT8 may be important (455, 541). The observation that ZnT8A reactive to extracellular ZnT8 regions was the first appearing islet autoantibody (prior to IAA/GADA) (455) suggests that ZnT8A responses may not always be a secondary humoral response in T1D and that ZnT8A may be able to bind ZnT8 at the  $\beta$ -cell surface of functional/intact  $\beta$ -cells as ZnT8 is the only antigen (to date) known to be trafficked to the cell surface during GSIS. During stimulated GSIS, ZnT8's exposed TMD (aa60-266) on the  $\beta$ -cell surface (rat INS-1E cell line) was shown to be recognised by ZnT8A in human serum (426, 542). However, it is not known whether bound ZnT8A could be pathogenic to  $\beta$ -cells, but a subclass of cell surface reactive ICA were shown to be preferentially lytic for rat  $\beta$ -cells many years ago (543). If further corroborated, this could enhance the predictive utility of ZnT8A in T1D and may explain many features of C-terminal ZnT8A: less commonly detected in young

children and more common in late childhood-adolescence, typically appear near T1D diagnosis, and more common in individuals positive for at least one other islet autoantibody, predominantly IA-2A (287, 290, 292). These features could be explained by repeated ZnT8 antigen stimulation of T-cells/B-cells and maturation of the ZnT8A response resulting in epitope spreading from other regions towards the C-terminal. Additionally, this may explain the heterogeneity in epitope specificity determined in the present study, as this may reflect the response following epitope spreading. An assessment of ZnT8A reactivity to extracellular and C-terminal ZnT8 over follow-up should clarify any temporal changes and/or intermolecular epitope spreading of ZnT8A and whether this would benefit T1D prediction and/or ZnT8A detection methods. These studies in GADA and IA-2A responses have benefitted T1D prediction, and therefore, this is a pertinent future study (317, 330, 337).

To our knowledge, there was not a formal study determining IgM/IgG/IgA prevalence in ZnT8A responses. Therefore, based on previous findings of IgG subclasses in GADA/IA-2A/IAA responses (317), we were confident that investigations of IgG subclasses in ZnT8A responses were the most logical choice for investigating SPs and RPs. Whilst the C-terminal region is currently exclusively studied in T1D, considering the epitope specificity may have important connotations for future investigations of ZnT8A IgG subclasses in relation to T1D risk. Data for GADA and IA-2A suggest that multiple IgG subclasses and antigen epitope spreading reflect high-titre humoral responses (317). In this study, we found that over a range of titre, ZnT8A responses in SPs/RPs and the ZnT8A seroconverter cohort were predominantly IgG1-restricted reflective of early autoantibody responses (244) with little differences in the frequency of specific IgG subclasses between those who progressed at different rates. However, the frequency of IgG4 appeared rare. As IgG4 is thought to be associated with chronic antigen exposure, the low but detectable prevalence of IgG4 in ZnT8A responses could

also suggest that the C-terminal of ZnT8 is not the earliest region that ZnT8A targets in T1D (242, 243).

When ZnT8A IgG subclasses were tested in a subset of new-onset T1D patients over a range of titres, the proportion of IgG1-restricted and IgG-unrestricted responses was comparable. This suggests that the spectrum of IgG subclasses becomes more prevalent closer to onset; therefore, ZnT8A IgG subclasses may identify rapid progression very close to onset or, conversely, may identify individuals who are more/less likely to rapidly lose their ZnT8A response after T1D onset, which appears particularly common in ZnT8A responses (443, 493). If an IgG subclass particularly important for ZnT8A could be identified, it is feasible this test could be incorporated into screening strategies; however, routine assaying would also require the use of established QCs and StDS thresholds based on a healthy population, which we have established for GADA and IA-2A but was more challenging for ZnT8A.

Clearly, the most common finding in ZnT8A responses prior to and at T1D diagnosis was the dynamic changes and heterogeneity between individuals. Whilst this project was unable to ascertain whether these ZnT8A characteristics inferred T1D risk or were influenced by age at sampling/onset due to the small sample size and the limited number of individuals >21 years of age, the observations, and the approach taken to characterise the ZnT8A humoral response in this project, are novel and provides a plethora of question generating preliminary data and optimised methods for larger and further investigations of T1D risk prediction.

---

## 5.2 Islet autoimmunity & residual $\beta$ -cell function

---

At diagnosis, islet autoantibodies provide an important biomarker to classify diabetes for research. Clinically, islet autoantibody testing is likely to be more useful within 3-5 years of a diabetes diagnosis as C-peptide is not reliable within this time frame (57, 544, 545). Consequently, relying on C-peptide alone could significantly delay the determination of severe insulin deficiency when clinicians suspect misdiagnosis (11, 544). Although biochemical autoantibody tests are not currently recommended in the National Institute for Health and Care Excellence (NICE) guidelines, rapid point-of-care tests are being developed for clinician use, and general population studies are being undertaken, the utility of autoantibodies for diagnosis and diabetes management may be on the horizon. Islet autoantibody detection closer to diagnosis has proven useful for diabetes classification, particularly in cases aged >30 years, where misdiagnosis is most common, but presently, islet autoantibody tests are not routine in clinical practice (11, 48, 546). The contribution of ZnT8 to ICA staining should be confirmed as ICA testing on monkey pancreas is still clinically performed routinely by some NHS laboratories to aid diabetes classification. Differential ICA staining and, by extension, lower sensitivity may be anticipated if ZnT8A epitopes do not recognise monkey ZnT8 in the pancreas tissue. As IAA detection is precluded by sample haemolysis, insulin treatment, and assay variability, which prevents assay harmonisation, detection of ZnT8A is more beneficial to complement GADA/IA-2A for clinical diabetes classification. One study found that >10 years, testing for ZnT8A as opposed to IAA did not lead to a loss of diagnostic sensitivity for T1D (275).

After diagnosis, islet autoantibodies represent a window into ongoing autoimmune responses and  $\beta$ -cell function. Many cross-sectional studies have explored the prevalence of autoantibodies after diagnosis and are often conducted in small cohorts of individuals of

European ancestry with many different study parameters. Few studies have been able to account for the presence and titres of all major islet autoantibodies at and after T1D onset in the same individuals. To our knowledge, the work reported in this thesis is the largest and only study that has been able to determine the prevalence of ZnT8A, GADA, and IA-2A at multiple serum sampling after T1D onset up to >30 years disease duration. Therefore, the responses described in this thesis reflects true autoantibody persistence/loss during disease and not just prevalence. We found that loss of all autoantibody responses is predominantly influenced by low titres at onset followed by longer disease duration and younger age-at-onset. However, genetic factors associated with autoantibody loss, independent of non-genetic covariates, revealed antigen-specific effects that differed from associations at the time of diagnosis in GADA and IA-2A responses but were comparable in ZnT8A responses.

Studies exploring islet autoantibodies after diagnosis have shown waning responses, but these have not always been consistent due to differences between autoantibody specificities (443, 493). Earlier studies (before 2007) do not include ZnT8A (307, 493, 547, 548), whilst many later studies either focus on ZnT8A (347, 428, 443) or have not measured ZnT8A (39, 498, 500). Where studied, the rate of autoantibody loss varies, but generally, GADA are the most prevalent, followed by IA-2A, and ZnT8A are the least common after diagnosis (266). The data presented in this thesis and other studies, when accounting for baseline autoantibody titres at onset, suggests that IA-2A are as persistent as GADA and that ZnT8A is rapidly lost (review in press)(307, 443, 493). Prior to the discovery of ZnT8A, the loss of ICA was shown to occur more rapidly than GADA and IA-2A responses (307, 493, 548), suggesting that undiscovered islet autoantibodies around this time (like ZnT8A) were lost more rapidly than GADA or IA-2A. The degree of ICA staining is thought to represent the total humoral response to  $\beta$ -cell antigens, with the degree of staining proportional to islet autoimmunity present in serum. Both GAD and IA-2 antigens have been confirmed as major contributors to the ICA complex.

However, no study has confirmed this for ZnT8 and the newly discovered TSPAN-7, but presumably, both are partly responsible for ICA staining (268, 549).

The data from previous reports and this project suggests ZnT8A responses are highly dynamic prior to and after T1D onset compared to other humoral responses. The ZnT8A humoral response may reflect a specific stage of  $\beta$ -cell destruction/function/mass through loss of antigenic stimulus given its high  $\beta$ -cell specificity and expression. Therefore, of all islet autoantibody responses, ZnT8A may be more likely to be associated with insulin/C-peptide production. Whilst ZnT8A and C-peptide have both been shown to decline rapidly, post-diagnosis ZnT8A levels did not appear to correlate with C-peptide within 2.5 to 12 years after diagnosis (443). Similarly, within the first 11 years of diagnosis, the presence of ZnT8A and detectable C-peptide were not correlated (548). However, levels of ZnT8A were associated with C-peptide levels in multivariate analysis adjusted for age and duration of diabetes in one cross-sectional study at a median 15 years after onset (448). Autoantibodies were also informative for modelling C-peptide after diagnosis in a recent cross-sectional study within the first decade of diabetes, but these associations were influenced by other factors such as genetic risk and age-at-onset (450). From these cross-sectional studies, autoantibody positivity, especially for ZnT8A, may provide some information about future  $\beta$ -cell function, but the relationship is complex. The loss of C-peptide after diagnosis does not appear to occur at a consistent rate but is clinically robust  $>3$  years disease duration, and this may be part of the reason for the variability between studies (57, 544). It is highly likely that longitudinal and concurrent testing of C-peptide/ZnT8A is required to fully elucidate whether a relationship exists. Establishing the relationship would be hugely beneficial for monitoring  $\beta$ -cell function and diabetes management as presently, testing for ZnT8A would be cheaper than C-peptide. As one of the strongest predictors of autoantibody loss/persistence after T1D onset in all autoantibody responses, it would be of interest to elucidate whether autoantibody titre is related

to residual  $\beta$ -cell function/mass and/or a useful marker of ongoing islet autoimmunity towards residual  $\beta$ -cells. We did not further investigate the relationship between autoantibody prevalence/loss and  $\beta$ -cell function (C-peptide detected by UCPCR) due to a previous report from BOX (449), but additional urine samples are currently being collected from the same individuals to update this analysis in the future.

Understanding ongoing/attenuating islet autoimmunity is likely to be more important when/if therapeutic agents can regenerate/preserve residual  $\beta$ -cell mass/function. Intriguingly, in the recent clinical trial of Teplizumab (T-cell depleting immunotherapy) in at-risk relatives, the pre-specified analysis suggested Teplizumab was more effective at maintaining  $\beta$ -cell function in individuals without ZnT8A (220), reinforcing the idea of an interaction. Currently, it is unclear whether islet autoantibodies could infer therapeutic efficacy or  $\beta$ -cell function in other therapies or in individuals clinically diagnosed with T1D. Autoantibodies may be more important biomarkers for antigen-specific immune interventions, still in the early phases of clinical trials (533). As yet, primary intervention trials have focused on insulin (300, 306, 550) and GAD65 (551, 552) as primary targets of the immune response, but data suggesting that the extracellular region of ZnT8 could be an earlier target of the immune response may lead to ZnT8 becoming a focus of future study. However, the data in this thesis underlining the heterogeneity of humoral ZnT8A responses suggest ZnT8-specific intervention strategies to delay T1D progression may prove difficult.

After diagnosis, islet autoantibodies may also be important for eligibility of islet/stem cell transplant, a treatment aimed at restoring glucose homeostasis in those with T1D. Islet autoantibodies may provide biomarkers for identifying reoccurring  $\beta$ -cell autoimmunity and determining transplantation outcomes. For example, in 25 subjects that received solitary pancreas transplants, 4 (16%) autoantibody changes (seroconversion after transplant,

seroconversion to mAutoab+ve status, or increasing autoantibody titre) was associated with loss of graft function and the addition of ZnT8A to GADA and IA-2A increased the predictive utility of autoantibodies for loss of graft function (553). Before the transplant, islet autoantibodies appear not to influence graft function strongly, but autoantibody seroconversion after transplant is a significant risk factor for re-occurring T1D. The appearance of ZnT8A and increasing ZnT8A levels increased the likelihood of T1D re-emergence in some patient case studies, but this may not be exclusive to ZnT8A responses (441, 554). However, the presence of the *SLC30A8* T allele (rs13266634), presence of *HLA-A\*24*, and higher BMI were independent risk factors for poor graft function in islet allograft recipients (403). However, these findings have not been corroborated yet. The rapid loss of ZnT8A, as shown in this thesis, may make ZnT8A a more specific marker of reoccurring  $\beta$ -cell autoimmunity because the response will usually have disappeared before transplant, unlike IA-2A and GADA.

---

### 5.3 Conclusion

---

In this study, we sought to address many questions about the comparatively under-investigated ZnT8A humoral response pertaining to wider T1D research gaps at different stages of the disease.

Methods were developed and optimised to investigate characteristics of ZnT8A responses (titres, affinity, IgG subclasses, and C-terminal ZnT8 epitope specificity) before and close to T1D diagnosis in select individuals to understand longitudinal islet autoimmunity and its potential implications for T1D risk prediction and/or detection methods. The data collected suggests that ZnT8A responses are dynamic, and individuals display large degrees of heterogeneity in their ZnT8A humoral responses regardless of the specific characteristic investigated. Whilst this precludes the ability to draw robust conclusions for future T1D risk

prediction, it nevertheless indicates that predictive models of T1D that incorporate ZnT8A status should be carefully considered. Larger studies that incorporate and are powered to examine characteristics of ZnT8A responses longitudinally from seroconversion are required to understand whether individually or combined, they impact T1D risk prediction. Ideally, a study without pre-selection for mAutoab+ve status, age, or genetics (DR3/DR4) that incorporates features of ZnT8A (C-terminal ZnT8 and extracellular ZnT8 antigenic constructs: titre, affinity, and epitope specificity), and genes associated with the development of ZnT8A (*HLA-A\*24*, *FCRL3/1q23*, and SNPs in *SLC30A8*), as IgG subclasses did not appear to be promising but should not be fully excluded from future research. There is scope within the BOX study to conduct such a study utilising the developed methods from this project. Presently, there are 70 individuals in BOX that developed ZnT8A prior to T1D diagnosis and provided at least two serum samples. Additionally, there are 400 islet autoantibody positive individuals who were ZnT8A negative in the first available sample but have longitudinal samples that could be investigated for ZnT8A seroconversion pending additional funding. However, the heterogeneity of the data collected suggests that ZnT8-specific intervention strategies to delay T1D progression may prove difficult but many facets of the ZnT8 humoral response remains to be fully elucidated. Nevertheless, the methods developed can be adapted for other islet autoantibody investigations inside/out of the Bristol research department.

Non-genetic and genetic factors associated with longitudinal ZnT8A, GADA, and IA-2A responses after the clinical onset of T1D were determined. Regardless of autoantibody specificity, autoantibody positivity was more likely to be maintained in individuals with long-duration T1D that had high baseline titres at diagnosis. Loss of autoantibody responses is predominantly influenced by low titres at onset followed by longer disease duration and younger age-at-onset, but there were distinct antigen-specific genetic factors that may reflect different humoral responses. Understanding why some individuals maintain autoantibodies for

decades may provide insights into  $\beta$ -cell survival and/or function in longstanding T1D cases in relation to clinical outcomes and intervention trials. However, the findings in this study strongly suggest that this requires autoantibody data close to diagnosis, which many historical studies have lacked. An extension of this work would be linking the autoantibody data from these individuals to residual  $\beta$ -cell function. This is plausible as UCPCR samples are currently being collected from these BOX participants.

A fluid-phase Nluc-ZnT8 LIPS method to detect ZnT8RA/ZnT8WA simultaneously was optimised and validated to replace the conventionally used fluid-phase RIA. Not only were ZnT8A levels highly correlated between Nluc-ZnT8 LIPS and both monomeric ZnT8R/ZnT8W RIAs, but Nluc-ZnT8 LIPS had also improved sensitivity and identified an additional small subset of at-risk relatives that had a 20-year diabetes risk of 26%. However, the Nluc-ZnT8 LIPS assay does not have a greater capacity for automation than RIAs in its current format but can be incorporated into a multiplex assay as a primary screening strategy for islet autoimmunity. Beyond this, future avenues of this work would be to adapt the Nluc-ZnT8 LIPS assay into a bridge-type plate format that has the capacity of integrating into an automated high throughput multiplex assay for future general population screening.

## Chapter 6 - References

---

1. Chiang JL, Kirkman MS, Laffel LM, Peters AL, Type 1 Diabetes Sourcebook A. Type 1 diabetes through the life span: a position statement of the American Diabetes Association. *Diabetes Care*. 2014;37(7):2034-54.
2. Kawasaki E. ZnT8 and type 1 diabetes. *Endocr J*. 2012;59(7):531-7.
3. Theofilopoulos AN, Kono DH, Baccala R. The multiple pathways to autoimmunity. *Nat Immunol*. 2017;18(7):716-24.
4. Gan MJ, Albanese-O'Neill A, Haller MJ. Type 1 diabetes: current concepts in epidemiology, pathophysiology, clinical care, and research. *Curr Probl Pediatr Adolesc Health Care*. 2012;42(10):269-91.
5. Patterson CC, Gyurus E, Rosenbauer J, Cinek O, Neu A, Schober E, et al. Trends in childhood type 1 diabetes incidence in Europe during 1989-2008: evidence of non-uniformity over time in rates of increase. *Diabetologia*. 2012;55(8):2142-7.
6. Redondo MJ, Oram RA, Steck AK. Genetic Risk Scores for Type 1 Diabetes Prediction and Diagnosis. *Curr Diab Rep*. 2017;17(12):129.
7. Gardner SG, Bingley PJ, Sawtell PA, Weeks S, Gale EA. Rising incidence of insulin dependent diabetes in children aged under 5 years in the Oxford region: time trend analysis. The Bart's-Oxford Study Group. *BMJ*. 1997;315(7110):713-7.
8. Zhang B, Kumar RB, Dai H, Feldman BJ. A plasmonic chip for biomarker discovery and diagnosis of type 1 diabetes. *Nat Med*. 2014;20(8):948-53.
9. Atkinson MA, Eisenbarth GS, Michels AW. Type 1 diabetes. *Lancet*. 2014;383(9911):69-82.
10. Thomas NJ, Jones SE, Weedon MN, Shields BM, Oram RA, Hattersley AT. Frequency and phenotype of type 1 diabetes in the first six decades of life: a cross-sectional, genetically stratified survival analysis from UK Biobank. *Lancet Diabetes Endocrinol*. 2018;6(2):122-9.
11. Thomas NJ, Lynam AL, Hill AV, Weedon MN, Shields BM, Oram RA, et al. Type 1 diabetes defined by severe insulin deficiency occurs after 30 years of age and is commonly treated as type 2 diabetes. *Diabetologia*. 2019;62(7):1167-72.
12. Bingley PJ, Bonifacio E, Williams AJ, Genovese S, Bottazzo GF, Gale EA. Prediction of IDDM in the general population: strategies based on combinations of autoantibody markers. *Diabetes*. 1997;46(11):1701-10.
13. Fonolleda M, Murillo M, Vazquez F, Bel J, Vives-Pi M. Remission Phase in Paediatric Type 1 Diabetes: New Understanding and Emerging Biomarkers. *Horm Res Paediatr*. 2017;88(5):307-15.
14. Knip M, Luopajarvi K, Harkonen T. Early life origin of type 1 diabetes. *Semin Immunopathol*. 2017;39(6):653-67.
15. Steck AK, Larsson HE, Liu X, Veijola R, Toppari J, Hagopian WA, et al. Residual beta-cell function in diabetes children followed and diagnosed in the TEDDY study compared to community controls. *Pediatr Diabetes*. 2017.
16. Mobasser M, Shirmohammadi M, Amiri T, Vahed N, Hosseini Fard H, Ghojzadeh M. Prevalence and incidence of type 1 diabetes in the world: a systematic review and meta-analysis. *Health Promot Perspect*. 2020;10(2):98-115.
17. Butalia S, Kaplan GG, Khokhar B, Rabi DM. Environmental Risk Factors and Type 1 Diabetes: Past, Present, and Future. *Can J Diabetes*. 2016;40(6):586-93.

18. Diamond Project Group. Incidence and trends of childhood Type 1 diabetes worldwide 1990-1999. *Diabet Med.* 2006;23(8):857-66.
19. Gonzalez EL, Johansson S, Wallander MA, Rodriguez LA. Trends in the prevalence and incidence of diabetes in the UK: 1996-2005. *J Epidemiol Community Health.* 2009;63(4):332-6.
20. Matzaraki V, Kumar V, Wijmenga C, Zhernakova A. The MHC locus and genetic susceptibility to autoimmune and infectious diseases. *Genome Biol.* 2017;18(1):76.
21. Lounici Boudiaf A, Bouziane D, Smara M, Meddour Y, Haffaf EM, Oudjit B, et al. Could ZnT8 antibodies replace ICA, GAD, IA2 and insulin antibodies in the diagnosis of type 1 diabetes? *Curr Res Transl Med.* 2018;66(1):1-7.
22. Dabelea D, Mayer-Davis EJ, Andrews JS, Dolan LM, Pihoker C, Hamman RF, et al. Clinical evolution of beta cell function in youth with diabetes: the SEARCH for Diabetes in Youth study. *Diabetologia.* 2012;55(12):3359-68.
23. Noble JA, Valdes AM. Genetics of the HLA region in the prediction of type 1 diabetes. *Curr Diab Rep.* 2011;11(6):533-42.
24. Robert AA, Al-Dawish A, Mujammami M, Dawish MAA. Type 1 Diabetes Mellitus in Saudi Arabia: A Soaring Epidemic. *Int J Pediatr.* 2018;2018:9408370.
25. International Diabetes Federation. *IDF Diabetes Atlas 9th ed 2019* [Available from: <https://www.diabetesatlas.org>].
26. Christoffersson G, Rodriguez-Calvo T, von Herrath M. Recent advances in understanding Type 1 Diabetes. *F1000Res.* 2016;5.
27. Raymond NT, Jones JR, Swift PG, Davies MJ, Lawrence G, McNally PG, et al. Comparative incidence of Type I diabetes in children aged under 15 years from South Asian and White or Other ethnic backgrounds in Leicestershire, UK, 1989 to 1998. *Diabetologia.* 2001;44 Suppl 3:B32-6.
28. Soderstrom U, Aman J, Hjern A. Being born in Sweden increases the risk for type 1 diabetes - a study of migration of children to Sweden as a natural experiment. *Acta Paediatr.* 2012;101(1):73-7.
29. Karvonen M, Pitkaniemi J, Tuomilehto J. The onset age of type 1 diabetes in Finnish children has become younger. The Finnish Childhood Diabetes Registry Group. *Diabetes Care.* 1999;22(7):1066-70.
30. Patterson CC, Dahlquist GG, Gyurus E, Green A, Soltesz G, Group ES. Incidence trends for childhood type 1 diabetes in Europe during 1989-2003 and predicted new cases 2005-20: a multicentre prospective registration study. *Lancet.* 2009;373(9680):2027-33.
31. Patterson C, Guariguata L, Dahlquist G, Soltesz G, Ogle G, Silink M. Diabetes in the young - a global view and worldwide estimates of numbers of children with type 1 diabetes. *Diabetes Res Clin Pract.* 2014;103(2):161-75.
32. Dunger DB, Sperling MA, Acerini CL, Bohn DJ, Daneman D, Danne TP, et al. European Society for Paediatric Endocrinology/Lawson Wilkins Pediatric Endocrine Society consensus statement on diabetic ketoacidosis in children and adolescents. *Pediatrics.* 2004;113(2):e133-40.
33. Bluestone JA, Herold K, Eisenbarth G. Genetics, pathogenesis and clinical interventions in type 1 diabetes. *Nature.* 2010;464(7293):1293-300.
34. Rawshani A, Sattar N, Franzen S, Rawshani A, Hattersley AT, Svensson AM, et al. Excess mortality and cardiovascular disease in young adults with type 1 diabetes in relation to age at onset: a nationwide, register-based cohort study. *Lancet.* 2018;392(10146):477-86.
35. Steffes MW, Sibley S, Jackson M, Thomas W. Beta-cell function and the development of diabetes-related complications in the diabetes control and complications trial. *Diabetes Care.* 2003;26(3):832-6.

36. Jeyam A, Colhoun H, McGurnaghan S, Blackbourn L, McDonald TJ, Palmer CNA, et al. Clinical Impact of Residual C-Peptide Secretion in Type 1 Diabetes on Glycemia and Microvascular Complications. *Diabetes Care*. 2021;44(2):390-8.
37. Oram RA, Jones AG, Besser RE, Knight BA, Shields BM, Brown RJ, et al. The majority of patients with long-duration type 1 diabetes are insulin microsecretors and have functioning beta cells. *Diabetologia*. 2014;57(1):187-91.
38. Oram RA, McDonald TJ, Shields BM, Hudson MM, Shepherd MH, Hammersley S, et al. Most people with long-duration type 1 diabetes in a large population-based study are insulin microsecretors. *Diabetes Care*. 2015;38(2):323-8.
39. Keenan HA, Sun JK, Levine J, Doria A, Aiello LP, Eisenbarth G, et al. Residual insulin production and pancreatic  $\beta$ -cell turnover after 50 years of diabetes: Joslin Medalist Study. *Diabetes*. 2010;59(11):2846-53.
40. Yu MG, Keenan HA, Shah HS, Frodsham SG, Pober D, He Z, et al. Residual beta cell function and monogenic variants in long-duration type 1 diabetes patients. *J Clin Invest*. 2019;129(8):3252-63.
41. Campbell-Thompson M. Organ donor specimens: What can they tell us about type 1 diabetes? *Pediatr Diabetes*. 2015;16(5):320-30.
42. Leete P, Willcox A, Krogvold L, Dahl-Jorgensen K, Foulis AK, Richardson SJ, et al. Differential Insulinitic Profiles Determine the Extent of beta-Cell Destruction and the Age at Onset of Type 1 Diabetes. *Diabetes*. 2016;65(5):1362-9.
43. Leete P, Oram RA, McDonald TJ, Shields BM, Ziller C, team Ts, et al. Studies of insulin and proinsulin in pancreas and serum support the existence of aetiopathological endotypes of type 1 diabetes associated with age at diagnosis. *Diabetologia*. 2020.
44. Eisenbarth GS. Type I diabetes mellitus. A chronic autoimmune disease. *N Engl J Med*. 1986;314(21):1360-8.
45. Miller KM, Foster NC, Beck RW, Bergenstal RM, DuBose SN, DiMeglio LA, et al. Current state of type 1 diabetes treatment in the U.S.: updated data from the T1D Exchange clinic registry. *Diabetes Care*. 2015;38(6):971-8.
46. Beran D, Yudkin JS, de Courten M. Access to care for patients with insulin-requiring diabetes in developing countries: case studies of Mozambique and Zambia. *Diabetes Care*. 2005;28(9):2136-40.
47. Pickup JC, Freeman SC, Sutton AJ. Glycaemic control in type 1 diabetes during real time continuous glucose monitoring compared with self monitoring of blood glucose: meta-analysis of randomised controlled trials using individual patient data. *BMJ*. 2011;343:d3805.
48. Hope SV, Wienand-Barnett S, Shepherd M, King SM, Fox C, Khunti K, et al. Practical Classification Guidelines for Diabetes in patients treated with insulin: a cross-sectional study of the accuracy of diabetes diagnosis. *Br J Gen Pract*. 2016;66(646):e315-22.
49. Zghebi SS, Steinke DT, Carr MJ, Rutter MK, Emsley RA, Ashcroft DM. Examining trends in type 2 diabetes incidence, prevalence and mortality in the UK between 2004 and 2014. *Diabetes Obes Metab*. 2017;19(11):1537-45.
50. McDonald TJ, Colclough K, Brown R, Shields B, Shepherd M, Bingley P, et al. Islet autoantibodies can discriminate maturity-onset diabetes of the young (MODY) from Type 1 diabetes. *Diabet Med*. 2011;28(9):1028-33.
51. Patel KA, Weedon MN, Shields BM, Pearson ER, Hattersley AT, McDonald TJ, et al. Zinc Transporter 8 Autoantibodies (ZnT8A) and a Type 1 Diabetes Genetic Risk Score Can Exclude Individuals With Type 1 Diabetes From Inappropriate Genetic Testing for Monogenic Diabetes. *Diabetes Care*. 2018.
52. de Leiva A, Mauricio D, Corcoy R. Diabetes-related autoantibodies and gestational diabetes. *Diabetes Care*. 2007;30 Suppl 2:S127-33.

53. Bingley PJ. Clinical applications of diabetes antibody testing. *J Clin Endocrinol Metab.* 2010;95(1):25-33.
54. The Diabetes Control and Complications Trial Research Group. Effect of intensive therapy on residual beta-cell function in patients with type 1 diabetes in the diabetes control and complications trial. A randomized, controlled trial. The Diabetes Control and Complications Trial Research Group. *Ann Intern Med.* 1998;128(7):517-23.
55. Greenbaum CJ, Beam CA, Boulware D, Gitelman SE, Gottlieb PA, Herold KC, et al. Fall in C-peptide during first 2 years from diagnosis: evidence of at least two distinct phases from composite Type 1 Diabetes TrialNet data. *Diabetes.* 2012;61(8):2066-73.
56. Madsbad S, Faber OK, Binder C, McNair P, Christiansen C, Transbol I. Prevalence of residual beta-cell function in insulin-dependent diabetics in relation to age at onset and duration of diabetes. *Diabetes.* 1978;27 Suppl 1:262-4.
57. Shields BM, McDonald TJ, Oram R, Hill A, Hudson M, Leete P, et al. C-Peptide Decline in Type 1 Diabetes Has Two Phases: An Initial Exponential Fall and a Subsequent Stable Phase. *Diabetes Care.* 2018;41(7):1486-92.
58. Pociot F. Type 1 diabetes genome-wide association studies: not to be lost in translation. *Clin Transl Immunology.* 2017;6(12):e162.
59. Robertson CC, Inshaw JRJ, Onengut-Gumuscu S, Chen WM, Santa Cruz DF, Yang H, et al. Fine-mapping, trans-ancestral and genomic analyses identify causal variants, cells, genes and drug targets for type 1 diabetes. *Nat Genet.* 2021;53(7):962-71.
60. Risch N. Assessing the role of HLA-linked and unlinked determinants of disease. *Am J Hum Genet.* 1987;40(1):1-14.
61. Redondo MJ, Steck AK, Pugliese A. Genetics of type 1 diabetes. *Pediatr Diabetes.* 2018;19(3):346-53.
62. Sfriso P, Ghirardello A, Botsios C, Tonon M, Zen M, Bassi N, et al. Infections and autoimmunity: the multifaceted relationship. *J Leukoc Biol.* 2010;87(3):385-95.
63. Regnell SE, Lernmark A. Early prediction of autoimmune (type 1) diabetes. *Diabetologia.* 2017;60(8):1370-81.
64. Gale EA, Gillespie KM. Diabetes and gender. *Diabetologia.* 2001;44(1):3-15.
65. Pociot F, Lernmark A. Genetic risk factors for type 1 diabetes. *Lancet.* 2016;387(10035):2331-9.
66. Redondo MJ, Rewers M, Yu L, Garg S, Pilcher CC, Elliott RB, et al. Genetic determination of islet cell autoimmunity in monozygotic twin, dizygotic twin, and non-twin siblings of patients with type 1 diabetes: prospective twin study. *BMJ.* 1999;318(7185):698-702.
67. Redondo MJ, Yu L, Hawa M, Mackenzie T, Pyke DA, Eisenbarth GS, et al. Heterogeneity of type I diabetes: analysis of monozygotic twins in Great Britain and the United States. *Diabetologia.* 2001;44(3):354-62.
68. Redondo MJ, Jeffrey J, Fain PR, Eisenbarth GS, Orban T. Concordance for islet autoimmunity among monozygotic twins. *N Engl J Med.* 2008;359(26):2849-50.
69. Lambert AP, Gillespie KM, Thomson G, Cordell HJ, Todd JA, Gale EA, et al. Absolute risk of childhood-onset type 1 diabetes defined by human leukocyte antigen class II genotype: a population-based study in the United Kingdom. *J Clin Endocrinol Metab.* 2004;89(8):4037-43.
70. Lima-Junior Jda C, Pratt-Riccio LR. Major Histocompatibility Complex and Malaria: Focus on *Plasmodium vivax* Infection. *Front Immunol.* 2016;7:13.
71. Dendrou CA, Petersen J, Rossjohn J, Fugger L. HLA variation and disease. *Nat Rev Immunol.* 2018.
72. Meyer D, VR CA, Bitarello BD, DY CB, Nunes K. A genomic perspective on HLA evolution. *Immunogenetics.* 2018;70(1):5-27.

73. Valdes AM, Thomson G, Type 1 Diabetes Genetics C. Several loci in the HLA class III region are associated with T1D risk after adjusting for DRB1-DQB1. *Diabetes Obes Metab.* 2009;11 Suppl 1:46-52.
74. Atkinson MA, Eisenbarth GS. Type 1 diabetes: new perspectives on disease pathogenesis and treatment. *Lancet.* 2001;358(9277):221-9.
75. Schumacher FR, Delamarre L, Jhunjhunwala S, Modrusan Z, Phung QT, Elias JE, et al. Building proteomic tool boxes to monitor MHC class I and class II peptides. *Proteomics.* 2017;17(1-2).
76. Wiczorek M, Abualrous ET, Sticht J, Alvaro-Benito M, Stolzenberg S, Noe F, et al. Major Histocompatibility Complex (MHC) Class I and MHC Class II Proteins: Conformational Plasticity in Antigen Presentation. *Front Immunol.* 2017;8:292.
77. Bakela K, Athanassakis I. Soluble major histocompatibility complex molecules in immune regulation: highlighting class II antigens. *Immunology.* 2018;153(3):315-24.
78. Redondo MJ, Steck AK, Pugliese A. Genetics of type 1 diabetes. *Pediatr Diabetes.* 2017.
79. Wyatt RC, Lanzoni G, Russell MA, Gerling I, Richardson SJ. What the HLA-I!-Classical and Non-classical HLA Class I and Their Potential Roles in Type 1 Diabetes. *Curr Diab Rep.* 2019;19(12):159.
80. Shiina T, Hosomichi K, Inoko H, Kulski JK. The HLA genomic loci map: expression, interaction, diversity and disease. *J Hum Genet.* 2009;54(1):15-39.
81. Braud VM, Allan DS, McMichael AJ. Functions of nonclassical MHC and non-MHC-encoded class I molecules. *Curr Opin Immunol.* 1999;11(1):100-8.
82. Noble JA, Valdes AM, Varney MD, Carlson JA, Moonsamy P, Fear AL, et al. HLA class I and genetic susceptibility to type 1 diabetes: results from the Type 1 Diabetes Genetics Consortium. *Diabetes.* 2010;59(11):2972-9.
83. Nejentsev S, Howson JM, Walker NM, Szeszko J, Field SF, Stevens HE, et al. Localization of type 1 diabetes susceptibility to the MHC class I genes HLA-B and HLA-A. *Nature.* 2007;450(7171):887-92.
84. Valdes AM, Erlich HA, Noble JA. Human leukocyte antigen class I B and C loci contribute to Type 1 Diabetes (T1D) susceptibility and age at T1D onset. *Hum Immunol.* 2005;66(3):301-13.
85. Baschal EE, Baker PR, Eyring KR, Siebert JC, Jasinski JM, Eisenbarth GS. The HLA-B 3906 allele imparts a high risk of diabetes only on specific HLA-DR/DQ haplotypes. *Diabetologia.* 2011;54(7):1702-9.
86. Noble JA, Valdes AM, Bugawan TL, Apple RJ, Thomson G, Erlich HA. The HLA class I A locus affects susceptibility to type 1 diabetes. *Hum Immunol.* 2002;63(8):657-64.
87. Tait BD, Colman PG, Morahan G, Marchinovska L, Dore E, Gellert S, et al. HLA genes associated with autoimmunity and progression to disease in type 1 diabetes. *Tissue Antigens.* 2003;61(2):146-53.
88. Howson JM, Walker NM, Clayton D, Todd JA, Type 1 Diabetes Genetics C. Confirmation of HLA class II independent type 1 diabetes associations in the major histocompatibility complex including HLA-B and HLA-A. *Diabetes Obes Metab.* 2009;11 Suppl 1:31-45.
89. Mbunwe E, Van der Auwera BJ, Vermeulen I, Demeester S, Van Dalem A, Balti EV, et al. HLA-A\*24 is an independent predictor of 5-year progression to diabetes in autoantibody-positive first-degree relatives of type 1 diabetic patients. *Diabetes.* 2013;62(4):1345-50.
90. Long AE, Gillespie KM, Aitken RJ, Goode JC, Bingley PJ, Williams AJ. Humoral responses to islet antigen-2 and zinc transporter 8 are attenuated in patients carrying HLA-A\*24 alleles at the onset of type 1 diabetes. *Diabetes.* 2013;62(6):2067-71.

91. Nakanishi K, Inoko H. Combination of HLA-A24, -DQA1\*03, and -DR9 contributes to acute-onset and early complete beta-cell destruction in type 1 diabetes: longitudinal study of residual beta-cell function. *Diabetes*. 2006;55(6):1862-8.
92. Valdes AM, Thomson G, Erlich HA, Noble JA. Association between type 1 diabetes age of onset and HLA among sibling pairs. *Diabetes*. 1999;48(8):1658-61.
93. Horton R, Wilming L, Rand V, Lovering RC, Bruford EA, Khodiyar VK, et al. Gene map of the extended human MHC. *Nat Rev Genet*. 2004;5(12):889-99.
94. Delli AJ, Vaziri-Sani F, Lindblad B, Elding-Larsson H, Carlsson A, Forsander G, et al. Zinc transporter 8 autoantibodies and their association with SLC30A8 and HLA-DQ genes differ between immigrant and Swedish patients with newly diagnosed type 1 diabetes in the Better Diabetes Diagnosis study. *Diabetes*. 2012;61(10):2556-64.
95. Erlich H, Valdes AM, Noble J, Carlson JA, Varney M, Concannon P, et al. HLA DR-DQ haplotypes and genotypes and type 1 diabetes risk: analysis of the type 1 diabetes genetics consortium families. *Diabetes*. 2008;57(4):1084-92.
96. Insel RA, Dunne JL, Atkinson MA, Chiang JL, Dabelea D, Gottlieb PA, et al. Staging presymptomatic type 1 diabetes: a scientific statement of JDRF, the Endocrine Society, and the American Diabetes Association. *Diabetes Care*. 2015;38(10):1964-74.
97. Jacobsen LM, Posgai A, Seay HR, Haller MJ, Brusko TM. T Cell Receptor Profiling in Type 1 Diabetes. *Curr Diab Rep*. 2017;17(11):118.
98. Ilonen J, Kiviniemi M, Lempainen J, Simell O, Toppari J, Vejjola R, et al. Genetic susceptibility to type 1 diabetes in childhood - estimation of HLA class II associated disease risk and class II effect in various phases of islet autoimmunity. *Pediatr Diabetes*. 2016;17 Suppl 22:8-16.
99. Kostic AD, Gevers D, Siljander H, Vatanen T, Hyotylainen T, Hamalainen AM, et al. The dynamics of the human infant gut microbiome in development and in progression toward type 1 diabetes. *Cell Host Microbe*. 2015;17(2):260-73.
100. Achenbach P, Bonifacio E, Koczwara K, Ziegler AG. Natural history of type 1 diabetes. *Diabetes*. 2005;54 Suppl 2:S25-31.
101. Ikegami H, Fujisawa T, Kawabata Y, Noso S, Ogihara T. Genetics of type 1 diabetes: similarities and differences between Asian and Caucasian populations. *Ann N Y Acad Sci*. 2006;1079:51-9.
102. Kawabata Y, Ikegami H, Kawaguchi Y, Fujisawa T, Shintani M, Ono M, et al. Asian-specific HLA haplotypes reveal heterogeneity of the contribution of HLA-DR and -DQ haplotypes to susceptibility to type 1 diabetes. *Diabetes*. 2002;51(2):545-51.
103. Gillespie KM, Bain SC, Barnett AH, Bingley PJ, Christie MR, Gill GV, et al. The rising incidence of childhood type 1 diabetes and reduced contribution of high-risk HLA haplotypes. *Lancet*. 2004;364(9446):1699-700.
104. Noble JA, Valdes AM, Thomson G, Erlich HA. The HLA class II locus DPB1 can influence susceptibility to type 1 diabetes. *Diabetes*. 2000;49(1):121-5.
105. Cucca F, Dudbridge F, Loddo M, Mulargia AP, Lampis R, Angius E, et al. The HLA-DPB1--associated component of the IDDM1 and its relationship to the major loci HLA-DQB1, -DQA1, and -DRB1. *Diabetes*. 2001;50(5):1200-5.
106. Cruz TD, Valdes AM, Santiago A, Frazer de Llado T, Raffel LJ, Zeidler A, et al. DPB1 alleles are associated with type 1 diabetes susceptibility in multiple ethnic groups. *Diabetes*. 2004;53(8):2158-63.
107. Erlich HA, Rotter JI, Chang JD, Shaw SJ, Raffel LJ, Klitz W, et al. Association of HLA-DPB1\*0301 with IDDM in Mexican-Americans. *Diabetes*. 1996;45(5):610-4.
108. Valdes AM, Noble JA, Genin E, Clerget-Darpoux F, Erlich HA, Thomson G. Modeling of HLA class II susceptibility to Type I diabetes reveals an effect associated with DPB1. *Genet Epidemiol*. 2001;21(3):212-23.

109. Barrett JC, Clayton DG, Concannon P, Akolkar B, Cooper JD, Erlich HA, et al. Genome-wide association study and meta-analysis find that over 40 loci affect risk of type 1 diabetes. *Nat Genet.* 2009;41(6):703-7.
110. Oram RA, Patel K, Hill A, Shields B, McDonald TJ, Jones A, et al. A Type 1 Diabetes Genetic Risk Score Can Aid Discrimination Between Type 1 and Type 2 Diabetes in Young Adults. *Diabetes Care.* 2016;39(3):337-44.
111. Pociot F, Akolkar B, Concannon P, Erlich HA, Julier C, Morahan G, et al. Genetics of type 1 diabetes: what's next? *Diabetes.* 2010;59(7):1561-71.
112. Concannon P, Rich SS, Nepom GT. Genetics of type 1A diabetes. *N Engl J Med.* 2009;360(16):1646-54.
113. Onengut-Gumuscu S, Chen WM, Burren O, Cooper NJ, Quinlan AR, Mychaleckyj JC, et al. Fine mapping of type 1 diabetes susceptibility loci and evidence for colocalization of causal variants with lymphoid gene enhancers. *Nat Genet.* 2015;47(4):381-6.
114. Bell GI, Horita S, Karam JH. A polymorphic locus near the human insulin gene is associated with insulin-dependent diabetes mellitus. *Diabetes.* 1984;33(2):176-83.
115. Todd JA. Genetic analysis of type 1 diabetes using whole genome approaches. *Proc Natl Acad Sci U S A.* 1995;92(19):8560-5.
116. Carry PM, Vanderlinden LA, Johnson RK, Dong F, Steck AK, Frohnert BI, et al. DNA methylation near the INS gene is associated with INS genetic variation (rs689) and type 1 diabetes in the Diabetes Autoimmunity Study in the Young. *Pediatr Diabetes.* 2020.
117. Pugliese A, Zeller M, Fernandez A, Jr., Zalcberg LJ, Bartlett RJ, Ricordi C, et al. The insulin gene is transcribed in the human thymus and transcription levels correlated with allelic variation at the INS VNTR-IDD2 susceptibility locus for type 1 diabetes. *Nat Genet.* 1997;15(3):293-7.
118. Barratt BJ, Payne F, Lowe CE, Hermann R, Healy BC, Harold D, et al. Remapping the insulin gene/IDD2 locus in type 1 diabetes. *Diabetes.* 2004;53(7):1884-9.
119. Bennett ST, Lucassen AM, Gough SC, Powell EE, Undlien DE, Pritchard LE, et al. Susceptibility to human type 1 diabetes at IDD2 is determined by tandem repeat variation at the insulin gene minisatellite locus. *Nat Genet.* 1995;9(3):284-92.
120. Pugliese A, Miceli D. The insulin gene in diabetes. *Diabetes Metab Res Rev.* 2002;18(1):13-25.
121. Undlien DE, Bennett ST, Todd JA, Akselsen HE, Ikaheimo I, Reijonen H, et al. Insulin gene region-encoded susceptibility to IDD2 maps upstream of the insulin gene. *Diabetes.* 1995;44(6):620-5.
122. Pugliese A, Awdeh ZL, Alper CA, Jackson RA, Eisenbarth GS. The paternally inherited insulin gene B allele (1,428 FokI site) confers protection from insulin-dependent diabetes in families. *J Autoimmun.* 1994;7(5):687-94.
123. Vafiadis P, Bennett ST, Todd JA, Nadeau J, Grabs R, Goodyer CG, et al. Insulin expression in human thymus is modulated by INS VNTR alleles at the IDD2 locus. *Nat Genet.* 1997;15(3):289-92.
124. Rewers M, Ludvigsson J. Environmental risk factors for type 1 diabetes. *Lancet.* 2016;387(10035):2340-8.
125. de Goffau MC, Luopajarvi K, Knip M, Ilonen J, Ruohtula T, Harkonen T, et al. Fecal microbiota composition differs between children with beta-cell autoimmunity and those without. *Diabetes.* 2013;62(4):1238-44.
126. Cardwell CR, Stene LC, Joner G, Davis EA, Cinek O, Rosenbauer J, et al. Birthweight and the risk of childhood-onset type 1 diabetes: a meta-analysis of observational studies using individual patient data. *Diabetologia.* 2010;53(4):641-51.

127. Koczwara K, Bonifacio E, Ziegler AG. Transmission of maternal islet antibodies and risk of autoimmune diabetes in offspring of mothers with type 1 diabetes. *Diabetes*. 2004;53(1):1-4.
128. Lund-Blix NA, Dydensborg Sander S, Stordal K, Nybo Andersen AM, Ronningen KS, Joner G, et al. Infant Feeding and Risk of Type 1 Diabetes in Two Large Scandinavian Birth Cohorts. *Diabetes Care*. 2017;40(7):920-7.
129. Stordal K, Lundeby KM, Brantsaeter AL, Haugen M, Nakstad B, Lund-Blix NA, et al. Breast-feeding and Infant Hospitalization for Infections: Large Cohort and Sibling Analysis. *J Pediatr Gastroenterol Nutr*. 2017;65(2):225-31.
130. Yeung WC, Rawlinson WD, Craig ME. Enterovirus infection and type 1 diabetes mellitus: systematic review and meta-analysis of observational molecular studies. *BMJ*. 2011;342:d35.
131. Paronen J, Knip M, Savilahti E, Virtanen SM, Ilonen J, Akerblom HK, et al. Effect of cow's milk exposure and maternal type 1 diabetes on cellular and humoral immunization to dietary insulin in infants at genetic risk for type 1 diabetes. Finnish Trial to Reduce IDDM in the Genetically at Risk Study Group. *Diabetes*. 2000;49(10):1657-65.
132. Karjalainen J, Martin JM, Knip M, Ilonen J, Robinson BH, Savilahti E, et al. A bovine albumin peptide as a possible trigger of insulin-dependent diabetes mellitus. *N Engl J Med*. 1992;327(5):302-7.
133. Knip M, Virtanen SM, Akerblom HK. Infant feeding and the risk of type 1 diabetes. *Am J Clin Nutr*. 2010;91(5):1506S-13S.
134. EURODIAB Substudy 2 Study Group. Vitamin D supplement in early childhood and risk for Type I (insulin-dependent) diabetes mellitus. The EURODIAB Substudy 2 Study Group. *Diabetologia*. 1999;42(1):51-4.
135. Teddy Study Group. The Environmental Determinants of Diabetes in the Young (TEDDY) Study. *Ann N Y Acad Sci*. 2008;1150:1-13.
136. Richardson SJ, Horwitz MS. Is type 1 diabetes "going viral"? *Diabetes*. 2014;63(7):2203-5.
137. Rodriguez-Calvo T, Sabouri S, Anquetil F, von Herrath MG. The viral paradigm in type 1 diabetes: Who are the main suspects? *Autoimmun Rev*. 2016;15(10):964-9.
138. Krogvold L, Edwin B, Buanes T, Frisk G, Skog O, Anagandula M, et al. Detection of a low-grade enteroviral infection in the islets of langerhans of living patients newly diagnosed with type 1 diabetes. *Diabetes*. 2015;64(5):1682-7.
139. Lee HS, Briese T, Winkler C, Rewers M, Bonifacio E, Hyoty H, et al. Next-generation sequencing for viruses in children with rapid-onset type 1 diabetes. *Diabetologia*. 2013;56(8):1705-11.
140. Strachan DP. Hay fever, hygiene, and household size. *BMJ*. 1989;299(6710):1259-60.
141. Okada H, Kuhn C, Feillet H, Bach JF. The 'hygiene hypothesis' for autoimmune and allergic diseases: an update. *Clin Exp Immunol*. 2010;160(1):1-9.
142. Pundziute-Lycka A, Urbonaite B, Dahlquist G. Infections and risk of Type I (insulin-dependent) diabetes mellitus in Lithuanian children. *Diabetologia*. 2000;43(10):1229-34.
143. McKinney PA, Okasha M, Parslow RC, Law GR, Gurney KA, Williams R, et al. Early social mixing and childhood Type 1 diabetes mellitus: a case-control study in Yorkshire, UK. *Diabet Med*. 2000;17(3):236-42.
144. EURODIAB Substudy 2 Study Group. Infections and vaccinations as risk factors for childhood type I (insulin-dependent) diabetes mellitus: a multicentre case-control investigation. EURODIAB Substudy 2 Study Group. *Diabetologia*. 2000;43(1):47-53.
145. Stene LC, Magnus P, Lie RT, Sovik O, Joner G. Maternal and paternal age at delivery, birth order, and risk of childhood onset type 1 diabetes: population based cohort study. *BMJ*. 2001;323(7309):369.

146. Patterson CC, Carson DJ, Hadden DR. Epidemiology of childhood IDDM in Northern Ireland 1989-1994: low incidence in areas with highest population density and most household crowding. Northern Ireland Diabetes Study Group. *Diabetologia*. 1996;39(9):1063-9.
147. Cardwell CR, Carson DJ, Yarnell J, Shields MD, Patterson CC. Atopy, home environment and the risk of childhood-onset type 1 diabetes: a population-based case-control study. *Pediatr Diabetes*. 2008;9(3 Pt 1):191-6.
148. Boerner BP, Sarvetnick NE. Type 1 diabetes: role of intestinal microbiome in humans and mice. *Ann N Y Acad Sci*. 2011;1243:103-18.
149. Manichanh C, Varela E, Martinez C, Antolin M, Llopis M, Dore J, et al. The gut microbiota predispose to the pathophysiology of acute postradiotherapy diarrhea. *Am J Gastroenterol*. 2008;103(7):1754-61.
150. Gronlund MM, Lehtonen OP, Eerola E, Kero P. Fecal microflora in healthy infants born by different methods of delivery: permanent changes in intestinal flora after cesarean delivery. *J Pediatr Gastroenterol Nutr*. 1999;28(1):19-25.
151. Salminen S, Gibson GR, McCartney AL, Isolauri E. Influence of mode of delivery on gut microbiota composition in seven year old children. *Gut*. 2004;53(9):1388-9.
152. Turnbaugh PJ, Hamady M, Yatsunenko T, Cantarel BL, Duncan A, Ley RE, et al. A core gut microbiome in obese and lean twins. *Nature*. 2009;457(7228):480-4.
153. Davis-Richardson AG, Ardisson AN, Dias R, Simell V, Leonard MT, Kemppainen KM, et al. *Bacteroides dorei* dominates gut microbiome prior to autoimmunity in Finnish children at high risk for type 1 diabetes. *Front Microbiol*. 2014;5:678.
154. Endesfelder D, zu Castell W, Ardisson A, Davis-Richardson AG, Achenbach P, Hagen M, et al. Compromised gut microbiota networks in children with anti-islet cell autoimmunity. *Diabetes*. 2014;63(6):2006-14.
155. Chang SW, Lee HC. Vitamin D and health - The missing vitamin in humans. *Pediatr Neonatol*. 2019;60(3):237-44.
156. Prietl B, Treiber G, Pieber TR, Amrein K. Vitamin D and immune function. *Nutrients*. 2013;5(7):2502-21.
157. Zipitis CS, Akobeng AK. Vitamin D supplementation in early childhood and risk of type 1 diabetes: a systematic review and meta-analysis. *Arch Dis Child*. 2008;93(6):512-7.
158. Walter M, Kaupper T, Adler K, Foersch J, Bonifacio E, Ziegler AG. No effect of the 1 $\alpha$ ,25-dihydroxyvitamin D<sub>3</sub> on beta-cell residual function and insulin requirement in adults with new-onset type 1 diabetes. *Diabetes Care*. 2010;33(7):1443-8.
159. Bizzarri C, Pitocco D, Napoli N, Di Stasio E, Maggi D, Manfrini S, et al. No protective effect of calcitriol on beta-cell function in recent-onset type 1 diabetes: the IMDIAB XIII trial. *Diabetes Care*. 2010;33(9):1962-3.
160. Campbell-Thompson ML, Atkinson MA, Butler AE, Chapman NM, Frisk G, Gianani R, et al. The diagnosis of insulinitis in human type 1 diabetes. *Diabetologia*. 2013;56(11):2541-3.
161. In't Veld P. Insulinitis in human type 1 diabetes: The quest for an elusive lesion. *Islets*. 2011;3(4):131-8.
162. Gepts W. Pathologic anatomy of the pancreas in juvenile diabetes mellitus. *Diabetes*. 1965;14(10):619-33.
163. Foulis AK, Liddle CN, Farquharson MA, Richmond JA, Weir RS. The histopathology of the pancreas in type 1 (insulin-dependent) diabetes mellitus: a 25-year review of deaths in patients under 20 years of age in the United Kingdom. *Diabetologia*. 1986;29(5):267-74.
164. Willcox A, Richardson SJ, Bone AJ, Foulis AK, Morgan NG. Analysis of islet inflammation in human type 1 diabetes. *Clin Exp Immunol*. 2009;155(2):173-81.
165. Schmidt MB. Uber die beziehung der Langerhans' schen Inselndes pancreas zum diabetes mellitus. *Muench Med Wochenschr*. 1902;49:51-4.

166. Lecompte PM. Insulinitis in early juvenile diabetes. *AMA Arch Pathol.* 1958;66(4):450-7.
167. Gepts W, De Mey J. Islet cell survival determined by morphology. An immunocytochemical study of the islets of Langerhans in juvenile diabetes mellitus. *Diabetes.* 1978;27 Suppl 1:251-61.
168. Foulis AK, Farquharson MA, Hardman R. Aberrant expression of class II major histocompatibility complex molecules by B cells and hyperexpression of class I major histocompatibility complex molecules by insulin containing islets in type 1 (insulin-dependent) diabetes mellitus. *Diabetologia.* 1987;30(5):333-43.
169. Bottazzo GF, Dean BM, McNally JM, MacKay EH, Swift PG, Gamble DR. In situ characterization of autoimmune phenomena and expression of HLA molecules in the pancreas in diabetic insulinitis. *N Engl J Med.* 1985;313(6):353-60.
170. Foulis AK, McGill M, Farquharson MA. Insulinitis in type 1 (insulin-dependent) diabetes mellitus in man--macrophages, lymphocytes, and interferon-gamma containing cells. *J Pathol.* 1991;165(2):97-103.
171. In't Veld P, Lievens D, De Grijse J, Ling Z, Van der Auwera B, Pipeleers-Marichal M, et al. Screening for insulinitis in adult autoantibody-positive organ donors. *Diabetes.* 2007;56(9):2400-4.
172. Gianani R, Putnam A, Still T, Yu L, Miao D, Gill RG, et al. Initial results of screening of nondiabetic organ donors for expression of islet autoantibodies. *J Clin Endocrinol Metab.* 2006;91(5):1855-61.
173. Campbell-Thompson M, Fu A, Kaddis JS, Wasserfall C, Schatz DA, Pugliese A, et al. Insulinitis and beta-Cell Mass in the Natural History of Type 1 Diabetes. *Diabetes.* 2016;65(3):719-31.
174. In't Veld P. Insulinitis in human type 1 diabetes: a comparison between patients and animal models. *Semin Immunopathol.* 2014;36(5):569-79.
175. Campbell-Thompson ML, Atkinson MA, Butler AE, Giepmans BN, von Herrath MG, Hyoty H, et al. Re-addressing the 2013 consensus guidelines for the diagnosis of insulinitis in human type 1 diabetes: is change necessary? *Diabetologia.* 2017;60(4):753-5.
176. Itoh N, Hanafusa T, Miyazaki A, Miyagawa J, Yamagata K, Yamamoto K, et al. Mononuclear cell infiltration and its relation to the expression of major histocompatibility complex antigens and adhesion molecules in pancreas biopsy specimens from newly diagnosed insulin-dependent diabetes mellitus patients. *J Clin Invest.* 1993;92(5):2313-22.
177. Imagawa A, Hanafusa T, Tamura S, Moriwaki M, Itoh N, Yamamoto K, et al. Pancreatic biopsy as a procedure for detecting in situ autoimmune phenomena in type 1 diabetes: close correlation between serological markers and histological evidence of cellular autoimmunity. *Diabetes.* 2001;50(6):1269-73.
178. Krogvold L, Edwin B, Buanes T, Ludvigsson J, Korsgren O, Hyoty H, et al. Pancreatic biopsy by minimal tail resection in live adult patients at the onset of type 1 diabetes: experiences from the DiViD study. *Diabetologia.* 2014;57(4):841-3.
179. Tauriainen S, Salmela K, Rantala I, Knip M, Hyoty H. Collecting high-quality pancreatic tissue for experimental study from organ donors with signs of beta-cell autoimmunity. *Diabetes Metab Res Rev.* 2010;26(7):585-92.
180. Campbell-Thompson M, Wasserfall C, Kaddis J, Albanese-O'Neill A, Staeva T, Nierras C, et al. Network for Pancreatic Organ Donors with Diabetes (nPOD): developing a tissue biobank for type 1 diabetes. *Diabetes Metab Res Rev.* 2012;28(7):608-17.
181. Panzer JK, Hiller H, Cohrs CM, Almaca J, Enos SJ, Beery M, et al. Pancreas tissue slices from organ donors enable in situ analysis of type 1 diabetes pathogenesis. *JCI Insight.* 2020;5(8).

182. Chen YG, Mathews CE, Driver JP. The Role of NOD Mice in Type 1 Diabetes Research: Lessons from the Past and Recommendations for the Future. *Front Endocrinol (Lausanne)*. 2018;9:51.
183. Serreze DV, Chen YG. Of mice and men: use of animal models to identify possible interventions for the prevention of autoimmune type 1 diabetes in humans. *Trends Immunol*. 2005;26(11):603-7.
184. Kindt TJ, Goldsby, R.A., Osborne, B.A. *Kuby Immunology*. WHFreeman & Co Ltd: Sixth Edition. 2006.
185. Pugliese A. Autoreactive T cells in type 1 diabetes. *J Clin Invest*. 2017;127(8):2881-91.
186. Dang M, Rockell J, Wagner R, Wenzlau JM, Yu L, Hutton JC, et al. Human type 1 diabetes is associated with T cell autoimmunity to zinc transporter 8. *J Immunol*. 2011;186(10):6056-63.
187. Xing Y, Hogquist KA. T-cell tolerance: central and peripheral. *Cold Spring Harb Perspect Biol*. 2012;4(6).
188. Wardemann H, Yurasov S, Schaefer A, Young JW, Meffre E, Nussenzweig MC. Predominant autoantibody production by early human B cell precursors. *Science*. 2003;301(5638):1374-7.
189. Rathmell JC, Cooke MP, Ho WY, Grein J, Townsend SE, Davis MM, et al. CD95 (Fas)-dependent elimination of self-reactive B cells upon interaction with CD4+ T cells. *Nature*. 1995;376(6536):181-4.
190. Nemazee D. Mechanisms of central tolerance for B cells. *Nat Rev Immunol*. 2017;17(5):281-94.
191. Chaplin DD. Overview of the immune response. *J Allergy Clin Immunol*. 2010;125(2 Suppl 2):S3-23.
192. Kaiko GE, Horvat JC, Beagley KW, Hansbro PM. Immunological decision-making: how does the immune system decide to mount a helper T-cell response? *Immunology*. 2008;123(3):326-38.
193. Buckner JH, Ziegler SF. Regulating the immune system: the induction of regulatory T cells in the periphery. *Arthritis Res Ther*. 2004;6(5):215-22.
194. Levings MK, Bacchetta R, Schulz U, Roncarolo MG. The role of IL-10 and TGF-beta in the differentiation and effector function of T regulatory cells. *Int Arch Allergy Immunol*. 2002;129(4):263-76.
195. Moore KW, de Waal Malefyt R, Coffman RL, O'Garra A. Interleukin-10 and the interleukin-10 receptor. *Annu Rev Immunol*. 2001;19:683-765.
196. Letterio JJ, Roberts AB. Regulation of immune responses by TGF-beta. *Annu Rev Immunol*. 1998;16:137-61.
197. James EA, Mallone R, Kent SC, DiLorenzo TP. T-Cell Epitopes and Neo-epitopes in Type 1 Diabetes: A Comprehensive Update and Reappraisal. *Diabetes*. 2020;69(7):1311-35.
198. Eerligh P, van Lummel M, Zaldumbide A, Moustakas AK, Duinkerken G, Bondinas G, et al. Functional consequences of HLA-DQ8 homozygosity versus heterozygosity for islet autoimmunity in type 1 diabetes. *Genes Immun*. 2011;12(6):415-27.
199. Kent SC, Chen Y, Bregoli L, Clemmings SM, Kenyon NS, Ricordi C, et al. Expanded T cells from pancreatic lymph nodes of type 1 diabetic subjects recognize an insulin epitope. *Nature*. 2005;435(7039):224-8.
200. Babon JA, DeNicola ME, Blodgett DM, Crevecoeur I, Buttrick TS, Maehr R, et al. Analysis of self-antigen specificity of islet-infiltrating T cells from human donors with type 1 diabetes. *Nat Med*. 2016;22(12):1482-7.

201. Christianson SW, Shultz LD, Leiter EH. Adoptive transfer of diabetes into immunodeficient NOD-scid/scid mice. Relative contributions of CD4+ and CD8+ T-cells from diabetic versus prediabetic NOD.NON-Thy-1a donors. *Diabetes*. 1993;42(1):44-55.
202. Campbell IL, Kay TW, Oxbrow L, Harrison LC. Essential role for interferon-gamma and interleukin-6 in autoimmune insulin-dependent diabetes in NOD/Wehi mice. *J Clin Invest*. 1991;87(2):739-42.
203. Katz JD, Benoist C, Mathis D. T helper cell subsets in insulin-dependent diabetes. *Science*. 1995;268(5214):1185-8.
204. Pilstrom B, Bjork L, Bohme J. Demonstration of a TH1 cytokine profile in the late phase of NOD insulinitis. *Cytokine*. 1995;7(8):806-14.
205. Hultgren B, Huang X, Dybdal N, Stewart TA. Genetic absence of gamma-interferon delays but does not prevent diabetes in NOD mice. *Diabetes*. 1996;45(6):812-7.
206. Lee MS, Mueller R, Wicker LS, Peterson LB, Sarvetnick N. IL-10 is necessary and sufficient for autoimmune diabetes in conjunction with NOD MHC homozygosity. *J Exp Med*. 1996;183(6):2663-8.
207. Tian J, Lehmann PV, Kaufman DL. Determinant spreading of T helper cell 2 (Th2) responses to pancreatic islet autoantigens. *J Exp Med*. 1997;186(12):2039-43.
208. de Jersey J, Snelgrove SL, Palmer SE, Teteris SA, Mullbacher A, Miller JF, et al. Beta cells cannot directly prime diabetogenic CD8 T cells in nonobese diabetic mice. *Proc Natl Acad Sci U S A*. 2007;104(4):1295-300.
209. Hamilton-Williams EE, Palmer SE, Charlton B, Slattery RM. Beta cell MHC class I is a late requirement for diabetes. *Proc Natl Acad Sci U S A*. 2003;100(11):6688-93.
210. Tsai S, Shamel A, Santamaria P. CD8+ T cells in type 1 diabetes. *Adv Immunol*. 2008;100:79-124.
211. Wong FS, Karttunen J, Dumont C, Wen L, Visintin I, Pilip IM, et al. Identification of an MHC class I-restricted autoantigen in type 1 diabetes by screening an organ-specific cDNA library. *Nat Med*. 1999;5(9):1026-31.
212. Daniel D, Wegmann DR. Protection of nonobese diabetic mice from diabetes by intranasal or subcutaneous administration of insulin peptide B-(9-23). *Proc Natl Acad Sci U S A*. 1996;93(2):956-60.
213. Buckner JH. Mechanisms of impaired regulation by CD4(+)CD25(+)FOXP3(+) regulatory T cells in human autoimmune diseases. *Nat Rev Immunol*. 2010;10(12):849-59.
214. Long SA, Cerozaletti K, Bollyky PL, Tatum M, Shilling H, Zhang S, et al. Defects in IL-2R signaling contribute to diminished maintenance of FOXP3 expression in CD4(+)CD25(+) regulatory T-cells of type 1 diabetic subjects. *Diabetes*. 2010;59(2):407-15.
215. Brusko T, Wasserfall C, McGrail K, Schatz R, Viener HL, Schatz D, et al. No alterations in the frequency of FOXP3+ regulatory T-cells in type 1 diabetes. *Diabetes*. 2007;56(3):604-12.
216. Lindley S, Dayan CM, Bishop A, Roep BO, Peakman M, Tree TI. Defective suppressor function in CD4(+)CD25(+) T-cells from patients with type 1 diabetes. *Diabetes*. 2005;54(1):92-9.
217. Brusko TM, Wasserfall CH, Clare-Salzler MJ, Schatz DA, Atkinson MA. Functional defects and the influence of age on the frequency of CD4+ CD25+ T-cells in type 1 diabetes. *Diabetes*. 2005;54(5):1407-14.
218. Tang Q, Adams JY, Penaranda C, Melli K, Piaggio E, Sgouroudis E, et al. Central role of defective interleukin-2 production in the triggering of islet autoimmune destruction. *Immunity*. 2008;28(5):687-97.
219. D'Alise AM, Auyeung V, Feuerer M, Nishio J, Fontenot J, Benoist C, et al. The defect in T-cell regulation in NOD mice is an effect on the T-cell effectors. *Proc Natl Acad Sci U S A*. 2008;105(50):19857-62.

220. Herold KC, Bundy BN, Long SA, Bluestone JA, DiMeglio LA, Dufort MJ, et al. An Anti-CD3 Antibody, Teplizumab, in Relatives at Risk for Type 1 Diabetes. *N Engl J Med.* 2019;381(7):603-13.
221. Sims EK, Bundy BN, Stier K, Serti E, Lim N, Long SA, et al. Teplizumab improves and stabilizes beta cell function in antibody-positive high-risk individuals. *Sci Transl Med.* 2021;13(583).
222. Assan R, Feutren G, Sirmaj J, Laborie C, Boitard C, Vexiau P, et al. Plasma C-peptide levels and clinical remissions in recent-onset type I diabetic patients treated with cyclosporin A and insulin. *Diabetes.* 1990;39(7):768-74.
223. Keymeulen B, Vandemeulebroucke E, Ziegler AG, Mathieu C, Kaufman L, Hale G, et al. Insulin needs after CD3-antibody therapy in new-onset type 1 diabetes. *N Engl J Med.* 2005;352(25):2598-608.
224. Orban T, Bundy B, Becker DJ, DiMeglio LA, Gitelman SE, Goland R, et al. Co-stimulation modulation with abatacept in patients with recent-onset type 1 diabetes: a randomised, double-blind, placebo-controlled trial. *Lancet.* 2011;378(9789):412-9.
225. Rigby MR, DiMeglio LA, Rendell MS, Felner EI, Dostou JM, Gitelman SE, et al. Targeting of memory T cells with alefacept in new-onset type 1 diabetes (T1DAL study): 12 month results of a randomised, double-blind, placebo-controlled phase 2 trial. *Lancet Diabetes Endocrinol.* 2013;1(4):284-94.
226. Roep BO, Thomaidou S, van Tienhoven R, Zaldumbide A. Type 1 diabetes mellitus as a disease of the beta-cell (do not blame the immune system?). *Nat Rev Endocrinol.* 2021;17(3):150-61.
227. Schroeder HW, Jr., Cavacini L. Structure and function of immunoglobulins. *J Allergy Clin Immunol.* 2010;125(2 Suppl 2):S41-52.
228. Yu K, Lieber MR. Current insights into the mechanism of mammalian immunoglobulin class switch recombination. *Crit Rev Biochem Mol Biol.* 2019;54(4):333-51.
229. Stavnezer J, Guikema JE, Schrader CE. Mechanism and regulation of class switch recombination. *Annu Rev Immunol.* 2008;26:261-92.
230. Mauri C, Ehrenstein MR. The 'short' history of regulatory B cells. *Trends Immunol.* 2008;29(1):34-40.
231. Wolf SD, Dittel BN, Hardardottir F, Janeway CA, Jr. Experimental autoimmune encephalomyelitis induction in genetically B cell-deficient mice. *J Exp Med.* 1996;184(6):2271-8.
232. Fillatreau S, Sweenie CH, McGeachy MJ, Gray D, Anderton SM. B cells regulate autoimmunity by provision of IL-10. *Nat Immunol.* 2002;3(10):944-50.
233. Achour A, Simon Q, Mohr A, Seite JF, Youinou P, Bendaoud B, et al. Human regulatory B cells control the TFH cell response. *J Allergy Clin Immunol.* 2017;140(1):215-22.
234. van de Veen W, Stanic B, Wirz OF, Jansen K, Globinska A, Akdis M. Role of regulatory B cells in immune tolerance to allergens and beyond. *J Allergy Clin Immunol.* 2016;138(3):654-65.
235. Silveira PA, Grey ST. B cells in the spotlight: innocent bystanders or major players in the pathogenesis of type 1 diabetes. *Trends Endocrinol Metab.* 2006;17(4):128-35.
236. Alberts B, Johnson, A., Lewis, J., Raff, M., Roberts, K., Walter, P. *Molecular Biology of the Cell* 4th edition. B cells and antibodies. New York: Garland Science. 2002.
237. Lightman SM, Utley A, Lee KP. Survival of Long-Lived Plasma Cells (LLPC): Piecing Together the Puzzle. *Front Immunol.* 2019;10:965.
238. Brynjolfsson SF, Persson Berg L, Olsen Ekerhult T, Rimkute I, Wick MJ, Martensson IL, et al. Long-Lived Plasma Cells in Mice and Men. *Front Immunol.* 2018;9:2673.

239. Chang HD, Tokoyoda K, Hoyer B, Alexander T, Khodadadi L, Mei H, et al. Pathogenic memory plasma cells in autoimmunity. *Curr Opin Immunol.* 2019;61:86-91.
240. Valenzuela NM, Schaub S. The Biology of IgG Subclasses and Their Clinical Relevance to Transplantation. *Transplantation.* 2018;102(1S Suppl 1):S7-S13.
241. Grey HM, Kunkel HG. H Chain Subgroups of Myeloma Proteins and Normal 7s Gamma-Globulin. *J Exp Med.* 1964;120:253-66.
242. Bruhns P, Iannascoli B, England P, Mancardi DA, Fernandez N, Jorieux S, et al. Specificity and affinity of human Fcγ receptors and their polymorphic variants for human IgG subclasses. *Blood.* 2009;113(16):3716-25.
243. Vidarsson G, Dekkers G, Rispens T. IgG subclasses and allotypes: from structure to effector functions. *Front Immunol.* 2014;5:520.
244. Bonifacio E, Scirpoli M, Kredel K, Fuchtenbusch M, Ziegler AG. Early autoantibody responses in prediabetes are IgG1 dominated and suggest antigen-specific regulation. *J Immunol.* 1999;163(1):525-32.
245. Zouali M, Jefferis R, Eyquem A. IgG subclass distribution of autoantibodies to DNA and to nuclear ribonucleoproteins in autoimmune diseases. *Immunology.* 1984;51(3):595-600.
246. Millward A, Hussain MJ, Peakman M, Pyke DA, Leslie RD, Vergani D. Characterization of islet cell antibody in insulin dependent diabetes: evidence for IgG1 subclass restriction and polyclonality. *Clin Exp Immunol.* 1988;71(2):353-6.
247. Parker AR, Skold M, Ramsden DB, Oejo-Vinyals JG, Lopez-Hoyos M, Harding S. The Clinical Utility of Measuring IgG Subclass Immunoglobulins During Immunological Investigation for Suspected Primary Antibody Deficiencies. *Lab Med.* 2017;48(4):314-25.
248. Stapleton NM, Andersen JT, Stemerding AM, Bjarnarson SP, Verheul RC, Gerritsen J, et al. Competition for FcRn-mediated transport gives rise to short half-life of human IgG3 and offers therapeutic potential. *Nat Commun.* 2011;2:599.
249. de Lange GG. Polymorphisms of human immunoglobulins: Gm, Am, Em and Km allotypes. *Exp Clin Immunogenet.* 1989;6(1):7-17.
250. Calonga-Solis V, Malheiros D, Beltrame MH, Vargas LB, Dourado RM, Issler HC, et al. Unveiling the Diversity of Immunoglobulin Heavy Constant Gamma (IGHG) Gene Segments in Brazilian Populations Reveals 28 Novel Alleles and Evidence of Gene Conversion and Natural Selection. *Front Immunol.* 2019;10:1161.
251. Damelang T, Rogerson SJ, Kent SJ, Chung AW. Role of IgG3 in Infectious Diseases. *Trends Immunol.* 2019;40(3):197-211.
252. Chu TH, Patz EF, Jr., Ackerman ME. Coming together at the hinges: Therapeutic prospects of IgG3. *MAbs.* 2021;13(1):1882028.
253. Yamamoto M, Tabeya T, Naishiro Y, Yajima H, Ishigami K, Shimizu Y, et al. Value of serum IgG4 in the diagnosis of IgG4-related disease and in differentiation from rheumatic diseases and other diseases. *Mod Rheumatol.* 2012;22(3):419-25.
254. Bloem SJ, Roep BO. The elusive role of B lymphocytes and islet autoantibodies in (human) type 1 diabetes. *Diabetologia.* 2017;60(7):1185-9.
255. Arif S, Leete P, Nguyen V, Marks K, Nor NM, Estorninho M, et al. Blood and islet phenotypes indicate immunological heterogeneity in type 1 diabetes. *Diabetes.* 2014;63(11):3835-45.
256. Pescovitz MD, Greenbaum CJ, Krause-Steinrauf H, Becker DJ, Gitelman SE, Goland R, et al. Rituximab, B-lymphocyte depletion, and preservation of beta-cell function. *N Engl J Med.* 2009;361(22):2143-52.
257. Edwards JC, Szczepanski L, Szechinski J, Filipowicz-Sosnowska A, Emery P, Close DR, et al. Efficacy of B-cell-targeted therapy with rituximab in patients with rheumatoid arthritis. *N Engl J Med.* 2004;350(25):2572-81.

258. Noorchashm H, Noorchashm N, Kern J, Rostami SY, Barker CF, Naji A. B-cells are required for the initiation of insulinitis and sialitis in nonobese diabetic mice. *Diabetes*. 1997;46(6):941-6.
259. Serreze DV, Chapman HD, Varnum DS, Hanson MS, Reifsnyder PC, Richard SD, et al. B lymphocytes are essential for the initiation of T cell-mediated autoimmune diabetes: analysis of a new "speed congenic" stock of NOD.Ig mu null mice. *J Exp Med*. 1996;184(5):2049-53.
260. Serreze DV, Fleming SA, Chapman HD, Richard SD, Leiter EH, Tisch RM. B lymphocytes are critical antigen-presenting cells for the initiation of T cell-mediated autoimmune diabetes in nonobese diabetic mice. *J Immunol*. 1998;161(8):3912-8.
261. Hu CY, Rodriguez-Pinto D, Du W, Ahuja A, Henegariu O, Wong FS, et al. Treatment with CD20-specific antibody prevents and reverses autoimmune diabetes in mice. *J Clin Invest*. 2007;117(12):3857-67.
262. Fiorina P, Vergani A, Dada S, Jurewicz M, Wong M, Law K, et al. Targeting CD22 reprograms B-cells and reverses autoimmune diabetes. *Diabetes*. 2008;57(11):3013-24.
263. Greeley SA, Katsumata M, Yu L, Eisenbarth GS, Moore DJ, Goodarzi H, et al. Elimination of maternally transmitted autoantibodies prevents diabetes in nonobese diabetic mice. *Nat Med*. 2002;8(4):399-402.
264. Wong FS, Hu C, Xiang Y, Wen L. To B or not to B--pathogenic and regulatory B cells in autoimmune diabetes. *Curr Opin Immunol*. 2010;22(6):723-31.
265. Bottazzo GF, Florin-Christensen A, Doniach D. Islet-cell antibodies in diabetes mellitus with autoimmune polyendocrine deficiencies. *Lancet*. 1974;2(7892):1279-83.
266. Lampasona V, Liberati D. Islet Autoantibodies. *Curr Diab Rep*. 2016;16(6):53.
267. Palmer JP, Asplin CM, Clemons P, Lyen K, Tatpati O, Raghu PK, et al. Insulin antibodies in insulin-dependent diabetics before insulin treatment. *Science*. 1983;222(4630):1337-9.
268. Baekkeskov S, Aanstoot HJ, Christgau S, Reetz A, Solimena M, Cascalho M, et al. Identification of the 64K autoantigen in insulin-dependent diabetes as the GABA-synthesizing enzyme glutamic acid decarboxylase. *Nature*. 1990;347(6289):151-6.
269. Rabin DU, Pleasic SM, Palmer-Crocker R, Shapiro JA. Cloning and expression of IDDM-specific human autoantigens. *Diabetes*. 1992;41(2):183-6.
270. Wenzlau JM, Juhl K, Yu L, Moua O, Sarkar SA, Gottlieb P, et al. The cation efflux transporter ZnT8 (Slc30A8) is a major autoantigen in human type 1 diabetes. *Proc Natl Acad Sci U S A*. 2007;104(43):17040-5.
271. McLaughlin KA, Richardson CC, Ravishankar A, Brigatti C, Liberati D, Lampasona V, et al. Identification of Tetraspanin-7 as a Target of Autoantibodies in Type 1 Diabetes. *Diabetes*. 2016;65(6):1690-8.
272. Vaziri-Sani F, Oak S, Radtke J, Lernmark K, Lynch K, Agardh CD, et al. ZnT8 autoantibody titers in type 1 diabetes patients decline rapidly after clinical onset. *Autoimmunity*. 2010;43(8):598-606.
273. Bravis V, Kaur A, Walkey HC, Godsland IF, Misra S, Bingley PJ, et al. Relationship between islet autoantibody status and the clinical characteristics of children and adults with incident type 1 diabetes in a UK cohort. *BMJ Open*. 2018;8(4):e020904.
274. Long AE, Gillespie KM, Rokni S, Bingley PJ, Williams AJ. Rising incidence of type 1 diabetes is associated with altered immunophenotype at diagnosis. *Diabetes*. 2012;61(3):683-6.
275. Vermeulen I, Weets I, Asanghanwa M, Ruige J, Van Gaal L, Mathieu C, et al. Contribution of antibodies against IA-2beta and zinc transporter 8 to classification of diabetes diagnosed under 40 years of age. *Diabetes Care*. 2011;34(8):1760-5.

276. Dickerson MT, Dadi PK, Butterworth RB, Nakhe AY, Graff SM, Zaborska KE, et al. Tetraspanin-7 regulation of L-type voltage-dependent calcium channels controls pancreatic beta-cell insulin secretion. *J Physiol*. 2020;598(21):4887-905.
277. Williams CL, Long AE. What has zinc transporter 8 autoimmunity taught us about type 1 diabetes? *Diabetologia*. 2019;62(11):1969-76.
278. Rewers M, Norris JM, Eisenbarth GS, Erlich HA, Beaty B, Klingensmith G, et al. Beta-cell autoantibodies in infants and toddlers without IDDM relatives: diabetes autoimmunity study in the young (DAISY). *J Autoimmun*. 1996;9(3):405-10.
279. Rewers M, Bugawan TL, Norris JM, Blair A, Beaty B, Hoffman M, et al. Newborn screening for HLA markers associated with IDDM: diabetes autoimmunity study in the young (DAISY). *Diabetologia*. 1996;39(7):807-12.
280. Nejentsev S, Sjoroos M, Soukka T, Knip M, Simell O, Lovgren T, et al. Population-based genetic screening for the estimation of Type 1 diabetes mellitus risk in Finland: selective genotyping of markers in the HLA-DQB1, HLA-DQA1 and HLA-DRB1 loci. *Diabet Med*. 1999;16(12):985-92.
281. Kimpimaki T, Kulmala P, Savola K, Kupila A, Korhonen S, Simell T, et al. Natural history of beta-cell autoimmunity in young children with increased genetic susceptibility to type 1 diabetes recruited from the general population. *J Clin Endocrinol Metab*. 2002;87(10):4572-9.
282. Ziegler AG, Hummel M, Schenker M, Bonifacio E. Autoantibody appearance and risk for development of childhood diabetes in offspring of parents with type 1 diabetes: the 2-year analysis of the German BABYDIAB Study. *Diabetes*. 1999;48(3):460-8.
283. Bingley PJ, Gale EA. Incidence of insulin dependent diabetes in England: a study in the Oxford region, 1985-6. *BMJ*. 1989;298(6673):558-60.
284. Mahon JL, Sosenko JM, Rafkin-Mervis L, Krause-Steinrauf H, Lachin JM, Thompson C, et al. The TrialNet Natural History Study of the Development of Type 1 Diabetes: objectives, design, and initial results. *Pediatr Diabetes*. 2009;10(2):97-104.
285. Dorchy H. [Screening, prediction and prevention of type 1 diabetes. Role of the Belgian Diabetes Registry]. *Rev Med Brux*. 1999;20(1):15-20.
286. So M, Speake C, Steck AK, Lundgren M, Colman PG, Palmer JP, et al. Advances in Type 1 Diabetes Prediction using Islet Autoantibodies: Beyond a Simple Count. *Endocr Rev*. 2021.
287. Ziegler AG, Rewers M, Simell O, Simell T, Lempainen J, Steck A, et al. Seroconversion to multiple islet autoantibodies and risk of progression to diabetes in children. *JAMA*. 2013;309(23):2473-9.
288. Vehik K, Bonifacio E, Lernmark A, Yu L, Williams A, Schatz D, et al. Hierarchical Order of Distinct Autoantibody Spreading and Progression to Type 1 Diabetes in the TEDDY Study. *Diabetes Care*. 2020;43(9):2066-73.
289. Achenbach P, Lampasona V, Landherr U, Koczwara K, Krause S, Grallert H, et al. Autoantibodies to zinc transporter 8 and SLC30A8 genotype stratify type 1 diabetes risk. *Diabetologia*. 2009;52(9):1881-8.
290. Ziegler AG, Bonifacio E, Group B-BS. Age-related islet autoantibody incidence in offspring of patients with type 1 diabetes. *Diabetologia*. 2012;55(7):1937-43.
291. Gorus FK, Balti EV, Messaoui A, Demeester S, Van Dalem A, Costa O, et al. Twenty-Year Progression Rate to Clinical Onset According to Autoantibody Profile, Age, and HLA-DQ Genotype in a Registry-Based Group of Children and Adults With a First-Degree Relative With Type 1 Diabetes. *Diabetes Care*. 2017;40(8):1065-72.
292. De Grijse J, Asanghanwa M, Nouthe B, Albrecher N, Goubert P, Vermeulen I, et al. Predictive power of screening for antibodies against insulinoma-associated protein 2 beta (IA-2beta) and zinc transporter-8 to select first-degree relatives of type 1 diabetic patients with risk

of rapid progression to clinical onset of the disease: implications for prevention trials. *Diabetologia*. 2010;53(3):517-24.

293. Yu L, Rewers M, Gianani R, Kawasaki E, Zhang Y, Verge C, et al. Antiislet autoantibodies usually develop sequentially rather than simultaneously. *J Clin Endocrinol Metab*. 1996;81(12):4264-7.

294. Vermeulen I, Weets I, Costa O, Asanghanwa M, Verhaeghen K, Decochez K, et al. An important minority of prediabetic first-degree relatives of type 1 diabetic patients derives from seroconversion to persistent autoantibody positivity after 10 years of age. *Diabetologia*. 2012;55(2):413-20.

295. Endesfelder D, Zu Castell W, Bonifacio E, Rewers M, Hagopian WA, She JX, et al. Time-Resolved Autoantibody Profiling Facilitates Stratification of Preclinical Type 1 Diabetes in Children. *Diabetes*. 2019;68(1):119-30.

296. Bingley PJ, Wherrett DK, Shultz A, Rafkin LE, Atkinson MA, Greenbaum CJ. Type 1 Diabetes TrialNet: A Multifaceted Approach to Bringing Disease-Modifying Therapy to Clinical Use in Type 1 Diabetes. *Diabetes Care*. 2018;41(4):653-61.

297. Giannopoulou EZ, Winkler C, Chmiel R, Matzke C, Scholz M, Beyerlein A, et al. Islet autoantibody phenotypes and incidence in children at increased risk for type 1 diabetes. *Diabetologia*. 2015;58(10):2317-23.

298. Krischer JP, Liu X, Vehik K, Akolkar B, Hagopian WA, Rewers MJ, et al. Predicting Islet Cell Autoimmunity and Type 1 Diabetes: An 8-Year TEDDY Study Progress Report. *Diabetes Care*. 2019;42(6):1051-60.

299. Bingley PJ, Gale EA, European Nicotinamide Diabetes Intervention Trial G. Progression to type 1 diabetes in islet cell antibody-positive relatives in the European Nicotinamide Diabetes Intervention Trial: the role of additional immune, genetic and metabolic markers of risk. *Diabetologia*. 2006;49(5):881-90.

300. Ziegler AG, Achenbach P, Berner R, Casteels K, Danne T, Gundert M, et al. Oral insulin therapy for primary prevention of type 1 diabetes in infants with high genetic risk: the GPPAD-POInT (global platform for the prevention of autoimmune diabetes primary oral insulin trial) study protocol. *BMJ Open*. 2019;9(6):e028578.

301. Krischer JP, Lynch KF, Schatz DA, Ilonen J, Lernmark A, Hagopian WA, et al. The 6 year incidence of diabetes-associated autoantibodies in genetically at-risk children: the TEDDY study. *Diabetologia*. 2015;58(5):980-7.

302. Krischer JP, Liu X, Lernmark A, Hagopian WA, Rewers MJ, She JX, et al. The Influence of Type 1 Diabetes Genetic Susceptibility Regions, Age, Sex, and Family History on the Progression From Multiple Autoantibodies to Type 1 Diabetes: A TEDDY Study Report. *Diabetes*. 2017;66(12):3122-9.

303. Smith MJ, Rihanek M, Wasserfall C, Mathews CE, Atkinson MA, Gottlieb PA, et al. Loss of B-Cell Anergy in Type 1 Diabetes Is Associated With High-Risk HLA and Non-HLA Disease Susceptibility Alleles. *Diabetes*. 2018;67(4):697-703.

304. Bingley PJ, Christie MR, Bonifacio E, Bonfanti R, Shattock M, Fonte MT, et al. Combined analysis of autoantibodies improves prediction of IDDM in islet cell antibody-positive relatives. *Diabetes*. 1994;43(11):1304-10.

305. Wherrett DK, Chiang JL, Delamater AM, DiMeglio LA, Gitelman SE, Gottlieb PA, et al. Defining pathways for development of disease-modifying therapies in children with type 1 diabetes: a consensus report. *Diabetes Care*. 2015;38(10):1975-85.

306. Writing Committee for the Type 1 Diabetes TrialNet Oral Insulin Study G, Krischer JP, Schatz DA, Bundy B, Skyler JS, Greenbaum CJ. Effect of Oral Insulin on Prevention of Diabetes in Relatives of Patients With Type 1 Diabetes: A Randomized Clinical Trial. *JAMA*. 2017;318(19):1891-902.

307. Decochez K, De Leeuw IH, Keymeulen B, Mathieu C, Rottiers R, Weets I, et al. IA-2 autoantibodies predict impending type I diabetes in siblings of patients. *Diabetologia*. 2002;45(12):1658-66.
308. Verge CF, Gianani R, Kawasaki E, Yu L, Pietropaolo M, Jackson RA, et al. Prediction of type I diabetes in first-degree relatives using a combination of insulin, GAD, and ICA512bdc/IA-2 autoantibodies. *Diabetes*. 1996;45(7):926-33.
309. Gorus FK, Balti EV, Vermeulen I, Demeester S, Van Dalem A, Costa O, et al. Screening for insulinoma antigen 2 and zinc transporter 8 autoantibodies: a cost-effective and age-independent strategy to identify rapid progressors to clinical onset among relatives of type 1 diabetic patients. *Clin Exp Immunol*. 2013;171(1):82-90.
310. Hao W, Gitelman S, DiMeglio LA, Boulware D, Greenbaum CJ, Type 1 Diabetes TrialNet Study G. Fall in C-Peptide During First 4 Years From Diagnosis of Type 1 Diabetes: Variable Relation to Age, HbA1c, and Insulin Dose. *Diabetes Care*. 2016;39(10):1664-70.
311. Redondo MJ, Sosenko J, Libman I, McVean JFF, Tosur M, Atkinson MA, et al. Single Islet Autoantibody at Diagnosis of Clinical Type 1 Diabetes is Associated With Older Age and Insulin Resistance. *J Clin Endocrinol Metab*. 2020;105(5).
312. Long AE, Wilson IV, Becker DJ, Libman IM, Arena VC, Wong FS, et al. Characteristics of slow progression to diabetes in multiple islet autoantibody-positive individuals from five longitudinal cohorts: the SNAIL study. *Diabetologia*. 2018;61(6):1484-90.
313. Gillespie KM, Long AE. What Have Slow Progressors Taught Us About T1D-Mind the Gap! *Curr Diab Rep*. 2019;19(10):99.
314. Steck AK, Vehik K, Bonifacio E, Lernmark A, Ziegler AG, Hagopian WA, et al. Predictors of Progression From the Appearance of Islet Autoantibodies to Early Childhood Diabetes: The Environmental Determinants of Diabetes in the Young (TEDDY). *Diabetes Care*. 2015;38(5):808-13.
315. Naserke HE, Ziegler AG, Lampasona V, Bonifacio E. Early development and spreading of autoantibodies to epitopes of IA-2 and their association with progression to type 1 diabetes. *J Immunol*. 1998;161(12):6963-9.
316. Achenbach P, Koczwara K, Knopff A, Naserke H, Ziegler AG, Bonifacio E. Mature high-affinity immune responses to (pro)insulin anticipate the autoimmune cascade that leads to type 1 diabetes. *J Clin Invest*. 2004;114(4):589-97.
317. Achenbach P, Warncke K, Reiter J, Naserke HE, Williams AJ, Bingley PJ, et al. Stratification of type 1 diabetes risk on the basis of islet autoantibody characteristics. *Diabetes*. 2004;53(2):384-92.
318. Yu L, Boulware DC, Beam CA, Hutton JC, Wenzlau JM, Greenbaum CJ, et al. Zinc transporter-8 autoantibodies improve prediction of type 1 diabetes in relatives positive for the standard biochemical autoantibodies. *Diabetes Care*. 2012;35(6):1213-8.
319. Yu L, Dong F, Miao D, Fouts AR, Wenzlau JM, Steck AK. Proinsulin/Insulin autoantibodies measured with electrochemiluminescent assay are the earliest indicator of prediabetic islet autoimmunity. *Diabetes Care*. 2013;36(8):2266-70.
320. Steck AK, Johnson K, Barriga KJ, Miao D, Yu L, Hutton JC, et al. Age of islet autoantibody appearance and mean levels of insulin, but not GAD or IA-2 autoantibodies, predict age of diagnosis of type 1 diabetes: diabetes autoimmunity study in the young. *Diabetes Care*. 2011;34(6):1397-9.
321. Bosi E, Boulware DC, Becker DJ, Buckner JH, Geyer S, Gottlieb PA, et al. Impact of Age and Antibody Type on Progression From Single to Multiple Autoantibodies in Type 1 Diabetes Relatives. *J Clin Endocrinol Metab*. 2017;102(8):2881-6.

322. Jacobsen LM, Bocchino L, Evans-Molina C, DiMeglio L, Goland R, Wilson DM, et al. The risk of progression to type 1 diabetes is highly variable in individuals with multiple autoantibodies following screening. *Diabetologia*. 2020;63(3):588-96.
323. Bingley PJ, Boulware DC, Krischer JP, Type 1 Diabetes TrialNet Study G. The implications of autoantibodies to a single islet antigen in relatives with normal glucose tolerance: development of other autoantibodies and progression to type 1 diabetes. *Diabetologia*. 2016;59(3):542-9.
324. Wyatt RC, Brigatti C, Liberati D, Grace SL, Gillard BT, Long AE, et al. The first 142 amino acids of glutamate decarboxylase do not contribute to epitopes recognized by autoantibodies associated with Type 1 diabetes. *Diabet Med*. 2018;35(7):954-63.
325. Williams AJ, Lampasona V, Wyatt R, Brigatti C, Gillespie KM, Bingley PJ, et al. Reactivity to N-Terminally Truncated GAD65(96-585) Identifies GAD Autoantibodies That Are More Closely Associated With Diabetes Progression in Relatives of Patients With Type 1 Diabetes. *Diabetes*. 2015;64(9):3247-52.
326. Kawasaki E, Yu L, Rewers MJ, Hutton JC, Eisenbarth GS. Definition of multiple ICA512/phogrin autoantibody epitopes and detection of intramolecular epitope spreading in relatives of patients with type 1 diabetes. *Diabetes*. 1998;47(5):733-42.
327. Kawasaki E, Nakamura K, Kuriya G, Satoh T, Kuwahara H, Kobayashi M, et al. Autoantibodies to insulin, insulinoma-associated antigen-2, and zinc transporter 8 improve the prediction of early insulin requirement in adult-onset autoimmune diabetes. *J Clin Endocrinol Metab*. 2010;95(2):707-13.
328. Wenzlau JM, Liu Y, Yu L, Moua O, Fowler KT, Rangasamy S, et al. A common nonsynonymous single nucleotide polymorphism in the SLC30A8 gene determines ZnT8 autoantibody specificity in type 1 diabetes. *Diabetes*. 2008;57(10):2693-7.
329. Hampe CS, Hammerle LP, Bekris L, Ortqvist E, Persson B, Lernmark A. Stable GAD65 autoantibody epitope patterns in type 1 diabetes children five years after onset. *J Autoimmun*. 2002;18(1):49-53.
330. Schlosser M, Banga JP, Madec AM, Binder KA, Strebelow M, Rjasanowski I, et al. Dynamic changes of GAD65 autoantibody epitope specificities in individuals at risk of developing type 1 diabetes. *Diabetologia*. 2005;48(5):922-30.
331. Schlosser M, Koczwarra K, Kenk H, Strebelow M, Rjasanowski I, Wassmuth R, et al. In insulin-autoantibody-positive children from the general population, antibody affinity identifies those at high and low risk. *Diabetologia*. 2005;48(9):1830-2.
332. Long AE, Gooneratne AT, Rokni S, Williams AJ, Bingley PJ. The role of autoantibodies to zinc transporter 8 in prediction of type 1 diabetes in relatives: lessons from the European Nicotinamide Diabetes Intervention Trial (ENDIT) cohort. *J Clin Endocrinol Metab*. 2012;97(2):632-7.
333. Jia X, He L, Miao D, Waugh K, Geno Rasmussen C, Dong F, et al. High-affinity ZnT8 autoantibodies by electrochemiluminescence assay improve risk prediction for type 1 diabetes. *J Clin Endocrinol Metab*. 2021.
334. Castano L, Ziegler AG, Ziegler R, Shoelson S, Eisenbarth GS. Characterization of insulin autoantibodies in relatives of patients with type I diabetes. *Diabetes*. 1993;42(8):1202-9.
335. Hall TR, Thomas JW, Padoa CJ, Torn C, Landin-Olsson M, Ortqvist E, et al. Longitudinal epitope analysis of insulin-binding antibodies in type 1 diabetes. *Clin Exp Immunol*. 2006;146(1):9-14.
336. Hampe CS, Hammerle LP, Bekris L, Ortqvist E, Kockum I, Rolandsson O, et al. Recognition of glutamic acid decarboxylase (GAD) by autoantibodies from different GAD antibody-positive phenotypes. *J Clin Endocrinol Metab*. 2000;85(12):4671-9.

337. Bonifacio E, Lampasona V, Bernasconi L, Ziegler AG. Maturation of the humoral autoimmune response to epitopes of GAD in preclinical childhood type 1 diabetes. *Diabetes*. 2000;49(2):202-8.
338. Lampasona V, Bearzatto M, Genovese S, Bosi E, Ferrari M, Bonifacio E. Autoantibodies in insulin-dependent diabetes recognize distinct cytoplasmic domains of the protein tyrosine phosphatase-like IA-2 autoantigen. *J Immunol*. 1996;157(6):2707-11.
339. Bonifacio E, Lampasona V, Bingley PJ. IA-2 (islet cell antigen 512) is the primary target of humoral autoimmunity against type 1 diabetes-associated tyrosine phosphatase autoantigens. *J Immunol*. 1998;161(5):2648-54.
340. McLaughlin KA, Richardson CC, Williams S, Bonifacio E, Morgan D, Feltbower RG, et al. Relationships between major epitopes of the IA-2 autoantigen in Type 1 diabetes: Implications for determinant spreading. *Clin Immunol*. 2015;160(2):226-36.
341. Elvers KT, Geoghegan I, Shoemark DK, Lampasona V, Bingley PJ, Williams AJ. The core cysteines, (C909) of islet antigen-2 and (C945) of islet antigen-2beta, are crucial to autoantibody binding in type 1 diabetes. *Diabetes*. 2013;62(1):214-22.
342. Trajkovski M, Mziaut H, Altkruger A, Ouwendijk J, Knoch KP, Muller S, et al. Nuclear translocation of an ICA512 cytosolic fragment couples granule exocytosis and insulin expression in  $\beta$ -cells. *J Cell Biol*. 2004;167(6):1063-74.
343. Curnock RM, Reed CR, Rokni S, Broadhurst JW, Bingley PJ, Williams AJ. Insulin autoantibody affinity measurement using a single concentration of unlabelled insulin competitor discriminates risk in relatives of patients with type 1 diabetes. *Clinical and Experimental Immunology*. 2012;167(1):67-72.
344. Mayr A, Schlosser M, Grober N, Kenk H, Ziegler AG, Bonifacio E, et al. GAD autoantibody affinity and epitope specificity identify distinct immunization profiles in children at risk for type 1 diabetes. *Diabetes*. 2007;56(6):1527-33.
345. Bender C, Schlosser M, Christen U, Ziegler AG, Achenbach P. GAD autoantibody affinity in schoolchildren from the general population. *Diabetologia*. 2014;57(9):1911-8.
346. Krause S, Chmiel R, Bonifacio E, Scholz M, Powell M, Furmaniak J, et al. IA-2 autoantibody affinity in children at risk for type 1 diabetes. *Clin Immunol*. 2012;145(3):224-9.
347. Howson JM, Krause S, Stevens H, Smyth DJ, Wenzlau JM, Bonifacio E, et al. Genetic association of zinc transporter 8 (ZnT8) autoantibodies in type 1 diabetes cases. *Diabetologia*. 2012;55(7):1978-84.
348. Bauer W, Veijola R, Lempainen J, Kiviniemi M, Harkonen T, Toppari J, et al. Age at Seroconversion, HLA Genotype, and Specificity of Autoantibodies in Progression of Islet Autoimmunity in Childhood. *J Clin Endocrinol Metab*. 2019;104(10):4521-30.
349. Genovese S, Bonfanti R, Bazzigaluppi E, Lampasona V, Benazzi E, Bosi E, et al. Association of IA-2 autoantibodies with HLA DR4 phenotypes in IDDM. *Diabetologia*. 1996;39(10):1223-6.
350. Ye J, Long AE, Pearson JA, Taylor H, Bingley PJ, Williams AJ, et al. Attenuated humoral responses in HLA-A\*24-positive individuals at risk of type 1 diabetes. *Diabetologia*. 2015;58(10):2284-7.
351. Mire-Sluis AR, Gaines Das R, Lernmark A. The World Health Organization International Collaborative Study for islet cell antibodies. *Diabetologia*. 2000;43(10):1282-92.
352. Gleichmann H, Bottazzo GF. Progress toward standardization of cytoplasmic islet cell-antibody assay. *Diabetes*. 1987;36(5):578-84.
353. Verge CF, Stenger D, Bonifacio E, Colman PG, Pilcher C, Bingley PJ, et al. Combined use of autoantibodies (IA-2) autoantibody, GAD autoantibody, insulin autoantibody, cytoplasmic islet cell antibodies) in type 1 diabetes - Combinatorial Islet Autoantibody Workshop. *Diabetes*. 1998;47(12):1857-66.

354. Bingley PJ, Bonifacio E, Shattock M, Gillmor HA, Sawtell PA, Dunger DB, et al. Can islet cell antibodies predict IDDM in the general population? *Diabetes Care*. 1993;16(1):45-50.
355. Boehm BO, Seissler J, Gluck M, Manfras BJ, Thomas H, Schmidt K, et al. The level and the persistence of islet cell antibodies in healthy schoolchildren are associated with polymorphic residues of the HLA-DQ beta chain. *Dis Markers*. 1991;9(5):273-80.
356. Williams AJ, Bingley PJ, Bonifacio E, Palmer JP, Gale EA. A novel micro-assay for insulin autoantibodies. *J Autoimmun*. 1997;10(5):473-8.
357. Petersen JS, Hejnaes KR, Moody A, Karlsen AE, Marshall MO, Hoier-Madsen M, et al. Detection of GAD65 antibodies in diabetes and other autoimmune diseases using a simple radioligand assay. *Diabetes*. 1994;43(3):459-67.
358. Brooking H, Ananieva-Jordanova R, Arnold C, Amoroso M, Powell M, Betterle C, et al. A sensitive non-isotopic assay for GAD65 autoantibodies. *Clin Chim Acta*. 2003;331(1-2):55-9.
359. Rahmati K, Lernmark A, Becker C, Foltyn-Zadura A, Larsson K, Ivarsson SA, et al. A comparison of serum and EDTA plasma in the measurement of glutamic acid decarboxylase autoantibodies (GADA) and autoantibodies to islet antigen-2 (IA-2A) using the RSR radioimmunoassay (RIA) and enzyme linked immunosorbent assay (ELISA) kits. *Clin Lab*. 2008;54(7-8):227-35.
360. Miao D, Guyer KM, Dong F, Jiang L, Steck AK, Rewers M, et al. GAD65 autoantibodies detected by electrochemiluminescence assay identify high risk for type 1 diabetes. *Diabetes*. 2013;62(12):4174-8.
361. Chen S, Willis J, Maclean C, Ananieva-Jordanova R, Amoroso MA, Brooking H, et al. Sensitive non-isotopic assays for autoantibodies to IA-2 and to a combination of both IA-2 and GAD65. *Clin Chim Acta*. 2005;357(1):74-83.
362. Dunseath G, Ananieva-Jordanova R, Coles R, Powell M, Amoroso M, Furmaniak J, et al. Bridging-type enzyme-linked immunoassay for zinc transporter 8 autoantibody measurements in adult patients with diabetes mellitus. *Clin Chim Acta*. 2015;447:90-5.
363. Yu L, Miao D, Scrimgeour L, Johnson K, Rewers M, Eisenbarth GS. Distinguishing persistent insulin autoantibodies with differential risk: nonradioactive bivalent proinsulin/insulin autoantibody assay. *Diabetes*. 2012;61(1):179-86.
364. Amoroso M, Achenbach P, Powell M, Coles R, Chlebowska M, Carr L, et al. 3 Screen islet cell autoantibody ELISA: A sensitive and specific ELISA for the combined measurement of autoantibodies to GAD65, to IA-2 and to ZnT8. *Clin Chim Acta*. 2016;462:60-4.
365. Gu Y, Zhao ZY, Waugh K, Miao DM, Jia XF, Cheng J, et al. High-throughput multiplexed autoantibody detection to screen type 1 diabetes and multiple autoimmune diseases simultaneously. *Ebiomedicine*. 2019;47:365-72.
366. Liberati D, Wyatt RC, Brigatti C, Marzinotto I, Ferrari M, Bazzigaluppi E, et al. A novel LIPS assay for insulin autoantibodies. *Acta Diabetol*. 2018;55(3):263-70.
367. Tsai CT, Robinson PV, Spencer CA, Bertozzi CR. Ultrasensitive Antibody Detection by Agglutination-PCR (ADAP). *ACS Cent Sci*. 2016;2(3):139-47.
368. Cortez FJ, Gebhart D, Robinson PV, Seftel D, Pourmandi N, Owyong J, et al. Sensitive detection of multiple islet autoantibodies in type 1 diabetes using small sample volumes by agglutination-PCR. *PLoS One*. 2020;15(11):e0242049.
369. Burbelo PD, Gunti S, Keller JM, Morse CG, Deeks SG, Lionakis MS, et al. Ultrarapid Measurement of Diagnostic Antibodies by Magnetic Capture of Immune Complexes. *Sci Rep*. 2017;7(1):3818.
370. Bottazzo GF, Gleichmann H. Immunology and Diabetes Workshops - Report of the 1st International Workshop on the Standardization of Cytoplasmic Islet Cell Antibodies - Summary of a Workshop Organized by the Juvenile-Diabetes-Foundation-International Held in Monte-Carlo on 31 October and 1 November 1985. *Diabetologia*. 1986;29(2):125-6.

371. Schlosser M, Mueller PW, Torn C, Bonifacio E, Bingley PJ, Participating L. Diabetes Antibody Standardization Program: evaluation of assays for insulin autoantibodies. *Diabetologia*. 2010;53(12):2611-20.
372. Bingley PJ, Bonifacio E, Mueller PW. Diabetes Antibody Standardization Program: first assay proficiency evaluation. *Diabetes*. 2003;52(5):1128-36.
373. Torn C, Mueller PW, Schlosser M, Bonifacio E, Bingley PJ, Participating L. Diabetes Antibody Standardization Program: evaluation of assays for autoantibodies to glutamic acid decarboxylase and islet antigen-2. *Diabetologia*. 2008;51(5):846-52.
374. Lampasona V, Schlosser M, Mueller PW, Williams AJ, Wenzlau JM, Hutton JC, et al. Diabetes antibody standardization program: first proficiency evaluation of assays for autoantibodies to zinc transporter 8. *Clin Chem*. 2011;57(12):1693-702.
375. Lampasona V, Pittman DL, Williams AJ, Achenbach P, Schlosser M, Akolkar B, et al. Islet Autoantibody Standardization Program 2018 Workshop: Interlaboratory Comparison of Glutamic Acid Decarboxylase Autoantibody Assay Performance. *Clin Chem*. 2019;65(9):1141-52.
376. Carvalho S, Molina-Lopez J, Parsons D, Corpe C, Maret W, Hogstrand C. Differential cytolocalization and functional assays of the two major human SLC30A8 (ZnT8) isoforms. *J Trace Elem Med Biol*. 2017;44:116-24.
377. Chimienti F, Devergnas S, Favier A, Seve M. Identification and cloning of a beta-cell-specific zinc transporter, ZnT-8, localized into insulin secretory granules. *Diabetes*. 2004;53(9):2330-7.
378. Chimienti F, Devergnas S, Pattou F, Schuit F, Garcia-Cuenca R, Vandewalle B, et al. In vivo expression and functional characterization of the zinc transporter ZnT8 in glucose-induced insulin secretion. *J Cell Sci*. 2006;119(Pt 20):4199-206.
379. Davidson HW, Wenzlau JM, O'Brien RM. Zinc transporter 8 (ZnT8) and beta cell function. *Trends Endocrinol Metab*. 2014;25(8):415-24.
380. Hutton JC, Penn EJ, Peshavaria M. Low-molecular-weight constituents of isolated insulin-secretory granules. Bivalent cations, adenine nucleotides and inorganic phosphate. *Biochem J*. 1983;210(2):297-305.
381. Lemaire K, Chimienti F, Schuit F. Zinc transporters and their role in the pancreatic beta-cell. *J Diabetes Investig*. 2012;3(3):202-11.
382. Emdin SO, Dodson GG, Cutfield JM, Cutfield SM. Role of zinc in insulin biosynthesis. Some possible zinc-insulin interactions in the pancreatic B-cell. *Diabetologia*. 1980;19(3):174-82.
383. Rutter GA, Chimienti F. SLC30A8 mutations in type 2 diabetes. *Diabetologia*. 2015;58(1):31-6.
384. Daniels MJ, Jagielnicki M, Yeager M. Structure/Function Analysis of human ZnT8 (SLC30A8): A Diabetes Risk Factor and Zinc Transporter. *Curr Res Struct Biol*. 2020;2:144-55.
385. Wenzlau JM, Frisch LM, Gardner TJ, Sarkar S, Hutton JC, Davidson HW. Novel antigens in type 1 diabetes: the importance of ZnT8. *Curr Diab Rep*. 2009;9(2):105-12.
386. Ahlqvist E, Storm P, Karajamaki A, Martinell M, Dorkhan M, Carlsson A, et al. Novel subgroups of adult-onset diabetes and their association with outcomes: a data-driven cluster analysis of six variables. *Lancet Diabetes Endocrinol*. 2018.
387. Salem SD, Saif-Ali R, Ismail IS, Al-Hamodi Z, Muniandy S. Contribution of SLC30A8 variants to the risk of type 2 diabetes in a multi-ethnic population: a case control study. *BMC Endocr Disord*. 2014;14:2.
388. Sladek R, Rocheleau G, Rung J, Dina C, Shen L, Serre D, et al. A genome-wide association study identifies novel risk loci for type 2 diabetes. *Nature*. 2007;445(7130):881-5.

389. Scott LJ, Mohlke KL, Bonnycastle LL, Willer CJ, Li Y, Duren WL, et al. A genome-wide association study of type 2 diabetes in Finns detects multiple susceptibility variants. *Science*. 2007;316(5829):1341-5.
390. Diabetes Genetics Initiative of Broad Institute of H, Mit LU, Novartis Institutes of BioMedical R, Saxena R, Voight BF, Lyssenko V, et al. Genome-wide association analysis identifies loci for type 2 diabetes and triglyceride levels. *Science*. 2007;316(5829):1331-6.
391. Zeggini E, Weedon MN, Lindgren CM, Frayling TM, Elliott KS, Lango H, et al. Replication of genome-wide association signals in UK samples reveals risk loci for type 2 diabetes. *Science*. 2007;316(5829):1336-41.
392. Merriman C, Huang Q, Rutter GA, Fu D. Lipid-tuned Zinc Transport Activity of Human ZnT8 Protein Correlates with Risk for Type-2 Diabetes. *J Biol Chem*. 2016;291(53):26950-7.
393. Flannick J, Thorleifsson G, Beer NL, Jacobs SB, Grarup N, Burt NP, et al. Loss-of-function mutations in SLC30A8 protect against type 2 diabetes. *Nat Genet*. 2014;46(4):357-63.
394. Fu Y, Tian W, Pratt EB, Dirling LB, Shyng SL, Meshul CK, et al. Down-regulation of ZnT8 expression in INS-1 rat pancreatic beta cells reduces insulin content and glucose-inducible insulin secretion. *PLoS One*. 2009;4(5):e5679.
395. Lemaire K, Ravier MA, Schraenen A, Creemers JW, Van de Plas R, Granvik M, et al. Insulin crystallization depends on zinc transporter ZnT8 expression, but is not required for normal glucose homeostasis in mice. *Proc Natl Acad Sci U S A*. 2009;106(35):14872-7.
396. Pound LD, Sarkar SA, Benninger RK, Wang Y, Suwanichkul A, Shadoan MK, et al. Deletion of the mouse Slc30a8 gene encoding zinc transporter-8 results in impaired insulin secretion. *Biochem J*. 2009;421(3):371-6.
397. Nicolson TJ, Bellomo EA, Wijesekara N, Loder MK, Baldwin JM, Gyulkhandanyan AV, et al. Insulin storage and glucose homeostasis in mice null for the granule zinc transporter ZnT8 and studies of the type 2 diabetes-associated variants. *Diabetes*. 2009;58(9):2070-83.
398. Wijesekara N, Dai FF, Hardy AB, Giglou PR, Bhattacharjee A, Koshkin V, et al. Beta cell-specific Znt8 deletion in mice causes marked defects in insulin processing, crystallisation and secretion. *Diabetologia*. 2010;53(8):1656-68.
399. Skarstrand H, Krupinska E, Haataja TJ, Vaziri-Sani F, Lagerstedt JO, Lernmark A. Zinc transporter 8 (ZnT8) autoantibody epitope specificity and affinity examined with recombinant ZnT8 variant proteins in specific ZnT8R and ZnT8W autoantibody-positive type 1 diabetes patients. *Clin Exp Immunol*. 2015;179(2):220-9.
400. Skarstrand H, Lernmark A, Vaziri-Sani F. Antigenicity and epitope specificity of ZnT8 autoantibodies in type 1 diabetes. *Scand J Immunol*. 2013;77(1):21-9.
401. Gohlke H, Ferrari U, Koczwara K, Bonifacio E, Illig T, Ziegler AG. SLC30A8 (ZnT8) Polymorphism is Associated with Young Age at Type 1 Diabetes Onset. *Rev Diabet Stud*. 2008;5(1):25-7.
402. Myles S, Davison D, Barrett J, Stoneking M, Timpson N. Worldwide population differentiation at disease-associated SNPs. *BMC Med Genomics*. 2008;1:22.
403. Balke EM, Demeester S, Lee D, Gillard P, Hilbrands R, Van de Velde U, et al. SLC30A8 polymorphism and BMI complement HLA-A\*24 as risk factors for poor graft function in islet allograft recipients. *Diabetologia*. 2018;61(7):1623-32.
404. Wenzlau JM, Frisch LM, Hutton JC, Davidson HW. Mapping of conformational autoantibody epitopes in ZNT8. *Diabetes Metab Res Rev*. 2011;27(8):883-6.
405. Wenzlau J, Frisch L, Gardner T, Sarkar S, Hutton JC, Davidson H. Novel antigens in type 1 diabetes: The importance of ZnT8. *Curr Diabetes Rep*. 2009;9(2):105-12.
406. Xu K, Zha M, Wu X, Yu Z, Yu R, Xu X, et al. Association between rs13266634 C/T polymorphisms of solute carrier family 30 member 8 (SLC30A8) and type 2 diabetes, impaired

- glucose tolerance, type 1 diabetes--a meta-analysis. *Diabetes Res Clin Pract.* 2011;91(2):195-202.
407. Wenzlau JM, Hutton JC. Novel diabetes autoantibodies and prediction of type 1 diabetes. *Curr Diab Rep.* 2013;13(5):608-15.
408. Bafaro E, Liu Y, Xu Y, Dempski RE. The emerging role of zinc transporters in cellular homeostasis and cancer. *Signal Transduct Target Ther.* 2017;2.
409. Eide DJ. Zinc transporters and the cellular trafficking of zinc. *Biochim Biophys Acta.* 2006;1763(7):711-22.
410. Parsons DS, Hogstrand C, Maret W. The C-terminal cytosolic domain of the human zinc transporter ZnT8 and its diabetes risk variant. *FEBS J.* 2018;285(7):1237-50.
411. Xue J, Xie T, Zeng W, Jiang Y, Bai XC. Cryo-EM structures of human ZnT8 in both outward- and inward-facing conformations. *Elife.* 2020;9.
412. Lu M, Chai J, Fu D. Structural basis for autoregulation of the zinc transporter YiiP. *Nat Struct Mol Biol.* 2009;16(10):1063-7.
413. Lu M, Fu D. Structure of the zinc transporter YiiP. *Science.* 2007;317(5845):1746-8.
414. Weijers RN. Three-dimensional structure of beta-cell-specific zinc transporter, ZnT-8, predicted from the type 2 diabetes-associated gene variant SLC30A8 R325W. *Diabetol Metab Syndr.* 2010;2(1):33.
415. Catapano MC, Parsons DS, Kotuniak R, Mladenka P, Bal W, Maret W. Probing the Structure and Function of the Cytosolic Domain of the Human Zinc Transporter ZnT8 with Nickel(II) Ions. *Int J Mol Sci.* 2021;22(6).
416. Gorus FK, Goubert P, Semakula C, Vandewalle CL, De Schepper J, Scheen A, et al. IA-2-autoantibodies complement GAD65-autoantibodies in new-onset IDDM patients and help predict impending diabetes in their siblings. *The Belgian Diabetes Registry. Diabetologia.* 1997;40(1):95-9.
417. Vandewalle CL, Falorni A, Svanholm S, Lernmark A, Pipeleers DG, Gorus FK. High diagnostic sensitivity of glutamate decarboxylase autoantibodies in insulin-dependent diabetes mellitus with clinical onset between age 20 and 40 years. *The Belgian Diabetes Registry. J Clin Endocrinol Metab.* 1995;80(3):846-51.
418. Buzzetti R, Zampetti S, Maddaloni E. Adult-onset autoimmune diabetes: current knowledge and implications for management. *Nat Rev Endocrinol.* 2017;13(11):674-86.
419. Fournalos S, Dotta F, Greenbaum CJ, Palmer JP, Rolandsson O, Colman PG, et al. Latent autoimmune diabetes in adults (LADA) should be less latent. *Diabetologia.* 2005;48(11):2206-12.
420. Hussein H, Ibrahim F, Sobngwi E, Gautier JF, Boudou P. Zinc transporter 8 autoantibodies assessment in daily practice. *Clin Biochem.* 2017;50(1-2):94-6.
421. Andersen CD, Bennet L, Nystrom L, Lindblad U, Lindholm E, Groop L, et al. Worse glycaemic control in LADA patients than in those with type 2 diabetes, despite a longer time on insulin therapy. *Diabetologia.* 2013;56(2):252-8.
422. Sorgjerd EP, Skorpen F, Kvaloy K, Midthjell K, Grill V. Prevalence of ZnT8 antibody in relation to phenotype and SLC30A8 polymorphism in adult autoimmune diabetes: results from the HUNT study, Norway. *Autoimmunity.* 2013;46(1):74-9.
423. Hawa MI, Buchan AP, Ola T, Wun CC, DeMicco DA, Bao W, et al. LADA and CARDS: a prospective study of clinical outcome in established adult-onset autoimmune diabetes. *Diabetes Care.* 2014;37(6):1643-9.
424. Kozhakhmetova A, Wyatt RC, Caygill C, Williams C, Long AE, Chandler K, et al. A quarter of patients with type 1 diabetes have co-existing non-islet autoimmunity; the findings of a UK population-based family study. *Clin Exp Immunol.* 2018.
425. Thorsen SU, Pipper CB, Mortensen HB, Pociot F, Johannesen J, Svensson J. No Contribution of GAD-65 and IA-2 Autoantibodies around Time of Diagnosis to the Increasing

- Incidence of Juvenile Type 1 Diabetes: A 9-Year Nationwide Danish Study. *Int J Endocrinol.* 2016;2016:8350158.
426. Huang Q, Merriman C, Zhang H, Fu D. Coupling of Insulin Secretion and Display of a Granule-resident Zinc Transporter ZnT8 on the Surface of Pancreatic Beta Cells. *J Biol Chem.* 2017;292(10):4034-43.
427. Hermann R, Laine AP, Veijola R, Vahlberg T, Simell S, Lahde J, et al. The effect of HLA class II, insulin and CTLA4 gene regions on the development of humoral beta cell autoimmunity. *Diabetologia.* 2005;48(9):1766-75.
428. Andersson C, Vaziri-Sani F, Delli A, Lindblad B, Carlsson A, Forsander G, et al. Triple specificity of ZnT8 autoantibodies in relation to HLA and other islet autoantibodies in childhood and adolescent type 1 diabetes. *Pediatr Diabetes.* 2013;14(2):97-105.
429. Enee E, Kratzer R, Arnoux JB, Barilleau E, Hamel Y, Marchi C, et al. ZnT8 is a major CD8+ T cell-recognized autoantigen in pediatric type 1 diabetes. *Diabetes.* 2012;61(7):1779-84.
430. Xu X, Gu Y, Bian L, Shi Y, Cai Y, Chen Y, et al. Characterization of immune response to novel HLA-A2-restricted epitopes from zinc transporter 8 in type 1 diabetes. *Vaccine.* 2016;34(6):854-62.
431. Scotto M, Afonso G, Larger E, Raverdy C, Lemonnier FA, Carel JC, et al. Zinc transporter (ZnT)8(186-194) is an immunodominant CD8+ T cell epitope in HLA-A2+ type 1 diabetic patients. *Diabetologia.* 2012;55(7):2026-31.
432. Culina S, Lalanne AI, Afonso G, Cerosaletti K, Pinto S, Sebastiani G, et al. Islet-reactive CD8(+) T cell frequencies in the pancreas, but not in blood, distinguish type 1 diabetic patients from healthy donors. *Sci Immunol.* 2018;3(20).
433. Nayak DK, Calderon B, Vomund AN, Unanue ER. ZnT8-reactive T cells are weakly pathogenic in NOD mice but can participate in diabetes under inflammatory conditions. *Diabetes.* 2014;63(10):3438-48.
434. Niegowska M, Rapini N, Piccinini S, Mameli G, Caggiu E, Manca Bitti ML, et al. Type 1 Diabetes at-risk children highly recognize *Mycobacterium avium* subspecies paratuberculosis epitopes homologous to human Znt8 and Proinsulin. *Sci Rep.* 2016;6:22266.
435. Puff R, Haupt F, Winkler C, Assfalg R, Achenbach P, Ziegler AG. [Early diagnosis, early care--"Fr1da" screening of children for type 1 diabetes]. *MMW Fortschr Med.* 2016;158(4):65-6.
436. Faccinetti NI, Guerra LL, Penas Steinhardt A, Iacono RF, Frechtel GD, Trifone L, et al. Characterization of zinc transporter 8 (ZnT8) antibodies in autoimmune diabetic patients from Argentinian population using monomeric, homodimeric, and heterodimeric ZnT8 antigen variants. *Eur J Endocrinol.* 2016;174(2):157-65.
437. Yang L, Luo S, Huang G, Peng J, Li X, Yan X, et al. The diagnostic value of zinc transporter 8 autoantibody (ZnT8A) for type 1 diabetes in Chinese. *Diabetes Metab Res Rev.* 2010;26(7):579-84.
438. Kawasaki E, Nakamura K, Kuriya G, Satoh T, Kobayashi M, Kuwahara H, et al. Zinc transporter 8 autoantibodies in fulminant, acute-onset, and slow-onset patients with type 1 diabetes. *Diabetes Metab Res Rev.* 2011;27(8):895-8.
439. Gomes KF, Semzezem C, Batista R, Fukui RT, Santos AS, Correia MR, et al. Importance of Zinc Transporter 8 Autoantibody in the Diagnosis of Type 1 Diabetes in Latin Americans. *Sci Rep.* 2017;7(1):207.
440. Wenzlau JM, Hutton JC, Davidson HW. New antigenic targets in type 1 diabetes. *Curr Opin Endocrinol Diabetes Obes.* 2008;15(4):315-20.
441. Burke GW, 3rd, Chen LJ, Ciancio G, Pugliese A. Biomarkers in pancreas transplant. *Curr Opin Organ Transplant.* 2016;21(4):412-8.

442. Wan H, Merriman C, Atkinson MA, Wasserfall CH, McGrail KM, Liang Y, et al. Proteoliposome-based full-length ZnT8 self-antigen for type 1 diabetes diagnosis on a plasmonic platform. *Proc Natl Acad Sci U S A*. 2017;114(38):10196-201.
443. Wenzlau JM, Walter M, Gardner TJ, Frisch LM, Yu L, Eisenbarth GS, et al. Kinetics of the post-onset decline in zinc transporter 8 autoantibodies in type 1 diabetic human subjects. *J Clin Endocrinol Metab*. 2010;95(10):4712-9.
444. Ingemansson S, Vaziri-Sani F, Lindblad U, Gudbjornsdottir S, Torn C, Diss-Study G. Long-term sustained autoimmune response to beta cell specific zinc transporter (ZnT8, W, R, Q) in young adult patients with preserved beta cell function at diagnosis of diabetes. *Autoimmunity*. 2013;46(1):50-61.
445. Nielsen LB, Vaziri-Sani F, Porksen S, Andersen ML, Svensson J, Bergholdt R, et al. Relationship between ZnT8Ab, the SLC30A8 gene and disease progression in children with newly diagnosed type 1 diabetes. *Autoimmunity*. 2011;44(8):616-23.
446. Juusola M, Parkkola A, Harkonen T, Siljander H, Ilonen J, Akerblom HK, et al. Positivity for Zinc Transporter 8 Autoantibodies at Diagnosis Is Subsequently Associated With Reduced beta-Cell Function and Higher Exogenous Insulin Requirement in Children and Adolescents With Type 1 Diabetes. *Diabetes Care*. 2016;39(1):118-21.
447. Richardson CC, Dromey JA, McLaughlin KA, Morgan D, Bodansky HJ, Feltbower RG, et al. High frequency of autoantibodies in patients with long duration type 1 diabetes. *Diabetologia*. 2013.
448. Wang L, Lovejoy NF, Faustman DL. Persistence of prolonged C-peptide production in type 1 diabetes as measured with an ultrasensitive C-peptide assay. *Diabetes Care*. 2012;35(3):465-70.
449. Williams GM, Long AE, Wilson IV, Aitken RJ, Wyatt RC, McDonald TJ, et al. Beta cell function and ongoing autoimmunity in long-standing, childhood onset type 1 diabetes. *Diabetologia*. 2016;59(12):2722-6.
450. Williams MD, Bacher R, Perry DJ, Grace CR, McGrail KM, Posgai AL, et al. Genetic Composition and Autoantibody Titers Model the Probability of Detecting C-Peptide Following Type 1 Diabetes Diagnosis. *Diabetes*. 2021;70(4):932-43.
451. Bonifacio E, Yu L, Williams AK, Eisenbarth GS, Bingley PJ, Marcovina SM, et al. Harmonization of glutamic acid decarboxylase and islet antigen-2 autoantibody assays for national institute of diabetes and digestive and kidney diseases consortia. *J Clin Endocrinol Metab*. 2010;95(7):3360-7.
452. Andersson C, Larsson K, Vaziri-Sani F, Lynch K, Carlsson A, Cedervall E, et al. The three ZNT8 autoantibody variants together improve the diagnostic sensitivity of childhood and adolescent type 1 diabetes. *Autoimmunity*. 2011;44(5):394-405.
453. Marcus P, Yan X, Bartley B, Hagopian W. LIPS islet autoantibody assays in high-throughput format for DASP 2010. *Diabetes Metab Res Rev*. 2011;27(8):891-4.
454. Raab J, Haupt F, Scholz M, Matzke C, Warncke K, Lange K, et al. Capillary blood islet autoantibody screening for identifying pre-type 1 diabetes in the general population: design and initial results of the Fr1da study. *BMJ Open*. 2016;6(5):e011144.
455. Gu Y, Merriman C, Guo Z, Jia X, Wenzlau J, Li H, et al. Novel autoantibodies to the beta-cell surface epitopes of ZnT8 in patients progressing to type-1 diabetes. *J Autoimmun*. 2021;122:102677.
456. Williams AJ, Aitken RJ, Chandler MA, Gillespie KM, Lampasona V, Bingley PJ. Autoantibodies to islet antigen-2 are associated with HLA-DRB1\*07 and DRB1\*09 haplotypes as well as DRB1\*04 at onset of type 1 diabetes: the possible role of HLA-DQA in autoimmunity to IA-2. *Diabetologia*. 2008;51(8):1444-8.
457. Gillespie KM. *Type-1 Diabetes: Methods and Protocols*. Walker JM, editor. Springer New York: Humana Press: Springer Nature; 2018 26/05/2018. 213 p.

458. Wyatt R, Williams AJ. Islet Autoantibody Analysis: Radioimmunoassays. *Methods Mol Biol.* 2016;1433:57-83.
459. Bingley PJ, Williams AJ, Colman PG, Gellert SA, Eisenbarth G, Yu L, et al. Measurement of islet cell antibodies in the Type 1 Diabetes Genetics Consortium: efforts to harmonize procedures among the laboratories. *Clin Trials.* 2010;7(1 Suppl):S56-64.
460. Sosenko JM, Skyler JS, Palmer JP, Krischer JP, Yu L, Mahon J, et al. The prediction of type 1 diabetes by multiple autoantibody levels and their incorporation into an autoantibody risk score in relatives of type 1 diabetic patients. *Diabetes Care.* 2013;36(9):2615-20.
461. Sosenko JM, Krischer JP, Palmer JP, Mahon J, Cowie C, Greenbaum CJ, et al. A risk score for type 1 diabetes derived from autoantibody-positive participants in the diabetes prevention trial-type 1. *Diabetes Care.* 2008;31(3):528-33.
462. Sosenko JM, Skyler JS, Mahon J, Krischer JP, Beam CA, Boulware DC, et al. Validation of the Diabetes Prevention Trial-Type 1 Risk Score in the TrialNet Natural History Study. *Diabetes Care.* 2011;34(8):1785-7.
463. Jia X, Gu Y, High H, Yu L. Islet autoantibodies in disease prediction and pathogenesis. *Diabetol Int.* 2020;11(1):6-10.
464. Hoppu S, Ronkainen MS, Kulmala P, Akerblom HK, Knip M, Childhood Diabetes in Finland Study G. GAD65 antibody isotypes and epitope recognition during the prediabetic process in siblings of children with type I diabetes. *Clin Exp Immunol.* 2004;136(1):120-8.
465. Hoppu S, Harkonen T, Ronkainen MS, Akerblom HK, Knip M, Childhood Diabetes in Finland Study G. IA-2 antibody epitopes and isotypes during the prediabetic process in siblings of children with type 1 diabetes. *J Autoimmun.* 2004;23(4):361-70.
466. Hoppu S, Ronkainen MS, Kimpimaki T, Simell S, Korhonen S, Ilonen J, et al. Insulin autoantibody isotypes during the prediabetic process in young children with increased genetic risk of type 1 diabetes. *Pediatr Res.* 2004;55(2):236-42.
467. Seissler J, Eikamp K, Schott M, Scherbaum WA, Group DS. IA-2 autoantibodies restricted to the IgG4 subclass are associated with protection from type 1 diabetes. *Horm Metab Res.* 2002;34(4):186-91.
468. Jefferis R, Reimer CB, Skvaril F, de Lange G, Ling NR, Lowe J, et al. Evaluation of monoclonal antibodies having specificity for human IgG sub-classes: results of an IUIS/WHO collaborative study. *Immunol Lett.* 1985;10(3-4):223-52.
469. Dozio N, Belloni C, Girardi AM, Genovese S, Sodoyez JC, Bottazzo GF, et al. Heterogeneous IgG subclass distribution of islet cell antibodies. *J Autoimmun.* 1994;7(1):45-53.
470. Omar MA, Srikanta S, Eisenbarth GS. Human islet cell antibodies: immunoglobulin class and subclass distribution defined by monoclonal antibodies. *Diabetes Res.* 1987;4(4):155-7.
471. Schatz DA, Barrett DJ, Maclaren NK, Riley WJ. Polyclonal nature of islet cell antibodies in insulin-dependent diabetes. *Autoimmunity.* 1988;1(1):45-50.
472. Dean BM, Bottazzo GF, Cudworth AG. IgG subclass distribution in organ specific autoantibodies. The relationship to complement fixing ability. *Clin Exp Immunol.* 1983;52(1):61-6.
473. Peakman M, Lobo-Yeo A, Mieli-Vergani G, Davies ET, Mowat AP, Vergani D. Characterization of anti-liver kidney microsomal antibody in childhood autoimmune chronic active hepatitis: evidence for IgG1 subclass restriction, polyclonality and non cross-reactivity with hepatocyte surface antigens. *Clin Exp Immunol.* 1987;69(3):543-9.
474. Hawa MI, Fava D, Medici F, Deng YJ, Notkins AL, De Mattia G, et al. Antibodies to IA-2 and GAD65 in type 1 and type 2 diabetes: isotype restriction and polyclonality. *Diabetes Care.* 2000;23(2):228-33.

475. Goding JW. Use of staphylococcal protein A as an immunological reagent. *J Immunol Methods*. 1978;20:241-53.
476. Kronvall G, Williams RC, Jr. Differences in anti-protein A activity among IgG subgroups. *J Immunol*. 1969;103(4):828-33.
477. Akerstrom B, Bjorck L. A physicochemical study of protein G, a molecule with unique immunoglobulin G-binding properties. *J Biol Chem*. 1986;261(22):10240-7.
478. Hillman M, Torn C, Landin-Olsson M, group Ds. The glutamic acid decarboxylase 65 immunoglobulin G subclass profile differs between adult-onset type 1 diabetes and latent autoimmune diabetes in adults (LADA) up to 3 years after clinical onset. *Clin Exp Immunol*. 2009;157(2):255-60.
479. Hillman M, Torn C, Thorgeirsson H, Landin-Olsson M. IgG4-subclass of glutamic acid decarboxylase antibody is more frequent in latent autoimmune diabetes in adults than in type 1 diabetes. *Diabetologia*. 2004;47(11):1984-9.
480. Wenzlau JM, Moua O, Liu Y, Eisenbarth GS, Hutton JC, Davidson HW. Identification of a major humoral epitope in Slc30A8 (ZnT8). *Ann N Y Acad Sci*. 2008;1150:252-5.
481. Williams AJ, Somerville M, Rokni S, Bonifacio E, Yu L, Eisenbarth G, et al. Azide and Tween-20 reduce binding to autoantibody epitopes of islet antigen-2; implications for assay performance and reproducibility. *J Immunol Methods*. 2009;351(1-2):75-9.
482. Altschul SF, Gish W, Miller W, Myers EW, Lipman DJ. Basic local alignment search tool. *J Mol Biol*. 1990;215(3):403-10.
483. Kawasaki E, Oikawa Y, Okada A, Kanatsuna N, Kawamura T, Kikuchi T, et al. Zinc transporter 8 autoantibodies complement glutamic acid decarboxylase and insulinoma-associated antigen-2 autoantibodies in the identification and characterization of Japanese type 1 diabetes. *J Diabetes Investig*. 2020;11(5):1181-7.
484. Gray VE, Hause RJ, Fowler DM. Analysis of Large-Scale Mutagenesis Data To Assess the Impact of Single Amino Acid Substitutions. *Genetics*. 2017;207(1):53-61.
485. So M, O'Rourke C, Bahnson HT, Greenbaum CJ, Speake C. Autoantibody Reversion: Changing Risk Categories in Multiple-Autoantibody-Positive Individuals. *Diabetes Care*. 2020;43(4):913-7.
486. Graham J, Hagopian WA, Kockum I, Li LS, Sanjeevi CB, Lowe RM, et al. Genetic effects on age-dependent onset and islet cell autoantibody markers in type 1 diabetes. *Diabetes*. 2002;51(5):1346-55.
487. Sharma A, Liu X, Hadley D, Hagopian W, Chen WM, Onengut-Gumuscu S, et al. Identification of non-HLA genes associated with development of islet autoimmunity and type 1 diabetes in the prospective TEDDY cohort. *J Autoimmun*. 2018;89:90-100.
488. Qu HQ, Polychronakos C. The effect of the MHC locus on autoantibodies in type 1 diabetes. *J Med Genet*. 2009;46(7):469-71.
489. Long AE, George G, Williams CL. Persistence of islet autoantibodies after diagnosis in type 1 diabetes. *Diabet Med*. 2021:e14712.
490. Jaeger C, Allendorfer J, Hatziagelaki E, Dyrberg T, Bergis KH, Federlin K, et al. Persistent GAD 65 antibodies in longstanding IDDM are not associated with residual beta-cell function, neuropathy or HLA-DR status. *Horm Metab Res*. 1997;29(10):510-5.
491. Brorsson CA, Onengut S, Chen WM, Wenzlau J, Yu L, Baker P, et al. Novel Association Between Immune-Mediated Susceptibility Loci and Persistent Autoantibody Positivity in Type 1 Diabetes. *Diabetes*. 2015;64(8):3017-27.
492. Wenzlau JM, Frisch LM, Hutton JC, Fain PR, Davidson HW. Changes in Zinc Transporter 8 Autoantibodies Following Type 1 Diabetes Onset: The Type 1 Diabetes Genetics Consortium Autoantibody Workshop. *Diabetes Care*. 2015;38 Suppl 2:S14-20.

493. Savola K, Sabbah E, Kulmala P, Vahasalo P, Ilonen J, Knip M. Autoantibodies associated with Type 1 diabetes mellitus persist after diagnosis in children. *Diabetologia*. 1998;41(11):1293-7.
494. Williams AJ, Norcross AJ, Chandler KA, Bingley PJ. Non-specific binding to protein A Sepharose and protein G Sepharose in insulin autoantibody assays may be reduced by pre-treatment with glycine or ethanolamine. *J Immunol Methods*. 2006;314(1-2):170-3.
495. Gillespie KM, Valovin SJ, Saunby J, Hunter KM, Savage DA, Middleton D, et al. HLA class II typing of whole genome amplified mouth swab DNA. *Tissue Antigens*. 2000;56(6):530-8.
496. Bunce M, O'Neill CM, Barnardo MC, Krausa P, Browning MJ, Morris PJ, et al. Phototyping: comprehensive DNA typing for HLA-A, B, C, DRB1, DRB3, DRB4, DRB5 & DQB1 by PCR with 144 primer mixes utilizing sequence-specific primers (PCR-SSP). *Tissue Antigens*. 1995;46(5):355-67.
497. Plagnol V, Howson JM, Smyth DJ, Walker N, Hafler JP, Wallace C, et al. Genome-wide association analysis of autoantibody positivity in type 1 diabetes cases. *PLoS Genet*. 2011;7(8):e1002216.
498. Howson JM, Stevens H, Smyth DJ, Walker NM, Chandler KA, Bingley PJ, et al. Evidence that HLA class I and II associations with type 1 diabetes, autoantibodies to GAD and autoantibodies to IA-2, are distinct. *Diabetes*. 2011;60(10):2635-44.
499. Tridgell DM, Spiekerman C, Wang RS, Greenbaum CJ. Interaction of onset and duration of diabetes on the percent of GAD and IA-2 antibody-positive subjects in the type 1 diabetes genetics consortium database. *Diabetes Care*. 2011;34(4):988-93.
500. Wilmot-Roussel H, Levy DJ, Carette C, Caillat-Zucman S, Boitard C, Timsit J, et al. Factors associated with the presence of glutamic acid decarboxylase and islet antigen-2 autoantibodies in patients with long-standing type 1 diabetes. *Diabetes Metab*. 2013;39(3):244-9.
501. Kozhakhmetova A, Wyatt RC, Caygill C, Williams C, Long AE, Chandler K, et al. A quarter of patients with type 1 diabetes have co-existing non-islet autoimmunity: the findings of a UK population-based family study. *Clin Exp Immunol*. 2018;192(3):251-8.
502. Jostins L, Ripke S, Weersma RK, Duerr RH, McGovern DP, Hui KY, et al. Host-microbe interactions have shaped the genetic architecture of inflammatory bowel disease. *Nature*. 2012;491(7422):119-24.
503. Smyth DJ, Plagnol V, Walker NM, Cooper JD, Downes K, Yang JH, et al. Shared and distinct genetic variants in type 1 diabetes and celiac disease. *N Engl J Med*. 2008;359(26):2767-77.
504. Smyth DJ, Cooper JD, Bailey R, Field S, Burren O, Smink LJ, et al. A genome-wide association study of nonsynonymous SNPs identifies a type 1 diabetes locus in the interferon-induced helicase (IFIH1) region. *Nat Genet*. 2006;38(6):617-9.
505. Winkler C, Lauber C, Adler K, Grallert H, Illig T, Ziegler AG, et al. An interferon-induced helicase (IFIH1) gene polymorphism associates with different rates of progression from autoimmunity to type 1 diabetes. *Diabetes*. 2011;60(2):685-90.
506. Chu X, Pan CM, Zhao SX, Liang J, Gao GQ, Zhang XM, et al. A genome-wide association study identifies two new risk loci for Graves' disease. *Nat Genet*. 2011;43(9):897-901.
507. Oram RA, Sims EK, Evans-Molina C. Beta cells in type 1 diabetes: mass and function; sleeping or dead? *Diabetologia*. 2019;62(4):567-77.
508. Meier JJ, Bhushan A, Butler AE, Rizza RA, Butler PC. Sustained beta cell apoptosis in patients with long-standing type 1 diabetes: indirect evidence for islet regeneration? *Diabetologia*. 2005;48(11):2221-8.

509. Burbelo PD, Lebovitz EE, Notkins AL. Luciferase immunoprecipitation systems for measuring antibodies in autoimmune and infectious diseases. *Transl Res.* 2015;165(2):325-35.
510. Hall MP, Unch J, Binkowski BF, Valley MP, Butler BL, Wood MG, et al. Engineered luciferase reporter from a deep sea shrimp utilizing a novel imidazopyrazinone substrate. *ACS Chem Biol.* 2012;7(11):1848-57.
511. Thorne N, Inglese J, Auld DS. Illuminating insights into firefly luciferase and other bioluminescent reporters used in chemical biology. *Chem Biol.* 2010;17(6):646-57.
512. Burbelo PD, Kisailus AE, Peck JW. Detecting protein-protein interactions using Renilla luciferase fusion proteins. *Biotechniques.* 2002;33(5):1044-8, 50.
513. Smirnova DV, Ugarova NN. Firefly Luciferase-based Fusion Proteins and their Applications in Bioanalysis. *Photochem Photobiol.* 2017;93(2):436-47.
514. Tannous BA, Kim DE, Fernandez JL, Weissleder R, Breakefield XO. Codon-optimized Gaussia luciferase cDNA for mammalian gene expression in culture and in vivo. *Mol Ther.* 2005;11(3):435-43.
515. Dyer BW, Ferrer FA, Klinedinst DK, Rodriguez R. A noncommercial dual luciferase enzyme assay system for reporter gene analysis. *Anal Biochem.* 2000;282(1):158-61.
516. Wurdinger T, Badr C, Pike L, de Kleine R, Weissleder R, Breakefield XO, et al. A secreted luciferase for ex vivo monitoring of in vivo processes. *Nat Methods.* 2008;5(2):171-3.
517. Andreu N, Zelmer A, Fletcher T, Elkington PT, Ward TH, Ripoll J, et al. Optimisation of bioluminescent reporters for use with mycobacteria. *PLoS One.* 2010;5(5):e10777.
518. Burbelo PD, Beck LH, Jr., Waldman M. Detection and monitoring PLA2R autoantibodies by LIPS in membranous nephropathy. *J Immunol Methods.* 2017;444:17-23.
519. Badr CE, Tannous BA. Bioluminescence imaging: progress and applications. *Trends Biotechnol.* 2011;29(12):624-33.
520. Smirnova NA, Haskew-Layton RE, Basso M, Hushpulian DM, Payappilly JB, Speer RE, et al. Development of Nrf2-luciferase reporter and its application for high throughput screening and real-time monitoring of Nrf2 activators. *Chem Biol.* 2011;18(6):752-65.
521. Burbelo PD, Hirai H, Leahy H, Lernmark A, Ivarsson SA, Iadarola MJ, et al. A new luminescence assay for autoantibodies to mammalian cell-prepared insulinoma-associated protein 2. *Diabetes Care.* 2008;31(9):1824-6.
522. Burbelo PD, Chaturvedi A, Notkins AL, Gunti S. Luciferase-Based Detection of Antibodies for the Diagnosis of HPV-Associated Head and Neck Squamous Cell Carcinoma. *Diagnostics (Basel).* 2019;9(3).
523. Burbelo PD, Hirai H, Issa AT, Kingman A, Lernmark A, Ivarsson SA, et al. Comparison of radioimmunoprecipitation with luciferase immunoprecipitation for autoantibodies to GAD65 and IA-2beta. *Diabetes Care.* 2010;33(4):754-6.
524. Ustinova J, Zusinaite E, Utt M, Metskula K, Reimand K, Huchaiah V, et al. Development of a luciferase-based system for the detection of ZnT8 autoantibodies. *J Immunol Methods.* 2014;405:67-73.
525. Ling Y, Jiang P, Li N, Yan Q, Wang X. A luciferase immunoprecipitation assay for the detection of proinsulin/insulin autoantibodies. *Clin Biochem.* 2018;54:51-5.
526. Banfi G, Salvagno GL, Lippi G. The role of ethylenediamine tetraacetic acid (EDTA) as in vitro anticoagulant for diagnostic purposes. *Clin Chem Lab Med.* 2007;45(5):565-76.
527. Bingley PJ, Bonifacio E, Gale EA. Can we really predict IDDM? *Diabetes.* 1993;42(2):213-20.
528. Bonifacio E, Hummel M, Walter M, Schmid S, Ziegler AG. IDDM1 and multiple family history of type 1 diabetes combine to identify neonates at high risk for type 1 diabetes. *Diabetes Care.* 2004;27(11):2695-700.

529. Yu L, Liu Y, Miao D, Wenzlau J, Davidson H, Hutton J, et al. Triple chimeric islet autoantigen IA2-ZnT8WR to facilitate islet autoantibody determination. *J Immunol Methods*. 2010;353(1-2):20-3.
530. Steck AK, Fouts A, Miao D, Zhao Z, Dong F, Sosenko J, et al. ECL-IAA and ECL-GADA Can Identify High-Risk Single Autoantibody-Positive Relatives in the TrialNet Pathway to Prevention Study. *Diabetes Technol Ther*. 2016;18(7):410-4.
531. Burbelo PD, Keller J, Wagner J, Klimavicz JS, Bayat A, Rhodes CS, et al. Serological diagnosis of pulmonary Mycobacterium tuberculosis infection by LIPS using a multiple antigen mixture. *BMC Microbiol*. 2015;15:205.
532. St John A, Price CP. Existing and Emerging Technologies for Point-of-Care Testing. *Clin Biochem Rev*. 2014;35(3):155-67.
533. Dayan CM, Besser REJ, Oram RA, Hagopian W, Vatish M, Bendor-Samuel O, et al. Preventing type 1 diabetes in childhood. *Science*. 2021;373(6554):506-10.
534. Miller KM, Hermann J, Foster N, Hofer SE, Rickels MR, Danne T, et al. Longitudinal Changes in Continuous Glucose Monitoring Use Among Individuals With Type 1 Diabetes: International Comparison in the German and Austrian DPV and U.S. T1D Exchange Registries. *Diabetes Care*. 2020;43(1):e1-e2.
535. Foster NC, Beck RW, Miller KM, Clements MA, Rickels MR, DiMeglio LA, et al. State of Type 1 Diabetes Management and Outcomes from the T1D Exchange in 2016-2018. *Diabetes Technol Ther*. 2019;21(2):66-72.
536. Ziegler AG, Kick K, Bonifacio E, Haupt F, Hippich M, Dunstheimer D, et al. Yield of a Public Health Screening of Children for Islet Autoantibodies in Bavaria, Germany. *JAMA*. 2020;323(4):339-51.
537. The Eurodiab Ace Study Group. Familial risk of type I diabetes in European children. The Eurodiab Ace Study Group and The Eurodiab Ace Substudy 2 Study Group. *Diabetologia*. 1998;41(10):1151-6.
538. Sims EK, Geyer S, Johnson SB, Libman I, Jacobsen LM, Boulware D, et al. Who Is Enrolling? The Path to Monitoring in Type 1 Diabetes TrialNet's Pathway to Prevention. *Diabetes Care*. 2019;42(12):2228-36.
539. Dahlquist GG, Mustonen LR. Clinical onset characteristics of familial versus nonfamilial cases in a large population-based cohort of childhood-onset diabetes patients. *Diabetes Care*. 1995;18(6):852-4.
540. Parkkola A, Harkonen T, Ryhanen SJ, Ilonen J, Knip M, Finnish Pediatric Diabetes R. Extended family history of type 1 diabetes and phenotype and genotype of newly diagnosed children. *Diabetes Care*. 2013;36(2):348-54.
541. Shruthi S, Mohan V, Maradana MR, Aravindhan V. In silico identification and wet lab validation of novel cryptic B cell epitopes in ZnT8 zinc transporter autoantigen. *Int J Biol Macromol*. 2019;127:657-64.
542. Merriman C, Huang Q, Gu W, Yu L, Fu D. A subclass of serum anti-ZnT8 antibodies directed to the surface of live pancreatic beta-cells. *J Biol Chem*. 2018;293(2):579-87.
543. Dobersen MJ, Scharff JE. Preferential lysis of pancreatic B-cells by islet cell surface antibodies. *Diabetes*. 1982;31(5 Pt 1):459-62.
544. Jones AG, Hattersley AT. The clinical utility of C-peptide measurement in the care of patients with diabetes. *Diabet Med*. 2013;30(7):803-17.
545. Foteinopoulou E, Clarke CAL, Pattenden RJ, Ritchie SA, McMurray EM, Reynolds RM, et al. Impact of routine clinic measurement of serum C-peptide in people with a clinician-diagnosis of type 1 diabetes. *Diabet Med*. 2021;38(7):e14449.
546. Thomas NJ, Walkey, H.C., Kaur, A., Misra, S., Oliver, N.S., Colclough, K., Weedon, M. N., Johnston, D. G., Hattersley, A.T., Patel, K.A. The Absence of Islet Autoantibodies in

- Clinically Diagnosed Older-Adult Onset Type 1 Diabetes Suggests an Alternative Pathology, Advocating for Routine Testing in This Age Group. medRxiv 2021032221252507. 2021.
547. Douek IF, Gillespie KM, Dix RJ, Bingley PJ, Gale EA. Three generations of autoimmune diabetes: an extended family study. *Diabetologia*. 2003;46(10):1313-8.
548. Borg H, Marcus C, Sjoblad S, Fernlund P, Sundkvist G. Islet cell antibody frequency differs from that of glutamic acid decarboxylase antibodies/IA2 antibodies after diagnosis of diabetes. *Acta Paediatr*. 2000;89(1):46-51.
549. Bonifacio E, Lampasona V, Genovese S, Ferrari M, Bosi E. Identification of protein tyrosine phosphatase-like IA2 (islet cell antigen 512) as the insulin-dependent diabetes-related 37/40K autoantigen and a target of islet-cell antibodies. *J Immunol*. 1995;155(11):5419-26.
550. Skyler JS, Krischer JP, Wolfsdorf J, Cowie C, Palmer JP, Greenbaum C, et al. Effects of oral insulin in relatives of patients with type 1 diabetes: The Diabetes Prevention Trial--Type 1. *Diabetes Care*. 2005;28(5):1068-76.
551. Ludvigsson J, Krisky D, Casas R, Battelino T, Castano L, Greening J, et al. GAD65 antigen therapy in recently diagnosed type 1 diabetes mellitus. *N Engl J Med*. 2012;366(5):433-42.
552. Wherrett DK, Bundy B, Becker DJ, DiMeglio LA, Gitelman SE, Goland R, et al. Antigen-based therapy with glutamic acid decarboxylase (GAD) vaccine in patients with recent-onset type 1 diabetes: a randomised double-blind trial. *Lancet*. 2011;378(9788):319-27.
553. Occhipinti M, Lampasona V, Vistoli F, Bazzigaluppi E, Scavini M, Boggi U, et al. Zinc transporter 8 autoantibodies increase the predictive value of islet autoantibodies for function loss of technically successful solitary pancreas transplant. *Transplantation*. 2011;92(6):674-7.
554. Vendrame F, Hopfner YY, Diamantopoulos S, Viridi SK, Allende G, Snowwhite IV, et al. Risk Factors for Type 1 Diabetes Recurrence in Immunosuppressed Recipients of Simultaneous Pancreas-Kidney Transplants. *Am J Transplant*. 2016;16(1):235-45.
555. Nygaard SB, Larsen A, Knuhtsen A, Rungby J, Smidt K. Effects of zinc supplementation and zinc chelation on in vitro beta-cell function in INS-1E cells. *BMC Res Notes*. 2014;7:84.
556. Tsonkova VG, Sand FW, Wolf XA, Grunnet LG, Kirstine Ringgaard A, Ingvorsen C, et al. The EndoC-betaH1 cell line is a valid model of human beta cells and applicable for screenings to identify novel drug target candidates. *Mol Metab*. 2018;8:144-57.
557. Merriman C, Fu D. Down-regulation of the islet-specific zinc transporter-8 (ZnT8) protects human insulinoma cells against inflammatory stress. *J Biol Chem*. 2019;294(45):16992-7006.

## Appendix A. ZnT8A affinity studies

---

---

### A.1. Generation of recombinant ZnT8 protein in-house

---

---

#### A.1.1. Cloning of C-terminal ZnT8 into the pET49b(+) vector

---

##### A.1.1.1. Buffers & Reagents

---

Tris base, acetic acid, and Ethylenediaminetetraacetic acid (EDTA) (TAE) – 50X stock commercially available (Fisher Scientific, Hampton, New Hampshire, USA) diluted to 1X (10ml in 490ml ddH<sub>2</sub>O), pH 8.3.

Chloramphenicol – 34mg/ml stock solution prepared with 100% ethanol, filter sterilised through a 0.22µm filter (Merck Millipore, Sigma Aldrich, Dorset, UK), and frozen at -20°C. A 1:1000 dilution in LB ÷ agar was used (34µg/ml).

Kanamycin – 50mg/ml stock solution prepared with ddH<sub>2</sub>O, filter sterilised through a 0.22µm filter (Merck Millipore, Sigma), and frozen at -20°C. A 1:1000 dilution in LB ± agar was used (50µg/ml).

##### A.1.1.2. Generating the ZnT8 construct insert

---

A previous body of work by Dr K. Elvers (Bristol, UK) involved the successful cloning of IA-2 (aa647-979) into the pET49b(+) vector (Novagen, Sigma) for IA-2 protein expression (2011-2013, described in detail in (457)). To allow the cleavage at the human rhinovirus (HRV) 3C protease for subsequent protein purification using an anti-GST or anti-HIS column, primers were designed to clone ZnT8 into the cloning region of the pET49b(+) vector to add a GST tag and a 6x histidine tag to the C-terminus of C-terminal ZnT8; the major variant ZnT8R was selected. The primers included specific flanking recognition sequences for tailored restriction enzymes *XmaI* and *XhoI* (**Figure A:1**). To build the ZnT8 insert, a 20 cycle PCR reaction was set-up using the Taq PCR core kit (Qiagen, Hilden, Germany) in a recipe detailed below (**Table A:1**).

## Appendix A. ZnT8A affinity studies

atgtccctatactaggttattgaaaattaagggccttgtgcaaccactcgacttcttttgaatatcttgaagaaaaatgaagagcat  
 ttgtatgagcgcgatgaaggtataaaatggcgaaacaaaaagttgaattgggttggagttccaatcttcttattatattgatgggat  
 gttaaattaacacagctcatggccatcatagcttatatagctgacaagcacaacatgttgggtggttgcctcaaaagagcgtgcagagattc  
 aatgcttgaaggagcggtttggatattagatacgggtttcgagaattgcataatagtaaagactttgaaactcctcaaaagttgatttcttagc  
 aagctacctaagatgctgaaaatgttcgaagatcgtttatgtcataaaacatattaaatgggtgatcatgtaaccatcctgaactcatgtt  
 atgacgctcttgatgttgtttatacatggaccaatgtgcctggatgcgttcccaaaattagttgttttaaaaaacgtattgaagctatccca  
 caaattgataagtaacttgaatccagcaagtatatagcatggcctttgcagggtggaagccacgttgggtggtggcgaccatcctccaa  
 aatcggatggttcaactagtggtgggtggcgttctaataacaatcctcctactcctactcctcatctagtggttctggtcatcaccatcaccatcacc  
 ggctcttgaagtcctttcagggaccgggAAGGACTTCTCCATCTTACTCATGGAAGGTGTGCCAAAGAG  
 CCTGAATTACAGTGGTGTGAAAGAGCTTATTTTAGCAGTTCGACGGGGTGTCTGTCTGTGCA  
 CAGCCTGCACATCTGGTCTCTAACAATGAATCAAGTAATTCTCTCAGCTCATGTTGCTAC  
 AGCAGCCAGCCGGGACAGCCAAGTGGTTCGGAGAGAAATTGCTAAAGCCCTTAGCAAAA  
 GCTTTACGATGCACTCACTCACCATTCAGATGGAATCTCCAGTTGACCAGGACCCCGACT  
 GCCTTTTCTGTGAAGACCCCTGTGACTgataatctcgag

**Figure A:1 – FASTA sequence of the cloning site of pET49b(+) vector with ZnT8 insert & flanking restriction enzyme recognition sites**

Bold; GST tag; Red; 6 x His tag; Green; human rhinovirus (HRV) 3C protease; Yellow: *XmaI* restriction enzyme recognition site; Blue; *XhoI* restriction enzyme recognition site; Grey: rs13266634 SNP site encoding R325 (CCG); Underlined: Sequence used to design primers with *XmaI* and *XhoI* flanking recognition sites; Capital text: C-terminal (aa268-269) ZnT8 insert sequence.

PCR Reagent	Volume (µl)	Final Concentration
<b>10x PCR Buffer</b>	5	1X
<b>dNTPs</b>	1	200mM
<b>10µM Forward Primer (31bp)</b>	1.13	125ng
<b>10µM Reverse Primer (32bp)</b>	1.12	125ng
<b>Template ZnT8 DNA (aa268-369)</b>	1	≤1ug
<b>Sterile H<sub>2</sub>O</b>	40.5	N/A
<b>Taq Polymerase</b>	0.3	1.5 units

**Table A:1 – PCR recipe for ZnT8 cloning**

The volumes and final concentrations of reagents used in a 50µl PCR reaction mix. PCR thermocycling was set at 94°C for 30 secs for initial denaturation followed by denaturing set at 94°C for 30secs, annealing at 55°C for 1 min, Taq polymerase elongation at 72°C for 2mins and a final extension at 72°C for 10mins before a new cycle. This was repeated for a 20 cycle PCR reaction to exponentially generate copies of ZnT8 insert from the pCMVTnT vector, routinely used for standard ZnT8A detection by RIA.

To confirm successful PCR, 5µl of the ZnT8 PCR product was mixed with 1µl of 6X purple loading dye (New England Biolabs, Ipswich, MA, USA) and run on a 1% agarose gel made with a 100bp ladder (New England Biolabs) in 1X TAE for 35mins at 110V (**Figure A:2**).

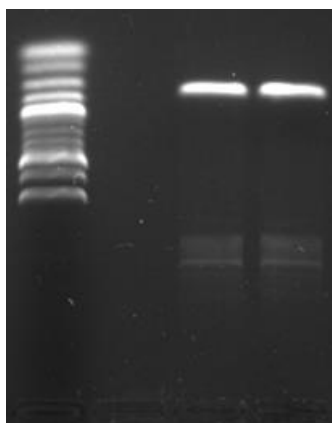


*Figure A:2 – Gel image of generating the ZnT8 insert for cloning into the pET49b(+) vector*

Lane 1: 100 bp ladder; Lane 2: Empty; Lanes 3 and 4: PCR product of ZnT8 insert (~325 bp) made in two different reactions for confirmation.

To remove possible contaminants and primer dimerisation (evident in the gel above), a PCR clean-up kit (Qiagen) was conducted to purify the remaining 45µl according to manufacturer instructions. To concentrate the DNA, the purified PCR product was ethanol precipitated (2 volumes of 100% ethanol and 1/10 volume of 3M Potassium Acetate was added, centrifuged at 13,000rpm for 20mins and the supernatant was carefully removed), washed with 70% ethanol and left to air-dry at RT for 1 hour. The PCR product was then rehydrated in 10µl sterile H<sub>2</sub>O and stored at -20°C until restriction enzyme digest.

### **A.1.1.3. Inserting the ZnT8 construct into the pET49b(+) vector**

---

The ZnT8 construct and pET49b(+) vector was digested in a 50µl reaction mix with 1ul of restriction enzymes *XhoI* and *XmaI* (New England BioLabs), 5µl 10X CutSmart buffer (New England BioLabs), and ddH<sub>2</sub>O for 2 hours at 37°C. Following incubation, the total reaction mixes were run on a 1% agarose gel with 100bp and 1kb ladders (New England Biolabs) in 1X TAE for 35mins at 110V (**Figure A:3**).

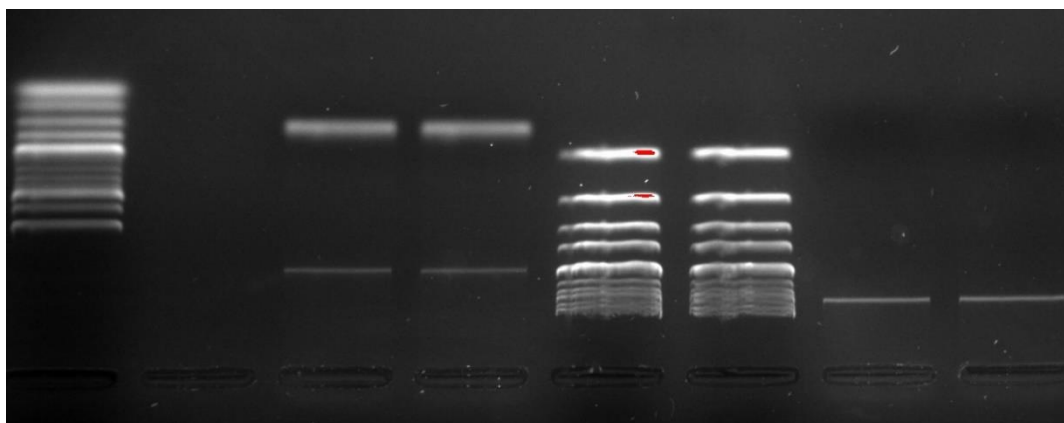


**Figure A:3 – Gel image of *XmaI* & *XhoI* double digest on the ZnT8 insert & pET49b(+) vector**

Lane 1: 100bp ladder; Lane 2: empty; Lane 3 and 4: ZnT8 insert; Lane 5 & 6: 1000bp ladder; Lane 7 and 8: pET49b(+) vector. Two double digest reactions were run to confirm successful double digest of ZnT8 insert and pET49b(+) vector using *XmaI* and *XhoI* restriction enzymes. ZnT8 insert estimated ~325bp and pET49b(+) estimated ~5772bp following double digest. The gel image indicates that PCR products are of estimated lengths.

Gel extraction was then conducted according to the manufacturer's instructions (Qiagen). To concentrate the resultant DNA (50µl), the purified PCR product was ethanol precipitated (2 volumes of 100% ethanol and 1/10 volume of 3M Potassium Acetate was added, centrifuged at 13,000rpm for 20mins, and the supernatant was carefully removed), washed with 70% ethanol, and left to air-dry at RT for 1 hour. Purified DNA digests of ZnT8 insert and pET49b(+) vector were resuspended in 10µl sterile ddH<sub>2</sub>O, mixed, and added in a 1:3 ratio to a 20µl ligation reaction mix containing T4 ligase (Sigma), 2X Ligase buffer (Sigma), and ddH<sub>2</sub>O for a 2-hour incubation at RT.

#### **A.1.1.4. Transformation of plasmids into *E. Coli***

To 50µl of chemically competent DH5α *Escherichia Coli* (*E. Coli*) cells (Invitrogen), 2µl of ligated plasmid was added and incubated on ice for 30mins. To allow entry of the ligated plasmid into these cells, the mixture was then heat shocked for 30 secs at 42°C and placed back on ice for a further 2mins. After heat shocking, 500µl of sterile SOC medium (Invitrogen) was added to the cells and incubated on a shaking platform at 225rpm for 1 hour at 37°C.

## Appendix A. ZnT8A affinity studies

To select cells containing the plasmid, cells were spread onto LB agar plates with 50µg/ml Kanamycin (Sigma) to select for the ZnT8/pET49b(+) plasmid containing the resistance gene and incubated overnight at 37°C. To amplify the single colonies containing the ZnT8/pET49b(+) plasmid, a selection of single colonies was selected and further incubated on a fresh agar plate containing 50µg/ml Kanamycin overnight at 37°C.

### A.1.1.5. Confirmation of ZnT8 Cloning into pET49b(+) vector

Following transformation, single DH5α *E. Coli* colonies were heat-shocked at 95°C for 10mins and screened for plasmids containing the ZnT8 insert in a 15µl PCR reaction using the plasmid as template DNA, the primers designed for generating the insert ZnT8 construct, and reagents from a Qiagen Taq Core Unit kit (**Table A:2**).

PCR Reagent	Volume (µl)	Final Concentration
10x CoralLoad PCR Buffer*	1.5	1X
10mM dNTPs*	0.3	200mM
10µM Forward Primer (31bp)	0.75	0.5µM
10µM Reverse Primer (32bp)	0.75	0.5µM
Template DNA ( <i>E. Coli</i> Colonies)	1	≤1µg
Sterile H <sub>2</sub> O	10.6	N/A
Taq Polymerase*	0.1	0.5 units

*Table A:2 – PCR recipe for screening E.Coli colonies for the ZnT8 insert*

The volumes and final concentrations of reagents used in a 15µl PCR reaction mix; \* indicates reagents from the Qiagen Taq Core Unit Kit. Before using as template DNA, cells from colonies were picked, diluted in 50µl of sterile ddH<sub>2</sub>O and heat-shocked at 95°C on a heating block for 10 minutes. PCR thermocycling was set at 94°C for 5mins for initial denaturation followed by denaturation at 94°C for 30secs, annealing at 55°C for 30secs, Taq polymerase elongation at 72°C for 1min and a final extension at 72°C for 10mins. This is repeated for a 35 cycle PCR reaction to exponentially generate copies of ZnT8 insert from the pET49b(+) vector.

Following PCR, 10µl of the reaction mix was loaded and run on a 1% agarose gel made with 1X TAE for 35mins at 110V. The expected length of the ZnT8 insert is 325bp, and the pet49b(+) vector is 57772bp. Colonies screening positive for a DNA band around 300bp (**Figure A:4**) was purified from liquid cultures (5ml LB broth and 50µg/ml Kanamycin incubated overnight at 37°C on a shaking platform set at 225rpm) using a miniprep kit to manufacturer's instructions (Qiagen).

## Appendix A. ZnT8A affinity studies

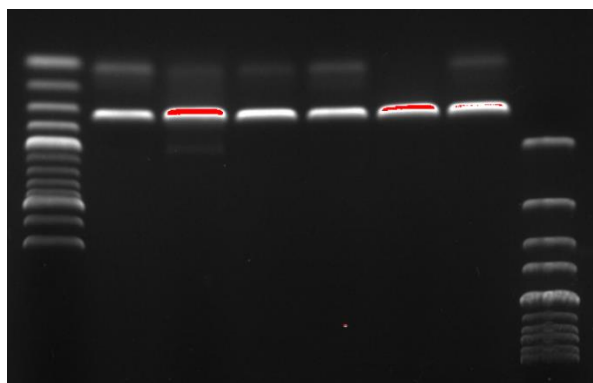


**Figure A:4 – Screening *E. Coli* colonies for ZnT8 insert on a 1% agarose gel**

Lane 1: 100bp ladder; Lane 2-7: 6 single *E.Coli* colonies; Lane 8: 1000bp ladder. Bands in between 300-400bp are indicative of the ZnT8 insert (~325bp). Bands around 100bp and 500bp could indicate primer dimerisation or other contaminants in the PCR reaction. High yields of DNA are highlighted in red. The *E.Coli* colony in Lane 6 was chosen for subsequent purification due to the high yield and clean band.

Purified plasmids were prepared for sequencing (Eurofins Genomics, Ebersberg, Germany) using the standard T7 promoter primer (to sequence the beginning of the pET49b(+) vector cloning site) and two designed primers specific to ZnT8 (**Table A:3**) to confirm cloning of ZnT8 into the pET49b(+) vector (**Figure A:5**).

Primer	Primer Sequence (5'-3')
<b>pET49b(+) T7 Promoter Primer</b>	TAATACGACTCACTATAGGGG
<b>ZnT8 Primer 1 (Forward)</b>	<u>TACAGCAGCCAGC</u> <b>CGG</b> <b>G</b>
<b>ZnT8 Primer 2 (Reverse Complement)</b>	<b>GTCACAGGGGTCTTCAC</b>

**Table A:3 – Primers to confirm ZnT8 cloning into pET49b(+) vector**

Underlined: Primer 1; Bold: Primer 2. Grey/underlined: R325W polymorphism site encoding ZnT8R.

## Appendix A. ZnT8A affinity studies

atgtccctatactaggttattggaaaattaaggcccttgcaaccactcgacttcttttgaatatcttgaagaaaaatgaagagcat  
ttgatgagcgcgatgaaggtgataaatggcgaaacaaaagtttgaattgggtttggagtttccaatcttccttattatattgatggtgat  
gttaaattaacacagctctatggccatcatagcttatagctgacaagcacaacatgttgggtggttgcctcaaaagagcgtgcagagattc  
aatgcttgaaggagcggttttggatattagatacgggttttcgagaattgcatatagtaaagactttgaaactcctcaagttgatttcttagc  
aagctacctgaaatgctgaaaatgttcgaagatcgtttatgtcataaaacatatttaaagtgatcatgtaacccatcctgacttcatgttgt  
atgacgctcttgatgttgtttatacatggaccaatgtgcctggatgcgttcccaaaattagtttgttttaaaaaacgtattgaagetatccca  
caaattgataagtaacttgaatccagcaagtatatagcatggcctttgcagggtggcaagccacgtttggtggtggegaccatcctccaa  
aatcggatggtcaactagtggtggtggcggttetaataacaatcctcctactcctactccatctagtggttctggtcaccatcaccatcacc  
ggccttgaagtcctttcagggaaccgggAAGGACTTCTCCATCTTACTCATGGAAGGTGTGCCAAAGAG  
CCTGAATTACAGTGGTGTGAAAGAGCTTATTTAGCAGTCGACGGGGTGCTGTCTGTGCA  
CAGCTGCACATCTGGTCTCTAACAATGAATCAAGTAATTCTCTCAGCTCATGTTGC**TAC**  
**AGCAGCCAGCCGGG**ACAGCCAAGTGGTTCGGAGAGAAATTGCTAAAGCCCTTAGCAAAA  
GCTTTACGATGCACTCACTACCATTAGATGGAATCTCCAGTTGACCAGGACCCCGACT  
GCCTTTTCTGTGAAGACCCCTGTGACtgataatctcgag

*Figure A:5 – FASTA sequence of the cloning site of pET49b(+) vector with ZnT8 insert & sequencing primers*

Bold; GST tag; Red; 6 x His tag; Green; human rhinovirus (HRV) 3C protease; Yellow: *XmaI* restriction enzyme recognition site; Blue; *XhoI* restriction enzyme recognition site; Grey: rs13266634 SNP site encoding R325 (CCG); Capital text: C-terminal (aa268-269) ZnT8 insert sequence; Red: ZnT8 Primer 1 (forward) used for sequencing of clone; Capital and bold text: ZnT8 Primer 2 (reverse complement) used for sequencing of clone.

---

### A.1.2. Protein expression of ZnT8 in E. Coli

#### A.1.2.1. Transformation of ZnT8/pET49b(+) plasmids into E.Coli Rosetta<sup>TM</sup> (DE3) pLysS cells

Rosetta<sup>TM</sup>(DE3)pLysS cells are BL21 derivatives designed to enhance the expression of eukaryotic proteins that contain codons rarely used in *E.coli*. The DE3 and pLysS strain of these cells are suitable for genes cloned in pET vectors with subsequent induction of protein expression using Isopropyl  $\beta$ -d-1-thiogalactopyranoside (IPTG) by suppressing the T7 RNA polymerase enzyme (457).

Plasmid DNA from an *E.Coli* colony with confirmed sequencing of the ZnT8 insert in the pET49b(+) vector was transformed into *E.Coli* Rosetta<sup>TM</sup>(DE3)pLysS cells (Novagen, Sigma) following a similar protocol as detailed in 2.4.2.2.2 with a few modifications according to the

## Appendix A. ZnT8A affinity studies

manufacturer's instructions; 1µl of plasmid DNA to 20µl Rosetta<sup>TM</sup>(DE3)pLysS cells, 250µl SOC medium, and selective LB+/-agar containing 15µg/ml kanamycin and 34µg/ml chloramphenicol. Successful transformation was confirmed by conducting the original PCR reaction run to generate the ZnT8 insert (**Figure A:6**).

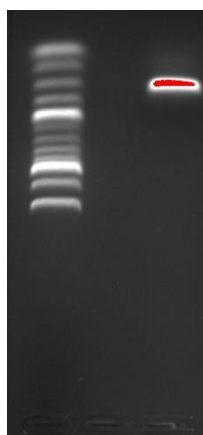


*Figure A:6 – Gel image confirming the transformation of ZnT8/pET49b(+) into Rosetta<sup>TM</sup>(DE3)pLysS cells*

Lane 1: 100bp ladder; Lane 2: empty; Lane 3; Single Rosetta<sup>TM</sup>(DE3)pLysS colony containing ZnT8 insert (~325bp) at high concentrations (red for saturated pixels) in the absence of other contaminants in the PCR reaction.

### **A.1.2.2. Generation of glycerol socks for long-term storage of ZnT8/pET49b(+) plasmids**

---

Glycerol stocks of single colonies of ZnT8/pET49b(b) were generated as previously described (2.4.2.2.4) with the modification of using 15µg/ml Kanamycin and 34µg/ml chloramphenicol as selective antibiotics.

### **A.1.2.3. Expression of ZnT8 in Rosetta<sup>TM</sup>(DE3)pLysS cells**

---

#### Reagents

1M Isopropyl-β-D-thiogalactoside (IPTG) stock solution – IPTG (2.38g) dissolved in ddH<sub>2</sub>O (10ml) and filter sterilised through a 0.22µM syringe filter (Merck Millipore, Sigma).

## Appendix A. ZnT8A affinity studies

### Large-scale expression of ZnT8 in Rosetta™(DE3)pLysS cells

A single colony of Rosetta™(DE3)pLysS cells containing ZnT8/pET49b(+) was inoculated into a 50ml LB starter culture containing 15µg/ml Kanamycin and 34µg/ml chloramphenicol. The 50ml starter culture was incubated for 16 hours at 37°C on an orbital shaking platform set at 225rpm. Following 16 hours, the starter culture was used to inoculate a 1L LB secondary culture containing 15µg/ml Kanamycin and 34µg/ml chloramphenicol to an optical density (OD)<sub>600 nm</sub> of 0.1 absorbance measured using 1ml by a spectrophotometer. The 1L secondary culture was further incubated (37°C/225rpm) and monitored every hour until the OD<sub>600 nm</sub> reached 0.8 absorbance (exponential phase of bacterial growth). A 1ml aliquot was taken (baseline; lag phase), pelleted (13,000rpm for 1min), and both the cell pellet and supernatant were separated, measured at OD<sub>600 nm</sub>, and frozen at -20°C for analysis of expression by sodium dodecyl sulfate polyacrylamide gel electrophoresis (SDS-PAGE; Error! Reference source not found.).

With an OD<sub>600 nm</sub> of 0.8, expression was induced by adding 1mM IPTG in the 1L secondary culture. After 2 hours of further incubation at 37°C/225rpm, 1mM IPTG is added and further incubated at 37°C/225rpm for 2 hours. Over these 4 hours, 1ml aliquots were taken (expression time course), pelleted (13,000rpm for 1min), and both the cell pellet and supernatant were separated, measured at OD<sub>600 nm</sub>, and frozen at -20°C for analysis of expression by SDS-PAGE (Error! Reference source not found.).

The 1L secondary culture after 4 hours of induced expression is centrifuged at 8,000rpm for 20 minutes at 4°C. After the removal of the supernatant, the cell pellet is resuspended in 15ml LB containing 15% glycerol, moved to a 50ml falcon tube, and is frozen at -80°C until cell lysis using the French Press (Error! Reference source not found.).

#### **A.1.2.4. SDS-PAGE protein gels to confirm ZnT8 protein expression**

##### *Buffers & Reagents*

Resolving gel buffer – 1.5M Tris base with hydrochloric acid (HCl), pH 8.8.

Stacking gel buffer – 0.5M Tris base with HCl, pH 6.8.

SDS running buffer – Tris-glycine (1X). For a 10X stock solution, 30.2g Tris base and 144g glycine was dissolved in 800ml ddH<sub>2</sub>O, and once mixed, 10g SDS was added to bring the volume to 1L. A 1/10 dilution was made for a 1X working solution.

2 x sample loading buffer (non-reducing): 1M Tris-HCl (0.5ml), pH 7, 20% SDS (2.5ml), glycerol (2ml), and 2mg bromophenol blue was mixed and made up to 10ml with ddH<sub>2</sub>O.

30% Acrylamide/Bis-acrylamide Available from VWR, Radnor, Pennsylvania, USA.

Sodium dodecyl sulfate (SDS) – 1M SDS was diluted 1/10 in ddH<sub>2</sub>O.

Tetramethylethylenediamine (TEMED)- Available from Sigma.

Ammonium persulfate (APS) – 1M APS diluted 1/10 in ddH<sub>2</sub>O.

Isopropanol – Commercially available (Fisher Scientific).

Precision Plus Protein™ All Blue Prestained Protein Standards – Commercially available from BioRad (Hercules, California, USA).

Brilliant Blue R Staining Solution (1L) – Commercially available (Sigma)

Destain solution – methanol (150ml) and glacial acetic acid (50ml) is mixed and made up to 500ml with ddH<sub>2</sub>O.

## Appendix A. ZnT8A affinity studies

### SDS-PAGE

SDS-PAGE using the Mini-PROTEAN Tetra cell kit (BioRad) was conducted according to the protocol described by Elvers & Williams (2016) (457); described in **Table A:4**, on the following page. The time course of protein expression by SDS-PAGE analysis confirmed the successful expression of ZnT8 with a GST tag in *E.Coli* Rosetta<sup>TM</sup>(DE3)pLysS cells with a molecular weight of 38.22 kilodaltons (kDa) (**Figure A:7**).

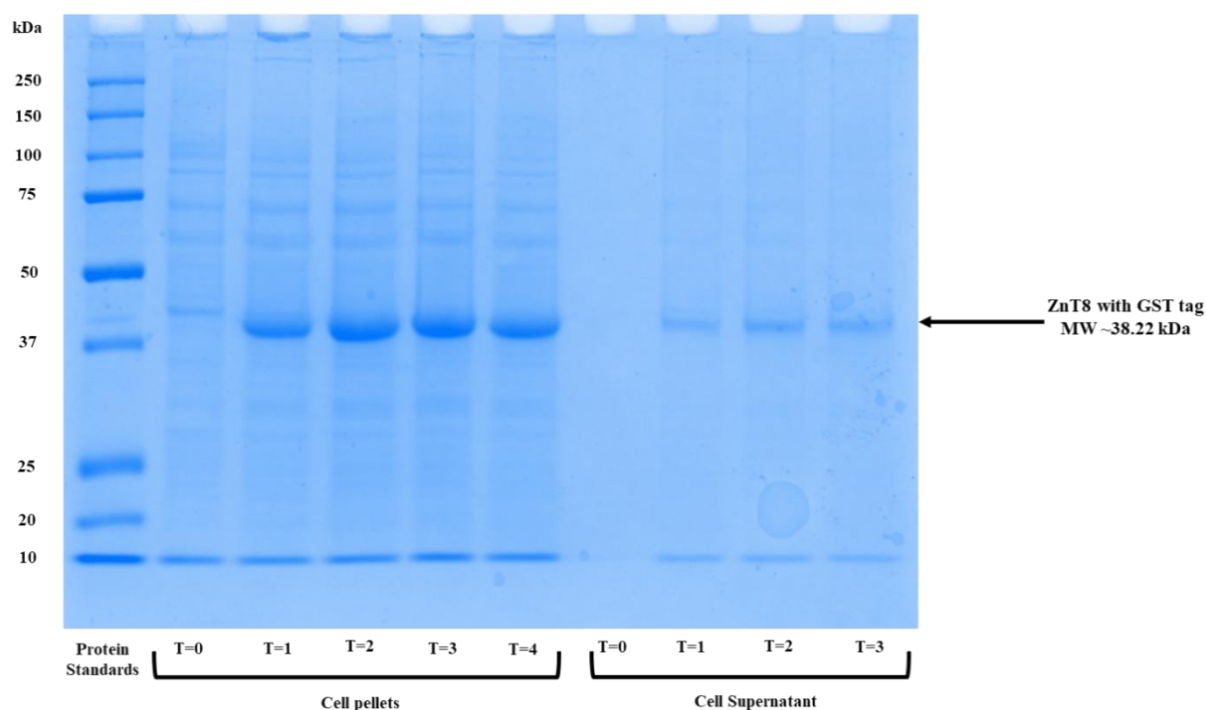


**Figure A:7 – SDS-PAGE gel showing the time course of expression of ZnT8 with GST tag in *E.Coli* Rosetta<sup>TM</sup>(DE3)pLysS cells**

Time course (T)=0-4 refers to baseline, 1hr, 2hrs, 3hrs and 4hrs, respectively. Protein expressed was induced at baseline and T=2. kDa: kilodalton molecular weight (MW).

Appendix A. ZnT8A affinity studies

Step	Reagents/Equipment	Volume	Protocol comments
<b>1. Preparing the 12% separating gel</b>	ddH <sub>2</sub> O 30% Acrylamide/Bis-acrylamide Resolving gel buffer 10% SDS TEMED 10% APS	5.3ml 6.4ml 4ml 160µl 16µl 160µl	Reagents added in order and poured between two mini glass plates assembled in the gel casting frame.
<b>2. Set the separating gel</b>	100% Isopropanol	1ml	Air is excluded to allow the separating gel to set. Once set, the isopropanol was removed.
<b>3. Preparing the 6% stacking gel</b>	ddH <sub>2</sub> O 30% Acrylamide/Bis-acrylamide Stacking gel buffer 10% SDS TEMED 10% APS	5.3ml 2ml 2.5ml 100µl 10µl 100µl	Reagents added in order and poured between two mini glass plates assembled in the gel casting frame. A 10-well gel comb was inserted & left to set. Once set, the gel was loaded into the gel buffer dam.
<b>4. Preparing samples for SDS-PAGE</b>	1X SDS running buffer Probe sonicator.	500µl	Thaw cell pellets & supernatant from protein expression. Resuspend cell pellets in SDS running buffer and sonicate. Collect supernatant by centrifuging sonicated cells at 13,000rpm 1 minute. Resuspend cell pellet in SDS-running buffer. Supernatants & cell pellets will be run on the SDS-PAGE gel.
<b>5. Loading the SDS-PAGE gel</b>	1X SDS running buffer 2 x sample loading buffer Sonicated cell supernatant & pellet Precision Plus Protein™ All Blue Prestained Protein Standards	1L 15µl 35µl 7µl	Fill gel tank and gel buffer dam with SDS running buffer. Mix sonicated cell supernatant & pellet with sample loading buffer and load 40µl into wells (2-10) of the gel. Thaw protein standard and load into well 1 of pre-made gel.
<b>6. Running &amp; imaging the SDS-PAGE gel</b>	Brilliant Blue R staining solution Destain solution	50ml 80ml	Run for 35-45mins at 110V. Gels are stained in Brilliant Blue R staining solution for 1h. After 1hr, gels are destained for 1 hour (50rpm at RT), replenished with destain solution and left overnight. Gels are imaged on a BioRad Imager using the Mini-PROTEAN gel programme & exported at 600dpi.

*Table A:4 – SDS-PAGE methodology*

Mini-PROTEAN Tetra Cell (BioRad) kit was used for all equipment supplies required for SDS-PAGE.

---

### A.1.3. Protein purification of recombinant ZnT8

---

#### **A.1.3.1. Buffer & Reagents**

---

Lysis buffer – 50mM Tris-HCl (pH 7.5), 150mM NaCl, and 1mM Dithiothreitol (DTT).

Binding buffer A for GSTrap – 50mM Tris-HCl (pH 7.5), 100mM NaCl, and 1mM DTT.

High Salt wash buffer B for GSTrap – 50mM Tris-HCl (pH 8), 300mM NaCl, and 1mM DTT.

Elution buffer C for GSTrap – 50mM Tris-HCl (pH 8) and 10mM reduced glutathione.

EDTA – 0.5M EDTA solution (pH 8).

cComplete™ ULTRA Tablets – EDTA-free, EASYpack Protease Inhibitor Cocktail (Sigma).

GSTrap™ – FF 5ml volume (Sigma)

#### **A.1.3.2. Using a French Press to Lyse Rosetta™(DE3)pLysS cells containing recombinant ZnT8**

---

The French Press lyses cells by applying high pressure and forcing the cells through a tiny hole in the press. The frozen cell pellet from expression is thawed at RT, passed through the pre-chilled (kept at 4°C overnight ~16 hours) French Press central apparatus twice and collected on ice.

The collected lysed cells were resuspended in 120ml lysis buffer and centrifuged at 8000rpm for 20 minutes at 4°C. The supernatant was collected and centrifuged again at 8000rpm for 20 minutes at 4°C. The supernatant was collected and fractioned into 30ml aliquots. Per 20ml of collected supernatant, 1 cComplete™ ULTRA Tablet and 100µl 0.5M EDTA was added. Once the tablet had dissolved, aliquots were gently mixed by swirling and frozen at -20°C until purification.

### **A.1.3.3. Purification of ZnT8 using FPLC**

---

Fast protein liquid chromatography (FPLC) using a GSTrap<sup>TM</sup> 5ml (Sigma) column was used to purify the soluble ZnT8-GST fusion protein from the supernatant of the lysed cells from the French Press. One 30ml aliquot of frozen cell supernatant from the French Press was thawed at RT with the addition of 300µl of 0.5M EDTA and 2.5ml of 2 dissolved cOmplete<sup>TM</sup> ULTRA Tablets in binding buffer A. Whilst defrosting, the supernatant was gently vortexed until fully thawed/aqueous.

Using the GE AKTA Prime System (Cytiva - Fisher Scientific, formerly GE Life Sciences) comprised of an automated programmable control system, pump, fraction collector, and the PrimeView software, the protocol described in (457) was followed (**Table A:5**).

Step	Protocol
<b>1. Priming the buffers lines &amp; equilibrate the GSTrap™ column</b>	<ul style="list-style-type: none"> <li>- Perform a system wash method of lines A and B with binding buffer A and high salt wash buffer B, respectively.</li> <li>- Connect the GSTrap™ column to the system and equilibrate with 5-10mls of binding buffer A at a flow rate of 1ml/min. Press pause.</li> </ul>
<b>2. Loading &amp; washing the cell supernatant</b>	<ul style="list-style-type: none"> <li>- Place the tubing from line A into the thawed cell supernatant, alter the flow rate to 0.8ml/min and press continue. As the expressed protein is loaded onto the column, the ultraviolet (UV) light absorbance at 280nm will increase indicating increasing protein concentration. Collect the flow through as the supernatant is loaded.</li> <li>- When all the cell supernatant is loaded, press pause, move line A back into binding buffer A and press continue to allow all the supernatant remaining in line A to be loaded onto the column.</li> </ul>
<b>3. Wash column</b>	<ul style="list-style-type: none"> <li>- Wash the column by 10 column volumes (50ml) in high salt wash buffer B at a flow rate of 0.8ml/min.</li> <li>- As the column is washed in this buffer, the conductivity detector that monitors salt concentration will increase.</li> <li>- Load high salt wash buffer B until the conductivity line returns to baseline. Collect the effluent for later analysis by SDS-PAGE.</li> </ul>
<b>4. Elution of the protein</b>	<ul style="list-style-type: none"> <li>- Remove column from the system and remove the B line from the high salt buffer B into elution buffer C. Perform a system wash to fill line B with elution buffer C.</li> <li>- Re-connect the GSTrap™ to the system. Perform a manual run with a flow rate of 1ml/min and the fraction collector set to 1ml fractions to collect eluted protein into ~20 fractions.</li> </ul>
<b>5. Add reagents to prevent protein degradation</b>	<ul style="list-style-type: none"> <li>- To each 1ml fractions where the UV absorption indicated the eluted protein, add 50ul of 0.1M EDTA and 100ul of 1cOmplete™ ULTRA Tablet dissolved in 1ml ddH<sub>2</sub>O. Gently mix by swirling and store at 4°C until SDS-PAGE analysis.</li> </ul>
<b>6. SDS-PAGE analysis</b>	<ul style="list-style-type: none"> <li>- Analyse load, flow through, and collected fractions that the FPLC showed increased protein concentrations (indicated by the UV absorbance).</li> </ul>

*Table A:5 – Methodology of purifying the ZnT8-GST fusion protein using a GSTrap™ column & FPLC (GE AKTA Prime System).*

#### **A.1.3.4. SDS-PAGE analysis of FPLC purified ZnT8-GST fusion protein**

The chromatogram (not shown) showed a very small peak of UV absorbance between fractions 9-14 (selected for SDS-PAGE analysis) with a long plateau beyond fraction 13. The SDS-PAGE gel was prepared according to the previously described method (**Table A:4**) on the load, flow-through, and fractions 8 to 14 collected from the FPLC purification of the ZnT8-GST fusion protein (**Figure A:8**). The protein bands between 50-60kDa in fractions 8-14 show eluted protein with a higher molecular weight than expected or observed after protein expression (~38.22kDa). This may be due to protein insolubility/precipitation, protein modification, and/or protein retardation during elution.

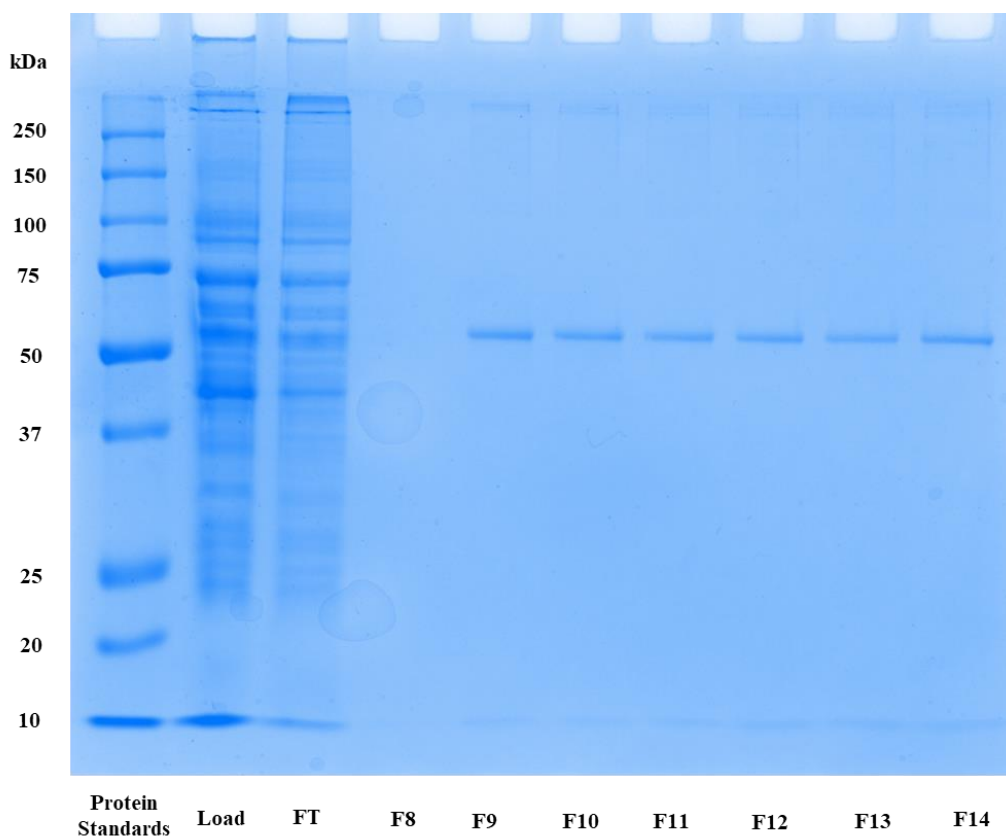


*Figure A:8 – SDS-PAGE gel of FPLC eluted fractions*

FT: flow through; F8-F14: fractions 8-14. The SDS-PAGE bands between 50-60kDa are much larger than expected and observed after protein expression ~38.22kDa.

### **A.1.3.5. Protein quantification of purified ZnT8-GST fusion protein**

All samples that were analysed by SDS-PAGE were quantified using the Qubit™ Protein Assay kit according to manufacturer instructions (Thermo Fisher) (**Table A:6**). The protein concentrations in eluted fractions 9-14 confirm the peak of eluted protein; however, there is no way of ascertaining the precise identity of the protein(s) present in the eluted fractions using SDS-PAGE alone, and most of the protein content did not bind the GST column suggesting there is a significant technical issue.

<b>FPLC eluted fractions</b>	<b>Protein concentration (mg/ml)</b>
<b>Load</b>	4.500
<b>Flow through</b>	4.480
<b>Fraction 8</b>	0.276
<b>Fraction 9</b>	0.532
<b>Fraction 10</b>	0.684
<b>Fraction 11</b>	0.658
<b>Fraction 12</b>	0.514
<b>Fraction 13</b>	0.546
<b>Fraction 14</b>	0.816

*Table A:6 – Protein concentrations of eluted FPLC fractions quantified using the Qubit™ Protein Assay kit (Thermo)*

## Appendix B. ZnT8A IgG subclass studies

### B.1. Clones & source of monoclonal anti-human IgG subclass antibodies used in seminal T1D studies

<b>Study (date)</b>	<b>Anti-rat IgM (control)</b>	<b>IgG1</b>	<b>IgG2</b>	<b>IgG3</b>	<b>IgG4</b>
<b>Bonifacio <i>et al.</i> (1999)§</b>	Cat no. quoted 34152D PharminGen (BD)	Cat no. quoted 35052D PharminGen (BD)	Cat no. quoted 35072D PharminGen (BD)	Cat no. quoted 35082D PharminGen (BD)	Cat no. quoted 35092D PharminGen (BD)
<b>Achenbach <i>et al.</i> (2004)§</b>	Clone G20-127 BD	Clone G17-1 BD	Clone G18-21 BD	Clone G18-3 BD*	Clone JDC-14 BD
<b>Hoppu <i>et al.</i> (2004)</b>	Clone G53-238 PharminGen (BD)	Clone G17-21 PharminGen (BD)	Clone G18-21 PharminGen (BD)	Clone HP6050 Southern Biotech	Clone JDC-14 PharminGen (BD)
<b>This project (2015-21)</b>	Clone G53-238 BD	Clone G17-1 BD	Clone G18-21 (BD)	Clone HP6047 (Invitrogen/ Sigma)*	Clone JDC-14 (BD)

*Table B:1 – Clones & source of monoclonal anti-human IgG-subclass antibodies used in seminal T1D studies*

\* Only a change in the clone of IgG3 between Achenbach *et al.* (2004) & this PhD project as the G18-3 clone was no longer commercially available from BD. The current HP6047 IgG3 clone binds to the light chain/hinge region of IgG3 and, therefore, is likely to be more sensitive than previous clones.

---

## B.2. GADA & IA-2A IgG subclass RIA standardisation

---

---

### B.2.1. Materials & methods

---

#### **B.2.1.1. Standardisation sample sets**

---

##### *Healthy schoolchildren*

A total of 2860 healthy schoolchildren [1488 (52.0%) male; 1372 (48.0%) female; median age at sampling 11.4 years (range 9.0-13.8 years); 88.6% of Caucasian ethnicity] from the general population were recruited from schools in Oxford and Windsor between 1989 and 1991 and were screened in-house for all known autoantibody positivity using established and standardised methods at that time (ICA/GADA/IA-2A/IAA) (12, 354).

From the 2860 healthy schoolchildren, a subset with high serum volume was tested to establish GADA and IA-2A IgG subclass-specific thresholds based on the SD obtained: GADA [n=49; 28 males (57.1%); median age at sample 11.1 years (range 9.4-13.1)] and IA-2A [n=48; 28 males (58.3%); median age at sample 11.1 years (9.4-13.1)] in the respective IgG subclass RIAs. For ZnT8RA/ZnT8WA IgG subclass RIAs, establishing IgG subclass-specific thresholds was not cost-effective and may not be useful in predicting disease risk given that the responses appear highly IgG1-dominant/restricted and would require screening of many more samples (results presented in **2.3.3-2.3.3.2**).

*Type 1 diabetes patients*

For GADA and IA-2A, samples from the T1D patients from the IgG subclass screening sample set (n=12 for GADA and n=35 for IA-2A; **Table 2:10**) and a subset of additional samples taken from T1D patients of moderate-high autoantibody titres **Table B:2**; n=15 for GADA and n=22 for IA-2A), were compared to the subset of healthy school children to establish IgG subclass-specific StDS positivity thresholds.

Autoantibody	n individuals	n samples	Median (range) autoantibody titre*	Median (range) age at diagnosis (years)	Median (range) age at sample (years)	Median (range) of diabetes duration (years)
GADA	20	26	203.2 (34.1-1159.4)	19.1 (4.7-50.1)	21.6 (10.2-49.9)	2.8 (-0.2-13.0)
IA-2A	36	56	277.3 (55.2-504.1)	12.3 (5.9-41.7)	15.0 (6.9-44.7)	1.4 (0.4-6.4)

*Table B:2 – T1D patient standardisation sample set*

Selected samples were selected to encompass around diagnosis and after diagnosis, moderate to high autoantibody titres, and were considered if sample volume availability was plentiful.

### **B.2.1.2. Statistical analysis**

A rudimentary GADA/IA-2A IgG subclass-specific detection thresholds was initially established using the IgG subclass-specific mean  $\Delta$ CPM + SD obtained in healthy ~50 healthy schoolchildren and was compared to the T1D patients from the screening sample set (**Table 2:10**). This was used to evaluate the assay background/non-specific binding in a healthy population relative to the binding observed in a patient population.

To further evaluate the use of an assay threshold, the mean  $\Delta$ CPM of IgG subclasses in each sample was converted into a StDS calculated by: [(IgG subclass or PGS mean  $\Delta$ CPM – mean  $\Delta$ CPM of healthy schoolchildren)  $\div$  SD mean  $\Delta$ CPM of healthy schoolchildren, described previously (244). An SDS >3 relative to each IgG subclass was considered positive as this

## Appendix B. ZnT8A IgG subclass studies

threshold offered the greatest compromise between assay sensitivity and specificity. Mann Whitney U tests were used to compare median StDS between T1D patients and healthy schoolchildren.

---

### B.2.2. Results

---

Using a 3 StDS threshold captures the dominant IgG subclass (IgG1) & total IgG (PGs) in all GADA & IA-2A positive T1D patients.

The IgG subclass-specific mean  $\Delta$ CPM and SD obtained from the healthy schoolchildren for GADA and IA-2A responses are detailed in **Table B:3**.

Using a detection threshold (mean  $\Delta$ CPM >100) for all immunoprecipitates, the IgG subclass detection prevalence in the GADA positive T1D patient sample set (n=26; **Figure B:1**) was: IgG1, 100% (n=26); IgG2, 26.9% (n=7); IgG3 34.6% (n=9); IgG4, 23.1% (n=6); and PGS, 100% (n=26).

Similarly, the IgG prevalence in the IA-2A positive T1D patient sample set (n=56, **Figure B:1**) was: IgG1, 100% (n=56); IgG2, 53.6% (n=30); IgG3, 39.3% (n=22); IgG4, 66.1% (n=37); and PGS, 100% (n=56).

Appendix B. ZnT8A IgG subclass studies

Autoantibody & number of healthy schoolchildren subjects tested	IgG1		IgG2		IgG3		IgG4		PGS	
	Mean ΔCPM (SD)	StDS Threshold								
<b>GADA (n=49)</b>	30.5 (27.1)	57.6	5.3 (11.7)	17.0	28.6 (60.3)	88.9	27.8 (33.2)	61.0	223.7 (133.6)	357.3
<b>IA-2A (n=48)</b>	38.8 (29.9)	68.7	9.9 (14.8)	24.7	15.0 (47.3)	62.3	11.8 (23.0)	34.8	52.4 (65.2)	117.6

Table B:3 – IgG subclasses & total IgG in healthy schoolchildren for IgG detection thresholds

Detection thresholds = mean Δ counts per minute (CPM) + standard deviation (SD) of healthy schoolchildren subjects tested for the respective autoantibody.

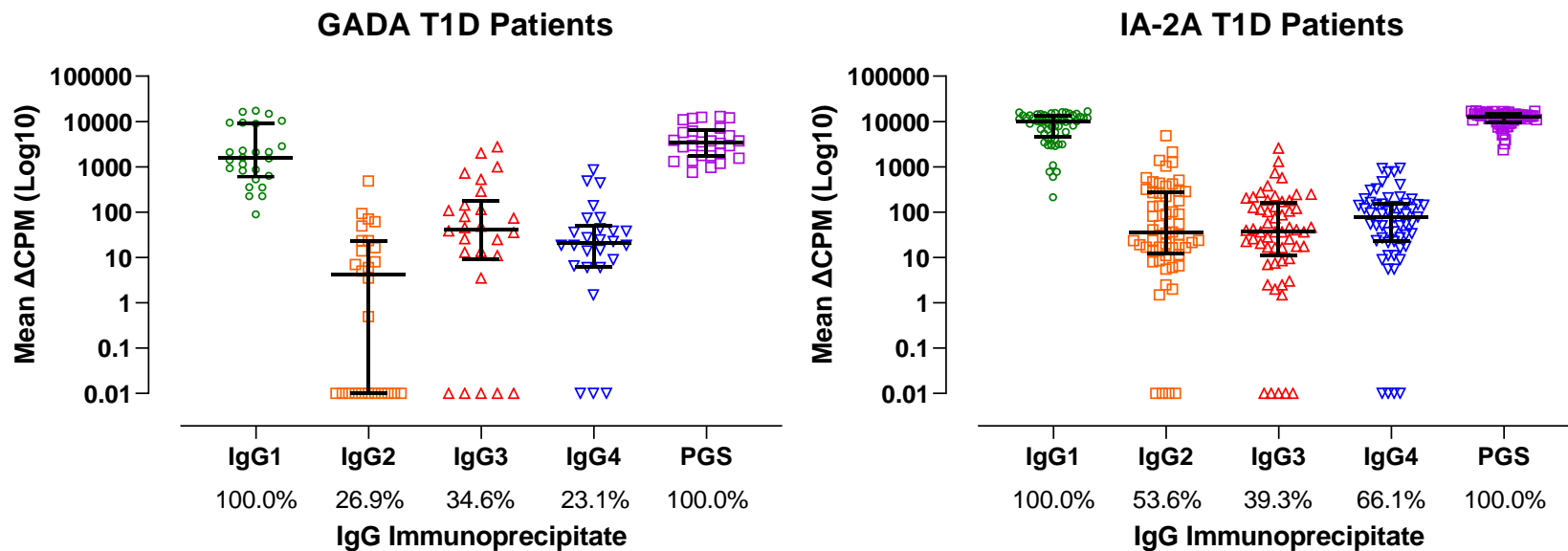


Figure B:1 – Prevalence of IgG subclasses in GADA & IA-2A T1D standardisation sample sets using the IgG detection thresholds

Samples from the T1D patient standardisation sample set were tested for GADA (n=26) and IA-2A (n=56) IgG subclasses. GADA detection thresholds based on the mean ΔCPM + SD of 49 healthy schoolchildren: IgG1, 57.6; IgG2, 17.0; IgG3, 88.9; IgG4, 61.0; and PGS, 357.3. IA-2A detection thresholds based on the mean ΔCPM + SD of 48 healthy schoolchildren: IgG1, 68.7; IgG2, 24.7; IgG3, 62.3; IgG4, 34.8; and PGS, 117.6.

## Appendix B. ZnT8A IgG subclass studies

As expected, the prevalence of any IgG subclass was higher in T1D patients than healthy schoolchildren for both GADA (**Figure B:2**) and IA-2A (**Figure B:3**) ( $p < 0.0001-0.003$ ). For any GADA or IA-2A IgG subclass RIAs, a threshold of 3 StDS would classify 2-4.2% ( $n=1-2$ ) of healthy schoolchildren, 15.4%-100% ( $n=4-26$ ) GADA T1D patients, and 25-100% of IA-2A T1D patients as positive across all 4 IgG subclasses. Despite a few healthy schoolchildren having an StDS  $>3$ , which could be due to assay variability in select samples, an StDS  $>3$  reduced assay background in the anti-rat IgM control and, therefore, is likely to improve overall assay specificity above utilising a detection threshold based  $>100$  mean  $\Delta$ CPM only.

StDS also confirmed that assay background (non-specific binding) was generally higher in T1D patients than healthy schoolchildren ( $p=0.049$  for GADA and  $p=0.044$  for IA-2A, data not shown). However, it cannot be ruled out that this could be due to serum sample quality.

To remove any IgG subclass binding in the healthy schoolchildren population, the StDS positivity threshold should be set at 6 and 7 for GADA and IA-2A, respectively. However, the small gain in specificity (1-2%) compromises a greater loss of sensitivity (loss of 7-27%) across all IgG subclasses in GADA and IA-2A responses. Therefore, an StDS  $>3$  offers the greatest compromise in sensitivity and specificity.

The IgG subclass-specific StDS thresholds should benefit future investigations in at-risk individuals or T1D patients.

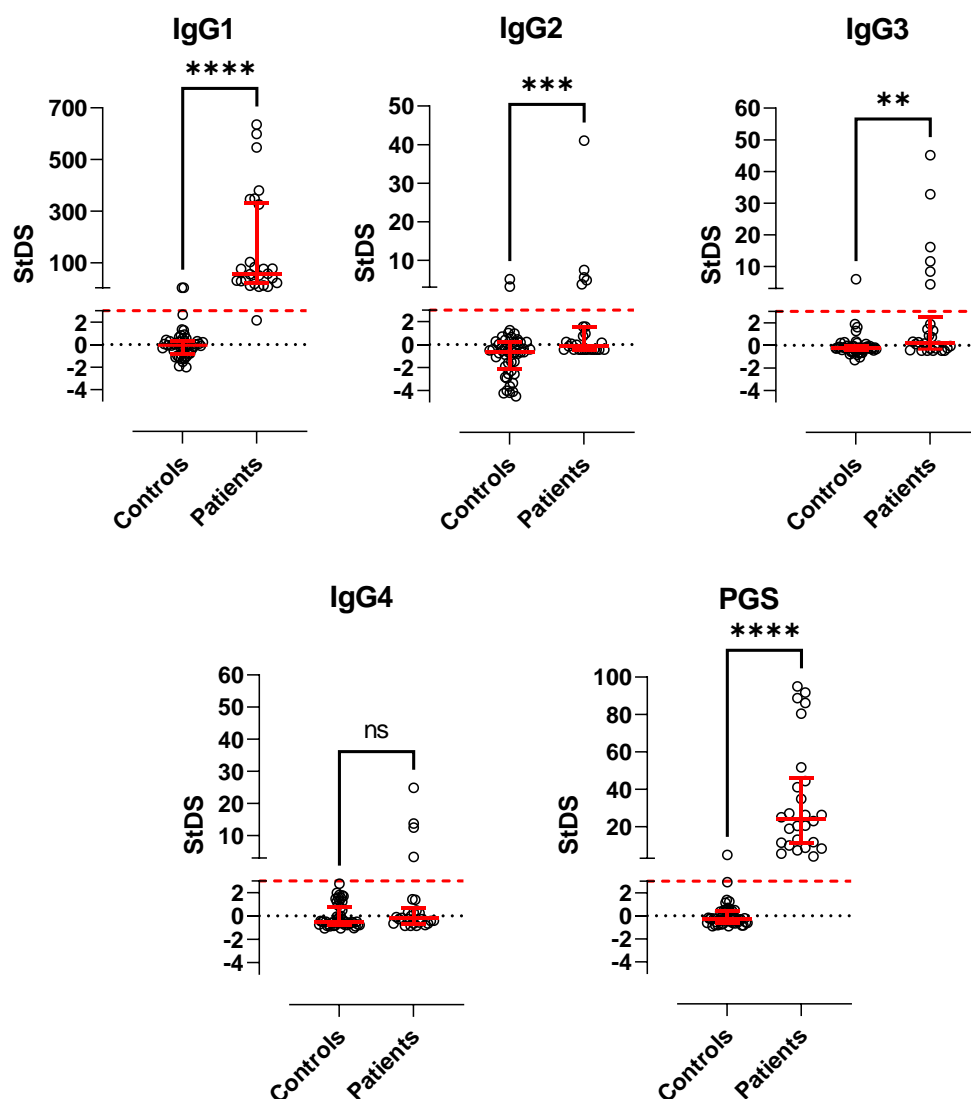


**Figure B:2 – StDS between healthy schoolchildren & T1D patients in the GADA IgG subclass RIA**

Red bars denote median and interquartile ranges. The red dashed line denotes the 3 StDS positivity threshold relative to the respective IgG subclass. NS: Not significant  $\alpha > 0.05$ ; \*  $p < 0.049$ ; \*\*  $p = 0.003$ ; \*\*\*  $p = 0.0004$ ; \*\*\*\*  $p < 0.0001$  by Mann Whitney U test. This confirmed that the IgM assay background and non-specific binding is higher in T1D patients ( $p = 0.049$ ; data not shown), but for all IgG subclasses but IgG4 (due to its low prevalence;  $p = 0.18$ ), T1D patients had much higher binding than healthy schoolchildren ( $p = 0.003 - < 0.0001$ ).

## Appendix B. ZnT8A IgG subclass studies

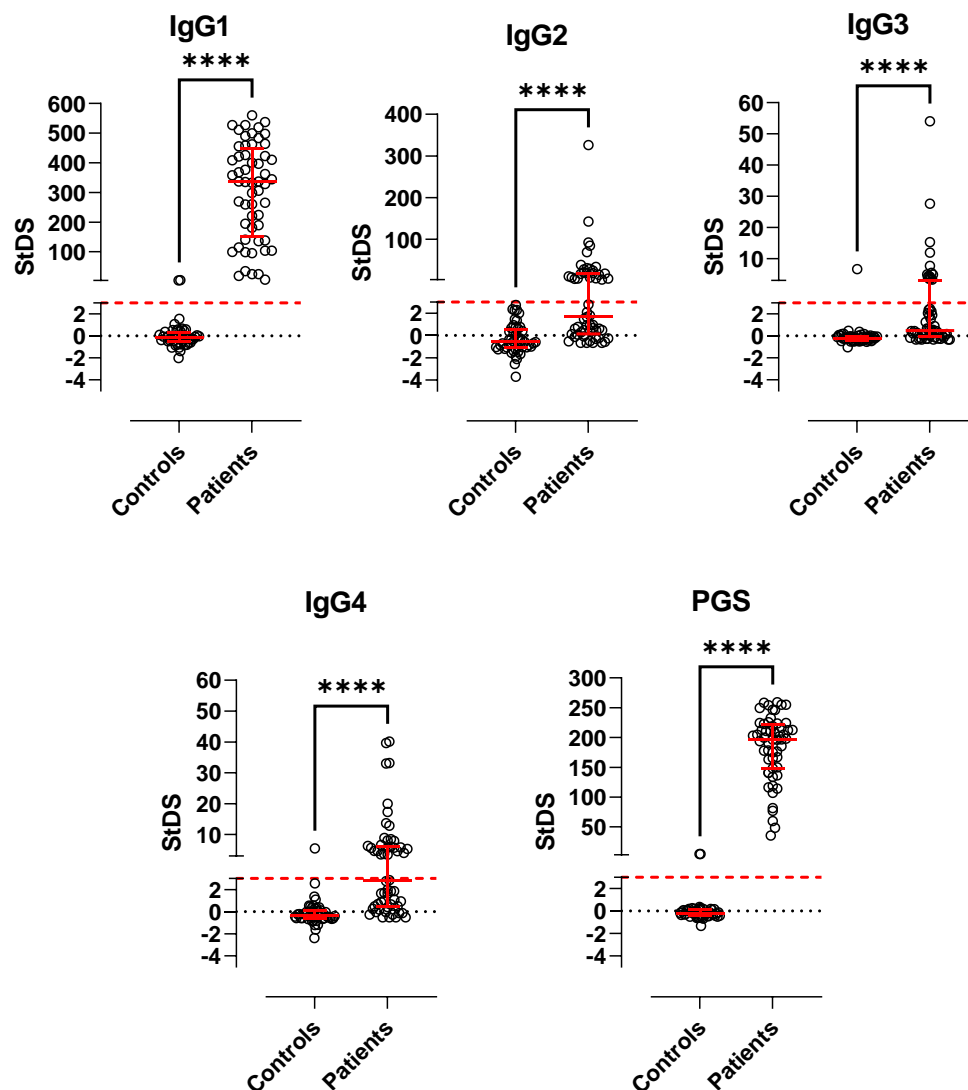


**Figure B:3 – StDS between healthy schoolchildren & T1D patients in the IA-2A IgG subclass RIA**

Red bars denote median and interquartile ranges. The red dashed line denotes the 3 StDS positivity threshold relative to the respective IgG subclass. \*  $p < 0.05$ ; \*\*\*\*  $p < 0.0001$  by Mann Whitney U test. This confirmed that the IgM assay background and non-specific binding is higher in T1D patients ( $p = 0.044$ ; data not shown), but for all IgG subclasses, T1D patients had much higher binding than healthy schoolchildren (all  $p < 0.0001$ ).

## Appendix C. ZnT8A epitope studies

### C.1. Cloning strategy to generate the ZnT8 construct encoding murine REKK (TGQ-)

#### C.1.1. Buffers & Reagents

Tris base, acetic acid, and Ethylenediaminetetraacetic acid (EDTA) (TAE) – 50X stock commercially available (Fisher Scientific, Hampton, New Hampshire, USA) diluted to 1X (10ml in 490ml ddH<sub>2</sub>O), pH 8.3.

#### C.1.2. Generating the murine REKK ZnT8 insert

Primers with specific flanking recognition sequences for *XhoI* and *HindIII* restriction enzymes were designed to generate a PCR product with TGQ encoded and aa340 removed (TGQ-).

**Figure C:1** details the human C-terminal ZnT8 FASTA sequence with the murine REKK sequences and the designed primers.

GCACTCGAGAATTCGCCGCCACCATGGAGAAAGGACTTCTCCATCTTACTCATGGAAGGTGTGCCAAA  
GAGCCTGAATTACAGTGGTGTGAAAGAGCTTATTTAGCAGTCGACGGGGTGCTGTCTGTGCACAG  
CCTGCACATCTGGTCTCTAACAAATGAATCAAGTAATTCTCTCAGCTCATGTTGCTACAGCAGCCAGCC  
GGGACAGCCAAGTGGTTCGGACGGGAATTGCTCAGGCCCTTTCAGCTTTACGATGCACTCACTCA  
CCATTGAGATGGAATCTCCAGTTGACCAGGACCCCGACTGCCTTTTCTGTGAAGACCCCTGTGACTA  
GGA

*Figure C:1 – FASTA sequence of human C-terminal ZnT8 with the cloning strategy for generating the murine REKK (TGQ-) ZnT8 construct utilising flanking restriction enzyme recognition sites*

FASTA sequence is detailed in the 5→3 orientation. Dark blue highlight: the beginning of C-terminal ZnT8 (aa268). Underlined: Forward (5→3) and reverse (3→5) primers. Red/bold: *XhoI* restriction enzyme recognition site. Dark blue/bold: *HindIII* restriction enzyme recognition site with the grey highlighting a nucleotide that was changed from AGC to TCA, which both encode serine, but TCA enabled the incorporation of the *HindIII* recognition site. Yellow: R325. Orange: R332T. Light blue: E333G. Green: K336Q. The amino acid 340 was removed at the beginning of the *HindIII* recognition site.

## Appendix C. ZnT8A epitope studies

To build the ZnT8 murine REKK insert, a 35-cycle PCR reaction was set up using the Taq PCR core kit (Qiagen, Hilden, Germany) in a recipe detailed below (**Table C:1**).

PCR Reagent	Volume (µl)	Final Concentration
10x PCR Buffer	5	1X
dNTPs	1	200mM
10µM Forward Primer (31bp)	2.5	125ng
10µM Reverse Primer (32bp)	2.5	125ng
Template ZnT8 DNA (aa268-369)	1	≤1ug
Sterile H <sub>2</sub> O	37.4	N/A
Taq Polymerase	0.3	1.5 units

PCR step	Temperature (°C)	Time (Min)	Cycles
Initial	94	0.5	
Denaturation	94	0.5	X35
Annealing	55	1	
Elongation	72	2	
Final	72	10	

*Table C:1 – PCR recipe & accompanying PCR cycle for generating ZnT8 murine REKK insert*

The volumes and final concentrations of reagents used in a 50µl PCR reaction mix. The pCMVTnT vector containing C-terminal ZnT8 (aa268-369) was used as template DNA.

To confirm successful PCR, 5µl of the ZnT8 PCR product was mixed with 1µl of 6X purple loading dye (New England Biolabs, Ipswich, MA, USA) and run on a 1% agarose gel made with a 1000bp ladder (New England Biolabs) in 1X TAE for 35mins at 110V (**Figure C:2**).

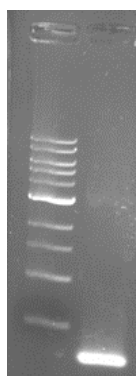


*Figure C:2 – Gel image of generating the ZnT8 murine REKK insert*

Lane 1: 1000bp ladder; Lane 2: PCR product of ZnT8 insert (estimated ~252 bp).

## Appendix C. ZnT8A epitope studies

To remove possible contaminants, a PCR clean-up kit (Qiagen) was conducted to purify the remaining 45µl according to manufacturer instructions. To concentrate the DNA, the purified PCR product was ethanol precipitated (2 volumes of 100% ethanol and 1/10 volume of 3M Potassium Acetate was added, centrifuged at 13,000rpm for 20mins, and the supernatant was carefully removed), washed with 70% ethanol and left to air-dry at RT for 1 hour. The PCR product was then rehydrated in 10µl sterile H<sub>2</sub>O and stored at -20°C until restriction enzyme digest.

---

### C.1.3. Cloning the ZnT8 murine REKK back into the ZnT8 pCMVTnT vector

---

The ZnT8 murine REKK construct and the ZnT8 pCMVTnT vector (1µg) was digested in a 50µl reaction mix with 1µl of restriction enzymes *XhoI* and *HindIII* (New England BioLabs), 5µl 10X CutSmart buffer (New England BioLabs), and sterile ddH<sub>2</sub>O for 2 hours at 37°C. Following incubation, the total reaction mixes were run on a 1% agarose gel with 100bp and 1kb ladders (New England Biolabs) in 1X TAE for 35mins at 110V (**Figure C:3**).

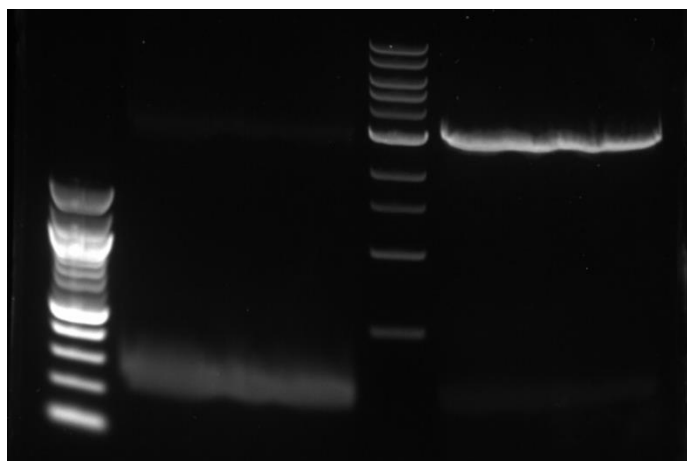


*Figure C:3 – Gel image of XhoI & HindIII double digest on the ZnT8 murine REKK insert & the ZnT8 pCMVTnT vector*

Lane 1: 100bp ladder; Lane 2: ZnT8 murine REKK insert; Lane 3: 1000bp ladder; Lane 4: ZnT8 pCMVTnT vector. Two double digest reactions were run to confirm successful double digest of ZnT8 murine REKK insert and the ZnT8 pCMVTnT vector using *XhoI* and *HindIII* restriction enzymes. ZnT8 insert estimated ~252bp, and the ZnT8 pCMVTnT vector estimated ~2951bp following double digest but size may be skewed due to the high agarose concentration of the gel.

## Appendix C. ZnT8A epitope studies

Gel extraction was then conducted according to the manufacturer's instructions (Qiagen). To concentrate the resultant DNA (50µl), the purified PCR product was ethanol precipitated (2 volumes of 100% ethanol and 1/10 volume of 3M Potassium Acetate was added, centrifuged at 13,000rpm for 20mins, and the supernatant was carefully removed), washed with 70% ethanol, and left to air-dry at RT for 1 hour. Purified DNA digests of ZnT8 insert and pET49b(+) vector were resuspended in 10µl sterile ddH<sub>2</sub>O, mixed, and added in a 1:3 ratio to a 20µl ligation reaction mix containing T4 ligase (Sigma), 2X Ligase buffer (Sigma), and ddH<sub>2</sub>O for a 2-hour incubation at RT. The ligated plasmid was then transformed into DH5α *E. Coli* cells, detailed previously (2.4.2.2.2).

---

### C.1.4. Confirmation of ZnT8 Murine REKK Cloning into the ZnT8 pCMVTnT vector

---

Following transformation and purification of plasmids from single colonies (2.4.2.2.2), plasmids were sent for sequencing using standard SP6 primers (Eurofins, described previously) as well as two specifically designed primers (**Table C:2**) and successful cloning was confirmed utilising BLAST (**Figure C:4**).

Primer	Primer Sequence (5→3)
ZnT8 Murine Primer 1	TACAGCAGCCAG <u>C</u> CGGG
ZnT8 Murine Primer 2	CAACGACCGCAAAAAGGTAT*

*Table C:2 – Primers used to confirm successful cloning of ZnT8 murine REKK into the ZnT8 pCMVTnT vector*

Primer 1: underlined denotes the rs13266634 SNP at aa325 encoding R325. \* Primer 2 was run to sequence the pCMvTnT vector downstream of C-terminal ZnT8 to check for significant alterations.

## Appendix C. ZnT8A epitope studies

GCACTCGAGAATTCGCCGCCACCATGGAG**AAG**GACTTCTCCATCTTACTCATGGAAGGTGTGCCAAA  
GAGCCTGAATTACAGTGGTGTGAAAGAGCTTATTTTAGCAGTCGACGGGGTGCTGTCTGTGCACAG  
CCTGCACATCTGGTCTCTAACAATGAATCAAGTAATTCTCTCAGCTCATGTTGCT**TACAGCAGCCAGCC**  
**GGG**GACAGCCAAGTGGTTCGG**ACGGGA**ATTGCT**CAG**GCCCTTT**CAAGCTTT**ACGATGCACTCACTCA  
CCATTGAGATGGAATCTCCAGTTGACCAGGACCCCGACTGCCTTTTCTGTGAAGACCCCTGTGACTA  
GGA

**Figure C:4 – FASTA sequence of human C-terminal ZnT8 with the successful cloning of ZnT8 murine REKK (TgQ-) into the pCMvTnT vector with the cloning and sequencing primers detailed**

FASTA sequence is detailed in the 5→3 orientation. Dark blue highlight: the beginning of C-terminal ZnT8 (aa268). Underlined: Forward (5→3) and reverse (3→5) PCR primers. Red/bold: *XhoI* restriction enzyme recognition site. Dark blue/bold: *HindIII* restriction enzyme recognition site with the grey highlighting a nucleotide that was changed from AGC to TCA, which both encode serine, but TCA enabled the incorporation of the *HindIII* recognition site. Yellow: R325. Orange: R332T. Light blue: E333G. Green: K336Q. The amino acid 340 was removed at the beginning of the *HindIII* recognition site. Orange: Primer 1 was designed for successful sequencing of the ZnT8 murine REKK construct. Primer 2 was run to sequence the pCMvTnT vector downstream of C-terminal ZnT8 to check for significant alterations (not shown in the figure).

---

## C.2. Primer sequences of C-terminal ZnT8 mutations

---

All primers used to generate mutations in C-terminal ZnT8 are detailed in **Table C:3**, below.

Appendix C. ZnT8A epitope studies

Mutation	C-terminal amino acid position	Primer Sequences (5' → 3')
C361-S	361	F: GACCAGGACCCCGAC <b>AGC</b> CTTTTCTGTGAAG (31bp) R: CTTACAGAAAAG <b>GCT</b> GTCTGGGGTCTCTGGTC (31bp)
C364-S	364	F: CCCGACTGCCTTTT <b>CA</b> GTGAAGACCCCTGTG (31bp) R: CACAGGGGTCTT <b>CACT</b> GAAAAGGCAGTCGGG (31bp)
C368-S*	368	F: TTTTCTGTGAAGACCC <b>CA</b> GTGACTAGGAATTCACG (35bp) R: CGTGAATTCCTAGT <b>CACT</b> GGGGTCTTACAGAAAA (35bp)
C361/C364-S	361 & 364	F: CCCGAC <b>AGC</b> CTTTT <b>CA</b> GTGAAGACCCCTGTG (31bp) R: CACAGGGGTCTT <b>CACT</b> GAAAAG <b>GCT</b> GTCTGGG (31bp)
C361/C368-S*	361 & 368	N/A
R325-Q	325	F: ACAGCAGCCAG <b>CCAG</b> GACAGCCAAGTG (27bp) R: CACTTGGCTGT <b>CC</b> TGGCTGGCTGCTGT (27bp)
R325-W	325	F: CTACAGCAGCCAG <b>CTGG</b> GACAGCCAAGTG (29bp) R: CACTTGGCTGT <b>CCC</b> AGCTGGCTGCTGTAG (29bp)
E333-A	333	F: CCAAGTGGTTCGGAGAG <b>GCA</b> ATTGCTAAAGCCCTTA (35bp) R: TAAGGGCTTTAGCAAT <b>TGCT</b> TCCGAACCACTTGG (35bp)
E333-S	332	F: CAGCCAAGTGGTTCGGAGAT <b>TCA</b> ATTGCTAAAGCCCTTAGC (40bp) R: GCTAAGGGCTTTAGCAAT <b>TGAT</b> TCCGAACCACTTGGCTG (40bp)
EK-A	333 & 340	F: <b>CA</b> ATTGCTAAAGCCCTTAG <b>CGCA</b> AGCTTTACGATGCACTCAC (42bp) R: GTGAGTGCATCGTAAAG <b>CTTGC</b> GCTAAGGGCTTTAGCAAT <b>TG</b> (42bp)
EK-S	333 & 340	F: GAT <b>TCA</b> ATTGCTAAAGCCCTTAG <b>AGC</b> AGCTTTACGATGCACTCA (44bp) R: TGAGTGCATCGTAAAG <b>CTGCT</b> GCTAAGGGCTTTAGCAAT <b>TGATC</b> (44bp)
REK-A	332, 333 & 340	F: ACAGCCAAGTGGTTCGG <b>GCAGCA</b> ATTGCTAAAGCCC (36bp) R: GGGCTTTAGCAAT <b>TGCTG</b> CCCGAACCACTTGGCTGT (36bp)
REK-S	332, 333 & 340	F: GCCAAGTGGTTCGG <b>AGCTCA</b> ATTGCTAAAGCCC (33bp) R: GGGCTTTAGCAAT <b>TGAGCT</b> CCGAACCACTTGGC (33bp)
REKK-A	332, 333, 336 & 340	F: GTGGTTCGG <b>GCAGCA</b> ATTGCT <b>GCAG</b> CCCTTAG <b>CGC</b> (35bp) R: <b>GCG</b> CTAAGGG <b>CTGCAGCA</b> AT <b>TGCTG</b> CCCGAACCAC (35bp)
REKK-S	332, 333, 336 & 340	F: AGTGGTTCGG <b>AGCTCA</b> ATTGCT <b>AGCG</b> CCCTTAGCAGC (37bp) R: GCTGCTAAGGG <b>CGCTAGCA</b> AT <b>TGAGCT</b> CCGAACCACT (37bp)
Murine REKK (TGQ-)	332, 333, 336 & 340	F: GCACTCGAG <b>A</b> ATTCGCCGCCACCATGGAGA (30bp) R: TAAAGCT <b>TGA</b> AAGGG <b>CTGAGCA</b> AT <b>TCCCGT</b> CCGAACCACTTGGCTGT (52bp)

Table C:3 – Primer sequences of C-terminal ZnT8 mutations

N/A: Not applicable; F: Forward primer; R: Reverse primer. Serine or alanine amino acid substitutions was conducted by SDM using primers designed by Agilent (Santa Clara, USA) QuikChange II SDM Instruction Manual and were PAGE-purified at 0.05pmol/μl (Sigma). Bold denotes the location of the amino acid mutation (s). The generation of a ZnT8 construct encoding murine REKK (TGQ-) was conducted through molecular cloning strategies: red denotes the location of amino acid deletion at aa340; dark grey highlight denotes the *XhoI* restriction enzyme recognition site sequence; light grey denotes the *HindIII* restriction enzyme recognition site sequence.\* To generate the ZnT8 construct with the double C361/C368-S mutation, SDM was conducted using the ZnT8 construct with C361S as template DNA and C368-S forward and reverse primers.

---

## **Appendix D. Characterisation of islet autoantibodies after T1D onset**

---

---

### **D.1. Seminal T1D studies reporting autoantibody prevalence**

---

Predominantly, studies that have reported islet autoantibody positivity after T1D onset have been conducted in European-Caucasian populations, usually focused on GADA and IA-2A responses, and have primarily been cross-sectional (**Table D:1**). There have been no reports of a strong association between post-diagnosis islet autoantibody responses and C-peptide/ $\beta$ -cell function to date.

Appendix D. Characterisation of islet autoantibodies after T1D onset

Study (year) Population Autoab Method	Definition of Diabetes	N	Age (years) at diagnosis (range)	Years from diagnosis (range)	AutoAb +ve (%)	GADA +ve (%)	IA-2A +ve (%)	ZnT8A +ve (%)	Main Findings
<b>Savola <i>et al.</i> (1998)</b>  <b>Longitudinal study University of Oulu (Finland)</b>  <b><u>Autoab Detection method:</u> RIA (well-validated)</b>	Diagnosed between 1983-1986	90	8.2 <sup>b</sup> (0.9-15.6)	Samples taken at 0, 2, 5, & 10 yrs	1+ve at 10yrs: 67  ≥2+ve at 10yrs: 46	0yrs: 62  2yrs: 53  5yrs: 32  10yrs: 25	0yrs: 79  2yrs: 74  5yrs: 66  10yrs: 58	¥	- ICA, IA-2A & GADA decreased with increasing disease duration. - 33% & 17% of individuals gained higher GADA and IA-2A levels, respectively.  - GADA loss more rapid with age at diagnosis <10years in first 2 years of disease.  - Titres can remain stable or increase despite reducing β-cell function (C-peptide).
<b>Wenzlau <i>et al.</i> (2010)</b>  <b>Longitudinal &amp; Cross-sectional Barbara Davis Centre (USA)</b>  <b><u>Autoab Detection method:</u> RIA<sup>Denver</sup> (harmonised &amp; well- validated)</b>	<b><u>Four groups:</u></b>  1) 21 new-Dx (<6 weeks)  2) 61 new-Dx (<6 weeks) from BDC  3) 282 long- standing T1D: provided one sample at f-up  4) 142 long- standing T1Ds: provided >1 f-up samples.	1) 21  2) 61  3) 282  4) 142	1) 20.3 <sup>a</sup> (12.2-34.6)  2) 9.8 <sup>a</sup> (1.6-36.7)  3) 11.4 <sup>a</sup> (0.5-52.7)  4) 8.9 <sup>a</sup> (1.0-40.3)	1) 3-month intervals up to 2.5yrs  2) 7 <sup>b</sup> (4.0-12.3) with 0.5-1yr f-up to 7yrs  3) 26.3 <sup>a</sup> (12-57.1)  4) 23.4 <sup>a</sup> (6.9-48.4) with f-up samples (3.0- 10.9)	1) 1+ve: 14.3 ≥2+ve: 85.7	1) 85.7 from 97.2  2) 32.4 from 63  3) 21  4) ¥	1) 90.5 from 90.5  2) 47.5 from 73.8  3) 19.5  4) ¥	1) 76.2 from 85.7  2) 42.6 from 80.3  3) 6.3  4) ¥	1) GADA & ZnT8A +ve decreased but IA-2A was unchanged at 2.5yrs disease duration.  2) Positivity & titres decreased for GADA, IA-2A & ZnT8A. ZnT8A dropped by >80%. 27.6% had detectable C-peptide (>0.02pmol/ml). C-peptide not related to any AutoAb prevalence.  3 & 4) ZnT8A & IA-2A titre but not GADA continued to decline up to 30yrs disease duration. <2% of individuals seroconverted during this time but titres of GADA increased frequently which may explain the plateau of GADA prevalence.

Appendix D. Characterisation of islet autoantibodies after T1D onset

<p><b>Keenan <i>et al.</i> (2010)</b></p> <p><b>Cross-sectional Joslin 50-Year Medals (USA across 42 states)</b></p> <p><b><u>Autoab Detection method:</u> RIA (well-validated)</b></p>	<p>T1D (insulin-dependent) with a duration &gt;50yrs</p>	<p>411 (47%)</p>	<p>11<sup>b</sup> (6.5±)</p>	<p>56.2<sup>b</sup> (5.8±)</p>	<p>1 AutoAb +ve: 29.7</p>	<p>18.4</p>	<p>14.9</p>	<p>¥</p>	<p>- Presence of GADA &amp; IA-2A not associated with random C-peptide.</p> <p>- IA-2A+ve was only found in individuals ≤0.2nmol/L C-peptide.</p>
<p><b>Wang <i>et al.</i> (2012)</b></p> <p><b>Cross-sectional Massachusetts General Hospital</b></p> <p><b><u>Autoab Detection method:</u> RIA<sup>Munich</sup> (well-validated)</b></p>	<p>Clinical diagnosis of diabetes</p>	<p>182</p>	<p>13<sup>a</sup> (1-56)</p>	<p>15<sup>a</sup> (0-73)</p>	<p>¥</p>	<p>50.4</p>	<p>36.2</p>	<p>28.3</p>	<p>- GADA was most prevalent, followed by IA-2A &amp; ZnT8A.</p> <p>- IA-2A &amp; ZnT8A but not GADA positively correlated with C-peptide. ZnT8A remained associated following multivariate analysis.</p> <p>- Number of autoabs did not correlate with C-peptide.</p>
<p><b>Richardson <i>et al.</i> (2013)</b></p> <p><b>Cross-sectional Golden Years Cohort</b></p> <p><b><u>Autoab Detection method:</u> RIA (well-validated)</b></p>	<p>T1D (insulin-dependent) with a duration &gt;50years</p>	<p>343</p>	<p>14<sup>b</sup> (0-36)</p>	<p>55<sup>b</sup> (51-75)</p>	<p>1 AutoAb +ve: 57</p>	<p>48.4</p>	<p>5.8</p>	<p>24.6</p>	<p>- GADA associated with age-at-onset &gt;18yrs but not duration of diabetes or presence of DR3.</p> <p>- IA-2A associated with DR4 &amp; was present at lower levels.</p>
<p><b>Wilmot-Roussel <i>et al.</i> (2013)</b></p> <p><b>Cross-sectional France</b></p> <p><b><u>Autoab Detection method:</u> Commercial RIA (Cisbio Bioassays) validated.</b></p>	<p>T1D &gt;10yrs duration.</p> <p>Criteria: &lt;20 years of age, &amp;/or ketoacidosis, &amp;/or autoab+ve &amp; strict insulin dependency.</p>	<p>430</p>	<p>12<sup>a</sup> (1-70)</p>	<p>19<sup>a</sup> (10-65)</p>	<p>1 AutoAb +ve: 42</p> <p>≥2 AutoAb +ve: 14</p>	<p>46</p>	<p>25</p>	<p>¥</p>	<p>- GADA associated with female gender &amp; DR3. IA-2A associated with DR4 only at short disease duration. No HbA1c, or insulin dose associations.</p> <p>- Autoab+ve associated with older age-at-onset, &amp; shorter disease duration with similar trends between GADA &amp; IA-2A. Titre remained unchanged.</p>

Appendix D. Characterisation of islet autoantibodies after T1D onset

<p><b>Inglemansson <i>et al.</i> (2013)</b></p> <p><b>The Diabetes Incidence Society in Sweden (DISS)</b></p> <p><b><u>Autoab Detection method:</u></b> <b>RIA (well-validated)</b></p>	<p>Diagnosed type 1 diabetes 15-34 years of age.</p> <p>Samples taken at onset and 5-6 years disease duration</p>	<p>270</p> <p>200 with 5-year follow-up</p> <p>70 with 6-year follow-up</p> <p>266 with full autoantibody data</p>	<p>26<sup>b</sup> (15-34)</p>	<p>5<sup>c</sup> (5-6)</p>	<p>¥</p>	<p>52 (67% at Dx)</p>	<p>38 (44% at Dx)</p>	<p>ZnT8RA: 14 (26% at onset)</p> <p>ZnT8WA: 11 (26% at onset)</p> <p>ZnT8QA: 10 (23% at onset)</p>	<p>- Levels of all ZnT8A specificities decreased &lt;5yrs of disease but ZnT8RA &amp; ZnT8WA were more likely to be maintained in individuals with detectable C-peptide at diagnosis during this time frame. - Only frequencies of GADA and IA-2A quoted.</p> <p>- Co-existing GADA correlated with lower levels of ZnT8WA.</p> <p>- No gender, age, or BMI association with ZnT8A.</p>
<p><b>Brorsson <i>et al.</i> (2015)</b></p> <p><b>Type 1 diabetes genetic consortium (T1DGC)</b></p> <p><b><u>Autoab Detection method:</u></b> <b>RIA (well-validated)</b></p>	<p>FDRs from 4,312 multiplex families with a clinical diagnosis of T1D</p>	<p>7,077 T1D-affected FDRs (siblings)</p>	<p>9<sup>a</sup> (±7.52)</p>	<p>7<sup>a</sup> (±10.06)</p> <p>25% of samples taken &lt;3yrs of diagnosis</p>		<p>45</p>	<p>47.1</p>	<p>53.77 (&lt;3yrs disease duration only)</p>	<p>- Female gender &amp; an older age-at-onset was associated with GADA positivity but not IA-2A or ZnT8A using adjusted logistic regression.</p> <p>- Disease duration had a negative association with GADA, IA-2A &amp; ZnT8A positivity.</p>
<p><b>Williams <i>et al.</i> (2016)</b></p> <p><b>Cross-sectional Bart's-Oxford (BOX) family study (UK)</b></p> <p><b><u>Autoab Detection method:</u></b> <b>RIA<sup>Bristol</sup> (harmonised &amp; well-validated)</b></p>	<p>Individuals diagnosed &lt;21yrs &amp; their FDRs.</p>	<p>144</p>	<p>11.7<sup>a</sup> (1.4-22.1)</p>	<p>23<sup>a</sup> (12-29)</p>	<p>1 AutoAb +ve 10yrs: 65.2</p> <p>≥2 AutoAb +ve ≥10yrs: 25.0</p>	<p>38.0 ≥10yrs</p>	<p>65.0 ≥10yrs</p>	<p>18.4 of 104 tested ≥10yrs</p>	<p>- Persistent IA-2A was more common in females.</p> <p>- Persistent IA-2A &amp; ZnT8A was associated with an older-age-at-onset &gt;9 and &gt;1 yrs, respectively.</p> <p>- Level of UCPCR was related to age-at-onset but not diabetes duration, &amp; baseline or f-up islet autoab status.</p>

*Table D:1 – Seminal T1D studies of islet autoantibody positivity after T1D diagnosis*

<sup>a</sup> Median; <sup>b</sup> Mean; <sup>c</sup> Mode; ¥ Unknown/Undetermined/Not Reported; ± SD (standard deviation); RIA: Radioimmunoassay with laboratory location denoted for most validated & harmonised methods with Bristol.

## D.2. Prevalence of ZnT8RA & ZnT8WA at onset & longitudinal follow-up

For the assessment of ZnT8A responses at onset and longitudinal follow-up, the maximum ZnT8A result (AU) between ZnT8RA and ZnT8WA RIAs was used for analysis as responses over follow-up were comparable (**Figure D:1**).

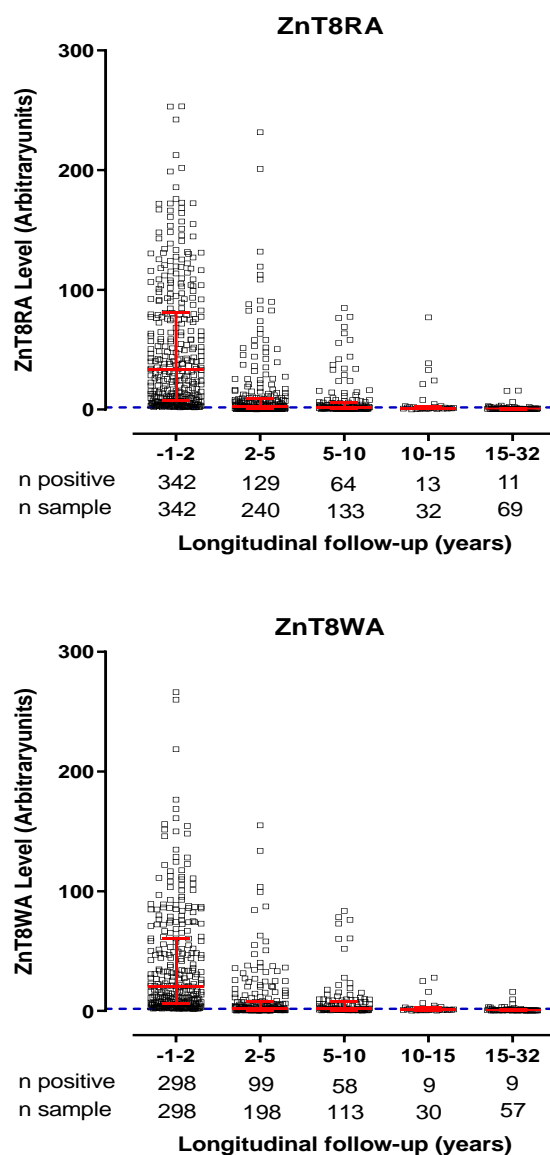


*Figure D:1 – Longitudinal ZnT8RA & ZnT8WA levels from T1D onset*

Individuals positive for ZnT8RA and/or ZnT8WA by RIA out of a T1D cohort of 577 individuals that provided one sample at onset (-1-2 years) and at least one sample at longitudinal follow-up (2-32 years). Autoantibody levels are expressed as arbitrary units (AU). The blue dashed line denotes the positivity threshold at 1.8 AU for both major ZnT8A responses. Red error bars denote respective median units and interquartile ranges. Autoantibody prevalence and median autoantibody titre at longitudinal follow-up compared to onset decreased as a function of increasing disease duration for ZnT8RA and ZnT8WA responses corrected for multiple analysis ( $p_{\text{corr}} < 0.0001$ ). The prevalence of ZnT8RA and ZnT8WA over follow-up was comparable, and the maximum ZnT8A level was used for multivariate analysis and comparison with GADA and IA-2A responses for simplicity.

## D.3. Prevalence of autoantibodies at onset & longitudinal follow-up

### D.3.1. Single autoantibody positives

Multivariate logistic regression would be underpowered since single autoantibody positives comprised a small proportion of the total cohort (n=94; 16.3%), but cohort characteristics, longitudinal prevalence, and longitudinal autoantibody titres were investigated.

#### D.3.1.1. GADA

The characteristics of single GADA positives are detailed in **Table D:2**.

Variable	Number (%)
<b>Gender (n=63)</b>	
Male	29 (46.0)
Female	34 (54.0)
<b>Age at onset (n = 63)</b>	
0.74-7.52 years	12 (19.1)
7.52-10.73 years	3 (4.8)
10.73-13.76 years	20 (31.7)
>13.76– 54.6 years	28 (44.4)
<b>Autoantibody Level (n=63)</b>	
14-64 DK units/ml	15 (23.8)
64-182 DK units/ml	17 (27.0)
182-548 DK units/ml	11 (17.5)
548-1492 DK units/ml	20 (31.7)
<b>HLA Class II (n=54)</b>	
High (DR3-DQ2/DR4-DQ8)	14 (25.9)
Moderate (DQ2/DQ2, DQ8/DQ8, DQ2/X, DQ8/X)	35 (64.8)
Low (X/X, DQ6/X)	5 (9.3)
<b>HLA Class I</b>	
HLA-A*24 Negative (n=48)	34 (70.8)
HLA-B*18 Negative (n=44)	40 (90.9)
HLA-B*39 Negative (n=43)	41 (95.3)

*Table D:2 – Cohort description of single GADA positives & all variables investigated for association with autoantibody loss after onset of T1D*

All available results (n) from 63 individuals single GADA positive at onset that were longitudinally followed-up from type 1 diabetes onset to 29 years disease duration. For Non-HLA SNPs, underlined alleles identify the minor allele.

## Appendix D. Characterisation of islet autoantibodies after T1D onset

In single GADA positive T1D subjects at onset [10.9%; 63/577; median GADA level 177.8 DK units/ml (range 13.7-1268.6)], 76.2% (48/63) remained positive at final sampling [median 5.83 years (range 2.0-28.8)] with a median GADA level of 49.6 DK units/ml (range 0.0-1248.5 DK units/ml). The median autoantibody level for single GADA positives decreased as a function of increasing disease duration at follow-up ( $p < 0.05$ - $0.0001$ ), but the magnitude of titre loss was variable (**Table D:3**).

Whilst there was evidence of a linear trend accounting for missing values ( $p < 0.001$ ), heterogeneity and unequal variance in GADA loss between all pairs of data across longitudinal follow-up was confirmed by the Geisser-Greenhouse correction  $\epsilon < 1$  (**Table D:4**). This can be observed more clearly when longitudinal GADA levels are plotted with subjects with higher GADA titres at onset, more likely to maintain positivity over follow-up as expected (**Figure D:2**).

Descriptive Statistic	GADA Levels (DK units/ml)				
	-1-2 years n=63	2-5 years n=49	5-10 years n=29	10-15 years n=10	15-32 years n=14
Mean (SEM)	371.8 (47.11)	260.7 (49.67)	137.9 (56.5)	65.1 (22.5)	115.5 (53.2)
SD	371.0	340.5	304.5	71.2	199.2
CV%	99.78	130.6	220.8	109.3	172.5
Median (IQR)	183.2 (65.65, 731.7)	71.9 (24.1, 507.3)	24.9 (6.4, 89.6)	43.1 (25.7, 73.9)	18.1 (7.2, 194.6)
Range	13.7-1269.0	0.3-1325.0	0.0-1141.0	0.0-252.4	0.0-732.7

*Table D:3 – Descriptive statistics for levels of GADA over longitudinal follow-up in single GADA positives*

SEM – standard error of the mean; SD – standard deviation; CV% - coefficient of variation (%); IQR – interquartile ranges.

Linear trend & GLM assessment of variance over longitudinal follow-up	GADA
Linear trend across follow-up	$2.0 \times 10^{-4}$ (***)
Slope (95% CI)	-52.6 (-26.1, -79.1)
Means different across follow-up (sig. level)	$2.0 \times 10^{-4}$ (***)
Geisser-Greenhouse correction $\epsilon$	0.6
n missing values	148

Table D:4 – Linear trend and GLM assessment of variance over longitudinal follow-up in single GADA positives

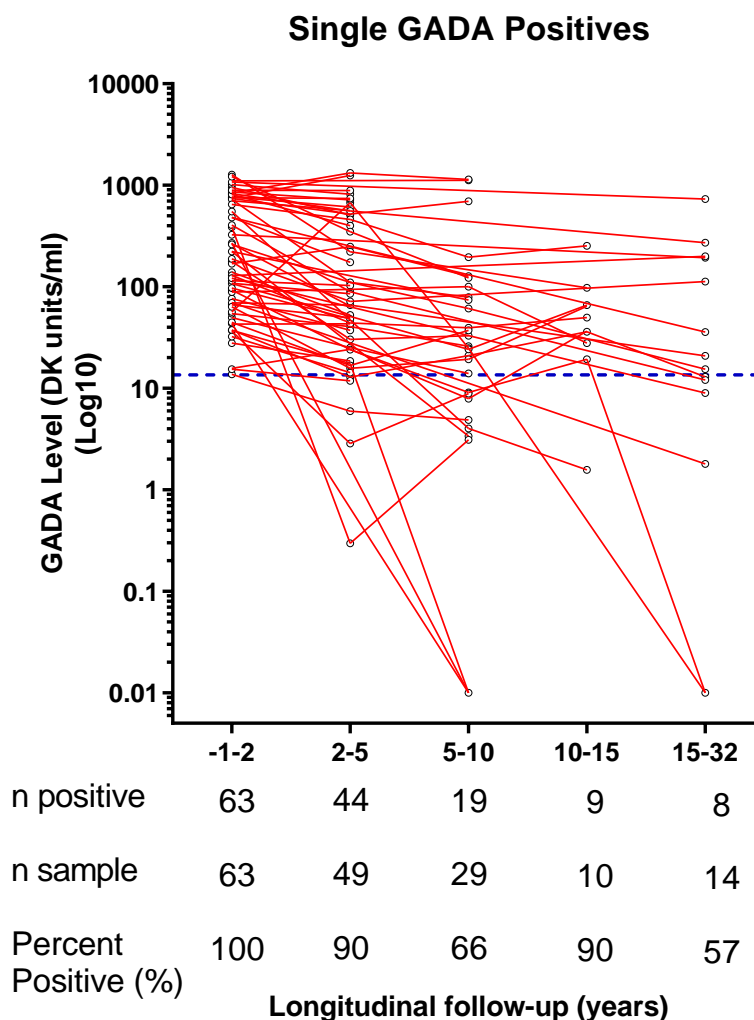


Figure D:2 – Longitudinal single GADA positive responses

Individuals single GADA positive (n=63) by RIA out of 577 T1D individuals that provided one sample at onset (-1-2 years) and at least one sample at longitudinal follow-up (2-29 years). Autoantibody levels are expressed as Diabetic Kidney (DK) units/ml and plotted on a logarithmic scale for resolution. Autoantibody levels equal to zero were transformed to 0.01 DK unit/ml to allow points to be plotted. The blue dashed line denotes the GADA positivity threshold (13.5 DK units/ml) based on the 97th percentile of 1000 adults (274).

## Appendix D. Characterisation of islet autoantibodies after T1D onset

The variables associated with longitudinal GADA loss at final follow-up could not be fully evaluated in the single GADA positive subset due to the small sample size. Despite this, individuals with a single GADA autoantibody response can produce a range of GADA levels [n=20 (31.7%) had GADA levels at the highest quartile 548-1492 DK units/ml] and may be more common in individuals diagnosed older [n=48 (76.2%) diagnosed >11 years], which is comparable to GADA responses in the presence of co-existing autoantibodies.

### D.3.1.2. IA-2A

The characteristics of single IA-2A positives are detailed in **Table D:5**.

Variable	Number (%)
<b>Gender (n=22)</b>	
Male	13 (59.1)
Female	9 (40.9)
<b>Age at onset (n = 22)</b>	
0.74-7.52 years	12 (54.5)
7.52-10.73 years	6 (27.3)
10.73-13.76 years	3 (13.6)
>13.76– 54.6 years	1 (4.5)
<b>Autoantibody Level (n=22)</b>	
1-99 DK units/ml	10 (45.5)
99-269 DK units/ml	7 (31.8)
269-354 DK units/ml	4 (18.2)
354-541 DK units/ml	1 (4.5)
<b>HLA Class II (n=20)</b>	
High (DR3-DQ2/DR4-DQ8)	8 (40.0)
Moderate (DQ2/DQ2, DQ8/DQ8, DQ2/X, DQ8/X)	8 (40.0)
Low (X/X, DQ6/X)	4 (20.0)
<b>HLA Class I</b>	
HLA-A*24 Negative (n=19)	15 (78.9)
HLA-B*18 Negative (n= 17)	15 (88.2)
HLA-B*39 Negative (n= 16)	14 (82.4)

**Table D:5 – Cohort description of single IA-2A positives & all variables investigated for association with autoantibody loss after onset of T1D**

All available results (n) from 22 individuals single IA-2A positive at onset that were longitudinally followed-up from type 1 diabetes onset to 26 years disease duration. For Non-HLA SNPs, underlined alleles identify the minor allele.

## Appendix D. Characterisation of islet autoantibodies after T1D onset

In single IA-2A positive subjects at onset [3.8%; 22/577; median IA-2A level 118.2 DK units/ml (range 1.5-355.7)], 54.5% (12/22) remained positive at final sampling [median 10.1 years (range 2.9-26.3)] with a median IA-2A level of 1.7 DK units/ml (range 0.0-328.0 DK units/ml). The median autoantibody level for single IA-2A positives decreased as a function of increasing disease duration at follow-up ( $p < 0.05-0.01$ ), but the magnitude of titre loss was variable (**Table D:6**).

Descriptive Statistic	IA-2A Levels (DK units/ml)				
	-1-2 years n=22	2-5 years n=13	5-10 years n=16	10-15 years n=6	15-32 years n=5
Mean (SEM)	141.9 (26.03)	55.2 (28.03)	21.3 (12.3)	9.6 (6.2)	14.1 (13.3)
SD	122.1	101.0	49.2	15.2	29.8
CV%	86.04	182.9	231.0	158.6	212.3
Median (IQR)	118.2 (7.1, 256.3)	11.1 (2.2, 48.1)	2.0 (1.0, 21.0)	1.4 (0.53, 21.4)	1.2 (0.2, 34.4)
Range	1.5-355.7	0.0-328.0	0.0-198.6	0.2-38.1	0.0-67.4

*Table D:6 – Descriptive statistics for levels of IA-2A over longitudinal follow-up in single IA-2A positives at T1D onset*

SEM – standard error of the mean; SD – standard deviation; CV% - coefficient of variation (%); IQR – interquartile ranges.

The variables associated with longitudinal IA-2A loss at final follow-up could not be fully evaluated in the single IA-2A positive subset due to the small sample size. However, the data suggests that perhaps individuals with a single IA-2A autoantibody response may be more likely to have lower levels of IA-2A at onset and may be more common in individuals diagnosed younger, but no robust conclusions can be drawn. The sample size was too small for mixed-model GLMs to estimate variance and linear trend. However, a negative linear trend can be observed when plotted on a logarithmic scale with subjects with higher IA-2A titres at onset more likely to maintain positivity over follow-up as expected (**Figure D:3**).

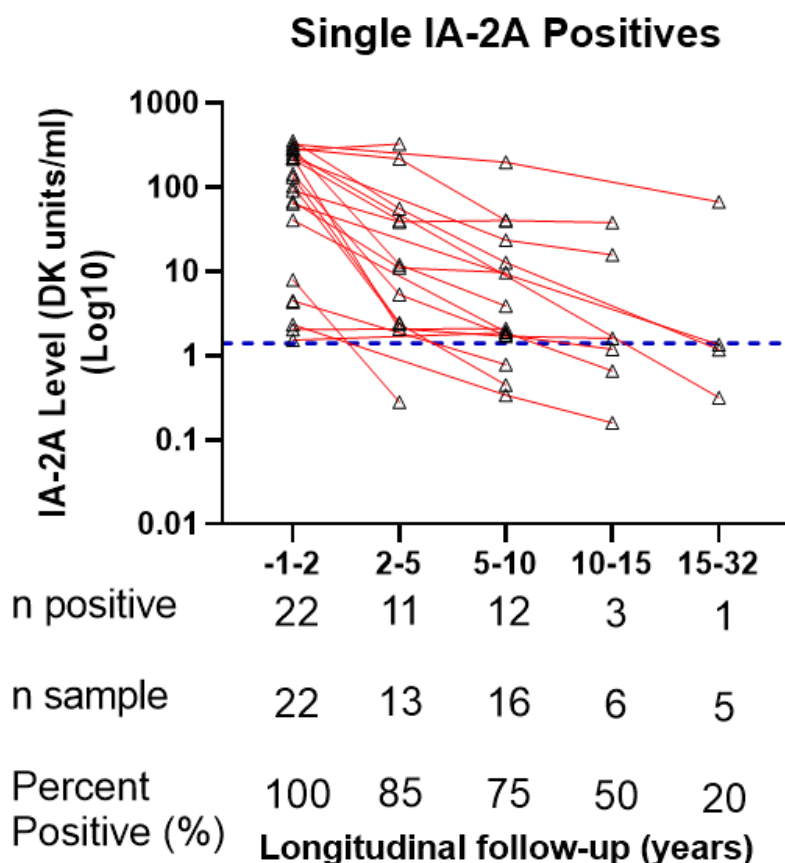


*Figure D:3 – Longitudinal single IA-2A positive responses*

Individuals single IA-2A positive (n=22) by RIA out of 577 T1D individuals that provided one sample at onset (-1-2 years) and at least one sample at longitudinal follow-up (2.9-26.3 years). Autoantibody levels are expressed as Diabetic Kidney (DK) units/ml and plotted on a logarithmic scale for resolution. Autoantibody levels equal to zero were transformed to 0.01 DK unit/ml to allow points to be plotted. The blue dashed line denotes the IA-2A positivity threshold (1.4 DK units/ml) based on the 98th of 500 adults (274).

### D.3.1.3. ZnT8A

The characteristics of single IA-2A positives are detailed in **Table D:7**.

Appendix D. Characterisation of islet autoantibodies after T1D onset

Variable	Number (%)
<b>Gender (n=9)</b>	
Male	8 (88.9)
Female	1 (11.1)
<b>Age at onset (n = 9)</b>	
0.74-7.52 years	2 (22.2)
7.52-10.73 years	4 (44.4)
10.73-13.76 years	1 (11.1)
>13.76– 54.6 years	2 (22.2)
<b>Autoantibody Level (n=9)</b>	
2-8 AU	5 (55.6)
8-33 AU	1 (11.1)
33-85 AU	3 (33.3)
85-266 AU	0 (0.0)
<b>HLA Class II (n=)</b>	
High (DR3-DQ2/DR4-DQ8)	3 (33.3)
Moderate (DQ2/DQ2, DQ8/DQ8, DQ2/X, DQ8/X)	5 (55.6)
Low (X/X, DQ6/X)	1 (11.1)
<b>HLA Class I</b>	
HLA-A*24 Negative (n=9)	8 (88.9)
HLA-B*18 Negative (n= 8)	7 (87.5)
HLA-B*39 Negative (n= 8)	7 (87.5)

*Table D:7 – Cohort description of single ZnT8A positives & all variables investigated for association with autoantibody loss after T1D onset*

In single ZnT8A positive subjects at onset [1.6%; 9/577; median ZnT8A level 7.5 AU (range 3.7-54.9)], 22.2% (2/9) remained positive at final sampling [median 9.9 years (range 3.7-29.4)] with a median ZnT8A level of 0.9 AU (range 0.4-3.2 AU). Median autoantibody ZnT8A level over longitudinal follow-up could only be assessed between onset and 2-5 years (>5 pairs), and there was no difference ( $p>0.05$ ). The variables associated with longitudinal ZnT8A loss at final follow-up could not be fully evaluated in the single ZnT8A positive subset due to the small sample size. Likewise, descriptive statistics and mixed-model GLMs would not be informative on such a small sample size. However, a negative linear trend can be observed when plotted on a logarithmic scale with individuals with low-level ZnT8A (55.6% <8AU) rapidly losing ZnT8A as expected (**Figure D:4**).

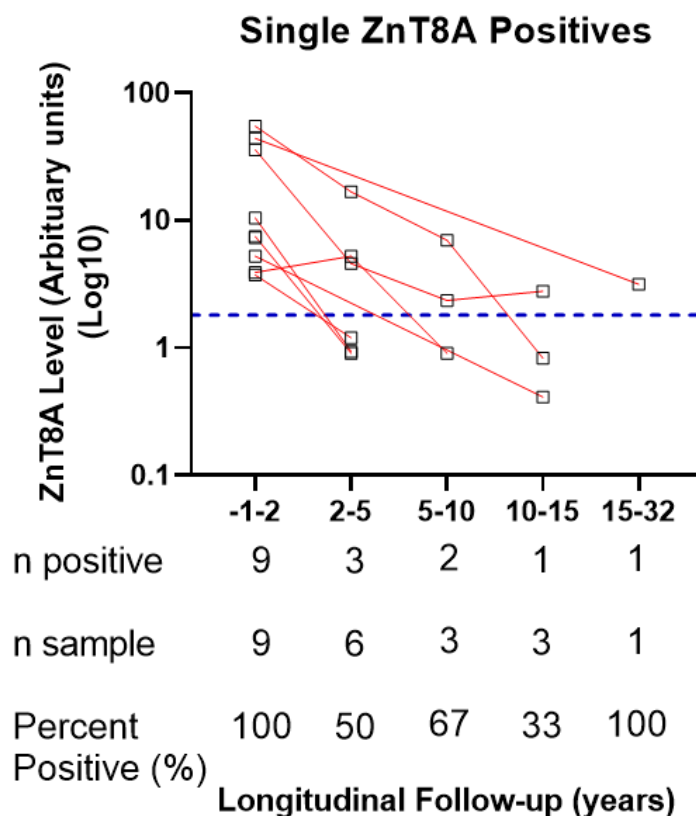


*Figure D:4 – Longitudinal single ZnT8A positive responses*

Individuals single ZnT8A positive (n=9) by RIA out of 577 T1D individuals that provided one sample at onset (-1-2 years) and at least one sample at longitudinal follow-up 3.7-29.4 years). Autoantibody levels are expressed as arbitrary units (AU) and plotted on a logarithmic scale for resolution. Autoantibody levels equal to zero were transformed to 0.01 AU to allow points to be plotted. The blue dashed line denotes the ZnT8A positivity threshold (1.8AU) based on the 97.5th of 523 healthy schoolchildren (274).

---

#### D.4. Patterns of autoantibody titre over longitudinal follow-up

---

Previous reports have indicated that autoantibody responses before T1D onset show waxing and waning patterns over follow-up and, that after T1D onset, can have increased titres (which has only been reproducibly found for GADA (493)). Therefore, it was of interest to characterise these patterns in individuals who provided  $\geq 2$  longitudinal samples. Few studies have been able to characterise this in-depth in a large cohort of individuals prospectively followed-up.

---

#### D.4.1. Prevalence of increasing autoantibody titres after T1D onset

---

Any longitudinal follow-up sample that had a higher autoantibody titre compared with initial sampling around T1D onset (baseline) was selected independent of the magnitude. Other available samples from the same individual that did not have a higher titre compared to baseline were omitted but included in the waxing-waning section where applicable.

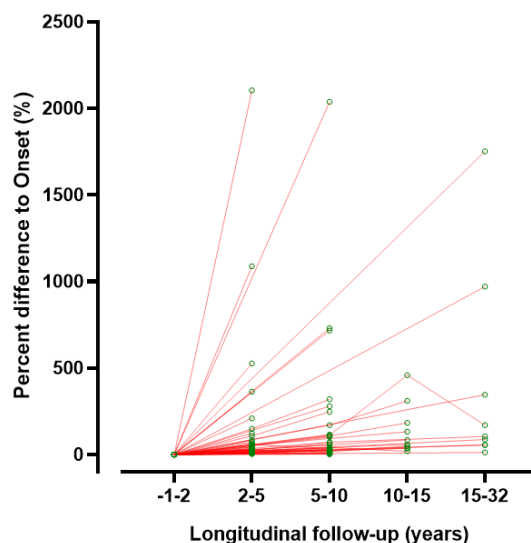
##### D.4.1.1. GADA

---

In GADA positive individuals at onset, 67 (14.0%; n=487 positive at onset) had at least one follow-up sample with higher GADA levels than baseline. Of 68, 53 (77.9%), 13 (19.1%), and 2 (2.9%) had 1, 2, or 3 longitudinal samples with higher GADA titres compared to baseline, respectively. The median GADA titre and median percent difference increased from baseline over longitudinal follow-up (time categories all  $p < 0.01$ - $0.0001$ ) (**Figure D:5**).

The prevalence of increasing GADA titres after onset appeared unrelated to the quartile of baseline GADA level [Q1 (n=20; 29.4%); Q2 (n=16; 23.5%); Q3 (n=14; 20.6%); Q4 (n=18; 26.5%)] and can occur in long-duration T1D. It is important to note that the sample availability over longitudinal follow-up also decreased from these individuals, with 55.2% (n=37), 43.3% (n=29), 14.9 (n=10), and 13.2% (n=9) providing samples within 2-5 years, 5-10 years, 10-15 years, and 15-32 years of onset, respectively.

## Appendix D. Characterisation of islet autoantibodies after T1D onset



	Onset	Longitudinal Follow-up			
	-1-2yrs	2-5yrs	5-10yrs	10-15yrs	15-32yrs
n samples	68	37	29	10	9
Median (IQR) GADA level (DK units/ml)	154.5 (56.6, 609.7)	448.7 (111.5, 939.5)	419.7 (173.8, 867.0)	509.9 (35.8, 1124.0)	521.3 (240.7, 795.0)
Median (IQR) Percent Difference to Onset (%)	0	30.9 (11.4, 78.1)	40.3 (19.5, 142.5)	71.5 (37.3, 214.9)	104.3 (55.3, 657.9)
Number of samples per quartile of GADA at onset	Q1: 20 Q2: 16 Q3: 14 Q4: 18	Q1: 10 Q2: 7 Q3: 7 Q4: 13	Q1: 6 Q2: 9 Q3: 6 Q4: 8	Q1: 4 Q2: 1 Q3: 2 Q4: 3	Q1: 3 Q2: 2 Q3: 3 Q4: 1

**Figure D:5 – Increasing GADA titres after T1D onset**

A plot of percent difference of GADA level compared to onset was calculated using the formula  $[100 * (\text{follow-up result} - \text{onset result} / \text{onset result})]$ . Median GADA level and percent difference increased from baseline (onset) over longitudinal follow-up by pairwise Wilcoxon signed-rank tests ( $p < 0.01$ - $0.0001$  across all time points).

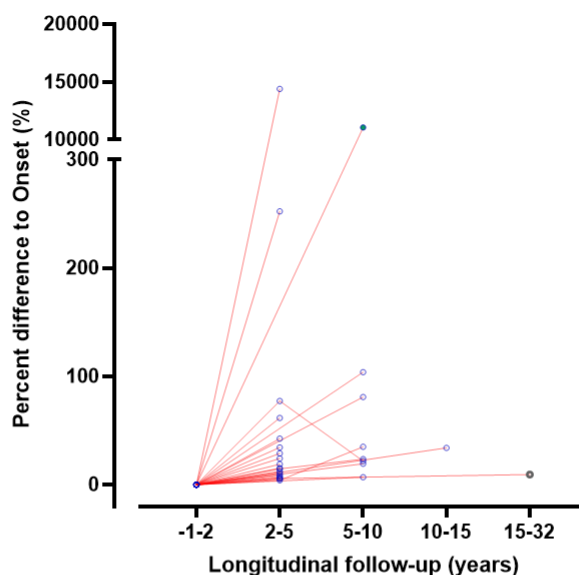
### D.4.1.2. IA-2A

In IA-2A positive individuals at onset, 25 (5.5%;  $n=452$  positive at onset) had at least one follow-up sample with higher IA-2A levels than at baseline. Of these 25 individuals, 21 (84.0%) and 4 (16.0%) had 1 or 2 longitudinal samples with higher IA-2A titres than baseline, respectively. The median IA-2A titre median percent difference increased from baseline increased over longitudinal follow-up ( $p < 0.0001$ - $0.05$ ) (**Figure D:6**).

The prevalence of increasing IA-2A titres after onset is lower than GADA and appeared to be almost equally distributed between individuals with a lower [Q1/Q2: 41.7% ( $n=10$ )] or upper [Q3/Q4: 60% ( $n=15$ )] quartile of IA-2A at onset. This indicates that increasing titre can occur

## Appendix D. Characterisation of islet autoantibodies after T1D onset

at all baseline IA-2A titres and that extrapolated IA-2A titre above the higher assay standard (>250 DK units/ml) can still show increased titres. Only 1 individual with an IA-2A titre in the highest quartile (354.3-541.2 DK units/ml) had a higher IA-2A titre at 5-10 years follow-up with a 7.1% difference to onset. Importantly, only 1 sample was available at 10-15 years and 15-32 years and, therefore, cannot be analysed. Due to the limited data, it is difficult to draw any conclusions about when increasing IA-2A titre may be most prevalent over longitudinal follow-up but may still occur >10 years disease duration.



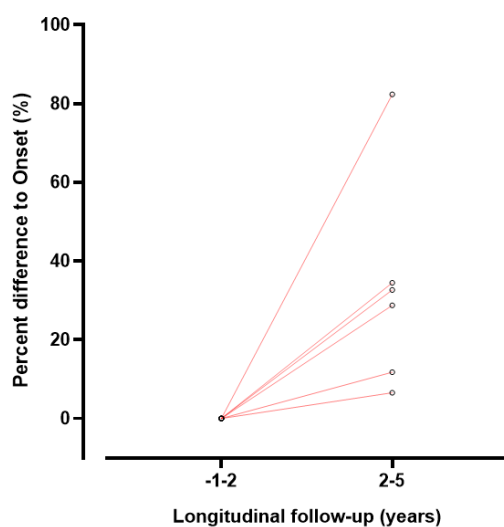
	Onset	Longitudinal Follow-up			
	-1-2yrs	2-5yrs	5-10yrs	10-15yrs	15-32yrs
n samples	25	19	8	1	1
Median (IQR) IA-2A level (DK units/ml)	274.3 (105.4, 311.8)	328.0 (260.2, 360.2)	335.8 (171.8, 412.1)	67.23 (N/A)	296.5 (N/A)
Median (IQR) Percent Difference to Onset (%)	0	15.3 (7.7, 42.5)	29.2 (20.0, 98.2)	33.9 (N/A)	9.4 (N/A)
Number of samples per quartile of IA-2A at onset	Q1: 5 Q2: 5 Q3: 14 Q4: 1	Q1: 3 Q2: 4 Q3: 11 Q4: 0	Q1: 1 Q2: 2 Q3: 3 Q4: 1	Q1: 1	Q3: 1

**Figure D:6 – Increasing IA-2A titres after T1D onset**

A plot of percent difference of IA-2A level compared to onset was calculated using the formula  $[100 * (\text{follow-up result} - \text{onset result}) / \text{onset result}]$ . Median IA-2A level and percent difference increased over longitudinal follow-up by pairwise Wilcoxon signed-rank tests where comparisons were possible ( $p < 0.05$ - $0.0001$ ). Due to limited sample availability, the assessment of IA-2A levels in these individuals >10 years disease duration cannot be assessed.

### D.4.1.3. ZnT8A

In ZnT8A positive individuals at onset, 6 (1.5%; n=395 positive at onset) had at least one follow-up sample with higher ZnT8A titres than baseline. All 6 individuals provided 1 longitudinal sample at 2-5 years disease duration. The median ZnT8A titre and median percent difference from baseline increased at 2-5 years disease duration ( $p < 0.05$ , **Figure D:7**). The prevalence of increasing ZnT8A titres is rare compared to GADA and IA-2A but can still occur in individuals with a range of baseline ZnT8A titre [Q1: 50.0% (n=3); Q3: 33.3% (n=2); Q4: 16.4% (n=1)]. Due to limited data, any observations about increasing ZnT8A  $\geq 5$  years disease duration cannot be made, but the rapid loss of ZnT8A and low positivity prevalence beyond 5 years suggests that gain of ZnT8A would be extremely rare.



	Onset	Longitudinal Follow-up
	-1-2yrs	2-5yrs
n samples	6	6
Median (IQR) ZnT8A level (AU)	23.9 (3.6, 83.0)	31.7 (3.9, 123.8)
Median (IQR) Percent Difference to Onset (%)	0	30.7 (10.5, 46.4)
Number of samples per quartile of ZnT8A at onset	Q1: 3 Q2: 0 Q3: 2 Q4: 1	Q1: 3 Q2: 0 Q3: 2 Q4: 1

**Figure D:7 – Increasing ZnT8A titres after T1D onset**

A plot of percent difference of ZnT8A level compared to onset was calculated using the formula  $[100 * (\text{follow-up result} - \text{onset result}) / \text{onset result}]$ . Median ZnT8A level and percent difference increased over longitudinal follow-up by pairwise Wilcoxon signed-rank tests ( $p < 0.05$ ). The identification of only 6 individuals from 395 ZnT8A positive T1D subjects at onset suggests increasing ZnT8A is very rare.

---

#### D.4.2. Waxing-waning autoantibody patterns after T1D onset

---

All individuals that showed fluctuating autoantibody levels (>10 units) in at least two samples over longitudinal follow-up were selected; individuals with a decreasing autoantibody level over all follow-up samples compared to the previously available sample were omitted. To investigate and compare mean fold-change over time, all longitudinal samples were compared to the respective autoantibody positivity threshold. All longitudinal samples from these individuals were included for a full assessment of autoantibody profiles. However, given the inappropriate use of linear modelling and missing values from unavailable samples, analysis by the Friedman test (non-parametric one-way ANOVA) was not possible.

There was no evidence of wax-waning patterns in ZnT8A responses, but a subset of GADA and IA-2A positive individuals showed various wax-waning patterns to differing magnitudes. However, it cannot be ruled out that assay variability could account for some degree of variation.

##### D.4.2.1. GADA

---

A total of 69 individuals (14.2% of 487 positive at onset) that provided at least two follow-up samples had fluctuating (waxing-waning) levels of GADA over longitudinal follow-up. The fold-change in GADA level over follow-up compared to baseline demonstrates the heterogeneity between individuals but segregating the data according to quartiles of baseline GADA level shows wax-waning patterns occurred in all quartiles of baseline GADA level (Q1: n=13; Q2: n=19; Q3: 17; Q4: n=20) (**Figure D:8**).

## Appendix D. Characterisation of islet autoantibodies after T1D onset

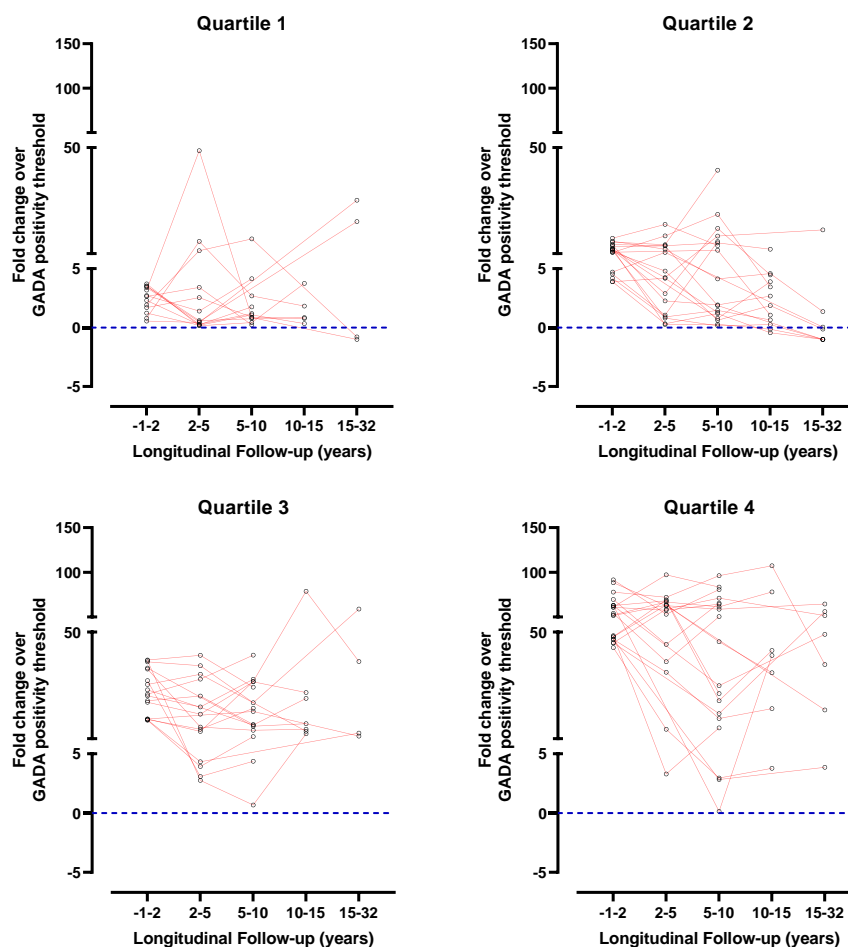


*Figure D:8 – Fold-change in GADA level corrected to the RIA positivity threshold over longitudinal follow-up (waxing-waning patterns)*

Plots of the fold-change in GADA level compared to the RIA positivity threshold organised by quartile of baseline GADA level. Fold-change was calculated using the formula  $[(\text{sample value} - \text{RIA threshold}) \div \text{RIA threshold}]$ .

### D.4.2.2. IA-2A

A total of 26 individuals (5.8% of 452 positive at onset) that provided at least two follow-up samples had fluctuating (waxing-waning) levels of IA-2A over longitudinal follow-up. The fold-change in IA-2A level over follow-up compared to baseline demonstrates the heterogeneity between individuals but segregating the data according to quartiles of baseline IA-2A level shows wax-waning patterns occurred in all quartiles of baseline IA-2A level (Q1: n=6; Q2: n=10; Q3: 6; Q4: n=4) but was rarer than GADA responses (**Figure D:9**).

Appendix D. Characterisation of islet autoantibodies after T1D onset

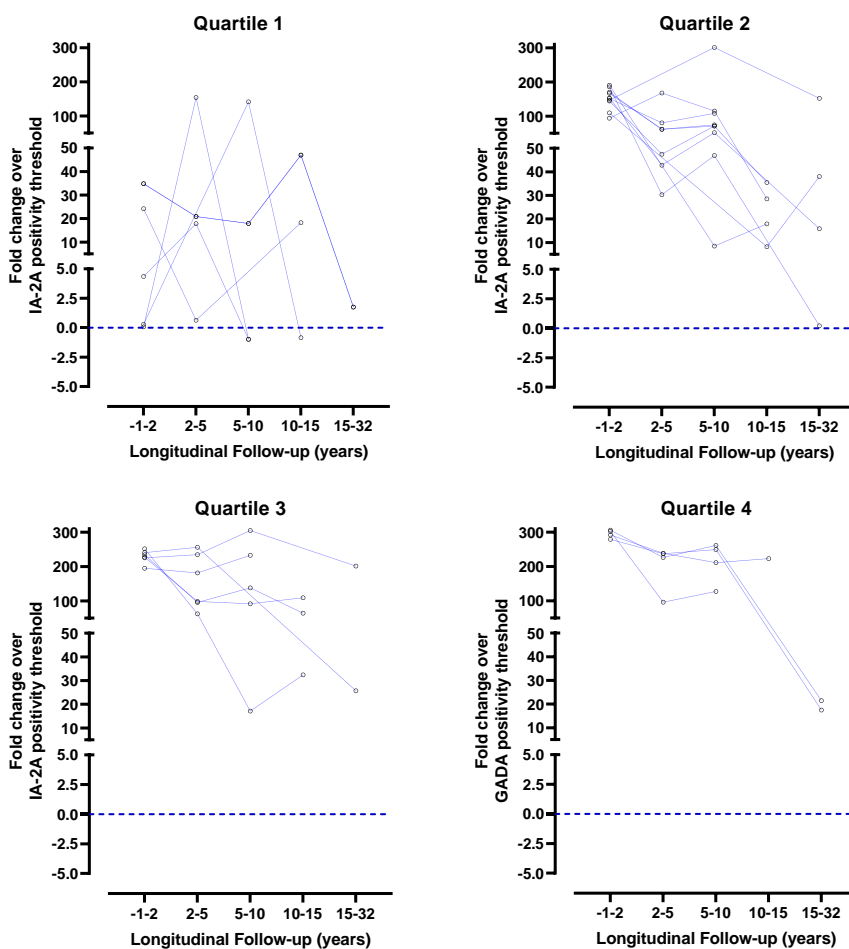


*Figure D:9 – Fold-change in IA-2A level corrected to the RIA positivity threshold over longitudinal follow-up (waxing-waning patterns)*

Plots of the fold-change in IA-2A level compared to the RIA positivity threshold organised by quartile of baseline GADA level. Fold-change was calculated using the formula  $[(\text{sample value} - \text{RIA threshold}) \div \text{RIA threshold}]$ .

## D.4.3. Testing for Gaussian Distribution

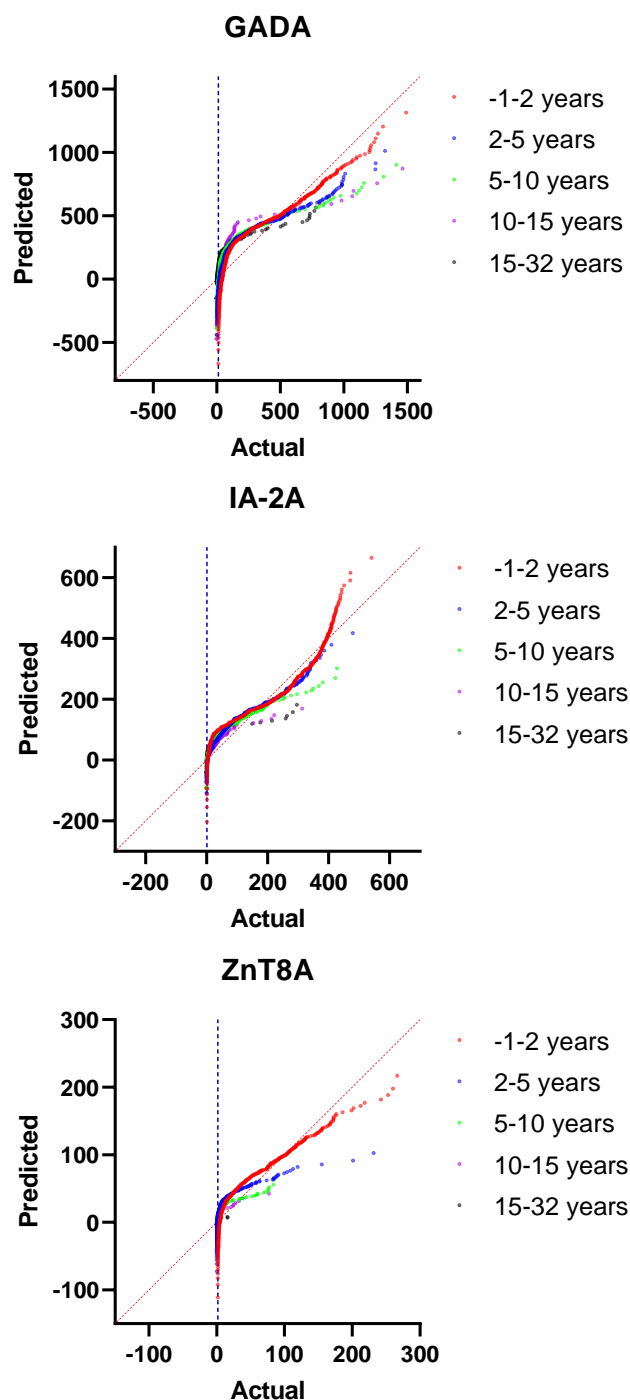


Figure D:10 – QQ plots using raw autoantibody data to test for Gaussian distribution

QQ plots using the raw longitudinal autoantibody data to test for normality. A Gaussian distribution would form a straight line where  $X=Y$  (red dashed line). The blue dotted line denotes positivity thresholds for the respective autoantibody by radioimmunoassay. D'Agostino-Pearson normality omnibus  $K_2$  test provides strong evidence that longitudinal autoantibody data were not sampled from a Gaussian population, as expected ( $p < 0.0001$ ).

## D.4.4. Descriptive statistics of mean autoantibody titres over longitudinal follow-up

Descriptive Statistic	Longitudinal GADA Levels (DK units/ml)				
	-1-2 years n=487	2-5 years n=346	5-10 years n=251	10-15 years n=97	15-32 years n=112
Mean (SEM)	323.9 (14.6)	196.5 (14.7)	150.8 (16.5)	142.7 (28.9)	126.1 (22.4)
SD	321.7	274.0	261.5	284.4	236.6
CV%	99.3	139.5	173.4	199.2	187.7
Median (IQR)	181.6 (63.8, 547.8)	63.9 (20.4, 251.3)	33.1 (11.2, 150.0)	36.5 (14.8, 107.5)	15.5 (0.1, 93.2)
Range	13.5-148	0.0-1325	0.0-1415	0.0-1463	0.0-987.3
Missing values (n)	0	141	236	390	375

Table D:8 – Descriptive statistics of GADA titres over longitudinal follow-up

SEM: standard error of the mean; SD: standard deviation; CV: coefficient of variation (%); IQR: interquartile ranges; DK: Diabetic Kidney.

Descriptive Statistic	Longitudinal IA-2A Levels (DK units/ml)				
	-1-2 years n=452	2-5 years n=311	5-10 years n=246	10-15 years n=89	15-32 years n=108
Mean (SEM)	231.0 (6.7)	100.9 (6.1)	59.0 (5.4)	35.0 (5.6)	26.5 (5.7)
SD	141.9	107.7	84.5	53.2	59.7
CV%	61.4	106.7	143.3	151.9	225.6
Median (IQR)	269.8 (100.1, 354.5)	61.4 (11.8, 171.6)	23.1 (1.9, 82.0)	15.75 (2.7, 313.8)	3.765 (0.0, 296.5)
Range	1.429-541.2	0.0-480.0	0.0-427.9	0.0-313.8	0.0-296.5
Missing values (n)	0	141	206	363	344

Table D:9 – Descriptive statistics of IA-2A titres over longitudinal follow-up

SEM: standard error of the mean; SD: standard deviation; CV: coefficient of variation (%); IQR: interquartile ranges; DK: Diabetic Kidney.

Descriptive Statistic	Longitudinal ZnT8A Levels (AU)				
	-1-2 years n=395	2-5 years n=265	5-10 years n=149	10-15 years n=38	15-32 years n=77
Mean (SEM)	52.9 (2.7)	14.8 (1.9)	10.7 (1.6)	8.2 (2.5)	1.5 (0.3)
SD	54.3	30.2	19.4	15.4	2.6
CV%	102.6	203.7	182.1	187.6	178.0
Median (IQR)	33.4 (7.6, 84.7)	2.9 (0.9, 12.8)	2.1 (1.0, 9.0)	1.2 (0.80, 5.4)	0.7 (0.5, 1.2)
Range	1.8-266.3	0.2-231.6	0.29-84.9	0.0-77.0	0.2-15.9
Missing values (n)	0	130	246	357	318

Table D:10 – Descriptive statistics of ZnT8A titres over longitudinal follow-up

SEM: standard error of the mean; SD: standard deviation; CV: coefficient of variation (%); IQR: interquartile ranges; AU: Arbitrary units.

### D.4.4.1. Mean Differences in autoantibody titre between groups of longitudinal follow-up

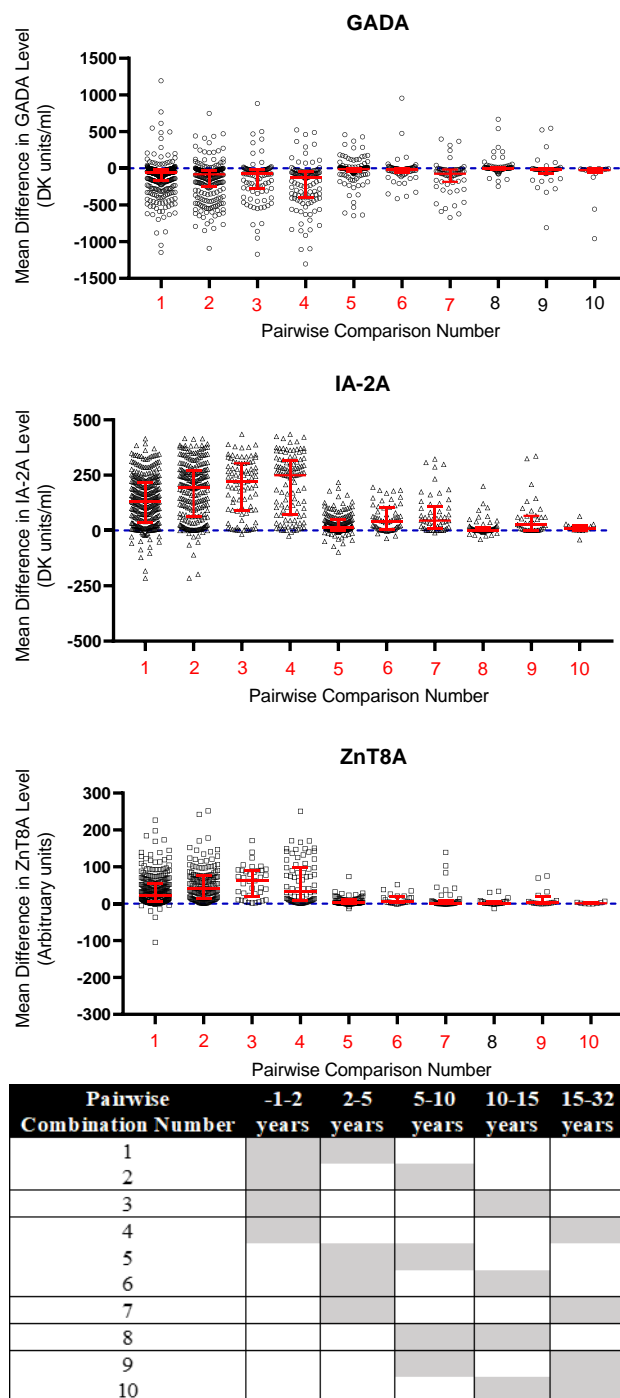


*Figure D:11 – Mean differences in GADA, IA-2A, & ZnT8A level between all combinations of longitudinal follow-up*

Red error bars denote respective median units and interquartile ranges. The blue dashed line indicates zero mean difference in the respective autoantibody titre. Pairwise combination numbers in red indicate significant mean differences in autoantibody titre between the longitudinal follow-up groups ( $p < 0.05$ - $0.0001$  with Tukey's multiple comparisons test).

---

## D.5. Non-genetic associations of longitudinal loss at final follow-up

---

### D.5.1. Longitudinal autoantibody positivity & titre by quartile of autoantibody titre present at T1D onset

---

The longitudinal prevalence of autoantibody positivity was investigated by quartile of autoantibody titre at T1D onset to ascertain whether the effect of autoantibody titre at T1D onset on autoantibody loss at final follow-up could have been influenced by the degree of bias in available serum samples and/or missing data points when considered in a multivariate logistic regression model. Interrogating the data in this way confirmed that the number of available/missing serum samples across all autoantibody titres in all autoantibody responses was comparable (**Table D:11**, **Table D:12**, and **Table D:13** for GADA, IA-2A, and ZnT8A, respectively).

Appendix D. Characterisation of islet autoantibodies after T1D onset

Descriptive Statistic	AutoAb Quartile at onset	Longitudinal GADA Prevalence & Titre (DK units/ml)				
		-1-2 years	2-5 years	5-10 years	10-15 years	15-32 years
Percent Positive/Percent Negative	Q1	100/0	48/52	40/60	56/44	27/73
	Q2	100/0	88/12	72/28	68/32	25/75
	Q3	100/0	98/2	92/8	96/4	64/36
	Q4	100/0	99/1	90/10	95/5	86/14
Median (IQR)	Q1	34.6 (22.2, 49.3)	13.0 (5.9, 25.4)	10.4 (4.5, 21.2)	18.1 (5.7, 29.1)	3.1 (0.0, 18.8)
	Q2	99.6 (77.2, 128.3)	44.0 (22.0, 70.4)	23.9 (10.9, 42.0)	22.4 (10.2, 63.1)	0.0 (0.0, 13.6)
	Q3:	336.4 (247.1, 449.2)	138.0 (72.0, 253.9)	73.9 (36.1, 159.0)	71.8 (30.7, 136.7)	18.6 (6.9, 82.7)
	Q4:	771.2 (650.0, 908.8)	562.0 (313.7, 814.4)	297.0 (78.9, 695.6)	154.3 (76.8, 823.0)	95.5 (0.0, 589.9)
Range	Q1	13.5-63.9	0.0-1250.0	0.0-504.0	0.0-124.0	0.0-540.2
	Q2	65.1-177.8	3.3-296.1	0.0-852.1	1.6-661.8	0.0-126.7
	Q3	181.6-544.4	0.0-999.3	0.0-556.9	10.6-1078.0	0.0-987.3
	Q4	547.8-1492	4.9-1325.0	0.0-1415.0	1.6-1462	0.0-883.9
Total available samples/number of missing values	Q1	123/0	91/32	72/51	27/96	22/101
	Q2	120/0	89/31	57/63	25/95	28/92
	Q3	122/0	90/32	63/59	25/97	33/89
	Q4	122/0	76/47	59/63	20/102	29/93

*Table D:11 – Longitudinal GADA positivity & titre by autoantibody quartile at T1D onset*

Categorisation of longitudinal GADA responses by the quartile of GADA level present at onset. Proportions of individuals positive (%) in available longitudinal samples with complete GADA data (with missing data detailed across follow-up). Median and interquartile ranges (IQRs) and range of GADA levels are detailed to demonstrate variation within each quartile of GADA levels. As expected from the multivariate logistic regression modelling, a higher proportion of individuals remain positive over longitudinal follow-up if high levels (higher quartiles) were present at T1D onset ( $p < 0.0001$ ).

Appendix D. Characterisation of islet autoantibodies after T1D onset

Descriptive Statistic	AutoAb Quartile at onset	Longitudinal IA-2A Prevalence & Titre (DK units/ml)				
		-1-2 years	2-5 years	5-10 years	10-15 years	15-32 years
Percent Positive/Percent Negative	Q1	100/0	55/45	33/67	25/75	8/92
	Q2	100/0	96/4	83/17	84/16	50/50
	Q3	100/0	99/1	99/1	100/0	91/9
	Q4	100/0	99/1	97/3	100/0	86/14
Median (IQR)	Q1	16.0 (4.8, 46.0)	1.6 (0.2, 10.2)	0.4 (0.0, 2.0)	0.4 (0.0, 1.9)	0.0 (0.0, 0.0)
	Q2	199.2 (139.6, 233.6)	42.1 (13.8, 89.9)	16.0 (2.3, 39.8)	12.9 (3.0, 25.3)	1.2 (0.0, 4.2)
	Q3	301.9 (286.6, 330.9)	109.0 (53.5, 240.9)	58.4 (26.5, 99.5)	34.3 (8.7, 72.5)	16.1 (4.0, 71.6)
	Q4	391.8 (373.7, 410.8)	168.7 (70.2, 262.1)	74.1 (24.3, 175.6)	40.7 (21.8, 77.8)	14.7 (5.0, 29.0)
Range	Q1	1.4-98.5	0.0-217.2	0.0-199.7	0.0-67.2	0.0-5.0
	Q2	99.0-268.3	0.0-340.0	0.0-422.4	0.1-69.9	0.0-214.4
	Q3	268.8-354.0	0.3-480.0	0.0-427.9	2.8-219.4	0.2-296.5
	Q4	354.3-541.2	0.0-370.9	0.3-381.1	2.6-313.8	0.5-72.4
Total available samples/number of missing values	Q1	112/0	69/43	58/53	20/92	25/87
	Q2	113/0	84/29	56/47	25/88	26/87
	Q3	113/0	86/27	50/63	22/91	35/78
	Q4	114/0	72/42	72/42	22/92	22/92

*Table D:12 – Longitudinal IA-2A positivity & level by autoantibody quartile at T1D onset*

Categorisation of longitudinal IA-2A responses by the quartile of IA-2A level present at onset. Proportions of individuals positive (%) in available longitudinal samples with complete IA-2A data (with missing data detailed across follow-up). Median and interquartile ranges (IQRs) and range of IA-2A levels are detailed to demonstrate variation within each quartile of IA-2A level. As expected from the multivariate logistic regression modelling, a higher proportion of individuals remain positive over longitudinal follow-up if high levels (higher quartiles) were present at T1D onset ( $p < 0.0001$ ).

Appendix D. Characterisation of islet autoantibodies after T1D onset

Descriptive Statistic	AutoAb Quartile at onset	Longitudinal ZnT8A Prevalence & Titre (AU)				
		-1-2 years	2-5 years	5-10 years	10-15 years	15-32 years
Percent Positive/Percent Negative	Q1	100/0	14/86	12/88	0/100	5/95
	Q2	100/0	37/63	33/67	38/62	5/95
	Q3	100/0	82/18	60/40	33/67	13/87
	Q4	100/0	93/7	91/9	63/37	48/52
Median (IQR)	Q1	3.5 (2.4, 5.3)	0.9 (0.6, 1.4)	0.8 (0.6, 1.3)	0.4 (0.1, 0.7)	0.6 (0.4, 0.7)
	Q2	17.5 (11.5, 24.9)	1.2 (0.7, 4.2)	1.3 (0.7, 2.2)	1.2 (0.8, 2.9)	0.5 (0.4, 0.6)
	Q3	54.9 (42.9, 74.1)	5.3 (2.3, 14.9)	2.3 (1.2, 6.2)	1.1 (0.9, 2.3)	0.9 (0.5, 1.2)
	Q4	119.6 (103.1, 154.6)	32.9 (8.3, 71.1)	15.5 (5.0, 47.0)	12.0 (1.1, 27.1)	1.2 (0.8, 3.1)
Range	Q1	1.8-7.6	0.3-5.4	0.3-3.5	0.0-0.8	0.3-2.4
	Q2	7.8-32.7	0.3-15.6	0.4-9.8	0.4-4.5	0.2-1.9
	Q3	33.3-84.6	0.2-87.9	0.4-60.6	0.7-3.4	0.3-15.8
	Q4	84.7-266.3	0.8-231.6	0.9-84.9	0.6-77.0	0.3-15.9
Total available samples/number of missing values	Q1	99/0	69/30	17/82	5/94	19/80
	Q2	98/0	65/33	40/58	8/90	19/79
	Q3	99/0	71/28	47/52	9/90	16/83
	Q4	99/0	60/39	45/54	16/83	23/76

*Table D:13 – Longitudinal ZnT8A positivity & level by autoantibody quartile at T1D onset*

Categorisation of longitudinal ZnT8A responses by the quartile of ZnT8A level present at onset. Proportions of individuals positive (%) in available longitudinal samples with complete ZnT8A data (with missing data detailed across follow-up). Median and interquartile ranges (IQRs) and range of ZnT8A levels are detailed to demonstrate variation within each quartile of ZnT8A level. As expected from the multivariate logistic regression modelling, a higher proportion of individuals remain positive over longitudinal follow-up if high levels (higher quartiles) were present at T1D onset ( $p < 0.0001$ ).

D.5.2. Longitudinal autoantibody prevalence & titres according to age at T1D onset considered by T1DE subtypes

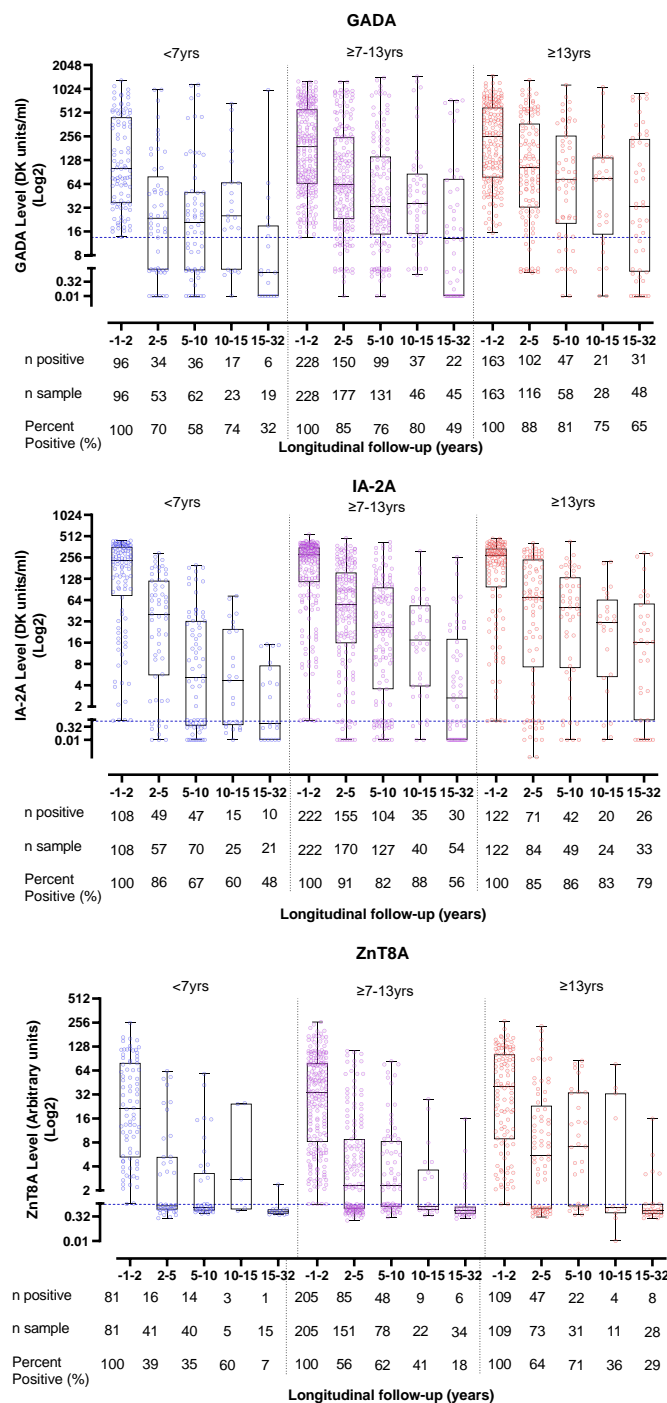


Figure D:12 – Longitudinal autoantibody prevalence & titres according to T1DE categories of T1D age at onset

Percent positive (%) out of the number of serum samples with available autoantibody data for GADA, IA-2A, and ZnT8A according to T1DE age at onset (T1DE1 <7yrs; T1DE2 ≥13yrs). An age at onset ≥7yrs was associated with decreased risk of autoantibody loss at final follow-up for all autoantibody responses (p=0.004-0.011), which was comparable to when age at onset was considered as quartiles. There was a higher proportion of subjects with the highest two quartiles of GADA and IA-2A titres at onset in T1DE2 subjects compared with T1DE1 subjects (p=0.010 and p=0.043, respectively). However, no difference in the quartile of ZnT8A titre at onset was observed between the two T1DEs.

## Appendix E. Development of Nluc-ZnT8 LIPS for ZnT8A detection

### E.1. Autoantibody detection in matched serum & EDTA-preserved plasma samples

Autoantibody RIA (n positive out of 27)	Median autoantibody units in serum (range)	Median autoantibody units in plasma (range)	Change in autoantibody positivity or level
<b>GADA</b> (6)	129.6 (36.6-493.8)	151.7 (39.7-456.1)	Little change
<b>IA-2A</b> (4)	18.4 (4.6-161.3)	14.5 (3.7-186.0)	Little change
<b>IAA</b> (12)	45.1 (0.8-104.5)	44.1 (0.7-135.4)	Little change
<b>ZnT8RA</b> (3)	4.8 (2.6-18.8)	1.8 (1.2-4.1)	Reduction in ZnT8RA binding & positivity.
<b>ZnT8WA</b> (2)	32.1 (4.5-59.7)	14.1 (2.3-26.0)	Reduction in ZnT8WA binding but not positivity.

*Table E:1 – Autoantibody positivity in anonymised matched serum & plasma samples*

Units derived from logarithmic standard curves by RIA are expressed in Diabetes Kidney (DK) units/ml for GADA and IA-2A and arbitrary units (AU) for IAA, ZnT8RA and ZnT8WA. Out of a total of 27 anonymised individuals that had matched serum and plasma samples, 7 were positive for  $\geq 2$  autoantibodies, and 4 were single autoantibody positive; 6 were positive for GADA, 4 were positive for IA-2A, and 3 were positive for ZnT8RA and/or ZnT8WA. It is not known whether the IAA detected is directed to endogenous or exogenous insulin and, therefore, cannot be considered as true positives.

---

## E.2. Nluc-ZnT8 LIPS optimisation

---

### E.2.1. Glycine-blocked PAS immunoprecipitate

---

To investigate whether glycine-blocked (GB)-PAS immunoprecipitate would increase assay sensitivity and specificity, the same concentration was added (6.25µl/well) and incubated for 2.5 hours at room temperature with 4M/25µl LU of Nluc-R+W-ZnT8 dual heterodimer antigen. It was of interest that GB-PAS may reduce non-specific ZnT8A binding in negative controls with greater discrimination from low ZnT8A positive patients. Therefore, samples from the main optimisation sample set and IASP2016 workshop with good volume and low ZnT8A level (<15 AU by monomeric ZnT8RA/ZnT8WA RIAs) were selected:

- 4 Internal ZnT8 RIA standards
- 6 Internal ZnT8 RIA controls (5 positive and 1 negative)
- 2 T1D patients (<15AU in ZnT8RA/ZnT8WA RIAs)
- 1 Anonymised healthy negative control
- 9 Samples from the IASP2016 workshop
  - 7 New-onset T1D patients (<15AU in ZnT8RA/ZnT8Wa RIAs)
  - 2 Negative controls

There was no difference in either the median LU or SNR acquired utilising unblocked PAS (standard) and GB-PAS ( $p>0.05$ ): median SNR of standard PAS 6.6 (range 0.3-73.2); median SNR of GB-PAS 6.3 (range 0.3-46.7)]. However, it is worth noting that the SNR of the highest internal standard was much lower in GB-PAS (46.7) than standard PAS (73.2), but all other samples were comparable (**Figure E:1**).

## Appendix E. Development of Nluc-ZnT8 LIPS for ZnT8A detection

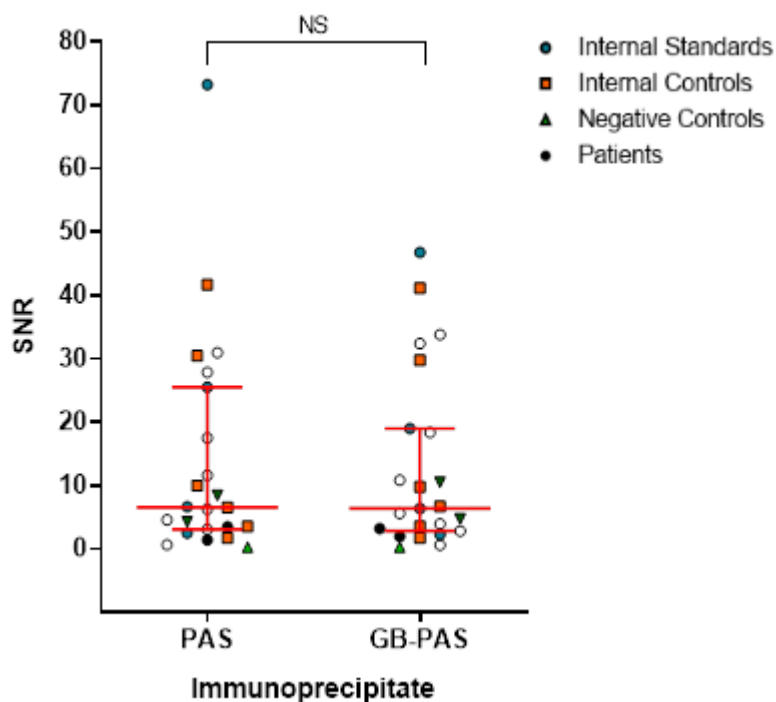


*Figure E:1 – Nluc-ZnT8 LIPS Optimisation: Glycine-blocked PAS (GB-PGS) immunoprecipitate (SNR)*

A plot of signal to noise ratio (SNR) comparing standard PAS and glycine-blocked (GB)-PAS at a volume of 6.25 $\mu$ l/well. Both immunoprecipitates were incubated with 4M/25 $\mu$ l of Nluc-R+W-ZnT8 dual heterodimer antigen construct for 2.5 hours at RT. Red bars denote the median and interquartile ranges. NS: Not significant by pairwise Wilcoxon signed-rank test.

**Experimental conclusion:** Using GB-PAS did not offer any significant improvement in ZnT8A binding or assay background over PAS when incubated at the same volume and concentration (6.25 $\mu$ l/50 $\mu$ l per well). Therefore, it was not implemented.

---

## E.2.2. Expression & preparation of the Nluc-tagged ZnT8 antigen construct

---

### **E.2.2.1. Purification of the Nluc-tagged ZnT8 antigen construct with ZnCl<sub>2</sub>**

---

As ZnCl<sub>2</sub> is corrosive, hazardous to aquatic life, and is an irritant, careful consideration of the maximum concentration appropriate for a routine assay was important. A study of zinc supplementation on the function of rat INS-1E cells (that show β-cell-like activity) indicated that 1mM ZnCl<sub>2</sub> caused a 52% reduction in cell viability compared to only 17% at 0.4mM (555). Another study observed an increase in ZnT8 expression in the β-cell line EndoC-βH1 (comparable stimulation and functionality to human β-cells (556)) when dosed with 600μM extracellular zinc peaked at 10μM (557). Therefore, to investigate the effect of ZnCl<sub>2</sub> on ZnT8A binding to the Nluc-R+W-ZnT8 dual heterodimer construct in the LIPS assay, 1mM was chosen as the maximum concentration, and 0.1mM was chosen as the lower concentration for practical ease.

The Nluc-R+W-ZnT8 dual heterodimer construct was expressed according to the optimised Nluc-GAD65 LIPS protocol (**Table 4:5**) but was purified through a NAP5<sup>TM</sup> desalting column (GE Healthcare) in TBST-0.5% buffer containing 0.1% BSA (v/v) and either 0mM, 0.1mM (v/v), or 1mM (v/v) ZnCl<sub>2</sub> (Sigma). The remainder of the optimised Nluc-ZnT8 LIPS protocol was followed. This assay used samples from the main optimisation sample set:

- 4 Internal ZnT8 RIA standards
- 6 Internal ZnT8 RIA controls (5 positive and 1 negative)
- 9 T1D patients
- 5 Healthy negative controls

## Appendix E. Development of Nluc-ZnT8 LIPS for ZnT8A detection

The median SNR [8.9 (range 0.4-78.0);  $p=0.044$ ] of the Nluc-R+W-ZnT8 dual heterodimer construct purified with 0.1mM was slightly increased when independently ranked and compared with, the absence of  $ZnCl_2$  [median SNR 8.4 (range 0.4-74.7)]. The marginally beneficial effect of  $ZnCl_2$  was not replicated at a concentration of 1mM [median SNR 7.6 (range 0.4-81.3);  $p>0.05$ ] (**Figure E:2**).

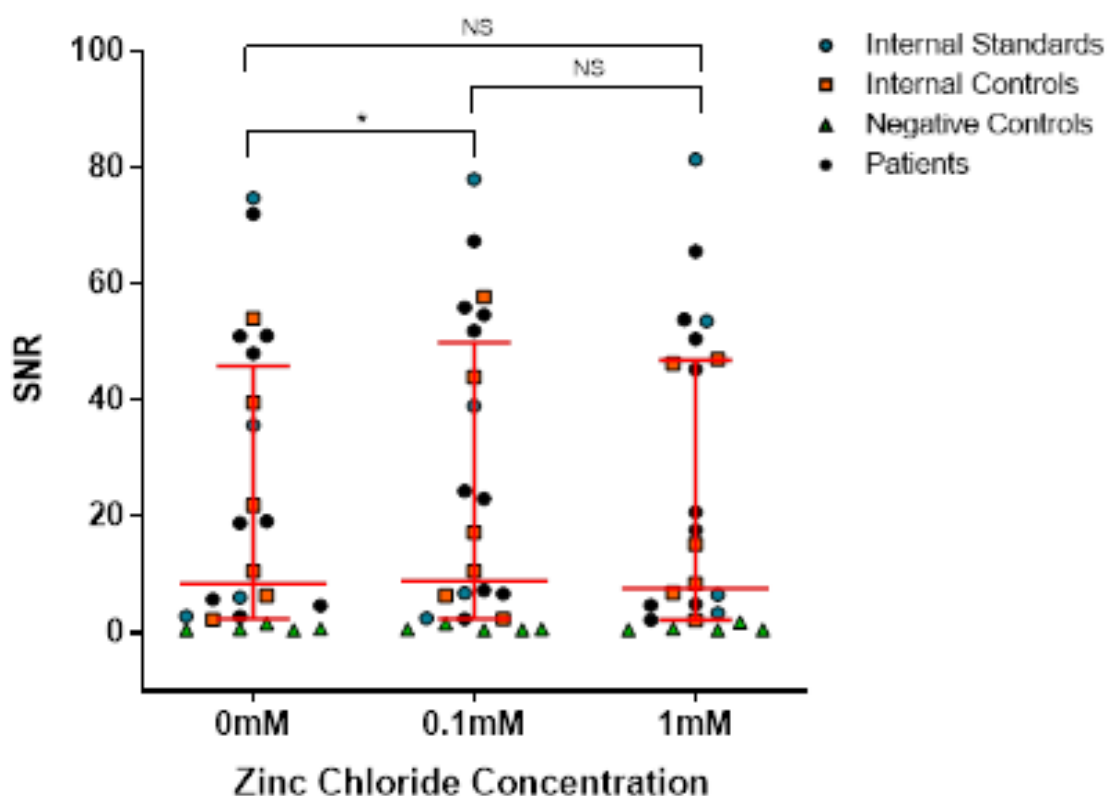


*Figure E:2 – Nluc-ZnT8 LIPS Optimisation: Purification of Nluc-R+W-ZnT8 dual heterodimer construct with  $ZnCl_2$  (SNR)*

A plot of signal to noise ratio (SNR) from investigating the Nluc-R+W-ZnT8 dual heterodimer construct purified with buffers containing 0mM (standard protocol), 0.1mM (v/v), or 1mM (v/v)  $ZnCl_2$ . The remainder of the optimised Nluc-ZnT8 LIPS protocol was followed. Red bars denote median and interquartile ranges. NS: Not Significant less than alpha value 0.05; \* $p<0.05$ ; \*\* $p<0.01$  by pairwise Wilcoxon signed-rank tests.

**Experimental Conclusion:** Despite some evidence to suggest that the presence of 0.1mM ZnCl<sub>2</sub> may benefit ZnT8A binding in some T1D patients and internal standards/controls, the assay background of the negative controls was virtually unchanged, and therefore, there was little to no benefit to lowering the assay background. When accounting for assay background using SNR, the benefit of 0.1mM ZnCl<sub>2</sub> was weak, close to the alpha value (p=0.044). Therefore, the presence of ZnCl<sub>2</sub> does not strongly improve assay performance. To maintain assay harmonisation within the department and with international collaborators conducting LIPS assays for other T1D autoantibodies, the presence of ZnCl<sub>2</sub> during Nluc-antigen purification was excluded.

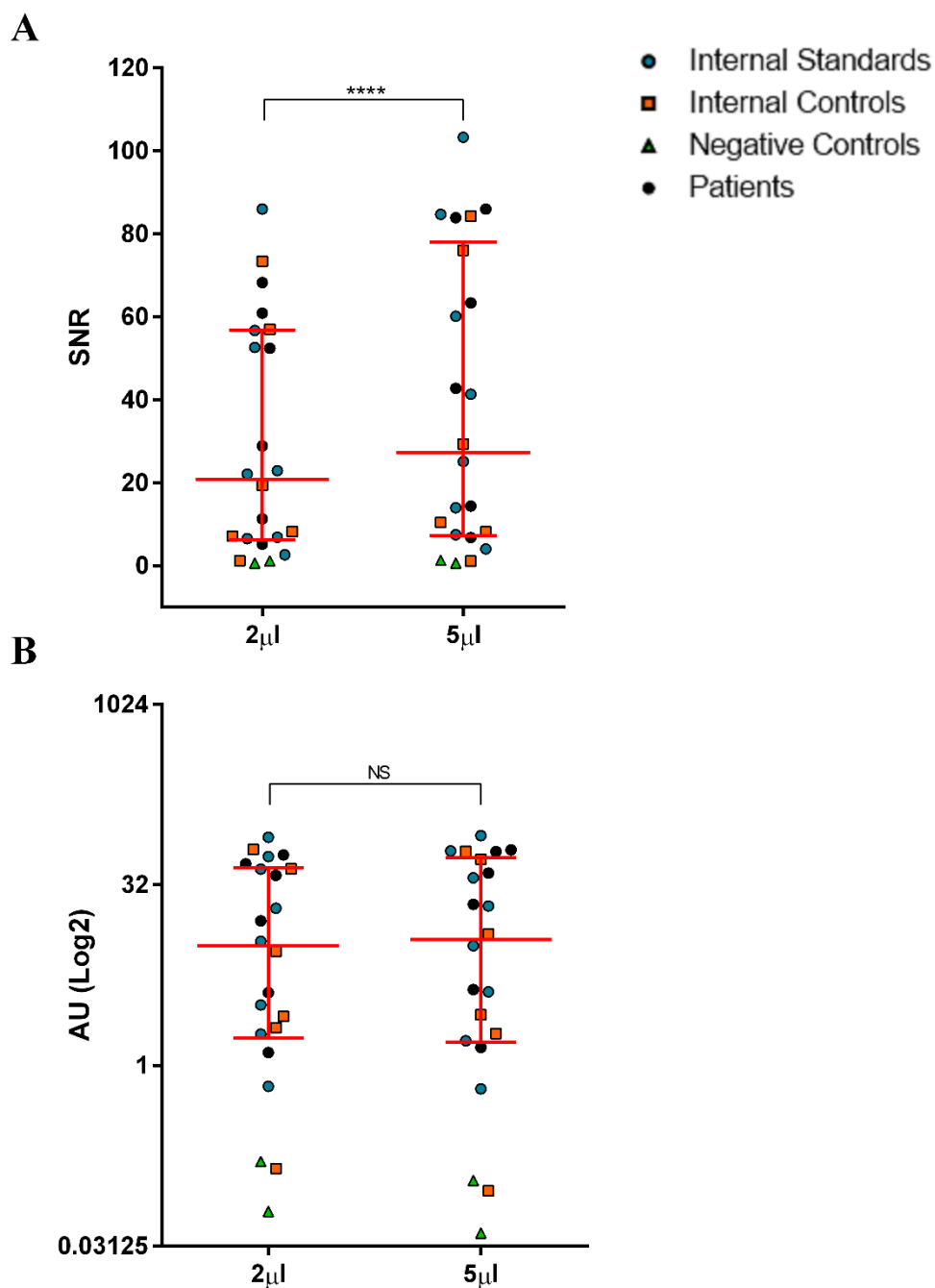
### **E.2.2.2. Quantity of 1mM methionine in Nluc-ZnT8 expression reaction mix**

---

To investigate whether the volume of 1mM methionine (minimum 2µl; maximum 5µl) and the reduction of nuclease free water (7µl/4µl) present in the 50µl Nluc expression reaction mix with 1mg of Nluc-R+W-ZnT8 dual heterodimer antigen would increase ZnT8A binding and/or lower assay backgrounds, the 0.45µM preparation protocol at 4M/25µl LU was tested across two independent assays. The assays included the full set of internal ZnT8 RIA standards (n=8) for AU determination and samples from the main optimisation sample set:

- 8 Internal ZnT8 RIA standards
- 6 Internal ZnT8 RIA controls
- 6 T1D patients
- 2 Healthy negative controls

The median LU [ $6.15 \times 10^5$  (range  $1.41 \times 10^4$ - $2.35 \times 10^6$ )] and median SNR [27.23 (range 0.62-103.3)] of the Nluc-R+W-ZnT8 dual heterodimer expressed with 5µl (maximum) 1mM methionine was slightly increased when independently ranked and compared with 2µl (minimum) 1mM methionine (standard protocol) [median LU  $5.22 \times 10^5$  (range  $1.63 \times 10^4$ - $2.16 \times 10^6$ ); median SNR 20.73 (range 0.65-85.95), both  $p < 0.0001$ ] (SNR presented in **Figure E:3A**). Whilst increasing the volume of 1mM methionine may offer an improvement on assay sensitivity and specificity according to raw data, the logarithmic fit and rank of AUs derived are highly comparable [2µl 1mM methionine median AU 9.91 (range 0.06-79.73); 5µl 1mM methionine median AU 11.20 (range 0.04-82.51)] (**Figure E:3B**).



### Volume of 1mM Methionine in Nluc-ZnT8 Expression Reaction Mix

**Figure E:3 – Nluc-ZnT8 LIPS Optimisation: Volume of 1mM methionine in Nluc-ZnT8 expression reaction mix (SNR/AU)**

Plots of signal to noise ratio (SNR; **A**) and arbitrary units (AU; **B**) comparing the standard 2µl 1mM methionine with 5µl 1mM methionine in the Nluc-ZnT8 expression reaction mix that also contains 1mg of Nluc-R+W-ZnT8 dual heterodimer (1µl\*) pCMvTnT plasmid, 40µl of the SP6 master mix (Promega) and nuclease-free water to make up to a 50µl total volume (7µl/4µl\*). Following Nluc expression, the Nluc-R+W-ZnT8 dual heterodimer construct was prepared for a LIPS assay following the 0.45µM filter unit preparation protocol at a concentration of 4M/25µl LU. Each data point represents four replicates from two independent experiments. Red bars denote the median and interquartile ranges. NS: Not Significant less than alpha value 0.05; \*\*\*\*p<0.0001 by pairwise Wilcoxon signed-rank test. \*Volumes of Nluc pCMvTnT plasmid and nuclease-free water are dependent on the PCMVtnt plasmid concentration; volumes of pCMvTnT plasmid range from 1-5µl and nuclease-free water range from 0-7µl. Therefore, 2µl and 5µl 1mM methionine represent the minimum and maximum quantities that can be present.

## Appendix E. Development of Nluc-ZnT8 LIPS for ZnT8A detection

**Experimental conclusion:** Increasing the quantity of 1mM methionine and decreasing nuclease-free water in the Nluc-ZnT8 expression reaction mix may improve LU/SNR but does not greatly influence the AUs derived. Therefore, it is unlikely that the presence of methionine is a rate-limiting reagent to Nluc-R+W-ZnT8 dual heterodimer antigen expression, but if the concentration of the plasmid permits a higher volume of methionine and a lower volume of nuclease-free water, then this may be preferable.

## E.2.3. Detection of luminescence

## E.2.3.1. Intra-assay &amp; Inter-assay variation of the internal logarithmic standard curve according to substrate incubation length in Nluc-ZnT8 LIPS

Parameter	Standard Number	5 second incubation		15-minute incubation		60-minute incubation	
		Experiment 1	Experiment 2	Experiment 1	Experiment 2	Experiment 1	Experiment 2
<b>Experiment 1 Curve Fit</b>	8	R <sup>2</sup> = 0.93 Equation: y = 2.4186ln(x) - 28.662	R <sup>2</sup> = 0.94 Equation: y = 2.3456ln(x) - 28.016	R <sup>2</sup> = 0.96 Equation: y = 2.5089ln(x) - 30.422	R <sup>2</sup> = 0.95 Equation: y = 2.3673ln(x) - 28.575	R <sup>2</sup> = 0.96 Equation: y = 2.5271ln(x) - 30.341	R <sup>2</sup> = 0.96 Equation: y = 2.3753ln(x) - 28.791
<b>Intra-assay LU Variation for each Internal ZnT8 RIA Standard CV (%)<sup>a</sup></b>	1	5.36	2.54	2.93	7.39	3.39	3.12
	2	3.57	2.53	1.80	1.32	1.16	2.84
	3	2.47	2.70	1.58	0.11	1.77	1.27
	4	9.55	3.99	7.06	4.10	7.24	3.28
	5	9.72	10.67	12.63	16.18	12.90	15.83
	6	0.87	9.13	4.89	4.26	4.61	3.33
	7	4.75	13.94	12.60	15.15	13.40	13.76
	8	1.31	3.98	2.32	2.81	2.88	2.21
<b>Inter-assay LU Variation for each Internal ZnT8 RIA Standard CV (%)<sup>b</sup></b>	1	10.90		4.67		15.39	
	2	14.21		4.70		16.10	
	3	4.74		3.99		14.15	
	4	11.76		7.25		14.71	
	5	10.31		13.51		18.04	
	6	7.35		4.08		5.26	
	7	16.26		11.45		15.24	
	8	2.49		5.75		5.71	

Table E:2 – Nluc-ZnT8 LIPS Optimisation: Intra-assay & inter-assay variability of the logarithmic standard curve according to substrate incubation length

<sup>a</sup> Calculated from two duplicates <sup>b</sup> calculated from four replicates across two experiments using the formula  $[100 \times (\text{standard deviation} \div \text{mean LU})]$ .

